



Méthodes numériques pour la dynamique des structures non-linéaires incompressibles à deux échelles.

Patrice Hauret

► To cite this version:

Patrice Hauret. Méthodes numériques pour la dynamique des structures non-linéaires incompressibles à deux échelles.. Mathématiques générales [math.GM]. Ecole Polytechnique X, 2004. Français. NNT : . pastel-00000961

HAL Id: pastel-00000961

<https://pastel.hal.science/pastel-00000961>

Submitted on 27 Jul 2010

HAL is a multi-disciplinary open access archive for the deposit and dissemination of scientific research documents, whether they are published or not. The documents may come from teaching and research institutions in France or abroad, or from public or private research centers.

L'archive ouverte pluridisciplinaire **HAL**, est destinée au dépôt et à la diffusion de documents scientifiques de niveau recherche, publiés ou non, émanant des établissements d'enseignement et de recherche français ou étrangers, des laboratoires publics ou privés.



POLYTECHNIQUE

Thèse présentée pour obtenir le grade de
DOCTEUR DE L'ÉCOLE POLYTECHNIQUE
Spécialité: Mathématiques Appliquées

par

PATRICE HAURET

Méthodes numériques pour la dynamique des structures non-linéaires incompressibles à deux échelles

Soutenue le lundi 20 Septembre 2004 devant le jury composé de:

François	Jouve	
Tod	Laursen	(rapporteur)
Claude	Le Bris	(président)
Patrick	Le Tallec	(directeur de thèse)
Frédéric	Nataf	
Olivier	Pironneau	(rapporteur)
Ali	Rezgui	

Méthodes numériques pour la dynamique des structures non-linéaires incompressibles à deux échelles

Patrice Hauret

A la mémoire de Jean-Marc et Lana,

A mes parents et grands-parents,

Remerciements

Le travail présenté dans les pages suivantes doit énormément à l'attention constante et aux encouragements de mon directeur de thèse, Patrick Le Tallec, qui s'est toujours montré d'une remarquable disponibilité malgré l'impressionnante charge de son emploi du temps, acceptant bien volontiers de prendre du temps à chaque fois que je faisais irruption dans son bureau de l'Administration de l'Ecole Polytechnique, papiers en mains et bien évidemment sans rendez-vous. Il m'a fait un grand honneur d'encadrer ce travail, et j'ai eu beaucoup de plaisir à être son étudiant : merci Patrick pour cet encadrement que je crois exceptionnel.

Les chapitres à venir doivent également beaucoup à une collaboration fructueuse avec la Manufacture Française des Pneumatiques Michelin, essentiellement en la personne d'Ali Rezgui qui a la responsabilité du service "Etudes et Recherches" au Centre de Technologies de Ladoux. Par des contacts fréquents, l'entreprise partenaire a su manifester son attachement à ce travail et aux applications possibles dans le cadre de la simulation numérique du roulage des pneumatiques. C'est une véritable satisfaction que de savoir son travail suivi et utilisé. En particulier, je tiens à te remercier, Ali, pour m'avoir accueilli durant six mois à Clermont-Ferrand afin de matérialiser ce partenariat à la fois instructif et enrichissant.

En ce qui concerne l'implémentation académique des outils présentés ici, je dois beaucoup à François Jouve du Centre de Mathématiques Appliquées de l'Ecole Polytechnique. Dès mon stage de DEA, il a mis à ma disposition son code de calcul mécanique SOL et a accepté avec bienveillance la prolifération de mes routines dans le code initial. Il m'a beaucoup encouragé et les nombreuses discussions que nous avons pu avoir ont été pour moi très importantes pour l'organisation des idées de ce travail.

Par ailleurs, que les deux rapporteurs de ce mémoire, Tod Laursen et Olivier Pironneau, trouvent ici ma reconnaissance pour l'attention qu'ils ont porté à l'appréciation du manuscrit, et pour les remarques toujours constructives qui ont été formulées et qui alimenteront probablement la poursuite de recherches complémentaires. Que Claude Le Bris et Frédéric Nataf reçoivent également l'expression de ma sympathie pour avoir accepté de faire partie du jury. Rencontrés tous deux en qualité de Professeurs, l'un à l'Ecole Nationale des Ponts et Chaussées, l'autre au sein du DEA Analyse Numérique de Paris 6, ils ont contribué à me rendre attractif cet univers si particulier de la recherche scientifique.

Ayant été formé à l'Ecole Nationale des Ponts et Chaussées, ce fut pour moi un grand honneur lorsqu'Alexandre Ern, responsable du cours de Calcul Scientifique de l'Ecole,

m'offrit de prendre en charge une petite classe d'étudiants de première année. J'ai été extrêmement sensible à la confiance qu'il m'a témoignée, d'autant plus que cette expérience a beaucoup compté dans mes années de thèse. Merci très sincèrement à ceux qui ont été mes étudiants : ils m'ont apporté sans doute plus qu'ils ne l'imaginent. Merci également aux collègues plus expérimentés qui m'ont accueilli dans l'équipe enseignante : Eric Cancès, Jean-Frédéric Gerbeau et Bruno Sportisse, qui enseignaient tous déjà alors que j'entrais aux Ponts à Marne-La-Vallée. Eric Cancès a été une personnalité centrale dans mes choix, et je tiens vivement à lui témoigner ma reconnaissance pour le goût qu'il sait transmettre à ses étudiants. J'en profite pour adresser mes plus vifs remerciements à ceux qui ont été mes enseignants dans cette Ecole, en particulier Mikhaël Balabane et Serge Piperno. Je leur dois sans doute, ainsi qu'à l'environnement stimulant du CERMICS de m'être engagé sur cette voie.

Le Centre de Mathématiques Appliquées de l'Ecole Polytechnique a été le refuge où est né ce travail, dirigé d'une main experte par Vincent Giovangigli qu'il convient de remercier pour l'ambiance conviviale qu'il contribue à faire régner dans ce laboratoire. Orchestrant la vie de tous les jours et ses contingences, je tiens à remercier Jeanne Bailleul, Geo Boléat, Liliane Doaré et Véronique Oriol qui nous rendent surmontables - et avec le sourire ! - les méandres de l'administration. Face aux dangers sournois de l'informatique, merci à tous ceux, experts, qui ont supporté ma présence épiphyte, en particulier Sylvain Ferrand, notre ingénieur système, Erwan Le Pennec qui partait avec le sérieux handicap d'occuper le bureau voisin, mais également François Jouve et Aldjia Mazari. D'ailleurs, Aldjia, soit également remerciée pour ton implication dans les relations contractuelles du laboratoire avec l'extérieur qui permettent des collaborations comme celles-ci, et pour la diversité des fonctions que tu assures simultanément. Ma pensée amicale va aussi à tous ceux qui contribuent à faire vivre ce laboratoire, chercheurs permanents, post-doctorants, invités ou thésards. Que chacun veuille bien trouver ici un témoignage de ma plus sincère sympathie pour les bons moments passés dans et hors des murs du laboratoire.

En terre auvergnate, je voudrais remercier les personnes du service "Etudes et Recherches" de la Manufacture Française des Pneumatiques Michelin pour avoir été d'agrables collègues et hôtes à la fois, sous l'autorité hiérarchique de François Lestang. J'adresse à tous ma reconnaissance pour leur accueil. Mon amicale pensée va à Jean-Michel Bellard, Stéphane Cohade mon accueillant comparse de bureau, Philippe Edmond de Boussiers, Adeline Eynard, Pascal Landereau, Pierre Lapouméroulie sans oublier bien sûr la maman de tout l'étage : Colette de la Perrotière, ainsi que tous ceux qui ont contribué à rendre agréable les six mois de mon séjour clermontois. Merci enfin à Jean-Michel Vacherand et Ludovic Gréverie avec lesquels le CEMRACS 2001, organisé par Yves Achdou, Frédéric Nataf et Claude Le Bris, fut l'occasion d'une collaboration fructueuse en acoustique du pneumatique.

Enfin, un immense merci va à tous les Autres, non les moindres, présences amicales, humaines, parents, proches et très proches de ces années indélébiles à bien des égards. En particulier à tous Ceux, vacanciers de l'APF, ou laissés pour compte de notre Société, qui

par leur courage et leur grandeur m'ont infiniment plus appris sur ce qui nous contruit que mes mots ne sauraient le dire, je dédie ces quelques pages de sueur. Je ne peux leur adresser que de petites choses, ils m'ont appris l'Essentiel. Merci aussi, et combien, à mes parents pour m'avoir soutenu, parfois au delà de leurs convictions propres, ce qui n'est que plus admirable, dans mes choix et dans ce projet professionnel qui me guide sous peu vers la Californie.

En vous souhaitant une lecture aussi agréable qu'il a été enrichissant pour moi d'écrire ces pages.

Palaiseau, le 20 Septembre 2004,
Patrice Hauret

Table des matières

1	Introduction	11
1.1	Position du problème	11
1.1.1	Le pneumatique	11
1.1.2	Quelques enjeux pour la simulation	13
1.1.3	Sources de difficultés	14
1.2	Travail de thèse et contributions	16
2	Eléments de mécanique des milieux continus	23
2.1	Dynamique des milieux continus	23
2.1.1	Cinématique	23
2.1.2	Système de l'élastodynamique	25
2.1.3	Problème mixte en déplacement-pression	26
2.2	Hyperélasticité	27
2.2.1	Energie emmagasinée	27
2.2.2	Forme indépendante du référentiel	29
2.2.3	Isotropie	30
2.3	Viscoélasticité	32
2.4	Contact sans frottement	35
3	Time integration in nonlinear elastodynamics	39
3.1	Introduction	40
3.2	Quasi-incompressible elastodynamics	42
3.2.1	The incompressible model	42
3.2.2	Variational quasi-incompressible formulation	43
3.2.3	Conservation properties	44
3.3	Efficiency and semi-explicit strategies	46
3.3.1	A centered explicit scheme	47
3.3.2	A semi-implicit scheme	53
3.3.3	Computational complexity of the semi-implicit scheme	55
3.4	Conservation analysis for some usual schemes	56
3.4.1	General concepts	56

3.4.2	Midpoint based schemes	57
3.4.3	Trapezoidal rule	58
3.4.4	Midpoint scheme	64
3.4.5	Exactly conservative schemes	68
3.5	Dissipative schemes	72
3.5.1	Conservation analysis for the HHT scheme	72
3.5.2	A new dissipative scheme in the nonlinear framework	78
3.6	Extensions of the conservative approach	80
3.6.1	Frictionless contact	80
3.6.2	Viscoelasticity	86
3.7	Numerical experiment	90
3.7.1	A simple cantilever beam	90
3.7.2	Ball impact	93
3.8	Conclusion	99
4	A stabilized discontinuous mortar formulation	103
4.1	Introduction	104
4.2	Nonconforming setting	106
4.2.1	Position of the problem	106
4.2.2	Discretization	107
4.2.3	Approximate problem	110
4.3	Well-posedness	113
4.3.1	Inf-sup condition	113
4.3.2	Local rigid motions	115
4.3.3	Minimal Lagrange multipliers spaces	117
4.3.4	Standard result of coercivity	120
4.4	Uniform coercivity	122
4.4.1	Fundamental assumptions	123
4.4.2	Generalized Korn's inequality	124
4.4.3	A Scott & Zhang like interpolation operator for mortar methods . .	125
4.4.4	Uniform coercivity result	138
4.4.5	Existence result for problem (4.7)	139
4.5	Error estimates in elastostatics	140
4.5.1	Approximation of displacements	140
4.5.2	Approximation of fluxes	146
4.6	Generalization to elastodynamics	148
4.6.1	Position of the problem	149
4.6.2	A midpoint nonconforming fully discrete approximation.	150
4.6.3	Convergence analysis	153
4.7	Analysis of discontinuous mortar spaces	167
4.7.1	Stabilized first order elements	167
4.7.2	A counter example	169

4.7.3	Numerical validation	171
4.7.4	A useful lemma	175
4.7.5	Second order stabilized interface elements	177
4.8	Some numerical issues	183
4.8.1	Penalized formulation.	183
4.8.2	Exact integration of the constraint	188
4.9	Numerical tests for discontinuous mortar-elements	189
4.10	Appendix A : Mesh-dependent norms.	202
4.11	Appendix B : Dependence of the constant in Korn's inequalities	205
4.11.1	Poincaré-Friedrichs inequalities	206
4.11.2	Dependence of the constant in Korn's second inequality	207
4.11.3	Semi-norm estimates	211
4.11.4	Conclusion	215
5	Mortiers : contributions industrielles	219
5.1	Introduction	219
5.2	Formulation mortier sur une surface courbe	221
5.2.1	Construction des espaces tangents	222
5.2.2	Construction du carreau.	223
5.2.3	Projection sur la surface	225
5.2.4	Contrainte mortier	228
5.3	Algorithme d'assemblage	230
5.3.1	Algorithme	230
5.4	Essais numériques	232
5.4.1	Recollements au tour de roue	232
5.4.2	Recollement d'un pain unique	235
5.4.3	Mortiers et dynamique	235
5.5	Conclusion	238
6	Two-scale Dirichlet-Neumann preconditioners	241
6.1	Introduction	242
6.2	A mortar formulation	244
6.2.1	Continuous problem	244
6.2.2	Discretization	245
6.3	Two-scale preconditioners.	250
6.3.1	Introduction	251
6.3.2	Two possible definitions for $\hat{\mathbf{D}}_0$	252
6.4	Condition number analysis	256
6.4.1	Factorization	256
6.4.2	Spectral equivalence for the simple Dirichlet-Neumann	257
6.4.3	Spectral equivalence for the enhanced Dirichlet Neumann	262
6.5	Algorithm	270

6.6	Numerical tests	271
6.6.1	A basic two-scale model	271
6.6.2	Extension to a quasi-Newton method	276
6.7	Conclusion	279
7	Conclusion	281

Chapitre 1

Introduction

Le travail exposé dans ce mémoire consiste en une étude mathématique et numérique d'outils permettant la simulation de la dynamique de structures complexes non-linéaires, quasi-incompressibles, et présentant deux échelles de longueurs caractéristiques. Pour être plus précis concernant ce dernier point, les structures considérées sont supposées comporter des détails géométriques fins sur leur bord.

Cette étude, réalisée en partenariat avec la Manufacture Française des Pneumatiques Michelin, est largement motivée par l'importance de calculs dynamiques en roulage du pneumatique afin de prédire la valeur de différentes grandeurs physiques : contraintes dans les matériaux, pressions de contact au sol ou encore rayonnement acoustique. Dans ce cadre, les difficultés d'obtention de simulations complètes et réalistes pour des coûts de calcul raisonnables sont liées à la complexité de la géométrie, au comportement des matériaux, au mode de sollicitation par contact, ou encore à l'intervention de différentes échelles de longueur, de temps ou de rigidité caractéristiques de la structure.

Après une description de l'anatomie du pneumatique, nous mentionnons quelques uns des enjeux de la simulation numérique lors de la phase de conception. Nous soulignons ensuite les propriétés intrinsèques de la structure qui rendent ces études délicates. Enfin, nous délimitons les problèmes qui occupent le reste de ce mémoire, et esquissons la démarche adoptée. Référence est faite au contenu des chapitres et aux contributions apportées.

1.1 Position du problème

1.1.1 Le pneumatique

Le pneumatique voit le jour en 1895 sous une forme rudimentaire pour équiper les premières automobiles. Dès les origines, il exploite les propriétés viscoélastiques du caoutchouc, matière naturelle polymérisée issue du traitement de la sève d'hévéa, et principalement formée de polyisoprène (cf. figure 1.1). Il s'est peu à peu complexifié pour adopter l'architecture dite radiale en 1946, et il comporte aujourd'hui plus de 200 matériaux et

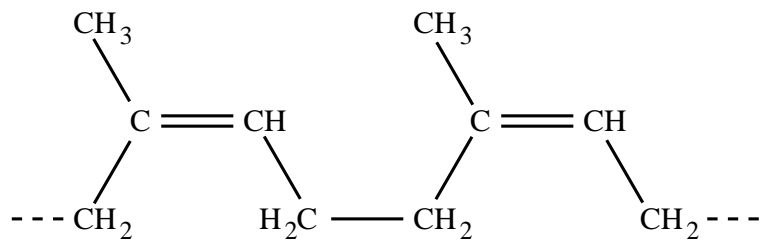


FIG. 1.1 – Molécule de polyisoprène.

30 semi-finis. On trouve sur la figure 1.2 une vue en coupe d'un pneumatique de tourisme type assorti d'un croquis qui en détaille les différents constituants.

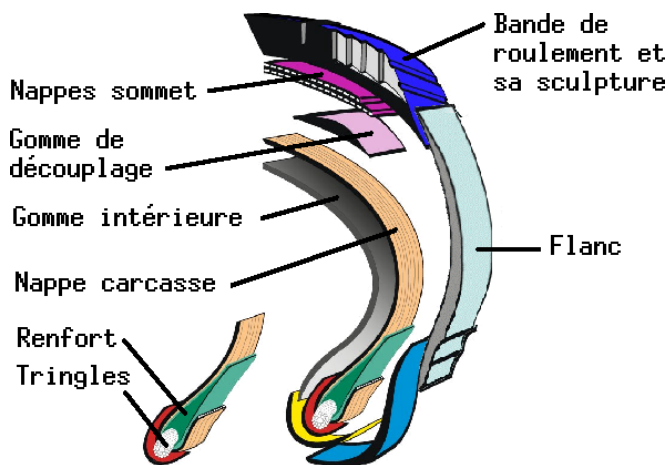


FIG. 1.2 – Pneumatique de tourisme type en coupe transversale (en haut) et croquis des différents constituants (en bas).

Un pneumatique, c'est bien évidemment une cavité de révolution arimée sur la jante de la roue d'un véhicule par l'intermédiaire d'une tringle. Il contient de l'air sous pression afin d'amortir les irrégularités de la route, ce à quoi contribue également le caractère viscoélastique du caoutchouc qui le compose. L'agencement de nappes anisotropes en nylon et en acier assure la reprise des contraintes dans le matériau et permet de maximiser la superficie de la zone de contact, principalement en ce qui concerne la nappe dite carcasse. Enfin, la bande de roulement, sculptée, assure le contact avec la route. Par temps pluvieux, les sculptures permettent de chasser l'eau sur les côtés du pneu tandis que leurs arêtes réalisent l'adhérence avec la route. A cet égard, il faut mentionner que la complexité des sculptures actuelles permet de faire apparaître de nouvelles arêtes au fur et à mesure de l'usure du caoutchouc de la bande de roulement afin de maintenir un niveau d'adhérence satisfaisant. Concernant la forme et la répartition des sculptures, il importe de mentionner qu'elles ne se répètent pas périodiquement sur le tour de roue. Ceci a pour effet d'élever la fréquence des premiers modes propres de la structure en brisant sa symétrie. De la sorte, le rayonnement acoustique du pneu aux plus basses fréquences, très inconfortables, est réduit. En général, trois tailles de sculptures se succèdent aléatoirement sur la circonférence, tandis que transversalement, l'orientation des sculptures varie, ce qui est illustré sur la figure 1.3.



FIG. 1.3 – Sur la circonférence, trois tailles de sculptures se succèdent (à gauche). Transversalement, l'orientation des sculptures varie (à droite).

1.1.2 Quelques enjeux pour la simulation

Tout d'abord, il importe de prendre conscience de la violence des sollicitations subies par un pneumatique en roulage. Un pneumatique de voiture de tourisme, gonflé sous une pression supérieure à 2 bars, n'est en contact avec le sol que sur une surface de 150 centimètres carrés, soit la surface d'une carte postale sur laquelle viennent s'appuyer plusieurs

centaines de kilogrammes. En outre, à une vitesse de 80 kilomètres par heure, un pneumatique fait approximativement un tour en 80 millisecondes, ce qui implique que chaque sculpture est écrasée au sol et libérée en environ une milliseconde. L'intensité et la rapidité de telles sollicitations nécessitent de s'assurer du parfait comportement mécanique de la structure. En outre, la difficulté d'effectuer des mesures dynamiques précises dans ces conditions rend tout à fait pertinent le recours à la simulation numérique.

Simuler la dynamique en grandes déformations d'un pneumatique en roulement, c'est prévoir la valeur des efforts de contact, donc le niveau d'adhérence au sol de la structure, mais c'est aussi obtenir la répartition des contraintes dans les matériaux, donnée particulièrement inaccessible à l'expérience et cependant cruciale pour estimer leur niveau de sollicitation. En ligne de mire, se trouve le besoin de prévoir leur usure dans le temps et donc la durée de vie du pneumatique à conditions d'utilisation fixées. Aussi, si de nombreux tests en usine s'attachent à certifier le niveau de fiabilité des structures, l'outil numérique s'avère de nos jours indispensable durant la phase de conception car il permet de limiter le recours à des prototypes.

Outre le problème de la dynamique en grandes déformations, se pose celui du rayonnement acoustique du pneumatique lors du roulement. Cette prévision est d'importance puisque lorsqu'une voiture de tourisme excède les 70 kilomètres par heure, on estime que le bruit rayonné par les frottements au sol et aérodynamique devient prépondérant devant le bruit rayonné par le moteur. En raison d'un intérêt croissant des pouvoirs publics pour la qualité de l'environnement sonore, comme en témoigne la norme européenne 2001/43 CE, une pression s'exerce sur les manufacturiers afin de limiter le rayonnement acoustique des pneumatiques.

1.1.3 Sources de difficultés

Il convient de reconnaître que le pneumatique présente un certain nombre de caractéristiques intrinsèques qui sont des sources importantes de difficultés tant en termes de modélisation que de simulation numérique des phénomènes étudiés. Ces propriétés dont nous allons dresser un portrait sommaire concernent la physique du problème, le comportement des matériaux utilisés, la géométrie de l'objet et la façon dont il est sollicité.

Dans le cadre de la dynamique en grandes déformations, la première difficulté tient au fait que nous sortons du cadre bien balisé des problèmes linéaires. Plus précisément, nous sommes confrontés à une première non-linéarité dite géométrique, qui est liée au fait que les lois de comportement des matériaux sont exprimées dans une configuration de référence distincte de la configuration actuelle, conformément à l'approche lagrangienne. La dynamique ne peut donc plus être simulée par décomposition sur les modes propres de la structure, ce qui est standard en élastodynamique linéaire, et une attention toute particulière doit être portée au choix des schémas numériques d'intégration en temps, très

sensibles en termes de stabilité aux non-linéarités de la physique.

Une seconde difficulté est liée aux propriétés des matériaux en présence. Ainsi, le caoutchouc possède une loi de comportement non-linéaire viscoélastique, laquelle fait intervenir une variable interne du matériau dont l'évolution doit être calculée au cours de la dynamique. De plus, il se trouve être l'un des rares matériaux quasi-incompressibles, contrainte cinématique qui est elle-même non-linéaire dans le cadre de grandes déformations. L'incompressibilité impose l'utilisation de schémas d'intégration en temps au moins partiellement implicites pour la structure. En effet, les ondes de pression hydrostatique dans le caoutchouc se propagent à des vitesses de l'ordre de 5000 mètres par seconde. Pour être stable, un schéma explicite doit utiliser des pas de temps suffisamment petits pour décrire la propagation de ces ondes, et l'extrême petitesse de tels pas de temps rendrait prohibitive la durée de la simulation.

Quant aux nappes métalliques qui constituent la carcasse radiale, outre leur anisotropie, mentionnons qu'elles doivent être considérées comme des coques par leur finesse. Du point de vue numérique, ce caractère de coque doit être mis à profit, faute de quoi on s'expose à une lenteur de convergence par raffinement de maillage liée à la dégradation des constantes dans les estimations éléments-finis tridimensionnelles usuelles. Dans ce cadre, se pose le problème du couplage entre ladite nappe traitée comme une coque, et le caoutchouc qui l'enserre. A ce propos, on pourra consulter les travaux d'Anca Ferent [Fer02] sur les formulations de coques tridimensionnelles.

Par ailleurs, les modules d'Young du caoutchouc et de l'acier qui constituent les nappes sont dans un rapport de 1 à 1 000 000. Il en résulte un très mauvais conditionnement naturel de la sculpture qui nuit sévèrement à l'utilisation de méthodes itératives.

Le caractère à deux échelles de la géométrie du pneumatique constitue la troisième source de difficultés, et non la moindre. En effet, la dimension caractéristique du pneumatique est de l'ordre de 60 centimètres, coïncidant avec le diamètre de l'architecture, alors que les sculptures mesurent quelques centimètres. En termes de fréquences fondamentales, disons que l'architecture possède un premier mode propre vers 100 Hertz tandis qu'une sculpture possède ce premier mode propre au voisinage de 2000 Hertz. A cause de la non-linéarité du matériau, les oscillations à ces deux échelles sont couplées et interagissent, ce qui interdit de découpler architecture et sculptures dans la résolution dynamique du problème. L'obligation de résoudre simultanément le problème à ces deux niveaux de finesse est à l'origine d'un coût de calcul important.

Enfin, la sollicitation du pneumatique résulte naturellement du contact frottant sur le sol (par exemple avec une loi de type Coulomb). Ainsi, s'ajoutent aux difficultés précédentes la noire complexité de la gestion du contact, ainsi que le caractère non-symétrique du problème considéré.

Prendre en compte la totalité de ces éléments pour simuler la dynamique du pneumatique en grandes déformations est certes affaire de puissance de calcul, mais pas seulement. En effet, développer des méthodes dédiées, c'est aller dans le sens d'une meilleure compréhension de la physique et de méthodes numériques adaptées qui permettent un allègement

considérable du coût informatique de simulation.

Pensant à ce stade avoir rendu compte de la difficulté de simuler entièrement le roulage d'un pneumatique sur une route chaotique, nous allons mentionner pour être plus complets, les difficultés inhérentes à la simulation de l'acoustique. Les prévisions acoustiques s'appuyant couramment sur les équations linéarisées de la dynamique en domaine fréquentiel, le cadre semble évidemment plus simple. Néanmoins, l'acoustique du pneumatique a ceci de particulier qu'il faudrait idéalement tenir compte du phénomène de "pompage" de l'air dans les sculptures, ce qui pose le problème d'un calcul difficile en interaction fluide-structure. Si on se limite aux vibrations de la structure, quelques difficultés demeurent cependant. Tout d'abord, il n'est pas aisément d'obtenir une caractérisation fréquentielle du modèle de viscoélasticité linéarisé, crucial quant au comportement acoustique de la structure. D'autre part, résoudre le problème de l'acoustique requiert préalablement l'extraction des modes propres du système. Ceci serait particulièrement peu coûteux en l'absence de sculptures, ou plus exactement pour un pneumatique axisymétrique. En effet, pour calculer les modes propres d'une structure axisymétrique, on peut procéder par séparation de variables entre la variable angulaire et les variables restantes -radiale et transverse- et obtenir ainsi les modes propres tridimensionnels pour le coût de calculs quasiment bidimensionnels. Tant que la longueur d'onde des vibrations considérées est grande devant la taille des sculptures du pneu, on peut légitimement négliger ces dernières et ainsi se contenter d'un calcul axisymétrique. Néanmoins, au-delà de 1500 Hertz, la présence des sculptures devient cruciale, ce qui nécessite un calcul modal vraiment tridimensionnel et suscite la question suivante : est-il possible de calculer avec une bonne précision la réponse fréquentielle du problème tridimensionnel par une correction (peu coûteuse) de la réponse du problème axisymétrique ?

Nous présentons maintenant les contributions de ce mémoire quant au traitement de certaines de ces problématiques.

1.2 Travail de thèse et contributions

Cette thèse s'intéresse à la simulation numérique de la dynamique des structures quasi-incompressibles en grandes déformations, présentant une loi de comportement hyperélastique non-linéaire et une géométrie à deux échelles. Nous esquissons ici la démarche adoptée et présentons le contenu des chapitres de cette thèse en mettant en relief nos contributions. En préambule, le chapitre 2 rappelle quelques notions essentielles de dynamique des milieux continus. Il est l'occasion d'introduire les principes fondamentaux de mécanique des milieux continus permettant de formaliser le problème mécanique qui nous occupe.

INTÉGRATION EN TEMPS - CHAPITRE 3

Tout d'abord, l'intégration numérique en temps des équations de l'élastodynamique non-linéaire, a fortiori incompressible, pose certaines difficultés. En particulier, la contrainte d'incompressibilité rend impossible toute stratégie explicite d'intégration, et nous montrons au chapitre 3 qu'une stratégie semi-implicite en pression a la même complexité qu'un schéma totalement implicite à cause de la non-linéarité. Nous devons donc nous résoudre à considérer des schémas totalement implicites, mais toujours à cause de la non-linéarité, leur stabilité reste un problème majeur. En effet, lorsque le pas de temps n'est pas suffisamment petit, la plupart des schémas issus du cadre linéaire donnent lieu à une explosion de l'énergie totale du système discret. Se pose alors le problème de la conservation de l'énergie par l'intégrateur, ce qui constitue un critère de stabilité fondamental. La conservation de l'impulsion et du moment cinétique représente par ailleurs une bonne information sur le respect des groupes de symétrie : translations et rotations.

Si le schéma de point milieu conserve exactement l'énergie et l'impulsion discrètes dans un cadre linéarisé, ses généralisations non-linéaires n'héritent pas forcément de bonnes propriétés de conservation pour des pas de temps physiquement significatifs. Nous présentons au chapitre 3 une analyse rigoureuse de conservation pour deux généralisations du schéma de point milieu. Ces analyses dictent en outre la forme naturelle de ses généralisations non-linéaires assurant la conservation de l'énergie et des moments dans le cadre incompressible. O.Gonzalez propose dans [Gon00] un schéma de cette famille particulièrement intéressant en pratique, car fournissant une expression explicite des termes de contrainte figurant dans le schéma.

Si l'utilisation de schémas linéairement dissipatifs (de rayon spectral inférieur ou égal à 1) comme celui de Hilber-Hughes-Taylor (voir [HHT77]) ne résout pas fondamentalement le problème de la maîtrise de l'énergie par rapport au schéma de point milieu, nous menons une analyse précise de conservation pour le schéma HHT qui fournit de précieux renseignements. Tout d'abord, nous mettons en évidence dans le cadre linéarisé, l'existence d'une énergie discrète modifiée régularisée qui décroît dans la dynamique et fait intervenir une petite contribution des effets d'accélération. Par ailleurs, cette analyse nous permet de proposer la formulation d'un schéma d'intégration en temps dissipatif pour cette même énergie modifiée dans le cadre non-linéaire. Les analyses précédentes sont confirmées par des études numériques. Cette étude a été publiée sous la forme suivante :

[HT02] Conservation analysis for integration schemes in quasi-incompressible nonlinear elastodynamics, P. Hauret and P. Le Tallec, CMAP Technical report # 499, 2002.

[THR02] Efficient solvers for the dynamic analysis of nonlinear multiscale structures, P. Le Tallec, P. Hauret and A. Rezgui, Proceedings of the Fifth World Congress on Computational Mechanics WCCM V, 2002, H.A Mang and F.G. Rammerstorfer and J. Eberhardsteiner eds.

[TH03b] *Nonlinear schemes and multiscale preconditioners for time evolution problems in constrained structural dynamics*, P. Le Tallec and P. Hauret, Proceedings of the 2nd MIT Conference on Computational Fluid and Solid Mechanics, Ed. K.-J. Bathe, Boston, June 2003.

Dans ce chapitre, nous montrons également que la technique de correction énergétique introduite par [Gon00] peut être généralisée à différents problèmes. Tout d'abord, le problème de l'élastodynamique avec impact passe pour être particulièrement raide et sensible au choix de l'intégrateur. En témoignent les travaux réalisés par Laursen, Armero et leurs collaborateurs [LC97, AP98]. Néanmoins, si ces premiers travaux proposent une intégration numérique temporelle exactement conservative, c'est au prix d'une modification des contraintes cinématiques satisfaites aux pas de temps entiers. Deux travaux consécutifs de Laursen et ses collaborateurs [LL02, LL03] permettent de corriger ce travers dans les cadres glissant et frottant, en agissant sur la maîtrise du saut de vitesse à travers l'impact. Ce point de vue utilise la résolution d'un problème annexe sur le saut des vitesses. C'est sans y recourir que nous proposons ici dans le cadre pénalisé, une formulation conservative des efforts de contact glissant dérivant de [Gon00] ne faisant pas intervenir de condition de persistence, et utilisant les contraintes de Kuhn et Tucker usuelles aux pas de temps entiers.

Lorsque le coefficient de pénalisation tend vers l'infini, il est bien connu que des oscillations de la pression de contact se manifestent. Ce phénomène, lié à l'absence de limite forte (par manque de compacité) pour la solution dynamique lorsque le coefficient de pénalisation tend vers l'infini, peut être montré mathématiquement dans le cadre de l'élastodynamique linéaire (voir le travail de [Sca04]). L'obtention d'une limite forte passe par l'introduction d'une viscosité, qui peut être introduite dans la formulation même du contact par la prise en compte d'une condition sur la vitesse de pénétration, comme il est proposé dans [TP93, AP98]. Une alternative consiste à introduire une viscoélasticité volumique du matériau. Dans cette voie, nous montrons qu'un bilan énergétique discret exact peut être obtenu dans le cadre viscoélastique introduit par [TRK93] pour un schéma que nous introduisons et qui étend la technique d'O.Gonzalez.

Enfin, la stratégie d'écriture de schémas conservatifs peut être étendue aux problèmes d'interaction fluide-structure en formulation ALE (Arbitrary Lagrangian Eulerian) quitte à utiliser des variables non-conservatives pour le fluide. Cette généralisation a fait l'objet de la publication suivante :

[TH03a] *Energy conservation in fluid-structure interactions*, P. Le Tallec and P. Hauret, Numerical methods for scientific computing, variational problems and applications, 2003, Y. Kuznetsov, P. Neittanmaki and O. Pironneau eds.

INTÉGRATION EN ESPACE - CHAPITRE 4

A l'issue de ce chapitre 3, le problème qui nous intéresse est maintenant discréétisé en temps et nous devons résoudre un système non-linéaire par pas de temps, ce que nous faisons par une méthode de Newton-Raphson. Focalisons nous sur l'un des problèmes tangents, tout à fait semblable à un problème d'élastostatique linéaire pour discuter de la discréétisation en espace à adopter et des techniques de résolution.

Si nous utilisions un maillage conforme pour mailler notre domaine à deux échelles, la finesse du maillage des zones fines (les sculptures) se propagerait à la zone grossière (l'architecture), occasionnant un coût de calcul accru lié à une surprécision de la solution dans la zone grossière. Il peut donc être intéressant de mailler séparément les sous-problèmes grossier et fins. En outre, s'agissant d'un pneumatique, l'architecture qui est axisymétrique peut être maillée à faible coût par révolution d'un maillage de la tranche. Seules les sculptures nécessitent un maillage véritablement tridimensionnel. Se pose donc le problème de la formulation non-conforme du problème en déplacements, pour lequel nous adoptons le cadre des méthodes de mortiers introduites dans [BMP93, BMP94] et consistant à imposer la continuité de la solution sur l'interface architecture/sculpture au sens faible contre un espace \mathcal{M} de multiplicateurs de Lagrange. La formulation initiale des mortiers proposée par C. Bernardi, Y. Maday et A. Patera présente cependant quelques difficultés numériques :

- la définition de \mathcal{M} au bord des interfaces est complexe en 3D si plus de 2 sous-domaines s'y intersectent,
- la base contrainte des déplacements est non-locale sur l'interface, ce qui peut engendrer de petites oscillations non-physiques.

Le premier point peut être résolu, comme indiqué dans [Ses98], en abaissant le degré des polynômes de \mathcal{M} si les déplacements sont au moins approchés par des polynômes du second degré. Le deuxième point trouve une solution dans [Woh00] par l'adoption de multiplicateurs de Lagrange construits sur une base duale de la base initiale. Pour concilier ces avantages, nous proposons au chapitre 4 une formulation mortier discontinue stabilisée, idée déjà introduite dans [BM00] pour des formulations dites à trois champs dans le cadre d'une approximation au premier ordre. Elle est ici introduite dans le cadre des formulations à deux champs pour des déplacements de degré 1 et 2. Outre le cas élastostatique standard, la preuve de convergence optimale vers la solution du problème continu est généralisée à l'élastodynamique linéaire. Par ailleurs, les formulations de type mortiers constituant un cadre naturel en décomposition de domaine (voir [Tal93, AKP95, AMW99, Ste99, Woh01]), il s'agit d'assurer la non-dégradation des différentes estimations lorsque le nombre de sous-domaines croît et que leur taille diminue. Un tel résultat s'obtient en s'assurant de la non-dégradation de la constante de coercivité du problème élastostatique. Un tel travail a été mené par J.Gopalakrishnan puis S. Brenner [Gop99, Bre03] dans le cadre de problèmes elliptiques scalaires avec interfaces planes, et étendu au cas vectoriel récemment dans [Bre04]. Un résultat analogue à [Bre04] est ici montré, mais pour des décompositions présentant des interfaces courbes, et en proposant une généralisation de l'opérateur d'interpolation de Scott et Zhang [SZ90] permettant d'approcher optimalement et de façon

stable en norme de l'énergie, un déplacement non-conforme par un déplacement conforme. Enfin, ce chapitre est l'occasion de discuter de détails pratiques de mise en oeuvre dans le cadre de problèmes tridimensionnels d'élasticité. Des cas tests numériques permettent de valider l'étude théorique. Ce travail a été publié sous la forme :

[HT04b] A stabilized discontinuous mortar formulation for elastostatics and elastodynamics problems, Part I : abstract framework, P. Hauret and P. Le Tallec, CMAP Technical Report # 553, 2004.

[HT04c] A stabilized discontinuous mortar formulation for elastostatics and elastodynamics problems, Part II : discontinuous Lagrange multipliers, P. Hauret and P. Le Tallec, CMAP Technical Report # 554, 2004.

SOLVEUR - CHAPITRE 6

La matrice du système linéaire à résoudre, issue de la discréétisation précédente, est assez coûteuse à inverser par une méthode directe pour des problèmes industriels à cause de la présence simultanée de deux échelles de description. Or, nous aimeraisons résoudre ce système pour un coût de calcul comparable à celui du système grossier (architecture seule) quitte à supposer que la détermination de la solution fine puisse se faire pour un coût faible connaissant la solution grossière. Nous commençons par supposer que les sculptures sont disjointes et de faible taille, de sorte que l'inversion des matrices de rigidité des sculptures peut se faire en parallèle, rendant minime le coût de calcul de la solution fine. Nous introduisons alors deux préconditionneurs à deux échelles de type Dirichlet-Neumann, permettant de résoudre le problème itérativement par gradient conjugué. Ces préconditionnements sont dits à deux échelles, en ce sens qu'utilisés dans une méthode de gradient conjugué, le nombre d'itérations pour obtenir la convergence souhaitée est indépendant du nombre de sculptures et de leur taille. Le premier préconditionneur s'inspire des méthodes usuelles de type Dirichlet-Neumann [QV99] et allie simplicité et qualité de résultats, mais fait apparaître une faiblesse lorsque les sous-problèmes fins sont soumis à une condition aux limites de Dirichlet. A des fins d'amélioration, nous introduisons un espace grossier donnant lieu au deuxième préconditionneur proposé, et montrons l'indépendance de comportement vis-à-vis de conditions aux limites essentielles. Le nombre de conditionnement obtenu reste dépendant du rapport des modules d'Young des sous-problèmes grossier et fin, limitation naturelle des préconditionneurs de type Dirichlet-Neumann. Ces préconditionnements sont proposés, analysés et testés au chapitre 6, et nous montrons également numériquement que moyennant une rigidité suffisante de l'architecture, ils peuvent donner lieu à des méthodes de quasi-Newton efficaces. Le travail de ce chapitre a été proposé pour publication :

[HT04a] *Dirichlet-Neumann preconditioners for elliptic problems with small disjoint geometric refinements on the boundary*, P. Hauret and P. Le Tallec, CMAP Technical Report # 552, 2004.

Les tests numériques académiques réalisés dans ces trois chapitres ont été réalisés sur la base du code académique SOL développé au Centre de Mathématiques Appliquées de l’Ecole Polytechnique par François Jouve. L’outil a été étendu au cours de ce travail afin de permettre des calculs dynamiques, incompressibles, ainsi que le recollement par mortiers de maillages incompatibles et la résolution itérative de problèmes par les préconditionne-ments proposés.

Cette thèse a par ailleurs été l’occasion d’un transfert de méthodes vers la Manufacture Française des Pneumatiques Michelin, et de leur implémentation au sein du code de calcul interne. L’implémentation réalisée comprend :

- l’initialisation et la simulation du roulage d’un pneumatique,
- le recollement de maillages incompatibles entre architecture et sculpture, après for-mulation d’une contrainte de recollement sur interface régularisée par patch Hermite, dans l’esprit de Puso [Pus04], décrite dans les grandes lignes au chapitre 5.

Ces aspects font l’objet d’une note technique confidentielle [Hau04].

Un peu en marge du sujet de cette thèse, mentionnons que l’édition 2001 du CEMRACS (Centre d’Eté Mathématique de Recherche Avancée en Calcul Scientifique) organisée par Yves Achdou, Claude Le Bris et Frédéric Nataf, a été l’occasion de se pencher sur un problème d’acoustique à deux échelles du pneumatique. Le contenu de ce travail est résumé dans ce paragraphe tiré de Matapli, la revue de la SMAI (Société de Mathématiques Appliquées Industrielles) :

L’étude de la réponse acoustique du pneumatique est d’un grand intérêt en termes de confort dans un véhicule mais elle est rendue coûteuse par son caractère multi-échelle. Une façon de simplifier le problème est de réaliser une homogénéisation angulaire du pneumatique, laquelle trouve néanmoins ses limites à moyennes fréquences, dès lors que les modes de vibration des pains de sculpture sont excités. L’idée de la démarche proposée par P. Le Tallec (École Polytechnique) et développée au CEM-RACS par P. Hauret (École Polytechnique) pour la société Michelin était d’utiliser un couplage entre le modèle homogénéisé et les modèles locaux des pains afin d’en corriger la réponse acoustique aux moyennes fré-quences.

Cette méthode, inspirée de la parution de [LB99], a été développée en collaboration avec Ludovic Gréverie et Jean-Michel Vacherand (Michelin). Son cadre d’application est celui de la réponse acoustique au voisinage des premières fréquences propres des pains de sculp-ture. Son lien avec les méthodes de Dirichlet-Neumann est l’exploitation d’une méthode

de complément de Schur afin de représenter une rigidité corrigée de la structure grossière.

Les chapitres sont rédigés de façon aussi indépendante que possible afin de permettre une lecture ponctuelle. En outre, afin de permettre une meilleure communication dans le cadre de ce travail qui s'inscrit dans un partenariat international et de faciliter le travail du rapporteur américain, les chapitres ultérieurs, excepté celui de rappels qui suit et le chapitre 5 traitant de contributions industrielles, sont rédigés en langue anglaise.

Chapitre 2

Eléments de mécanique des milieux continus

Afin de faciliter la lecture du présent travail et de formuler en totalité le problème mécanique qui le motive, nous rappelons ici quelques éléments de dynamique des milieux continus. Le cadre de l'hyperélasticité, privilégié par la suite, y est détaillé. Une formulation viscoélastique issue de [TRK93] est également introduite afin de fournir le cadre complet de modélisation de la dynamique du pneumatique. Enfin, pour compléter la description présentée, mention est faite de la formulation du contact sans frottement. Pour tout détail complémentaire en ce qui concerne la mécanique des milieux continus, on pourra consulter les ouvrages de référence suivant qui exposent le point de vue de la géométrie [MH83, Arn89, MR94], de l'analyse [Cia88, Tal94b] ou de la mécanique [Sal88, Tal99]. Les références [Joh85, Lau02, Wri02] concernent plus particulièrement les problèmes liés au contact.

2.1 Dynamique des milieux continus

2.1.1 Cinématique

Considérons dans l'intervalle de temps $[0, T]$ la déformation d'un solide dont l'intérieur de la configuration de référence est noté Ω . On peut supposer que l'adhérence $\overline{\Omega}$ de Ω coïncide avec le domaine occupé par la structure au temps $t = 0$, mais celà n'a rien d'obligatoire. Nous désignons par $\varphi : [0, T] \times \overline{\Omega} \rightarrow \mathbb{R}^3$ le champ des déplacements, en ce sens que $\varphi(t, x)$ est la position à l'instant $t \in [0, T]$ du point $x \in \overline{\Omega}$. A chaque instant $t \in [0, T]$, on notera $\varphi(t) = \varphi(t, \cdot)$ et on suppose que l'application $\varphi(t)$ est injective sur Ω pour une raison de non-interpénétration du matériau dans lui-même. Néanmoins, $\varphi(t)$ n'est pas forcément injective sur $\overline{\Omega}$ afin de permettre les phénomènes d'auto-contact. En outre, pour tout $t \in [0, T]$, l'application $\varphi(t)$ respecte l'orientation des champs de vecteurs afin d'interdire un "retournement" du domaine sur lui-même ce qui se traduit par

$\det \nabla \varphi(t) > 0$ sur Ω . De plus, on montre dans [Cia88] que si $\varphi(t)$ est continue sur Ω et en l'absence d'auto-contact, alors le bord du domaine déformé $\partial\varphi(t, \Omega)$ est l'image par $\varphi(t)$ du bord de la configuration de référence, c'est-à-dire que :

$$\partial\varphi(t, \Omega) = \varphi(t, \partial\Omega). \quad (2.1)$$

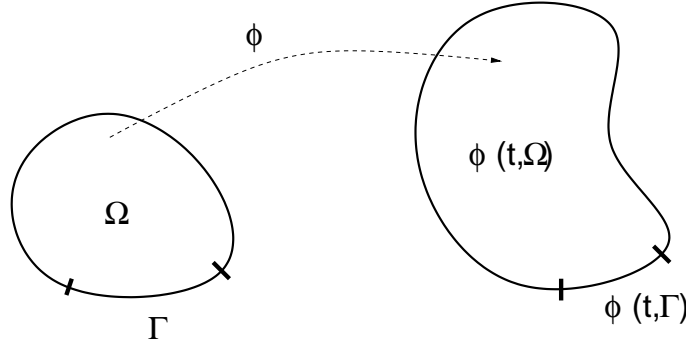


FIG. 2.1 – Déformation de la configuration de référence Ω .

De plus, le champ de déplacements doit satisfaire les contraintes cinématiques du problème à tout instant. En particulier, à chaque instant $t \in [0, T]$, on impose le déplacement $\varphi_D(t)$ sur la partie $\Gamma_D(t) \subset \partial\Omega$ du bord de Ω :

$$\forall t \in [0, T], \quad \varphi(t, x) = \varphi_D(t, x), \quad x \in \Gamma_D(t). \quad (2.2)$$

En vertu de la relation (2.1), cela est équivalent à dire qu'à l'instant t , les déplacements sont connus sur la partie $\varphi(t, \Gamma_D(t))$ du bord du domaine déformé.

Une contrainte cinématique tout aussi fondamentale dans la suite de notre étude réside dans l'incompressibilité du matériau. Une telle contrainte d'incompressibilité s'écrit sous la forme :

$$\det \nabla \varphi(t, x) = 1, \quad \text{presque partout.} \quad (2.3)$$

En effet, la préservation du volume impose que pour toute partie $A \subset \Omega$, on doit avoir pour tout $t \in [0, T]$:

$$\int_A d\hat{x} = \int_{\varphi(t, A)} dx,$$

et le changement de variable $x = \varphi(t, \hat{x})$ implique donc :

$$\int_A d\hat{x} = \int_A \det \nabla \varphi(t, \hat{x}) d\hat{x}, \quad \forall A \subset \Omega,$$

ce qui est bien la contrainte annoncée (2.3). On préfère souvent à cette contrainte ponctuelle une contrainte variationnelle, et quitte à introduire l'espace \mathcal{P} des pressions hydrostatiques, la contrainte d'incompressibilité devient :

$$\int_{\Omega} (\det \nabla \varphi - 1) q = 0, \quad \forall q \in \mathcal{P}. \quad (2.4)$$

A tout instant $t \in [0, T]$, on désignera par $\mathcal{U}(t)$ l'ensemble des champs de déplacements "suffisamment réguliers" $\varphi(t) : \Omega \rightarrow \mathbb{R}^3$ satisfaisant les contraintes cinématiques du problème, c'est-à-dire les déplacements imposés sur $\Gamma_D(t)$ et l'incompressibilité au sens variationnel (2.4). Ainsi, l'ensemble des déplacements cinématiquement admissibles se définit par :

$$\mathcal{U}(t) = \left\{ \psi \in \mathcal{U}^c(t), \int_{\Omega} (\det \nabla \psi - 1) q = 0, \quad \forall q \in \mathcal{P} \right\},$$

où l'espace affine $\mathcal{U}^c(t)$ des déplacements compressibles est défini par :

$$\mathcal{U}^c(t) = \left\{ \psi : \mathbb{R}^3 \rightarrow \mathbb{R}^3 \text{ "assez régulier", } \psi = \varphi_D(t), \text{ sur } \Gamma_D(t) \right\}.$$

2.1.2 Système de l'élastodynamique

Il s'agit maintenant de rappeler le système d'équations permettant de déterminer le champ de déformation φ dans un solide en fonction de ses caractéristiques et des sollicitations appliquées.

Notons $\rho : \Omega \rightarrow \mathbb{R}_+^*$ la masse volumique du solide. A l'instant $t \in [0, T]$, lorsque le solide occupe le domaine déformé $\varphi(t, \Omega)$, on lui impose la force volumique $\tilde{f}_\varphi(t, x) \in \mathbb{R}^3$ en tout point $x \in \varphi(t, \Omega)$ et la force surfacique $\tilde{g}_\varphi(t, x) \in \mathbb{R}^3$ en tout point $x \in \varphi(t, \Gamma_N(t))$. A tout instant $t \in [0, T]$, on a désigné par $\Gamma_N(t) = \partial\Omega \setminus \Gamma_D(t)$ la partie complémentaire de $\Gamma_D(t)$ sur le bord de la configuration de référence Ω .

Par des bilans locaux de conservation de la quantité de mouvement dans le matériau du domaine déformé $\varphi(t, \Omega)$ à tout instant $t \in [0, T]$, puis en utilisant le changement de variables lagrangien φ dans la formulation variationnelle de ces bilans, on établit classiquement qu'il existe un champ de tenseurs du second ordre,

$$\Pi^c : [0, T] \times \Omega \rightarrow \mathbb{R}^{3 \times 3}, \quad (2.5)$$

dit champ du premier tenseur des contraintes de Piola-Kirchhoff, et que les équations de la dynamique consistent à trouver à tout instant $t \in [0, T]$, le champ de déplacements $\varphi(t) \in \mathcal{U}(t)$ tel que :

$$\begin{aligned} & \int_{\Omega} \rho(x) \frac{\partial^2 \varphi}{\partial t^2}(t, x) \cdot v(x) dx + \int_{\Omega} \Pi^c(t, x) : \nabla v(x) dx \\ &= \int_{\Omega} f(t, x) \cdot v(x) dx + \int_{\Gamma_N(t)} g(t, x) \cdot v(x) dx, \quad \forall v \in d_{\varphi(t)} \mathcal{U}(t). \end{aligned} \quad (2.6)$$

Cette formulation est également connue sous le nom de principe des puissances virtuelles, et $d_{\varphi(t)}\mathcal{U}(t)$ y désigne l'espace vectoriel tangent à $\mathcal{U}(t)$ en $\varphi(t) \in \mathcal{U}(t)$, c'est-à-dire que :

$$d_{\varphi(t)}\mathcal{U}(t) = \left\{ v \in d_{\varphi(t)}\mathcal{U}^c(t), \quad \int_{\Omega} q (\operatorname{cof} \nabla \varphi(t)) : \nabla v = 0, \quad \forall q \in \mathcal{P} \right\},$$

où $\operatorname{cof} M$ désigne la matrice des cofacteurs de la matrice $M \in \mathbb{R}^{3 \times 3}$, et :

$$d_{\varphi(t)}\mathcal{U}^c(t) = \{v : \mathbb{R}^3 \rightarrow \mathbb{R}^3 \text{ "assez régulier", } v = 0, \text{ sur } \Gamma_D(t)\}.$$

De plus, on a introduit les forces suivantes, exprimées dans la configuration de référence :

$$\begin{cases} f(t, x) = \tilde{f}_{\varphi}(t, \varphi(t, x)) \det \nabla \varphi(t, x), & x \in \Omega, \\ g(t, x) = \left|(\nabla \varphi(t, x))^{-1} \cdot n(x)\right| \tilde{g}_{\varphi}(t, \varphi(t, x)) \det \nabla \varphi(t, x), & x \in \Gamma_N(t), \end{cases} \quad (2.7)$$

où n désigne la normale unitaire extérieure à $\Gamma_N(t)$. Naturellement, les forces f et g dépendent a priori du champ de déplacements φ , même si nous avons délibérément omis de faire figurer cette dépendance. Lorsque f et g sont réellement indépendantes du champ de déplacements, on parle de forces mortes. Dans la formulation (2.6), le champ de tenseurs Π^c ne prend pas en compte la propriété d'incompressibilité du matériau. Il s'agit donc du champ de tenseurs des contraintes du matériau compressible associé.

2.1.3 Problème mixte en déplacement-pression

La formulation (2.6) à l'instant $t \in [0, T]$ fait intervenir la contrainte d'incompressibilité à la fois dans l'espace $\mathcal{U}(t)$ des déplacements cinématiquement admissibles et dans l'espace tangent $d_{\varphi(t)}\mathcal{U}(t)$. A des fins d'approximation variationnelle, il est bien souvent commode de faire apparaître séparément la contrainte d'incompressibilité, ce que nous faisons ici.

Nous notons $\mathcal{U}^c(t)$ l'espace affine des déplacements compressibles admissibles au temps $t \in [0, T]$, et introduisons l'opérateur de contrainte suivant :

$$B_{\varphi(t)} : d_{\varphi(t)}\mathcal{U}^c(t) \rightarrow \mathcal{P}',$$

qui agit de l'espace tangent $d_{\varphi(t)}\mathcal{U}^c(t)$ vers l'espace \mathcal{P}' des formes linéaires continues sur \mathcal{P} et se définit par la forme bilinéaire :

$$\langle B_{\varphi(t)}v, q \rangle_{\mathcal{P}', \mathcal{P}} = \int_{\Omega} q(x) (\operatorname{cof} \nabla \varphi(t, x)) : \nabla v(x) dx,$$

pour tous $(v, q) \in d_{\varphi(t)}\mathcal{U}^c(t) \times \mathcal{P}$. Par ailleurs, on se donne la forme linéaire continue $T_{\varphi(t)} \in d_{\varphi(t)}\mathcal{U}^c(t)'$ définie par :

$$\begin{aligned} & \langle T_{\varphi(t)}, v \rangle_{d_{\varphi(t)}\mathcal{U}^c(t)', d_{\varphi(t)}\mathcal{U}^c(t)} && (2.8) \\ &= \int_{\Omega} \rho(x) \frac{\partial^2 \varphi}{\partial t^2}(t, x) \cdot v(x) dx + \int_{\Omega} \Pi^c(t, x) : \nabla v(x) dx \\ & - \int_{\Omega} f(t, x) \cdot v(x) dx - \int_{\Gamma_N(t)} g(t, x) \cdot v(x) dx, \end{aligned}$$

pour tout $v \in d_{\varphi(t)}\mathcal{U}^c(t)$. Ainsi, la formulation (2.6) implique classiquement avec un minimum d'hypothèses de régularité, que pour tout temps $t \in [0, T]$, le champ de déplacements solution $\varphi(t) \in \mathcal{U}^c(t)$ est tel que :

$$T_{\varphi(t)} \in (\text{Ker } B_{\varphi(t)})^\perp = \text{Im } B_{\varphi(t)}^t.$$

Il existe donc formellement un multiplicateur de Lagrange $p(t) \in \mathcal{P}$, dit pression hydrostatique, tel que :

$$T_{\varphi(t)} = B_{\varphi(t)}^t p(t),$$

si bien que la formulation contrainte (2.6) revient à trouver pour tout $t \in [0, T]$, le champ de déplacements $\varphi(t) \in \mathcal{U}^c(t)$ et la pression hydrostatique $p(t) \in \mathcal{P}$ tels que :

$$\begin{aligned} & \int_{\Omega} \rho(x) \frac{\partial^2 \varphi}{\partial t^2}(t, x) \cdot v(x) dx \\ & + \int_{\Omega} (\Pi^c(t, x) - p(t, x) \text{ cof } \nabla \varphi(t, x)) : \nabla v(x) dx \\ & = \int_{\Omega} f(t, x) \cdot v(x) dx + \int_{\Gamma_N} g(t, x) \cdot v(x) dx, \quad \forall v \in d_{\varphi(t)}\mathcal{U}^c(t), \end{aligned} \tag{2.9}$$

et :

$$\int_{\Omega} q(x) (\det \nabla \varphi(t, x) - 1) dx = 0, \quad \forall q \in \mathcal{P}. \tag{2.10}$$

Il s'agit du problème mixte en déplacement-pression usuel utilisé pour les problèmes hyperélastiques incompressibles. On y voit apparaître le champ du premier tenseur des contraintes de Piola-Kirchhoff $\Pi : [0, T] \times \Omega \rightarrow \mathbb{R}^{3 \times 3}$ du matériau incompressible qui se définit par :

$$\Pi(t, x) = \Pi^c(t, x) - p(t, x) \text{ cof } \nabla \varphi(t, x), \quad \forall (t, x) \in [0, T] \times \Omega.$$

2.2 Hyperélasticité

2.2.1 Energie emmagasinée

A ce stade, il importe de se donner une loi de comportement, c'est-à-dire une expression du premier tenseur des contraintes de Piola-Kirchhoff Π^c du matériau compressible en fonction de l'état de la structure. L'hypothèse d'élasticité consiste à supposer que le tenseur des contraintes $\Pi^c(t, x)$ à l'instant $t \in [0, T]$ et au point $x \in \Omega$ ne dépend en fait que des propriétés du matériau au point $x \in \Omega$ et du tenseur du second ordre gradient de déformation :

$$F = \nabla \varphi, \quad [0, T] \times \Omega.$$

On notera ainsi $\Pi^c(t, x) = \mathcal{L}(x, F(t, x))$ pour tout $(t, x) \in [0, T] \times \Omega$.

Nous restreignons encore ce cadre en introduisant l'hypothèse d'hyperélasticité, c'est-à-dire en supposant qu'aucune énergie n'est emmagasinée dans le matériau lors de cycles de charge-décharge admissibles. Plus précisément, on a la :

Definition 2.1. On dit qu'un matériau est hyperélastique si et seulement si pour tout champ de déplacements de la forme :

$$\varphi(t, x) = c(t) + F(t) \cdot x, \quad \forall (t, x) \in [0, \tau] \times \Omega,$$

et τ -périodique :

$$\varphi(0, x) = \varphi(\tau, x), \quad \forall x \in \Omega,$$

le travail fourni par le matériau compressible au cours d'une période est nul, en ce sens que :

$$\int_0^\tau \int_A \mathcal{L}(x, F(t)) : \dot{F}(t) dx dt = 0, \quad \forall A \subset \Omega. \quad (2.11)$$

Dans ce cadre (décrit dans [Tal94b]), on obtient la :

Proposition 2.1. Pour un matériau hyperélastique, il existe une fonctionnelle d'énergie emmagasinée $\hat{\mathcal{W}} : \Omega \times \mathbb{R}^{3 \times 3} \rightarrow \mathbb{R}$ continûment différentiable par rapport à son deuxième argument, telle que pour tout $x \in \Omega$ et tout $t \in [0, T]$:

$$\mathcal{L}(x, \nabla \psi) = \frac{\partial \hat{\mathcal{W}}}{\partial F}(x, \nabla \psi), \quad \forall \psi \in \mathcal{U}^c(t).$$

Preuve : Nous la rappelons ici. Tout d'abord, on établit un résultat préliminaire. En différentiant la relation (2.11) pour la variation δF de F , il vient en utilisant la convention de sommation implicite sur les indices répétés et une intégration par parties en temps :

$$\begin{aligned} 0 &= \int_0^\tau \int_A \left(\frac{\partial \mathcal{L}_{ij}}{\partial F_{kl}} \delta F_{kl} \frac{\partial F_{ij}}{\partial t} + \mathcal{L}_{ij} \frac{\partial}{\partial t} \delta F_{ij} \right) dx dt \\ &= \int_0^\tau \int_A \left(\frac{\partial \mathcal{L}_{ij}}{\partial F_{kl}} \delta F_{kl} \frac{\partial F_{ij}}{\partial t} - \left(\frac{\partial}{\partial t} \mathcal{L}_{ij} \right) \delta F_{ij} \right) dx dt \\ &= \int_0^\tau \int_A \left(\frac{\partial \mathcal{L}_{ij}}{\partial F_{kl}} \delta F_{kl} \frac{\partial F_{ij}}{\partial t} - \frac{\partial \mathcal{L}_{ij}}{\partial F_{mn}} \frac{\partial F_{mn}}{\partial t} \delta F_{ij} \right) dx dt \\ &= \int_0^\tau \int_A \left(\frac{\partial \mathcal{L}_{ij}}{\partial F_{kl}} - \frac{\partial \mathcal{L}_{kl}}{\partial F_{ij}} \right) \delta F_{kl} \frac{\partial F_{ij}}{\partial t} dx dt. \end{aligned}$$

En conséquence, pour presque tout $x \in \Omega$, on a :

$$\int_0^\tau \left(\frac{\partial \mathcal{L}_{ij}}{\partial F_{kl}}(x, F(t)) - \frac{\partial \mathcal{L}_{kl}}{\partial F_{ij}}(x, F(t)) \right) \delta F_{kl}(t) \frac{\partial F_{ij}}{\partial t}(t) dt = 0. \quad (2.12)$$

D'autre part, soit $F \in \mathbb{R}^{3 \times 3}$ un gradient de déformation. Pour tout $x \in \Omega$, on définit l'énergie accumulée par le champ de déplacements $\varphi(t, x) = tF \cdot x$ au point $x \in \Omega$ par :

$$\hat{\mathcal{W}}(x, F) = \int_0^1 \mathcal{L}(x, tF) : F dt.$$

On obtient alors pour toute variation $\delta F \in \mathbb{R}^{3 \times 3}$ de $F \in \mathbb{R}^{3 \times 3}$ en utilisant (2.12) :

$$\begin{aligned}\frac{\partial \hat{\mathcal{W}}}{\partial F}(x, F) : \delta F &= \int_0^1 \left(t \left(\frac{\partial \mathcal{L}}{\partial F}(x, tF) : \delta F \right) : F + \mathcal{L}(x, tF) : \delta F \right) dt \\ &= \int_0^1 \left(t \left(\frac{\partial \mathcal{L}}{\partial F}(x, tF) : F \right) : \delta F + \mathcal{L}(x, tF) : \delta F \right) dt \\ &= \int_0^1 \frac{d}{dt} (t \mathcal{L}(x, tF) : \delta F) dt \\ &= \mathcal{L}(x, F) : \delta F.\end{aligned}$$

Il s'agit bien du résultat annoncé. De plus, il résulte de (2.11) que la définition de $\hat{\mathcal{W}}$ ne dépend pas du champ de déplacements φ choisi. \square

En vertu de ce résultat, nous avons pour un matériau hyperélastique :

$$\Pi^c(t, x) = \mathcal{L}(t, F(t, x)) = \frac{\partial \hat{\mathcal{W}}}{\partial F}(x, F(t, x)), \quad \forall (t, x) \in [0, T] \times \Omega.$$

2.2.2 Forme indépendante du référentiel

Nous pouvons en outre préciser la forme de l'énergie emmagasinée $\hat{\mathcal{W}}$ du matériau hyperélastique dans le cadre d'hypothèses physiques adaptées. En particulier, il importe que l'énergie emmagasinée $\hat{\mathcal{W}}$ soit définie en chaque point d'une façon indépendante du choix du référentiel. Cette préoccupation légitime la définition suivante :

Définition 2.1. *On dit que l'énergie emmagasinée $\hat{\mathcal{W}} : \Omega \times \mathbb{R}^{3 \times 3} \rightarrow \mathbb{R}$ est indépendante du référentiel si pour toute rotation $Q \in SO^+(3)$, on a pour presque tout $x \in \Omega$:*

$$\hat{\mathcal{W}}(x, Q \cdot F) = \hat{\mathcal{W}}(x, F), \quad \forall F \in \mathbb{R}^{3 \times 3}, \det F > 0.$$

On obtient alors simplement une condition nécessaire et suffisante pour que l'énergie emmagasinée $\hat{\mathcal{W}}$ soit indépendante du référentiel.

Lemme 2.1. *L'énergie emmagasinée $\hat{\mathcal{W}}$ est indépendante du référentiel si et seulement s'il existe une fonctionnelle $\mathcal{W} : \Omega \times \mathbb{R}^{3 \times 3} \rightarrow \mathbb{R}$ telle que pour tout $x \in \Omega$ et tout $F \in \mathbb{R}^{3 \times 3}$ avec $\det F > 0$:*

$$\hat{\mathcal{W}}(x, F) = \mathcal{W}(x, F^t \cdot F). \tag{2.13}$$

Preuve : En effet, si un tel \mathcal{W} existe, on a pour presque tout $x \in \Omega$ et tout $F \in \mathbb{R}^{3 \times 3}$ tel que $\det F > 0$:

$$\hat{\mathcal{W}}(x, Q \cdot F) = \mathcal{W}(x, F^t \cdot Q^t \cdot Q \cdot F) = \mathcal{W}(x, F^t \cdot F) = \hat{\mathcal{W}}(x, F), \quad \forall Q \in SO^+(3),$$

ce qui revient précisément à dire que l'énergie emmagasinée $\hat{\mathcal{W}}$ est indépendante du référentiel choisi.

Réiproquement, si on adopte $Q = (F^t \cdot F)^{1/2} \cdot F^{-1} \in SO^+(3)$ dans la définition 2.1, puisqu'ainsi $\det Q = 1$, il vient :

$$\hat{\mathcal{W}}(x, F) = \hat{\mathcal{W}}(x, Q \cdot F) = \hat{\mathcal{W}}(x, F^t \cdot F).$$

□

Cette propriété légitime l'introduction du tenseur de Cauchy-Green à droite :

$$C = F^t \cdot F. \quad (2.14)$$

On peut alors préciser la forme du premier tenseur des contraintes de Piola-Kirchhoff. Pour ce faire, nous avons le :

Lemme 2.2. *Avec les notations (2.13) et (2.14), on obtient :*

$$\frac{\partial \hat{\mathcal{W}}}{\partial F}(x, F) = 2F \cdot \frac{\partial \mathcal{W}}{\partial C}(x, F^t \cdot F), \quad \forall x \in \Omega, \quad \forall F \in \mathbb{R}^{3 \times 3}, \det F > 0.$$

Preuve : On a par définition de \mathcal{W} , pour toute variation $\delta F \in \mathbb{R}^{3 \times 3}$ de $F \in \mathbb{R}^{3 \times 3}$:

$$\begin{aligned} \frac{\partial \hat{\mathcal{W}}}{\partial F} : \delta F &= \frac{\partial \mathcal{W}}{\partial C} : (\delta F^t \cdot F + F^t \cdot \delta F) \\ &= \left(2F \cdot \frac{\partial \mathcal{W}}{\partial C} \right) : \delta F, \end{aligned}$$

en utilisant le caractère symétrique de $\frac{\partial \mathcal{W}}{\partial C}$, d'où la preuve. □

En introduisant le second tenseur de Piola-Kirchhoff Σ^c tel que :

$$\Pi^c(t, x) = F(t, x) \cdot \Sigma^c(t, x), \quad (t, x) \in [0, T] \times \Omega, \quad (2.15)$$

on a donc dans le cas hyperélastique la forme générale de la loi de comportement :

$$\Sigma^c(t, x) = 2 \frac{\partial \mathcal{W}}{\partial C}(x, \nabla \varphi^t(t, x) \cdot \nabla \varphi(t, x)). \quad (2.16)$$

2.2.3 Isotropie

Nous terminons cette sous-section en rappelant que sous une hypothèse d'isotropie, la loi de comportement prend une forme particulière. On définit le caractère isotrope du matériau en termes d'énergie emmagasinée par la :

Définition 2.2. On dit que l'énergie emmagasinée $\hat{\mathcal{W}} : \Omega \times \mathbb{R}^{3 \times 3} \rightarrow \mathbb{R}$ caractérise un matériau isotrope si pour toute rotation $Q \in SO^+(3)$, on a pour presque tout $x \in \Omega$:

$$\hat{\mathcal{W}}(x, F \cdot Q) = \hat{\mathcal{W}}(x, F), \quad \forall F \in \mathbb{R}^{3 \times 3}, \det F > 0.$$

Nous renvoyons à ([Cia88], page 152) pour montrer que $\hat{\mathcal{W}}$ est une fonctionnelle d'énergie emmagasinée sous forme indépendante du référentiel et caractérisant un matériau isotrope si et seulement si elle s'écrit :

$$\hat{\mathcal{W}}(x, F) = \mathcal{I}(x, i(F^t \cdot F)),$$

où $i(F^t F) = (\text{tr } C, \text{tr cof } C, \det C)$ désigne les invariants principaux de la matrice $C = F^t \cdot F$. La loi de Mooney-Rivlin pour les matériaux isotropes incompressibles, qui adopte l'énergie quadratique par rapport aux invariants :

$$\mathcal{W}(C) = c_1 (\text{tr } C - 3)^2 + c_2 (\text{tr cof } C - 3)^2,$$

voit ainsi légitimer sa forme par ce résultat.

Enfin, en supposant que \mathcal{I} est deux fois continument différentiable par rapport aux invariants principaux $i(C)$ pour $C = F^t \cdot F = I_2$, on en déduit par un calcul explicite de sa dérivée seconde qu'il existe deux fonctions positives λ et μ définies sur Ω et dites coefficients de Lamé du matériau, telles que :

$$\frac{\partial^2 \mathcal{W}}{\partial C^2}(I_2) = \lambda I_2 \otimes I_2 + 2\mu I_4,$$

où I_2 et I_4 désignent respectivement les tenseurs unité d'ordre 2 et 4. On pourra trouver le détail de ce calcul dans ([Cia88], page 156). Ce dernier résultat permet de justifier la loi de comportement dite de Hooke en élasticité isotrope linéarisée. En effet, en linéarisant par exemple le système incompressible (2.9),(2.10) avec la loi (2.15),(2.16) autour du champ de déplacements identité $\varphi = id$, on obtient alors le problème consistant à trouver les champs des déplacements u et des pressions p , tels qu'à tout instant $t \in [0, T]$ on ait $u(t) \in \mathcal{V}(t)$ et $p(t) \in \mathcal{P}$ satisfaisant :

$$\begin{aligned} & \int_{\Omega} \rho(x) \frac{\partial^2 u}{\partial t^2}(t, x) \cdot v(x) dx \\ & + \int_{\Omega} (\mathbf{E}(x) : \varepsilon(u(t, x)) - p(t, x) \operatorname{div} u(t, x)) : \nabla v(x) dx \\ & = \int_{\Omega} f(t, x) \cdot v(x) dx + \int_{\Gamma_N} g(t, x) \cdot v(x) dx, \quad \forall v \in \mathcal{V}_0(t), \end{aligned}$$

et

$$\int_{\Omega} q(x) \operatorname{div} u(t, x) dx = 0, \quad \forall q \in \mathcal{P}.$$

Nous avons désigné par :

$$\mathcal{V}(t) = \{u : \Omega \rightarrow \mathbb{R}^3, u = \varphi_D(t) - id \text{ sur } \Gamma_D(t)\},$$

l'espace des déplacements cinématiquement admissibles à l'instant $t \in [0, T]$, et par :

$$\mathcal{V}_0(t) = \{u : \Omega \rightarrow \mathbb{R}^3, u = 0 \text{ sur } \Gamma_D(t)\},$$

l'espace vectoriel des fonctions test. Le tenseur d'élasticité d'ordre quatre, noté \mathbf{E} , est donné par la loi de Hooke :

$$\mathbf{E} = \frac{\partial^2 \mathcal{W}}{\partial C^2}(I_2) = \lambda I_2 \otimes I_2 + 2\mu I_4.$$

De plus, le tenseur de déformation linéarisé $\varepsilon(u)$ est défini comme la partie symétrique du gradient de u :

$$\varepsilon(u) = \frac{1}{2} (\nabla u + \nabla^t u),$$

et $\sigma = \mathbf{E} : \varepsilon(u)$ définit le tenseur des contraintes de Cauchy, avec :

$$\sigma = \lambda \operatorname{tr} \varepsilon(u) + 2\mu \varepsilon(u).$$

Le cadre de la dynamique hyperélastique incompressible présenté dans cette section est le cadre fondamental de ce travail.

2.3 Viscoélasticité

L'hypothèse d'hyperélasticité ne permettant pas de prendre en compte l'historique de déformation des matériaux, nous complétons ici la présentation précédente en introduisant le cadre viscoélastique, tel que décrit dans [TRK93, Tal94b].

Il est basé sur le modèle rhéologique de Kelvin-Voigt schématisé figure 2.2, en ce sens que l'expression du tenseur des contraintes en fonction du tenseur de Cauchy-Green à droite s'inspire de la relation entre la force f appliquée entre A et B et l'elongation l du système. Ledit système est composé de deux branches parallèles : la première est purement élastique et composée d'un ressort de raideur K_0 , d'elongation l . La deuxième, partiellement visqueuse, comprend un ressort de raideur K_e d'elongation l_e , et un vérin de coefficient de viscosité ν d'elongation l_v . Si la force f est exercée entre les extrémités A et B du système, son évolution est alors décrite par le système d'équations :

$$\begin{cases} f = K_0 l + K_e l_e, \\ \nu \dot{l}_v = K_e l_e, \\ l = l_e + l_v. \end{cases} \quad (2.17)$$

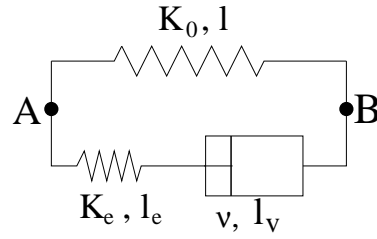


FIG. 2.2 – Modèle rhéologique de Kelvin-Voigt pour un matériau viscoélastique.

En grandes déformations, on considère par analogie que le champ de déformation F dans le matériau se décompose en une partie visqueuse F_v et une partie élastique F_e , et on écrit :

$$F = F_e \cdot F_v.$$

Par application du lemme de décomposition polaire (démontré par exemple dans [GvL83, Cia88]), il existe une matrice de rotation R telle que :

$$F_e = R \cdot (F_e^t \cdot F_e)^{1/2} = R \cdot C_e^{1/2},$$

où $C_e = F_e^t \cdot F_e$ désigne le tenseur de Cauchy-Green à droite de la partie élastique du champ de déplacements. Nous procédons de même sur la partie visqueuse des déplacements en supposant en outre que la rotation associée à la décomposition polaire de F_v a été intégralement reportée dans F_e et vaut donc l'identité, de sorte que :

$$F_v = C_v^{1/2},$$

où $C_v = F_v^t \cdot F_v$ désigne le tenseur de Cauchy-Green à droite de la partie visqueuse du champ de déplacements. Il vient donc que :

$$C = F_v^t \cdot F_e^t \cdot F_e \cdot F_v = C_v^{1/2} \cdot C_e \cdot C_v^{1/2}.$$

D'une façon consistante avec cette introduction, on associe à toute déformation du matériau, deux champs de tenseurs de Cauchy-Green à droite C et C_v , qui permettent de définir le tenseur de Cauchy-Green de la déformation élastique de la branche visqueuse :

$$C_e = C_v^{-1/2} \cdot C \cdot C_v^{-1/2}.$$

Si on suppose de plus que le matériau est incompressible dans son comportement élastique et visqueux, ces quantités sont alors contraintes, au moins dans un sens variationnel, par :

$$\det C_v = 1, \quad \det C = 1.$$

A tout état déformé caractérisé par C et C_v , on associe alors l'énergie de déformation suivante :

$$\tilde{\mathcal{W}}(C, C_v) = \tilde{\mathcal{W}}_0(C) + \tilde{\mathcal{W}}_e(C_v^{-1/2} \cdot C \cdot C_v^{-1/2}),$$

constituée de l'énergie de déformation de la branche élastique $\tilde{\mathcal{W}}_0$, et de l'énergie de déformation élastique de la branche visqueuse $\tilde{\mathcal{W}}_e$.

Reste à rendre compte de la deuxième équation de (2.17), c'est-à-dire de la dissipation due à la branche visqueuse. Lors d'une variation δC_v de C_v , on exprime l'énergie dissipée sous la forme $\phi(\dot{C}_v) : \delta C_v$ et le second principe de la thermodynamique impose :

$$\phi(\dot{C}_v) : \dot{C}_v \geq 0, \quad \forall \dot{C}_v.$$

On adopte classiquement :

$$\phi(\dot{C}_v) = -\nu \frac{\partial}{\partial t}(C_v^{-1}),$$

choix pour lequel nous explicitons la quantité $\phi(\dot{C}_v) : \dot{C}_v$. Par dérivation par rapport au temps t , la relation $C_v(t) \cdot C_v^{-1}(t) = I_2$ fournit :

$$\frac{\partial}{\partial t}(C_v) \cdot C_v^{-1} + C_v \cdot \frac{\partial}{\partial t}(C_v^{-1}) = 0,$$

de sorte que :

$$\frac{\partial}{\partial t}(C_v^{-1}) = -C_v^{-1} \cdot \frac{\partial}{\partial t}(C_v) \cdot C_v^{-1}.$$

Il s'ensuit que :

$$\phi(\dot{C}_v) = \nu C_v^{-1} \cdot \dot{C}_v \cdot C_v^{-1},$$

et donc le second principe de la thermodynamique est satisfait en ce sens que :

$$\phi(\dot{C}_v) : \dot{C}_v = \nu D_v : D_v \geq 0,$$

avec le tenseur de taux de déformation visqueux :

$$D_v = C_v^{-1/2} \cdot \dot{C}_v \cdot C_v^{-1/2}.$$

Dans ce cadre, nous obtenons l'expression du premier tenseur des contraintes de Piola-Kirchhoff :

$$\begin{aligned} \Pi &= 2F \cdot \frac{\partial \tilde{\mathcal{W}}}{\partial C}(C, C_v) - p \operatorname{cof} F \\ &= F \cdot \left(2 \frac{\partial \tilde{\mathcal{W}}}{\partial C}(C, C_v) - p \frac{1}{\det F} C^{-1} \right), \end{aligned} \tag{2.18}$$

où figure la pression hydrostatique $p \in \mathcal{P}$, associée à la contrainte d'incompressibilité :

$$\int_{\Omega} (\det F - 1) q = 0, \quad \forall q \in \mathcal{P}.$$

Conformément au second principe de la thermodynamique, la dissipation correspond exactement à la diminution de l'énergie élastique du système, de sorte que :

$$-\nu \frac{\partial}{\partial t}(C_v^{-1}) = -\frac{\partial \tilde{\mathcal{W}}}{\partial C_v}(C, C_v) + q \operatorname{cof} C_v, \quad (2.19)$$

où figure la pression $q \in \mathcal{Q}$ associée à la contrainte d'incompressibilité :

$$\int_{\Omega} (\det C_v - 1) q = 0, \quad \forall q \in \mathcal{Q}.$$

Nous introduisons alors la variable interne $A = C_v^{-1}$, et réécrivons (2.19) sous la forme :

$$\nu C_v^{-1} \cdot \dot{C}_v \cdot C_v^{-1} = C_v^{-1} \cdot \frac{\partial \tilde{\mathcal{W}}}{\partial A}(C, C_v) \cdot C_v^{-1} + q (\det C_v) C_v^{-1}. \quad (2.20)$$

En multipliant cette expression à gauche et à droite par C_v , il vient :

$$\nu \frac{\partial}{\partial t}(A^{-1}) = \frac{\partial \tilde{\mathcal{W}}}{\partial A}(C, C_v) + q \operatorname{cof} A. \quad (2.21)$$

Les équations de l'évolution viscoélastique consistent donc à trouver au sens variationnel à tout instant $t \in [0, T]$, le champ des déplacements $\varphi(t) \in \mathcal{U}^c(t)$, des pressions hydrostatiques $p(t) \in \mathcal{P}$, des variables internes $A(t) \in \mathcal{A}$ et des pressions associées $q(t) \in \mathcal{Q}$ tels que :

$$\begin{cases} \int_{\Omega} \rho \ddot{\varphi} \cdot \hat{\varphi} + \int_{\Omega} F \cdot \left(2 \frac{\partial \tilde{\mathcal{W}}}{\partial C}(C, A) - p \frac{C^{-1}}{\det F} \right) : \nabla \hat{\varphi} = \int_{\Omega} f \cdot \hat{\varphi} + \int_{\Gamma_N} g \cdot \hat{\varphi}, \\ \int_{\Omega} (\det F - 1) \hat{p} = 0, \\ \int_{\Omega} \left(\nu \frac{\partial}{\partial t}(A^{-1}) - \frac{\partial \tilde{\mathcal{W}}}{\partial A}(C, A) - q \operatorname{cof} A \right) : \hat{A} = 0, \\ \int_{\Omega} (\det A - 1) \hat{q} = 0, \end{cases} \quad (2.22)$$

pour tout $(\hat{\varphi}, \hat{p}, \hat{A}, \hat{q}) \in d_{\varphi(t)} \mathcal{U}^c(t) \times \mathcal{P} \times \mathcal{A} \times \mathcal{Q}$. Le caoutchouc est un excellent candidat au comportement viscoélastique. Le cadre du comportement viscoélastique nous servira essentiellement au chapitre 3 où nous proposons un schéma d'intégration en temps pour l'évolution viscoélastique possédant un bilan énergétique discret exact.

2.4 Contact sans frottement

Afin de donner une description complète du problème qui motive cette étude, il nous faut maintenant introduire la notion de force de contact. Soit Γ_c une partie du bord de Ω ,

où est susceptible de se produire un contact unilatéral (pour simplifier) contre une surface rigide Γ_r . Pour tout point $x \in \Gamma_c$, on définit le point $\bar{y}(x)$ de Γ_r le plus proche de x :

$$\bar{y}(x) = \arg \min_{y \in \Gamma_r} \|y - x\|_2.$$

Si on suppose la variété Γ_r différentiable, cela signifie qu'il existe un réel $g(x)$ (l'opposé de la distance de x à Γ_c) tel que :

$$\bar{y}(x) - x = g(x) \nu(\bar{y}(x)),$$

où $\nu(y)$ désigne le vecteur normal unitaire au point y de Γ_r , dirigé vers Γ_c en supposant que Ω se trouve d'un seul côté de la paroi Γ_r . On a ainsi :

$$g(x) = (\bar{y}(x) - x) \cdot \nu(\bar{y}(x)), \quad \forall x \in \Gamma_c.$$

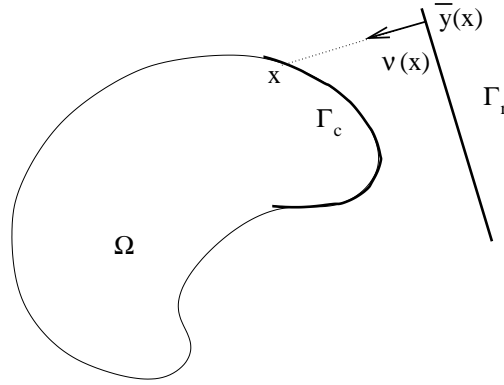


FIG. 2.3 – Configuration non-déformée Ω d'un solide, dont la partie Γ_c du bord est susceptible d'entrer en contact avec la paroi rigide Γ_r .

La contrainte de contact unilatéral se formule de manière non-variationnelle en disant que tout champ de déplacements φ doit être tel que :

$$g(\varphi(x)) \leq 0, \quad \forall x \in \Gamma_c.$$

En conséquence de cette contrainte, la réaction de contact exercée par Γ_r sur Γ_c s'écrit :

$$\tau(x) = -\lambda(x) \frac{\partial g}{\partial x}(\varphi(x)), \quad \forall x \in \Gamma_c,$$

où figure l'intensité λ de la force répulsive qui satisfait aux conditions de Karush, Kuhn et Tucker [Lue84, Cia92] :

$$\begin{cases} \lambda(x) \geq 0, \\ g(\varphi(x)) \leq 0, \\ \lambda(x)g(\varphi(x)) = 0, \quad \forall x \in \Gamma_c. \end{cases}$$

Par suite, il vient que :

$$\begin{aligned}\tau(x) &= -\lambda(x) \left[\left(\frac{\partial \bar{y}}{\partial x} - I_2 \right) \cdot \nu(\bar{y}(x)) + g(\varphi(x)) \nu(\bar{y}(x)) \cdot \left(\frac{\partial \nu}{\partial y} \cdot \frac{\partial \bar{y}}{\partial x} \right) \right] \\ &= -\lambda(x) \left(\frac{\partial \bar{y}}{\partial x} - I_2 \right) \cdot \nu(\bar{y}(x)), \text{ puisque } \lambda(x)g(\varphi(x)) = 0, \\ &= \lambda(x) \nu(\bar{y}(x)),\end{aligned}\tag{2.23}$$

puisque pour toute variation δx de $x \in \mathbb{R}^{3 \times 3}$, le vecteur $\frac{\partial \bar{y}}{\partial x} \cdot \delta x \in \mathbb{R}^{3 \times 3}$ est tangent à la variété Γ_r au point $\bar{y}(x)$. Il est donc naturellement orthogonal à $\nu(\bar{y}(x))$, et on obtient ainsi une force de réaction normale à la paroi rigide Γ_r . En conclusion, le problème d'évolution viscoélastique avec contact consiste à trouver à tout temps $t \in [0, T]$, le champ des déplacements $\varphi(t) \in \mathcal{U}^c(t)$, des pressions hydrostatiques $p(t) \in \mathcal{P}$, des variables internes $A(t) \in \mathcal{A}$ avec pressions associées $q(t) \in \mathcal{Q}$, et des pressions de contact $\lambda(t) \in \Lambda(t)$ tels que :

$$\left\{ \begin{array}{l} \int_{\Omega} \rho \ddot{\varphi} \cdot \hat{\varphi} + \int_{\Omega} F \cdot \left(2 \frac{\partial \tilde{\mathcal{W}}}{\partial C}(C, A) - p \frac{C^{-1}}{\det F} \right) : \nabla \hat{\varphi} = \int_{\Omega} f \cdot \hat{\varphi} + \int_{\Gamma_N} g \cdot \hat{\varphi} + \int_{\Gamma_r} \lambda(t) \nu(\bar{y}) \cdot \hat{\varphi}, \\ \int_{\Omega} (\det F - 1) \hat{p} = 0, \\ \int_{\Omega} \left(\nu \frac{\partial}{\partial t} (A^{-1}) - \frac{\partial \tilde{\mathcal{W}}}{\partial A}(C, A) - q \operatorname{cof} A \right) : \hat{A} = 0, \\ \int_{\Omega} (\det A - 1) \hat{q} = 0, \\ \lambda(t, x) \geq 0, \quad x \in \Gamma_c \text{ almost everywhere,} \\ \lambda(t, x)g(\varphi(t, x)) = 0, \quad x \in \Gamma_c \text{ almost everywhere.} \end{array} \right. \tag{2.24}$$

pour tout $(\hat{\varphi}, \hat{p}, \hat{A}, \hat{q}) \in d_{\varphi(t)} \mathcal{U}^c(t) \times \mathcal{P} \times \mathcal{A} \times \mathcal{Q}$.

Nous n'évoquerons pas dans ce travail, le traitement du contact frottant qui peut être lu par exemple dans [Joh85, Lau02, Wri02]. En effet, notre contribution dans ce domaine concerne essentiellement la formulation d'un schéma d'intégration en temps conservant l'énergie discrète en élastodynamique avec contact sans frottement ou parfaitement adhérent. Quant à elles, l'évaluation du glissement et l'expression des forces de frottement pourront être réalisées de manière tout à fait indépendante par la méthode voulue.

Les éléments de ce chapitre décrivent donc sommairement la manière usuelle de modéliser la dynamique de structures hyperélastiques ou viscoélastiques pouvant entrer en contact sur une partie de leur bord avec un corps rigide extérieur. Il fournit le cadre physique des développements du travail exposé dans les chapitres suivant.

Chapitre 3

Energy conservative/dissipative time integration in nonlinear elastodynamics

Résumé

Il est maintenant bien établi que la conservation/dissipation de l'énergie discrète joue un rôle fondamental en ce qui concerne la stabilité inconditionnelle des schémas d'intégration en temps pour l'élastodynamique non-linéaire. Dans ce chapitre, nous présentons une analyse théorique et numérique de l'évolution de l'énergie pour les schémas du second ordre de point milieu, de trapèze, et de Hilber-Hughes-Taylor [HHT77], comparés à des schémas conservatifs tels que [Gon00]. De plus, nous proposons des extensions de la technique de correction d'énergie proposée par O. Gonzalez pour un modèle viscoélastique issu de [TRK93], et les problèmes avec contact glissant, comme dans [LL02, AP98]. Enfin, en exploitant l'analyse proposée du schéma HHT, nous formulons une intégration en temps dissipative des termes d'inertie, précise à l'ordre deux, et se traduisant par l'obtention d'un schéma dissipatif pour une énergie régularisée prenant en compte une petite contribution des effets d'accélération. Le tout est illustré sur plusieurs essais numériques significatifs.

Abstract

It is now well established that discrete energy conservation/dissipation plays a key-role for the unconditional stability of time integration schemes in nonlinear elastodynamics. In this paper, we present a theoretical and numerical study of energy evolution for midpoint, trapezoidal and Hilber-Hughes-Taylor second order schemes, as compared with energy conserving schemes like [Gon00]. Moreover, we propose extensions of Gonzalez' energy correction to a viscoelastic model from [TRK93], and frictionless contact problems in the way of [LL02, AP98].

Finally, by exploiting the proposed analysis of the HHT scheme, we formulate a second order dissipative time integration of inertial terms, resulting in a dissipative scheme involving a regularized energy, taking into account a small contribution of accelerations.

3.1 Introduction

Time integration schemes for elastodynamics have been developed for a long time in a linear framework in which consistency and linear stability ensure convergence by time step refinement. Whereas the conditionally stable explicit centered method must be mentioned for its simplicity, the numerical stiffness of such mechanical problems has lead to the development of implicit methods, especially when dealing with incompressible materials, such as Houbolt, Wilson, Newmark or Hilber-Hughes-Taylor [HHT77] methods, that can be read in [Bat82, Cri97, GR93] among others. Nevertheless, when considering nonlinear problems, the previous implicit schemes lose their unconditional stability and nonlinear criteria of stability must be found.

In the Hamiltonian framework (i.e. with conservative loadings), a geometrical approach could consist in constructing numerical schemes whose flow is symplectic [HLW02, SSC94], entailing the conservation of the volume in the phase space. Nevertheless, such a condition is not always sufficient to ensure the stability of the numerical system for large time steps and for stiff problems. In the compressible case, this statement will be numerically assessed for the symplectic midpoint scheme. A deeper analysis is proposed by J.C.Simo and O.Gonzalez in [SG93]. In particular, the authors show that symplecticness is difficult to maintain in the case of kinematically constrained systems. More recently, a new geometric understanding of time integration schemes in the Lagrangian framework has lead to the concept of variational integrators, and seems quite promising [KMOW00, MW01].

Another way to stabilize the discrete solution can consist in imposing energy conservation as a constraint, by projection [NNR77, HLC78] or by Lie group methods [MK99]. In fact, by a mean value argument, Simo and Tarnow have shown in [ST92] that conservation could be achieved by choosing correctly the algorithmic definition of the second Piola-Kirchhoff stress tensor. Such an idea has lead to a very practical conservative scheme proposed by Gonzalez in [Gon00].

In the linear framework, *linearly dissipative* integration schemes, i.e. whose spectral radius is strictly less than unity, have been developed to avoid polynomial instabilities, arising for non-diagonalizable integrators with double unit eigenvalue. Nevertheless, when extended to the nonlinear framework, they do not ensure longterm stability as the evolution of energy cannot be controlled. Many works from Bauchau, Bottasso and their collaborators [BT96, BJ99, BB99, BBT01a, BBT01b, BBC02, BBT03] or Armero and Romero [AR01a, AR01b] or Bui [Bui03] among others, have proposed various strategies to obtain slightly dissipative time integration schemes, able to damp out unresolved high frequency modes, while maintaining a good accuracy. Whereas these works often develop a special discrete integration of the inertial term, or introduce a numerical Rayleigh damping (see [GR93]) at highest frequencies, we turn to good account the conservation analysis for the HHT scheme we propose, to provide a way of introducing energy dissipation in a conservative scheme such as [Gon00] by a non-trapezoidal second order approximation of the inertial term. In particular, as often, the dissipative contribution remains located in the inertial term, which makes easier to transpose it to various Lagrangian systems for which the potential energy remains integrated with a conservative method.

Among the most violent situations involving the dynamics of hyperelastic structures, the problem of impact is known to be particularly demanding. Over the last years, an increasing interest has been devoted to energy conserving time integration schemes for contact mechanics. In particular, in the framework of frictionless contact, both Laursen and Chawla [LC97] and Armero and Petöcz [AP98] have proposed an energy conserving approach. Nevertheless, as underlined in [LL02], both contributions encounter a difficulty in enforcing standard Kuhn-Tucker conditions associated to frictionless contact, so that they concede an interpenetration of the structures in interaction, vanishing as the time step goes to zero. This drawback is resolved by Laursen and Love in [LL02], by introducing a discrete jump in velocities during impact, making possible the enforcement of contact conditions at each time step, at the computational price of resolving a problem on the jump in velocities. In the framework of a penalized enforcement of the contact condition, and by adapting the correction technique from [Gon00], we propose an energy conserving scheme while enforcing the standard Kuhn-Tucker contact conditions at entire time steps.

On the other hand, because of the Dirac acceleration involved during perfect impact, which has Fourier components at all frequencies, oscillations of the normal contact pressure occur when the penalization coefficient tends to infinity. Indeed, the absence of strong convergence of the solution in the linearized framework is well understood from a mathematical point of view in the absence of viscosity (see [Sca04] for example) for a lack of compacity reason. The enforcement of a constraint on velocities, formally equivalent to a viscous contact force, used for example in [TP93, AP98] is known to provide the dissipation of the high frequency oscillations. An alternative consists in taking into account a real internal viscoelastic behavior in the material. In order to obtain an exact discrete energetic balance, we adapt again the technique from [Gon00], and propose a new scheme for the time integration of the viscoelastic model introduced in [TRK93].

When considering the dynamics of coupled problems, such as aeroelasticity [FLT98] or magneto-hydro-dynamics [GLB03] problems, of even more crucial importance is the stability of the coupled system, well described by energy evolution. We have shown in [TH03a] that the energy conserving approach presented herein could be extended to a fluid-structure interaction framework, with Arbitrary Lagrangian Eulerian description, by adopting special non-conservative variables in the fluid.

In section 2, we introduce the problem of nonlinear quasi-incompressible elastodynamics. In section 3, we show why completely implicit schemes are the only way to explore. Indeed, in the nonlinear framework, semi-implicit strategies are shown to have the same complexity as implicit ones. We propose in section 4, a precise conservation analysis of linearly conservative schemes such as midpoint and trapezoidal rules, identifying their major sources of instability in presence of an incompressibility kinematical constraint, which are avoided by [ST92, Gon00, LM01]. In section 5, based on a rigorous analysis of the conservation of the Hilber-Hughes-Taylor time integration scheme [HHT77], we propose a dissipative discretization of the inertial terms in a conservative scheme enabling to conciliate second order accuracy with an energy decaying property for a regularized energy involving acceleration effects. In section 6, we propose an extension of the energy correction technique from [Gon00] to obtain a conservative discrete integration of the viscoelasticity system from [TRK93], and of penalized contact pressures involved during impact enabling the enforcement of the standard Kuhn-Tucker conditions at time discretization points. Numerical tests in the hyperelastic framework are presented in section 6, and illustrate the present work.

3.2 Quasi-incompressible elastodynamics

3.2.1 The incompressible model

The open set $\Omega \subset \mathbb{R}^3$ denotes the interior of the reference configuration of a solid body and its time-dependent deformation is described by the following mapping :

$$\varphi : [0, T] \times \Omega \rightarrow \mathbb{R}^3. \quad (3.1)$$

The material is assumed to be incompressible in the sense that on $[0, T] \times \Omega$,

$$\det F = \det \nabla \varphi = 1. \quad (3.2)$$

The density of the material on the reference configuration is denoted by $\rho : \Omega \rightarrow \mathbb{R}_+^*$ and the body forces by $f : [0, T] \times \Omega \rightarrow \mathbb{R}^3$. On the subsets Γ_D and Γ_N of the boundary $\Gamma = \partial\Omega$ of the domain, the displacement $\underline{\varphi_D} : [0, T] \times \Gamma_D \rightarrow \mathbb{R}^3$ and the traction $\underline{g} : [0, T] \times \Gamma_N \rightarrow \mathbb{R}^3$ are prescribed. Moreover $\overline{\Gamma_D \cup \Gamma_N} = \Gamma$, $\Gamma_D \cap \Gamma_N = \emptyset$, and n is the outward normal unit vector.

The first Piola-Kirchhoff stress tensor in the material is denoted by Π and is given by the hyperelastic constitutive law :

$$\begin{aligned}\Pi &= \frac{\partial \hat{\mathcal{W}}}{\partial F} - p \operatorname{cof} F \\ &= F \cdot \left(2 \frac{\partial \mathcal{W}}{\partial C} - \frac{1}{(\det C)^{1/2}} p \operatorname{cof} C \right) \\ &= F \cdot \left(2 \frac{\partial \mathcal{W}}{\partial C} - 2p \frac{\partial \det C^{1/2}}{\partial C} \right) \\ &= F \cdot \Sigma.\end{aligned}$$

The symmetric tensor Σ is known as the second Piola-Kirchhoff stress tensor, $p : [0, T] \times \Omega \rightarrow \mathbb{R}$ denotes the hydrostatic pressure, $\hat{\mathcal{W}}$ and \mathcal{W} the stored elastic potentials respectively in term of the gradient F or the right Cauchy-Green strain tensor $C = F^t \cdot F$. The cofactor matrix of the matrix F is denoted by $\operatorname{cof} F = \partial_F \det F$.

3.2.2 Variational quasi-incompressible formulation

We introduce variational spaces for displacements, velocities and pressures :

$$\begin{cases} \mathcal{U}_0 \subset \{u \in W^{1,s}(\Omega)^3; \quad u = 0 \text{ on } \Gamma_D\}, \\ \mathcal{V} \subset \{w \in L^2(\Omega)^3\}, \\ \mathcal{P} \subset \{p \in L^q(\Omega); \quad \frac{3}{s} + \frac{1}{q} \leq 1\}. \end{cases} \quad (3.3)$$

We assume that $\rho \in L^\infty(\Omega)$, with $\rho \geq \rho_0 > 0$ almost everywhere on Ω , that $f \in L^2(0, T; L^{s^*}(\Omega))$ with $\frac{1}{s} + \frac{1}{s^*} = 1$, and that $\varphi_D \in L^2(0, T; W^{1-1/s, s}(\Gamma_D)^3)$. The elastic potentials $\hat{\mathcal{W}}$ and \mathcal{W} are assumed to be continuously differentiable with respect to their arguments. Then, the variational formulation of the hyperelastic incompressible elastodynamics problem we consider, consists in finding :

$$\begin{cases} \varphi - \varphi_D \in L^2(0, T; \mathcal{U}_0), \\ \dot{\varphi} \in L^2(0, T; \mathcal{V}), \\ \rho \ddot{\varphi} \in L^2(0, T; \mathcal{U}'_0), \\ p \in L^2(0, T; \mathcal{P}), \end{cases} \quad (3.4)$$

such as for almost every $t \in]0, T[$, any $v \in \mathcal{U}_0$ and any $q \in \mathcal{P}$:

$$\begin{cases} \langle \rho \ddot{\varphi}(t), v \rangle_{\mathcal{U}'_0, \mathcal{U}_0} + \int_{\Omega} \Pi(t) : \nabla v = \int_{\Omega} f(t) \cdot v, \\ \int_{\Omega} (\det \nabla \varphi(t) - 1 + \epsilon p(t)) q = 0. \end{cases} \quad (3.5)$$

Remark 3.1. Some remarks should be done concerning the formulation (3.5) :

- We have assumed that the surfacic traction g was vanishing to avoid a technical difficulty. Indeed, since the speed is in $L^2(\Omega)^3$, it has no trace on the boundary Γ_N and the surfacic work cannot be defined so easily without additional regularity study.
- The spaces \mathcal{U}_0 , \mathcal{V} and \mathcal{P} can be finite dimensional spaces in the framework of space discretized approximation.
- The compression term ϵp generalizes the problem to quasi-incompressible situations. $1/\epsilon$ has the physical meaning of a bulk modulus.
- To ensure the well posedness of the linearized problems coming from (3.5) around any admissible displacement φ and obtain the uniform convergence toward the incompressible limit as $\epsilon \rightarrow 0$, it is necessary to have the following compatibility condition (see [Bab73, Bre74]) :

$$\begin{aligned} & \exists \beta > 0, \quad \forall \varphi \in \varphi_D + \mathcal{U}_0, \\ & \inf_{q \in \mathcal{P}, \|q\|_{\mathcal{P}}=1} \sup_{v \in \mathcal{U}_0, \|v\|_{\mathcal{U}_0}=1} \int_{\Omega} q ((\operatorname{cof} \nabla \varphi) : \nabla v) \geq \beta. \end{aligned} \quad (3.6)$$

As far as we know, the proof of existence of a solution for (3.4) is presently out of reach, but we recall in the next subsection a crucial expected conservation property for such a solution, both from theoretical and numerical point of view.

3.2.3 Conservation properties

From a physical point of view, a solution of (3.4) is expected to satisfy the following conservation properties :

Proposition 3.1. Formally¹, the following conservation properties hold for a solution of (3.5) for any $t \in]0, T[$:

- Energy conservation.

$$\mathcal{E}(t) - \mathcal{E}(0) = \int_0^t \int_{\Omega} f \cdot \dot{\varphi}, \quad (3.7)$$

the total energy being defined by :

$$\mathcal{E}(t) = \frac{1}{2} \int_{\Omega} \rho \dot{\varphi}(t, x)^2 dx + \int_{\Omega} \hat{\mathcal{W}}(x, \nabla \varphi(t, x)) dx + \frac{\epsilon}{2} \int_{\Omega} p(t)^2. \quad (3.8)$$

- Angular momentum conservation (for $\Gamma_D = \emptyset$).

$$\mathcal{J}(t) - \mathcal{J}(0) = \int_0^t \int_{\Omega} \varphi \times f, \quad (3.9)$$

with :

$$\mathcal{J}(t) = \int_{\Omega} \rho \varphi(t, x) \times \dot{\varphi}(t, x) dx. \quad (3.10)$$

– Linear momentum conservation (for $\Gamma_D = \emptyset$).

$$\mathcal{I}(t) - \mathcal{I}(0) = \int_0^t \int_{\Omega} f, \quad (3.11)$$

with :

$$\mathcal{I}(t) = \int_{\Omega} \rho \dot{\varphi}(t, x) dx. \quad (3.12)$$

Proof : As announced, the present proof is formal. Concerning energy conservation, the variational formulation of the problem at time $t \in [0, T]$ entails for $v = \dot{\varphi}(t)$ that :

$$\int_{\Omega} \rho \ddot{\varphi}(t) \cdot \dot{\varphi}(t) + \int_{\Omega} \left(\frac{\partial \hat{\mathcal{W}}}{\partial F}(\nabla \varphi(t)) - p(t) \operatorname{cof} \nabla \varphi(t) \right) : \nabla \dot{\varphi}(t) = \int_{\Omega} f(t) \cdot \dot{\varphi}(t). \quad (3.13)$$

By a derivation in time of the incompressibility constraint :

$$\int_{\Omega} (\det \nabla \varphi(t) - 1 + \epsilon p(t)) q = 0, \quad \forall q \in \mathcal{P},$$

one gets that :

$$\int_{\Omega} ((\operatorname{cof} \nabla \varphi(t)) : \nabla \dot{\varphi}(t) + \epsilon \dot{p}(t)) q = 0, \quad \forall q \in \mathcal{P},$$

and by using this expression with $q = p(t)$ into (3.13) :

$$\int_{\Omega} \rho \ddot{\varphi}(t) \cdot \dot{\varphi}(t) + \int_{\Omega} \frac{\partial \hat{\mathcal{W}}}{\partial F}(\nabla \varphi(t)) : \nabla \dot{\varphi}(t) + \epsilon \int_{\Omega} \dot{p}(t) p(t) = \int_{\Omega} f(t) \cdot \dot{\varphi}(t).$$

which formally entails that :

$$\frac{d}{dt} \left(\frac{1}{2} \int_{\Omega} \rho \dot{\varphi}(t)^2 + \int_{\Omega} \hat{\mathcal{W}}(\nabla \varphi(t)) + \frac{\epsilon}{2} \int_{\Omega} p(t)^2 \right) = \int_{\Omega} f(t) \cdot \dot{\varphi}(t).$$

The announced formal energy conservation comes from an integration over $[0, t]$.

Concerning angular momentum conservation, for any $a \in \mathbb{R}^3$ we introduce the skew-symmetric matrix \mathbb{J}_a defined by :

$$\mathbb{J}_a \cdot w = a \times w, \quad \forall w \in \mathbb{R}^3.$$

By using the factorization $\Pi = F \cdot \Sigma$ of the first Piola-Kirchoff stress tensor, the variational formulation of the problem at time $t \in [0, T]$ entails for $v = a \times \varphi(t) = \mathbb{J}_a \cdot \varphi(t)$ that :

$$a \cdot \int_{\Omega} \rho \varphi(t) \times \ddot{\varphi}(t) + \int_{\Omega} (F(t) \cdot \Sigma(t)) : (\mathbb{J}_a \cdot \nabla \varphi(t)) = a \cdot \int_{\Omega} \varphi(t) \times f(t), \quad (3.14)$$

¹in the sense that these properties can only be derived from (3.5) if higher regularity than expected in (3.4) is assumed.

that is :

$$a \cdot \int_{\Omega} \rho \varphi(t) \times \ddot{\varphi}(t) + \int_{\Omega} (F(t) \cdot \Sigma(t) \cdot F^t(t)) : \mathbb{J}_a = a \cdot \int_{\Omega} \varphi(t) \times f(t),$$

and because $F(t) \cdot \Sigma(t) \cdot F^t(t)$ is a symmetric tensor because the second Piola-Kirchhoff stress tensor Σ is symmetric, and \mathbb{J}_a is skew-symmetric, one gets for all $a \in \mathbb{R}^3$:

$$a \cdot \int_{\Omega} \rho \varphi(t) \times \ddot{\varphi}(t) = a \cdot \int_{\Omega} \varphi(t) \times f(t),$$

and therefore :

$$\int_{\Omega} \rho \varphi(t) \times \ddot{\varphi}(t) = \int_{\Omega} \varphi(t) \times f(t).$$

This last expression can be written as :

$$\frac{d}{dt} \int_{\Omega} \rho \varphi(t) \times \dot{\varphi}(t) = \int_{\Omega} \varphi(t) \times f(t),$$

resulting in the announced formal angular momentum conservation by integration over $[0, t]$.

Concerning linear momentum conservation, the variational formulation of the problem at time $t \in [0, T]$ entails for any $v \in \mathbb{R}^3$ that :

$$v \cdot \int_{\Omega} \rho \ddot{\varphi}(t) = v \cdot \int_{\Omega} f(t),$$

and then :

$$\frac{d}{dt} \int_{\Omega} \rho \dot{\varphi}(t) = \int_{\Omega} f(t),$$

resulting in the announced formal linear momentum conservation by integration over $[0, t]$.

□

In coming sections, we are interested in the transposition of such expected properties for the continuous solution to the time discrete framework, that is when considering time integration schemes.

3.3 Efficiency and semi-explicit strategies

When regarding industrial computations, the necessity of obtaining low cost methods for time integration is obvious. The disadvantage of implicit methods is the introduction of a nonlinear problem at each time step, whose resolution has an expensive computational cost.

At the opposite, each time iteration of an explicit scheme would be economic to compute, but for stability reasons, the time step has to satisfy a Courant-Friedrichs-Lax (CFL)

condition, particularly restrictive for quasi-incompressible problems. Indeed, in a linearized framework, we show in section 3.3.1 that the time step must decrease as $\sqrt{\epsilon}$. In section 3.3.2, we propose a compromise between explicit and implicit strategies which consists in impliciting the compression term in the centered explicit scheme. Then, the CFL condition to satisfy for the time step in the linearized framework is proved to be far less restrictive : it must only ensure the stability of the explicit compressible scheme. Nevertheless, when extended to the nonlinear framework, this latter scheme proves to be more complex to handle than expected, which is developed in section 3.3.3 : it has the same computational complexity of a totally implicit strategy, and cannot be lightened.

3.3.1 A centered explicit scheme

In the case where quasi-incompressibility is ensured with $\epsilon > 0$, let us consider the centered explicit scheme using obvious notation :

$$\begin{cases} \int_{\Omega} \rho \ddot{\varphi}_n \cdot v + \int_{\Omega} \frac{\partial \hat{\mathcal{W}}}{\partial F}(\nabla \varphi_n) : \nabla v - \int_{\Omega} p_n \operatorname{cof} F_n : \nabla v = \int_{\Omega} f_n \cdot v, \\ \int_{\Omega} q (\det \nabla \varphi_{n+1} - 1 + \epsilon p_{n+1}) = 0, \end{cases} \quad (3.15)$$

for all $v \in \mathcal{U}_0$, $q \in \mathcal{P}$ and the centered discrete acceleration (see e.g. [Bat82]) :

$$\ddot{\varphi}_n = \frac{\varphi_{n+1} - 2\varphi_n + \varphi_{n-1}}{\Delta t_n^2}.$$

The n suffix denotes an approximate value at discrete time t_n and $\Delta t_n = t_{n+1} - t_n > 0$.

Linear stability

First, let us analyze the corresponding scheme for the time integration of incompressible linearized elastodynamics equations describing the evolution of the displacement u and the hydrostatic pressure p , namely :

$$\begin{cases} \int_{\Omega} \rho \ddot{u}_n \cdot v + \int_{\Omega} (\mathbf{E} : \varepsilon(u_n)) : \nabla v - \int_{\Omega} p_n \operatorname{div} v = \int_{\Omega} f_n \cdot v, \\ \int_{\Omega} q (\operatorname{div} u_{n+1} + \epsilon p_{n+1}) = 0, \end{cases} \quad (3.16)$$

for all $v \in \mathcal{U}_0$, $q \in \mathcal{P}$ and the centered discrete acceleration :

$$\ddot{u}_n = \frac{u_{n+1} - 2u_n + u_{n-1}}{\Delta t_n^2}.$$

Moreover, the elasticity tensor \mathbf{E} is given by :

$$\mathbf{E} = \frac{\partial^2 \mathcal{W}}{\partial C^2}(I_2),$$

where \mathcal{W} is the stored energy in terms of the Cauchy-Green strain tensor C , and I_2 the unit matrix in $\mathbb{R}^{3 \times 3}$. Assuming that the spaces \mathcal{U}_0 of displacements and \mathcal{P} of pressures have a finite dimension, the scheme (3.16) can be written as follows under obvious matricial notation :

$$\begin{cases} \frac{1}{\Delta t_n^2} M(U_{n+1} - 2U_n + U_{n-1}) + KU_n + B^t P_n = F_n \\ BU_{n+1} = \epsilon C P_{n+1}. \end{cases}$$

We deduce that :

$$\begin{aligned} U_{n+1} &= \Delta t_n^2 M^{-1} F_n + 2U_n - \Delta t_n^2 M^{-1} K U_n - \Delta t_n^2 M^{-1} B^t P_n - U_{n-1} \\ &= \Delta t_n^2 M^{-1} F_n + \left(2I_2 - \Delta t_n^2 M^{-1} K - \frac{1}{\epsilon} \Delta t_n^2 M^{-1} B^t C^{-1} B \right) U_n - U_{n-1}, \end{aligned}$$

resulting in the following matricial form of the integration scheme :

$$\begin{pmatrix} U_{n+1} \\ U_n \end{pmatrix} = \underbrace{\begin{pmatrix} A & -I_2 \\ I_2 & 0 \end{pmatrix}}_{\mathcal{H}} \begin{pmatrix} U_n \\ U_{n-1} \end{pmatrix} + \begin{pmatrix} \Delta t_n^2 M^{-1} F_n \\ 0 \end{pmatrix}, \quad (3.17)$$

with :

$$A = 2I_2 - \Delta t_n^2 M^{-1} K - \frac{1}{\epsilon} \Delta t_n^2 M^{-1} B^t C^{-1} B.$$

To obtain the convergence of the approximation toward the exact solution of the elastodynamics problem, it is standard (see [Bat82, RT98] for example) that a classical sufficient condition is that the spectral radius of the matrix \mathcal{H} be less than one. More precisely, let $X = (U, V)^t$ be an eigenvector of \mathcal{H} associated to the eigenvalue $\lambda \neq 0$. Then :

$$AU - \frac{1}{\lambda} U = \lambda U,$$

which is exactly by definition of A and from a left multiplication by $\frac{1}{\Delta t_n^2} M$:

$$\left(K + \frac{1}{\epsilon} B^t C^{-1} B \right) U = \left(2 - \frac{1}{\lambda} - \lambda \right) \frac{1}{\Delta t_n^2} M U.$$

As a consequence, there exists an eigenvalue ω_ϵ^2 of $K + \frac{1}{\epsilon} B^t C^{-1} B$ with respect to the mass matrix M such that :

$$\omega_\epsilon^2 \Delta t_n^2 - 2 = -\frac{1}{\lambda} - \lambda = -\frac{\lambda^2 + 1}{\lambda}.$$

Moreover, a direct calculus shows that the solutions λ of :

$$\frac{\lambda^2 + 1}{\lambda} = \alpha$$

satisfy $|\lambda| \leq 1$ iff $|\alpha| \leq 2$. Therefore, the spectral radius of the matrix \mathcal{H} is less than one iff for the highest eigenvalue $(\omega_\epsilon^{\max})^2$ of $K + \frac{1}{\epsilon}B^t C^{-1}B$ with respect to the mass matrix M , we have :

$$|(\omega_\epsilon^{\max})^2 \Delta t_n^2 - 2| \leq 2,$$

that is $\omega_\epsilon^{\max} \Delta t_n \leq 2$. Moreover :

$$\begin{aligned} (\omega_\epsilon^{\max})^2 &= \max_U \frac{\langle (K + \frac{1}{\epsilon}B^t C^{-1}B)U, U \rangle}{\langle MU, U \rangle} \\ &\geq (\omega_\infty^{\max})^2 + \frac{1}{\epsilon} \frac{\langle C^{-1}B\Phi, B\Phi \rangle}{\langle M\Phi, \Phi \rangle} = (\omega_\infty^{\max})^2 + \frac{c_0}{\epsilon}, \end{aligned} \quad (3.18)$$

where Φ is an eigenvector of the (compressible) stiffness matrix K with respect to the mass matrix M associated to the maximum eigenvalue $(\omega_\infty^{\max})^2$, that is :

$$K\Phi = (\omega_\infty^{\max})^2 M\Phi.$$

Then, for a time step Δt_n satisfying the stability condition $\omega_\epsilon^{\max} \Delta t_n \leq 2$, we get the following CFL condition :

$$\Delta t_n \leq \frac{2}{\omega_\epsilon^{\max}} \leq \frac{2}{\sqrt{(\omega_\infty^{\max})^2 + \frac{c_0}{\epsilon}}}.$$

Such a CFL condition becomes particularly restrictive for nearly incompressible models. Indeed, the right hand side goes to zero as $\sqrt{\epsilon}$.

Conservation analysis in the compressible framework

Even if in the quasi-incompressible framework this CFL condition makes the centered explicit scheme delicate to use, such a scheme can become interesting in the compressible framework, by using the following time iteration :

$$\int_{\Omega} \rho \ddot{\varphi}_n \cdot v + \int_{\Omega} \frac{\partial \hat{\mathcal{W}}}{\partial F}(\nabla \varphi_n) : \nabla v = \int_{\Omega} f_n \cdot v, \quad \forall v \in \mathcal{U}_0, \quad (3.19)$$

using the centered discrete acceleration :

$$\ddot{\varphi}_n = \frac{\varphi_{n+1} - 2\varphi_n + \varphi_{n-1}}{\Delta t_n^2}.$$

In the nonlinear framework, we prove for the centered explicit scheme :

Proposition 3.2. *In the discrete dynamics given by the explicit centered integration scheme (3.19), the following properties of discrete evolution hold :*

1. Discrete energy.

$$\mathcal{E}_{n+1} - \mathcal{E}_n = \mathfrak{P}_n + c_n \Delta t_n^2, \quad (3.20)$$

where the discrete energy is defined by :

$$\mathcal{E}_n = \frac{1}{2} \int_{\Omega} \rho \left(\frac{\varphi_n - \varphi_{n-1}}{\Delta t_n} \right)^2 + \int_{\Omega} \hat{\mathcal{W}}(F_n),$$

the discrete work of body forces by :

$$\mathfrak{P}_n = \int_{\Omega} f_n \cdot \left(\frac{\varphi_{n+1} - \varphi_{n-1}}{2\Delta t_n} \right),$$

and c_n depends on the discrete displacements, velocities but also of the acceleration $\ddot{\varphi}_n$.

2. Discrete angular momentum. If $\Gamma_D = \emptyset$, we have :

$$\mathcal{J}_{n+1} - \mathcal{J}_n = \mathfrak{M}_n + c_n \Delta t_n^3, \quad (3.21)$$

where the discrete angular momentum is defined by :

$$\mathcal{J}_n = \int_{\Omega} \rho \left(\frac{\varphi_{n-1} + \varphi_n}{2} \right) \times \left(\frac{\varphi_n - \varphi_{n-1}}{\Delta t_n} \right),$$

the discrete resultant moment is given by :

$$\mathfrak{M}_n = \int_{\Omega} \frac{\varphi_{n-1} + \varphi_{n+1}}{2} \times f_n.$$

and c_n only depends on the displacement φ_n and the acceleration $\ddot{\varphi}_n$.

3. Discrete linear momentum. If $\Gamma_D = \emptyset$, we have :

$$\mathcal{I}_{n+1} - \mathcal{I}_n = \mathfrak{F}_n, \quad (3.22)$$

where the discrete linear momentum is defined by :

$$\mathcal{I}_n = \int_{\Omega} \rho \left(\frac{\varphi_n - \varphi_{n-1}}{\Delta t_n} \right),$$

and the discrete resultant force by :

$$\mathfrak{F}_n = \int_{\Omega} f_n.$$

Proof :

- 1. Discrete energy evolution.** The proposed result can be easily obtained by using as a test function v in (3.19), the second order accurate velocity :

$$v = \frac{1}{2\Delta t_n}(\varphi_{n+1} - \varphi_{n-1}).$$

Then, the inertial term becomes :

$$\ddot{\varphi}_n \cdot v = \frac{1}{2\Delta t_n} \left(\frac{\varphi_{n+1} - \varphi_n}{\Delta t_n} \right)^2 - \frac{1}{2\Delta t_n} \left(\frac{\varphi_n - \varphi_{n-1}}{\Delta t_n} \right)^2.$$

Concerning the elastic contribution, we mainly use lemma 3.3 (page 67) and elementary Taylor's expansions to get :

$$\begin{aligned} & \frac{1}{2\Delta t_n} \frac{\partial \hat{\mathcal{W}}}{\partial F}(F_n) : (F_{n+1} - F_{n-1}) \\ &= \frac{1}{2\Delta t_n} \frac{\partial \hat{\mathcal{W}}}{\partial F} \left(\frac{F_{n+1} + F_{n-1}}{2} \right) : (F_{n+1} - F_{n-1}) \\ & \quad + \frac{1}{2\Delta t_n} \left(\frac{\partial \hat{\mathcal{W}}}{\partial F}(F_n) - \frac{\partial \hat{\mathcal{W}}}{\partial F} \left(\frac{F_{n+1} + F_{n-1}}{2} \right) \right) : (F_{n+1} - F_{n-1}), \\ &= \frac{\hat{\mathcal{W}}(F_{n+1}) - \hat{\mathcal{W}}(F_{n-1})}{2\Delta t_n} + c_n \Delta t_n^2 \frac{\partial^3 \hat{\mathcal{W}}}{\partial F^3}(F_*) \cdot (\nabla \dot{\varphi}_n)^3 \\ & \quad - \Delta t_n^2 \left(\frac{\partial^2 \hat{\mathcal{W}}}{\partial F^2}(F_*) : \nabla \dot{\varphi}_n \right) : \nabla \dot{\varphi}_n, \\ &= \frac{\hat{\mathcal{W}}(F_{n+1}) - \hat{\mathcal{W}}(F_n)}{\Delta t_n} + \frac{\hat{\mathcal{W}}(F_n) - \hat{\mathcal{W}}(F_{n+1})}{2\Delta t_n} + \frac{\hat{\mathcal{W}}(F_n) - \hat{\mathcal{W}}(F_{n-1})}{2\Delta t_n} \\ & \quad + \Delta t_n^2 \left(c_n \frac{\partial^3 \hat{\mathcal{W}}}{\partial F^3}(F_*) \cdot (\nabla \dot{\varphi}_n)^3 - \left(\frac{\partial^2 \hat{\mathcal{W}}}{\partial F^2}(F_*) : \nabla \ddot{\varphi}_n \right) : \nabla \dot{\varphi}_n \right), \end{aligned}$$

where F_* stands for various gradient tensors, and we have denoted by $\dot{\varphi}_n = (\varphi_{n+1} - \varphi_{n-1})/2\Delta t_n$ the second order accurate velocity at time t_n . Moreover, let us detail the two first terms of the energy error :

$$\begin{aligned} & \frac{\hat{\mathcal{W}}(F_n) - \hat{\mathcal{W}}(F_{n+1})}{2\Delta t_n} + \frac{\hat{\mathcal{W}}(F_n) - \hat{\mathcal{W}}(F_{n-1})}{2\Delta t_n} \\ &= \frac{1}{2} \frac{\partial \hat{\mathcal{W}}}{\partial F}(F_{n+1/2}^*) : \left(\frac{F_n - F_{n+1}}{\Delta t_n} \right) + \frac{1}{2} \frac{\partial \hat{\mathcal{W}}}{\partial F}(F_{n-1/2}^*) : \left(\frac{F_n - F_{n-1}}{\Delta t_n} \right) \\ &= -\frac{1}{2} \Delta t_n \frac{\partial \hat{\mathcal{W}}}{\partial F}(F_n) : \nabla \ddot{\varphi}_n \\ & \quad - \frac{1}{2} \Delta t_n \frac{\partial^2 \hat{\mathcal{W}}}{\partial F^2}(F_{n+1/4}^*) : \left(\frac{F_{n+1} - F_n}{\Delta t_n} \right) : \left(\frac{F_{n+1/2}^* - F_n}{\Delta t_n} \right) \\ & \quad - \frac{1}{2} \Delta t_n \frac{\partial^2 \hat{\mathcal{W}}}{\partial F^2}(F_{n-1/4}^*) : \left(\frac{F_n - F_{n-1}}{\Delta t_n} \right) : \left(\frac{F_n - F_{n-1/2}^*}{\Delta t_n} \right). \end{aligned}$$

Hence the energy conservation up to a Δt_n^2 term.

- 2. Discrete angular momentum evolution.** If $\Gamma_D = \emptyset$, by using the test function $v = a \times \frac{\varphi_n + \varphi_{n+1}}{2} = \mathbb{J}_a \cdot \frac{\varphi_n + \varphi_{n+1}}{2}$ in (3.19), the elastic term becomes :

$$\begin{aligned} & F_n \cdot \frac{\partial \mathcal{W}}{\partial C}(C_n) \cdot (F_n + F_{n+1})^t : \mathbb{J}_a \\ &= \frac{1}{2}(F_{n-1} + F_{n+1}) \cdot \frac{\partial \mathcal{W}}{\partial C}(C_n) \cdot (F_n + F_{n+1})^t : \mathbb{J}_a \\ &\quad - \frac{1}{2}(F_{n+1} - 2F_n + F_{n-1}) \cdot \frac{\partial \mathcal{W}}{\partial C}(C_n) \cdot (F_n + F_{n+1})^t : \mathbb{J}_a, \\ &= -\frac{\Delta t_n^2}{2} \nabla \ddot{\varphi}_n \cdot \frac{\partial \mathcal{W}}{\partial C}(C_n) \cdot (F_n + F_{n+1})^t : \mathbb{J}_a. \end{aligned}$$

Concerning the inertial terms, we get :

$$\begin{aligned} & \ddot{\varphi}_n \cdot v \\ &= \frac{1}{2\Delta t_n^2} a \cdot ((\varphi_{n-1} + \varphi_{n+1}) \times (\varphi_{n+1} - 2\varphi_n + \varphi_{n-1})), \\ &= \frac{1}{\Delta t_n^2} a \cdot (\varphi_n \times (\varphi_{n+1} + \varphi_{n-1})), \\ &= \frac{1}{\Delta t_n^2} a \cdot (\varphi_n \times (\varphi_{n+1} - \varphi_n) - \varphi_n \times (\varphi_n - \varphi_{n-1})), \\ &= \frac{1}{\Delta t_n} a \cdot \left(\left(\frac{\varphi_n + \varphi_{n+1}}{2} \right) \times \left(\frac{\varphi_{n+1} - \varphi_n}{\Delta t_n} \right) - \left(\frac{\varphi_{n-1} + \varphi_n}{2} \right) \times \left(\frac{\varphi_n - \varphi_{n-1}}{\Delta t_n} \right) \right). \end{aligned}$$

The sollicitation term exactly gives the contribution $a \cdot \mathfrak{M}_n$, and then we get :

$$\mathcal{J}_{n+1} - \mathcal{J}_n = \mathfrak{M}_n + c_n \Delta t_n^3.$$

- 3. Discrete linear momentum conservation.** It is straightforward by using constant test functions v in (3.19).

□

Remark 3.2. Not only energy conservation is satisfied up to a $O(\Delta t_n^2)$ additional term instead of $O(\Delta t_n^3)$ for midpoint based schemes presented in section 3.4.2, but the constant c_n depends on the acceleration of the system, whereas it only depends on the velocities in the case of the implicit trapezoidal scheme for example (as we will see in section 3.4.3). From the nonlinear point of view, it explains the extreme sensitivity of the present scheme with respect to the time step translated by the CFL condition in the linear framework.

Remark 3.3. Whereas the natural centered second order accurate expression of the velocity at time n is :

$$\dot{\varphi}_n = \frac{\varphi_{n+1} - \varphi_n}{2\Delta t_n},$$

the velocity appears under a upwind and first order accurate form in the expressions of the energy \mathcal{E}_n , the angular momentum \mathcal{J}_n and the linear momentum \mathcal{I}_n , that is :

$$\dot{\varphi}_n^{up} = \frac{\varphi_n - \varphi_{n-1}}{\Delta t_n}.$$

3.3.2 A semi-implicit scheme

To overcome the dependence of the previous integration scheme stability in the penalization coefficient ϵ , we propose the following semi-implicit scheme :

$$\begin{cases} \int_{\Omega} \rho \ddot{\varphi}_n \cdot v + \int_{\Omega} \frac{\partial \hat{\mathcal{W}}}{\partial F}(\nabla \varphi_n) : \nabla v - \frac{1}{2} \int_{\Omega} p_{n-1} \operatorname{cof} F_{n-1} : \nabla v \\ -\frac{1}{2} \int_{\Omega} p_{n+1} \operatorname{cof} F_{n+1} : \nabla v = \int_{\Omega} f_n \cdot v, \quad \forall v \in \mathcal{U}_0, \\ \int_{\Omega} q (\det \nabla \varphi_{n+1} - 1 + \epsilon p_{n+1}) = 0, \quad \forall q \in \mathcal{P}, \end{cases} \quad (3.23)$$

with the centered discrete acceleration :

$$\ddot{\varphi}_n = \frac{\varphi_{n+1} - 2\varphi_n + \varphi_{n-1}}{\Delta t_n^2}.$$

Linear stability

Let us analyze the corresponding scheme for the time integration of incompressible linearized elastodynamics equations describing the evolution of the displacement u and the hydrostatic pressure p , namely :

$$\begin{cases} \int_{\Omega} \rho \ddot{u}_n \cdot v + \int_{\Omega} \mathbf{E} : \varepsilon(u_n) : \nabla v - \frac{1}{2} \int_{\Omega} p_{n-1} \operatorname{div} v - \frac{1}{2} \int_{\Omega} p_{n+1} \operatorname{div} v = \int_{\Omega} f_n \cdot v, \\ \int_{\Omega} q (\operatorname{div} u_{n+1} + \epsilon p_{n+1}) = 0, \end{cases} \quad (3.24)$$

for all $v \in \mathcal{U}_0$, $q \in \mathcal{P}$. With the notation introduced in the previous subsection, the scheme (3.24) can be written as follows under obvious matricial notation :

$$\begin{cases} \frac{1}{\Delta t_n^2} M(U_{n+1} - 2U_n + U_{n-1}) + KU_n + \frac{1}{2} B^t (P_{n-1} + P_{n+1}) = F_n \\ BU_{n+1} = \epsilon CP_{n+1}. \end{cases}$$

As a consequence, we deduce that :

$$JU_{n+1} = F_n - JU_{n-1} + \left(\frac{2}{\Delta t_n^2} M - K \right) U_n,$$

with :

$$J = \frac{1}{\Delta t_n^2} M + \frac{1}{2\epsilon} B^t C^{-1} B,$$

and the semi-implicit scheme can be written as :

$$\begin{pmatrix} U_{n+1} \\ U_n \end{pmatrix} = \underbrace{\begin{pmatrix} J^{-1} \left(\frac{2}{\Delta t_n^2} M - K \right) & -I_2 \\ I_2 & 0 \end{pmatrix}}_{\mathcal{H}} \begin{pmatrix} U_n \\ U_{n-1} \end{pmatrix} + \begin{pmatrix} J^{-1} F_n \\ 0 \end{pmatrix}. \quad (3.25)$$

To obtain the convergence of the approximation toward the exact solution of the elastodynamics problem, it is standard (see [Bat82, RT98] for example) that a classical sufficient condition is that the spectral radius of the matrix \mathcal{H} be less than one. More precisely, let $X = (U, V)^t$ be an eigenvector of \mathcal{H} associated to the eigenvalue $\lambda \neq 0$. Then :

$$\left(\frac{2}{\Delta t_n^2} M - K \right) U = \left(\lambda + \frac{1}{\lambda} \right) JU, \quad (3.26)$$

and the present purpose is to determine a condition over Δt_n such that $|\lambda| \leq 1$. From (3.26), we get that :

$$\min_W \frac{W^t \left(\frac{2}{\Delta t_n^2} M - K \right) W}{W^t JW} \leq \left(\lambda + \frac{1}{\lambda} \right) \leq \max_W \frac{W^t \left(\frac{2}{\Delta t_n^2} M - K \right) W}{W^t JW}, \quad \forall W, \quad (3.27)$$

and from the previous subsection, a sufficient condition to get $|\lambda| \leq 1$ is that :

$$-2 \leq \frac{W^t \left(\frac{2}{\Delta t_n^2} M - K \right) W}{W^t JW} \leq 2, \quad \forall W. \quad (3.28)$$

Let Φ the matrix of the eigenvectors of the stiffness matrix K with respect to the mass matrix M , namely :

$$K\Phi = M\Phi D^2,$$

where D^2 is a diagonal matrix whose coefficients are the eigenvalues $(\omega_i^2)_{i \geq 1}$. Moreover, the orthonormality of the eigenvectors with respect to the mass matrix M is expressed as :

$$\Phi^t M \Phi = I_2.$$

Because the eigenvectors of the stiffness matrix K with respect to the mass matrix M spans the space of displacements, we can replace W by $W = \Phi X$ for all X in (3.28), leading to :

$$-2X^t \Phi^t J \Phi X \leq X^t \left(\frac{2}{\Delta t_n^2} I_2 - D^2 \right) X \leq 2X^t \Phi^t J \Phi X. \quad (3.29)$$

By definition of J and Φ , the right inequality in (3.29) means that :

$$-X^t D^2 X \leq \frac{1}{\epsilon} X^t \Phi^t B^t C^{-1} B \Phi X,$$

which is always true because the left hand side quantity is always negative, and the right hand side one is positive as the compression energy. The left inequality in (3.29) means that :

$$-\frac{1}{\epsilon} X^t \Phi^t B^t C^{-1} B \Phi X \leq \frac{4}{\Delta t_n^2} X^t X - X^t D^2 X,$$

and because the left hand side term is always negative, a sufficient stability condition is :

$$0 \leq \frac{4}{\Delta t_n^2} X^t X - X^t D^2 X,$$

that is in components :

$$0 \leq \sum_{i \geq 1} \left(\frac{4}{\Delta t_n^2} - \omega_i^2 \right) X_i^2.$$

We conclude denoting by $\omega^{max} = \max_{i \geq 1} \omega_i$, that a sufficient stability condition for the proposed semi-implicit scheme is :

$$\Delta t_n \leq \frac{2}{\omega^{max}}.$$

This last sufficient stability condition is independent of ϵ and then far less restrictive than the one of the totally explicit scheme. Moreover, this semi-implicit scheme can be used even for $\epsilon = 0$. This scheme consists in impliciting the compression term in the scheme, which is equivalent to project the centered explicit time iteration of the compressible problem on the manifold of incompressible displacements. Then, the CFL condition to satisfy for the time step in the linearized framework has been proved to be far less restrictive : it must only ensure the stability of the explicit compressible scheme.

3.3.3 Computational complexity of the semi-implicit scheme

We discuss now the implementation of the semi-implicit scheme (3.23) proposed in the nonlinear framework, and analyze its pertinence. Using a standard resolution by Newton method, the increments $\delta\varphi_{n+1}^{(k)}$ and $\delta p_{n+1}^{(k)}$ are solutions of tangent problems of the following type :

$$\begin{cases} \frac{1}{\Delta t_n^2} \int_{\Omega} \rho \delta\varphi_{n+1}^{(k)} \cdot v - \frac{1}{2} \int_{\Omega} p_{n+1} \left(\frac{\partial cof F_{n+1}^{(k)}}{\partial F_{n+1}^{(k)}} : \nabla \delta\varphi_{n+1}^{(k)} \right) : \nabla v \\ - \frac{1}{2} \int_{\Omega} \delta p_{n+1}^{(k)} cof F_{n+1}^{(k)} : \nabla v = \langle R_{n+1}^{(k)}, v \rangle, \quad \forall v \in \mathcal{U}_0, \\ \int_{\Omega} q \left(cof F_{n+1} : \nabla \delta\varphi_{n+1}^{(k)} + \epsilon \delta p_{n+1}^{(k)} \right) = - \langle S_{n+1}^{(k)}, v \rangle, \quad \forall q \in \mathcal{P}. \end{cases} \quad (3.30)$$

The only way to make it computable at low cost compared to an implicit scheme would be to invert only a pressure problem, which requires to adopt a lumped diagonal mass and to neglect the term in displacement :

$$\frac{1}{2} \int_{\Omega} p_{n+1} \left(\frac{\partial cof F_{n+1}^{(k)}}{\partial F_{n+1}^{(k)}} : \nabla v \right) : \nabla \delta\varphi_{n+1}^{(k)}. \quad (3.31)$$

This modification leads to a modified algorithm which we have observed not to converge in practice in nonlinear incompressible elasticity. Indeed, because the set of incompressible displacements is very nonlinear, the projection operator cannot be simplified. Thus, a displacement problem must be inverted and the associated cost is comparable to the cost of an implicit time step. Then, in our framework, totally implicit schemes seem to be the only way to explore.

3.4 Conservation analysis for some usual schemes

In nonlinear elastodynamics, discrete energy dissipation in the large sense (i.e. strict dissipation or conservation) is the natural criterion of stability for time integration schemes. Because in the linear framework, Newmark's trapezoidal scheme (see [Bat82]) is the typical example of schemes having a clear conservative behavior in terms of mechanical energy, it is rather natural to study its possible generalizations to the nonlinear framework. In particular, we provide a discrete conservation analysis for the midpoint and the trapezoidal schemes derived from Newmark's scheme in the nonlinear framework. The concepts underlined in these analysis lead to the design of energy conserving schemes, as proposed in [ST92, Gon00, LM01].

3.4.1 General concepts

We write (3.5) under a first order form, useful for time integration concepts :
For all $v \in \mathcal{U}_0$, $q \in \mathcal{P}$,

$$\begin{cases} \partial_t \int_{\Omega} \rho \dot{\varphi} \cdot v + \int_{\Omega} \Pi : \nabla v = \int_{\Omega} f \cdot v, & \text{in } \mathcal{D}'(0, T), \\ \partial_t \varphi(\cdot, x) = \dot{\varphi}(\cdot, x), & \text{in } \mathcal{D}'(0, T), \forall x \in \Omega, \\ \int_{\Omega} (\det \nabla \varphi(t) - 1 + \epsilon p(t)) q = 0, & \text{in } \mathcal{D}'(0, T). \end{cases} \quad (3.32)$$

The time interval $[0, T]$ is split into subintervals $[0, T] = \cup_{n=0}^N [t_n; t_{n+1}]$, with $\Delta t_n = t_{n+1} - t_n$. We will call numerical approximation of (3.32), any sequence $(\varphi_n, \dot{\varphi}_n, p_n)_{0 \leq n \leq N}$ of $(\mathcal{U}_0 \times \mathcal{V} \times \mathcal{P})^N$, given by an integration scheme of the type :

$$\begin{cases} \int_{\Omega} \rho \dot{\varphi}_{n+1} \cdot v = \int_{\Omega} \rho \dot{\varphi}_n \cdot v + \Delta t_n \left\langle P(\varphi_n, \varphi_{n+1}, \dot{\varphi}_n, \dot{\varphi}_{n+1}, p_n, p_{n+1}); v \right\rangle, & \forall v \in \mathcal{U}_0, \\ \varphi_{n+1} = \varphi_n + \Delta t_n Q(\varphi_n, \varphi_{n+1}, \dot{\varphi}_n, \dot{\varphi}_{n+1}), & \text{on } \Omega, \\ \Delta t_n \int_{\Omega} q G(\varphi_n, \varphi_{n+1}) = 0, & \forall q \in \mathcal{P}. \end{cases} \quad (3.33)$$

The concept of consistency is then defined by :

Definition 3.1. Let us assume that for all $x \in \Omega$, $f(\cdot, x) \in \mathcal{C}^\infty([0, T])$ and $\hat{\mathcal{W}}(x, \cdot) \in \mathcal{C}^\infty(\mathbb{R}^{3 \times 3})$. The scheme (3.33) is said to be consistent and accurate at order r with the problem (3.4) if for any solution (φ, p) of (3.4) satisfying $\varphi(\cdot, x) \in \mathcal{C}^\infty([0, T]; \mathbb{R}^3)$ and $p(\cdot, x) \in \mathcal{C}^\infty([0, T])$ for all $x \in \Omega$, we have :

$$\begin{cases} \int_{\Omega} \rho \dot{\varphi}(t_{n+1}) \cdot v = \int_{\Omega} \rho \dot{\varphi}(t_n) \cdot v \\ \quad + \Delta t_n \left\langle P(\varphi(t_n), \varphi(t_{n+1}), \dot{\varphi}(t_n), \dot{\varphi}(t_{n+1}), p(t_n), p(t_{n+1})) ; v \right\rangle + O(\Delta t_n^{r+1}), \\ \varphi(t_{n+1}) = \varphi(t_n) + \Delta t_n Q(\varphi(t_n), \varphi(t_{n+1}), \dot{\varphi}(t_n), \dot{\varphi}(t_{n+1})) + O(\Delta t_n^{r+1}), \quad \text{on } \Omega, \\ \int_{\Omega} q G(\varphi(t_n), \varphi(t_{n+1})) = O(\Delta t_n^r), \end{cases} \quad (3.34)$$

for all $v \in \mathcal{U}_0$ and $q \in \mathcal{P}$.

3.4.2 Midpoint based schemes

We analyze below some natural second order time integration schemes of the form :

$$\begin{cases} \int_{\Omega} \rho \dot{\varphi}_{n+1} \cdot v = \int_{\Omega} \rho \dot{\varphi}_n \cdot v - \Delta t_n \int_{\Omega} \Pi_{n+1/2} : \nabla v + \Delta t_n \int_{\Omega} \frac{f_n + f_{n+1}}{2} \cdot v, \\ \int_{\Omega} \varphi_{n+1} \cdot w = \int_{\Omega} \varphi_n \cdot w + \Delta t_n \int_{\Omega} \frac{\dot{\varphi}_n + \dot{\varphi}_{n+1}}{2} \cdot w, \\ \int_{\Omega} q \left(D_{n+1/2} - 1 + \epsilon \frac{p_n + p_{n+1}}{2} \right) = 0, \end{cases} \quad (3.35)$$

entirely determined by the expressions of $\Pi_{n+1/2}$ and $D_{n+1/2}$. We have the :

Lemma 3.1. The time integration scheme (3.35) is consistent and accurate at order $r \leq 2$ with the problem (3.4) if and only if by replacing the discrete approximations by the solution at discrete times $(t_n)_{n \geq 0}$, we get for all $n \geq 0$:

$$\begin{cases} \Delta t_n \int_{\Omega} \Pi_{n+1/2} : \nabla v = \int_{t_n}^{t_{n+1}} \int_{\Omega} \Pi : \nabla v + O(\Delta t_n^{r+1}), \quad \forall v \in \mathcal{U}_0, \\ \Delta t_n \int_{\Omega} q D_{n+1/2} = \int_{t_n}^{t_{n+1}} \int_{\Omega} q \det C^{1/2} + O(\Delta t_n^{r+1}), \quad \forall q \in \mathcal{P}. \end{cases} \quad (3.36)$$

Proof : Let (φ, p) a smooth solution in time of (3.4). We denote by $\varphi_n = \varphi(t_n)$, $\dot{\varphi}_n = \dot{\varphi}(t_n)$ and $p_n = p(t_n)$. The time integration scheme (3.35) is accurate at order r iff we have first

for all $v \in \mathcal{U}_0$:

$$\begin{aligned}
& \Delta t_n \int_{\Omega} \Pi_{n+1/2} : \nabla v \\
&= - \int_{\Omega} \rho \dot{\varphi}_{n+1} \cdot v + \int_{\Omega} \rho \dot{\varphi}_n \cdot v + \Delta t_n \int_{\Omega} \frac{f_n + f_{n+1}}{2} \cdot v + \Delta t_n \int_{\Gamma_N} \frac{g_n + g_{n+1}}{2} \cdot v + O(\Delta t_n^{r+1}), \\
&= - \int_{t_n}^{t_{n+1}} \int_{\Omega} \rho \ddot{\varphi} \cdot v + \int_{t_n}^{t_{n+1}} \int_{\Omega} f \cdot v + \int_{t_n}^{t_{n+1}} \int_{\Gamma_N} g \cdot v + O(\Delta t_n^{s+1}), \quad s = \min(r, 2), \\
&= \int_{t_n}^{t_{n+1}} \int_{\Omega} \Pi : \nabla v + O(\Delta t_n^{s+1}).
\end{aligned}$$

Secondly, the relation (3.34)-2 is straightforward because by Taylor's expansion, one gets on Ω that :

$$\varphi_{n+1} - \varphi_n = \int_{t_n}^{t_{n+1}} \dot{\varphi} = \frac{\Delta t_n}{2} (\dot{\varphi}_n + \dot{\varphi}_{n+1}) + O(\Delta t_n^3).$$

Thirdly, the relation (3.34)-3 means that for all $q \in \mathcal{P}$:

$$\begin{aligned}
\Delta t_n \int_{\Omega} q D_{n+1/2} &= \Delta t_n \int_{\Omega} q \left(1 - \epsilon \frac{p_n + p_{n+1}}{2} \right) + O(\Delta t_n^{r+1}) \\
&= \int_{t_n}^{t_{n+1}} \int_{\Omega} q (1 - \epsilon p) + O(\Delta t_n^{s+1}), \quad s = \min(r, 2), \\
&= \int_{t_n}^{t_{n+1}} \int_{\Omega} q \det C^{1/2} + O(\Delta t_n^{s+1}).
\end{aligned}$$

□

The choices analyzed in this paper corresponds to second order approximations.

3.4.3 Trapezoidal rule

When approximating the integrals in (3.36) by the trapezoidal rule, we get from lemma 3.1 that the corresponding time integration scheme is second order accurate. It corresponds to the choice :

$$\begin{cases} \Pi_{n+1/2} := \frac{1}{2} \left(\frac{\partial \hat{\mathcal{W}}}{\partial F}(F_n) + \frac{\partial \hat{\mathcal{W}}}{\partial F}(F_{n+1}) \right) - \frac{1}{2} (p_n \ cof F_n + p_{n+1} \ cof F_{n+1}), \\ D_{n+1/2} := \frac{1}{2} (\det F_n + \det F_{n+1}), \end{cases} \quad (3.37)$$

and in other words, we could say it is a stress averaging scheme. Concerning its discrete evolution properties, we prove the :

Proposition 3.3. *The trapezoidal rule achieves the following properties of discrete evolution :*

1. Discrete energy.

$$\mathcal{E}_{n+1} - \mathcal{E}_n = \mathfrak{P}_n + c_n \Delta t_n^3, \quad (3.38)$$

where the discrete work between times t_n and t_{n+1} is given by :

$$\mathfrak{P}_n = \int_{\Omega} \frac{f_n + f_{n+1}}{2} \cdot (\varphi_{n+1} - \varphi_n),$$

and the discrete energy at discrete time n by :

$$\mathcal{E}_n = \frac{1}{2} \int_{\Omega} \rho \dot{\varphi}_n^2 + \int_{\Omega} \hat{\mathcal{W}}(\nabla \varphi_n) + \frac{\epsilon}{2} \int_{\Omega} p_n^2.$$

The scalar c_n only depends on $\varphi_n, \dot{\varphi}_n, p_n, \varphi_{n+1}, \dot{\varphi}_{n+1}, p_{n+1}$, and on the approximate time derivative of the pressure $\frac{p_{n+1} - p_n}{\Delta t_n}$. We will say that c_n only depends on the approximate solution at times n and $n+1$.

2. Discrete angular momentum. If $\Gamma_D = \emptyset$,

$$\mathcal{J}_{n+1} - \mathcal{J}_n = \mathfrak{M}_n + c_n \Delta t_n^3, \quad (3.39)$$

where the resultant moment between times t_n and t_{n+1} is given by :

$$\mathfrak{M}_n = \Delta t_n \int_{\Omega} \frac{\varphi_n + \varphi_{n+1}}{2} \times \frac{f_n + f_{n+1}}{2},$$

and the angular momentum at discrete time n by :

$$\mathcal{J}_n = \int_{\Omega} \rho \varphi_n \times \dot{\varphi}_n.$$

The constant c_n only depends on the approximate solution at times n and $n+1$.

3. Discrete linear momentum. If $\Gamma_D = \emptyset$,

$$\mathcal{I}_{n+1} - \mathcal{I}_n = \mathfrak{F}_n, \quad (3.40)$$

where the resultant force between times t_n and t_{n+1} is given by :

$$\mathfrak{F}_n = \Delta t_n \int_{\Omega} \frac{f_n + f_{n+1}}{2},$$

and the discrete linear momentum at time n by :

$$\mathcal{I}_n = \int_{\Omega} \rho \dot{\varphi}_n.$$

Proof :

1. Energy evolution. We take $v = (\varphi_{n+1} - \varphi_n)/\Delta t$ in (3.35). The inertial term gives the discrete increase of kinetic energy :

$$\int_{\Omega} \rho (\dot{\varphi}_{n+1} - \dot{\varphi}_n) \cdot v = \frac{1}{2} \int_{\Omega} \rho \dot{\varphi}_{n+1}^2 - \frac{1}{2} \int_{\Omega} \rho \dot{\varphi}_n^2.$$

The work \mathfrak{P}_n is obtained as :

$$\Delta t_n \int_{\Omega} \frac{f_n + f_{n+1}}{2} \cdot v = \int_{\Omega} \frac{f_n + f_{n+1}}{2} \cdot (\varphi_{n+1} - \varphi_n).$$

The elastic term gives by a standard Taylor's expansion :

$$\begin{aligned} & \frac{1}{2} \left(\frac{\partial \hat{\mathcal{W}}}{\partial F}(F_n) + \frac{\partial \hat{\mathcal{W}}}{\partial F}(F_{n+1}) \right) : \nabla v \\ &= \frac{1}{2\Delta\tau_n} \left(\frac{\partial \hat{\mathcal{W}}}{\partial F}(F_n) + \frac{\partial \hat{\mathcal{W}}}{\partial F}(F_{n+1}) \right) : (F_{n+1} - F_n), \\ &= \frac{1}{\Delta\tau_n} \left(\hat{\mathcal{W}}_{n+1} - \hat{\mathcal{W}}_n \right) + \frac{c}{\Delta\tau_n} \frac{\partial^3 \mathcal{W}}{\partial F^3}(F_*) (F_{n+1} - F_n)^3, \\ &= \frac{1}{\Delta\tau_n} \left(\hat{\mathcal{W}}_{n+1} - \hat{\mathcal{W}}_n \right) + \frac{c}{8} \Delta t_n^2 \frac{\partial^3 \mathcal{W}}{\partial F^3}(F_*) (\nabla \dot{\varphi}_{n+1} + \nabla \dot{\varphi}_n)^3, \end{aligned}$$

for a given constant $0 < c < 1/8$ and an unknown matrix F_* .

Concerning the compression term :

$$\begin{aligned} & \frac{1}{2} (p_n \ cof F_n + p_{n+1} \ cof F_{n+1}) : \nabla v \\ &= \frac{1}{2\Delta t_n} (p_n \ cof F_n + p_{n+1} \ cof F_{n+1}) : (F_{n+1} - F_n), \\ &= \frac{1}{2\Delta t_n} \frac{p_n + p_{n+1}}{2} (cof F_n + cof F_{n+1}) : (F_{n+1} - F_n) \\ &\quad + \frac{1}{2\Delta t_n} \frac{p_{n+1} - p_n}{2} (cof F_{n+1} - cof F_n) : (F_{n+1} - F_n), \\ &= \frac{1}{\Delta t_n} \frac{p_n + p_{n+1}}{2} (\det F_{n+1} - \det F_n) \\ &\quad + c \frac{1}{\Delta t_n} \frac{p_n + p_{n+1}}{2} \frac{\partial^3 \det F}{\partial F^3}(F_{n+1} - F_n)^3 \\ &\quad + \frac{1}{2\Delta t_n} \frac{p_{n+1} - p_n}{2} (cof F_{n+1} - cof F_n) : (F_{n+1} - F_n), \end{aligned}$$

with $0 < c < 1/8$ from lemma 3.2 (page 63). Moreover, if the initial kinematic constraint holds :

$$\int_{\Omega} q (\det \nabla \varphi_0 - 1 + \epsilon p_0) = 0, \quad \forall q \in \mathcal{P},$$

then it holds at every discrete time. Then, using (3.35) :

$$\int_{\Omega} \frac{p_n + p_{n+1}}{2} (\det F_{n+1} - \det F_n) = \epsilon \int_{\Omega} \frac{p_n + p_{n+1}}{2} (p_{n+1} - p_n) = \frac{\epsilon}{2} \int_{\Omega} (p_{n+1}^2 - p_n^2).$$

Up to an integration over Ω , we have :

$$\begin{aligned} & \frac{1}{2} (p_n \ cof F_n + p_{n+1} \ cof F_{n+1}) : \nabla v \\ &= \epsilon \frac{p_{n+1}^2 - p_n^2}{2\Delta t_n} \\ &+ \frac{c}{8} \Delta t_n^2 \frac{p_n + p_{n+1}}{2} \frac{\partial^3 \det F}{\partial F^3} (\nabla \dot{\varphi}_n + \nabla \dot{\varphi}_{n+1})^3 \\ &+ \frac{\Delta t_n^2}{2} \frac{p_{n+1} - p_n}{2\Delta t_n} \frac{\partial^2 \det F}{\partial F^2} (F_*) (\nabla \dot{\varphi}_n + \nabla \dot{\varphi}_{n+1})^2, \end{aligned}$$

and the announced result holds :

$$\mathcal{E}_{n+1} - \mathcal{E}_n = \mathfrak{P}_n + c_n \Delta t_n^3,$$

with :

$$\begin{aligned} c_n &= \alpha \frac{\partial^3 \mathcal{W}}{\partial F^3} (F_*) (\nabla \dot{\varphi}_{n+1} + \nabla \dot{\varphi}_n)^3 + \beta \frac{p_n + p_{n+1}}{2} \frac{\partial^3 \det F}{\partial F^3} (\nabla \dot{\varphi}_n + \nabla \dot{\varphi}_{n+1})^3 \\ &- \frac{1}{4} \frac{p_{n+1} - p_n}{\Delta t_n} \frac{\partial^2 \det F}{\partial F^2} (F_*) (\nabla \dot{\varphi}_n + \nabla \dot{\varphi}_{n+1})^2. \end{aligned}$$

- 2. Angular momentum evolution.** If $\Gamma_D = \emptyset$, taking $v = a \times \frac{\varphi_n + \varphi_{n+1}}{2} = \mathbb{J}_a$. $\frac{\varphi_n + \varphi_{n+1}}{2}$ in (3.35), the elastic term becomes :

$$\begin{aligned} & \frac{1}{2} \left(\frac{\partial \hat{\mathcal{W}}}{\partial F}(F_n) + \frac{\partial \hat{\mathcal{W}}}{\partial F}(F_{n+1}) \right) \cdot (F_n + F_{n+1})^t : \mathbb{J}_a \\ &= \left(F_n \cdot \frac{\partial \mathcal{W}}{\partial C}(C_n) + F_{n+1} \cdot \frac{\partial \mathcal{W}}{\partial C}(C_{n+1}) \right) \cdot (F_n + F_{n+1})^t : \mathbb{J}_a, \\ &= \frac{1}{2} (F_n + F_{n+1}) \cdot \left(\frac{\partial \mathcal{W}}{\partial C}(C_n) + \frac{\partial \mathcal{W}}{\partial C}(C_{n+1}) \right) \cdot (F_n + F_{n+1})^t : \mathbb{J}_a \\ &+ \frac{1}{2} (F_{n+1} - F_n) \cdot \left(\frac{\partial \mathcal{W}}{\partial C}(C_{n+1}) - \frac{\partial \mathcal{W}}{\partial C}(C_n) \right) \cdot (F_n + F_{n+1})^t : \mathbb{J}_a. \end{aligned}$$

The first term vanishes because of the skew-symmetry of \mathbb{J}_a . Therefore, we get :

$$\begin{aligned} & \frac{1}{2} \left(\frac{\partial \hat{\mathcal{W}}}{\partial F}(F_n) + \frac{\partial \hat{\mathcal{W}}}{\partial F}(F_{n+1}) \right) \cdot (F_n + F_{n+1})^t : \mathbb{J}_a \\ &= \frac{1}{4} \Delta t_n (\nabla \dot{\varphi}_n + \nabla \dot{\varphi}_{n+1}) \cdot \left(\frac{\partial^2 \mathcal{W}}{\partial C^2}(C_*) : (C_{n+1} - C_n) \right) \cdot (F_n + F_{n+1})^t : \mathbb{J}_a, \\ &= \frac{1}{4} \Delta t_n (\nabla \dot{\varphi}_n + \nabla \dot{\varphi}_{n+1}) \cdot \left(\frac{\partial^2 \mathcal{W}}{\partial C^2}(C_*) : (\nabla \varphi_*^t \cdot (F_{n+1} - F_n)) \right) \cdot (F_n + F_{n+1})^t : \mathbb{J}_a, \\ &= \frac{1}{8} \Delta t_n^2 (\nabla \dot{\varphi}_n + \nabla \dot{\varphi}_{n+1}) \cdot \left(\frac{\partial^2 \mathcal{W}}{\partial C^2}(C_*) : (\nabla \varphi_*^t \cdot \nabla (\dot{\varphi}_n + \dot{\varphi}_{n+1})) \right) \cdot (F_n + F_{n+1})^t : \mathbb{J}_a. \end{aligned}$$

Concerning the momentum of compression terms, we have :

$$\begin{aligned} & \frac{1}{2} (p_n \operatorname{cof} F_n + p_{n+1} \operatorname{cof} F_{n+1}) \cdot (F_n + F_{n+1})^t : \mathbb{J}_a \\ &= \left(p_n F_n \cdot \frac{\partial \det C_n^{1/2}}{\partial C_n} + p_{n+1} F_{n+1} \cdot \frac{\partial \det C_{n+1}^{1/2}}{\partial C_{n+1}} \right) \cdot (F_n + F_{n+1})^t : \mathbb{J}_a, \\ &= \frac{1}{2} (F_n + F_{n+1}) \cdot \left(p_n \frac{\partial \det C_n^{1/2}}{\partial C_n} + p_{n+1} \frac{\partial \det C_{n+1}^{1/2}}{\partial C_{n+1}} \right) \cdot (F_n + F_{n+1})^t : \mathbb{J}_a \\ &\quad + \frac{1}{2} (F_{n+1} - F_n) \cdot \left(p_{n+1} \frac{\partial \det C_{n+1}^{1/2}}{\partial C_{n+1}} - p_n \frac{\partial \det C_n^{1/2}}{\partial C_n} \right) \cdot (F_n + F_{n+1})^t : \mathbb{J}_a, \end{aligned}$$

whose first term vanishes because of the skew-symmetry of \mathbb{J}_a . Therefore, we have simply :

$$\begin{aligned} & \frac{1}{2} (p_n \operatorname{cof} F_n + p_{n+1} \operatorname{cof} F_{n+1}) \cdot (F_n + F_{n+1})^t : \mathbb{J}_a \\ &= \frac{1}{4} \Delta t_n (\nabla \dot{\varphi}_n + \nabla \dot{\varphi}_{n+1}) \cdot \left(p_{n+1} \frac{\partial \det C_{n+1}^{1/2}}{\partial C_{n+1}} - p_n \frac{\partial \det C_n^{1/2}}{\partial C_n} \right) \cdot (F_n + F_{n+1})^t : \mathbb{J}_a. \end{aligned}$$

We detail the central factor :

$$\begin{aligned} & p_{n+1} \frac{\partial \det C_{n+1}^{1/2}}{\partial C_{n+1}} - p_n \frac{\partial \det C_n^{1/2}}{\partial C_n} \\ &= \frac{1}{2} (p_{n+1} - p_n) \left(\frac{\partial \det C_n^{1/2}}{\partial C_n} + \frac{\partial \det C_{n+1}^{1/2}}{\partial C_{n+1}} \right) \\ &\quad + \frac{1}{2} (p_n + p_{n+1}) \left(\frac{\partial \det C_{n+1}^{1/2}}{\partial C_{n+1}} - \frac{\partial \det C_n^{1/2}}{\partial C_n} \right), \\ &= \Delta t_n \frac{1}{2} \frac{p_{n+1} - p_n}{\Delta t_n} \left(\frac{\partial \det C_n^{1/2}}{\partial C_n} + \frac{\partial \det C_{n+1}^{1/2}}{\partial C_{n+1}} \right) \\ &\quad + \Delta t_n \frac{1}{4} (p_n + p_{n+1}) \left(\frac{\partial^2 \det C^{1/2}}{\partial C^2} (C_*) : (\nabla \varphi_*^t \cdot \nabla (\dot{\varphi}_n + \dot{\varphi}_{n+1})) \right) = A_n \Delta t_n, \end{aligned}$$

where A_n is a fourth order symmetric tensor depending on the approximate solution at times n and $n + 1$. Then, we have :

$$\begin{aligned} & \frac{1}{2} (p_n \operatorname{cof} F_n + p_{n+1} \operatorname{cof} F_{n+1}) \cdot (F_n + F_{n+1})^t : \mathbb{J}_a \\ &= \frac{1}{4} \Delta t_n^2 (\nabla \dot{\varphi}_n + \nabla \dot{\varphi}_{n+1}) \cdot A_n \cdot (F_n + F_{n+1})^t : \mathbb{J}_a. \end{aligned}$$

Let us introduce :

$$c_n^a := \Delta t_n^2 (\nabla \dot{\varphi}_n + \nabla \dot{\varphi}_{n+1}) \cdot$$

$$\left(A_n + \frac{1}{2} \frac{\partial^2 \mathcal{W}}{\partial C^2}(C_*) : (\nabla \varphi_*^t \cdot \nabla (\dot{\varphi}_n + \dot{\varphi}_{n+1})) \right) \cdot (F_n + F_{n+1})^t : \mathbb{J}_a,$$

the discrete momentum of the tensions in the material between times t_n and t_{n+1} along the $a \in \mathbb{R}^3$ direction. By linearity $c_n^a = c_n \cdot a$, for a $c_n \in \mathbb{R}^3$. Plugging this in (3.35), and from the identity $u \cdot (a \times w) = (w \times u) \cdot a$, we obtain that :

$$\begin{aligned} \int_{\Omega} \rho \frac{\varphi_n + \varphi_{n+1}}{2} \times \frac{\dot{\varphi}_{n+1} - \dot{\varphi}_n}{\Delta t_n} &= \int_{\Omega} \frac{\varphi_n + \varphi_{n+1}}{2} \times \frac{f_n + f_{n+1}}{2} \\ &+ \int_{\Gamma} \frac{\varphi_n + \varphi_{n+1}}{2} \times \frac{g_n + g_{n+1}}{2} - c_n. \end{aligned} \quad (3.41)$$

From (3.35)-2, we have :

$$\int_{\Omega} \rho \frac{\varphi_{n+1} - \varphi_n}{\Delta t_n} \times \frac{\dot{\varphi}_n + \dot{\varphi}_{n+1}}{2} = 0,$$

which from (3.41), implies :

$$\mathcal{J}_{n+1} - \mathcal{J}_n = \mathfrak{M}_n + c_n \Delta t_n^3.$$

3. Linear momentum conservation. If $\Gamma_D = \emptyset$, the result is straightforward by using any constant vector $v \in \mathbb{R}^3$ in (3.35). □

In the previous proof, we have used the simple lemma :

Lemma 3.2. *If $J \in \mathcal{C}^3(\mathbb{R}^{3 \times 3})$, then for all $F_n, F_{n+1} \in \mathbb{R}^{3 \times 3}$, there exists a constant $0 \leq c \leq 1/8$ and a matrix $F_* \in \mathbb{R}^{3 \times 3}$ such that :*

$$J(F_{n+1}) = J(F_n) + \frac{1}{2} \left(\frac{\partial J}{\partial F}(F_n) + \frac{\partial J}{\partial F}(F_{n+1}) \right) : (F_{n+1} - F_n) - c \frac{\partial^3 J}{\partial F^3}(F_*)(F_{n+1} - F_n)^3.$$

Proof : Let $f \in \mathcal{C}^3(\mathbb{R})$ and $a, b \in \mathbb{R}$. From successive integrations by parts, one gets that :

$$\begin{aligned} f(b) - f(a) &= \int_a^b f'(x) dx \\ &= \left[\left(x - \frac{a+b}{2} \right) f'(x) \right]_a^b - \int_a^b \left(x - \frac{a+b}{2} \right) f''(x) dx \\ &= (b-a) \frac{f'(a) + f'(b)}{2} + \int_a^b \left(\frac{x^2}{2} - \frac{a+b}{2}x + \frac{ab}{2} \right) f'''(x) dx, \end{aligned}$$

and from the mean value theorem, there exists $x_* \in]a, b[$ such that :

$$f(b) - f(a) = (b-a) \frac{f'(a) + f'(b)}{2} + (b-a) \underbrace{\left(\frac{x_*^2}{2} - \frac{a+b}{2}x_* + \frac{ab}{2} \right)}_{P(x_*)} f'''(x_*).$$

But the second order polynomial P admits a and b as roots and therefore $P(x_*) < 0$. Its minimum is reached for $x_* = \frac{a+b}{2}$ and $P(\frac{a+b}{2}) = -\frac{(b-a)^2}{8}$. Then, let us denote $P(x_*) = -c(x_*)(b-a)^2$ with $0 \leq c(x_*) \leq \frac{1}{8}$, resulting in :

$$f(b) - f(a) = \frac{f'(a) + f'(b)}{2}(b-a) - c(x_*)f'''(x_*)(b-a)^3.$$

The announced lemma is straightforward by applying this expansion to the function :

$$\begin{aligned} f : [0, 1] &\rightarrow \mathbb{R} \\ x &\mapsto J((1-x)F_n + xF_{n+1}), \end{aligned}$$

with $a = 0$ and $b = 1$. □

Remark 3.4. *Some key-ideas about the trapezoidal scheme :*

- In the compressible case, exact energy conservation is only achieved if $\hat{\mathcal{W}}$ is a quadratic elastic potential as a function of F . It is easy to check that angular momentum is then also conserved. Nevertheless, this assumption is not realistic because incompatible with :

$$\lim_{\det F \rightarrow 0} \hat{\mathcal{W}}(F) \rightarrow +\infty,$$

as shown in [Cia88].

- A crucial argument in the proof of energy evolution is that if the initial kinematic constraint holds :

$$\int_{\Omega} q (\det \nabla \varphi_0 - 1 + \epsilon p_0) = 0, \quad \forall q \in \mathcal{P},$$

then it holds at every discrete time.

- Energy and angular momentum conservations are achieved with an error term $c_n \Delta t^3$, and the dependance of c_n with respect to the approximate solution is quite regular. Nevertheless, an accretive behavior (local increase of energy or/and momentum) cannot be excluded for nonlinear problems with large time steps. It can entail numerical instability and a poor behavior with respect to the group of rotations. In fact, one can wonder if a control of the time step is possible in order to control the behavior of energy for example. Nevertheless, we observe numerically that when the time grows, the time step should become smaller and smaller to prevent energy from exploding, and far more the time step converges to zero.
- The perfect behavior of the scheme with respect to the group of translations is ensured by the exact conservation of linear momentum.

3.4.4 Midpoint scheme

When approximating the integrals in (3.36) by the midpoint rule, we get from lemma 3.1 that the corresponding time integration scheme is second order accurate. It corresponds

to the choice :

$$\begin{cases} \Pi_{n+1/2} = \frac{\partial \hat{\mathcal{W}}}{\partial F} \left(\frac{F_n + F_{n+1}}{2} \right) - \frac{p_n + p_{n+1}}{2} \text{cof} \left(\frac{F_n + F_{n+1}}{2} \right), \\ D_{n+1/2} = \det \left(\frac{F_n + F_{n+1}}{2} \right). \end{cases} \quad (3.42)$$

In other words, it results in a strain averaging scheme, and we show the following properties :

Proposition 3.4. *The midpoint scheme achieves the following discrete evolution properties :*

1. **Discrete energy evolution.** *For a constant time step Δt ,*

$$\mathcal{E}_{n+1} - \mathcal{E}_n = \mathfrak{P}_n + c_n \Delta t^3. \quad (3.43)$$

Here, c_n depends on the approximate solution at times n and $n+1$, but also of the discrete third order time derivative of acceleration : $\ddot{\varphi}_{n+1/2} = \frac{1}{2\Delta t^2}(\dot{\varphi}_{n+2} - \dot{\varphi}_{n+1} - \dot{\varphi}_n + \dot{\varphi}_{n+1})$.

2. **Discrete angular momentum conservation.** *If $\Gamma_D = \emptyset$,*

$$\mathcal{J}_{n+1} - \mathcal{J}_n = \mathfrak{M}_n. \quad (3.44)$$

3. **Discrete linear momentum conservation.** *If $\Gamma_D = \emptyset$,*

$$\mathcal{I}_{n+1} - \mathcal{I}_n = \mathfrak{F}_n. \quad (3.45)$$

Proof :

1. **Energy evolution.** We take $v = \frac{1}{2}(\dot{\varphi}_n + \dot{\varphi}_{n+1})$ in (3.35). The elastic and compression terms are the only one which differ from the trapezoidal case. For the elastic one, we have from lemma 3.3 with $0 \leq c \leq 1$:

$$\begin{aligned} & \frac{\partial \hat{\mathcal{W}}}{\partial F} \left(\frac{F_n + F_{n+1}}{2} \right) : \nabla v = \frac{1}{\Delta t_n} \frac{\partial \hat{\mathcal{W}}}{\partial F} \left(\frac{F_n + F_{n+1}}{2} \right) : (F_{n+1} - F_n), \\ &= \frac{\hat{\mathcal{W}}(F_{n+1}) - \hat{\mathcal{W}}(F_n)}{\Delta t_n} - \frac{c}{8} \Delta t_n^2 \frac{\partial^3 \hat{\mathcal{W}}}{\partial F^3} \left(\frac{F_n + F_{n+1}}{2} \right) \cdot (\nabla \dot{\varphi}_n + \nabla \dot{\varphi}_{n+1})^3. \end{aligned}$$

The main difficulty comes from the kinematic constraint. We denote $\square_{n+1/2} = \frac{1}{2}(\square_n + \square_{n+1})$ and $\frac{1}{2}(\dot{\square}_n + \dot{\square}_{n+1}) = \frac{1}{\Delta t_n}(\square_{n+1} - \square_n)$. We assume that the step time is a constant Δt , and introduce the interpolated displacement :

$$\bar{\varphi}_{n+1/2} = \frac{1}{2}(\varphi_{n+3/2} + \varphi_{n-1/2}) = \frac{1}{4}(\varphi_{n+2} + \varphi_{n+1} + \varphi_n + \varphi_{n-1}).$$

Then :

$$\begin{aligned}\bar{\varphi}_{n+1/2} - \varphi_{n+1/2} &= \frac{1}{4}(\varphi_{n+2} - \varphi_{n+1} - \varphi_n + \varphi_{n-1}) \\ &= \frac{\Delta t}{8}(\dot{\varphi}_{n+2} + \dot{\varphi}_{n+1} - \dot{\varphi}_n - \dot{\varphi}_{n-1}) \\ &= \frac{\Delta t^2}{4}(\ddot{\varphi}_{n+1} + \ddot{\varphi}_n),\end{aligned}$$

with $\ddot{\varphi}_n = \frac{\dot{\varphi}_{n+1} - \dot{\varphi}_{n-1}}{2\Delta t}$. The increase of displacement is defined by :

$$\begin{aligned}\delta &= \varphi_{n+3/2} - \varphi_{n-1/2} = \frac{1}{2}(\varphi_{n+2} + \varphi_{n+1} - \varphi_n - \varphi_{n-1}) \\ &= \frac{1}{2}(\dot{\varphi}_{n+3/2}\Delta t + \dot{\varphi}_{n-1/2}\Delta t + 2\varphi_{n+1} - 2\varphi_n) \\ &= 2\dot{\varphi}_{n+1/2}\Delta t + \frac{1}{2}\ddot{\varphi}_{n+1/2}\Delta t^3.\end{aligned}\tag{3.46}$$

From the kinematic constraint at half step time, we deduce :

$$\begin{aligned}\det F_{n+3/2} - \det F_{n-1/2} &= \left(\text{cof } \nabla \bar{\varphi}_{n+1/2} \right) : (\nabla \delta) + \frac{1}{24} \frac{\partial^2 \text{cof } F}{\partial F^2} (F_*) (\nabla \delta)^3 \\ &= -\epsilon (p_{n+3/2} - p_{n-1/2}).\end{aligned}\tag{3.47}$$

The work of pressure forces is therefore :

$$\begin{aligned}p_{n+1/2} \text{cof } F_{n+1/2} : \nabla \dot{\varphi}_{n+1/2} &= \\ p_{n+1/2} \left(\text{cof } \nabla \bar{\varphi}_{n+1/2} + \frac{\partial \text{cof } F}{\partial F} (F_{**}) : \left(F_{n+1/2} - \nabla \bar{\varphi}_{n+1/2} \right) \right) : \nabla \dot{\varphi}_{n+1/2} &= \\ p_{n+1/2} \left(\text{cof } \nabla \bar{\varphi}_{n+1/2} - \frac{\partial \text{cof } F}{\partial F} (F_{**}) : \left(\frac{1}{4}(\nabla \ddot{\varphi}_{n+1} + \nabla \ddot{\varphi}_n)\Delta t^2 \right) \right) : \nabla \dot{\varphi}_{n+1/2}.\end{aligned}$$

Since $\dot{\varphi}_{n+1/2} = \frac{\delta}{2\Delta t} - \frac{\Delta t^2}{4}\ddot{\varphi}_{n+1/2}$, we have :

$$\begin{aligned}p_{n+1/2} \text{cof } F_{n+1/2} : \nabla \dot{\varphi}_{n+1/2} &= \frac{1}{2\Delta t} p_{n+1/2} \left(\text{cof } \nabla \bar{\varphi}_{n+1/2} \right) : (\nabla \delta) \\ &\quad - \frac{\Delta t^2}{4} p_{n+1/2} \left(\text{cof } \nabla \bar{\varphi}_{n+1/2} \right) : \nabla \ddot{\varphi}_{n+1/2} \\ &\quad - \frac{\Delta t^2}{4} \frac{\partial \text{cof } F}{\partial F} (F_{**}) : (\nabla \ddot{\varphi}_{n+1} + \nabla \ddot{\varphi}_n) : \nabla \dot{\varphi}_{n+1/2}.\end{aligned}$$

The two last terms are of order 2 in Δt . To tackle the first one, we use (3.47) and up to a second order term in Δt , we get :

$$\begin{aligned}p_{n+1/2} \text{cof } F_{n+1/2} : \nabla \dot{\varphi}_{n+1/2} &= -\frac{\Delta t^2}{48} p_{n+1/2} \frac{\partial^2 \text{cof } F}{\partial F^2} (F_*) (\nabla \frac{\delta}{\Delta t})^3 \\ &\quad - \frac{\epsilon}{2\Delta t} p_{n+1/2} (p_{n+3/2} - p_{n-1/2}).\end{aligned}$$

By rewriting (3.46) for the quantity $p_{n+3/2} - p_{n-1/2}$, we have :

$$p_{n+1/2} \operatorname{cof} F_{n+1/2} : \nabla \dot{\varphi}_{n+1/2} = \frac{\epsilon}{2\Delta t} (p_{n+1}^2 - p_n^2),$$

up to a second order term in Δt .

- 2. Angular momentum conservation.** Assuming that $\Gamma_D = \emptyset$, we use $v = a \times \frac{\varphi_n + \varphi_{n+1}}{2} = \mathbb{J}_a \cdot \frac{\varphi_n + \varphi_{n+1}}{2}$ in (3.35). In the elastic part, we obtain the terms :

$$2 \left(\frac{F_n + F_{n+1}}{2} \right) \cdot \frac{\partial \mathcal{W}}{\partial C} (C_{n+1/2}^*) \cdot \left(\frac{F_n + F_{n+1}}{2} \right)^t : \mathbb{J}_a = 0,$$

and :

$$2 \left(\frac{p_n + p_{n+1}}{2} \right) \left(\frac{F_n + F_{n+1}}{2} \right) \cdot \frac{\partial \det C^{1/2}}{\partial C} (C_{n+1/2}^*) \cdot \left(\frac{F_n + F_{n+1}}{2} \right)^t : \mathbb{J}_a = 0,$$

that vanish because of the skew-symmetry of \mathbb{J}_a . The result proceeds then as in (3.41) but with $c_n = 0$.

- 3. Linear momentum conservation.** Direct derivation as in the trapezoidal case.

□

In the previous proof, we have used the simple lemma :

Lemma 3.3. *If $J \in \mathcal{C}^3(\mathbb{R}^{3 \times 3})$, then for all $F_n, F_{n+1} \in \mathbb{R}^{3 \times 3}$, there exists a constant $0 \leq c \leq 1$ and a matrix $F_* \in \mathbb{R}^{3 \times 3}$ such that :*

$$J(F_{n+1}) = J(F_n) + \frac{\partial J}{\partial E} \left(\frac{F_n + F_{n+1}}{2} \right) : (F_{n+1} - F_n) + c \frac{\partial^3 J}{\partial E^3} (F_*) (F_{n+1} - F_n)^3$$

Proof : Let $f \in \mathcal{C}^3(\mathbb{R})$ and $a, b \in \mathbb{R}$. From successive integrations by parts, one gets that :

$$\begin{aligned} & f(b) - f(a) \\ &= \int_a^b f'(x) dx = \int_a^{\frac{a+b}{2}} f'(x) dx + \int_{\frac{a+b}{2}}^b f'(x) dx \\ &= [(x-a)f'(x)]_{a}^{\frac{a+b}{2}} + [(x-b)f'(x)]_{\frac{a+b}{2}}^b \\ &\quad - \int_a^{\frac{a+b}{2}} (x-a)f''(x) dx - \int_{\frac{a+b}{2}}^b (x-b)f''(x) dx \\ &= (b-a)f' \left(\frac{a+b}{2} \right) + \int_a^{\frac{a+b}{2}} \left(\frac{x^2}{2} - ax + \frac{a^2}{2} \right) f'''(x) dx \\ &\quad + \int_{\frac{a+b}{2}}^b \left(\frac{x^2}{2} - bx + \frac{b^2}{2} \right) f'''(x) dx \\ &= (b-a)f' \left(\frac{a+b}{2} \right) + 2 \int_a^{\frac{a+b}{2}} \left(\frac{x^2}{2} - ax + \frac{a^2}{2} \right) (f'''(x) + f'''(a+b-x)) dx, \end{aligned}$$

and from the mean value theorem, there exists $x_* \in]a, \frac{a+b}{2}[$ such that :

$$f(b) - f(a) = (b-a)f' \left(\frac{a+b}{2} \right) + \underbrace{\left(\frac{x_*^2}{2} - ax_* + \frac{a^2}{2} \right)}_{P(x_*)} (f'''(x_*) + f'''(a+b-x_*) (b-a).$$

The second order polynomial P admits a as a double root and is an increasing function over the segment $[a, b]$ with $P(b) = \frac{(b-a)^2}{2}$. We denote $P(x_*) = \frac{1}{2}c(x_*)(b-a)^2$ with $0 \leq c(x_*) \leq 1$. Moreover, because of the continuity of f''' on $[a, b]$, the mean value theorem proves that there exists $x_{**} \in]a, b[$ such that $f'''(x_{**}) = \frac{1}{2}(f'''(x_*) + f'''(a+b-x_*)$. Therefore :

$$f(b) - f(a) = (b-a)f' \left(\frac{a+b}{2} \right) + c(x_*)f'''(x_{**})(b-a)^3.$$

The announced lemma is straightforward by applying this expansion to the function :

$$\begin{aligned} f : [0, 1] &\rightarrow \mathbb{R} \\ x &\mapsto J((1-x)F_n + xF_{n+1}), \end{aligned}$$

with $a = 0$ et $b = 1$.

□

Remark 3.5. Some key-points about the midpoint scheme :

- This scheme is known to be symplectic in the compressible framework (see [HLW02, SSC94, Gon96]). For small time steps, backward analysis shows the conservation of a discrete energy, close to the physical one up to a $O(\Delta t^2)$ term. Nevertheless, in practice, the desired time step may prove to be not sufficiently small to ensure such a property. Moreover, symplecticity is hard to obtain for constrained problems (see [SG93]); in particular, it is lost in the incompressible framework.
- For compressible materials with (unrealistic) quadratic elastic potential $\hat{\mathcal{W}}$, energy would be exactly conserved.
- The kinematic constraint at midpoint has bad consequences on energy conservation. In particular, it requires a very high regularity in time.
- Angular and linear momenta are exactly conserved, which is a proof of a perfect behavior of the scheme with respect to rotations and translations groups.

3.4.5 Exactly conservative schemes

At this stage, some remarks need to be done :

- The better conservation of energy achieved by the trapezoidal rule in comparison with the midpoint scheme, is due to the imposition of the kinematic constraint at time steps, and not at mid time steps. In (3.35), it is then natural to adopt :

$$D_{n+1/2} = \frac{1}{2} (\det F_n + \det F_{n+1}). \quad (3.48)$$

- The exact conservation of momenta performed by the midpoint scheme is due to the natural form of the first algorithmic stress tensor :

$$\Pi_{n+1/2} = \left(\frac{F_n + F_{n+1}}{2} \right) \cdot \Sigma_{n+1/2}, \quad (3.49)$$

with a symmetric second stress tensor $\Sigma_{n+1/2}$.

- Then, it is straightforward to check that exact energy conservation is achieved iff we can satisfy :

$$\frac{1}{2} \int_{\Omega} \Sigma_{n+1/2} : (C_{n+1} - C_n) = \int_{\Omega} \left(\mathcal{W}(C_{n+1}) + \frac{\epsilon}{2} p_{n+1}^2 \right) - \int_{\Omega} \left(\mathcal{W}(C_n) + \frac{\epsilon}{2} p_n^2 \right). \quad (3.50)$$

Remark 3.6. After finite element discretization, the integral over Ω in (3.50), could be replaced by the following relation :

$$\begin{aligned} \frac{1}{2} \Sigma_{n+1/2} : (C_{n+1} - C_n) &= \left(\mathcal{W}(C_{n+1}) + \frac{1}{2\epsilon} \mathbb{P}_{\mathcal{P}} (\det F_{n+1} - 1)^2 \right) \\ &\quad - \left(\mathcal{W}(C_n) + \frac{1}{2\epsilon} \mathbb{P}_{\mathcal{P}} (\det F_n - 1)^2 \right), \end{aligned}$$

where $\mathbb{P}_{\mathcal{P}}$ denotes the $L^2(\Omega)$ -projection over \mathcal{P} . It can be treated numerically by a subintegration technique.

A major goal is then to construct such a tensor $\Sigma_{n+1/2}$ satisfying (3.50). We extend the construction of Simo and Tarnow in [ST92] to the quasi-incompressible case by proving the :

Lemma 3.4. For all $n \geq 0$, there exist two scalar functions β_n and γ_n over Ω such that :

$$\begin{aligned} \Sigma_{n+1/2} &:= \left(\frac{\partial \mathcal{W}}{\partial C} (\beta_n C_n + (1 - \beta_n) C_{n+1}) + \frac{\partial \mathcal{W}}{\partial C} ((1 - \beta_n) C_n + \beta_n C_{n+1}) \right) \\ &\quad - \frac{p_n + p_{n+1}}{2} \left(\frac{\partial \det C^{1/2}}{\partial C} (\gamma_n C_n + (1 - \gamma_n) C_{n+1}) + \frac{\partial \det C^{1/2}}{\partial C} ((1 - \gamma_n) C_n + \gamma_n C_{n+1}) \right), \end{aligned}$$

satisfies (3.50), and the corresponding scheme is second order accurate when making the choices (3.48) and (3.49) for $D_{n+1/2}$ and $\Pi_{n+1/2}$ in the midpoint like scheme (3.35) . The corresponding scheme performs exact conservation for momenta and energy.

Proof : Let be given $x \in \Omega$ and two Cauchy-Green tensors C_n and C_{n+1} (given at the point $x \in \Omega$ of the material). We define the functions :

$$h(\beta) = \mathcal{W}(x, \beta C_n + (1 - \beta) C_{n+1}) - \mathcal{W}(x, (1 - \beta) C_n + \beta C_{n+1}), \quad \forall \beta \in [0, 1],$$

and :

$$k(\gamma) = \det(\gamma C_n + (1 - \gamma)C_{n+1})^{1/2} - \det((1 - \gamma)C_n + \gamma C_{n+1})^{1/2}, \quad \forall \gamma \in [0, 1].$$

By the mean value theorem, there exists a constant $\beta^* \in [0, 1]$ such that :

$$\mathcal{W}(x, C_{n+1}) - \mathcal{W}(x, C_n) = \frac{1}{2}(h_x(0) - h_x(1)) = -\frac{1}{2} \frac{dh_x}{d\beta}(\beta^*) = \frac{1}{2} \mathcal{S}_{n+1/2}^{\beta^*} : (C_{n+1} - C_n),$$

with the algorithmic compressible second Piola-Kirchhoff stress tensor :

$$\mathcal{S}_{n+1/2}^{\beta^*} = \frac{\partial \mathcal{W}}{\partial C}(x, \beta^* C_n + (1 - \beta^*)C_{n+1}) + \frac{\partial \mathcal{W}}{\partial C}(x, (1 - \beta^*)C_n + \beta^* C_{n+1}).$$

We obtain by the same argument the existence of a constant $\gamma^* \in [0, 1]$ such that :

$$(\det C_{n+1})^{1/2} - (\det C_n)^{1/2} = \frac{1}{2}(k_x(0) - k_x(1)) = -\frac{1}{2} \frac{dk_x}{d\gamma}(\gamma^*) = \frac{1}{2} G_{n+1/2}^{\gamma^*} : (C_{n+1} - C_n),$$

with the tensor $G_{n+1/2}^{\gamma^*}$ defined as :

$$G_{n+1/2}^{\gamma^*} = \frac{\partial \det C^{1/2}}{\partial C}(\gamma C_n + (1 - \gamma)C_{n+1}) + \frac{\partial \det C^{1/2}}{\partial C}((1 - \gamma)C_n + \gamma C_{n+1}).$$

If p_n and p_{n+1} are the algorithmic pressures at times n and $n+1$, we then introduce :

$$\Sigma_{n+1/2}(x) := \mathcal{S}_{n+1/2}^{\beta^*} + \frac{p_n(x) + p_{n+1}(x)}{2} G_{n+1/2}^{\gamma^*},$$

at $x \in \Omega$.

Extending this definition for all fields of Cauchy-Green tensors C_n and C_{n+1} and any $x \in \Omega$, we deduce by construction of $\Sigma_{n+1/2}$, β^* , γ^* and by definition of the (quasi)incompressibility constraint :

$$\begin{aligned} & \int_{\Omega} \Sigma_{n+1/2} : (C_{n+1} - C_n) \\ &= \int_{\Omega} \mathcal{S}_{n+1/2}^{\beta^*} : (C_{n+1} - C_n) + \int_{\Omega} \frac{p_n + p_{n+1}}{2} G_{n+1/2}^{\gamma^*} : (C_{n+1} - C_n) \\ &= 2 \int_{\Omega} \mathcal{W}(C_{n+1}) - \mathcal{W}(C_n) + \int_{\Omega} \frac{p_n + p_{n+1}}{2} (\det F_{n+1} - \det F_n) \\ &= 2 \int_{\Omega} \mathcal{W}(C_{n+1}) - \mathcal{W}(C_n) + \epsilon \int_{\Omega} \frac{p_n + p_{n+1}}{2} (p_{n+1} - p_n) \\ &= 2 \int_{\Omega} \mathcal{W}(C_{n+1}) - \mathcal{W}(C_n) + \epsilon \int_{\Omega} p_{n+1}^2 - p_n^2, \end{aligned}$$

which is exactly (3.50). Then, the corresponding scheme is energy conserving. The linear momentum is obviously conserved as for any scheme of the form (3.35), and the angular momentum is conserved because of the form (3.49) of the algorithmic algorithmic

Piola-Kirchhoff stress tensor. The second order accuracy comes from the direct Taylor's expansion :

$$\begin{aligned}\Sigma_{n+1/2} &= 2 \frac{\partial \mathcal{W}}{\partial C}(C_{n+1/2}) - \frac{p_n + p_{n+1}}{2} \frac{\partial \det C^{1/2}}{\partial C}(C_{n+1/2}) + O(C_{n+1} - C_n)^2 \\ &= 2 \frac{\partial \mathcal{W}}{\partial C}(C(t_{n+1/2})) - 2p(t_{n+1/2}) \frac{\partial \det C^{1/2}}{\partial C}(C(t_{n+1/2})) + O(\Delta t_n^2),\end{aligned}$$

where we have denoted by $C_{n+1/2} = (C_n + C_{n+1})/2$. \square

In [LM01], T.A Laursen and X.N. Meng propose a local procedure enabling the consistant determination of β_n in the compressible framework. Nevertheless, the difficulty of determining β_n and γ_n at each time step and at each Gauss point can be overcome by the proposal of Gonzalez in [Gon00], proposing to compute the stress at mid-interval by :

$$\begin{aligned}\Sigma_{n+1/2} := 2 \frac{\partial \mathcal{W}}{\partial C}(C_{n+1/2}) &+ 2 \left(\mathcal{W}(C_{n+1}) - \mathcal{W}(C_n) - \frac{\partial \mathcal{W}}{\partial C}(C_{n+1/2}) : \delta C_n \right) \frac{\delta C_n}{\delta C_n : \delta C_n} \\ &- (p_n + p_{n+1}) \left[\frac{\partial \det C^{1/2}}{\partial C}(C_{n+1/2}) + \right. \\ &\left. + \left(\det C_{n+1}^{1/2} - \det C_n^{1/2} - \frac{\partial \det C^{1/2}}{\partial C}(C_{n+1/2}) : \delta C_n \right) \frac{\delta C_n}{\delta C_n : \delta C_n} \right],\end{aligned}\tag{3.51}$$

with $C_{n+1/2} = \frac{1}{2}(C_n + C_{n+1})$, and $\delta C_n = C_{n+1} - C_n$. By construction, the resulting scheme satisfies (3.50) and therefore conserves energy, angular and linear momentum.

Remark 3.7. In the compressible framework with a quadratic elastic potential \mathcal{W} (e.g. Saint Venant-Kirchhoff material), energy conservation is achieved with :

$$\Sigma_{n+1/2} = \frac{\partial \mathcal{W}}{\partial C}(C_n) + \frac{\partial \mathcal{W}}{\partial C}(C_{n+1}).$$

Remark 3.8. In a Newton's method, nonlinear problems are solved by successive linearizations. Here, the linearized time integrator is not symmetric, which is a noticeable complication in numerical methods. An interesting idea, already mentioned in [AR01b], is to adopt the following perturbed expression :

$$\Sigma_{n+1/2} = 2 \frac{\partial \mathcal{W}}{\partial C}(C(\varphi_{n+1/2})) + \underbrace{\left(\Sigma_{n+1/2} - 2 \frac{\partial \mathcal{W}}{\partial C}(C(\varphi_{n+1/2})) \right)}_{(\dagger)},$$

where $C(\varphi_{n+1/2}) = \nabla^t \varphi_{n+1/2} \cdot \nabla \varphi_{n+1/2}$ is the midpoint right Cauchy-Green strain tensor, and in which no differentiation is made on the correction term denoted by (\dagger) . The disadvantage of the proposed quasi-Newton methods is a non-quadratic convergence, but the

practical overcost is negligible. This proposal proves to be much more efficient than simply adopting the midpoint tangent stiffness operator. Indeed, in this latter case, a complete preliminary midpoint prediction of the solution at each time step becomes necessary to obtain a good convergence.

Remark 3.9. When (3.5) is linearized around the undeformed configuration, the schemes presented in this section are reduced to the classical Newmark's trapezoidal rule, performing exact energy and linear momentum conservations. Because of the linearization, the angular momentum is no more conserved, neither for the continuous solution, nor for the approximate one. The spectral radius of the time integration operator is equal to one. The classical proof of this last statement can be found for example in [RT98].

3.5 Dissipative schemes

We discuss herein the extension of a *linearly dissipative* scheme to the nonlinear framework by analyzing the evolution of main invariants for a generalized Hilber-Hughes-Taylor [HHT77] scheme in the nonlinear framework. In particular, the control of the spectral radius of the linear scheme is proved not to entail energy dissipation in the nonlinear framework. Nevertheless, the proposed analysis shows that in the linear framework, dissipation property holds for a modified energy taking a small acceleration energy into account.

By using the analysis done for the HHT scheme, we propose a modification of the conserving scheme [Gon00] enabling a dissipation property for a modified energy.

3.5.1 Conservation analysis for the HHT scheme

In linear elastodynamics, it is necessary for stability reasons to use schemes whose spectral radius is $r \leq 1$, and even $r < 1$ because in this latest case :

1. possible polynomial instabilities are avoided (arising when $r = 1$ in presence of a multiple unit eigenvalue),
2. information is dissipated at highest frequencies, that has no physical meaning,
3. the condition number of the linear systems to be solved is improved,
4. there exist a quadratic form whose value diminishes along the discrete evolution.

A good example is the popular second order Hilber-Hughes-Taylor (HHT) scheme. We present here a nonlinear analysis of this scheme, showing that the above advantages are no more conserved in a nonlinear framework. Nevertheless, it is the occasion to show that in the linear framework, the scheme is strictly dissipative for a modified energy. For a given $\alpha \geq 0$, the natural extension of the HHT scheme [HHT77, Hug87] to nonlinear

elastodynamics is given by :

$$\begin{cases} \int_{\Omega} \rho \ddot{\varphi}_{n+1} \cdot v + \int_{\Omega} (\alpha \Pi_n + (1 - \alpha) \Pi_{n+1}) : \nabla v = \int_{\Omega} f_{n+1-\alpha} \cdot v + \int_{\Gamma_N} g_{n+1-\alpha} \cdot v, \\ \int_{\Omega} q (\det F_{n+1} - 1) = 0, \end{cases} \quad (3.52)$$

for all $v \in \mathcal{U}_0$ and $q \in \mathcal{P}$, with Newmark's relations :

$$\begin{cases} \varphi_{n+1} = \varphi_n + \Delta t_n \dot{\varphi}_n + \Delta t_n^2 \left(\left(\frac{1}{2} - \beta \right) \ddot{\varphi}_n + \beta \ddot{\varphi}_{n+1} \right), \\ \dot{\varphi}_{n+1} = \dot{\varphi}_n + \Delta t_n ((1 - \gamma) \ddot{\varphi}_n + \gamma \ddot{\varphi}_{n+1}). \end{cases}$$

We have denoted $\gamma = \frac{1}{2} + \alpha$, and $\beta = \frac{(1+\alpha)^2}{4}$. The notation $\square_{n+1-\alpha}$ classically stands for $\alpha \square_n + (1 - \alpha) \square_{n+1}$.

Remark 3.10. In the linear case, we recall that [HHT77, Hug87] :

- HHT scheme is the natural modification of the Newmark's scheme combining spectral dissipation and second order accuracy.
- The choice of $\gamma = \frac{1}{2} + \alpha$ ensures second order accuracy.
- For the Newmark's case (see [RT98]), the choice

$$\frac{1 + 2\alpha}{4} \leq \beta \leq \frac{(1 + \alpha)^2}{4},$$

corresponds to real eigenvalues for the integration operator, whereas :

$$\beta \geq \frac{(1 + \alpha)^2}{4},$$

corresponds to complex conjugate eigenvalues.

- The stability imposes $0 \leq \alpha \leq \frac{1}{2}$, with $\alpha = 0$ corresponding to the trapezoidal rule. The spectral radius decreases for $0 \leq \alpha \leq \frac{1}{3}$ and increases for $\frac{1}{3} \leq \alpha \leq \frac{1}{2}$.

In the nonlinear framework, we prove :

Proposition 3.5. We assume the time step to be constant. Then, the nonlinear HHT scheme (3.52) achieves the following discrete evolution properties :

1. **Discrete energy evolution.** Up to higher order terms depending only of time variations in force, we have :

$$\mathcal{E}_{n+1} - \mathcal{E}_n = \mathfrak{P}_n - \mathfrak{D}_n^\alpha \Delta t^2 + c_n \Delta t^3, \quad (3.53)$$

where c_n is defined as for the trapezoidal rule and depends on displacements and pressures at times n and $n + 1$, on the approximate velocity $V_{n+1/2} = \frac{1}{\Delta t}(\varphi_{n+1} -$

φ_n), and on the approximate pressure time derivative $\pi_{n+1/2} = \frac{1}{\Delta t}(p_{n+1} - p_n)$. The coefficient \mathfrak{D}_n^α has the following expression :

$$\begin{aligned}\mathfrak{D}_n^\alpha &= \frac{\alpha^2}{8} \int_\Omega \rho (\ddot{\varphi}_{n+1}^2 - \ddot{\varphi}_n^2) + \frac{\alpha^3}{4} \int_\Omega (\ddot{\varphi}_{n+1} - \ddot{\varphi}_n)^2 \\ &\quad + k \Delta t_n \int_\Omega \ddot{\Pi}_n : (\nabla V_{n+1/2}) + k \Delta t_n \int_\Omega \frac{\partial^2 f}{\partial t^2}(t_n) \cdot V_{n+1/2},\end{aligned}$$

where $\ddot{\Pi}_n$ is the centered second order finite difference :

$$\ddot{\Pi}_n = \frac{1}{\Delta t^2} (\Pi_{n-1} - 2\Pi_n + \Pi_{n+1}).$$

2. Discrete angular evolution. Up to higher order terms, we have :

$$\mathcal{J}_{n+1} - \mathcal{J}_n = \mathfrak{M}_n + c_n \Delta t^3, \quad (3.54)$$

where c_n depends on the approximate solution at times $n-1$, n and $n+1$, on the accelerations $\ddot{\varphi}_{n-1}$, $\ddot{\varphi}_n$ et $\ddot{\varphi}_{n+1}$, and on the approximate second order time derivatives $\frac{1}{\Delta t}(\pi_{n+1/2} - \pi_{n-1/2})$.

3. Discrete linear evolution. Up to higher order terms depending only of the time variations in force, we have :

$$\mathcal{I}_{n+1} - \mathcal{I}_n = \mathfrak{F}_n + c_n \Delta t^3, \quad (3.55)$$

where c_n only depends on the second order time derivative of f .

Proof : A linear combination of the discrete systems at times n and $n+1$, with respective coefficients $(1-\gamma) = \frac{1}{2} - \alpha$ and $\gamma = \frac{1}{2} + \alpha$ gives :

$$\begin{aligned}&\int_\Omega \rho \frac{\dot{\varphi}_{n+1} - \dot{\varphi}_n}{\Delta t_n} \cdot v + \int_\Omega \underbrace{k(\Pi_{n-1} - 2\Pi_n + \Pi_{n+1})}_{\mathfrak{R}_n} : \nabla v + \int_\Omega \frac{\Pi_n + \Pi_{n+1}}{2} : \nabla v = \\ &\int_\Omega \frac{f_n + f_{n+1}}{2} \cdot v + \int_\Omega \underbrace{k(f_{n-1} - 2f_n + f_{n+1})}_{\mathfrak{f}_n} \cdot v,\end{aligned} \quad (3.56)$$

with coefficient $k = \alpha(\frac{1}{2} - \alpha) > 0$ for $0 \leq \alpha \leq \frac{1}{2}$. With $\gamma = \frac{1}{2} + \alpha$ and $\beta = \frac{(1+\alpha)^2}{4}$, Newmark's relations are :

$$\begin{cases} \dot{\varphi}_{n+1} - \dot{\varphi}_n = \Delta t_n \left(\left(\frac{1}{2} - \alpha \right) \ddot{\varphi}_n + \left(\frac{1}{2} + \alpha \right) \ddot{\varphi}_{n+1} \right), \\ \varphi_{n+1} - \varphi_n = \Delta t_n \frac{\dot{\varphi}_n + \dot{\varphi}_{n+1}}{2} + \frac{\alpha^2 \Delta t_n^2}{4} (\ddot{\varphi}_{n+1} - \ddot{\varphi}_n). \end{cases} \quad (3.57)$$

The form (3.56),(3.57) of the scheme adds to the trapezoidal rule some “correction terms”. We only detail these additional contributions.

- 1. Energy evolution.** By using $v = (\varphi_{n+1} - \varphi_n)/\Delta t_n$ in (3.56), and the relations (3.57), the inertial term takes the form :

$$\begin{aligned}\int_{\Omega} \rho \frac{\dot{\varphi}_{n+1} - \dot{\varphi}_n}{\Delta t_n} \cdot v &= \int_{\Omega} \rho \frac{\dot{\varphi}_{n+1} - \dot{\varphi}_n}{\Delta t_n} \cdot \frac{\dot{\varphi}_n + \dot{\varphi}_{n+1}}{2} \\ &\quad + \Delta t_n \frac{\alpha^2}{4} \int_{\Omega} \rho \left(\left(\frac{1}{2} - \alpha \right) \ddot{\varphi}_n + \left(\frac{1}{2} + \alpha \right) \ddot{\varphi}_{n+1} \right) \cdot (\ddot{\varphi}_{n+1} - \ddot{\varphi}_n), \\ &= \frac{1}{2\Delta t_n} \int_{\Omega} \rho \dot{\varphi}_{n+1}^2 - \frac{1}{2\Delta t_n} \int_{\Omega} \rho \dot{\varphi}_n^2 \\ &\quad + \Delta t_n \frac{\alpha^2}{8} \int_{\Omega} \rho (\ddot{\varphi}_{n+1}^2 - \ddot{\varphi}_n^2) + \Delta t_n \frac{\alpha^3}{4} \int_{\Omega} (\ddot{\varphi}_{n+1} - \ddot{\varphi}_n)^2.\end{aligned}$$

The non-trapezoidal contribution to the stress terms is :

$$\int_{\Omega} \aleph_n : \nabla v = k\Delta t^2 \int_{\Omega} \ddot{\Pi}_n : (\nabla V_{n+1/2}),$$

defining the second order accurate finite difference approximations of the stress acceleration $\ddot{\Pi}_n$, and of the velocity $V_{n+1/2}$ by

$$\begin{aligned}\ddot{\Pi}_n &= \frac{1}{\Delta t^2} (\Pi_{n-1} - 2\Pi_n + \Pi_{n+1}), \\ V_{n+1/2} &= \frac{1}{\Delta t} (\varphi_{n+1} - \varphi_n).\end{aligned}$$

Concerning corrections on the force term, we have

$$\int_{\Omega} \mathfrak{f}_n \cdot v = k\Delta t^2 \int_{\Omega} \frac{\partial^2 f}{\partial t^2}(t_n) \cdot V_{n+1/2} + O(\Delta t^3).$$

As a consequence, up to higher orders in Δt concerning only the variations of f , we obtain :

$$\mathcal{E}_{n+1} - \mathcal{E}_n = \mathfrak{P}_n - \mathfrak{D}_n^\alpha \Delta t_n^3 + c_n \Delta t_n^3,$$

with :

$$\begin{aligned}\mathfrak{D}_n^\alpha &= \frac{\alpha^2}{8} \int_{\Omega} \rho (\ddot{\varphi}_{n+1}^2 - \ddot{\varphi}_n^2) + \frac{\alpha^3}{4} \int_{\Omega} (\ddot{\varphi}_{n+1} - \ddot{\varphi}_n)^2 \\ &\quad + k \int_{\Omega} \ddot{\Pi}_n : (\nabla V_{n+1/2}) + k \int_{\Omega} \frac{\partial^2 f}{\partial t^2}(t_n) \cdot V_{n+1/2}.\end{aligned}$$

- 2. Angular momentum evolution.** Assuming that $\Gamma_D = \emptyset$, we use $v = \mathbb{J}_a \cdot \frac{\varphi_n + \varphi_{n+1}}{2}$.

The non-trapezoidal contribution of stresses is :

$$\begin{aligned}\int_{\Omega} \aleph_n \cdot \left(\frac{F_n + F_{n+1}}{2} \right)^t : \mathbb{J}_a &= \underbrace{\int_{\Omega} \aleph_n \cdot \left(\frac{F_{n+1} + F_{n-1}}{2} \right)^t : \mathbb{J}_a}_{I_1} \\ &\quad + \underbrace{\frac{\Delta t}{2} \int_{\Omega} \aleph_n \cdot (\nabla V_{n-1/2})^t : \mathbb{J}_a}_{I_2}.\end{aligned}$$

We decompose \aleph_n by writing :

$$\begin{aligned}
 \aleph_n &= \left(\frac{F_{n+1} + F_{n-1}}{2} \right) \cdot (\Sigma_{n-1} - 2\Sigma_n + \Sigma_{n+1}) \\
 &\quad + \left(\frac{F_{n+1} - F_{n-1}}{2} \right) \cdot (\Sigma_{n+1} - \Sigma_{n-1}) + (F_{n+1} - 2F_n + F_{n-1}) \cdot \Sigma_n, \\
 &= \left(\frac{F_{n+1} + F_{n-1}}{2} \right) \cdot (\Sigma_{n-1} - 2\Sigma_n + \Sigma_{n+1}) \\
 &\quad + \frac{\Delta t}{2} (\nabla V_{n+1/2} + \nabla V_{n-1/2}) \cdot (\Sigma_{n+1} - \Sigma_{n-1}) \\
 &\quad + \Delta t (\nabla V_{n+1/2} - \nabla V_{n-1/2}) \cdot \Sigma_n.
 \end{aligned} \tag{3.58}$$

We denote the centered finite difference approximations of stress acceleration by :

$$\ddot{\Sigma}_n = \frac{1}{\Delta t^2} (\Sigma_{n-1} - 2\Sigma_n + \Sigma_{n+1}),$$

and of stress speed by :

$$\dot{\Sigma}_n = \frac{1}{2\Delta t} (\Sigma_{n+1} - \Sigma_{n-1}).$$

Considering Newmark's relations, we have :

$$\begin{aligned}
 V_{n+1/2} - V_{n-1/2} &= \Delta t \left(\left(\frac{1}{2} - \alpha \right) \ddot{\varphi}_{n-1} + \ddot{\varphi}_n + \left(\frac{1}{2} + \alpha \right) \ddot{\varphi}_{n+1} \right) \\
 &\quad + \Delta t^2 \frac{\alpha^2}{4} (\ddot{\varphi}_{n+1} - 2\ddot{\varphi}_n + \ddot{\varphi}_{n-1}).
 \end{aligned}$$

Then, we can rewrite \aleph_n as :

$$\begin{aligned}
 \aleph_n &= \overbrace{k\Delta t^2 \left(\frac{F_{n+1} + F_{n-1}}{2} \right) \cdot \ddot{\Sigma}_n}^{\aleph_n^1} \\
 &\quad + \underbrace{k\Delta t^2 (\nabla V_{n+1/2} + \nabla V_{n-1/2}) \cdot \dot{\Sigma}_n + k\Delta t^2 (\nabla (V_{n+1/2} - V_{n-1/2}) / \Delta t) \cdot \Sigma_n}_{\aleph_n^2}.
 \end{aligned}$$

By skew-symmetry of \mathbb{J}_a , \aleph_n^1 has a vanishing contribution in I_1 , whereas \aleph_n^2 has a second order contribution in I_1 . Contributions of \aleph_n in I_2 is at third order in Δt .

Concerning the additional resultant moment, up to a third order term :

$$\int_{\Omega} \mathfrak{f}_n \cdot v = k\Delta t^2 \int_{\Omega} \frac{\varphi_n + \varphi_{n+1}}{2} \times \frac{\partial^2 f}{\partial t^2}(t_n).$$

3. Linear momentum evolution. Assuming that $\Gamma_D = \emptyset$, the HHT scheme entails a second order error in the discrete resultant force, given by :

$$\int_{\Omega} \mathfrak{f}_n \simeq \Delta t^2 \int_{\Omega} \frac{\partial^2 f}{\partial t^2}(t_n),$$

up to a third order term.

□

Remark 3.11. Considering the linearized problem, we assume that $\hat{\mathcal{W}}$ is quadratic as a function of F , and that the incompressibility constraint is linearized. Then :

$$\int_{\Omega} \Pi_n : \nabla v = \int_{\Omega} \frac{\partial \hat{\mathcal{W}}}{\partial F} : \nabla v - p \operatorname{div} v, \quad \forall v \in \mathcal{U}_0.$$

If $f = 0$, we have $c_n = 0$ (i.e. the trapezoidal rule is energy conserving). Moreover, since :

$$\begin{aligned} \varphi_{n+1} - \varphi_n = & \frac{1}{2}(\varphi_{n+1} - \varphi_n) + \frac{1}{2}(\varphi_n - \varphi_{n-1}) \\ & + \frac{1}{2}(\varphi_{n+1} - \varphi_n) - \frac{1}{2}(\varphi_n - \varphi_{n-1}), \end{aligned} \tag{3.59}$$

we have up to an integration over Ω :

$$\begin{aligned} \Delta t^3 \ddot{\Pi}_n : \nabla V_{n+1/2} = & \hat{\mathcal{W}}(F_{n+1} - F_n) - \hat{\mathcal{W}}(F_n - F_{n-1}) \\ & + \frac{\epsilon}{2}(p_{n+1} - p_n)^2 - \frac{\epsilon}{2}(p_n - p_{n-1})^2 \\ & + \hat{\mathcal{W}}(F_{n+1} - 2F_n + F_{n-1}) \\ & + \frac{\epsilon}{2}(p_{n+1} - 2p_n + p_{n-1})^2. \end{aligned}$$

Then, the following quadratic form :

$$\begin{aligned} \mathcal{E}_n^{HHT} = & \frac{1}{2} \int_{\Omega} \rho \dot{\varphi}_n^2 + \int_{\Omega} \hat{\mathcal{W}}(F_n) + \frac{\epsilon}{2} \int_{\Omega} p_n^2 \\ & + \frac{\alpha^2 \Delta t^2}{8} \int_{\Omega} \rho \ddot{\varphi}_{n+1}^2 + k \Delta t^2 \hat{\mathcal{W}}(\dot{F}_{n-1/2}) + \frac{k\epsilon}{2} \Delta t^2 (\dot{p}_{n-1/2})^2, \end{aligned}$$

with $\dot{F}_{n-1/2} = (F_n - F_{n-1})/\Delta t$ and $\dot{p}_{n-1/2} = (p_n - p_{n-1})/\Delta t$, diminishes along the dynamics. More precisely :

$$\begin{aligned} \mathcal{E}_{n+1}^{HHT} - \mathcal{E}_n^{HHT} = & -\frac{\alpha^3 \Delta t^2}{4} \int_{\Omega} (\ddot{\varphi}_{n+1} - \ddot{\varphi}_n)^2 \\ & - k \Delta t^4 \int_{\Omega} \hat{\mathcal{W}}(\ddot{F}_n) - \frac{k\epsilon}{2} \Delta t^4 (\ddot{p}_n)^2 \leq 0. \end{aligned}$$

Therefore, for linear elastodynamics, there exist a quadratic form \mathcal{E}_n^{HHT} diminishing along the HHT discrete evolution. This comes from the fact that the spectral radius of the time integrator is less than one. Nevertheless, this quadratic form does not coincide with the usual mechanical energy. It introduces acceleration terms in the energy and high order terms in time in the dissipation, which are larger for larger frequencies.

- Remark 3.12.**
- If $\beta = \frac{1+2\alpha}{4}$, it is straightforward to check in the proof that the two first inertial terms in \mathfrak{D}_n^α disappear. In particular, there is no energy associated to acceleration effects.
 - Groups of symmetry are not well preserved by the discrete dynamics as momenta conservation is not preserved in the discrete dynamics. This remark confirms the work of Armero and Romero in [AR01a]; they prove the non-existence of relative equilibria for the HHT discrete dynamics in the case of a nonlinear spring-mass system.

3.5.2 A new dissipative scheme in the nonlinear framework

The previous analysis inspires us to propose a dissipative scheme for a modified energy taking into account acceleration effects, by using a second order non-trapezoidal Newmark time integration of the inertial term, while keeping Gonzalez energy conserving proposal for the algorithmic Piola-Kirchhoff stress tensor at midtime. More precisely, let us adopt the following integration scheme, in the compressible framework to lighten the presentation :

$$\int_{\Omega} \rho [(1-\gamma)\ddot{\varphi}_n + \gamma\ddot{\varphi}_{n+1}] \cdot v + \int_{\Omega} \Pi_{n+1/2} : \nabla v = \int_{\Omega} \frac{f_n + f_{n+1}}{2} \cdot v, \quad \forall v \in \mathcal{U}_0, \quad (3.60)$$

where $\Pi_{n+1/2}$ is the first Piola-Kirchhoff algorithmic stress tensor proposed in [Gon00] to achieve energy conservation, and described by equations (3.49) and (3.51), together with Newmark's relations :

$$\begin{cases} \varphi_{n+1} = \varphi_n + \Delta t_n \dot{\varphi}_n + \Delta t_n^2 \left(\left(\frac{1}{2} - \beta \right) \ddot{\varphi}_n + \beta \ddot{\varphi}_{n+1} \right), \\ \dot{\varphi}_{n+1} = \dot{\varphi}_n + \Delta t_n [(1-\gamma)\ddot{\varphi}_n + \gamma\ddot{\varphi}_{n+1}]. \end{cases} \quad (3.61)$$

Second order accuracy is ensured by considering $\gamma = \frac{1}{2} + \alpha$ with $\alpha = \eta \Delta t_n > 0$, and in the framework of the proposed conservation analysis, we adopt $\beta = (1+\alpha)^2/4$, as in the original HHT scheme. Then, we obtain the following result :

Proposition 3.6. *The scheme (3.60),(3.61) achieves the following properties :*

1. Discrete energy dissipation.

$$\tilde{\mathcal{E}}_{n+1} - \tilde{\mathcal{E}}_n = \mathfrak{P}_n - \frac{\alpha^3 \Delta t_n^2}{4} \int_{\Omega} (\ddot{\varphi}_{n+1} - \ddot{\varphi}_n) \leq \mathfrak{P}_n, \quad (3.62)$$

with the modified energy :

$$\tilde{\mathcal{E}}_n = \frac{\alpha^2 \Delta t_n^2}{8} \int_{\Omega} \rho \ddot{\varphi}_n^2 + \frac{1}{2} \int_{\Omega} \rho \dot{\varphi}_n^2 + \int_{\Omega} \hat{W}(\nabla \varphi_n).$$

2. Discrete angular momentum conservation. If $\Gamma_D = \emptyset$, we have :

$$\mathcal{J}_{n+1} - \mathcal{J}_n = \mathfrak{M}_n. \quad (3.63)$$

3. Discrete linear momentum conservation. If $\Gamma_D = \emptyset$, we have :

$$\mathcal{I}_{n+1} - \mathcal{I}_n = \mathfrak{F}_n. \quad (3.64)$$

The definitions of the discrete angular (resp. linear) momentum \mathcal{J}_n (resp. \mathcal{I}_n) and of the resultant moment (resp. force) \mathfrak{M}_n (resp. \mathfrak{F}_n) are the one given in Proposition 3.3.

Proof : The proof readily comes from the previous analysis of the HHT scheme. \square

Concerning the practical implementation of the present scheme, we propose to compute first the displacements φ_{n+1} such that for all $v \in \mathcal{U}_0$:

$$\begin{aligned} & \int_{\Omega} \rho \frac{\gamma}{\beta \Delta t_n^2} \varphi_{n+1} \cdot v + \int_{\Omega} \Pi_{n+1/2} : \nabla v = \\ & \int_{\Omega} \rho \frac{\gamma}{\beta \Delta t_n^2} \varphi_n \cdot v + \int_{\Omega} \rho \frac{\gamma}{\beta \Delta t_n} \dot{\varphi}_n \cdot v + \delta \int_{\Omega} \rho \ddot{\varphi}_n + \int_{\Omega} f \cdot v + \int_{\Gamma_N} g \cdot v + \int_{\Gamma_c} \tau_{n+1/2}^* \cdot v, \quad \forall v \in \mathcal{U}_0, \end{aligned}$$

with :

$$\delta = \gamma \frac{\frac{1}{2} - \beta}{\beta} - 1 + \gamma.$$

Then, the accelerations at time t_{n+1} are computed by :

$$\ddot{\varphi}_{n+1} = \frac{\varphi_{n+1} - \varphi_n}{\beta \Delta t_n^2} - \frac{\dot{\varphi}_n}{\beta \Delta t_n} - \frac{\frac{1}{2} - \beta}{\beta} \ddot{\varphi}_n,$$

and velocities by :

$$\dot{\varphi}_{n+1} = \dot{\varphi}_n + \Delta t_n [(1 - \gamma) \ddot{\varphi}_n + \gamma \ddot{\varphi}_{n+1}].$$

A practical issue deals with acceleration initialization. To do so, we propose to compute two time steps with a midpoint, a trapezoidal or a conservative scheme with initial displacements φ_0 and velocities $\dot{\varphi}_0$, and adopt the following initial data :

$$\begin{cases} \varphi'_0 = \varphi_1, \\ \dot{\varphi}'_0 = \dot{\varphi}_1, \\ \ddot{\varphi}'_0 = \frac{\dot{\varphi}_2 - \dot{\varphi}_0}{2 \Delta t_n}, \end{cases}$$

for the proposed dissipative scheme.

3.6 Extensions of the conservative approach

In this section, we illustrate the idea that the approach of energy conserving time integration schemes can be extended to various mechanical situations. In particular, we extend the finite difference energy correction from [Gon00] to time integration schemes for frictionless impact and viscoelasticity.

First, a conservative formulation of frictionless impact is proposed, enabling as in [LL02] the enforcement of the usual Kuhn-Tucker conditions at time discretization points.

On the other hand, we propose herein a conservative scheme in the viscoelastic framework, that is achieving the same energetic balance as the continuous viscoelastic system. The main goal of this approach is to avoid the pollution of the viscoelastic dissipation by numerical effects, potentially important as shown numerically in section 3.7 for purely hyperelastic systems.

Finally, in the case of fluid-structure interaction problems in Arbitrary Lagrangian Eulerian (ALE) formulation, we have proposed an energy conserving integration scheme provided special non-conservative variables are adopted in the fluid part. As this last issue is not fully related with the rest of the work, the contribution [TH03a] does not appear herein.

3.6.1 Frictionless contact

Over the last years, an increasing interest has been devoted to energy conserving time integration schemes for contact mechanics. In particular, in the framework of frictionless contact, both Laursen and Chawla [LC97] and Armero and Petöcz [AP98] have shown the interest of the persistency condition to obtain energy conservation in the discrete framework. Nevertheless, as underlined in [LL02], both contributions encounter a difficulty in enforcing standard Kuhn-Tucker conditions associated to frictionless contact, so that they concede an interpenetration of the structures in interaction, vanishing as the time step goes to zero. This drawback is resolved by Laursen and Love in [LL02], by introducing a discrete jump in velocities during impact, making possible the enforcement of contact conditions at each time step, at the computational price of resolving a problem on the jump in velocities. In the framework of a penalized enforcement of the contact condition, and by adapting the correction technique from [Gon00], we propose an energy conserving scheme while enforcing the standard Kuhn-Tucker contact conditions at entire time steps.

Let $\Omega^{(1)}$ and $\Omega^{(2)}$, two open sets in \mathbb{R}^3 representing the interior of the reference configurations of two solids potentially in contact on the parts $\Gamma_c^{(i)} \subset \partial\Omega^{(i)}$ ($i \in \{1, 2\}$) of their boundaries. For each $i \in \{1, 2\}$, $\square^{(i)}$ will denote the quantity \square relative to $\Omega^{(i)}$, and with the notation introduced above, we assume that $\Gamma_D^{(i)}$, $\Gamma_N^{(i)}$, and $\Gamma_c^{(i)}$ constitute a partition of the boundary $\partial\Omega^{(i)}$. In this presentation, $\Gamma_c^{(2)}$ will be considered as the master surface. Let us introduce for all $x \in \Gamma_c^{(1)}$, the closest-point projection :

$$\bar{y}(t, x) = \arg \min_{y \in \Gamma_c^{(2)}} \|\varphi^{(1)}(t, x) - \varphi^{(2)}(t, y)\|_2.$$

Assuming that the manifold $\Gamma_c^{(2)}$ is continuously differentiable, it follows that there exists a function $g : [0, T] \times \Gamma_c^{(1)} \rightarrow \mathbb{R}$ continuous with respect to the space variables, such that :

$$\varphi^{(1)}(t, x) - \varphi^{(2)}(t, \bar{y}(t, x)) = -g(t, x) \nu(t, \bar{y}(t, x)),$$

where $\nu(t, y)$ is the normal outward unit vector to $\varphi^{(2)}(t, \Gamma_c^{(2)})$ at time $t \in [0, T]$ and point $y \in \Gamma_c^{(2)}$. As a consequence, we get :

$$g(t, x) = -\left(\varphi^{(1)}(t, x) - \varphi^{(2)}(t, \bar{y}(t, x))\right) \cdot \nu(t, \bar{y}(t, x)),$$

and the non-penetration condition expresses as :

$$g(t, x) \leq 0,$$

for all displacements fields $\varphi^{(1)}$ and $\varphi^{(2)}$. Then, the weak form of the balance of linear momentum reads :

$$\begin{aligned} \sum_{i=1}^2 \int_{\Omega^{(i)}} \rho^{(i)} \ddot{\varphi}^{(i)} \cdot v^{(i)} + \int_{\Omega^{(i)}} \Pi^{(i)} : \nabla v^{(i)} &= \sum_{i=1}^2 \int_{\Omega^{(i)}} f^{(i)} \cdot v^{(i)} \\ &\quad - \underbrace{\int_{\Gamma_c^{(1)}} \lambda(t, x) \left(\frac{\partial g}{\partial \varphi^{(1)}} \cdot v^{(1)} + \frac{\partial g}{\partial \varphi^{(2)}} \cdot v^{(2)} \right)}_{G(v^{(1)}, v^{(2)})}, \end{aligned} \quad (3.65)$$

for all admissible virtual displacements $v^{(i)} \in \mathcal{U}_0(\Omega^{(i)})$, $i \in \{1, 2\}$, such that the Kuhn-Tucker conditions are satisfied :

$$\begin{cases} \lambda(t, x) \geq 0, \\ g(t, x) \leq 0, \\ \lambda(t, x)g(t, x) = 0, \end{cases} \quad (3.66)$$

for almost all $(t, x) \in [0, T] \times \Omega$ (see [Lau02]). Moreover, it is well known that the frictionless contact reaction is then normal to $\Gamma_c^{(1)}$, and as proved in [Lau02] for example, the following relation holds :

$$G(v^{(1)}, v^{(2)}) = - \int_{\Gamma_c^{(1)}} \lambda(t, x) \nu(t, \bar{y}(t, x)) \cdot \left[v^{(1)}(x) - v^{(2)}(\bar{y}(t, x)) \right].$$

For energy conservation purpose, the following persistency condition (see [SL92]) has to be added :

$$\lambda(t, x) \dot{g}(\varphi(t, x)) = 0. \quad (3.67)$$

The condition (3.67) means that normal contact reactions can only appear during persistent contact on the rigid surface.

Conservation properties in the continuous framework

The two-body system, assumed here to be compressible for simplicity, achieves usual conservation properties in the absence of external forces, as proved in [AP98] for example. Indeed, the work of normal contact reactions at time t , obtained as $G(\dot{\varphi}^{(1)}(t), \dot{\varphi}^{(2)}(t))$ vanishes :

$$\begin{aligned} G(\dot{\varphi}^{(1)}(t), \dot{\varphi}^{(2)}(t)) &= - \int_{\Gamma_c} \lambda(t, x) \nu(t, \bar{y}(t, x)) \cdot (\dot{\varphi}^{(1)}(t, x) - \dot{\varphi}^{(2)}(t, \bar{y}(t, x))) \\ &= \int_{\Gamma_c} \lambda(t, x) \left(\frac{\partial g}{\partial \varphi^{(1)}} \cdot \dot{\varphi}^{(1)}(t, x) + \frac{\partial g}{\partial \varphi^{(2)}} \cdot \dot{\varphi}^{(2)}(t, x) \right) \\ &= \int_{\Gamma_c} \lambda(t, x) \dot{g}(t, x) \\ &= 0. \end{aligned}$$

As a consequence, when the persistency condition (3.67) is enforced, the total energy of the two-body-system :

$$\mathcal{E}(t) = \sum_{i=1}^2 \mathcal{E}^{(i)}(t),$$

with :

$$\mathcal{E}^{(i)}(t) = \frac{1}{2} \int_{\Omega^{(i)}} \rho^{(i)} \ddot{\varphi}^{(i)}(t) + \int_{\Omega^{(i)}} \hat{\mathcal{W}}^{(i)}(\nabla \varphi^{(i)}(t)),$$

is conserved. The same statement can be established for angular and linear momentum. Indeed, the resultant moment of the contact forces with respect to any axis $a \in \mathbb{R}^3$ vanishes :

$$\begin{aligned} G(a \times \varphi^{(1)}(t), a \times \varphi^{(2)}(t)) &= -a \cdot \int_{\Gamma_c} \lambda(t, x) (\varphi^{(1)}(t, x) - \varphi^{(2)}(t, \bar{y}(t, x))) \times \nu(t, \bar{y}(t, x)) \\ &= a \cdot \int_{\Gamma_c} \lambda(t, x) g(t, x) \nu(t, \bar{y}(t, x)) \times \nu(t, \bar{y}(t, x)) \\ &= 0, \end{aligned}$$

which entails, in the absence of external efforts, the conservation of the two-body system angular momentum :

$$\mathcal{M}(t) = \sum_{i=1}^2 \mathcal{M}^{(i)}(t),$$

with :

$$\mathcal{M}^{(i)}(t) = \int_{\Omega} \rho^{(i)} \varphi^{(i)}(t) \times \dot{\varphi}^{(i)}(t).$$

Finally, for any translation $a \in \mathbb{R}^3$ of the two-body system, it is straightforward that $G(a, a) = 0$, which entails that the sum of resultant forces between the two bodies vanishes,

and in the absence of external efforts, the conservation of the two-body system linear momentum :

$$\mathcal{I}(t) = \sum_{i=1}^2 \mathcal{I}^{(i)}(t),$$

with :

$$\mathcal{I}^{(i)}(t) = \int_{\Omega} \rho^{(i)} \dot{\varphi}^{(i)}(t).$$

When the conditions (3.66) are enforced through a penalized formulation, the Lagrange multiplier λ is defined as :

$$\lambda = \frac{1}{\eta} g^+, \quad [0, T] \times \Omega,$$

with $g^+ = g$ if $g \geq 0$ and $g^+ = 0$ otherwise. Then, the persistency condition (3.67) is no more necessary to achieve energy conservation. The work of contact forces is given by :

$$\int_{\Gamma_c} \lambda(t, x) \dot{g}(t, x) = \frac{d}{dt} \left(\frac{1}{2\eta} \int_{\Gamma_c} (g^+)^2 \right),$$

resulting in the absence of external forces, in the conservation of a penalized total energy of the two-body system :

$$\mathcal{E}(t) = \frac{1}{2\eta} \int_{\Gamma_c} (g^+(t))^2 + \sum_{i=1}^2 \mathcal{E}^{(i)}(t).$$

A conserving time integration approach for frictionless contact

To reproduce in the discrete framework the previous conservation properties, we adapt the energy correction approach of [Gon00] and propose the following midtime approximation of the normal contact reaction :

$$G_{n+1/2}(v^{(1)}, v^{(2)}) = \int_{\Gamma_c^{(1)}} \Lambda_{n+1/2} \Delta g_{n+1/2} \cdot \left[v^{(1)}(x) - v^{(2)}(\bar{y}_{n+1/2}(x)) \right], \quad (3.68)$$

where $\bar{y}_{n+1/2}(x)$ is the projection of $\varphi_{n+1/2}^{(1)}(x)$ over $\varphi_{n+1/2}^{(2)}(\Gamma_c)$ with the notation :

$$\varphi_{n+1/2}^{(i)} = \frac{1}{2} \left(\varphi_n^{(i)} + \varphi_{n+1}^{(i)} \right).$$

Moreover, we propose to adopt :

$$\Delta g_{n+1/2} = -\nu_{n+1/2} + [g_{n+1} - g_n + \nu_{n+1/2} \cdot \delta \varphi_n] \frac{\delta \varphi_n}{\delta \varphi_n \cdot \delta \varphi_n},$$

where $\nu_{n+1/2}(x)$ is the normal outward unit vector to $\varphi_{n+1/2}^{(2)}(\Gamma_c^{(2)})$ at point $\bar{y}_{n+1/2}(x) \in \Gamma_c^{(2)}$, and :

$$\begin{cases} g_n(x) = -\left(\varphi_n^{(1)}(x) - \varphi_n^{(2)}(\bar{y}_n(x))\right) \cdot \nu_n(x), \\ \delta\varphi_n(x) = \left[\varphi_{n+1}^{(1)}(x) - \varphi_{n+1}^{(2)}(\bar{y}_{n+1/2}(x))\right] - \left[\varphi_n^{(1)}(x) - \varphi_n^{(2)}(\bar{y}_{n+1/2}(x))\right]. \end{cases}$$

With rather obvious notation, we have denoted by $\bar{y}_n(x)$ the projection of $\varphi_n^{(1)}(x)$ over $\varphi_n^{(2)}(\Gamma_c)$ and by $\nu_n(x)$ the outward normal unit vector to $\varphi_n^{(2)}(\Gamma_c)$ at point $\bar{y}_n(x)$. Finally, we propose :

$$\Lambda_{n+1/2} = \lambda_{n+1/2} + \left[\frac{\lambda_{n+1} g_{n+1} - \lambda_n g_n}{2} - \lambda_{n+1/2} \delta g_n \right] \frac{\delta g_n}{(\delta g_n)^2},$$

where $\lambda_{n+1/2} = g_{n+1/2}(x)^+/\eta$ in which $g_{n+1/2}(x)$ is the gap function g evaluated at point $x \in \Gamma_c^{(1)}$ for the displacements fields $\varphi_{n+1/2}^{(1)}$ and $\varphi_{n+1/2}^{(2)}$. Moreover, the following notation has been used :

$$\begin{cases} \lambda_n(x) = g_n^+(x)/\eta, \\ \delta g_n(x) = g_{n+1}(x) - g_n(x). \end{cases}$$

With this construction, the following properties hold :

Proposition 3.7. *The discrete work of frictionless contact forces we have defined in (3.68), achieves :*

1. exact discrete work, that is :

$$\begin{aligned} G_{n+1/2}(\varphi_{n+1}^{(1)} - \varphi_n^{(1)}, \varphi_{n+1}^{(2)} - \varphi_n^{(2)}) &= \frac{1}{2} \int_{\Gamma_c^{(1)}} \lambda_{n+1} g_{n+1} - \lambda_n g_n \\ &= \frac{1}{2\eta} \int_{\Gamma_c} (g_{n+1}^+)^2 - (g_n^+)^2 \end{aligned}$$

2. zero resultant force, that is :

$$G_{n+1/2}(a, a) = 0, \quad \forall a \in \mathbb{R}^3.$$

Proof : The zero resultant force is readily obtained from (3.68). Concerning discrete work, we have by construction :

$$\begin{aligned} G_{n+1/2}(\varphi_{n+1}^{(1)} - \varphi_n^{(1)}, \varphi_{n+1}^{(2)} - \varphi_n^{(2)}) &= \int_{\Gamma_c^{(1)}} \Lambda_{n+1/2} \Delta g_{n+1/2} \cdot \delta\varphi_n \\ &= \int_{\Gamma_c^{(1)}} \Lambda_{n+1/2} \delta g_n \\ &= \frac{1}{2} \int_{\Gamma_c^{(1)}} \lambda_{n+1} g_{n+1} - \lambda_n g_n, \end{aligned}$$

hence the proof. \square

Remark 3.13. A more simple energy conserving formulation is given by :

$$G_{n+1/2}(v^{(1)}, v^{(2)}) = \int_{\Gamma_c^{(1)}} N_{n+1/2} \cdot [v^{(1)}(x) - v^{(2)}(\bar{y}_{n+1/2}(x))] , \quad (3.69)$$

in which :

$$N_{n+1/2} = \lambda_{n+1/2} \nu_{n+1/2} - \left[\frac{\lambda_{n+1} g_{n+1} - \lambda_n g_n}{2} - \lambda_{n+1/2} \nu_{n+1/2} \cdot \delta \varphi_n \right] \frac{\delta \varphi_n}{\delta \varphi_n \cdot \delta \varphi_n},$$

with the above notation. Nevertheless, the section dealing with unilateral frictionless contact against a plane wall will illustrate a major difference between the two approaches (3.68) and (3.69).

Remark 3.14. In order to preserve symmetric tangent operators in a Newton's method, we propose not to differentiate correction terms, that is in the expressions of $\Delta g_{n+1/2}$ and $\Lambda_{n+1/2}$, the terms marked with a (\dagger) :

$$\begin{aligned} \Delta g_{n+1/2} &= -\nu_{n+1/2} + \underbrace{[g_{n+1} - g_n + \nu_{n+1/2} \cdot \delta \varphi_n]}_{(\dagger)} \frac{\delta \varphi_n}{\delta \varphi_n \cdot \delta \varphi_n}, \\ \Lambda_{n+1/2} &= \lambda_{n+1/2} + \underbrace{\left[\frac{\lambda_{n+1} g_{n+1} - \lambda_n g_n}{2} - \lambda_{n+1/2} \delta g_n \right]}_{(\dagger)} \frac{\delta g_n}{(\delta g_n)^2}. \end{aligned}$$

This proposal enables to solve the problem in the midtime displacements field $\varphi_{n+1/2}$, as in the proposed implementation of Gonzalez time integration scheme.

Unilateral frictionless contact against a plane wall

We analyze here the case of unilateral frictionless contact against a plane wall. Then, we assume that the infinite half space $\Omega^{(2)} = \mathbb{R}^2 \times \mathbb{R}_+$ is fixed and perfectly rigid, and that the deformable body of reference configuration $\Omega^{(1)}$ is submitted to a unilateral frictionless contact against the boundary $\Gamma_c^{(2)} = \mathbb{R}^2 \times \{0\}$ of $\Omega^{(2)}$. This assumption impose that the displacement fields $\varphi^{(2)} = id$ and its variations $v^{(2)}$ vanishes. Moreover, the outward normal unit vector ν is constant over $\Gamma_c^{(2)}$. Then, by using the above definitions, we get :

$$\begin{cases} \bar{y}_n(x) = \varphi_n(x) - (\varphi_n(x) \cdot \nu) \nu, \\ g_n(x) = -\varphi_n^{(1)}(x) \cdot \nu, \\ \delta \varphi_n(x) = \varphi_{n+1}^{(1)}(x) - \varphi_n^{(1)}(x) \end{cases}$$

and deduce that $\Delta g_{n+1/2}(x) = -\nu$, so that :

$$G_{n+1/2}(v^{(1)}, 0) = - \int_{\Gamma_c^{(1)}} \Lambda_{n+1/2} \nu \cdot v^{(1)},$$

for all $v^{(1)} \in \mathcal{U}_0(\Omega^{(1)})$. The fact, that the contact force remains normal to the wall explains the superiority of the proposed discrete formulation, when compared to the apparently simpler formulation (3.69). Indeed, the latter induces a non-physical variation of the contact force direction to achieve energy conservation, while (3.68) only plays on the intensity of the contact force. Moreover, we have noticed numerically the superiority of (3.68) in terms of number of iterations in Newton's algorithm in the framework of the previous implementation, since the formulation (3.69) implemented with the same strategy experiment difficulty in converging.

3.6.2 Viscoelasticity

The two-branch viscoelastic incompressible model presented in [Tal94b, TRK93] introduces in addition to the displacements and hydrostatic pressures fields φ, p of the hyperelastic framework, the symmetric positive second order tensor A of internal variables, which is physically the inverse of the right Cauchy-Green strain tensor of the viscous branch in the material, and the pressure q associated to the incompressibility constraint on A . The hyperelastic stored energy function $\mathcal{W}(C)$ in terms of the right Cauchy Green strain tensor becomes $\tilde{\mathcal{W}}(C, A)$ with typically :

$$\tilde{\mathcal{W}}(C, A) = \mathcal{W}(C) + \mathcal{W}_e(A^{1/2} \cdot C \cdot A^{1/2}),$$

where \mathcal{W}_e is the so-called stored energy of the elastic part in the viscous branch of the material. We also introduce the dissipation coefficient ν and the penalization coefficients ϵ and η associated to the incompressibility constraints. Then, for all $t \in [0, T]$ we look in a variational formal sense for the displacements $\varphi(t) \in \varphi_D(t) + \mathcal{U}_0$, the hydrostatic pressure $p(t) \in \mathcal{P}$, the second order tensor of internal variables $A(t) \in \mathcal{A}$ and the associated pressure $q(t) \in \mathcal{Q}$ such that :

$$\begin{cases} \int_{\Omega} \rho \ddot{\varphi}(t) \cdot \hat{\varphi} + \int_{\Omega} \left(2\nabla \varphi(t) \cdot \frac{\partial \tilde{\mathcal{W}}}{\partial C} - p(t) \operatorname{cof} \nabla \varphi(t) \right) : \nabla \hat{\varphi} = \int_{\Omega} f(t) \cdot \hat{\varphi}, \\ \int_{\Omega} (\det \nabla \varphi(t) - 1 + \epsilon p(t)) \hat{p} = 0, \\ \int_{\Omega} \left(\nu \partial_t (A(t)^{-1}) - \frac{\partial \tilde{\mathcal{W}}}{\partial A} - q(t) \operatorname{cof} A(t) \right) : \hat{A} = 0, \\ \int_{\Omega} (\det A(t) - 1 - \eta q(t)) \hat{q} = 0, \end{cases} \quad (3.70)$$

for all $(\hat{\varphi}, \hat{p}, \hat{A}, \hat{q}) \in \mathcal{U}_0 \times \mathcal{P} \times \mathcal{A} \times \mathcal{Q}$. The following proposition shows the conservation properties of the system.

Proposition 3.8. *For the viscoelastic variational problem (3.70), energy conservation holds in a formal sense :*

$$\mathcal{E}(t) - \mathcal{E}(0) = \int_0^t \left(\int_{\Omega} f(s) \cdot \dot{\varphi}(s) - \int_{\Omega} \nu D(s) : D(s) \right),$$

with the viscous deformation rate second order tensor :

$$D(s) = A(s)^{-1/2} \cdot \dot{A}(s) \cdot A(s)^{-1/2},$$

and the total energy :

$$\mathcal{E}(t) = \int_{\Omega} \rho \dot{\varphi}(t)^2 + \int_{\Omega} \tilde{\mathcal{W}}(C(t), A(t)) + \frac{\epsilon}{2} \int_{\Omega} p(t)^2 + \frac{\epsilon}{2} \int_{\Omega} q(t)^2.$$

Angular and linear momenta are also conserved, exactly as in proposition 1.

Proof : Concerning energy conservation, we consider the problem (3.70) at time t with $\hat{\varphi} = \dot{\varphi}(t)$ and $\hat{A} = \dot{A}(t)$, and we formally compute the time derivatives of the incompressibility constraints taking $\hat{p} = p(t)$ and $\hat{q} = q(t)$. Therefore, we get :

$$\begin{cases} \int_{\Omega} \rho \ddot{\varphi}(t) \cdot \dot{\varphi}(t) + \int_{\Omega} \frac{\partial \tilde{\mathcal{W}}}{\partial C} : \dot{C}(t) - \int_{\Omega} p(t) \operatorname{cof} F(t) : \dot{F}(t) = \int_{\Omega} f(t) \cdot \dot{\varphi}(t), \\ \int_{\Omega} (\operatorname{cof} F(t) : \dot{F}(t) + \epsilon \dot{p}(t)) p(t) = 0, \\ \int_{\Omega} -\nu D(t) : D(t) - \int_{\Omega} \frac{\partial \tilde{\mathcal{W}}}{\partial A} : \dot{A}(t) - \int_{\Omega} q(t) \operatorname{cof} A(t) : \dot{A}(t) = 0, \\ \int_{\Omega} (\operatorname{cof} A(t) : \dot{A}(t) - \eta \dot{q}(t)) q(t) = 0, \end{cases}$$

with the viscous deformation rate second order tensor :

$$D(t) = A(t)^{-1/2} \cdot \dot{A}(t) \cdot A(t)^{-1/2}.$$

By exploiting the time derivative of the incompressibility constraints, we deduce that :

$$\begin{cases} \int_{\Omega} \rho \ddot{\varphi}(t) \cdot \dot{\varphi}(t) + \int_{\Omega} \frac{\partial \tilde{\mathcal{W}}}{\partial C} : \dot{C}(t) + \epsilon \int_{\Omega} \dot{p}(t) p(t) = \int_{\Omega} f(t) \cdot \dot{\varphi}(t), \\ \int_{\Omega} \nu D(t) : D(t) + \int_{\Omega} \frac{\partial \tilde{\mathcal{W}}}{\partial A} : \dot{A}(t) + \eta \int_{\Omega} \dot{q}(t) q(t) = 0. \end{cases}$$

By summing these relations, we then get formally :

$$\begin{aligned} \frac{d}{dt} \left(\int_{\Omega} \rho \dot{\varphi}(t)^2 + \int_{\Omega} \tilde{\mathcal{W}}(C(t), A(t)) + \frac{\epsilon}{2} \int_{\Omega} p(t)^2 + \frac{\epsilon}{2} \int_{\Omega} q(t)^2 \right) \\ = \int_{\Omega} f(t) \cdot \dot{\varphi}(t) - \int_{\Omega} \nu D(t) : D(t), \end{aligned}$$

which gives the claimed energy conservation by time integration over $[0, t]$. Concerning angular and linear momenta, conservation is obtained with the same arguments as in the

proof of proposition 1. \square

Now, we propose a time integration scheme for the viscoelastic problem (3.70) respecting exactly the discrete energy conservation, and formulated as follows :

$$\begin{cases} \int_{\Omega} \rho \frac{\dot{\varphi}_{n+1} - \dot{\varphi}_n}{\Delta t_n} \cdot \hat{\varphi} + \int_{\Omega} \nu \left(\frac{A_n + A_{n+1}}{2} \cdot \frac{A_{n+1} - A_n}{\Delta t_n} \cdot \frac{A_n + A_{n+1}}{2} \right) : \hat{A} \\ + \mathcal{T}_{n+1/2}(\hat{\varphi}, \hat{A}) = \int_{\Omega} \frac{f_n + f_{n+1}}{2} \cdot \hat{\varphi}, \quad \forall (\hat{\varphi}, \hat{A}) \in \mathcal{U}_0 \times \mathcal{A}, \\ \int_{\Omega} (\det \nabla \varphi_{n+1} - 1 + \epsilon p_{n+1}) \hat{p} = 0, \quad \forall \hat{p} \in \mathcal{P}, \\ \int_{\Omega} (\det A_{n+1} - 1 - \eta q_{n+1}) \hat{q} = 0, \quad \forall \hat{q} \in \mathcal{Q}, \end{cases} \quad (3.71)$$

where the stress term $\mathcal{T}_{n+1/2}(\hat{\varphi}, \hat{A})$ is given for all $(\hat{\varphi}, \hat{A}) \in \mathcal{U}_0 \times \mathcal{A}$ by :

$$\begin{aligned} \mathcal{T}_{n+1/2}(\hat{\varphi}, \hat{A}) &= \\ 2 F_{n+1/2} \cdot \frac{\partial \tilde{\mathcal{W}}}{\partial C}(C_{n+1/2}, A_{n+1/2}) : \nabla \hat{\varphi} + \frac{\partial \tilde{\mathcal{W}}}{\partial A}(C_{n+1/2}, A_{n+1/2}) : \hat{A} \\ - 2 p_{n+1/2} F_{n+1/2} \cdot \frac{\partial \det C^{1/2}}{\partial C}(C_{n+1/2}) : \nabla \hat{\varphi} + q_{n+1/2} \operatorname{cof} A_{n+1/2} : \hat{A} \\ + \Delta t_n \left[\tilde{\mathcal{W}}(C_{n+1}, A_{n+1}) - \tilde{\mathcal{W}}(C_n, A_n) \right] \frac{2(\delta C_n : F_{n+1/2}^t \cdot \nabla \hat{\varphi}) + (\delta A_n : \hat{A})}{(\delta C_n : \delta C_n) + (\delta A_n : \delta A_n)} \\ - \Delta t_n \left[\frac{\partial \tilde{\mathcal{W}}}{\partial C}(C_{n+1/2}, A_{n+1/2}) : \delta C_n + \frac{\partial \tilde{\mathcal{W}}}{\partial A}(C_{n+1/2}, A_{n+1/2}) : \delta A_n \right] \times \\ \times \frac{2(\delta C_n : F_{n+1/2}^t \cdot \nabla \hat{\varphi}) + (\delta A_n : \hat{A})}{(\delta C_n : \delta C_n) + (\delta A_n : \delta A_n)} \\ - 2 p_{n+1/2} \left[\det C_{n+1}^{1/2} - \det C_n^{1/2} - \frac{\partial \det C^{1/2}}{\partial C}(C_{n+1/2}) : \delta C_n \right] \frac{\delta C_n : F_{n+1/2}^t \cdot \nabla \hat{\varphi}}{\delta C_n : \delta C_n} \\ + q_{n+1/2} \left[\det A_{n+1} - \det A_n - \operatorname{cof} A_{n+1/2} : \delta A_n \right] \frac{\delta A_n : \hat{A}}{\delta A_n : \delta A_n}. \end{aligned} \quad (3.72)$$

We have adopted the notation $\square_{n+1/2} = \frac{\square_n + \square_{n+1}}{2}$ and $\delta \square_n = \square_{n+1} - \square_n$, and the formulation is completed by Newmark's trapezoidal rule :

$$\frac{\varphi_{n+1} - \varphi_n}{\Delta t_n} = \frac{\dot{\varphi}_n + \dot{\varphi}_{n+1}}{2}.$$

The expression of $\mathcal{T}_{n+1/2}(\hat{\varphi}, \hat{A})$ given by (3.72) is a second order accurate approximation in time of the continuous expression :

$$\int_{\Omega} 2F \cdot \frac{\partial \mathcal{W}}{\partial C}(C, A) : \nabla \hat{\varphi} + \int_{\Omega} \frac{\partial \mathcal{W}}{\partial C}(C, A) : \hat{A},$$

at time $t_{n+1/2}$, and therefore the time integration scheme (3.71) is second order accurate. In the definition (3.72) of $\mathcal{T}_{n+1/2}(\hat{\varphi}, \hat{A})$, the four last lines correspond to energy correction terms enabling energy conservation in the way proposed by O. Gonzalez ([Gon00]).

We show the following conservation properties for (3.71) :

Proposition 3.9. *The discrete solution given by (3.71) satisfies the following discrete conservation properties :*

1. Discrete energy conservation.

$$\mathcal{E}_{n+1} - \mathcal{E}_n = \int_{\Omega} \frac{f_n + f_{n+1}}{2} \cdot \frac{\dot{\varphi}_n + \dot{\varphi}_{n+1}}{2} - \int_{\Omega} \nu D_{n+1/2} : D_{n+1/2},$$

with the discrete total energy :

$$\mathcal{E}_n = \frac{1}{2} \int_{\Omega} \rho \dot{\varphi}_n^2 + \int_{\Omega} \tilde{\mathcal{W}}(C_n, A_n) + \frac{\epsilon}{2} \int_{\Omega} p_n^2 + \frac{\eta}{2} \int_{\Omega} q_n^2,$$

and the discrete deformation rate tensor :

$$D_{n+1/2} = \left(\frac{A_n + A_{n+1}}{2} \right)^{1/2} \cdot \frac{A_{n+1} - A_n}{\Delta t_n} \cdot \left(\frac{A_n + A_{n+1}}{2} \right)^{1/2}.$$

2. Discrete angular and linear momenta conservations hold with the same expressions as in the hyperelastic case.

Proof : Energy conservation comes by taking $\hat{\varphi} = \frac{\varphi_{n+1} - \varphi_n}{\Delta t_n}$ and $\hat{A} = \frac{A_{n+1} - A_n}{\Delta t_n}$ in (3.71). By construction of $\mathcal{T}_{n+1/2}$, we get :

$$\begin{aligned} \mathcal{T}_{n+1/2} \left(\frac{\varphi_{n+1} - \varphi_n}{\Delta t_n}, \frac{A_{n+1} - A_n}{\Delta t_n} \right) &= \frac{1}{\Delta t_n} \int_{\Omega} \tilde{\mathcal{W}}(C_{n+1}, A_{n+1}) - \tilde{\mathcal{W}}(C_n, A_n) \\ &\quad - \frac{1}{\Delta t_n} \int_{\Omega} p_{n+1/2} \left(\det C_{n+1}^{1/2} - \det C_n^{1/2} \right) + \frac{1}{\Delta t_n} \int_{\Omega} q_{n+1/2} \left(\det A_{n+1} - \det A_n \right), \end{aligned}$$

and by using the quasi-incompressibility constraints :

$$\mathcal{T}_{n+1/2} \left(\frac{\varphi_{n+1} - \varphi_n}{\Delta t_n}, \frac{A_{n+1} - A_n}{\Delta t_n} \right) = \frac{1}{\Delta t_n} \int_{\Omega} \tilde{\mathcal{W}}(C_{n+1}, A_{n+1}) - \tilde{\mathcal{W}}(C_n, A_n)$$

$$+ \frac{\epsilon}{2\Delta t_n} \int_{\Omega} (p_{n+1}^2 - p_n^2) + \frac{\eta}{2\Delta t_n} \int_{\Omega} (q_{n+1}^2 - q_n^2).$$

As a consequence, we get :

$$\begin{aligned} & \int_{\Omega} \rho \frac{\dot{\varphi}_{n+1} - \dot{\varphi}_n}{\Delta t_n} \cdot \frac{\varphi_{n+1} - \varphi_n}{\Delta t_n} + \int_{\Omega} \nu D_{n+1/2} : D_{n+1/2} \\ & + \frac{1}{\Delta t_n} \int_{\Omega} \tilde{W}(C_{n+1}, A_{n+1}) - \tilde{W}(C_n, A_n) + \frac{\epsilon}{2\Delta t_n} \int_{\Omega} (p_{n+1}^2 - p_n^2) + \frac{\eta}{2\Delta t_n} \int_{\Omega} (q_{n+1}^2 - q_n^2) \\ & = \int_{\Omega} \frac{f_n + f_{n+1}}{2} \cdot \frac{\varphi_{n+1} - \varphi_n}{\Delta t_n}, \end{aligned}$$

with :

$$D_{n+1/2} = \left(\frac{A_n + A_{n+1}}{2} \right)^{1/2} \cdot \frac{A_{n+1} - A_n}{\Delta t_n} \cdot \left(\frac{A_n + A_{n+1}}{2} \right)^{1/2}.$$

We have used herein the fact that $\text{tr}(A \cdot B) = \text{tr}(B \cdot A)$ implying with $B = \left(\frac{A_n + A_{n+1}}{2} \right)^{1/2}$ that :

$$D_{n+1/2} : D_{n+1/2} = \text{tr} \left[\frac{A_n + A_{n+1}}{2} \cdot \frac{A_{n+1} - A_n}{\Delta t_n} \cdot \frac{A_n + A_{n+1}}{2} \cdot \frac{A_{n+1} - A_n}{\Delta t_n} \right].$$

The announced discrete energy conservation result is then straightforward by using Newmark's trapezoidal rule :

$$\frac{\varphi_{n+1} - \varphi_n}{\Delta t_n} = \frac{\dot{\varphi}_n + \dot{\varphi}_{n+1}}{2},$$

and a multiplication by Δt_n . Concerning discrete momenta conservation, the proof for Gonzalez scheme in the hyperelastic framework exactly applies. \square

3.7 Numerical experiment

In this section, we illustrate the analysis proposed in this chapter. First, the bad conservation of standard time integration schemes such as midpoint, trapezoidal and HHT is underlined when compare to the energy conserving strategy from [Gon00]. On the case of a ball impact against a wall, we validate numerically the proposed energy conserving formulation for frictionless contact, and the energy dissipating approach.

3.7.1 A simple cantilever beam

In this section, we illustrate numerically the previous analysis in the case of a bidimensional quasi-incompressible cantilever beam in plane displacements (figure 3.1). The elastic potential is given by the Mooney-Rivlin constitutive law :

$$\mathcal{W}(C) = c_1 (\text{tr } C - 3) + c_2 (\text{tr cof } C - 3).$$

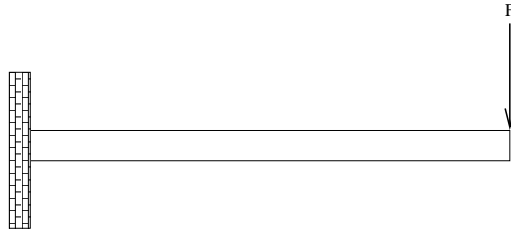


FIG. 3.1 – A cantilever beam with constant force F.

length	1 m
width	0.1 m
F	1000 N
ρ	1000 kg/m ³
c_1	2 MPa
c_2	0.2 MPa
$1/\epsilon$	2.E12 Pa
T	10 s
Δt	0.02 s
Newton's tolerance	1E-7

FIG. 3.2 – Physical data and numerical choices.

Data is presented on figure 3.2.

On the quadrangular mesh presented on figure 3.3, the discrete spaces \mathbb{Q}_1 and \mathbb{Q}_0 for displacements and pressures respectively are adopted. They are compatible in the sense that the following inf-sup condition relative to the linearized incompressibility constraint is satisfied (see [Bre74]) :

$$\exists \beta_h > 0, \quad \inf_{p \in \mathcal{P}, p \neq 0} \sup_{u \in \mathcal{U}_0, u \neq 0} \frac{\int_{\Omega} p \operatorname{div} u}{\|p\|_{L^2(\Omega)} \|u\|_{H^1(\Omega)^3}} \geq \beta_h,$$

provided the system is not fixed on its whole boundary, that is when the measure of $\partial\Omega \setminus \Gamma_D$ is strictly positive for the surfacic measure. The inf-sup constant β_h depends on the discretization and more precisely :

$$ch \leq \beta_h \leq Ch,$$

where c, C denote two constants independent of the discretization (see [GR86], page 164), and h is the diameter of the elements. A general description of the $\mathbb{Q}_1/\mathbb{Q}_0$ compatibility condition is presented in [Tal81].

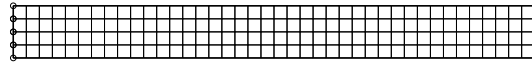


FIG. 3.3 – A 250 elements mesh of the beam.

Let f be a field of constant forces distributed on the tip of the cantilever beam whose resultant is :

$$F = \int_{\Omega} f.$$

Then, the field of forces f is derived from a potential and we ideally expect to observe the evolution of the following discrete quantity :

$$H_n = \int_{\Omega} f \cdot \varphi_n - \mathcal{E}_n.$$

The constant time step Δt is chosen so that to have approximatively 20 time steps per oscillation of the cantilever beam. With this value of Δt , 4 or 5 Newton's iterations per time step are necessary to solve the problem with the required accuracy (10^{-7} m) at least at the beginning of the simulation. Due to numerical instabilities, the number of Newton's iterations per time step can grow up ; the simulation is stopped when it exceeds 20.

Our first observation is that when H_n decreases (global increase of the energy of the system), the number of Newton's iterations per time step grows up until the method does not converge any more. As a consequence, trapezoidal, midpoint and HHT [HHT77] schemes cannot complete the simulation on the whole time interval $[0, T]$ for the specified parameters. Only the conservative Gonzalez scheme can achieve long term time integration without such an overcost.

Energy evolution is presented on figure 3.5. The worst energy conservation holds for the midpoint scheme, as shown in the previous analysis. With the selected parameters, HHT is globally energy growing. Gonzalez scheme is quasi-exactly conservative up to a very small error term depending on Newton's tolerance.

Concerning midpoint and trapezoidal schemes, the energy growth goes with numerical instabilities on velocities, as shown on figure 3.6.

To highlight the theoretical analysis done for the HHT scheme, figure 3.7 shows a zoom of energy evolution during one second of the dynamics, with displacements. It is worth noticing that in conformity with the analysis of (3.53), energy is dissipated when the beam goes up or down (acceleration of the dynamics) and grows when the deformation is in a neighborhood of the minimum or the maximum. This observation comes from the natural accelerations contribution in the natural energy \mathcal{E}^{HHT} of the scheme.

Moreover, concerning HHT scheme, it is difficult to adopt the right value of the dissipation parameter α . We have seen that the usual value $\alpha = 0.05$ proposed in [Cri97, HHT77] is not sufficient to ensure long term time integration in the nonlinear framework. At the opposite $\alpha = 0, 2$ entails overdissipation, as shown on figure 3.8.

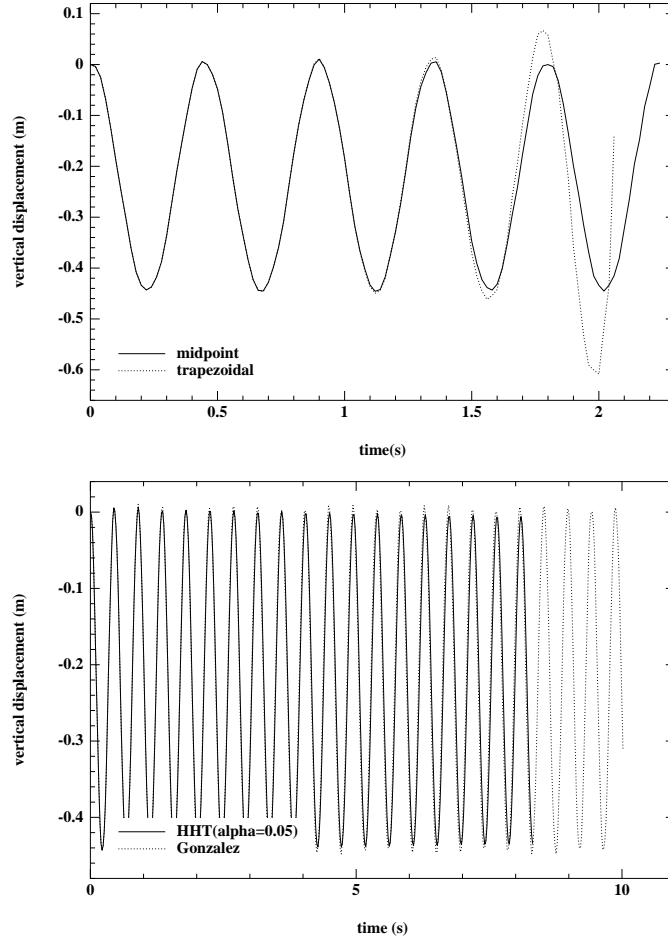


FIG. 3.4 – Vertical displacement of the tip of the cantilever beam. Simulation stops when the time step calculation exceeds 20 Newton’s iterations.

Remark 3.15. *The present numerical analysis holds for quasi-incompressible nonlinear elastodynamics, but the same phenomena can be observed in large displacements for compressible systems.*

3.7.2 Ball impact

For validation purposes concerning energy conservation for impact formulation, let us consider an axisymmetric ball with a small cylindrical hole as shown on figure 3.10, with data listed in figure 3.9.

Four snapshots of the impact simulation are shown on figure 3.11. As illustrated on figure

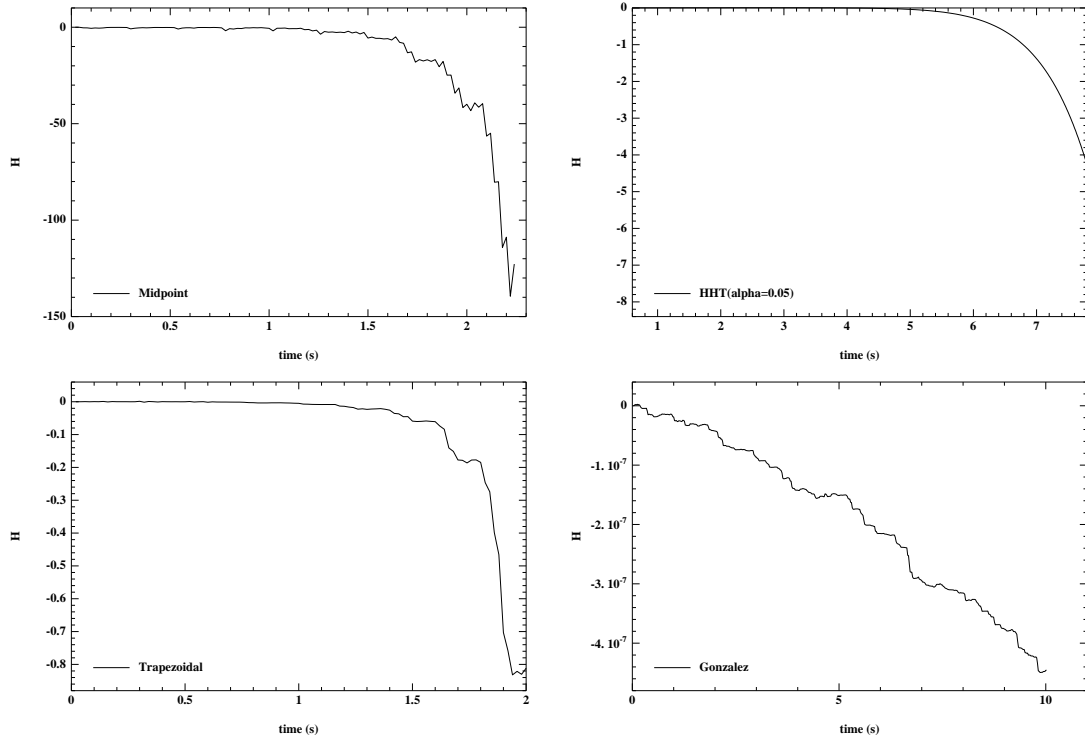


FIG. 3.5 – Evolution of the discrete total potential H (in Joules) as a function of time. As an indication, the maximal value of the deformation potential $\int_{\Omega} \mathcal{W}(C)$ is about 0.5 Joules.

3.12, the evolution of discrete energy in the ball during the dynamics is very sensitive to the time integration strategy.

In particular, the discrete energy explodes when using a midpoint scheme (or a trapezoidal scheme), and the deformation of the ball just before energy explosion is shown on figure 3.13. In particular, non-physical irregular displacements can be noticed around the hole. The conservative Gonzalez scheme enriched with our energy conserving impact formulation keeps its promise and the relative loss of energy through the impact is 1.8 E-4, only depending on the required accuracy in Newton's algorithm. The interest of our energy dissipative formulation is also confirmed, showing here the control of the mechanical energy in the ball. To complete this discussion, let us mention that when considering practical industrial use of time integration schemes for non-smooth dynamics, first order implicit schemes are sometimes preferred for their robustness. The best proof is the frequent use of implicit Euler strategies in coupled systems [TM01, GLB03]. In order to compare energy evolution when using first order strategy, we introduce the following time integration approach, obtained by a trapezoidal integration of the inertial term, and an implicit Euler

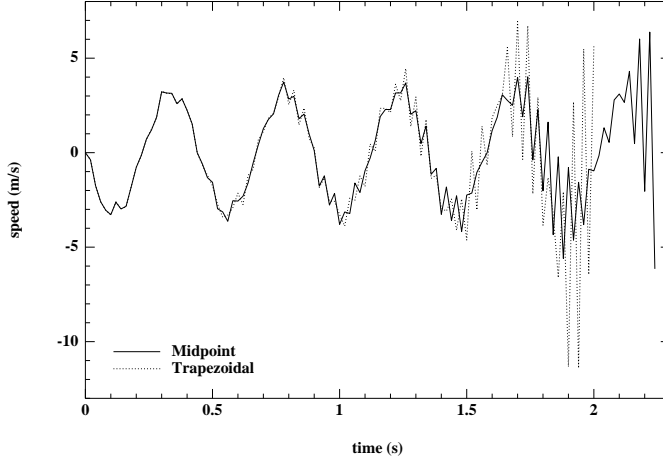


FIG. 3.6 – Instability of the vertical velocity at the tip of the cantilever beam, for midpoint and trapezoidal schemes.

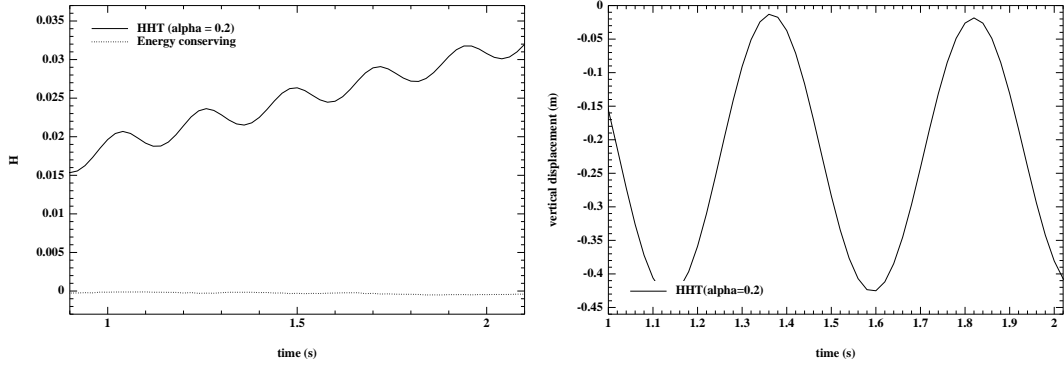


FIG. 3.7 – Zoom on total discrete potential and displacement for HHT scheme ($\alpha = 0.2$).

strategy for the stress part :

$$\begin{cases} \int_{\Omega} \rho \frac{\dot{\varphi}_{n+1} - \dot{\varphi}_n}{\Delta t_n} \cdot v + \int_{\Omega} \frac{\partial \hat{W}}{\partial F}(\nabla \varphi_{n+1}) : \nabla v = \int_{\Omega} \frac{f_n + f_{n+1}}{2} \cdot v, & \forall v \in \mathcal{U}_0, \\ \frac{\varphi_{n+1} - \varphi_n}{\Delta t_n} = \frac{\dot{\varphi}_n - \dot{\varphi}_{n+1}}{2}, \end{cases} \quad (3.73)$$

written here in the compressible framework. The kinematical constraint will be naturally satisfied by the displacements field φ_{n+1} at time t_{n+1} . It is a Euler-like degraded first order version of the trapezoidal second order time integration scheme. It can be readily checked with the analysis of section 4, that the Euler-Newmark scheme (3.73) is energy dissipating

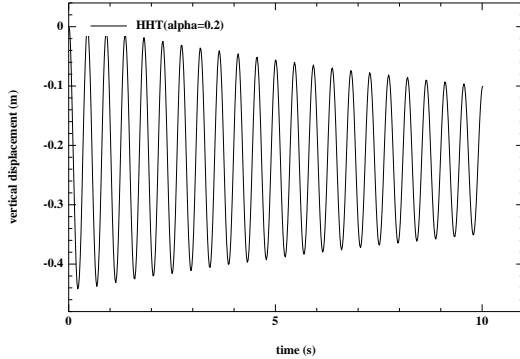


FIG. 3.8 – Overdissipation for vertical displacement at the tip of the beam for HHT scheme ($\alpha = 0.2$).

radius	0.1 m
density	1200 kg/m^3
Young's modulus	0.2 M Pa
Poisson's ratio	0.33
initial distance of the center of the ball to the wall	0.12 m
initial velocity	0.4 m/s
η	1.E-4
time step	0.002 s
T	1.0 s
# nodes in the mesh	11.160

FIG. 3.9 – Data for ball impact, made of a Saint-Venant Kirchhoff material.

whenever the stored energy $\hat{\mathcal{W}}(F)$ is locally convex. The ball impact simulation performed with this scheme proves to achieve global energy dissipation, with a 9 % relative loss of energy through the impact. To illustrate the better accuracy of our second order energy conserving/dissipating schemes, the figure 3.14 illustrates the evolution of elastic energy after impact.

A noticeable statement is that the computation of contact pressures is relatively independent of the considered scheme for the simulation, as illustrated on figure 3.15.

Finally, we use the present example to illustrate the well known sensitivity of contact pressures in the penalization coefficient η . Indeed, it is shown on figure 3.16 that when η is divided by 10, oscillations on the contact force appear. This phenomenon can be explained by the absence of strong limit for the linearized dynamics as η goes to zero (see for example [Sca04]) in the absence of viscosity. Such oscillations are typical of weak limits in two-scale

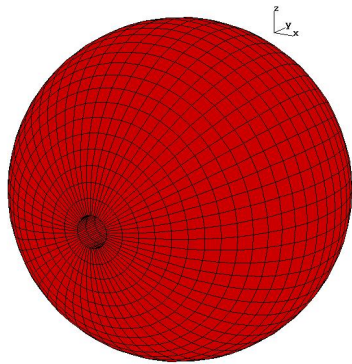


FIG. 3.10 – Mesh of the ball.

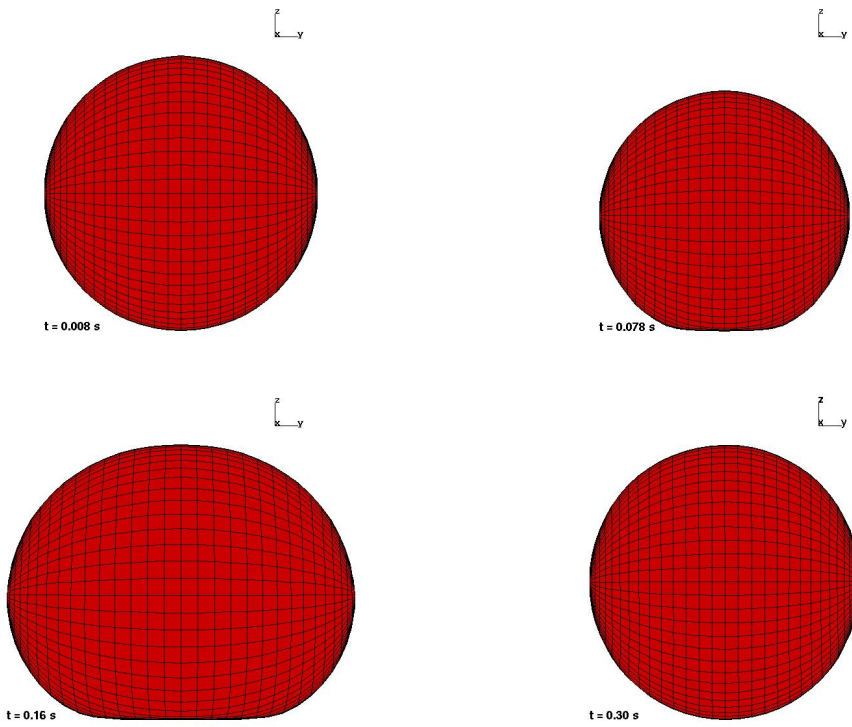


FIG. 3.11 – Snapshots of the impact simulation.

problems, as in [BLP78, All97]. The phenomenon is even much more visible in the case of a cube impact, described on figure (3.17).

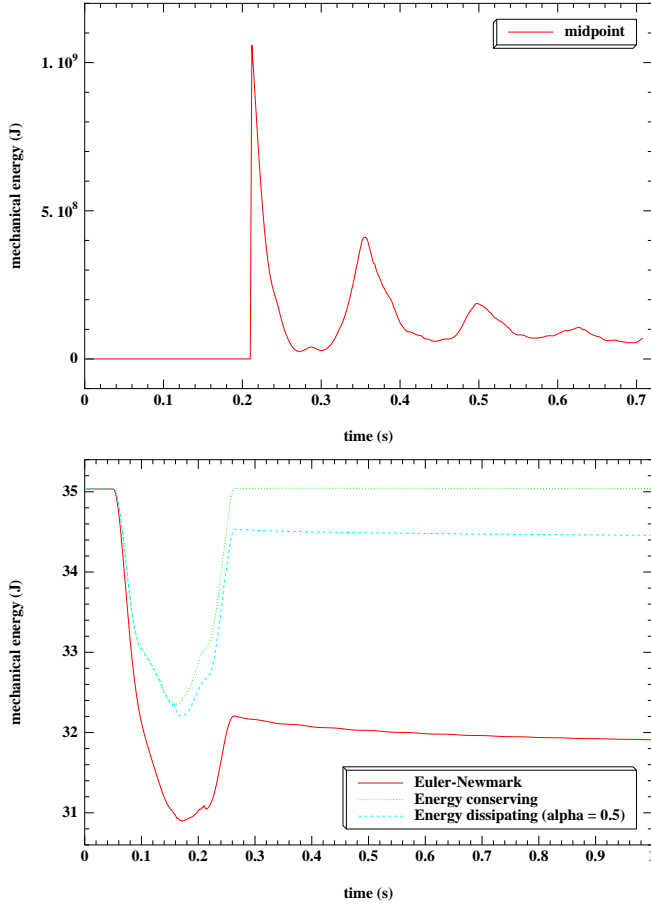


FIG. 3.12 – Evolution of the ball mechanical energy through impact for midpoint, Euler-Newmark, energy conserving, and dissipating ($\alpha = 0.5$) schemes.

From a mathematical point of view, the presence of viscosity enables to obtain compacity, enabling the possibility to build a converging sequence of solutions as $\eta \rightarrow 0$. From a physical point of view, viscosity would enable the dissipation of high frequency vibrations. In [AP98], the authors propose the enforcement of the persistency condition (3.67) at entire time steps in their formulation, then adding an energy term associated with this constraint. An alternative could consist in introducing a real internal viscoelastic behavior of the material in the structures. In this framework, the “conserving” scheme proposed in the viscoelastic framework could be exploited.

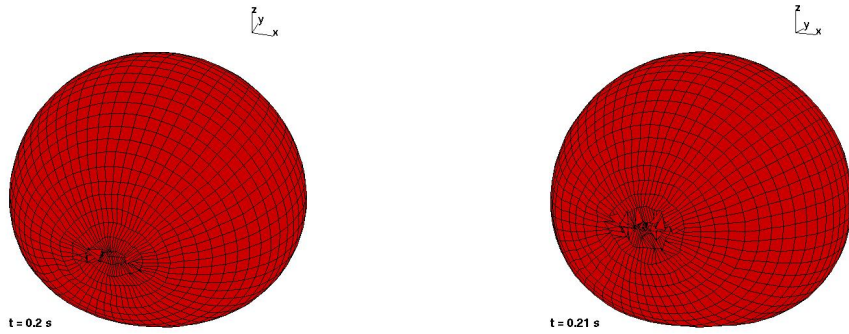


FIG. 3.13 – Snapshots at times $t = 0.2$ and 0.21 s, illustrating the deformation of the ball before energy explosion when using a midpoint time integration scheme.

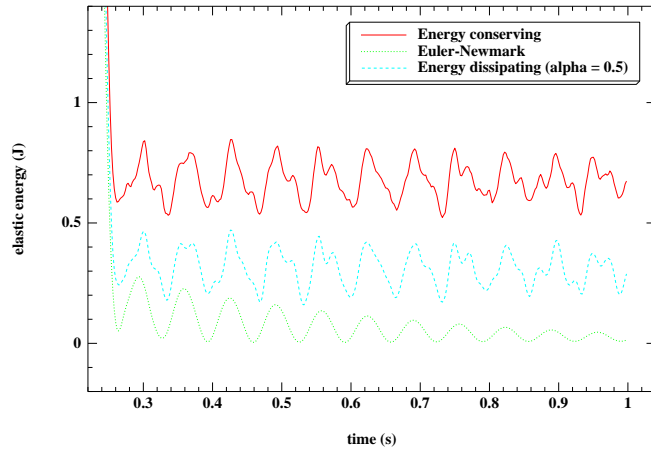


FIG. 3.14 – Evolution of elastic energy after impact for first order accuracy Euler-Newmark scheme, and second order accuracy energy conserving and dissipating ($\alpha = 0.5$) schemes.

3.8 Conclusion

In this chapter, we have proposed a detailed analysis of the non-conservative contributions of midpoint, trapezoidal and HHT time integration schemes in incompressible nonlinear elasticity, and compared it to an energy conserving scheme. Moreover, we have used the analysis done for the HHT method, to propose a new energy dissipative discrete integration in the nonlinear framework, involving a regularized energy taking small acceleration effects into account. Finally, by generalizing Gonzalez' energy correction method [Gon00], we have proposed a conservative strategy for penalized frictionless impact

enforcing the usual Kuhn-Tucker conditions at entire time steps. The analysis of these techniques is illustrated with numerical simulations. An extension to viscoelasticity is also proposed.

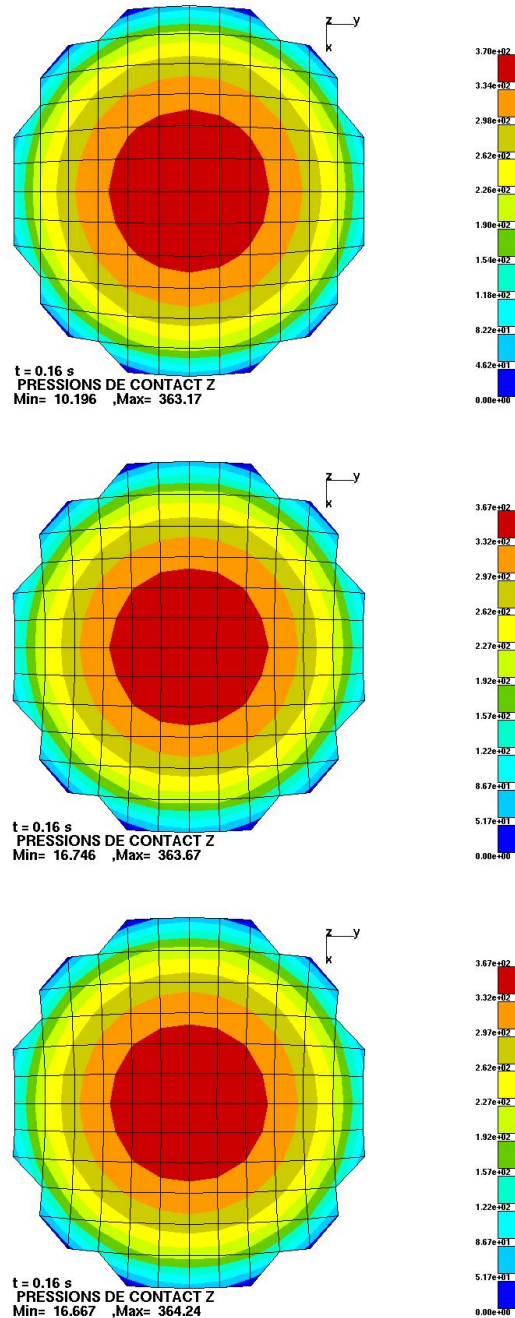


FIG. 3.15 – Contact pressures computed at time $t = 0.16 \text{ s}$, when energy penetration is maximal, for Euler-Newmark, midpoint and energy-conserving schemes.

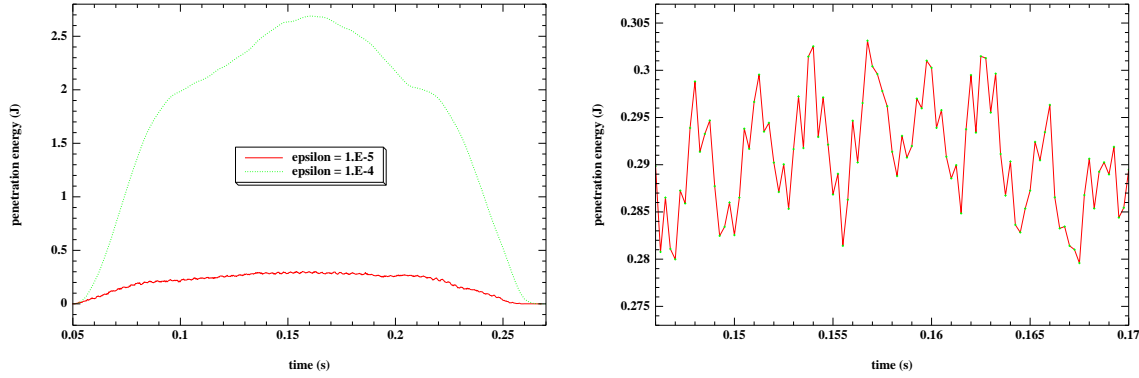


FIG. 3.16 – Evolution of penetration energy during ball impact for $\eta = 1.E-4$ and $\eta = 1.E-5$ (left), and zoom on the oscillations for $\epsilon = 1.E-5$ (right).

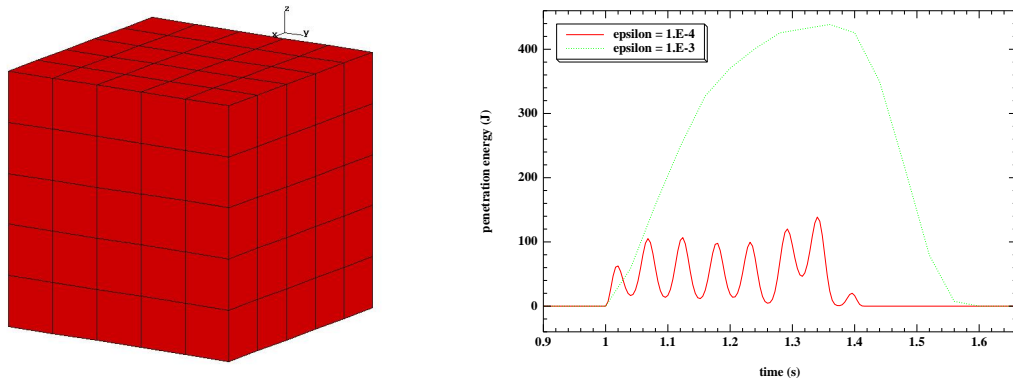


FIG. 3.17 – Oscillations of penetration energy for a cube impact problem, as the penalization coefficient η decrease.

Chapitre 4

A stabilized discontinuous mortar formulation for elastostatics and elastodynamics problems

Résumé

Dans ce chapitre, nous introduisons et analysons une formulation mortier stabilisée utilisant des multiplicateurs de Lagrange discontinus, pour des approximations aux éléments finis d'ordre 1 et 2 de la solution de problèmes d'élasticité linéarisée. Cette approche s'inscrit dans la continuité de Brezzi et Marini [BM00] qui utilisent de tels multiplicateurs pour une formulation dite à trois champs dans le cadre de problèmes elliptiques scalaires. Dans le cas d'un grand nombre de sous-domaines, nous montrons en outre l'indépendance de la constante de coercivité de la forme bilinéaire associée au problème d'élastostatique non-conforme par rapport au nombre de sous-domaines considérés et à leur taille, par extension au cas d'interfaces courbes des idées de Gopalakrishnan et Brenner [Gop99, Bre03, Bre04], et généralisation de l'opérateur d'interpolation de Scott et Zhang [SZ90]. De plus, nous rappelons la convergence optimale de la méthode en élastostatique linéarisée en utilisant les outils de Wohlmuth [Woh01], et procédons à une extension au cas de l'élastodynamique. Enfin, des choix concrets d'espaces sont proposés, les détails pratiques de mise en oeuvre sont indiqués, et des tests numériques viennent illustrer la présente analyse.

Abstract

We introduce and analyze first and second order stabilized discontinuous two-field mortar formulations for linearized elasticity problems, following the stabilization technique of Brezzi and Marini [BM00] introduced in the scalar elliptic case for a three-field formulation. By extension to the curved interfaces case of the ideas from Gopalakrishnan and Brenner [Gop99, Bre03, Bre04], and from the introduction a generalized Scott and Zhang interpolation operator [SZ90], we prove the independence of the coercivity constant of the broken elasticity bilinear form with respect to the number and the size of the subdomains. Moreover, we prove the optimal convergence of the method by mesh refinement by using the tools from Wohlmuth [Woh01] in the elastostatic case, and extend the result to the elastodynamic framework. Finally, we detail practical issues and present numerical tests to illustrate the present analysis.

4.1 Introduction

In this paper, we introduce, analyze and test a non-conforming formulation using stabilized discontinuous mortar elements to find the vector solution u of linearized elasticity problems such as :

$$\begin{cases} -\operatorname{div}(\mathbf{E} : \varepsilon(u)) = f, & \Omega \subset \mathbb{R}^d, (d = 2, 3) \\ u = 0, & \Gamma_D, \\ (\mathbf{E} : \varepsilon(u)) \cdot n = g, & \Gamma_N, \end{cases} \quad (4.1)$$

where the linearized strain tensor is classically given by :

$$\varepsilon(u) = \frac{1}{2} (\nabla u + \nabla^t u),$$

and the fourth order elasticity tensor \mathbf{E} is assumed to be elliptic over the set of symmetric matrices :

$$\exists \alpha > 0, \forall \xi \in \mathbb{R}^{d \times d}, \xi^t = \xi, \quad (\mathbf{E} : \xi) : \xi \geq \alpha \xi : \xi.$$

The analysis is also extended to the elastodynamics problem :

$$\begin{cases} \rho \frac{\partial^2 u}{\partial t^2} - \operatorname{div}(\mathbf{E} : \varepsilon(u)) = f, & [0, T] \times \Omega, \\ u = 0, & [0, T] \times \Gamma_D, \\ (\mathbf{E} : \varepsilon(u)) \cdot n = g, & [0, T] \times \Gamma_N, \\ u = u_0, & \{0\} \times \Omega, \\ \frac{\partial u}{\partial t} = \dot{u}_0, & \{0\} \times \Omega, \end{cases} \quad (4.2)$$

and we consider this analysis as a theoretical background for using discontinuous mortar elements in nonlinear elastodynamics.

Mortar methods have been introduced for the first time in [BMP93, BMP94] as a weak coupling between subdomains with nonconforming meshes, or between subproblems solved with different approximation methods. The main purpose was to overcome the very sub-optimal “ \sqrt{h} ” error estimate obtained with pointwise matching. The analysis of this method as a mixed formulation was first made in [Bel99].

Nevertheless, in spite of the optimal error convergence obtained with the original mortar elements, some numerical difficulties appear. First, the original space of Lagrange multipliers ensuring the weak coupling is rather difficult to build in 3D on the boundary of the interfaces when more than two subdomains have a common intersection (see [BM97, BD98]). Moreover, the original constrained space has a non-local basis on the non-conforming artificial interfaces, which may lead to small spurious oscillations of the approximate solution.

To overcome the first difficulty, one idea is given in [Ses98] when displacements are at least approximated by second order polynomials. The introduced Lagrange multipliers have a lower order, still enabling optimal error estimates, and no special treatment is needed on the boundary of the interfaces. To overcome the second difficulty, dual mortar spaces are proposed in [Woh00, Woh01], enabling the localization of the mortar kinematical constraint. In order to benefit from the advantages of these two approaches, we propose to introduce stabilized low order discontinuous mortar elements. This idea has already been introduced for a first order three-field mortar formulation in [BM00], and we exploit it herein in the two-field framework for first and second order elements when dealing with elastostatics and elastodynamics problems.

Mortar formulations also provide a natural framework for domain decomposition, as observed by [Tal93, AKP95, AMW99, AAKP99, Ste99] and the references therein. A large number of subdomains and their small size is therefore a basic difficulty to overcome. To get an optimal use of such domain decomposition methods, it is then crucial that the constants arising in the analysis of the mortar formulation remain independent (or at least weakly dependent) on the number and the size of the subdomains. One can readily check that the only potential dependence on such parameters is hidden in the coercivity constant of the broken bilinear form associated to the linearized elastostatics problem. In the framework of elliptic scalar problems, both [Gop99, Bre03] and [BM00] have shown the independence of the coercivity constant with respect to the number and the size of the subdomains, respectively when considering two and three-field mortar formulations with plane interfaces. An extension to the vector elasticity case has been proposed by [Bre04]. By definition of a generalized Scott and Zhang [SZ90] interpolation operator, we simplify and extend herein the result to potentially curved interfaces.

In section 2, the fundamental assumptions and results arising in mortar element methods to approximate the solution of the elastostatics problem (4.1) are recalled. Well-posedness results are recalled in section 3. Moreover, we prove in section 4, the indepen-

dence of the coercivity constant with respect to the number and the size of the subdomains. In section 5, we recall the optimal convergence of the method by mesh refinement, and generalize the analysis to the elastodynamics problem (4.2) in section 6. We propose in section 7 the analysis of stabilized discontinuous mortar elements, proving the satisfaction of the fundamental assumptions. In section 8, some practical issues are pointed out : the choice of an appropriate penalization term, and the exact integration of the constraint. We present numerical tests in section 9 to confirm the previous analysis.

4.2 Nonconforming setting

4.2.1 Position of the problem

Let $\Omega \subset \mathbb{R}^d$ ($d = 2, 3$), be an open set partitioned into K subsets $(\Omega_k)_{1 \leq k \leq K}$. We denote by $\gamma_{kl} = \overline{\Omega_k} \cap \overline{\Omega_l}$ the interface between Ω_k and Ω_l , and the skeleton of the internal interfaces is denoted by $\mathcal{S} = \bigcup_{k,l \geq 1} \gamma_{kl}$. On the part Γ_D of the boundary $\partial\Omega$, an homogeneous Dirichlet boundary condition is imposed. Concerning the coefficients of the fourth order elasticity tensor \mathbf{E} , we assume that the stress tensor is symmetric whatever the deformation is in the material, namely for almost all $x \in \Omega$:

$$\forall \xi \in \mathbb{R}^{d \times d}, \xi^t = \xi, \quad \mathbf{E}(x) : \xi \text{ is a symmetric matrix.}$$

Moreover, in the theoretical analysis, we will suppose that for all $k \geq 1$, there exists two constants c_k and C_k , such that for almost all $x \in \Omega_k$:

$$\forall \xi \in \mathbb{R}^{d \times d}, \xi^t = \xi, \quad c_k \xi : \xi \leq (\mathbf{E}(x) : \xi) : \xi \leq C_k \xi : \xi. \quad (4.3)$$

If the material of the subdomain Ω_k has a Young modulus E_k , both c_k and C_k are proportional to E_k .

We introduce the following spaces :

$$H_*^1(\Omega) = \{v \in H^1(\Omega)^d, v|_{\Gamma_D} = 0\},$$

$$H_*^1(\Omega_k) = \{v \in H^1(\Omega_k)^d, v|_{\Gamma_D \cap \partial\Omega_k} = 0\},$$

$$X = \left\{ v \in L^2(\Omega)^d, \quad v_k = v|_{\Omega_k} \in H_*^1(\Omega_k), \forall k \right\} = \prod_{k=0}^K H_*^1(\Omega_k),$$

X being endowed with the H^1 broken norm :

$$\|v\|_X = \left(\sum_{k=0}^K \|v\|_{H^1(\Omega_k)^d}^2 \right)^{\frac{1}{2}}.$$

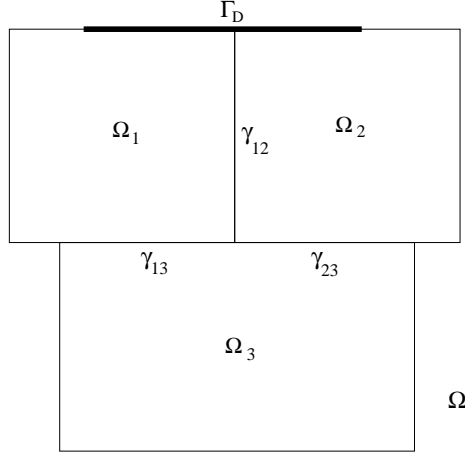


FIG. 4.1 – A decomposition of Ω into subdomains.

Here, in order to be scale independent when dealing with a large number of subdomains, we use a scale invariant definition of the H^1 norm :

$$\|v\|_{H^1(\Omega_k)^d}^2 = \frac{1}{(L_k)^2} \|v\|_{L^2(\Omega_k)^d}^2 + \|\nabla v\|_{L^2(\Omega_k)^{d \times d}}^2,$$

L_k being a characteristic length of Ω_k , for instance its diameter.

We are interested in finding $u \in H_*^1(\Omega)$ such that :

$$a(u, v) = l(v), \quad \forall v \in H_*^1(\Omega), \tag{4.4}$$

where the continuous coercive bilinear form a is defined by :

$$a(u, v) = \int_{\Omega} (\mathbf{E} : \boldsymbol{\varepsilon}(u)) : \boldsymbol{\varepsilon}(v), \quad \forall u, v \in H_*^1(\Omega),$$

and the continuous linear form l by :

$$l(v) = \int_{\Omega} f \cdot v + \int_{\Gamma_N} g \cdot v, \quad \forall v \in H_*^1(\Omega).$$

This problem is classically well-posed by Lax-Milgram lemma, the Korn's inequality (see [DL72]) ensuring the coercivity of the bilinear form a over $H_*^1(\Omega) \times H_*^1(\Omega)$.

4.2.2 Discretization

We introduce here a non-conforming discretization of the problem (4.4) using mortar elements to be further defined later on. The discrete problem is proved to be well-posed and error estimates are derived in the mesh-dependent norms already introduced and used in [AT95, Woh99]. Some useful elementary trace and lifting results for the related mesh-dependent spaces are reviewed and detailed in appendix 4.10.

The mesh

For each $1 \leq k \leq K$, we consider a family of shape regular *affine meshes* $(\mathcal{T}_{k;h_k})_{h_k>0}$ on the subdomain Ω_k . This means that each element T is the image of a reference element \hat{T} by an affine mapping J_T . For each $T \in \mathcal{T}_{k;h_k}$, we will denote its diameter :

$$h(T) = \text{diam}(T),$$

and the local mesh size by :

$$h_k = \sup_{T \in \mathcal{T}_{k;h_k}} h(T).$$

Then, a nonconforming family of domain based meshes $(\mathcal{T}_h)_{h>0}$ over Ω is obtained by :

$$\mathcal{T}_h = \bigcup_{k=1}^K \mathcal{T}_{k;h_k}, \quad h = \max_{1 \leq k \leq K} h_k.$$

The skeleton $\mathcal{S} = \bigcup_{k,l \geq 1} \gamma_{kl}$ is partitioned into M interfaces $(\Gamma_m)_{1 \leq m \leq M}$, and can then be decomposed as $\mathcal{S} = \bigcup_{1 \leq m \leq M} \Gamma_m$. Moreover, we assume that for each $1 \leq m \leq M$, there exists at least one domain Ω_k with $k \geq 1$ such that $\Gamma_m \subset \partial\Omega_k$, and denote $k(m) := k$ the name of one of these subdomains, taken once for all for each interface. This side will said to be the non-mortar (or slave) side.

For each $1 \leq m \leq M$, Γ_m inherits a family of meshes $(\mathcal{F}_{m;\delta_m})_{\delta_m>0}$, obtained as the trace of the volumic mesh $(\mathcal{T}_{k(m);h_{k(m)}})_{h_{k(m)}>0}$ of the slave subdomain over Γ_m . We have denoted by :

$$\delta_m = \sup_{F \in \mathcal{F}_{m;\delta_m}} h(F).$$

We also denote by $\bar{\delta}_m$ the size of the mesh on the mortar side :

$$\bar{\delta}_m = \sup_{T \in \mathcal{T}_{l;h_l}, l \neq k(m)} \text{diam}(T \cap \Gamma_m).$$

Then, a family of interface meshes $(\mathcal{F}_\delta)_{\delta>0}$ can be defined over \mathcal{S} by :

$$\mathcal{F}_\delta = \bigcup_{m=1}^M \mathcal{F}_{m;\delta_m}, \quad \delta = \max_{1 \leq m \leq M} \delta_m.$$

For each $F \in \mathcal{F}_{m;\delta_m}$, we denote by $T(F) \in \mathcal{T}_{k(m);h_{k(m)}}$ the unique element $T \in \mathcal{T}_{k(m);h_{k(m)}}$ such that $T \cap \mathcal{S} = F$.

Moreover, the following assumption is made :

Assumption 4.1. $F \in \mathcal{F}_\delta$ is always an entire face of $T(F) \in \mathcal{T}_h$.

In other words, the construction of the interfaces $(\Gamma_m)_{1 \leq m \leq M}$ respects the mesh of the slave sides. An example of situation obeying to assumption 1 is given on figure 4.2.

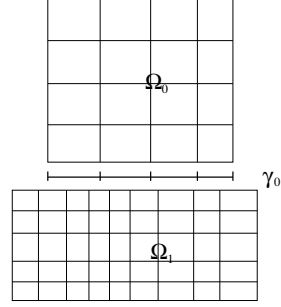


FIG. 4.2 – A situation where the mesh $\mathcal{F}_{1;\delta_1}$ of the interface γ_{01} is inherited from the mesh $\mathcal{T}_{0;h_0}$ of Ω_0 . The assumption 1 would be violated if at the opposite, Ω_1 were the slave side.

Remark 4.1. *For simplicity, the mesh is assumed to be affine but the following results are still valid for regular quasi-uniform quadrangular meshes, at least in 2D (see [GR86]). In fact, the only assumptions to satisfy are the following standard inequalities :*

$$\begin{cases} |\hat{w}|_{H^m(\hat{K})} \leq C \operatorname{diam}(K)^m \operatorname{meas}(K)^{-\frac{1}{2}} |w|_{H^m(K)}, \\ |w|_{H^m(K)} \leq C \operatorname{diam}(K)^{-m} \operatorname{meas}(K)^{\frac{1}{2}} |\hat{w}|_{H^m(\hat{K})}, \end{cases}$$

between the semi-norms of the function w defined on a mesh-element K and its transformation \hat{w} defined on the corresponding reference element \hat{K} .

Remark 4.2. *In the following sections, C will stand for various constants independent of the discretization.*

Interface mesh-dependent spaces

We define here some mesh-dependent trace spaces, endowed with useful mesh-dependent norms already introduced and used in [AT95, Woh99]. For each $1 \leq m \leq M$, they are defined by :

$$\mathbb{H}_\delta^{1/2}(\Gamma_m) = \{\phi \in L^2(\Gamma_m)^d, \|\phi\|_{\delta,\frac{1}{2},m}^2 = \sum_{F \in \mathcal{F}_{m;\delta_m}} \frac{1}{h(F)} \|\phi\|_{L^2(F)^d}^2 < +\infty\},$$

$$\mathbb{H}_\delta^{-1/2}(\Gamma_m) = \{\lambda \in L^2(\Gamma_m)^d, \|\lambda\|_{\delta,-\frac{1}{2},m}^2 = \sum_{F \in \mathcal{F}_{m;\delta_m}} h(F) \|\lambda\|_{L^2(F)^d}^2 < +\infty\},$$

endowed respectively with the norms $\|\cdot\|_{\delta,\frac{1}{2},m}$ and $\|\cdot\|_{\delta,-\frac{1}{2},m}$. The product spaces $\mathbb{W}_\delta = \prod_{k=1}^K \mathbb{H}_\delta^{1/2}(\Gamma_m)$ and $\mathbb{M}_\delta = \prod_{k=1}^K \mathbb{H}_\delta^{-1/2}(\Gamma_m)$, are then respectively endowed with the

norms :

$$\|\phi\|_{\delta, \frac{1}{2}} = \left(\sum_{m=1}^M \|\phi\|_{\delta, \frac{1}{2}, m}^2 \right)^{1/2},$$

$$\|\lambda\|_{\delta, -\frac{1}{2}} = \left(\sum_{m=1}^M \|\lambda\|_{\delta, -\frac{1}{2}, m}^2 \right)^{1/2}.$$

They can be viewed as dual spaces by means of the the L^2 inner product :

$$\int_S \phi \cdot \lambda \leq \|\lambda\|_{\delta, -\frac{1}{2}} \|\phi\|_{\delta, \frac{1}{2}}, \quad \forall (\phi, \lambda) \in \mathbb{W}_\delta \times \mathbb{M}_\delta. \quad (4.5)$$

Some elementary results about these spaces can be found in appendix. Their advantage is that the corresponding norms are easily computable, enabling a posteriori estimates [Woh99] and efficient penalization strategies as shown in section 5.

4.2.3 Approximate problem

Nonconforming formulation

Let us define the discrete subspaces of degree q inside each subdomain :

$$X_{k;h_k} = \{p \in H_*^1(\Omega_k) \cap \mathcal{C}^0(\Omega_k)^d, \quad p|_T \in \mathcal{P}_q(T), \forall T \in \mathcal{T}_{k;h_k}\} \oplus \mathcal{B}_{k;h_k},$$

with $\mathcal{P}_q = [\mathbb{P}_q]^d$ or $[\mathbb{Q}_q]^d$. We have denoted by \mathbb{P}_q (resp. \mathbb{Q}_q) the space of polynomials of total (resp. partial) degree q , and have introduced the possibility of adding a space $\mathcal{B}_{k;h_k}$ of interface bubble stabilization to be constructed later on. The corresponding product space is denoted by :

$$X_h = \prod_{k=0}^K X_{k;h_k} \subset X.$$

We introduce the following trace spaces on the non-mortar side :

$$W_{m;\delta_m} = \{p|_{\Gamma_m}, p \in X_{k(m);h_{k(m)}}\}, \quad W_{m;\delta_m}^0 = W_{m;\delta_m} \cap H_0^1(\Gamma_m)^d,$$

and the corresponding product space $W_\delta^0 = \prod_{m=1}^M W_{m;\delta_m}^0$ endowed with the mesh-dependent norm $\|\cdot\|_{\delta, \frac{1}{2}}$.

In order to formulate the weak continuity constraint, the following spaces of discontinuous Lagrange multipliers are defined :

$$M_{m;\delta_m} = \{p \in L^2(\Gamma_m)^d, \quad p|_F \in \mathcal{P}_{q-1}(F), \forall F \in \mathcal{F}_{m,\delta_m}\}, \quad (4.6)$$

as well as the product space $M_\delta = \prod_{m=1}^M M_{m;\delta_m}$, endowed with the mesh-dependent norm $\|\cdot\|_{\delta,-\frac{1}{2}}$ and $M = \prod_{m=1}^M L^2(\Gamma_m)^d$. The following continuous bilinear form is then introduced to impose interface weak continuity :

$$\begin{aligned} b : X \times M &\rightarrow \mathbb{R} \\ (v, \lambda) &\mapsto b(v, \lambda) = \sum_{m=1}^M \int_{\Gamma_m} [v]_m \cdot \lambda_m, \end{aligned}$$

with $[v]_m = v_{k(m)} - v_l$, on $\gamma_{k(m)l} \subset \Gamma_m$. Then, the constrained space of discrete unknowns can be defined as :

$$V_h = \{u_h \in X_h, b(u_h, \lambda_h) = 0, \forall \lambda_h \in M_\delta\}.$$

In order to formulate the non-conforming approximate problem, it is standard to consider the broken elliptic form :

$$\begin{aligned} \tilde{a} : X \times X &\rightarrow \mathbb{R} \\ (u, v) &\mapsto \tilde{a}(u, v) = \sum_{k=1}^K a_k(u_k, v_k), \end{aligned}$$

with :

$$a_k(u_k, v_k) = \int_{\Omega_k} (\mathbf{E} : \boldsymbol{\varepsilon}(u_k)) : \boldsymbol{\varepsilon}(v_k).$$

We are then interested in finding $(u_h, \lambda_h) \in X_h \times M_\delta$, such that :

$$\begin{cases} \tilde{a}(u_h, v_h) + b(v_h, \lambda_h) = l(v_h), & \forall v_h \in X_h, \\ b(u_h, \mu_h) = 0, & \forall \mu_h \in M_\delta. \end{cases} \quad (4.7)$$

In other words, we solve our variational problem on the product space X_h under the kinematic continuity constraint $b(\cdot, \cdot) = 0$.

Remark 4.3. *The theory proposed herein also applies to situations involving continuous Lagrange multipliers defined on spaces like :*

$$M_{m;\delta_m} = \{p \in \mathcal{C}^0(\Gamma_m), p|_F \in \mathcal{P}_q(F), \forall F \in \mathcal{F}_{m;\delta_m}\}.$$

Fundamental assumptions

In order to ensure the well-posedness of the problem (4.7), some fundamental assumptions have to be made. Concerning the compatibility of X_h and M_δ , we assume :

Assumption 4.2. For each interface $1 \leq m \leq M$, there exists an operator :

$$\pi_m : \mathbb{H}_\delta^{1/2}(\Gamma_m) \rightarrow W_{m;\delta_m}^0,$$

such that for all $v \in \mathbb{H}_\delta^{1/2}(\Gamma_m)$:

$$\int_{\Gamma_m} (\pi_m v) \cdot \mu = \int_{\Gamma_m} v \cdot \mu, \quad \forall \mu \in M_{m;\delta_m},$$

with :

$$\|\pi_m v\|_{\delta, \frac{1}{2}, m} \leq C_m \|v\|_{\delta, \frac{1}{2}, m}.$$

This assumption means that the projection perpendicular to the multiplier space onto the trace space $W_{m;\delta_m}^0$ with zero extension is continuous. This assumption will have to be checked for each choice of discretization. Its major consequence lies in the fact that the weak-continuity constraint is onto, as shown in the next section.

Concerning the coercivity of \tilde{a} over $V \times V$, where V is a constrained subspace of X to be defined in that section, we have to consider Lagrange multipliers spaces which are sufficiently rich on the interfaces to kill local rigid motions, which are defined by :

Definition 4.1. A displacement field $r \in H^1(\Omega)^d$ over $\Omega \subset \mathbb{R}^d$ is said to be a rigid motion of Ω iff :

$$\int_{\Omega} \varepsilon(r) : \varepsilon(w) = 0, \quad \forall w \in H^1(\Omega)^d,$$

which we denote $r \in \mathcal{R}(\Omega)$.

For that purpose, we introduce the following assumption over the Lagrange multipliers spaces :

Assumption 4.3. For all $1 \leq m \leq M$, we assume that there exists two integers $1 \leq k, l \leq K$ such that $\Gamma_m = \gamma_{kl}$ and a minimal Lagrange multiplier space M_{kl} such that $M_{kl} \subset M_{m;\delta_m}$ independently of the discretization. Moreover, we assume that for all $v \in X$ which is locally a rigid motion both over the subdomains Ω_k and Ω_l , that is $v|_{\Omega_k} \in \mathcal{R}(\Omega_k)$ and $v|_{\Omega_l} \in \mathcal{R}(\Omega_l)$, we have :

$$\int_{\gamma_{kl}} [v] \cdot \mu = 0 \quad \forall \mu \in M_{kl} \quad \implies [v]_{kl} = 0, \tag{4.8}$$

where the jump of v over γ_{kl} is denoted by $[v]_{kl}$.

Under assumption 4.3, the constrained subspace V of X on which the coercivity of the broken bilinear form \tilde{a} holds, is defined as :

$$V = \{v \in X, \quad \int_{\gamma_{kl}} [v] \cdot \mu = 0, \quad \forall \mu \in M_{kl}, \quad 1 \leq k, l \leq K\}.$$

Remark 4.4. In the scalar case, as shown in [BMP94], this assumption would be reduced to impose that constant functions belong to the minimal Lagrange multipliers spaces $(M_{kl})_{1 \leq k, l \leq K}$.

4.3 Well-posedness

4.3.1 Inf-sup condition

The main consequence of assumption 4.2 is the inf-sup condition satisfied by the bilinear form b expressing the mortar condition :

Proposition 4.1. Under assumption 4.2, there exists a constant $\beta > 0$ such that :

$$\inf_{\lambda_h \in M_\delta \setminus \{0\}} \sup_{u_h \in X_h \setminus \{0\}} \frac{b(u_h, \lambda_h)}{\|\lambda_h\|_{\delta, -\frac{1}{2}} \|u_h\|_X} \geq \beta, \quad (4.9)$$

where β is of the form :

$$\beta = C \min_{1 \leq m \leq M} \frac{1}{(C_m)^2},$$

where the constant C_m is the stability constant of π_m defined in assumption 4.2, for all $1 \leq m \leq M$, and C is independent of the discretization and of the number of subdomains.

Proof : For completeness, we recall the proof from [Woh01]. Let $\lambda \in M_\delta$. For all $1 \leq m \leq M$, denoting by $\lambda_m := \lambda|_{\Gamma_m}$ we have by construction :

$$\|\lambda_m\|_{\delta, -\frac{1}{2}, m} = \sup_{\phi \in \mathbb{H}_\delta^{1/2}(\Gamma_m)} \frac{\int_{\Gamma_m} \lambda_m \cdot \phi}{\|\phi\|_{\delta, \frac{1}{2}, m}},$$

and by definition of the projection π_m and by using assumption 4.2 :

$$\|\lambda_m\|_{\delta, -\frac{1}{2}, m} \leq C_m \sup_{\phi \in \mathbb{H}_\delta^{1/2}(\Gamma_m)} \frac{\int_{\Gamma_m} \lambda_m \cdot \pi_m \phi}{\|\pi_m \phi\|_{\delta, \frac{1}{2}, m}} \leq C_m \max_{\phi \in W_{m; \delta_m}^0} \frac{\int_{\Gamma_m} \lambda_m \cdot \phi}{\|\phi\|_{\delta, \frac{1}{2}, m}}.$$

Let $\phi_{\lambda_m} \in W_{m; \delta_m}^0$ be the function reaching the maximum with $\|\phi_{\lambda_m}\|_{\delta, \frac{1}{2}, m} = 1$, hence :

$$\int_{\Gamma_m} \lambda_m \cdot \phi_{\lambda_m} \geq \frac{1}{C_m} \|\lambda_m\|_{\delta, -\frac{1}{2}, m}. \quad (4.10)$$

We use the discrete extension by zero operator over the Lagrange nodes of the volumic mesh $\tilde{\mathcal{R}}_{m; h_m} : W_{m; \delta_m}^0 \rightarrow X_h$ (introduced in definition 4.2 of the appendix, page 203) to define :

$$u_m = \tilde{\mathcal{R}}_{m; h_m} \phi_{\lambda_m}.$$

Then, because $\phi_{\lambda_m} \in W_{m;\delta_m}^0$, its extension u_m has zero trace on all interfaces except Γ_m and thus it is obtained that :

$$b(u_m, \lambda_m) = \int_{\Gamma_m} \phi_{\lambda_m} \cdot \lambda_m. \quad (4.11)$$

Now, let us define the function $u_h \in X_h$ by :

$$u_h = \sum_{m=1}^M b(u_m, \lambda_m) u_m.$$

As a consequence, using (4.11) and (4.10) :

$$b(u_h, \lambda) = \sum_{m=1}^M b(u_m, \lambda_m)^2 \geq \sum_{m=1}^M \frac{1}{C_m^2} \|\lambda_m\|_{\delta, -\frac{1}{2}, m}^2 \geq \min_{1 \leq m \leq M} \frac{1}{(C_m)^2} \|\lambda\|_{\delta, -\frac{1}{2}}^2. \quad (4.12)$$

Using the locality of the supports of the $(u_m)_m$ on disjoint small strips around the $(\Gamma_m)_m$ and lemma 4.19 of the appendix (page 203) :

$$\begin{aligned} \|u_h\|_X^2 &= \sum_{m=1}^M b(u_m, \lambda_m)^2 \|u_m\|_{H^1(\Omega_{k(m)})^d}^2 \\ &\leq C \sum_{m=1}^M b(u_m, \lambda_m)^2 \|\phi_{\lambda_m}\|_{\delta, \frac{1}{2}, m}^2 = C \sum_{m=1}^M b(u_m, \lambda_m)^2. \end{aligned}$$

Then, by (4.11) and the Cauchy-Schwartz inequality (4.5) :

$$\|u_h\|_X^2 \leq C \sum_{m=1}^M \left(\int_{\Gamma_m} \phi_{\lambda_m} \cdot \lambda_m \right)^2 \leq C \sum_{m=1}^M \|\lambda_m\|_{\delta, -\frac{1}{2}, m}^2 = C \|\lambda\|_{\delta, -\frac{1}{2}}^2. \quad (4.13)$$

Therefore, by construction, for all $\lambda \in M_\delta$, there exists a $u_h \in X_h$ such that :

$$\frac{b(u_h, \lambda)}{\|u_h\|_X} \geq C \min_{1 \leq m \leq M} \frac{1}{(C_m)^2} \|\lambda\|_{\delta, -\frac{1}{2}},$$

which ends the proof. \square

Remark 4.5. In the absence of any triple point on the interface, that is if any function defined on Γ_m has zero trace on all other interfaces Γ_l , $l \neq m$, the previous proposition remains true even if one replaces $W_{m;\delta_m}^0$ by $W_{m;\delta_m}$ in assumption 4.2.

4.3.2 Local rigid motions

The set of rigid motions is spanned with translations and elementary rotations, as recalled in the following simple lemma :

Lemma 4.1. *A tridimensional rigid motion $r \in \mathcal{R}(\Omega)$ with $\Omega \subset \mathbb{R}^3$ is a linear combination of the three translations :*

$$t_1(x) = e_1, \quad t_2(x) = e_2, \quad t_3(x) = e_3, \quad x \in \Omega,$$

where (e_1, e_2, e_3) is the canonical basis of \mathbb{R}^3 , and the three elementary rotations :

$$\begin{cases} r_1(x) = e_1 \times x = \begin{pmatrix} 0 \\ -x_3 \\ x_2 \end{pmatrix}, \\ r_2(x) = e_2 \times x = \begin{pmatrix} x_3 \\ 0 \\ -x_1 \end{pmatrix}, \\ r_3(x) = e_3 \times x = \begin{pmatrix} -x_2 \\ x_1 \\ 0 \end{pmatrix}, \quad x \in \Omega. \end{cases}$$

A bidimensional rigid motion $r \in \mathcal{R}(\Omega)$ with $\Omega \subset \mathbb{R}^2$ is a linear combination of the translations t_1, t_2 and of the elementary rotation :

$$r(x) = \begin{pmatrix} -x_2 \\ x_1 \end{pmatrix}, \quad x \in \Omega.$$

Proof : By definition of a rigid motion $v \in \mathcal{R}(\Omega)$, it follows that the symmetrized gradient $\varepsilon(v)$ vanishes almost everywhere in Ω . Let us notice that for all $1 \leq i, j, l \leq d$, the following equality holds in the sense of distributions :

$$\frac{\partial^2 v_i}{\partial x_j \partial x_l} = \frac{\partial}{\partial x_j} \varepsilon_{il}(v) + \frac{\partial}{\partial x_l} \varepsilon_{ij}(v) - \frac{\partial}{\partial x_i} \varepsilon_{jl}(v), \text{ in } \mathcal{D}'(\Omega),$$

where the indices i, j, l , denote the components of v and x in \mathbb{R}^d . The fact that $\varepsilon(v)$ vanishes almost everywhere in Ω implies that for all $1 \leq i, j, l \leq d$:

$$\frac{\partial^2 v_i}{\partial x_j \partial x_l} = 0, \text{ in } \mathcal{D}'(\Omega).$$

By a classical result from distribution theory ([Sch66], page 60) and provided Ω is connected, each scalar function v_i for all $1 \leq i \leq d$ is an affine function, namely $v_i(x) =$

$a_i + \sum_{j=1}^d b_{ij}x_j$ for almost all $x \in \Omega$. Since $\varepsilon_{ii}(v) = 0$, we get $b_{ii} = 0$ and because $\varepsilon_{ij}(v) = 0$, we get $b_{ij} = -b_{ji}$. As a consequence, we obtain for $d = 3$:

$$\begin{cases} v_1(x) = a_1 - b_{21}x_2 + b_{13}x_3, \\ v_2(x) = a_2 + b_{21}x_1 - b_{32}x_3, \\ v_3(x) = a_3 - b_{13}x_1 + b_{32}x_2, \quad \forall x \in \Omega, \end{cases}$$

and for $d = 2$:

$$\begin{cases} v_1(x) = a_1 - b_{21}x_2, \\ v_2(x) = a_2 + b_{21}x_1, \quad \forall x \in \Omega, \end{cases}$$

which ends the proof. \square

Remark 4.6. Another way to understand rigid motions in the linear framework comes from the nonlinear one. Indeed, in nonlinear elasticity, if we denote by $\varphi : \Omega \rightarrow \mathbb{R}^3$ the deformation of the reference configuration in the sense that $\varphi(\Omega)$ is the deformed domain, the associated strain tensor is defined by :

$$E(\varphi) = \frac{1}{2} (\nabla^t \varphi \cdot \nabla \varphi - id).$$

As shown in [Cia88], if Ω is a connected open set in \mathbb{R}^3 and $\varphi \in C^1(\Omega; \mathbb{R}^3)$, then $E(\varphi) = 0$ iff φ is a rotation or a translation. In particular, let us introduce the rotation of angle θ with respect to e_3 :

$$R_\theta^3(x) = \begin{pmatrix} x_1 \cos \theta - x_2 \sin \theta \\ x_1 \sin \theta + x_2 \cos \theta \\ x_3 \end{pmatrix}.$$

For all $\theta \in \mathbb{R}$, we have $E(R_\theta^3) = 0$ and therefore by differentiation with respect to θ for $\theta = 0$, it is obtained that :

$$dE_{id} \left(\frac{\partial R_\theta^3}{\partial \theta} \Big|_{\theta=0} (x) \right) = 0,$$

which is exactly :

$$\varepsilon(e_3 \times x) = 0.$$

We have then justified the fact that elementary rotations are rigid motions in the linearized framework. The case of translations is simpler. Indeed, let T_k^3 the translation of vector ke_3 , that is :

$$T_k^3(x) = x + ke_3.$$

For all $k \in \mathbb{R}$, we have $E(T_k^3) = 0$, entailing by differentiation with respect to k for $k = 0$:

$$dE_{id} \left(\frac{\partial T_k^3}{\partial k} \Big|_{k=0} (x) \right) = 0,$$

which is exactly :

$$\varepsilon(e_3) = 0.$$

4.3.3 Minimal Lagrange multipliers spaces

For instance, the implication (4.8) of assumption 4.3 is true when the traces of first order polynomial displacements over the interfaces belong to the Lagrange multipliers spaces, as shown in the next lemma.

Lemma 4.2. *By choosing M_{kl} as the restriction to γ_{kl} of first order polynomial displacements, i.e.:*

$$M_{kl} = M_1(\gamma_{kl}) = \mathbb{P}_1(\Omega)^d|_{\gamma_{kl}} := \{v|_{\gamma_{kl}}, \quad v \in \mathbb{P}_1(\Omega)^d\}, \quad 1 \leq k, l \leq K,$$

where $\mathbb{P}_1(\Omega)$ is the space of first order polynomials over Ω , the implication (4.8) of assumption 4.3 holds.

Proof : Let us assume that $v \in X$ is such that its restriction $v_k = v|_{\Omega_k}$ (resp. $v_l = v|_{\Omega_l}$) to Ω_k (resp. Ω_l) is a local rigid motion. Assuming that :

$$\int_{\gamma_{kl}} [v] \cdot \mu = 0, \quad \forall \mu \in M_1(\gamma_{kl}),$$

and because by construction the jump $[v]_{\gamma_{kl}}$ of v across γ_{kl} belongs to $M_1(\gamma_{kl})$, we can choose $\mu = [v]_{\gamma_{kl}}$, so that :

$$\int_{\gamma_{kl}} [v]^2 = 0 \implies [v]_{\gamma_{kl}} = 0 \text{ on } \gamma_{kl}.$$

Hence the proof. □

Remark 4.7. When considering second order approximations for the displacements, first order polynomials must belong to the space of Lagrange multipliers in order to achieve an optimal rate of convergence, as shown in the proof of proposition 4.7, page 141. The choice of M_{kl} given by lemma 4.2 is then natural. Nevertheless, when considering first order approximations of the displacements, and when more than two subdomains share a common edge, it is impossible for stability reason to conserve all the affine functions in the spaces of Lagrange multipliers. In particular, the order of Lagrange multipliers should be reduced on the interface elements having a non-empty intersection with the boundary of the interface, as pointed out in [BMP93, BMP94] for the scalar case.

It is possible to weaken the assumption of lemma 4.2, for instance by using piecewise constant Lagrange multipliers, at least over interfaces having a tensor product structure.

Lemma 4.3. *We assume that for all $1 \leq k, l \leq K$ such that Ω_k and Ω_l have a non-empty intersection, the interface $\gamma_{kl} = \partial\Omega_k \cap \partial\Omega_l$ between the subdomains is planar. Denoting by G_{kl} its center of gravity defined by :*

$$G_{kl} = \frac{1}{\text{meas}(\Gamma_{kl})} \int_{\Gamma_{kl}} x \, dx,$$

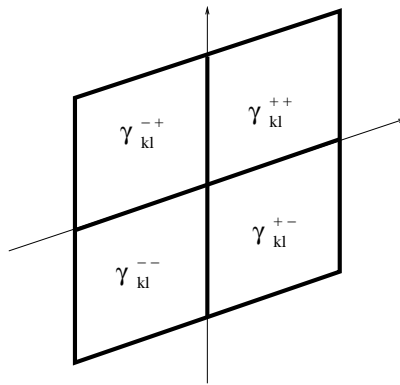
we can characterize γ_{kl} by :

$$\gamma_{kl} = \{x \in \mathbb{R}^3, \quad x - G_{kl} = \xi_1 f_1 + \xi_2 f_2, \quad (\xi_1, \xi_2) \in [-1, 1]^2\},$$

where $f_1, f_2 \in \mathbb{R}^3$ are linearly independent. We introduce the following partition over γ_{kl} :

$$\begin{cases} \gamma_{kl}^{++} = \{\xi_1 f_1 + \xi_2 f_2; \quad \xi_1 \in [0; 1] \text{ and } \xi_2 \in [0; 1]\}, \\ \gamma_{kl}^{+-} = \{\xi_1 f_1 + \xi_2 f_2; \quad \xi_1 \in [0; 1] \text{ and } \xi_2 \in [-1; 0]\}, \\ \gamma_{kl}^{--} = \{\xi_1 f_1 + \xi_2 f_2; \quad \xi_1 \in [-1; 0] \text{ and } \xi_2 \in [-1; 0]\}, \\ \gamma_{kl}^{-+} = \{\xi_1 f_1 + \xi_2 f_2; \quad \xi_1 \in [-1; 0] \text{ and } \xi_2 \in [0; 1]\}, \end{cases}$$

and assume that M_{kl} is made of piecewise constant functions over the sets γ_{kl}^{++} , γ_{kl}^{+-} , γ_{kl}^{--} and γ_{kl}^{-+} . Then, the assertion (4.8) of assumption 4.3 holds.



Proof : Let $v \in X$ such that its restriction $v_k = v|_{\Omega_k}$ (resp. $v_l = v|_{\Omega_l}$) to Ω_k (resp. Ω_l) is a local rigid motion, and :

$$\int_{\gamma_{kl}} (v_k - v_l) \cdot \mu = 0, \quad \forall \mu \in M_{kl}. \quad (4.14)$$

As $[v]_{kl} = (v_k - v_l) \in \mathcal{R}(\gamma_{kl})$ is a rigid motion of the interface γ_{kl} , there exist constant vectors $t, a \in \mathbb{R}^3$ such that :

$$[v]_{kl}(x) = t + a \times (x - G_{kl}), \quad x \in \gamma_{kl}.$$

If we consider constant vector functions μ in (4.14), it is obtained that :

$$t \cdot \mu \operatorname{meas}(\gamma_{kl}) + (\mu \times a) \cdot \int_{\gamma_{kl}} (x - G_{kl}) = t \cdot \mu \operatorname{meas}(\gamma_{kl}) = 0,$$

for all constant vectors $\mu \in \mathbb{R}^3$, entailing that $t = 0$.

Now, let us prove that $a = 0$. We can decompose it into :

$$a = \alpha_1 f_1 + \alpha_2 f_2 + \alpha_3 f_3, \text{ with } f_3 = f_1 \times f_2,$$

and then obtain from (4.14) :

$$\int_{[-1;1]^2} (\alpha_1 f_1 + \alpha_2 f_2 + \alpha_3 f_3) \times (\xi_1 f_1 + \xi_2 f_2) \cdot \mu d\xi_1 d\xi_2 = 0,$$

for all functions μ that are constant over the sets γ_{kl}^{++} , γ_{kl}^{+-} , γ_{kl}^{--} and γ_{kl}^{-+} . Then :

$$\begin{aligned} & \alpha_1 \int_{[-1;1]^2} \xi_2 (f_3 \cdot \mu) d\xi_1 d\xi_2 - \alpha_2 \int_{[-1;1]^2} \xi_1 (f_3 \cdot \mu) d\xi_1 d\xi_2 \\ & + \alpha_3 \int_{[-1;1]^2} (\xi_1 ((f_3 \times f_1) \cdot \mu) + \xi_2 ((f_3 \times f_2) \cdot \mu)) d\xi_1 d\xi_2 = 0, \end{aligned} \quad (4.15)$$

for all functions μ that are constant over the sets γ_{kl}^{++} , γ_{kl}^{+-} , γ_{kl}^{--} and γ_{kl}^{-+} . For all $\xi_1 \in [-1; 1]$, let us define :

$$\mu(x) = \mu(\xi_1 f_1 + \xi_2 f_2) = \begin{cases} f_3, & \xi_2 \in [0; 1], \\ -f_3, & \xi_2 \in [-1; 0], \end{cases}$$

in (4.15), which leads to :

$$4\alpha_1 \int_0^1 \xi_2 d\xi_2 = 2\alpha_1 = 0 \implies \alpha_1 = 0.$$

By chosing for all $\xi_2 \in [-1; 1]$:

$$\mu(x) = \mu(\xi_1 f_1 + \xi_2 f_2) = \begin{cases} f_3, & \xi_1 \in [0; 1], \\ -f_3, & \xi_1 \in [-1; 0], \end{cases}$$

in (4.15), it is obtained that :

$$-4\alpha_2 \int_0^1 \xi_1 d\xi_1 = -2\alpha_2 = 0 \implies \alpha_2 = 0.$$

When chosing now for all $\xi_2 \in [-1; 1]$:

$$\mu(x) = \mu(\xi_1 f_1 + \xi_2 f_2) = \begin{cases} f_2, & \xi_1 \in [0; 1], \\ -f_2, & \xi_1 \in [-1; 0], \end{cases}$$

it is obtained that :

$$4\alpha_3 \int_0^1 \xi_1 d\xi_1 = 2\alpha_3 = 0 \implies \alpha_3 = 0.$$

We conclude that $[v]_{kl} = 0$, hence the proof. \square

Remark 4.8. In the proof of lemma 4.3, the space of Lagrange multipliers we have used to check the implication (4.8) of assumption 4.3, is in fact a subspace of dimension 3 of the proposed space M_{kl} .

4.3.4 Standard result of coercivity

We are now ready to recall the standard coercivity result for the bilinear form :

$$\tilde{d}(u, v) := \sum_{k=1}^K d_k(u, v), \quad \forall u, v \in V$$

with :

$$d_k(u, v) := \int_{\Omega_k} \varepsilon(u) : \varepsilon(v), \quad \forall u, v \in V.$$

The now standard proof, done by contradiction as in [BMP93] for example in the scalar case, does not guarantee the independence on the number and the size of the subdomains. We recall it nevertheless for completeness, and illustrate the way local rigid motions are controlled.

Proposition 4.2. *Let Ω be a bounded C^1 connected open set. The assumption 4.3 is supposed to be satisfied. Then, there exists a constant $C > 0$ possibly depending on the number and sizes of subdomains such that for all $v \in V$, the following inequality holds :*

$$\sum_{k=1}^K \int_{\Omega_k} \varepsilon(v) : \varepsilon(v) \geq C \left(\sum_{k=1}^K \frac{1}{\text{diam}(\Omega_k)^2} \int_{\Omega_k} v^2 + \int_{\Omega_k} \nabla v : \nabla v \right).$$

Proof : Let us assume that the inequality is false. Then, there exists a sequence $(v_n)_{n \geq 1}$ in V such that :

$$\sum_{k=1}^K \int_{\Omega_k} \varepsilon(v_n) : \varepsilon(v_n) \leq \frac{1}{n}, \quad \sum_{k=1}^K \frac{1}{\text{diam}(\Omega_k)^2} \int_{\Omega_k} (v_n)^2 + \int_{\Omega_k} \nabla v_n : \nabla v_n = 1. \quad (4.16)$$

From (4.16), $(v_n)_{n \geq 1}$ is bounded in X , and we can extract a subsequence still denoted by $(v_n)_{n \geq 1}$ converging to v , weakly in X and strongly in $L^2(\Omega)^d$ by the Rellich-Kondrachov theorem ([Bré99], page 169). It comes that $(v_n)_{n \geq 1}$ is a Cauchy sequence in $L^2(\Omega)^d$. Moreover, from (4.16), we obtain that for all $1 \leq k \leq K$, $(\varepsilon(v_n))_{n \geq 1}$ is strongly convergent to zero in $L^2(\Omega_k)^{d \times d}$, and as a consequence, is a Cauchy sequence in $L^2(\Omega_k)^{d \times d}$. Therefore, for all $1 \leq k \leq K$, $(v_n)_{n \geq 1}$ is a Cauchy sequence for the norm :

$$\frac{1}{\text{diam}(\Omega_k)^2} \int_{\Omega_k} (v_n)^2 + \int_{\Omega_k} \varepsilon(v_n) : \varepsilon(v_n),$$

and then for the norm of $H^1(\Omega_k)^d$ by the Korn's inequality (proposition 4.3). We deduce that $(v_n)_{n \geq 1}$ strongly converges to v in $X = \prod_{k=1}^K H_*^1(\Omega_k)$ by completeness of X . From (4.16), it comes that $\varepsilon(v|_{\Omega_k}) = 0$, i.e. $v|_{\Omega_k}$ is a rigid motion for all $1 \leq k \leq K$.

Let us prove now that $v \in V$. We have for all $1 \leq m \leq M$, and $\mu \in M_{m; \delta_m}$:

$$\int_{\Gamma_m} [v] \cdot \mu = \int_{\Gamma_m} [v_n] \cdot \mu + \int_{\Gamma_m} [v - v_n] \cdot \mu,$$

and by using that $v_n \in V$ and the convergence of v_n to v in $H^1(\Omega_{k(m)})^d$, and therefore the convergence of their traces in $L^2(\Gamma_m)^d$ by the trace theorem, we get :

$$\int_{\Gamma_m} [v] \cdot \mu = 0, \quad \forall \mu \in M_{m;\delta_m}.$$

The assumption 4.3 entails that the jump of v across all the interfaces $(\Gamma_m)_{1 \leq m \leq M}$ vanishes, making v a rigid motion over Ω . Because $v = 0$ on Γ_D , we deduce that v vanishes on the whole domain Ω , which is in contradiction with :

$$\sum_{k=1}^K \frac{1}{\text{diam}(\Omega_k)^2} \int_{\Omega_k} (v_n)^2 + \int_{\Omega_k} \nabla v_n : \nabla v_n = 1,$$

proving the proposition. \square

In the previous proof, we have used the well-known :

Proposition 4.3 (Korn's inequality). *Let Ω be a bounded C^1 connected open set. There exists a constant C_Ω independent of the diameter of Ω such that :*

$$\int_{\Omega} \varepsilon(v) : \varepsilon(v) + \frac{1}{\text{diam}(\Omega)^2} \int_{\Omega} v^2 \geq C_\Omega \left(\int_{\Omega} \nabla v : \nabla v + \frac{1}{\text{diam}(\Omega)^2} \int_{\Omega} v^2 \right),$$

for all functions v such that $\int_{\Omega} \varepsilon(v) : \varepsilon(v) + \frac{1}{\text{diam}(\Omega)^2} \int_{\Omega} v^2$ is bounded.

The Korn's inequality is a consequence of the following lemma (see [DL72], page 112, for a proof) :

Lemma 4.4. *Let $\Omega \subset \mathbb{R}^d$ be a bounded C^1 connected open set, and $f \in \mathcal{D}'(\Omega)$ a real valued distribution such that $f \in H^{-1}(\Omega)$ and for all $1 \leq i \leq d$, the derivative $\partial f / \partial x_i$ in the sense of distributions belongs to $H^{-1}(\Omega)$, where $H^{-1}(\Omega)$ is the dual space of $H_0^1(\Omega)$. Then the distribution f can be identified to a function by means of the L^2 inner product and $f \in L^2(\Omega)$.*

Again following [DL72], we get the proof of the Korn's inequality.

Proof : First, we assume that Ω has a unit diameter. The following space

$$E = \{v \in L^2(\Omega)^d; \varepsilon(v) \in L^2(\Omega)^{d \times d}\}$$

is an Hilbert space when endowed with the norm :

$$\|v\|_E = \left(\int_{\Omega} \varepsilon(v) : \varepsilon(v) + \int_{\Omega} v^2 \right)^{1/2}, \quad \forall v \in E.$$

For all $1 \leq i, j, k \leq d$, the following expression holds in $\mathcal{D}'(\Omega)$:

$$\frac{\partial^2 v_i}{\partial x_j \partial x_k} = \frac{\partial}{\partial x_j} \varepsilon_{ik}(v) + \frac{\partial}{\partial x_k} \varepsilon_{ij}(v) - \frac{\partial}{\partial x_i} \varepsilon_{jk}(v). \quad (4.17)$$

As $v \in E$, then $\varepsilon_{ij}(v) \in L^2(\Omega)$ and then $\partial \varepsilon_{ij}/\partial x_k \in H^{-1}(\Omega)$. From (4.17) we get that :

$$\frac{\partial^2 v_i}{\partial x_j \partial x_k} \in H^{-1}(\Omega),$$

and from lemma 4.4, we conclude that for all $1 \leq i, k \leq d$:

$$\frac{\partial v_i}{\partial x_k} \in L^2(\Omega),$$

and then $v \in H^1(\Omega)^d$. We have proved that $E \subset H^1(\Omega)^d$, and then $E = H^1(\Omega)^d$. Let $T : H^1(\Omega)^d \rightarrow E$ the canonical embedding from $H^1(\Omega)^d$ to E . The application T is linear, continuous because for all $v \in H^1(\Omega)^d$, $\|v\|_E \leq \|v\|_{H^1(\Omega)^d}$ and onto because we have proved that if $v \in E$, then $v \in H^1(\Omega)^d$. From the theorem of the open application (see [Bré99]), there exists a constant C such that for all $v \in E$:

$$\|v\|_{H^1(\Omega)^d} \leq C\|v\|_E.$$

If Ω has not a unit diameter, there exists an homotethy φ and a bounded \mathcal{C}^1 -connected open set $\hat{\Omega} \subset \mathbb{R}^d$ with unit diameter such that $\varphi(\hat{\Omega}) = \Omega$. As a consequence, by the change of variables φ and by using the previous result over $\hat{\Omega}$, we get :

$$\begin{aligned} \int_{\Omega} \varepsilon(v) : \varepsilon(v) + \frac{1}{\text{diam}(\Omega)^2} \int_{\Omega} v^2 &= \text{diam}(\Omega)^{d-2} \left(\int_{\hat{\Omega}} \hat{\varepsilon}(\hat{v}) : \hat{\varepsilon}(\hat{v}) + \int_{\hat{\Omega}} \hat{v}^2 \right) \\ &\geq \text{diam}(\Omega)^{d-2} C_{\hat{\Omega}} \left(\int_{\hat{\Omega}} \hat{\nabla} \hat{v} : \hat{\nabla} \hat{v} + \int_{\hat{\Omega}} \hat{v}^2 \right) \\ &= C_{\hat{\Omega}} \left(\int_{\Omega} \nabla v : \nabla v + \frac{1}{\text{diam}(\Omega)^2} \int_{\Omega} v^2 \right), \end{aligned}$$

which ends the proof. \square

4.4 Uniform coercivity

We improve herein the previous coercivity result by showing the independence of the coercivity constant with respect to the number, the size and the shape of the subdomains. Such a result is known for scalar elliptic problems, when interfaces are plane, as proved in [Gop99, Bre03]. A proof for the vector case is also proposed in a recent publication [Bre04]. The originality of our approach is that it uses a generalization of the Scott and Zhang interpolation [SZ90], and is valid for curved interfaces.

4.4.1 Fundamental assumptions

Let us introduce the assumptions used in the present section. First, we assume that each subdomain is a “compact deformation” of a reference domain, the reference domains being in finite number. More precisely :

Assumption 4.4. *It is assumed that :*

1. *there exists a finite collection of reference domains $(\hat{\Omega}_j)_{1 \leq j \leq J}$ of unit diameter, of compact sets $(\mathcal{K}_j)_{1 \leq j \leq J}$ and of maps $\varphi_j : \hat{\Omega}_j \times \mathcal{K}_j \rightarrow \mathbb{R}^d$, $1 \leq j \leq J$ such that for all $1 \leq j \leq J$:*

$$\text{diam}(\varphi_j(\hat{\Omega}_j, p)) = 1, \quad \forall p \in \mathcal{K}_j,$$

and the following application :

$$\begin{aligned} \mathcal{K}_j &\rightarrow W^{1,\infty}(\hat{\Omega}_j)^d, \\ p &\mapsto \varphi_j(\cdot, p), \end{aligned}$$

is continuous;

2. *for all $1 \leq j \leq J$, there exists a constant $C_j > 0$ such that :*

$$\det \frac{\partial \varphi_j}{\partial \hat{x}}(\hat{x}, p) \geq C_j, \quad \forall p \in \mathcal{K}_j, \text{ for almost all } \hat{x} \in \hat{\Omega}_j;$$

in other words, for all $p \in \mathcal{K}_j$, $\varphi_j(\cdot, p)$ is a uniform homeomorphism ;

3. *for all $(\Omega_k)_{1 \leq k \leq K}$ there exists a j with $1 \leq j \leq J$ and an element $p \in \mathcal{K}_j$ such that within a scaling factor :*

$$\frac{1}{\text{diam}(\Omega_k)} \Omega_k = \varphi_j(\hat{\Omega}_j, p).$$

Moreover, we consider that :

4. *there exists a finite collection of reference interfaces $(\hat{\gamma}_j)_{1 \leq j \leq J}$, with $\hat{\gamma}_j \subset \partial \hat{\Omega}_j$, $1 \leq j \leq J$, and that the application :*

$$\begin{aligned} \mathcal{K}_j &\rightarrow W^{1,\infty}(\hat{\gamma}_j)^d, \\ p &\mapsto \varphi_j(\cdot, p), \end{aligned}$$

is continuous,

5. *for all $1 \leq j \leq J$, there exists a constant $C_j > 0$ such that :*

$$\det \frac{\partial \varphi_j}{\partial \hat{x}}(\hat{x}, p) \geq C_j, \quad \forall p \in \mathcal{K}_j, \text{ for almost all } \hat{x} \in \hat{\gamma}_j,$$

and when γ is a part of the boundary of $\Omega_k = \varphi_j(\hat{\Omega}_j, p)$, we assume that :

6. $\frac{1}{\text{diam}(\gamma)} \gamma = \varphi_j(\hat{\gamma}_j, p).$

7. there exists three constants $\kappa, \kappa', \kappa'' > 0$ such that for all $1 \leq k \leq K$:

$$\begin{cases} \rho(\Omega_k) \geq \kappa \operatorname{diam}(\Omega_k), \\ \operatorname{diam}(\gamma_{kl}) \geq \kappa' \operatorname{diam}(\Omega_k), \quad 1 \leq l \leq K, \\ |\gamma_{kl}| \geq \kappa'' \operatorname{diam}(\Omega_k)^{d-1}, \end{cases} \quad (4.18)$$

where $\rho(\Omega_k)$ denotes the diameter of the largest ball contained in Ω_k . The constants κ, κ' and κ'' must remain independent of the number and the size of the subdomains. As a consequence of (4.18), the number of subdomains sharing a common intersection remains bounded by a fixed integer P , independently of the chosen regular decomposition.

The assumptions 1 to 6 are used to show a technical result of shape-independence of the constant in Korn-like inequalities with proper scaling, detailed in appendix B (section 4.11, page 205). Assumption 7 will be used to show our interpolation estimates.

To deal with curved interfaces in the framework of Scott-Zhang like interpolation, we will need the technical assumption 4.5, page 127, precized in the definition of the interpolation operator. The present coercivity result will be shown on the constrained space :

$$V = \{v \in X, \quad \int_{\gamma_{kl}} [v] \cdot \mu = 0, \quad \forall \mu \in \mathbb{P}_1(\gamma_{kl})^d\}$$

Remark 4.9. In this section, we use the Lagrange multipliers spaces $M_{kl} = \mathbb{P}_1(\gamma_{kl})^d$. Nevertheless, one can adopt any M_{kl} such that for all $v \in L^2(\gamma_{kl})^d$, there exists a solution $\pi_{\gamma_{kl}} v \in \mathbb{P}_1(\gamma_{kl})^d$ of :

$$\int_{\gamma_{kl}} \pi_{\gamma_{kl}} v \cdot \mu = \int_{\gamma_{kl}} v \cdot \mu, \quad \forall \mu \in M_{kl},$$

satisfying :

$$\|\pi_{\gamma_{kl}} v\|_{L^2(\gamma_{kl})^d} \leq C \sup_{\mu \in M_{kl}} \frac{\int_{\gamma_{kl}} v \cdot \mu}{\|\mu\|_{L^2(\gamma_{kl})^d}}, \quad (4.19)$$

with a constant C independent of the interface γ_{kl} . The statement (4.19) is true when adopting Lagrange multipliers satisfying the assumption 4.3, but the constant a priori depends on the shape of the interface γ_{kl} .

In this section, we assume that all these assumptions are satisfied.

4.4.2 Generalized Korn's inequality

We will use hereafter the two following generalized Korn's inequalities reviewed and detailed in appendix 4.11, page 205, for domains satisfying the assumptions of section 4.4.1.

Lemma 4.5. *There exists a constant C_P such that for all Ω_k and γ_{kl} satisfying the conditions defined in section 4.4.1, the following inequality holds for all $v \in H^1(\Omega_k)^d$:*

$$\|v\|_{H^1(\Omega_k)^d}^2 \leq C_P \left(\frac{1}{\text{diam}(\Omega_k)} \left(\sup_{\mu \in M_{kl}} \frac{\int_{\gamma_{kl}} v \cdot \mu}{\|\mu\|_{L^2(\gamma_{kl})^d}} \right)^2 + d_k(v, v) \right),$$

where C_P does not depend on Ω_k and γ_{kl} .

Lemma 4.6. *There exists a constant C_N such that for all Ω_k and γ_{kl} satisfying the conditions defined in section 4.4.1, the following inequality holds for all $v \in H^1(\Omega_k)^d$:*

$$\|v\|_{H^1(\Omega_k)^d}^2 \leq C_N \left(\frac{1}{\text{diam}(\Omega_k)^2} \left(\sup_{r \in \mathcal{R}(\Omega_k)} \frac{\int_{\Omega_k} v \cdot r}{\|r\|_{L^2(\Omega_k)^d}} \right)^2 + d_k(v, v) \right),$$

where C_N does not depend on Ω_k and γ_{kl} .

Then, we deduce the following trace lemma :

Lemma 4.7. *There exists a constant C_T such that for all Ω_k and γ_{kl} satisfying the conditions defined in section 4.4.1, the following inequality holds for all $v \in H^1(\Omega_k)^d$:*

$$\frac{1}{\text{diam}(\Omega_k)} \left(\sup_{\mu \in M_{kl}} \frac{\int_{\gamma_{kl}} v \cdot \mu}{\|\mu\|_{L^2(\gamma_{kl})^d}} \right)^2 \leq C_T \left(\frac{1}{\text{diam}(\Omega_k)^2} \left(\sup_{r \in \mathcal{R}(\Omega_k)} \frac{\int_{\Omega_k} v \cdot r}{\|r\|_{L^2(\Omega_k)^d}} \right)^2 + d_k(v, v) \right),$$

where C_T does not depend on Ω_k and γ_{kl} .

Proof : By using the Cauchy-Schwarz inequality, the Sobolev trace theorem (with proper scaling) and the lemma 4.6, we get :

$$\begin{aligned} \frac{1}{\text{diam}(\Omega_k)} \left(\sup_{\mu \in M_{kl}} \frac{\int_{\gamma_{kl}} v \cdot \mu}{\|\mu\|_{L^2(\gamma_{kl})^d}} \right)^2 &\leq \frac{1}{\text{diam}(\Omega_k)} \int_{\gamma_{kl}} v^2 \\ &\leq C \left(\frac{1}{\text{diam}(\Omega_k)^2} \int_{\Omega_k} v^2 + \int_{\Omega_k} |\nabla v|^2 \right) \\ &\leq CC_N \left(\frac{1}{\text{diam}(\Omega_k)^2} \left(\sup_{r \in \mathcal{R}(\Omega_k)} \frac{\int_{\Omega_k} v \cdot r}{\|r\|_{L^2(\Omega_k)^d}} \right)^2 + d_k(v, v) \right), \end{aligned}$$

hence the proof. □

4.4.3 A Scott & Zhang like interpolation operator for mortar methods

The proposed interpolation operator builds a conforming approximation of a non-conforming function defined in the constrained space V of functions whose jump is orthogonal to interface Lagrange multipliers, with the usual stability properties shown in [SZ90], even when considering curved interfaces between the subdomains.

Construction of a coarse conforming basis - Let us introduce a coarse conforming triangulation \mathcal{T}_H of Ω , as shown on figure 4.3, which satisfies the following conditions :

1. Each $T \in \mathcal{T}_H$ is totally included in a subdomain Ω_k .
2. The tetrahedra in \mathcal{T}_H possibly have curved faces along the skeleton interface \mathcal{S} .
3. The tetrahedra $T \in \mathcal{T}_H$ in Ω_k are such that $\rho(T) \geq C \text{diam}(\Omega_k)$, with $\rho(T)$ the diameter of the largest ball included in T .

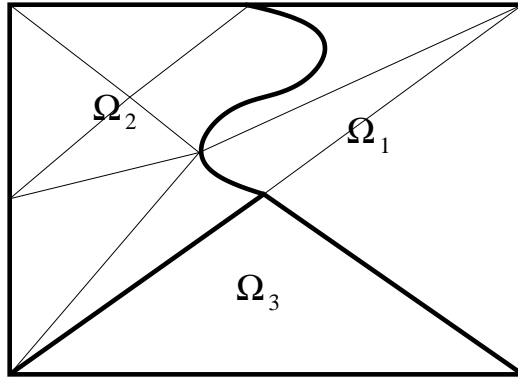


FIG. 4.3 – A coarse conforming triangulation \mathcal{T}_H of $\Omega = \Omega_1 \cup \Omega_2 \cup \Omega_3$ satisfying conditions 1 and 2.

We define on \mathcal{T}_H the following conforming approximation space :

$$X_H = \{v \in H^1(\Omega), \quad v|_T \in \mathbb{P}_1(T), \quad T \in \mathcal{T}_H\},$$

where $\mathbb{P}_1(T)$ denotes the space of affine applications over T . The vertices of the coarse conforming triangulation \mathcal{T}_H are denoted by $(M_i)_{1 \leq i \leq I}$, and the associated nodal basis of X_H by $(\phi_i)_{1 \leq i \leq I}$ such that :

$$\phi_i(M_j) = \delta_{ij},$$

using the Kronecker symbol $\delta_{ij} = 1$ for $i = j$ and 0 otherwise.

Set of interfaces - Let us denote by Z_S the set of interfaces γ_{kl} between two adjacent subdomains, and by \mathring{Z} the set of internal faces of the triangulation \mathcal{T}_H , that is the faces of the triangles $T \in \mathcal{T}_H$, which are not included in the skeleton interface \mathcal{S} . The total set of interfaces is then defined by :

$$Z = Z_S \cup \mathring{Z}.$$

To deal with curved interfaces in the framework of Scott-Zhang like interpolation, we need the following assumption :

Assumption 4.5. There exists a constant $C > 0$ such that for each node M_i of the coarse triangulation \mathcal{T}_H , there exists an interface $\gamma_i \in Z$ with $M_i \in \gamma_i$ such that for all matrix $B \in \mathbb{R}^{d \times d}$, we have :

$$\frac{1}{|\gamma_i|} \int_{\gamma_i} |B \cdot (x - G_{\gamma_i})|^2 dx \geq C \lambda(B, \gamma_i)^2 \operatorname{diam}(\gamma_i)^2, \quad (4.20)$$

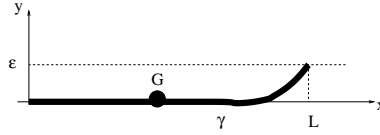
where G_γ is the center of gravity of γ , i.e :

$$G_\gamma = \frac{1}{|\gamma|} \int_{\gamma} x dx,$$

and $\lambda(B, \gamma)$ the maximal singular value of B on γ :

$$\lambda(B, \gamma)^2 = \sup_{x \in \gamma} \frac{|B \cdot (x - G_\gamma)|^2}{|x - G_\gamma|^2}.$$

Remark 4.10. The assumption 4.5 means that for all node M_i of the coarse triangulation \mathcal{T}_H , there exists an interface sharing M_i and having a finite “length” along the principal direction of displacement for all affine fields of displacements. As a counter-example, let us consider the curved interface depicted in the following picture :



and the linear function $v(x, y) = \epsilon^{-1}y = B \cdot \mathbf{x}$. It follows that $\lambda(B, \gamma)^2 \simeq \frac{1}{L^2}$ and

$$\frac{1}{|\gamma_i|} \int_{\gamma_i} |B \cdot (x - G_{\gamma_i})|^2 dx \simeq \frac{1}{L} \int_0^\epsilon (\epsilon^{-1}y)^2 dy \simeq \frac{\epsilon}{L}.$$

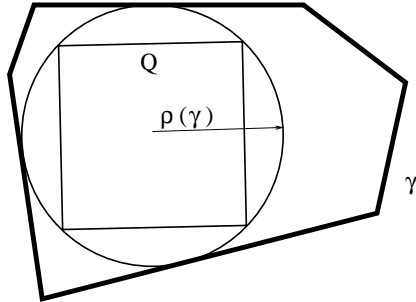
As a consequence, the assertion (4.20) is not satisfied on γ uniformly in ϵ . The reason is that in this case, γ is nearly orthogonal to the principal direction of displacement.

Nevertheless, the assertion (4.20) is satisfied for any plane interface γ whatever the matrix $B \in \mathbb{R}^{d \times d}$, as shown in the following lemma :

Lemma 4.8. The assumption 4.5 is satisfied when choosing as γ_i any plane interface sharing the node M_i , provided γ_i is shape regular that is :

$$\rho(\gamma_i) \geq C \operatorname{diam}(\gamma_i).$$

Proof : The present proof is done in three dimensions. Let γ be a plane interface, and Q a square of maximal edge length ($= \rho(\gamma)/\sqrt{2}$) included in the largest ball contained in γ (as shown in the following picture).



We write $x - G_\gamma = x_1 e_1 + x_2 e_2 = J \cdot x$, where e_1 and e_2 are two orthogonal vectors such that $G_\gamma + \text{span}\{e_1, e_2\} = \gamma$. As the matrix $J^t \cdot B^t \cdot B \cdot J$ is symmetric semi-definite positive, it can be diagonalized and we still denote by e_1 and e_2 its eigenvectors, associated to the eigenvalues μ_1^2 and μ_2^2 with $\mu_2^2 \geq \mu_1^2$. Finally, we choose among all the possible squares Q , the one whose edges are parallel to the eigenvectors :

$$Q = \{x_1 e_1 + x_2 e_2; \quad x_1 \in [X_1 - a, X_1 + a], x_2 \in [X_2 - a, X_2 + a]\},$$

where the center of the largest ball in γ is $G_\gamma + X_1 e_1 + X_2 e_2$, and $2a = \rho(\gamma)/\sqrt{2}$. Then, we get :

$$\begin{aligned} \frac{1}{|\gamma|} \int_{\gamma} |B \cdot (x - G_\gamma)|^2 &\geq \frac{1}{|\gamma|} \int_Q |B \cdot (x - G_\gamma)|^2 \\ &\geq \frac{1}{|\gamma|} \int_{X_1-a}^{X_1+a} \int_{X_2-a}^{X_2+a} (\mu_1^2(x_1)^2 + \mu_2^2(x_2)^2) dx_1 dx_2 \\ &\geq \frac{2a}{3|\gamma|} (\mu_1^2((X_1+a)^3 - (X_1-a)^3) + \mu_2^2((X_2+a)^3 - (X_2-a)^3)). \end{aligned}$$

Moreover, we have :

$$\begin{aligned} (X_1+a)^3 - (X_1-a)^3 &= 2a((X_1+a)^2 + (X_1+a)(X_1-a) + (X_1-a)^2) \\ &= 2a(3X_1^2 + a^2) \\ &\geq 2a^3, \end{aligned}$$

leading to :

$$\begin{aligned} \frac{1}{|\gamma|} \int_{\gamma} |B \cdot (x - G_\gamma)|^2 &\geq \frac{2a}{3|\gamma|} 2a^3 (\mu_1^2 + \mu_2^2) \\ &\geq \frac{2a}{3|\gamma|} 2a^3 \mu_2^2. \end{aligned}$$

From shape regularity, we have $|\gamma| \leq C \text{diam}(\gamma)^2 \leq C \rho(\gamma)^2 = 2Ca^2$, and therefore :

$$\begin{aligned} \frac{1}{|\gamma|} \int_{\gamma} |B \cdot (x - G_\gamma)|^2 &\geq Ca^2 \mu_2^2 \\ &\geq C \text{diam}(\gamma)^2 \mu_2^2, \end{aligned}$$

but by definition :

$$\mu_2^2 = \lambda(B, \gamma)^2,$$

which ends the proof. \square

The main consequence from assumption 4.5 is the simple :

Lemma 4.9. *Under assumption 4.5, there exists a constant $C > 0$ such that for all locally affine functions $v \in \mathbb{P}_1(\Omega)^d$, we can find at each node M of the coarse mesh \mathcal{T}_H , an interface $\gamma \ni M$ for which :*

$$\|v\|_{L^\infty(\gamma)^d}^2 \leq C \frac{1}{|\gamma|} \|v\|_{L^2(\gamma)^d}^2.$$

Proof : Let v be locally in $\mathbb{P}_1(\Omega)^d$. For all $\gamma \in Z$, there exists a vector $v(G_\gamma) \in \mathbb{R}^d$ and a matrix $B \in \mathbb{R}^{d \times d}$ such that :

$$v(x) = v(G_\gamma) + B \cdot (x - G_\gamma), \quad \forall x \in \gamma,$$

the matrix B being independent of the choice of $\gamma \in Z$. From assumption 4.5, we can always find at each node M_i of the coarse mesh \mathcal{T}_H , an interface $\gamma = \gamma_i$ such that (4.20) is satisfied. Then :

$$\|v\|_{L^\infty(\gamma)}^2 \leq 2|v(G_\gamma)|^2 + 2\lambda(B, \gamma)^2 \text{diam}(\gamma)^2,$$

and from assumption 4.5, we deduce :

$$\begin{aligned} \frac{1}{|\gamma|} \|v\|_{L^2(\gamma)}^2 &= v(G_\gamma)^2 + \frac{1}{|\gamma|} \int_\gamma |B \cdot (x - G_\gamma)|^2 \\ &\geq C(v(G_\gamma)^2 + \lambda(B, \gamma)^2 \text{diam}(\gamma)^2) \\ &\geq C\|v\|_{L^\infty(\gamma)}^2. \end{aligned}$$

\square

Conforming approximation - For all functions $v \in X$, we are now ready to define the conforming approximation $\mathbf{P}v \in H_*^1(\Omega)$ by :

$$\mathbf{P}v = \sum_{i \geq 1} p_i v(M_i) \phi_i, \tag{4.21}$$

where :

$$p_i v = \pi_{\gamma_i} v,$$

in which π_γ is the $L^2(\gamma)^d$ projection over $\mathbb{P}_1(\gamma)^d$ (the restrictions to γ of functions in $\mathbb{P}_1(\Omega)^d$), and $\gamma_i \in Z$ is among the interfaces sharing M_i , the one which maximizes :

$$\mathcal{A}(\gamma) = \inf_{B \in \mathbb{R}^{d \times d}} \frac{1}{\lambda(B, \gamma)^2 \text{diam}(\gamma)^2} \frac{1}{|\gamma|} \int_\gamma |B \cdot (x - G_\gamma)|^2 dx.$$

Let us notice that in the expression $\pi_{\gamma_i} v$, we choose arbitrarily the side of γ_i on which the trace of v is taken. When considering $v \in V$ with the constrained space :

$$V = \{v \in X, \int_{\gamma_{kl}} [v] \cdot \mu = 0, \quad \forall \mu \in \mathbb{P}_1(\gamma_{kl})^d, 1 \leq k, l \leq K\},$$

this choice has no influence because :

$$\int_{\gamma_i} v^+ \cdot \mu = \int_{\gamma_i} v^- \cdot \mu, \quad \forall \mu \in \mathbb{P}_1(\gamma_i)^d,$$

entailing that $\pi_{\gamma_i} v^+ = \pi_{\gamma_i} v^-$.

Remark 4.11. In this section, we use the Lagrange multipliers spaces $M_{kl} = \mathbb{P}_1(\gamma_{kl})^d$. Nevertheless, one can adopt any M_{kl} such that for all $v \in L^2(\gamma_{kl})^d$, there exists a solution $\pi_{\gamma_{kl}} v \in \mathbb{P}_1(\gamma_{kl})^d$ of :

$$\int_{\gamma_{kl}} \pi_{\gamma_{kl}} v \cdot \mu = \int_{\gamma_{kl}} v \cdot \mu, \quad \forall \mu \in M_{kl},$$

satisfying :

$$\|\pi_{\gamma_{kl}} v\|_{L^2(\gamma_{kl})^d} \leq C \sup_{\mu \in M_{kl}} \frac{\int_{\gamma_{kl}} v \cdot \mu}{\|\mu\|_{L^2(\gamma_{kl})^d}}. \quad (4.22)$$

Such a statement is true when adopting Lagrange multipliers satisfying the assumption 4.3, but the constant a priori depends on the shape of the interface γ_{kl} .

Proposition 4.4. The interpolation operator $\mathbf{P} : \prod_{k=1}^K H^1(\Omega_k)^d \rightarrow (X_H)^d$ defined by (4.21) satisfies the following local inequality for all $1 \leq k \leq K$:

$$\|v - \mathbf{P}v\|_{H^1(\Omega_k)^d}^2 \leq C \left(\sum_{l \in \mathcal{N}(\Omega_k)} d_l(v, v) + \frac{1}{\text{diam}(\Omega_k)} \int_{\mathcal{S}_k} (\pi[v])^2 \right), \quad (4.23)$$

where $\mathcal{N}(\Omega_k)$ denotes the set of indices of the subdomains sharing a vertex with Ω_k , and d_k is the bilinear form over $H^1(\Omega_k)^d \times H^1(\Omega_k)^d$ defined as :

$$d_k(u, v) = \int_{\Omega_k} \varepsilon(u) : \varepsilon(v), \quad \forall u, v \in H^1(\Omega_k)^d.$$

Moreover, we have denoted by \mathcal{S}_k the union of the neighboring interfaces of Ω_k :

$$\mathcal{S}_k = \bigcup_{l, m \in \mathcal{N}(\Omega_k)} \gamma_{lm},$$

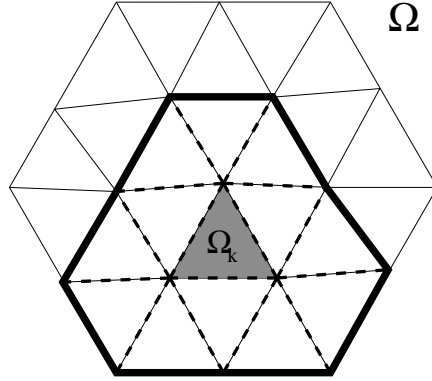


FIG. 4.4 – A triangular domain decomposition of $\Omega \subset \mathbb{R}^2$, with illustration of the subdomains $(\Omega_l)_{l \in \mathcal{N}(\Omega_k)}$ sharing a vertex with Ω_k (inside the dark thick line), and of the reunion \mathcal{S}_k of the neighboring interfaces of Ω_k (in dotted lines).

and :

$$\pi[v](x) = \pi_\gamma[v](x), \quad \text{for all } x \in \gamma, \text{ with } \gamma \in Z_S.$$

Moreover, when the decomposition into subdomains satisfies the conditions defined in section 4.4.1, the constant C is independent of the diameter and the shape of the subdomains. The definitions of $\mathcal{N}(\Omega_k)$ and \mathcal{S}_k are illustrated on figure 4.4.

Proof : The proof is decomposed into 4 parts. For convenience, we will denote by \mathcal{O}_k the neighborhood of Ω_k defined as :

$$\mathcal{O}_k = \bigcup_{l \in \mathcal{N}(\Omega_k)} \Omega_l.$$

1. Range of $\mathbb{P}_1(\mathcal{O}_k)^d$.

Let us consider the affine displacement $v \in \mathbb{P}_1(\mathcal{O}_k)^d$. For all $\gamma \in Z \cap \mathcal{O}_k$, the trace of v over γ belongs to $\mathbb{P}_1(\gamma)^d$ by definition, and therefore :

$$\pi_\gamma v = v, \quad \text{on } \gamma.$$

As a consequence, we obtain for all $i \geq 1$ satisfying $M_i \in \overline{\Omega_k}$, that $p_i v = v$, hence :

$$(\mathbf{P}v)|_{\Omega_k} = \sum_{i \geq 1, M_i \in \overline{\Omega_k}} v(M_i) \phi_i = v|_{\Omega_k},$$

because $v|_{\Omega_k} \in (X_H)^d$.

2. Stability of \mathbf{P} in $L^2(\Omega_k)^d$.

Let $v \in X$. It is readily obtained from definition (4.21), that :

$$\begin{aligned} \|\mathbf{P}v\|_{L^2(\Omega_k)^d}^2 &\leq \max_{i, M_i \in \overline{\Omega}_k} |p_i v(M_i)|^2 \int_{\Omega_k} \left(\sum_{1 \leq i \leq I} |\phi_i| \right)^2 \\ &\leq \max_{i, M_i \in \overline{\Omega}_k} \|\pi_{\gamma_i} v\|_{L^\infty(\gamma_i)^d}^2 \int_{\Omega_k} \left(\sum_{1 \leq i \leq I} |\phi_i| \right)^2. \end{aligned}$$

Under assumption 4.5, we obtain from lemma 4.9 that :

$$\|\pi_{\gamma_i} v\|_{L^\infty(\gamma_i)^d}^2 \leq C \frac{1}{|\gamma_i|} \|\pi_{\gamma_i} v\|_{L^2(\gamma_i)^d}^2,$$

and because π_{γ_i} is the $L^2(\gamma_i)^d$ projection over $\mathbb{P}_1(\gamma_i)^d$, we get :

$$\|\pi_{\gamma_i} v\|_{L^2(\gamma_i)^d}^2 \leq \|v\|_{L^2(\gamma_i)^d}^2,$$

resulting in :

$$\|\mathbf{P}v\|_{L^2(\Omega_k)^d}^2 \leq \max_{i, M_i \in \overline{\Omega}_k} \frac{1}{|\gamma_i|} \|v\|_{L^2(\gamma_i)^d}^2 \int_{\Omega_k} \left(\sum_{1 \leq i \leq I} |\phi_i| \right)^2. \quad (4.24)$$

As γ_i is a part of the boundary of a domain $\Omega_{l(i)}$ corresponding to the side of γ_i on which the trace of v is taken, we get from the Sobolev trace theorem that :

$$\frac{1}{\text{diam}(\Omega_{l(i)})} \|v\|_{L^2(\gamma_i)^d}^2 \leq C \left(\frac{1}{\text{diam}(\Omega_{l(i)})^2} \int_{\Omega_{l(i)}} v^2 + \int_{\Omega_{l(i)}} |\nabla v|^2 \right), \quad (4.25)$$

with C uniformly bounded due to the shape regularity of $\Omega_{l(i)}$. Moreover, we have :

$$\int_{\Omega_k} \left(\sum_{1 \leq i \leq I} |\phi_i| \right)^2 = \int_{\Omega_k} dx = |\Omega_k|, \quad (4.26)$$

because by construction $\sum_{1 \leq i \leq I} |\phi_i| = 1$. We deduce by exploiting the expressions (4.25) and (4.26) in (4.24) that :

$$\begin{aligned} \|\mathbf{P}v\|_{L^2(\Omega_k)^d}^2 &\leq C \max_{i, M_i \in \overline{\Omega}_k} \frac{|\Omega_k|}{|\gamma_i|} \text{diam}(\Omega_{l(i)}) \left(\frac{1}{\text{diam}(\Omega_{l(i)})^2} \int_{\Omega_{l(i)}} v^2 + \int_{\Omega_{l(i)}} |\nabla v|^2 \right) \\ &\leq C \max_{i, M_i \in \overline{\Omega}_k} \frac{|\Omega_k|}{|\Omega_{l(i)}|} \text{diam}(\Omega_{l(i)})^2 \left(\frac{1}{\text{diam}(\Omega_{l(i)})^2} \int_{\Omega_{l(i)}} v^2 + \int_{\Omega_{l(i)}} |\nabla v|^2 \right) \end{aligned}$$

because from the shape regularity conditions (4.18), we get :

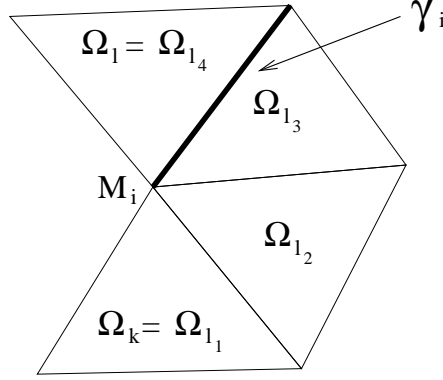
$$\begin{aligned} |\gamma_i| \operatorname{diam}(\Omega_{l(i)}) &\geq \kappa'' \operatorname{diam}(\Omega_{l(i)})^{d-1} \operatorname{diam}(\Omega_{l(i)}) \\ &= \kappa'' \operatorname{diam}(\Omega_{l(i)})^d \\ &\geq C \kappa'' |\Omega_{l(i)}|. \end{aligned}$$

Therefore, there exists a subdomain Ω_l sharing a node with Ω_k such that :

$$\frac{1}{\operatorname{diam}(\Omega_l)^2} \|\mathbf{P}v\|_{L^2(\Omega_k)^d}^2 \leq C \frac{|\Omega_k|}{|\Omega_l|} \left(\frac{1}{\operatorname{diam}(\Omega_l)^2} \int_{\Omega_l} v^2 + \int_{\Omega_l} |\nabla v|^2 \right),$$

after a division of the two sides of the inequality by $\operatorname{diam}(\Omega_l)^2$.

Let us show now that $\operatorname{diam}(\Omega_l) \leq C \operatorname{diam}(\Omega_k)$. From the shape regularity (4.18) of the decomposition, we can build a sequence of (less than) P adjacent subdomains $(\Omega_{l_m})_{1 \leq m \leq P}$ such that Ω_{l_m} and $\Omega_{l_{m+1}}$ share the interface $\gamma_{l_m l_{m+1}}$ with $\Omega_{l_1} = \Omega_k$ and $\Omega_{l_P} = \Omega_l$, as illustrated on the following figure (for triangular subdomains) :



From the shape regularity (4.18) of the decomposition into subdomains, we then have :

$$\begin{aligned} \operatorname{diam}(\Omega_{l_{m+1}}) &\leq \frac{1}{\kappa'} \operatorname{diam}(\gamma_{l_m l_{m+1}}) \\ &\leq \frac{1}{\kappa'} \operatorname{diam}(\Omega_{l_m}), \end{aligned} \tag{4.27}$$

and by iteration of (4.27), we get :

$$\operatorname{diam}(\Omega_l) \leq \frac{1}{(\kappa')^P} \operatorname{diam}(\Omega_k). \tag{4.28}$$

Considering that the roles of Ω_k and Ω_l can be swapped in the previous inequality (4.28), we deduce that $|\Omega_k| \leq C |\Omega_l|$ from the shape regularity (4.18) of the

decomposition because :

$$\begin{aligned} |\Omega_k| &\leq C \operatorname{diam}(\Omega_k)^d \\ &\leq C \frac{1}{(\kappa')^{dP}} \operatorname{diam}(\Omega_l)^d \\ &\leq C \frac{1}{(\kappa')^{dP}} \frac{1}{\kappa^d} \rho(\Omega_l)^d \\ &\leq C \frac{1}{(\kappa')^{dP}} \frac{1}{\kappa^d} |\Omega_l|. \end{aligned}$$

As a consequence, we obtain from (4.27) with a still generic use of the constant C , that there exists a subdomain Ω_l sharing a node with Ω_k such that :

$$\frac{1}{\operatorname{diam}(\Omega_k)^2} \|\mathbf{P}v\|_{L^2(\Omega_k)}^2 \leq C \left(\frac{1}{\operatorname{diam}(\Omega_l)^2} \int_{\Omega_l} v^2 + \int_{\Omega_l} |\nabla v|^2 \right). \quad (4.29)$$

3. Stability of \mathbf{P} in $H^1(\Omega_k)^d$.

Proceeding as previously, we get for all $v \in X$ the following bound on the $H^1(\Omega_k)^d$ semi-norm of the interpolate function $\mathbf{P}v$:

$$\begin{aligned} |\mathbf{P}v|_{H^1(\Omega_k)^d}^2 &\leq \max_{1 \leq i \leq I} |p_i v(M_i)|^2 \int_{\Omega_k} \left(\sum_{1 \leq i \leq I} |\nabla \phi_i| \right)^2 \\ &\leq C \max_{i, M_i \in \overline{\Omega}_k} \frac{\operatorname{diam}(\Omega_{l(i)})^2}{|\Omega_{l(i)}|} \left(\frac{1}{\operatorname{diam}(\Omega_{l(i)})^2} \int_{\Omega_{l(i)}} v^2 + \int_{\Omega_{l(i)}} |\nabla v|^2 \right) \int_{\Omega_k} \left(\sum_{1 \leq i \leq I} |\nabla \phi_i| \right)^2. \end{aligned} \quad (4.30)$$

Moreover, by decomposing the last integral over Ω_k into a sum of integrals over the triangles of the coarse triangulation \mathcal{T}_H belonging to Ω_k :

$$\int_{\Omega_k} \left(\sum_{1 \leq i \leq I} |\nabla \phi_i| \right)^2 = \sum_{T \in \mathcal{T}_H, T \subset \Omega_k} \int_T \left(\sum_{1 \leq i \leq I} |\nabla \phi_i| \right)^2,$$

and using the fact that for all tetrahedra $T \in \mathcal{T}_H$ belonging to Ω_k , we have the standard result :

$$|\nabla \phi_i| \leq C \frac{1}{\rho(T)} \leq C \frac{1}{\operatorname{diam}(\Omega_k)},$$

using the assumption 3- made for the coarse triangulation \mathcal{T}_H , we conclude that :

$$\int_{\Omega_k} \left(\sum_{1 \leq i \leq I} |\nabla \phi_i| \right)^2 \leq \frac{C}{\operatorname{diam}(\Omega_k)^2} |\Omega_k|. \quad (4.31)$$

Hence from (4.30) and (4.31), we get by using the same arguments of shape regularity of the decomposition as in the previous part of the proof that there exists a subdomain Ω_l sharing a node with Ω_k (the same as in (4.29)) such that :

$$\|\mathbf{P}v\|_{H^1(\Omega_k)}^2 \leq C \left(\frac{1}{diam(\Omega_l)^2} \int_{\Omega_l} v^2 + \int_{\Omega_l} |\nabla v|^2 \right).$$

4. Approximation property

For all $v \in X$ the interpolation $\mathbf{P}v \in (X_H)^d$ satisfies from the two previous points of the proof, the following stability property :

$$\|\mathbf{P}v\|_{H^1(\Omega_k)^d}^2 \leq C \|v\|_{H^1(\Omega_l)^d}^2. \quad (4.32)$$

For all rigid motion $p \in \mathcal{R}(\mathcal{O}_k)$, which is a fortiori a linear function of $\mathbb{P}_1(\mathcal{O}_k)^d$, we have from point 1 that $\mathbf{P}p = p$ on Ω_k , resulting in the following bounds by using the triangular inequality and the stability estimate (4.32) :

$$\begin{aligned} \|v - \mathbf{P}v\|_{H^1(\Omega_k)^d}^2 &= \|v - p + \mathbf{P}(p - v)\|_{H^1(\Omega_k)^d}^2 \\ &\leq 2\|v - p\|_{H^1(\Omega_k)^d}^2 + 2\|\mathbf{P}(p - v)\|_{H^1(\Omega_k)^d}^2 \\ &\leq C \left(\|v - p\|_{H^1(\Omega_k)^d}^2 + \|v - p\|_{H^1(\Omega_l)^d}^2 \right) \\ &\leq C \sum_{l \in \mathcal{N}(\Omega_k)} \|v - p\|_{H^1(\Omega_l)^d}^2. \end{aligned}$$

By taking p as the extension over Ω of the rigid motion projection of v over Ω_k , we get from lemma 4.10, page 135 that :

$$\|v - \mathbf{P}v\|_{H^1(\Omega_k)^d}^2 \leq C \left(\sum_{l \in \mathcal{N}(\Omega_k)} d_l(v, v) + \frac{1}{diam(\Omega_k)} \int_{\mathcal{S}_k} (\pi[v])^2 \right),$$

which is exactly (4.23). □

In the previous proof, we have used the following lemma which is a generalization to non-conforming vector functions of the Deny-Lions [DL55] or Bramble-Hilbert [BH70] lemma involving the broken elasticity semi-norm.

Lemma 4.10. *There exists a constant $C > 0$ such that for all $v \in X$:*

$$\sum_{l \in \mathcal{N}(\Omega_k)} \|v - p\|_{H^1(\Omega_l)^d}^2 \leq C \left(\sum_{l \in \mathcal{N}(\Omega_k)} d_l(v, v) + \frac{1}{diam(\Omega_k)} \int_{\mathcal{S}_k} (\pi[v])^2 \right), \quad (4.33)$$

where $p \in \mathcal{R}(\Omega)$ is the rigid motion satisfying :

$$\int_{\Omega_k} p \cdot w = \int_{\Omega_k} v \cdot w, \quad \forall w \in \mathcal{R}(\Omega).$$

Moreover, provided the decomposition into subdomains satisfy the shape regularity condition defined in section 4.4.1, the constant C is independent of the size and the shape of the neighbor subdomains.

Proof : We prove herein the announced upper bound for the quantity

$$\sum_{l \in \mathcal{N}(\Omega_k)} \|v - p\|_{H^1(\Omega_l)^d}^2,$$

in which the rigid motion $p \in \mathcal{R}(\Omega)$ is defined by :

$$\int_{\Omega_k} p \cdot r = \int_{\Omega_k} v \cdot r, \quad \forall r \in \mathcal{R}(\Omega_k).$$

- First, it follows from lemma 4.6 that :

$$\|v - p\|_{H^1(\Omega_k)^d}^2 \leq C_N \left(\frac{1}{\text{diam}(\Omega_k)^2} \left(\sup_{r \in \mathcal{R}(\Omega_k)} \frac{\int_{\Omega_k} (v - p) \cdot r}{\|r\|_{L^2(\Omega_k)^d}} \right)^2 + d_k(v - p, v - p) \right) = C_N d_k(v, v),$$

by definition of the local rigid motion projection p .

- If Ω_l shares an interface with Ω_k , we obtain from lemmas 4.5 and 4.7 that :

$$\begin{aligned} & \|v - p\|_{H^1(\Omega_l)^d}^2 \\ & \leq C_P \left(\frac{1}{\text{diam}(\Omega_l)} \left(\sup_{\mu \in M_{kl}} \frac{\int_{\gamma_{kl}} (v - p)|_{\Omega_l} \cdot \mu}{\|\mu\|_{L^2(\gamma_{kl})^d}} \right)^2 + d_l(v, v) \right) \\ & \leq 2C_P \left(\frac{1}{\text{diam}(\Omega_l)} \left(\sup_{\mu \in M_{kl}} \frac{\int_{\gamma_{kl}} (v - p)|_{\Omega_k} \cdot \mu}{\|\mu\|_{L^2(\gamma_{kl})^d}} \right)^2 + d_l(v, v) + \frac{1}{\text{diam}(\Omega_l)} \int_{\gamma_{kl}} (\pi_{\gamma_{kl}}[v])^2 \right) \\ & \leq 2C_P \left(\frac{\text{diam}(\Omega_k)}{\text{diam}(\Omega_l)} C_T \left(\frac{1}{\text{diam}(\Omega_k)^2} \left(\sup_{r \in \mathcal{R}(\Omega_k)} \frac{\int_{\Omega_k} (v - p) \cdot r}{\|r\|_{L^2(\Omega_k)^d}} \right)^2 + d_k(v, v) \right) + d_l(v, v) \right) \\ & \quad + 2C_P \frac{1}{\text{diam}(\Omega_l)} \int_{\gamma_{kl}} (\pi_{\gamma_{kl}}[v])^2 \\ & = 2C_P \left(\frac{\text{diam}(\Omega_k)}{\text{diam}(\Omega_l)} C_T d_k(v, v) + d_l(v, v) \right) + 2C_P \frac{1}{\text{diam}(\Omega_l)} \int_{\gamma_{kl}} (\pi_{\gamma_{kl}}[v])^2 \\ & \leq C \left(d_k(v, v) + d_l(v, v) + \frac{1}{\text{diam}(\Omega_l)} \int_{\gamma_{kl}} (\pi_{\gamma_{kl}}[v])^2 \right), \end{aligned} \tag{4.34}$$

because we have $diam(\Omega_k) \leq Cdiam(\Omega_l)$ as in the step 2 of the proof of proposition 4.4.

- For other $l \in \mathcal{N}(\Omega_k)$, we proceed by the same technique used in the step 2 of the proof of proposition 4.4, by reasonning on a sequence of adjacent subdomains, and obtain as above :

$$\begin{aligned}
& \|v - p\|_{H^1(\Omega_{l_{m+1}})^d}^2 \\
& \leq C_P \left(\frac{1}{diam(\Omega_{l_{m+1}})} \left(\sup_{\mu \in M_{l_m l_{m+1}}} \frac{\int_{\gamma_{l_m l_{m+1}}}(v - p)|_{\Omega_{l_{m+1}}} \cdot \mu}{\|\mu\|_{L^2(\gamma_{l_m l_{m+1}})^d}} \right)^2 + d_{l_{m+1}}(v, v) \right) \\
& \leq 2C_P \left(\frac{1}{diam(\Omega_{l_{m+1}})} \left(\sup_{\mu \in M_{l_m l_{m+1}}} \frac{\int_{\gamma_{l_m l_{m+1}}}(v - p)|_{\Omega_{l_m}} \cdot \mu}{\|\mu\|_{L^2(\gamma_{l_m l_{m+1}})^d}} \right)^2 + d_{l_{m+1}}(v, v) \right) \\
& \quad + 2C_P \frac{1}{diam(\Omega_{l_{m+1}})} \int_{\gamma_{l_m l_{m+1}}} (\pi_{\gamma_{l_m l_{m+1}}}[v])^2 \\
& \leq 2C_P \frac{diam(\Omega_{l_m})}{diam(\Omega_{l_{m+1}})} C_T \left(\frac{1}{diam(\Omega_{l_m})^2} \left(\sup_{r \in \mathcal{R}(\Omega_{l_m})} \frac{\int_{\Omega_{l_m}}(v - p) \cdot r}{\|r\|_{L^2(\Omega_{l_m})^d}} \right)^2 + d_{l_m}(v - p, v - p) \right) \\
& \quad + 2C_P \left(d_{l_{m+1}}(v, v) + \frac{1}{diam(\Omega_{l_{m+1}})} \int_{\gamma_{l_m l_{m+1}}} (\pi_{\gamma_{l_m l_{m+1}}}[v])^2 \right) \\
& \leq 2C_P \left(\frac{diam(\Omega_{l_m})}{diam(\Omega_{l_{m+1}})} C_T \|v - p\|_{H^1(\Omega_{l_m})^d}^2 + d_{l_{m+1}}(v, v) + \frac{1}{diam(\Omega_{l_{m+1}})} \int_{\gamma_{l_m l_{m+1}}} (\pi_{\gamma_{l_m l_{m+1}}}[v])^2 \right),
\end{aligned}$$

from Cauchy-Schwarz inequality. From the shape regularity (4.18), it follows that $diam(\Omega_k) \leq Cdiam(\Omega_{l_{m+1}})$ and $diam(\Omega_{l_m}) \leq Cdiam(\Omega_{l_{m+1}})$ as in the step 2 of the proof of proposition 4.4, and we get :

$$\begin{aligned}
& \|v - p\|_{H^1(\Omega_{l_{m+1}})^d}^2 \\
& \leq CC_P \left(C_T \|v - p\|_{H^1(\Omega_{l_m})^d}^2 + d_{l_{m+1}}(v, v) + \frac{1}{diam(\Omega_k)} \int_{\gamma_{l_m l_{m+1}}} (\pi_{\gamma_{l_m l_{m+1}}}[v])^2 \right).
\end{aligned}$$

By induction on m and from (4.34), it is then obtained from $\#\mathcal{N}(\Omega_k) \leq P$ that :

$$\|v - p\|_{H^1(\Omega_l)^d}^2 \leq C(C_P C_T)^P C_N \left(\sum_{j \in \mathcal{N}(\Omega_k)} d_j(v, v) + \frac{1}{diam(\Omega_k)} \int_{\mathcal{S}_k} (\pi[v])^2 \right),$$

and therefore :

$$\begin{aligned} \sum_{l \in \mathcal{N}(\Omega_k)} \|v - p\|_{H^1(\Omega_l)^d}^2 &\leq C(C_P C_T)^P C_N \sum_{l \in \mathcal{N}(\Omega_k)} \left(\sum_{j \in \mathcal{N}(\Omega_k)} d_j(v, v) + \frac{1}{\text{diam}(\Omega_k)} \int_{S_k} (\pi[v])^2 \right) \\ &\leq CP(C_P C_T)^P C_N \left(\sum_{j \in \mathcal{N}(\Omega_k)} d_j(v, v) + \frac{1}{\text{diam}(\Omega_k)} \int_{S_k} (\pi[v])^2 \right), \end{aligned}$$

hence the proof. \square

Remark 4.12 (Satisfaction of a Dirichlet homogeneous boundary condition). If $v \in X$ satisfies a Dirichlet homogeneous boundary condition on the part Γ_D of the boundary of the domain Ω , its interpolation $\mathbf{P}v$ has the same boundary value on Γ_D provided :

- $\mathcal{T}_H \cap \Gamma_D$ is a (possibly curved) triangulation of Γ_D ,
- the nodes $M_i \in \Gamma_D$ are associated to faces $\gamma_i \in Z$ contained in Γ_D .

4.4.4 Uniform coercivity result

We improve herein the coercivity result from proposition 4.2 by showing that the coercivity constant is independent of the number and the size of the subdomains :

Proposition 4.5. *There exists a constant $C > 0$ independent of any decomposition of Ω into subdomains satisfying the assumptions of section 4.4.1, such that for all displacements fields $v \in X$:*

$$\|v\|_X^2 \leq C \left(\sum_{k=1}^K d_k(v, v) + \sum_{1 \leq k < l \leq K} \frac{1}{\text{diam}(\gamma_{kl})} \int_{\gamma_{kl}} (\pi_{\gamma_{kl}}[v])^2 \right). \quad (4.35)$$

Proof : For all $v \in V$, the conforming interpolate function $\mathbf{P}v \in (X_H)^d \subset H^1(\Omega)^d$ satisfies the same Dirichlet boundary condition as v (see remark 4.12) resulting in the usual coercivity result, only depending on the shape of Ω :

$$\tilde{d}(\mathbf{P}v, \mathbf{P}v) = d(\mathbf{P}v, \mathbf{P}v) \geq C \|\mathbf{P}v\|_{H^1(\Omega)^d}^2 = C \|\mathbf{P}v\|_X^2. \quad (4.36)$$

Consequently, we get from (4.36) and proposition 4.4 that :

$$\begin{aligned} \|v\|_X^2 &= \|v - \mathbf{P}v + \mathbf{P}v\|_X^2, \\ &\leq 2 \sum_{k=1}^K \|v - \mathbf{P}v\|_{H^1(\Omega_k)^d}^2 + 2 \sum_{k=1}^K \|\mathbf{P}v\|_{H^1(\Omega_k)^d}^2, \\ &\leq C \sum_{k=1}^K \left(\sum_{l \in \mathcal{N}(\Omega_k)} d_l(v, v) + \frac{1}{\text{diam}(\Omega_k)} \int_{S_k} (\pi[v])^2 \right) + C \tilde{d}(\mathbf{P}v, \mathbf{P}v), \end{aligned}$$

Moreover, we obtain by the triangular inequality and the use of proposition 4.4 that :

$$\begin{aligned}
\tilde{d}(\mathbf{P}v, \mathbf{P}v) &= \tilde{d}(\mathbf{P}v - v + v, \mathbf{P}v - v + v) \\
&\leq 2\tilde{d}(\mathbf{P}v - v, \mathbf{P}v - v) + 2\tilde{d}(v, v) \\
&\leq 2 \sum_{k=1}^K |\mathbf{P}v - v|_{H^1(\Omega_k)^d}^2 + 2\tilde{d}(v, v) \\
&\leq C \sum_{k=1}^K \left(\sum_{l \in \mathcal{N}(\Omega_k)} d_l(v, v) + \frac{1}{\text{diam}(\Omega_k)} \int_{\mathcal{S}_k} (\pi[v])^2 \right) + 2\tilde{d}(v, v),
\end{aligned}$$

which leads to the final estimate :

$$\|v\|_X^2 \leq C \left(\sum_{k=1}^K d_k(v, v) + \sum_{1 \leq k < l \leq K} \frac{1}{\text{diam}(\gamma_{kl})} \int_{\gamma_{kl}} (\pi_{\gamma_{kl}}[v])^2 \right), \quad \forall v \in X, \quad (4.37)$$

by exploiting the fact that $\#\mathcal{N}(\Omega_k) \leq P$, and $\text{diam}(\Omega_k) \geq \text{diam}(\gamma_{kl})$. \square

4.4.5 Existence result for problem (4.7)

From assumption 4.3, we have $V_h \subset V$ independently of the discretization, and get the uniform coercivity of the bilinear form \tilde{a} over $V_h \times V_h$. Indeed, for all $v_h \in V_h$, we get from (4.35) that :

$$\begin{aligned}
\tilde{a}(v_h, v_h) &= \sum_{k=1}^K \int_{\Omega_k} (\mathbf{E} : \boldsymbol{\varepsilon}(v_h)) : \boldsymbol{\varepsilon}(v_h) \\
&\geq \min_{k \geq 1}(c_k) \sum_{k=1}^K \int_{\Omega_k} \boldsymbol{\varepsilon}(v_h) : \boldsymbol{\varepsilon}(v_h) \\
&\geq C \min_{k \geq 1}(c_k) \left(\sum_{k=1}^K \frac{1}{\text{diam}(\Omega_k)^2} \int_{\Omega_k} (v_h)^2 + \int_{\Omega_k} |\nabla v_h|^2 \right),
\end{aligned}$$

because $\pi[v_h] = 0$ due to the fact that $v_h \in V$. The coercivity of the bilinear form \tilde{a} over $V_h \times V_h$ is then proved, with independence of the coercivity constant $\tilde{a} = C \min_{k \geq 1}(c_k)$ with respect to the number and the size of the subdomains. Let us remark that when the Young moduli of the subdomains are multiplied by a constant, \tilde{a} is multiplicatively as well. Since \tilde{a} is uniformly coercive over $V_h \times V_h$ and since (4.9) ensures that the weak-continuity constraint b over the interfaces is onto, the discrete problem (4.7) is well posed by using Babuska and Brezzi's theory of mixed problems [Bre74, Bab73] summarized in the following proposition :

Proposition 4.6. Let X_h and M_δ be two real reflexive Banach spaces respectively endowed with the norms $\|\cdot\|_{X_h}$ and $\|\cdot\|_{M_\delta}$. Let $\tilde{a} : X_h \times X_h \rightarrow \mathbb{R}$ and $b : X_h \times M_\delta \rightarrow \mathbb{R}$ two continuous bilinear forms, and $l : X_h \rightarrow \mathbb{R}$ a continuous linear form. Denoting by :

$$V_h = \{v_h \in X_h, \quad b(v_h, \mu_h) = 0, \forall \mu_h \in M_\delta\}$$

the kernel space of b , we assume that \tilde{a} is coercive over $V_h \times V_h$ in the sense that :

$$\exists \tilde{\alpha} > 0, \quad \tilde{a}(v_h, v_h) \geq \tilde{\alpha} \|v_h\|_{X_h}^2,$$

and that b satisfies the following inf-sup condition :

$$\exists \beta > 0, \quad \inf_{\mu_h \in M_\delta \setminus \{0\}} \sup_{v_h \in X_h \setminus \{0\}} \frac{b(v_h, \mu_h)}{\|v_h\|_{X_h} \|\mu_h\|_{M_\delta}} \geq \beta.$$

Then there exists a unique solution $(u_h, \lambda_h) \in X_h \times M_\delta$ of :

$$\begin{cases} \tilde{a}(u_h, v_h) + b(v_h, \lambda_h) = l(v_h), & \forall v_h \in X_h, \\ b(u_h, \mu_h) = 0, & \forall \mu_h \in M_\delta. \end{cases}$$

4.5 Error estimates in elastostatics

4.5.1 Approximation of displacements

We recall now the standard error estimates in elastostatics under the following assumption :

Assumption 4.6. For all $1 \leq m \leq M$, the family of interface meshes $(\mathcal{F}_{m;\delta_m})_{\delta_m > 0}$ over the non-mortar side is quasi-uniform, and $\bar{\delta}_m/\delta_m$ remains bounded independently of the chosen discretization.

First, we need the following lemma :

Lemma 4.11. For all $1 \leq m \leq M$, there exists an operator :

$$P_m : \mathbb{H}_\delta^{1/2}(\Gamma_m) \rightarrow W_{m;\delta_m},$$

such that for all $v \in \mathbb{H}_\delta^{1/2}(\Gamma_m)$:

$$\int_{\Gamma_m} (P_m v) \cdot \mu = \int_{\Gamma_m} v \cdot \mu, \quad \forall \mu \in M_{m;\delta_m},$$

with :

$$\|P_m v\|_{\delta, \frac{1}{2}, m} \leq C \|v\|_{\delta, \frac{1}{2}, m}.$$

Proof : For all $1 \leq m \leq M$, we have by using assumption 4.2 :

$$\begin{aligned} & \inf_{\lambda_h \in M_{m;\delta_m}} \sup_{\phi_h \in W_{m;\delta_m}} \frac{\int_{\Gamma_m} \lambda_h \cdot \phi_h}{\|\lambda_h\|_{\delta,\frac{1}{2},m} \|\phi_h\|_{\delta,-\frac{1}{2},m}} \geq \inf_{\lambda_h \in M_{m;\delta_m}} \sup_{\phi_h \in W_{m;\delta_m}^0} \frac{\int_{\Gamma_m} \lambda_h \cdot \phi_h}{\|\lambda_h\|_{\delta,\frac{1}{2},m} \|\phi_h\|_{\delta,-\frac{1}{2},m}} \\ & \geq \inf_{\lambda_h \in M_{m;\delta_m}} \sup_{\phi \in \mathbb{H}_\delta^{1/2}(\Gamma_m)} \frac{\int_{\Gamma_m} \lambda_h \cdot \pi_m \phi}{\|\lambda_h\|_{\delta,\frac{1}{2},m} \|\pi_m \phi\|_{\delta,-\frac{1}{2},m}} \\ & \geq \frac{1}{C_m} \inf_{\lambda_h \in M_{m;\delta_m}} \sup_{\phi \in \mathbb{H}_\delta^{1/2}(\Gamma_m)} \frac{\int_{\Gamma_m} \lambda_h \cdot \phi}{\|\lambda_h\|_{\delta,\frac{1}{2},m} \|\phi\|_{\delta,-\frac{1}{2},m}} = \frac{1}{C_m}. \end{aligned}$$

As $W_{m;\delta_m}$ is reflexive, this condition implies that the map $v_h \in W_{m;\delta_m} \rightarrow l \in M'_{m;\delta_m}$ with $l(\mu) = \int_{\Gamma_m} v_h \cdot \mu$ for all $\mu \in M_{m;\delta_m}$ is onto with a continuous inverse. In other words, it implies that for all $l \in M'_{m;\delta_m}$, there exists a $v_h \in W_{m;\delta_m}$ such that :

$$\int_{\Gamma_m} v_h \cdot \mu = l(\mu), \quad \forall \mu \in M_{m;\delta_m},$$

with

$$\|v_h\|_{\delta,\frac{1}{2},m} \leq \frac{1}{C_m} \|l\|_{M'_{m;\delta_m}}.$$

In particular, for all $v \in \mathbb{H}_\delta^{1/2}(\Gamma_m)$, we can define $l(\mu) = \int_{\Gamma_m} v \cdot \mu$ for all $\mu \in M_{m;\delta_m}$, and obtain the announced property. \square

Error estimates can then be established by the classical result.

Proposition 4.7. *If $u \in \prod_{k=1}^K H^{q+1}(\Omega_k)^d$ is solution of (4.4) with $(\mathbf{E} : \varepsilon(u)) \in \prod_{k=1}^K H^q(\Omega_k)^{d \times d}$ and $q \geq 1$, and $(u_h, \lambda_h) \in X_h \times M_\delta$ is solution of (4.7), the following error estimate holds :*

$$\|u - u_h\|_X \leq C \left(1 + \max_{1 \leq k \leq K} \frac{C_k}{\tilde{\alpha}} \right) \left(\sum_{k=1}^K h_k^{2q} |u|_{q+1,\mathbf{E},\Omega_k}^2 \right)^{1/2},$$

with :

$$|u|_{q+1,\mathbf{E},\Omega_k}^2 = |u|_{H^{q+1}(\Omega_k)^d}^2 + \frac{1}{C_k^2} \|\mathbf{E} : \varepsilon(u)\|_{H^q(\Omega_k)^{d \times d}}^2. \quad (4.38)$$

The constant C is independent of the number, the diameter, the Young moduli and the discretization of the subdomains. The coercivity constant of $\tilde{\alpha}$ over $V_h \times V_h$ is denoted by $\tilde{\alpha}$ and the coefficients $(C_k)_{1 \leq k \leq K}$ characterizing the elasticity tensor \mathbf{E} are defined by (4.3).

Remark 4.13. *The difference with the original result of Wohlmuth lies in the fact that the constants appearing in the proof do not depend any more on the number of subdomains. The result remains true if we replace in (4.38) q by any integer $1 \leq r \leq q$ because it relies on interpolation results which hold for any $1 \leq r \leq q$ given our choice of finite element.*

Proof : The proof can be found in [Woh01]. We review here the main steps. By a standard use of the second Strang's lemma [Str73], we have :

$$\|u - u_h\|_X \leq \left(1 + \frac{C_a}{\tilde{\alpha}}\right) \inf_{v_h \in V_h} \|u - v_h\|_X + \frac{1}{\tilde{\alpha}} \sup_{v_h \in V_h \setminus \{0\}} \frac{\tilde{a}(u, v_h) - l(v_h)}{\|v_h\|_X}, \quad (4.39)$$

where $C_a = C \max_{1 \leq k \leq K} C_k$ is the continuity constant of \tilde{a} , and is independent of h . We detail the estimates for the consistency error (the second term in (4.39)) and the approximation error (the first term in (4.39)).

Concerning the consistency error, because $(\mathbf{E} : \varepsilon(u)) \in \prod_{k=1}^K H^1(\Omega_k)^{d \times d}$, we have for all $v_h \in V_h$ by using the divergence formula :

$$\begin{aligned} \tilde{a}(u, v_h) - l(v_h) &= \sum_{k \geq 1} \int_{\Omega_k} (\mathbf{E} : \varepsilon(u)) : \nabla v_h - \int_{\Omega_k} f \cdot v_h - \int_{\Gamma_N} g \cdot v_h \\ &= - \sum_{k \geq 1} \int_{\Omega_k} (\operatorname{div}(\mathbf{E} : \varepsilon(u)) + f) \cdot v_h + \sum_{k \geq 1} \int_{\partial\Omega_k} ((\mathbf{E} : \varepsilon(u)) \cdot n_k) \cdot v_h \\ &\quad - \int_{\Gamma_N} g \cdot v_h, \end{aligned} \quad (4.40)$$

where n_k denotes the outward normal unit vector on Ω_k . Moreover, since $(\mathbf{E} : \varepsilon(u)) \in \prod_{k=1}^K H^1(\Omega_k)^{d \times d}$, we have for all $v \in \mathcal{C}_c^\infty(\Omega_k)^d$:

$$\int_{\Omega_k} f \cdot v = a(u, v) = \int_{\Omega_k} (\mathbf{E} : \varepsilon(u)) : \nabla v = - \int_{\Omega_k} \operatorname{div}(\mathbf{E} : \varepsilon(u)) \cdot v,$$

which entails by density of $\mathcal{C}_c^\infty(\Omega_k)^d$ in $L^2(\Omega_k)^d$, that :

$$\operatorname{div}(\mathbf{E} : \varepsilon(u)) + f = 0, \quad \text{in } L^2(\Omega_k)^d. \quad (4.41)$$

A fortiori, the result (4.41) entails that for all $v \in \prod_{k=1}^K H_*^1(\Omega_k)$:

$$- \sum_{k=1}^K \int_{\Omega_k} \operatorname{div}(\mathbf{E} : \varepsilon(u)) \cdot v = \int_{\Omega} f \cdot v,$$

which gives by subtracting the original problem (4.4) that :

$$\begin{aligned} \int_{\Gamma_N} g \cdot v &= \int_{\Omega} (\mathbf{E} : \varepsilon(u)) : \nabla v + \int_{\Omega} \operatorname{div}(\mathbf{E} : \varepsilon(u)) \cdot v, \quad \forall v \in H_*^1(\Omega), \\ &= \int_{\Gamma_N} ((\mathbf{E} : \varepsilon(u)) \cdot n) \cdot v, \quad \forall v \in H_*^1(\Omega), \end{aligned}$$

where the normal outward unit vector on Γ_N is denoted by n . As this final expression only depends on the restriction $v|_{\Gamma_N} \in H_{00}^{1/2}(\Gamma_N)^d$, we conclude that :

$$\int_{\Gamma_N} g \cdot \phi = \int_{\Gamma_N} ((\mathbf{E} : \varepsilon(u)) \cdot n) \cdot \phi, \quad \forall \phi \in H_{00}^{1/2}(\Gamma_N)^d. \quad (4.42)$$

As a consequence, by using (4.41) and (4.42) in (4.40), we get :

$$\tilde{a}(u, v_h) - l(v_h) = \sum_{1 \leq m \leq M} \int_{\Gamma_m} \lambda \cdot [v_h],$$

with $\lambda = (\mathbf{E} : \varepsilon(u)) \cdot n$, where the normal unit vector n is chosen to be outward to $\Omega_{k(m)}$ on Γ_m . Moreover, $[v_h]$ denotes the jump of v_h over \mathcal{S} . Then, we have to find an upper bound for the following quantity :

$$\sup_{v_h \in V_h} \frac{\int_{\mathcal{S}} \lambda \cdot [v_h]}{\|v_h\|_X}.$$

By construction of V_h , we have for all $\mu_h \in M_\delta$:

$$\int_{\mathcal{S}} \lambda \cdot [v_h] = \int_{\mathcal{S}} (\lambda - \mu_h) \cdot [v_h] \leq \|\lambda - \mu_h\|_{\delta, -\frac{1}{2}} \| [v_h] \|_{\delta, \frac{1}{2}}.$$

Moreover, we can prove that :

$$\inf_{\mu_h \in M_\delta} \|\lambda - \mu_h\|_{\delta, -\frac{1}{2}, m} \leq \delta_m^q \|\lambda\|_{H^{q-\frac{1}{2}}(\Gamma_m)}.$$

Indeed :

$$\begin{aligned} \inf_{\mu_h \in M_\delta} \|\lambda - \mu_h\|_{\delta, -\frac{1}{2}, m}^2 &= \inf_{\mu_h \in M_\delta} \sum_{F \in \mathcal{F}_{m; \delta_m}} h(F) \|\lambda - \mu_h\|_{L^2(F)^d}^2 \\ &\leq \delta_m \inf_{\mu_h \in M_\delta} \|\lambda - \mu_h\|_{L^2(\Gamma_m)^d}^2 \leq C \delta_m^{2q+1} \|\lambda\|_{H^q(\Gamma_m)^d}^2, \end{aligned}$$

because the space of polynomials of degree $q-1$ is included in $M_{m; \delta_m}$. We have also at order $q-1$:

$$\inf_{\mu_h \in M_\delta} \|\lambda - \mu_h\|_{\delta, -\frac{1}{2}, m}^2 \leq C \delta_m^{2q-1} \|\lambda\|_{H^{q-1}(\Gamma_m)^d}^2.$$

By interpolation between the H^{q-1} and the H^q norm (see [LM72]), we obtain :

$$\inf_{\mu_h \in M_\delta} \|\lambda - \mu_h\|_{\delta, -\frac{1}{2}, m}^2 \leq C \delta_m^{2q} \|\lambda\|_{H^{q-\frac{1}{2}}(\Gamma_m)^d}^2, \quad (4.43)$$

As a consequence, by summing the previous estimations over $m \geq 1$:

$$\begin{aligned} \inf_{\mu_h \in M_\delta} \|\lambda - \mu_h\|_{\delta, -\frac{1}{2}}^2 &= \sum_{m=1}^M \inf_{\mu_h \in M_\delta} \|\lambda - \mu_h\|_{\delta, -\frac{1}{2}, m}^2 \\ &\leq C \sum_{m=1}^M \delta_m^{2q} \|\lambda\|_{H^{q-\frac{1}{2}}(\Gamma_m)^d}^2 \leq C \sum_{k=1}^K h_k^{2q} \|\lambda\|_{H^{q-\frac{1}{2}}(\partial\Omega_k)^d}^2 \\ &\leq C \sum_{k=1}^K h_k^{2q} \|\mathbf{E} : \varepsilon(u)\|_{H^q(\Omega_k)^{d \times d}}^2, \end{aligned}$$

hence the following estimate :

$$\inf_{\mu_h \in M_\delta} \|\lambda - \mu_h\|_{\delta, -\frac{1}{2}}^2 \leq C \sum_{k=1}^K h_k^{2q} \|\mathbf{E} : \varepsilon(u)\|_{H^q(\Omega_k)^{d \times d}}^2. \quad (4.44)$$

Now, let us estimate $\|[v_h]\|_{\delta, \frac{1}{2}}$, by using the operators P_m introduced above. As $v_h \in V_h$, $[v_h]$ vanishes in the dual space $M'_{m; \delta_m}$ and therefore $P_m[v_h] = 0$. Then, for all $w_h \in W_{m; \delta_m}$ and using lemma 4.11 :

$$\|[v_h]\|_{\delta, \frac{1}{2}, m} \leq \|[v_h] - w_h - P_m([v_h] - w_h)\|_{\delta, \frac{1}{2}, m} \leq C \|[v_h] - w_h\|_{\delta, \frac{1}{2}, m}. \quad (4.45)$$

As the family of meshes over the non-mortar side is quasi-uniform by assumption 4, we have by a standard inverse inequality (see [EG02]) :

$$\|[v_h] - w_h\|_{\delta, \frac{1}{2}, m}^2 \leq \frac{1}{\delta_m} \|[v_h] - w_h\|_{L^2(\Gamma_m)^d}^2$$

Let w_h the L^2 projection of $[v_h]$ over $W_{m; \delta_m}$. We then have :

$$\|[v_h] - w_h\|_{L^2(\Gamma_m)^d}^2 \leq \|[v_h]\|_{L^2(\Gamma_m)^d}^2,$$

and by a classical interpolation result :

$$\|[v_h] - w_h\|_{L^2(\Gamma_m)^d}^2 \leq \|[v_h] - I_h[v_h]\|_{L^2(\Gamma_m)^d}^2 \leq C \delta_m^2 \|[v_h]\|_{H^1(\Gamma_m)^d}^2,$$

where I_h is the nodal interpolation over Γ_m . By interpolation between the L^2 and H^1 norms (see [LM72]), we obtain :

$$\|[v_h] - w_h\|_{L^2(\Gamma_m)^d}^2 \leq C \delta_m \|[v_h]\|_{H^{1/2}(\Gamma_m)^d}^2,$$

resulting in :

$$\|[v_h] - w_h\|_{\delta, \frac{1}{2}, m}^2 \leq C \|[v_h]\|_{H^{1/2}(\Gamma_m)^d}^2.$$

It is deduced from (4.45) that :

$$\|[v_h]\|_{\delta, \frac{1}{2}, m} \leq C \| [v_h] \|_{H^{1/2}(\Gamma_m)^d}, \quad \forall v_h \in V_h. \quad (4.46)$$

The consistency error is therefore of optimal order, and we get more precisely by using the Cauchy-Schwarz inequality and estimates (4.46) and (4.44) :

$$\begin{aligned} \left(\int_S \lambda \cdot [v_h] \right)^2 &\leq \left(\sum_{m=1}^M \| \lambda - \mu_h \|_{\delta, -\frac{1}{2}, m}^2 \right) \left(\sum_{m=1}^M \| [v_h] \|_{\delta, \frac{1}{2}, m}^2 \right), \quad \forall \mu_h \in M_\delta, \\ &\leq C \left(\sum_{k=1}^K h_k^{2q} \| \mathbf{E} : \varepsilon(u) \|_{H^q(\Omega_k)^{d \times d}}^2 \right) \left(\sum_{m=1}^M \| [v_h] \|_{H^{1/2}(\Gamma_m)^d}^2 \right) \end{aligned}$$

by taking the infimum over $\mu_h \in M_\delta$. We deduce from the trace theorem that :

$$\sup_{v_h \in V_h} \frac{\int_S \lambda \cdot [v_h]}{\|v_h\|_X} \leq C \left(\sum_{k=1}^K C_k^2 h_k^{2q} |u|_{q+1, \mathbf{E}, \Omega_k}^2 \right)^{1/2}.$$

Now, let us consider the approximation error. If I_h is the standard Lagrange interpolation operator over X_h , $w_h = I_h u$ does not satisfy the weak constraint on the jump $[w_h]$ over Γ_m . Then we define :

$$v_h = w_h - \sum_{m=1}^M \tilde{\mathcal{R}}_{m; h_m} \pi_m [w_h]_m \in V_h,$$

with the discrete extension by zero operators $\tilde{\mathcal{R}}_{m; h_m} : W_{m; \delta_m} \rightarrow X_h$ defined in the definition 4.2 of the appendix, page 203. As a consequence, from lemma 4.19 :

$$\|u - v_h\|_X^2 \leq C \left(\|u - w_h\|_X^2 + \sum_{m=1}^M \|\pi_m [w_h]_m\|_{\delta, \frac{1}{2}, m}^2 \right).$$

Moreover, from assumption 4.2 :

$$\sum_{m=1}^M \|\pi_m [w_h]_m\|_{\delta, \frac{1}{2}, m}^2 \leq C \sum_{m=1}^M \| [w_h]_m \|_{\delta, \frac{1}{2}, m}^2 = C \sum_{m=1}^M \| [u - w_h] \|_{\delta, \frac{1}{2}, m}^2.$$

We have also :

$$\begin{aligned} &\sum_{m=1}^M \| [u - w_h] \|_{\delta, \frac{1}{2}, m}^2 \\ &\leq 2 \sum_{m=1}^M \| u - w_h \|_{\partial \Omega_{k(m)}}^2 + 2 \sum_{m=1}^M \| u - w_h \|_{\partial \Omega_l, l \neq k(m)}^2, \end{aligned}$$

and use the quasi-uniformity of the non-mortar mesh to obtain :

$$\leq 2 \sum_{m=1}^M \|u - w_h|_{\partial\Omega_{k(m)}}\|_{\delta, \frac{1}{2}, m}^2 + 2 \sum_{m=1}^M \frac{\bar{\delta}_m}{\delta_m} \|u - w_h|_{\partial\Omega_l, l \neq k(m)}\|_{\delta, \frac{1}{2}, m}^2.$$

Using now the lemma 4.18 from the appendix, page 202, we get the following upper bound :

$$\begin{aligned} &\leq 2 \sum_{m=1}^M \sum_{T \in \mathcal{T}_h, T \subset \Omega_{k(m)}} \frac{1}{h(T)^2} \|u - w_h|_{\Omega_{k(m)}}\|_{L^2(T)^d}^2 + \|\nabla(u - w_h)|_{\Omega_{k(m)}}\|_{L^2(T)^{d \times d}}^2 \\ &+ 2 \sum_{m=1}^M \sum_{T \in \mathcal{T}_h, T \subset \Omega_l, l \neq k(m)} \frac{\bar{\delta}_m}{\delta_m} \left(\frac{1}{h(T)^2} \|u - w_h|_{\Omega_l, l \neq k(m)}\|_{L^2(T)^d}^2 + \|\nabla(u - w_h)|_{\Omega_l, l \neq k(m)}\|_{L^2(T)^{d \times d}}^2 \right). \end{aligned}$$

Then, by using a classical interpolation result and the assumption 4, we get :

$$\begin{aligned} \sum_{m=1}^M \|\pi_m[w_h]_m\|_{\delta, \frac{1}{2}, m}^2 &\leq C \left(1 + \max_{1 \leq m \leq M} \frac{\bar{\delta}_m}{\delta_m} \right) \sum_{k=1}^K h_k^{2q} |u|_{H^{q+1}(\Omega_k)^d}^2 \\ &\leq C \sum_{k=1}^K h_k^{2q} |u|_{H^{q+1}(\Omega_k)^d}^2. \end{aligned}$$

and the proof is complete. \square

Remark 4.14. It can be noticed by reading precisely the previous proof, that a better a priori estimate is obtained when the non-mortar side is taken as the coarsest side (to improve the approximation error) and/or the softer one (to improve the consistency error).

4.5.2 Approximation of fluxes

The convergence of Lagrange multipliers uses the inf-sup condition (4.9) and is established by the :

Proposition 4.8. If $u \in \prod_{k=1}^K H^{q+1}(\Omega_k)^d$ is solution of (4.4) with $(\mathbf{E} : \varepsilon(u)) \in \prod_{k=1}^K H^q(\Omega_k)^{d \times d}$ and $q \geq 1$, and $(u_h, \lambda_h) \in X_h \times M_\delta$ is solution of (4.7), the following error estimate on Lagrange multipliers holds :

$$\|\lambda - \lambda_h\|_{\delta, -\frac{1}{2}} \leq C \left(\sum_{k=1}^K h_k^{2q} |u|_{q+1, \mathbf{E}, \Omega_k}^2 \right)^{1/2},$$

with $\lambda = (\mathbf{E} : \varepsilon(u)) \cdot n$, where n is the normal unit vector on \mathcal{S} which is outward to $\Omega_{k(m)}$ for all $1 \leq m \leq M$. In more details, the constant C has the following dependence :

$$C = C' \max_{1 \leq k \leq K} C_k \left(1 + \frac{1}{\beta} \right) + C' \frac{\max_{1 \leq k \leq K} C_k}{\beta} \left(1 + \max_{1 \leq k \leq K} \frac{C_k}{\tilde{\alpha}} \right),$$

where the various constants denoted by C' do not depend on the number, the diameter, the Young moduli and the discretization of the subdomains.

Proof : As $(\mathbf{E} : \varepsilon(u)) \in \prod_{k=1}^K H^1(\Omega_k)^{d \times d}$, by a simple integration by part over each Ω_k , one can obtain from the continuous problem :

$$\tilde{a}(u, v) + b(v, \lambda) = l(v), \quad \forall v \in X.$$

Considering this equality with $v = v_h \in X_h \subset X$ and subtracting the approximate problem (4.7), we obtain :

$$b(v_h, \mu_h - \lambda_h) = \tilde{a}(u_h - u, v_h) + b(v_h, \mu_h - \lambda), \quad \forall v_h \in X_h, \forall \mu_h \in M_\delta. \quad (4.47)$$

Defining v_h from $\mu_h - \lambda_h$ by the same technique used for constructing u_h in the proof of (4.9), we deduce from (4.12), and using (4.47) :

$$\begin{aligned} \|\mu_h - \lambda_h\|_{\delta, -\frac{1}{2}}^2 &\leq C \frac{1}{\beta} b(v_h, \mu_h - \lambda_h) \\ &= C \frac{1}{\beta} \left(\tilde{a}(u_h - u, v_h) + \sum_{m=1}^M \int_{\Gamma_m} [v_h]|_{\Gamma_m} \cdot (\mu_h - \lambda) \right). \end{aligned}$$

But by construction :

$$[v_h]|_{\Gamma_m} = \phi_{\mu_h - \lambda_h} \int_{\Gamma_m} \phi_{\mu_h - \lambda_h} \cdot (\lambda_h - \mu_h),$$

hence since $\|\phi_{\mu_h - \lambda_h}\|_{\delta, \frac{1}{2}, m} = 1$, we get :

$$\begin{aligned} \int_{\Gamma_m} [v_h]|_{\Gamma_m} \cdot (\mu_h - \lambda) &= \int_{\Gamma_m} \phi_{\mu_h - \lambda_h} \cdot (\lambda_h - \mu_h) \int_{\Gamma_m} \phi_{\mu_h - \lambda_h} \cdot (\mu_h - \lambda) \\ &\leq \|\lambda_h - \mu_h\|_{\delta, -\frac{1}{2}, m} \|\mu_h - \lambda\|_{\delta, -\frac{1}{2}, m}. \end{aligned}$$

It remains that :

$$\begin{aligned} \|\mu_h - \lambda_h\|_{\delta, -\frac{1}{2}}^2 &\leq \frac{C}{\beta} \max_{1 \leq k \leq K} C_k \|u - u_h\|_X \|v_h\|_X \\ &\quad + \frac{C}{\beta} \left(\sum_{m=1}^M \|\mu_h - \lambda\|_{\delta, -\frac{1}{2}, m}^2 \right)^{1/2} \left(\sum_{m=1}^M \|\mu_h - \lambda_h\|_{\delta, -\frac{1}{2}, m}^2 \right)^{1/2} \end{aligned}$$

and recalling that $\|v_h\|_X \leq C \|\mu_h - \lambda_h\|_{\delta, -\frac{1}{2}}$ from (4.13), we obtain after division by $\|\mu_h - \lambda_h\|_{\delta, -\frac{1}{2}}$:

$$\|\mu_h - \lambda_h\|_{\delta, -\frac{1}{2}} \leq C \frac{1}{\beta} \left(\max_{1 \leq k \leq K} C_k \|u - u_h\|_X + \|\mu_h - \lambda\|_{\delta, -\frac{1}{2}} \right).$$

By the triangular inequality, we have :

$$\begin{aligned}\|\lambda - \lambda_h\|_{\delta, -\frac{1}{2}} &\leq \|\lambda - \mu_h\|_{\delta, -\frac{1}{2}} + \|\lambda_h - \mu_h\|_{\delta, -\frac{1}{2}} \\ &\leq C \frac{1}{\beta} \max_{1 \leq k \leq K} (C_k) \|u - u_h\|_X + \left(1 + C \frac{1}{\beta}\right) \|\lambda - \mu_h\|_{\delta, -\frac{1}{2}}, \quad \forall \mu_h \in M_\delta.\end{aligned}$$

Then, from proposition 4.7 and (4.44), the announced estimate is obtained. \square

4.6 Generalization to elastodynamics.

In this section, we analyze the use of mortar elements to solve the linear elastodynamics problem :

$$\begin{cases} \frac{\partial^2 u}{\partial t^2} - \operatorname{div}(\mathbf{E} : \varepsilon(u)) = f, & [0, T] \times \Omega, \\ (\mathbf{E} : \varepsilon(u)) \cdot \nu = g, & [0, T] \times \Gamma_N, \\ u = 0, & [0, T] \times \Gamma_D, \\ u = u_0, & \{0\} \times \Omega, \\ \frac{\partial u}{\partial t} = \dot{u}_0, & \{0\} \times \Omega, \end{cases} \quad (4.48)$$

with obvious notation. Let us only notice that the normal outward unit vector over a surface is now denoted by ν instead of n to avoid any possible confusion with the forthcoming numbering of the time steps.

First, the notation of the static case is adapted and a standard result of existence recalled in the elastodynamics framework. In the second subsection, a total approximation in space and time is introduced for the dynamical solution. It uses a mid-point finite difference time integration scheme which is interesting for energy conservation purpose, and a non-conforming finite element space approximation using a mortar weak-continuity constraint over the interfaces. We finally establish the convergence of the approximate solution to the continuous one, which is the main contribution of this section.

Moreover, an important remark has to be done with respect to this analysis. For first order problems in time, Lagrange multipliers are involved in the convergence analysis through the estimation of :

$$\inf_{\mu_h \in M_\delta} \|(\mathbf{E} : \varepsilon(u(t))) \cdot \nu - \mu_h\|_{\delta, -\frac{1}{2}},$$

as shown for example in [BMR01] for an eddy currents model. In the framework of second order problems in time, we underline the idea that the Lagrange multipliers are also involved through the estimation of :

$$\inf_{\mu_h \in M_\delta} \left\| \left(\mathbf{E} : \varepsilon \left(\frac{\partial u}{\partial t}(t) \right) \right) \cdot \nu - \mu_h \right\|_{\delta, -\frac{1}{2}},$$

entailing a higher sensitivity with respect to the choice of Lagrange multipliers. A time discontinuity in interface constraints would lead to a deterioration of convergence.

4.6.1 Position of the problem.

We formulate here the linear elastodynamics problem, using mainly the same notation as in the static case. The body forces are denoted by $f \in L^2(0, T; L^2(\Omega)^d)$, the density of the material by $\rho \in L^\infty(\Omega)$, which is assumed to be greater than a positive constant, and the initial conditions in displacement by $u_0 \in H^1(\Omega)^d$ and in velocity by $\dot{u}_0 \in L^2(\Omega)^d$. A surfacic force $g \in C^1(0, T; L^2(\Gamma_N)^d)$ which is regular in time is applied over the part Γ_N of the boundary $\partial\Omega$ and a Dirichlet boundary condition $u = 0$ is imposed on the complementary part $\Gamma_D = \partial\Omega \setminus \Gamma_N$ which can be of zero measure. The elastic properties of the material are the same as in the static case described above.

To give a precise meaning to the system (4.48), we define a solution as a displacement function :

$$u \in C^0(0, T; H_*^1(\Omega)) \cap C^1(0, T; L^2(\Omega)^d),$$

such that in the sense of distributions on $]0, T[$:

$$\frac{\partial^2}{\partial t^2} \int_{\Omega} \rho u(t) \cdot v + a(u(t), v) = \int_{\Omega} f(t) \cdot v + \int_{\Gamma_N} g(t) \cdot v, \quad \forall v \in H_*^1(\Omega). \quad (4.49)$$

It is now standard that :

Proposition 4.9. *Under the previous assumptions, there exists a unique displacement field $u \in C^0(0, T; H_*^1(\Omega)) \cap C^1(0, T; L^2(\Omega)^d)$, such that the equation (4.49) is satisfied in the sense of distributions on $]0, T[$. Moreover, the energy :*

$$\mathcal{E}(t) = \frac{1}{2} \int_{\Omega} \rho \left(\frac{\partial u}{\partial t}(t) \right)^2 + \frac{1}{2} a(u(t), u(t)),$$

is conserved, that is for all $t \in [0, T]$:

$$\mathcal{E}(t) = \mathcal{E}(0) + \int_0^t \int_{\Omega} f(s) \cdot \frac{\partial u}{\partial t}(s) ds + \int_0^t \int_{\Gamma_N} g(s) \cdot \frac{\partial u}{\partial t}(s) ds.$$

We refer to [LM72, RT98] for a proof of the proposition. It is classically done by :

– defining an approximation :

$$u_m(t) = \sum_{k=1}^m c_i(t) \varphi_i,$$

of the solution over the m first eigenmodes $(\varphi_i)_{i \geq 1}$ satisfying :

$$a(\varphi_i, v) = \omega_i^2 \int_{\Omega} \rho \varphi_i \cdot v, \quad \forall v \in H_*^1(\Omega),$$

with the eigenvalues $(\omega_i^2)_{i \geq 1}$,

- proving that the sequence of approximate solutions $(u_m)_{m \geq 1}$ is a Cauchy sequence in $\mathcal{C}^0(0, T; H_*^1(\Omega)) \cap \mathcal{C}^1(0, T; L^2(\Omega)^d)$, resulting in its convergence to a solution $u \in \mathcal{C}^0(0, T; H_*^1(\Omega)) \cap \mathcal{C}^1(0, T; L^2(\Omega)^d)$ of the problem (4.49).

The energy estimate for the solution u comes from the limit of energy estimates for the approximate solutions u_m . The uniqueness of the solution u is a straightforward consequence of the energy estimate.

4.6.2 A midpoint nonconforming fully discrete approximation.

We introduce here a space non-conforming fully discrete approximation of the solution of (4.48). First, at each time $t \in [0, T]$ the spaces $H_*^1(\Omega)$ and $L^2(\Omega)^d$ for the displacements and the velocities are replaced by the non-conforming finite element space V_h introduced in section 4.2.3, page 110, for the elastostatics problem. We then look for the displacements $u^h \in \mathcal{C}^0(0, T; V_h) \cap \mathcal{C}^1(0, T; V_h)$ such that in the sense of distributions on $]0, T[$:

$$\frac{\partial^2}{\partial t^2} \int_{\Omega} \rho u^h(t) \cdot v^h + \tilde{a}(u^h(t), v^h) = \int_{\Omega} f(t) \cdot v^h + \int_{\Gamma_N} g(t) \cdot v^h, \quad \forall v^h \in V_h. \quad (4.50)$$

The initial conditions in displacement and velocity take the form :

$$\begin{cases} u^h(0) = \mathcal{P}_h^1 u_0 & \in V_h, \\ \frac{\partial u^h}{\partial t}(0) = \mathcal{P}_h^0 \dot{u}_0 & \in V_h, \end{cases} \quad (4.51)$$

where \mathcal{P}_h^1 (resp. \mathcal{P}_h^0) denotes a projection from $H_*^1(\Omega)$ (resp. $L^2(\Omega)^d$) to V_h . Now, let $(t_n)_{n \in \mathbb{N}}$ a sequence of discrete times such that $t_n = n\Delta t$ for $n \in \mathbb{N}$. The use of a constant time step Δt enables the optimal time accuracy order established below. The formal integration of (4.50) and of the additional relation :

$$\frac{\partial}{\partial t} \int_{\Omega} u^h(t) \cdot v^h = \int_{\Omega} \frac{\partial u^h}{\partial t}(t) \cdot v^h, \quad \forall v^h \in V_h,$$

over $t \in [t_n, t_{n+1}]$ by the trapezoidal rule gives the following fully discrete system :

$$\begin{cases} \int_{\Omega} \rho \frac{\dot{u}_{n+1}^h - \dot{u}_n^h}{\Delta t} \cdot v_h + \tilde{a} \left(\frac{u_n^h + u_{n+1}^h}{2}, v_h \right) = \frac{L_n(v_h) + L_{n+1}(v_h)}{2}, \\ \frac{u_{n+1}^h - u_n^h}{\Delta t} = \frac{\dot{u}_n^h + \dot{u}_{n+1}^h}{2}. \end{cases} \quad (4.52)$$

We have introduced the virtual work of the applied forces at the discrete time t_n :

$$L_n(v_h) = \int_{\Omega} f(t_n) \cdot v_h + \int_{\Gamma_N} g(t_n) \cdot v_h, \quad \forall v_h \in V_h,$$

and have denoted by $u_n^h \in V_h$ (resp. $\dot{u}_n^h \in V_h$) the approximation in time of the space approximation $u^h(t_n) \in V_h$ of the displacement (resp. $\frac{\partial u^h}{\partial t}(t_n) \in V_h$ of the velocity), that is the fully discrete approximation of the displacement $u(t_n) \in H_*^1(\Omega)$ (resp. the velocity $\frac{\partial u}{\partial t}(t_n) \in L^2(\Omega)^d$). This trapezoidal finite difference scheme in time has been selected for its exact conservation properties with respect to the energy and to the linear momentum (see [ST92]).

The convergence analysis to come could be extended to other time integrators. The system has to be completed with the initial conditions :

$$\begin{cases} u_0^h = \mathcal{P}_h^1 u_0 & \in V_h, \\ \dot{u}_0^h = \mathcal{P}_h^0 \dot{u}_0 & \in V_h. \end{cases} \quad (4.53)$$

Knowing $u_n^h, \dot{u}_n^h \in V_h$ and after elimination of \dot{u}_{n+1}^h by (4.52)-2, we can then determine the fully discrete displacement $u_{n+1}^h \in V_h$ at the discrete time $t_{n+1} \in [0, T]$ by solving :

$$\begin{aligned} \int_{\Omega} \frac{2}{\Delta t^2} \rho u_{n+1}^h \cdot v_h + \frac{1}{2} \tilde{a} (u_{n+1}^h, v_h) &= \int_{\Omega} \rho \left(\frac{2}{\Delta t^2} u_n^h + \frac{2}{\Delta t} \dot{u}_n^h \right) \cdot v_h \\ &\quad - \frac{1}{2} \tilde{a} (u_n^h, v_h) \\ &\quad + \frac{L_n(v_h) + L_{n+1}(v_h)}{2}, \quad \forall v_h \in V_h, \end{aligned}$$

and the velocity $\dot{u}_{n+1}^h \in V_h$ is obtained by the simple computation :

$$\dot{u}_{n+1}^h = \frac{2}{\Delta t} (u_{n+1}^h - u_n^h) - \dot{u}_n^h.$$

The existence of a projection \mathbb{P}_h from $H_*^1(\Omega)$ to V_h is detailed in the following lemma :

Lemma 4.12. *If Γ_D has a positive measure, there exists a projection operator :*

$$\begin{aligned} \mathbb{P}_h : \quad H_*^1(\Omega) &\rightarrow V_h \\ u &\mapsto \mathbb{P}_h u, \end{aligned}$$

such that $\mathbb{P}_h u$ is the unique solution $u_h \in V_h$ of :

$$\tilde{a}(u_h, v_h) = \tilde{a}(u, v_h), \quad \forall v_h \in V_h.$$

Moreover, for all $u \in H_{\mathbf{E}}^{r+1}(\Omega)$ with $r \geq 1$, we have the following estimates :

$$\|u - \mathbb{P}_h u\|_X^2 \leq C \sum_{k=1}^K h_k^{2r} |u|_{r+1, \mathbf{E}, \Omega_k}^2,$$

$$\|u - \mathbb{P}_h u\|_{L^2(\Omega)}^2 \leq C \left(\sup_{1 \leq k \leq K} h_k^2 \right) \sum_{k=1}^K h_k^{2r} |u|_{r+1, \mathbf{E}, \Omega_k}^2.$$

Observation : the last inequality holds within a regularity condition, namely that the solution of all elasticity problems over Ω be in $H_{\mathbf{E}}^2(\Omega)$.

Remark 4.15. *The constant C in the estimates of proposition 4.12 is in fact of the form :*

$$C = C' \left(1 + \max_{k \geq 1} \frac{C_k}{\tilde{\alpha}} \right) \max_{k \geq 1} \frac{C_k}{\tilde{\alpha}},$$

where C' is independent of the discretization in space and time, of the number of sub-domains, and of the coercivity and continuity constants of the broken bilinear form \tilde{a} . Nevertheless, to simplify the present exposition, we will keep the generic notation C .

Proof : The existence of the projection \mathbb{P}_h is a straightforward consequence of the Lax-Milgram lemma. More precisely, for a given function $u \in H_*^1(\Omega)$, let us define the continuous linear form $l \in X'$ by :

$$l(v) = \tilde{a}(u, v), \quad \forall v \in X.$$

The function $u \in H_*^1(\Omega)$ is the unique solution of :

$$a(u, v) = l(v), \quad \forall v \in H_*^1(\Omega),$$

and $\mathbb{P}_h u$ is the unique solution u_h of :

$$\tilde{a}(u_h, v_h) = l(v_h), \quad \forall v_h \in V_h.$$

The error between u_h and u in the broken norm $\|\cdot\|_X$ is given in the proposition 4.7, resulting in the announced estimate. The estimation in the $L^2(\Omega)^d$ norm can be obtained by a Aubin-Nitsche argument (cf. [Aub87] for example) that we detail here. Let us assume that for all $\phi \in L^2(\Omega)^d$, there exist a solution $\zeta_\phi \in H_{\mathbf{E}}^2(\Omega)$ of :

$$\tilde{a}(v, \zeta_\phi) = \int_{\Omega} \phi \cdot v, \quad \forall v \in H_*^1(\Omega). \quad (4.54)$$

Indeed, we have assumed that the solution of all elasticity problems over Ω be in $H_{\mathbf{E}}^2(\Omega)$. First, because the application :

$$\begin{aligned} T : \quad H_{\mathbf{E}}^2(\Omega) \cap H_*^1(\Omega) &\rightarrow H_*^1(\Omega)' \\ \zeta &\mapsto T\zeta; \quad \langle T\zeta, v \rangle_{H_*^1(\Omega)', H^1(\Omega)} = \tilde{a}(v, \zeta), \end{aligned}$$

is linear, continuous and bijective, the inverse T^{-1} is continuous by the open application theorem [Bré99, Yos65]. As a consequence, the solution $\zeta_\phi \in H_{\mathbf{E}}^2(\Omega)$ of (4.54) satisfies :

$$\left(\sum_{k=1}^K C_k^2 |\zeta_\phi|_{2, \mathbf{E}, \Omega_k}^2 \right)^{1/2} \leq C \|\phi\|_{H_*^1(\Omega)'} \leq C \|\phi\|_{L^2(\Omega)^d}. \quad (4.55)$$

Now, let us prove the announced upper bound on $\|u - \mathbb{P}_h u\|_{L^2(\Omega)^d}$, by the Aubin-Nitsche technique. Namely :

$$\begin{aligned}\|u - \mathbb{P}_h u\|_{L^2(\Omega)^d} &= \sup_{\phi \in L^2(\Omega)^d \setminus \{0\}} \frac{\int_{\Omega} (u - \mathbb{P}_h u) \cdot \phi}{\|\phi\|_{L^2(\Omega)^d}} \\ &= \sup_{\phi \in L^2(\Omega)^d \setminus \{0\}} \frac{\tilde{a}(u - \mathbb{P}_h u, \zeta_{\phi})}{\|\phi\|_{L^2(\Omega)^d}},\end{aligned}$$

and by definition of \mathbb{P}_h , $\tilde{a}(u - \mathbb{P}_h u, v_h) = 0$ for all $v_h \in V_h$, resulting in the following expression for all $v_h \in V_h$, and ϕ realizing the supremum in the above inequality :

$$\begin{aligned}\|u - \mathbb{P}_h u\|_{L^2(\Omega)^d} &\leq \frac{\tilde{a}(u - \mathbb{P}_h u, \zeta_{\phi} - v_h)}{\|\phi\|_{L^2(\Omega)^d}}, \\ &\leq \frac{\tilde{a}(u - \mathbb{P}_h u, u - \mathbb{P}_h u)^{1/2} \tilde{a}(\zeta_{\phi} - v_h, \zeta_{\phi} - v_h)^{1/2}}{\|\phi\|_{L^2(\Omega)^d}}.\end{aligned}$$

By taking the infimum of the right hand side over $v_h \in V_h$, and by using the approximation property of \mathbb{P}_h in X (proposition 4.7), and the relation (4.55), we get :

$$\begin{aligned}\|u - \mathbb{P}_h u\|_{L^2(\Omega)^d} &\leq C \frac{\left(\sum_{k=1}^K h_k^{2r} |u|_{r+1, \mathbf{E}, \Omega_k}^2 \right)^{1/2} \left(\sum_{k=1}^K h_k^2 C_k^2 |\zeta_{\phi}|_{2, \mathbf{E}, \Omega_k}^2 \right)^{1/2}}{\|\phi\|_{L^2(\Omega)^d}} \\ &\leq C \left(\sum_{k=1}^K h_k^{2r} |u|_{r+1, \mathbf{E}, \Omega_k}^2 \right)^{1/2} \left(\sup_{1 \leq k \leq K} h_k \right).\end{aligned}$$

□

4.6.3 Convergence analysis

Now, we prove the convergence of the fully discrete approximation given by (4.52) to the continuous solution of (4.49). For that purpose, we introduce the following space :

$$H_{\mathbf{E}}^{q+1}(\Omega) = \{v \in H_*^1(\Omega); \quad \|v\|_{q+1, \mathbf{E}, \Omega} < +\infty\},$$

which is endowed with the following norm :

$$\|v\|_{q+1, \mathbf{E}, \Omega}^2 = \|v\|_{H^1(\Omega)^d}^2 + \sum_{k=1}^K \left(\|v\|_{H^{q+1}(\Omega_k)^d}^2 + \frac{1}{C_k^2} \|\mathbf{E} : \boldsymbol{\varepsilon}(v)\|_{H^q(\Omega_k)^{d \times d}}^2 \right).$$

We also denote as in proposition 4.7 :

$$|v|_{q+1, \mathbf{E}, \Omega_k}^2 = |v|_{H^{q+1}(\Omega_k)^d}^2 + \frac{1}{C_k^2} \|\mathbf{E} : \boldsymbol{\varepsilon}(v)\|_{H^q(\Omega_k)^{d \times d}}^2,$$

and state the main result of that section :

Proposition 4.10 (Error estimate). *If*

$$u \in \mathcal{C}^1(0, T; H_{\mathbf{E}}^{q+1}(\Omega)) \cap \mathcal{C}^2(0, T; \prod_{k=1}^K H^{r+1}(\Omega_k)^d) \cap \mathcal{C}^4(0, T; L^2(\Omega)^d)$$

is solution of (4.49) and $(u_n^h; \dot{u}_n^h)_{n \in \mathbb{N}}$ is the fully discrete solution of (4.52), then the following error estimate holds :

$$\begin{aligned} & \left\| \sqrt{\rho} \left(\dot{u}(t_{n+1/2}) - \frac{\dot{u}_n^h + \dot{u}_{n+1}^h}{2} \right) \right\|_{L^2(\Omega)^d}^2 + \tilde{\alpha} \left\| u(t_{n+1/2}) - \frac{u_n^h + u_{n+1}^h}{2} \right\|_X^2 \\ & \leq C \left(\|\mathcal{P}_h \dot{u}_0 - \dot{u}_0^h\|_{L^2(\Omega)^d}^2 + \|\mathcal{P}_h u_0 - u_0^h\|_X^2 \right) \\ & + C \left[\left(\frac{\Delta t}{t_0} \right)^4 \left\{ \tilde{\alpha} \sup_{t \in [0, T]} \|t_0^2 \ddot{u}(t)\|_X^2 + \sup_{t \in [0, T]} \|\sqrt{\rho} t_0^2 \ddot{u}(t)\|_{L^2(\Omega)^d}^2 + \frac{T}{t_0} \sup_{t \in [0, T]} \|\sqrt{\rho} t_0^3 \ddot{u}(t)\|_{L^2(\Omega)^d}^2 \right\} \right. \\ & + h^2 \frac{T}{t_0} \sum_{k=1}^K h_k^{2r} \left(\sup_{t \in [0, T]} |\sqrt{\rho} t_0 \ddot{u}(t)|_{r+1, \mathbf{E}, \Omega_k}^2 + \sup_{t \in [0, T]} |\sqrt{\rho} \dot{u}(t)|_{r+1, \mathbf{E}, \Omega_k}^2 \right) + \tilde{\alpha} \sum_{k=1}^K h_k^{2q} \sup_{t \in [0, T]} |u(t)|_{q+1, \mathbf{E}, \Omega_k}^2 \\ & \left. + \sum_{k=1}^K h_k^{2q} \frac{C_k^2}{\tilde{\alpha}} \left\{ \sup_{t \in [0, T]} |u(t)|_{q+1, \mathbf{E}, \Omega}^2 + \frac{T}{t_0} \sup_{t \in [0, T]} |t_0 \dot{u}(t)|_{q+1, \mathbf{E}, \Omega}^2 \right\} \right] \left(1 + \frac{\Delta t}{t_0} \right)^n, \end{aligned}$$

where C denotes various constants independent of the discretization in space and time, and $t_{n+1/2} = \frac{1}{2}(t_n + t_{n+1})$. Moreover, \mathcal{P}_h is the projection \mathbb{P}_h from $H_*^1(\Omega)$ to V_h given in lemma 4.12 if Γ_D has a positive measure, and is defined by (4.66) if Γ_D has a null measure, and r is any integer with $1 \leq r \leq q$. Finally, t_0 is a reference length of time.

In order to simplify the exposition of the proof, we assume that Γ_D has a positive measure so that the bilinear form a is coercive over $H_*^1(\Omega) \times H_*^1(\Omega)$. We will enumerate in the remark following the proof the necessary modifications when Γ_D has a null measure. The proof is inspired by the convergence proof introduced in [TM00] for fluid-structure analysis.

Proof : For clarity, the proof is decomposed into six parts. The time derivative of u will be sometimes denoted by \dot{u} to simplify notation.

1. The discrete evolution of error.

Let us define the projection on V_h of the error in displacements at time t_n by :

$$e u_n^h = \mathbb{P}_h u(t_n) - u_n^h,$$

and a new approximation $(V_n^h)_{n \geq 0}$ of velocities by :

$$\frac{1}{2} (V_n^h + V_{n+1}^h) = \frac{1}{\Delta t} (\mathbb{P}_h u(t_{n+1}) - \mathbb{P}_h u(t_n)),$$

with the initial condition $V_0^h = \mathbb{P}_h \dot{u}_0$. The gap between the fully discrete velocity \dot{u}_n^h and V_n^h is then defined by :

$$eV_n^h = V_n^h - \dot{u}_n^h.$$

We now establish the equation satisfied by these errors.

To do so, we first show that for all $t \in [0, T]$:

$$\int_{\Omega} \rho \frac{\partial^2 u}{\partial t^2}(t) \cdot v_h + \tilde{a}(u(t), v_h) = \int_{\Omega} f(t) \cdot v_h + \int_{\Gamma_N} g(t) \cdot v_h + \int_{\mathcal{S}} \lambda(t) \cdot [v_h], \quad \forall v_h \in V_h, \quad (4.56)$$

with $\lambda(t) = (\mathbf{E} : \varepsilon(u(t))) \cdot \nu$, where ν is the normal unit vector on \mathcal{S} which is outward to the non-mortar subdomain.

Due to the assumptions that for all $t \in [0, T]$, $(\mathbf{E} : \varepsilon(u(t))) \in \prod_{k=1}^K H^1(\Omega_k)^{d \times d}$ and that the time derivatives of u have a classical sense, we obtain from (4.49) that for all $t \in [0, T]$ and all $v \in \mathcal{C}_c^\infty(\Omega)^d$:

$$\int_{\Omega} \left(\rho \frac{\partial^2 u}{\partial t^2}(t) - \operatorname{div}(\mathbf{E} : \varepsilon(u(t))) - f(t) \right) \cdot v = 0.$$

By density of $\mathcal{C}_c^\infty(\Omega)^d$ in $L^2(\Omega)^d$ we have then that for all $t \in [0, T]$:

$$\rho \frac{\partial^2 u}{\partial t^2}(t) - \operatorname{div}(\mathbf{E} : \varepsilon(u(t))) - f(t) = 0, \quad \text{in } L^2(\Omega)^d. \quad (4.57)$$

Then, we can obtain some information about the natural boundary conditions. Indeed, we get a fortiori from (4.57) that :

$$\int_{\Omega} \left(\rho \frac{\partial^2 u}{\partial t^2}(t) - \operatorname{div}(\mathbf{E} : \varepsilon(u(t))) - f(t) \right) \cdot v = 0, \quad \forall v \in H_*^1(\Omega), \quad (4.58)$$

and by subtracting the original problem (4.49) to (4.58), we obtain for all $v \in H_*^1(\Omega)$:

$$\begin{aligned} \int_{\Gamma_N} g(t) \cdot v &= \int_{\Omega} (\mathbf{E} : \varepsilon(u(t))) : \nabla v + \int_{\Omega} \operatorname{div}(\mathbf{E} : \varepsilon(u(t))) \cdot v \\ &:= \int_{\Gamma_N} ((\mathbf{E} : \varepsilon(u(t))) \cdot \nu) \cdot v. \end{aligned}$$

Obviously, this relation does not depend on $v \in H_*^1(\Omega)$ but only on its trace $v|_{\Gamma_N} \in H_{00}^{1/2}(\Gamma_N)^d$, resulting in :

$$\int_{\Gamma_N} g(t) \cdot \phi = \int_{\Gamma_N} ((\mathbf{E} : \varepsilon(u(t))) \cdot \nu) \cdot \phi, \quad \forall \phi \in H_{00}^{1/2}(\Gamma_N)^d. \quad (4.59)$$

Now, we can show the relation (4.56). By exploiting the divergence formula, and the results (4.57) and (4.59), we get for all $t \in [0, T]$, and all $v_h \in V_h$:

$$\begin{aligned}\tilde{a}(u, v_h) &= \sum_{k=1}^K \int_{\Omega_k} (\mathbf{E} : \varepsilon(u(t))) : \varepsilon(v_h) \\ &= - \sum_{k=1}^K \int_{\Omega_k} \operatorname{div}(\mathbf{E} : \varepsilon(u(t))) \cdot v_h + \sum_{k=1}^K \int_{\partial\Omega_k} ((\mathbf{E} : \varepsilon(u(t))) \cdot \nu) \cdot v_h \\ &= \int_{\Omega} \left(f(t) - \rho \frac{\partial^2 u}{\partial t^2}(t) \right) \cdot v_h + \int_{\Gamma_N} g(t) \cdot v_h + \int_S \lambda(t) \cdot [v_h],\end{aligned}$$

resulting in the announced expression (4.56).

By computing the half sum of the expressions (4.56) for $t = t_n$ and $t = t_{n+1}$ and substracting the first line of the system (4.52), it comes that for all $v_h \in V_h$:

$$\begin{aligned}&\int_{\Omega} \rho \frac{V_{n+1}^h - V_n^h}{\Delta t} \cdot v_h - \int_{\Omega} \rho \frac{\dot{u}_{n+1}^h - \dot{u}_n^h}{\Delta t} \cdot v_h + \tilde{a} \left(\frac{u(t_n) - u_n^h}{2} + \frac{u(t_{n+1}) - u_{n+1}^h}{2}, v_h \right) \\ &= \int_{\Omega} \rho \frac{V_{n+1}^h - V_n^h}{\Delta t} \cdot v_h - \frac{1}{2} \int_{\Omega} \rho \left(\frac{\partial^2 u}{\partial t^2}(t_n) + \frac{\partial^2 u}{\partial t^2}(t_{n+1}) \right) \cdot v_h + \int_S \frac{\lambda(t_n) + \lambda(t_{n+1})}{2} \cdot [v_h],\end{aligned}$$

where we have added the term $\int_{\Omega} \rho \frac{V_{n+1}^h - V_n^h}{\Delta t} \cdot v_h$ on the both sides of the equality. From the lemma 4.12 and the definitions of eu_n^h and eV_n^h , we deduce that for all $v_h \in V_h$:

$$\begin{aligned}&\int_{\Omega} \rho \frac{eV_{n+1}^h - eV_n^h}{\Delta t} \cdot v_h + \tilde{a} \left(\frac{eu_n^h + eu_{n+1}^h}{2}, v_h \right) \\ &= \int_{\Omega} \rho \frac{V_{n+1}^h - V_n^h}{\Delta t} \cdot v_h - \frac{1}{2} \int_{\Omega} \rho \left(\frac{\partial^2 u}{\partial t^2}(t_n) + \frac{\partial^2 u}{\partial t^2}(t_{n+1}) \right) \cdot v_h + \int_S \frac{\lambda(t_n) + \lambda(t_{n+1})}{2} \cdot [v_h],\end{aligned}$$

that we sum up in the following expression :

$$\int_{\Omega} \rho \frac{eV_{n+1}^h - eV_n^h}{\Delta t} \cdot v_h + \tilde{a} \left(\frac{eu_n^h + eu_{n+1}^h}{2}, v_h \right) = E_{n+1/2}^a(v_h) + E_{n+1/2}^c(v_h). \quad (4.60)$$

We have denoted the approximation error in time and space by :

$$E_{n+1/2}^a(v_h) = \int_{\Omega} \sqrt{\rho} T_{n+1/2} \cdot v_h, \quad \forall v_h \in V_h,$$

with :

$$T_{n+1/2} = \sqrt{\rho} \frac{V_{n+1}^h - V_n^h}{\Delta t} - \frac{1}{2} \sqrt{\rho} \left(\frac{\partial^2 u}{\partial t^2}(t_n) + \frac{\partial^2 u}{\partial t^2}(t_{n+1}) \right),$$

and the consistency error by :

$$E_{n+1/2}^c(v_h) = \frac{1}{2} \int_S (\lambda(t_n) + \lambda(t_{n+1})) \cdot [v_h], \quad \forall v_h \in V_h.$$

It will be convenient to have estimations at midtime steps, and this is why we introduce the midtime quantities :

$$eV_{n+1/2}^h = \frac{eV_n^h + eV_{n+1}^h}{2}, \quad eu_{n+1/2}^h = \frac{eu_n^h + eu_{n+1}^h}{2},$$

whose evolution is given by averaging (4.60) between two consecutive time steps. We get for all $v_h \in V_h$:

$$\int_\Omega \rho \frac{eV_{n+1/2}^h - eV_{n-1/2}^h}{\Delta t} \cdot v_h + \tilde{a} \left(\frac{eu_{n-1/2}^h + eu_{n+1/2}^h}{2}, v_h \right) = E_n^a(v_h) + E_n^c(v_h), \quad (4.61)$$

where :

$$E_n^\square(v_h) = \frac{1}{2} \left(E_{n-1/2}^\square(v_h) + E_{n+1/2}^\square(v_h) \right), \quad \forall v_h \in V_h,$$

in which \square stands for “ a ” or “ c ”. In (4.61), we choose :

$$v_h = \frac{eu_{n+1/2}^h - eu_{n-1/2}^h}{\Delta t} = \frac{eV_{n-1/2}^h + eV_{n+1/2}^h}{2},$$

by construction of $(V_n^h)_{n \geq 0}$, which gives by summation on all time steps between 1 and n the main estimation of this first step of the proof :

$$\eta_{n+1/2}^h - \eta_{1/2}^h = \Delta t \sum_{i=1}^n E_i^a \left(\frac{eV_{i-1/2}^h + eV_{i+1/2}^h}{2} \right) + E_i^c \left(\frac{eu_{i+1/2}^h - eu_{i-1/2}^h}{\Delta t} \right), \quad (4.62)$$

with :

$$\eta_{n+1/2}^h = \frac{1}{2} \int_\Omega \rho eV_{n+1/2}^h \cdot eV_{n+1/2}^h + \frac{1}{2} \tilde{a}(eu_{n+1/2}^h, eu_{n+1/2}^h).$$

2. An upper bound for $\eta_{1/2}^h$.

We establish here an upper bound for $\eta_{1/2}^h$. By definition of $\eta_{1/2}^h$, we get by using the symmetry of \tilde{a} :

$$\begin{aligned} \eta_{1/2}^h &= \frac{1}{2} \int_\Omega \rho \left(\frac{eV_0^h + eV_1^h}{2} \right)^2 + \frac{1}{2} \tilde{a} \left(\frac{eu_0^h + eu_1^h}{2}, \frac{eu_0^h + eu_1^h}{2} \right) \\ &\leq \frac{1}{4} \int_\Omega \rho (eV_0^h)^2 + \frac{1}{4} \int_\Omega \rho (eV_1^h)^2 + \frac{1}{4} \tilde{a}(eu_0^h, eu_0^h) + \frac{1}{4} \tilde{a}(eu_1^h, eu_1^h). \end{aligned}$$

Using (4.60) with $n = 0$ and :

$$v_h = \frac{eu_1^h - eu_0^h}{\Delta t} = \frac{eV_0^h + eV_1^h}{2}$$

by construction, we obtain :

$$\begin{aligned} \frac{1}{2} \int_{\Omega} \rho(eV_1^h)^2 + \frac{1}{2} \tilde{a}(eu_1^h, eu_1^h) &= \frac{1}{2} \int_{\Omega} \rho(eV_0^h)^2 + \frac{1}{2} \tilde{a}(eu_0^h, eu_0^h) \\ &\quad + \frac{\Delta t}{2} E_{1/2}^a(eV_1^h) + E_{1/2}^c(eu_1^h - eu_0^h). \end{aligned}$$

The approximation term in the right hand side can be bounded by using the Cauchy-Schwarz inequality :

$$\begin{aligned} \frac{\Delta t}{2} E_{1/2}^a(eV_1^h) &\leq \|\Delta t T_{1/2}\|_{L^2(\Omega)^d} \left\| \frac{1}{2} \sqrt{\rho} eV_1^h \right\|_{L^2(\Omega)^d} \\ &\leq \frac{1}{2} \|\Delta t T_{1/2}\|_{L^2(\Omega)^d}^2 + \frac{1}{8} \int_{\Omega} \rho(eV_1^h)^2. \end{aligned}$$

Moreover :

$$\begin{aligned} \Delta t T_{1/2} &= \sqrt{\rho} \left(V_1^h - V_0^h - \frac{\Delta t}{2} (\ddot{u}(t_0) + \ddot{u}(t_1)) \right) \\ &= \sqrt{\rho} \left(\frac{2}{\Delta t} (\mathbb{P}_h u(t_1) - \mathbb{P}_h u(t_0)) - 2\mathbb{P}_h \dot{u}(t_0) - \frac{\Delta t}{2} (\ddot{u}(t_0) + \ddot{u}(t_1)) \right) \\ &= \sqrt{\rho} \left(\frac{2}{\Delta t} (u(t_1) - u(t_0)) - 2\dot{u}(t_0) - \frac{\Delta t}{2} (\ddot{u}(t_0) + \ddot{u}(t_1)) \right) \\ &\quad + \sqrt{\rho} (\mathbb{P}_h - id) \left(\frac{2}{\Delta t} (u(t_1) - u(t_0)) - 2\dot{u}(t_0) \right). \end{aligned} \tag{4.63}$$

We then use the lemma 4.12 and a Taylor's expansion with integral remainder to bound the second term in (4.63) as follows :

$$\begin{aligned} &\left\| \sqrt{\rho} (\mathbb{P}_h - id) \left(\frac{2}{\Delta t} (u(t_1) - u(t_0)) - 2\dot{u}(t_0) \right) \right\|_{L^2(\Omega)^d}^2 \\ &\leq C h^2 \sum_{k=1}^K h_k^{2r} \left| \frac{2\sqrt{\rho}}{\Delta t} (u(t_1) - u(t_0)) - 2\dot{u}(t_0) \right|_{r+1, \mathbf{E}, \Omega_k}^2 \\ &\leq C \left(\frac{\Delta t}{t_0} \right)^2 h^2 \sum_{k=1}^K h_k^{2r} \sup_{t \in [0, \Delta t]} |\sqrt{\rho} t_0 \ddot{u}(t)|_{r+1, \mathbf{E}, \Omega_k}^2. \end{aligned}$$

The first term in (4.63) is also bounded by the use of a Taylor's expansion with integral remainder, resulting in :

$$\Delta t^2 \|T_{1/2}\|_{L^2(\Omega)^d}^2 \leq C \left(\left(\frac{\Delta t}{t_0} \right)^4 \sup_{t \in [0, \Delta t]} \|\sqrt{\rho} t_0^2 \ddot{u}(t)\|_{L^2(\Omega)^d}^2 \right)$$

$$+ \left(\frac{\Delta t}{t_0} \right)^2 h^2 \sum_{k=1}^K h_k^{2r} \sup_{t \in [0, \Delta t]} |\sqrt{\rho} t_0 \ddot{u}(t)|_{r+1, \mathbf{E}, \Omega_k}^2 \Big).$$

For the consistency term, we use that $eu_1^h - eu_0^h \in V_h$, the Cauchy-Schwarz inequality, the inequality (4.46) page 145, and the error estimate (4.44) page 144 :

$$\|[v_h]\|_{\delta, \frac{1}{2}, m} \leq C \| [v_h] \|_{H^{1/2}(\Gamma_m)^d}, \quad \forall v_h \in V_h, \quad (4.64)$$

$$\inf_{\mu_h \in M_\delta} \|\lambda - \mu_h\|_{\delta, -\frac{1}{2}}^2 \leq C \sum_{k=1}^K h_k^{2q} \|\mathbf{E} : \varepsilon(u)\|_{H^q(\Omega_k)^{d \times d}}^2, \quad (4.65)$$

to obtain that :

$$\begin{aligned} E_{1/2}^c (eu_1^h - eu_0^h) &\leq \max_{i=0,1} \int_S \lambda(t_i) \cdot [eu_1^h - eu_0^h] \\ &\leq \max_{i=0,1} \int_S (\lambda(t_i) - \mu_h) \cdot [eu_1^h - eu_0^h], \quad \forall \mu_h \in M_\delta \\ &\leq \theta \max_{i=0,1} \inf_{\mu_h \in M_\delta} \|\lambda(t_i) - \mu_h\|_{\delta, -\frac{1}{2}} \frac{1}{\theta} \|eu_1^h - eu_0^h\|_X, \quad \forall \theta \in]0, +\infty[, \\ &\leq C\theta^2 \max_{i=0,1} \inf_{\mu_h \in M_\delta} \|\lambda(t_i) - \mu_h\|_{\delta, -\frac{1}{2}}^2 + \frac{1}{2\theta^2} \|eu_1^h - eu_0^h\|_X^2 \\ &\leq C\theta^2 \sum_{k=1}^K h_k^{2q} C_k^2 \sup_{t \in [0, \Delta t]} |u(t)|_{q+1, \mathbf{E}, \Omega_k}^2 + \frac{1}{\theta^2} \|eu_1^h\|_X^2 + \frac{1}{\theta^2} \|eu_0^h\|_X^2. \end{aligned}$$

As Γ_D has not a null measure, the bilinear form \tilde{a} is coercive over $V_h \times V_h$. Then, we choose $\theta^2 = 8/\tilde{\alpha}$ where $\tilde{\alpha}$ is the coercivity constant of \tilde{a} over $V_h \times V_h$, and obtain the final estimation :

$$\begin{aligned} &\frac{3}{8} \int_\Omega \rho(eV_1^h)^2 + \frac{3}{8} \tilde{a}(eu_1^h, eu_1^h) \leq \frac{1}{2} \int_\Omega \rho(eV_0^h)^2 + \frac{5}{8} \tilde{a}(eu_0^h, eu_0^h) \\ &+ C \left(\frac{\Delta t}{t_0} \right)^4 \sup_{t \in [0, \Delta t]} \|\sqrt{\rho} t_0^2 \ddot{u}(t)\|_{L^2(\Omega)^d}^2 \\ &+ C \left(\frac{\Delta t}{t_0} \right)^2 h^2 \sum_{k=1}^K h_k^{2r} \sup_{t \in [0, \Delta t]} |\sqrt{\rho} t_0 \ddot{u}(t)|_{r+1, \mathbf{E}, \Omega_k}^2 \\ &+ C \sum_{k=1}^K h_k^{2q} \frac{C_k^2}{\tilde{\alpha}} \sup_{t \in [0, \Delta t]} |u(t)|_{q+1, \mathbf{E}, \Omega_k}^2, \end{aligned}$$

hence :

$$\begin{aligned}
\eta_{1/2}^h &\leq C \left(\|\sqrt{\rho} e V_0^h\|_{L^2(\Omega)^d}^2 + \tilde{a}(e u_0^h, e u_0^h) + \left(\frac{\Delta t}{t_0} \right)^4 \sup_{t \in [0, \Delta t]} \|\sqrt{\rho} t_0^2 \ddot{u}(t)\|_{L^2(\Omega)^d}^2 \right) \\
&+ C \left(\frac{\Delta t}{t_0} \right)^2 h^2 \sum_{k=1}^K h_k^{2r} \sup_{t \in [0, \Delta t]} |\sqrt{\rho} t_0 \dot{u}(t)|_{r+1, \mathbf{E}, \Omega_k}^2 \\
&+ C \sum_{k=1}^K h_k^{2q} \frac{C_k^2}{\tilde{\alpha}} \sup_{t \in [0, \Delta t]} |u(t)|_{q+1, \mathbf{E}, \Omega_k}^2.
\end{aligned}$$

3. Time and space approximation error estimate.

We estimate here the space and time approximation error given by :

$$A = \Delta t \sum_{i=1}^n E_i^a \left(\frac{e V_{i-1/2}^h + e V_{i+1/2}^h}{2} \right).$$

By applying the Cauchy-Schwarz inequality, we obtain :

$$\begin{aligned}
A &\leq \frac{\Delta t}{t_0} \sum_{i=1}^n \left\| t_0 \frac{T_{i-1/2} + T_{i+1/2}}{2} \right\|_{L^2(\Omega)^d} \left\| \sqrt{\rho} \frac{e V_{i-1/2}^h + e V_{i+1/2}^h}{2} \right\|_{L^2(\Omega)^d} \\
&\leq \frac{\Delta t}{2t_0} \sum_{i=1}^n \left\| t_0 \frac{T_{i-1/2} + T_{i+1/2}}{2} \right\|_{L^2(\Omega)^d}^2 + \frac{\Delta t}{2t_0} \sum_{i=1}^n \left\| \sqrt{\rho} \frac{e V_{i-1/2}^h + e V_{i+1/2}^h}{2} \right\|_{L^2(\Omega)^d}^2 \\
&\leq \frac{\Delta t}{2t_0} \sum_{i=1}^n \left\| t_0 \frac{T_{i-1/2} + T_{i+1/2}}{2} \right\|_{L^2(\Omega)^d}^2 + \frac{\Delta t}{2t_0} \sum_{i=0}^n \left\| \sqrt{\rho} e V_{i+1/2}^h \right\|_{L^2(\Omega)^d}^2.
\end{aligned}$$

Let us remark that :

$$\begin{aligned}
T_{i+1/2} + T_{i-1/2} &= \sqrt{\rho} \frac{V_{i+1}^h - V_{i-1}^h}{\Delta t} - \sqrt{\rho} \frac{\ddot{u}(t_{i-1}) + 2\ddot{u}(t_i) + \ddot{u}(t_{i+1})}{2} \\
&= \sqrt{\rho} \frac{V_{i+1}^h + V_i^h - V_i^h - V_{i-1}^h}{\Delta t} - \sqrt{\rho} \frac{\ddot{u}(t_{i-1}) + 2\ddot{u}(t_i) + \ddot{u}(t_{i+1})}{2} \\
&= 2\sqrt{\rho} \frac{\mathbb{P}_h u(t_{i+1}) - 2\mathbb{P}_h u(t_i) + \mathbb{P}_h u(t_{i-1})}{\Delta t^2} - \sqrt{\rho} \frac{\ddot{u}(t_{i-1}) + 2\ddot{u}(t_i) + \ddot{u}(t_{i+1})}{2} \\
&= 2\sqrt{\rho} \frac{u(t_{i+1}) - 2u(t_i) + u(t_{i-1})}{\Delta t^2} - \sqrt{\rho} \frac{\ddot{u}(t_{i-1}) + 2\ddot{u}(t_i) + \ddot{u}(t_{i+1})}{2} \\
&+ 2\sqrt{\rho} (\mathbb{P}_h - id) \left(\frac{u(t_{i+1}) - 2u(t_i) + u(t_{i-1})}{\Delta t^2} \right).
\end{aligned}$$

Proceeding, as in the estimation of the approximation error of the second step of the proof,

we use the lemma 4.12 and Taylor's expansions with integral remainder to obtain :

$$\begin{aligned}
& \|T_{i+1/2} + T_{i-1/2}\|_{L^2(\Omega)^d}^2 \\
\leq & C \left(\Delta t^4 \sup_{t \in [0, T]} \|\sqrt{\rho} \ddot{u}(t)\|_{L^2(\Omega)^d}^2 \right. \\
& \left. + h^2 \sum_{k=1}^K h_k^{2r} \left| \sqrt{\rho} \frac{u(t_{i+1}) - 2u(t_i) + u(t_{i-1})}{\Delta t^2} \right|_{r+1, \mathbf{E}, \Omega_k}^2 \right) \\
\leq & \frac{C}{t_0^2} \left(\left(\frac{\Delta t}{t_0} \right)^4 \sup_{t \in [0, T]} \|\sqrt{\rho} t_0^3 \ddot{u}(t)\|_{L^2(\Omega)^d}^2 + h^2 \sum_{k=1}^K h_k^{2r} \sup_{t \in [0, T]} |\sqrt{\rho} t_0 \ddot{u}(t)|_{r+1, \mathbf{E}, \Omega_k}^2 \right)
\end{aligned}$$

Then :

$$\begin{aligned}
& \frac{\Delta t}{2t_0} \sum_{i=1}^{n-1} \left\| t_0 \frac{T_{i-1/2} + T_{i+1/2}}{2} \right\|_{L^2(\Omega)^d}^2 \leq \frac{T}{8t_0} t_0^2 \sup_{i < n} \|T_{i+1/2} + T_{i-1/2}\|_{L^2(\Omega)^d}^2 \\
& \leq C \frac{T}{8t_0} \left(\left(\frac{\Delta t}{t_0} \right)^4 \sup_{t \in [0, T]} \|\sqrt{\rho} t_0^3 \ddot{u}(t)\|_{L^2(\Omega)^d}^2 + h^2 \sum_{k=1}^K h_k^{2r} \sup_{t \in [0, T]} |\sqrt{\rho} t_0 \ddot{u}(t)|_{r+1, \mathbf{E}, \Omega_k}^2 \right).
\end{aligned}$$

4. Consistency error

We estimate here the consistency error given by :

$$B = \Delta t \sum_{i=1}^n E_i^c \left(\frac{eu_{i+1/2}^h - eu_{i-1/2}^h}{\Delta t} \right).$$

Using a reorganization of the terms (equivalent to a discrete integration by parts in time), we obtain :

$$\begin{aligned}
B &= \Delta t \sum_{i=1}^n \int_{\mathcal{S}} \left(\frac{\lambda(t_{i-1}) + 2\lambda(t_i) + \lambda(t_{i+1})}{4} \right) \cdot \left[\frac{eu_{i+1/2}^h - eu_{i-1/2}^h}{\Delta t} \right] \\
&= \Delta t \sum_{i=1}^{n-1} \int_{\mathcal{S}} \left(\frac{\lambda(t_{i-1}) + \lambda(t_i) - \lambda(t_{i+1}) - \lambda(t_{i+2})}{4\Delta t} \right) \cdot [eu_{i+1/2}^h] \\
&\quad + \int_{\mathcal{S}} \left(\frac{\lambda(t_{n-1}) + 2\lambda(t_n) + \lambda(t_{n+1})}{4} \right) \cdot [eu_{n+1/2}^h] \\
&\quad - \int_{\mathcal{S}} \left(\frac{\lambda(t_0) + 2\lambda(t_1) + \lambda(t_2)}{4} \right) \cdot [eu_{1/2}^h] \\
&= \Delta t D + E - F.
\end{aligned}$$

Concerning the $\Delta t D$ term, we proceed exactly as in the estimation of the consistency error of the second step of the proof. More precisely, we use that $[eu_{i+1/2}^h] \in V_h$, the

Cauchy-Schwarz inequality and the inequality (4.46), the estimation (4.43) and a Taylor's expansion to get :

$$\begin{aligned}
\Delta t D &= \frac{\Delta t}{t_0} \sum_{i=1}^{n-1} \int_S \left(t_0 \frac{\lambda(t_{i-1}) + \lambda(t_i) - \lambda(t_{i+1}) - \lambda(t_{i+2})}{4\Delta t} - \mu_h \right) \cdot [eu_{i+1/2}^h], \quad \forall \mu_h \in M_\delta, \\
&\leq \frac{\Delta t}{2t_0} \theta^2 \sum_{i=1}^{n-1} \left\| t_0 \frac{\lambda(t_{i-1}) + \lambda(t_i) - \lambda(t_{i+1}) - \lambda(t_{i+2})}{4\Delta t} - \mu_h \right\|_{\delta, -\frac{1}{2}}^2 \\
&\quad + \frac{\Delta t}{2\theta^2 t_0} \sum_{i=1}^{n-1} \|eu_{i+1/2}\|_X^2, \quad \forall \theta \in]0, +\infty[, \forall \mu_h \in M_\delta, \\
&\leq \frac{\Delta t}{2t_0} \theta^2 \sum_{i=1}^{n-1} \sum_{k=1}^K h_k^{2q} \left\| t_0 \frac{\lambda(t_{i-1}) + \lambda(t_i) - \lambda(t_{i+1}) - \lambda(t_{i+2})}{4\Delta t} \right\|_{H^{q-\frac{1}{2}}(\partial\Omega_k)^d}^2 \\
&\quad + \frac{\Delta t}{2\theta^2 t_0} \sum_{i=1}^{n-1} \|eu_{i+1/2}\|_X^2, \quad \forall \theta \in]0, +\infty[\\
&\leq C \frac{\Delta t}{t_0} \theta^2 \sum_{i=1}^{n-1} \sum_{k=1}^K h_k^{2q} \sup_{t \in [0, T]} \|t_0 \dot{\lambda}(t)\|_{H^{q-\frac{1}{2}}(\partial\Omega_k)^d}^2 + \frac{\Delta t}{2\theta^2 t_0} \sum_{i=1}^{n-1} \|eu_{i+1/2}\|_X^2, \quad \forall \theta \in]0, +\infty[\\
&\leq C \frac{T}{t_0} \theta^2 \sum_{k=1}^K h_k^{2q} C_k^2 \sup_{t \in [0, T]} |t_0 \dot{u}(t)|_{q+1, \mathbf{E}, \Omega_k}^2 + \frac{\Delta t}{2\theta^2 t_0} \sum_{i=1}^{n-1} \|eu_{i+1/2}\|_X^2, \quad \forall \theta \in]0, +\infty[,
\end{aligned}$$

and by choosing $\theta^2 = 1/\tilde{\alpha}$, we obtain :

$$\Delta t D \leq C \frac{T}{t_0} \sum_{k=1}^K h_k^{2q} \frac{C_k^2}{\tilde{\alpha}} \sup_{t \in [0, T]} |t_0 \dot{u}(t)|_{q+1, \mathbf{E}, \Omega_k}^2 + \frac{\Delta t}{2t_0} \sum_{i=1}^{n-1} \tilde{a}(eu_{i+1/2}, eu_{i+1/2}).$$

The terms E and F are easily bounded by using the same technique :

$$\begin{aligned}
E &\leq C \sum_{k=1}^K h_k^{2q} \frac{C_k^2}{\tilde{\alpha}} \sup_{t \in [0, T]} |u(t)|_{q+1, \mathbf{E}, \Omega}^2 + \frac{1}{4} \tilde{a}(eu_{n+1/2}^h, eu_{n+1/2}^h), \\
F &\leq C \left(\sum_{k=1}^K h_k^{2q} \frac{C_k^2}{\tilde{\alpha}} \sup_{t \in [0, T]} |u(t)|_{q+1, \mathbf{E}, \Omega}^2 + \tilde{a}(eu_{1/2}^h, eu_{1/2}^h) \right).
\end{aligned}$$

Moreover, the second term $\tilde{a}(eu_{1/2}^h, eu_{1/2}^h)$ in the upper bound of F can be bounded optimally by the second point of the present proof.

5. Estimate on $\eta_{n+1/2}^h$.

Putting together the estimations from the previous points, we obtain that :

$$\begin{aligned}
& \frac{1}{2} \left(1 - \frac{\Delta t}{t_0} \right) \int_{\Omega} \rho(eV_{n+1/2}^h)^2 + \frac{1}{4} \tilde{a}(eu_{n+1/2}^h, eu_{n+1/2}^h) \\
& \leq C \left(\int_{\Omega} \rho(eV_0^h)^2 + \tilde{a}(eu_0^h, eu_0^h) \right) \\
& + C \left(\frac{\Delta t}{t_0} \right)^4 \left\{ \sup_{t \in [0, T]} \|\sqrt{\rho} t_0^2 \ddot{u}(t)\|_{L^2(\Omega)^d}^2 + \frac{T}{t_0} \sup_{t \in [0, T]} \|\sqrt{\rho} t_0^3 \cdot \ddot{u}(t)\|_{L^2(\Omega)^d}^2 \right\} \\
& + C \left(\max_{1 \leq k \leq K} C_k \right) h^2 \left(\frac{T}{t_0} + \left(\frac{\Delta t}{t_0} \right)^2 \right) \sum_{k=1}^K h_k^{2r} \sup_{t \in [0, T]} |\sqrt{\rho} t_0 \ddot{u}(t)|_{r+1, \mathbf{E}, \Omega_k}^2 \\
& + C \sum_{k=1}^K h_k^{2q} \frac{C_k^2}{\tilde{\alpha}} \left\{ \sup_{t \in [0, T]} |u(t)|_{q+1, \mathbf{E}, \Omega}^2 + \frac{T}{t_0} \sup_{t \in [0, T]} |t_0 \dot{u}(t)|_{q+1, \mathbf{E}, \Omega}^2 \right\} \\
& + \frac{\Delta t}{2t_0} \sum_{i=0}^{n-1} \|\sqrt{\rho} eV_{i+1/2}^h\|_{L^2(\Omega)^d}^2 + \frac{\Delta t}{2t_0} \sum_{i=1}^{n-1} \tilde{a}(eu_{i+1/2}^h, eu_{i+1/2}^h).
\end{aligned}$$

We deduce by applying the discrete Gronwall's lemma 4.13, and for sufficiently small time steps ($\Delta t \leq t_0/2$) that :

$$\begin{aligned}
& \int_{\Omega} \rho(eV_{n+1/2}^h)^2 + \tilde{a}(eu_{n+1/2}^h, eu_{n+1/2}^h) \leq C \left(\|eV_0^h\|_{L^2(\Omega)^d}^2 + \tilde{a}(eu_0^h, eu_0^h) \right) \\
& + \left[C \left(\frac{\Delta t}{t_0} \right)^4 \left\{ \sup_{t \in [0, T]} \|\sqrt{\rho} t_0^2 \ddot{u}(t)\|_{L^2(\Omega)^d}^2 + \frac{T}{t_0} \sup_{t \in [0, T]} \|\sqrt{\rho} t_0^3 \cdot \ddot{u}(t)\|_{L^2(\Omega)^d}^2 \right\} \right. \\
& + C h^2 \frac{T}{t_0} \sum_{k=1}^K h_k^{2r} \sup_{t \in [0, T]} |\sqrt{\rho} t_0 \ddot{u}(t)|_{r+1, \mathbf{E}, \Omega_k}^2 \\
& \left. + C \sum_{k=1}^K h_k^{2q} \frac{C_k^2}{\tilde{\alpha}} \left\{ \sup_{t \in [0, T]} |u(t)|_{q+1, \mathbf{E}, \Omega}^2 + \frac{T}{t_0} \sup_{t \in [0, T]} |t_0 \dot{u}(t)|_{q+1, \mathbf{E}, \Omega}^2 \right\} \right] \left(1 + \frac{\Delta t}{t_0} \right)^n.
\end{aligned}$$

6. Conclusion.

We end this proof by establishing the announced error estimates on velocities and displacements. Concerning the estimate on velocities, let us remark that :

$$\dot{u}(t_{n+1/2}) - \frac{\dot{u}_n^h + \dot{u}_{n+1}^h}{2} = \dot{u}(t_{n+1/2}) - \frac{V_n^h + V_{n+1}^h}{2} + eV_{n+1/2}^h.$$

We have by definition :

$$\begin{aligned}
\dot{u}(t_{n+1/2}) - \frac{V_n^h + V_{n+1}^h}{2} &= \dot{u}(t_{n+1/2}) - \frac{\mathbb{P}_h u(t_{n+1}) - \mathbb{P}_h u(t_n)}{\Delta t}, \\
&= \dot{u}(t_{n+1/2}) - \frac{u(t_{n+1}) - u(t_n)}{\Delta t} + (id - \mathbb{P}_h) \left(\frac{u(t_{n+1}) - u(t_n)}{\Delta t} \right),
\end{aligned}$$

which entails that :

$$\begin{aligned} & \left\| \sqrt{\rho} \left(\dot{u}(t_{n+1/2}) - \frac{V_n^h + V_{n+1}^h}{2} \right) \right\|_{L^2(\Omega)^d}^2 \\ & \leq C \left(\left(\frac{\Delta t}{t_0} \right)^4 \sup_{t \in [0, T]} \|\sqrt{\rho} t_0^2 \ddot{u}(t)\|_{L^2(\Omega)^d}^2 + h^2 \sum_{k=1}^K h_k^{2r} \sup_{t \in [0, T]} |\sqrt{\rho} \dot{u}(t)|_{r+1, \mathbf{E}, \Omega_k}^2 \right). \end{aligned}$$

Therefore, we deduce the final estimate on velocities by the triangular inequality :

$$\begin{aligned} & \left\| \sqrt{\rho} \left(\dot{u}(t_{n+1/2}) - \frac{\dot{u}_n^h + \dot{u}_{n+1}^h}{2} \right) \right\|_{L^2(\Omega)^d}^2 \leq C \left(\|\sqrt{\rho} e V_0^h\|_{L^2(\Omega)^d}^2 + \tilde{a}(e u_0^h, e u_0^h) \right) \\ & + \left[C \left(\frac{\Delta t}{t_0} \right)^4 \left\{ \sup_{t \in [0, T]} \|\sqrt{\rho} t_0^2 \ddot{u}(t)\|_{L^2(\Omega)^d}^2 + \frac{T}{t_0} \sup_{t \in [0, T]} \|\sqrt{\rho} t_0^3 \ddot{u}(t)\|_{L^2(\Omega)^d}^2 \right\} \right. \\ & + C h^2 \frac{T}{t_0} \sum_{k=1}^K h_k^{2r} \left(\sup_{t \in [0, T]} |\sqrt{\rho} t_0 \ddot{u}(t)|_{r+1, \mathbf{E}, \Omega_k}^2 + \sup_{t \in [0, T]} |\sqrt{\rho} \dot{u}(t)|_{r+1, \mathbf{E}, \Omega_k}^2 \right) \\ & \left. + C \sum_{k=1}^K h_k^{2q} \frac{C_k^2}{\tilde{\alpha}} \left\{ \sup_{t \in [0, T]} |u(t)|_{q+1, \mathbf{E}, \Omega}^2 + \frac{T}{t_0} \sup_{t \in [0, T]} |t_0 \dot{u}(t)|_{q+1, \mathbf{E}, \Omega}^2 \right\} \right] \left(1 + \frac{\Delta t}{t_0} \right)^n. \end{aligned}$$

We end by the estimate on displacements. We remark that :

$$u(t_{n+1/2}) - \frac{u_n^h + u_{n+1}^h}{2} = u(t_{n+1/2}) - \frac{\mathbb{P}_h u(t_n) + \mathbb{P}_h u(t_{n+1})}{2} + e u_{n+1/2}^h.$$

Moreover, we notice that :

$$\begin{aligned} u(t_{n+1/2}) - \frac{\mathbb{P}_h u(t_n) + \mathbb{P}_h u(t_{n+1})}{2} &= u(t_{n+1/2}) - \frac{u(t_n) + u(t_{n+1})}{2} \\ &+ (id - \mathbb{P}_h) \left(\frac{u(t_n) + u(t_{n+1})}{2} \right), \end{aligned}$$

resulting in :

$$\begin{aligned} & \left\| u(t_{n+1/2}) - \frac{\mathbb{P}_h u(t_n) + \mathbb{P}_h u(t_{n+1})}{2} \right\|_X^2 \\ & \leq C \left(\left(\frac{\Delta t}{t_0} \right)^4 \sup_{t \in [0, T]} \|t_0^2 \ddot{u}(t)\|_X^2 + \sum_{k=1}^K h_k^{2q} \sup_{t \in [0, T]} |u(t)|_{q+1, \mathbf{E}, \Omega_k}^2 \right), \end{aligned}$$

and we conclude by the triangular inequality that :

$$\begin{aligned}
& \tilde{\alpha} \left\| u(t_{n+1/2}) - \frac{u_n^h + u_{n+1}^h}{2} \right\|_X^2 \\
& \leq C \left(\|\sqrt{\rho} eV_0^h\|_{L^2(\Omega)^d}^2 + \tilde{a}(eu_0^h, eu_0^h) \right) \\
& + C \left[\left(\frac{\Delta t}{t_0} \right)^4 \left\{ \tilde{\alpha} \sup_{t \in [0, T]} \|t_0^2 \ddot{u}(t)\|_X^2 + \sup_{t \in [0, T]} \|\sqrt{\rho} t_0^2 \ddot{u}(t)\|_{L^2(\Omega)^d}^2 + \frac{T}{t_0} \sup_{t \in [0, T]} \|\sqrt{\rho} t_0^3 \ddot{u}(t)\|_{L^2(\Omega)^d}^2 \right\} \right. \\
& + \left(\max_{1 \leq k \leq K} C_k \right) h^2 \frac{T}{t_0} \sum_{k=1}^K h_k^{2r} \sup_{t \in [0, T]} |\sqrt{\rho} t_0 \ddot{u}(t)|_{r+1, \mathbf{E}, \Omega_k}^2 + \tilde{\alpha} \sum_{k=1}^K h_k^{2q} \sup_{t \in [0, T]} |u(t)|_{q+1, \mathbf{E}, \Omega_k}^2 \\
& \left. + \sum_{k=1}^K h_k^{2q} \frac{C_k^2}{\tilde{\alpha}} \left\{ \sup_{t \in [0, T]} |u(t)|_{q+1, \mathbf{E}, \Omega}^2 + \frac{T}{t_0} \sup_{t \in [0, T]} |t_0 \dot{u}(t)|_{q+1, \mathbf{E}, \Omega}^2 \right\} \right] \left(1 + \frac{\Delta t}{t_0} \right)^n.
\end{aligned}$$

The proof is complete. \square

In the previous proof, we have used the following discrete Gronwall's lemma :

Lemma 4.13 (Gronwall). *Let $(w_n)_{n \in \mathbb{N}}$, a real valued sequence such that :*

$$w_n \leq a + k \sum_{i=0}^{n-1} w_i, \quad \forall n \geq 0,$$

with $a > 0$, and $k > 0$. Then, for all $n \in \mathbb{N}$:

$$w_n \leq a(1+k)^n.$$

Proof : Denoting by $y_n = \sum_{i=0}^n w_i$, we obtain for all $n \geq 1$:

$$y_n \leq (1+k)y_{n-1} + a,$$

and by induction :

$$y_n \leq (1+k)^n w_0 + a \sum_{i=0}^{n-1} (1+k)^i \leq a \sum_{i=0}^n (1+k)^i.$$

As a consequence, for all $n \geq 1$:

$$w_n \leq a + ky_{n-1} \leq a(1+k)^n,$$

which ends the proof. \square

Remark 4.16. *The proof of the convergence has been done in the case where the measure of Γ_D was positive. Let us mention the necessary modifications of the proof when it is not the case. The displacements have to be decomposed in the space of rigid motions :*

$$\mathcal{R} = \{v \in H^1(\Omega)^d, \quad a(v, w) = 0, \forall w \in H^1(\Omega)\},$$

and in the complementary :

$$\mathcal{V} = \{v \in H^1(\Omega)^d, \quad \int_{\Omega} v \cdot r = 0, \forall r \in \mathcal{R}\},$$

such that $H^1(\Omega)^d = \mathcal{R} \oplus \mathcal{V}$. The solution u of (4.49) can then be decomposed into $u = \bar{u} + u'$, with $\bar{u} \in \mathcal{C}^0(0, T; \mathcal{R}) \cap \mathcal{C}^1(0, T; \mathcal{R})$ such that in the sense of distributions over $]0, T[$:

$$\frac{\partial^2}{\partial t^2} \int_{\Omega} \rho \bar{u}(t) \cdot \bar{v} = \int_{\Omega} f(t) \cdot \bar{v} + \int_{\Gamma_N} g(t) \cdot \bar{v}, \quad \forall \bar{v} \in \mathcal{R},$$

and $u' \in \mathcal{C}^0(0, T; \mathcal{V}) \cap \mathcal{C}^1(0, T; \mathcal{W})$ such that in the sense of distributions over $]0, T[$:

$$\frac{\partial^2}{\partial t^2} \int_{\Omega} \rho u'(t) \cdot v' + a(u', v') = \int_{\Omega} f(t) \cdot v' + \int_{\Gamma_N} g(t) \cdot v', \quad \forall v' \in \mathcal{V},$$

with $\mathcal{W} = \{v \in L^2(\Omega)^d, \quad \int_{\Omega} v \cdot r = 0, \forall r \in \mathcal{R}\}$. The fully discrete approximation of u

at time t_n is $u_n^h = \bar{u}_n^h + u_n'^h$ in displacements and $\dot{u}_n^h = \dot{\bar{u}}_n^h + \dot{u}_n'^h$ in velocities. To find $(u_n'^h; \dot{u}_n'^h)_{n \geq 1}$, one has to replace V_h by :

$$V'_h = \{v_h \in V_h; \quad \int_{\Omega} v_h \cdot r = 0, \forall r \in \mathcal{R}\}$$

in (4.52). The previous proof gives an upper bound for :

$$\left\| \frac{\partial u'}{\partial t}(t_{n+1/2}) - \frac{\dot{u}_n'^h + \dot{u}_{n+1}^h}{2} \right\|_{L^2(\Omega)^d}^2 + \left\| u'(t_{n+1/2}) - \frac{u_n'^h + u_{n+1}^h}{2} \right\|_{H^1(\Omega)^d}^2,$$

because \tilde{a} is coercive over $V'_h \times V'_h$. To find $(\bar{u}_n^h; \dot{\bar{u}}_n^h)_{n \geq 1}$, one has to replace V_h by \mathcal{R} in (4.52). An upper bound on :

$$\left\| \frac{\partial \bar{u}}{\partial t}(t_{n+1/2}) - \frac{\dot{\bar{u}}_n^h + \dot{\bar{u}}_{n+1}^h}{2} \right\|_{L^2(\Omega)^d}^2,$$

is then obtained by the previous proof, which still applies. Indeed, it is noticeable that there is no consistency error because $\mathcal{R} \subset V_h$, and then, no need of coercivity. Putting together the estimates concerning the rigid motion part of the solution and the complementary part,

the announced estimate then remains the same when Γ_D has a null measure.

In this case, the projection \mathcal{P}_h of the proposition 4.10 can be constructed as follows. For all $u \in H^1(\Omega)^d$, we can build the decomposition $u = \bar{u} + u'$, with $\bar{u} \in \mathcal{R}$ and $u' \in \mathcal{V}$. The projection $\mathcal{P}_h u$ of $u \in H^1(\Omega)^d$ is then defined by :

$$\mathcal{P}_h u = \bar{u} + u'_h, \quad (4.66)$$

where $u'_h \in V'_h$ is such that :

$$\tilde{a}(u'_h, v'_h) = \tilde{a}(u', v'_h), \quad \forall v' \in V'_h.$$

4.7 Analysis of discontinuous mortar spaces

In this section, the fundamental assumption 4.2 on mortar spaces is checked for particular discrete spaces with discontinuous Lagrange multipliers, when a suitable stabilization on the interface is added. Let us mention that this assumption is equivalent to the following interface inf-sup conditions for $1 \leq m \leq M$:

$$\inf_{\mu_m \in M_{m; \delta_m}} \sup_{\phi_m \in W_{m; \delta_m}^0} \frac{\int_{\Gamma_m} \mu_m \cdot \phi_m}{\|\mu_m\|_{\delta, -\frac{1}{2}, m} \|\phi_m\|_{\delta, \frac{1}{2}, m}} \geq \beta'_m. \quad (4.67)$$

In subsection 3.1, we show that a $\mathbb{P}_1/\mathbb{P}_0$ approximation with interface bubble stabilization on u_h is compatible for u/λ , i.e satisfies assumption 4.2. This idea has been introduced in [BM00] for the so-called three-field formulation. In subsection 3.3, we propose a numerical procedure to check the compatibility condition (4.67). In subsection 3.4, we show a useful lemma enabling to check only a local inf-sup condition on the interface in the way of [BN83, Ste84, Ste90] for divergence free problems. We use it in the subsection 3.5 to prove (4.67) for a stabilized \mathbb{P}_2 or $\mathbb{Q}_2/\mathbb{P}_1$ – *discontinuous* formulation.

4.7.1 Stabilized first order elements

Here, we assume that λ is approximated by piecewise constants ($q = 1$), and u by continuous piecewise linear functions with bubbles on the interface \mathcal{S} (see figure 4.5). For each mesh element $F \in \mathcal{F}_\delta$ on the interface \mathcal{S} , an interface bubble can be defined on $T(F)$ in the way followed by [BM00]. If $T(F)$ is a triangle or a tetrahedron whose vertices are denoted by $(a_i)_i$ with the associated barycentric coordinates $(\lambda_i)_i$, an interface bubble b_F can be defined as :

$$b_F = \prod_{a_i \in \mathcal{S}} \lambda_i.$$

When considering a square or cubic reference element $\hat{Q} = [-1, 1]^d$, we can also define the face bubble associated with the face $\hat{F} = [-1, 1]^{d-1} \times \{-1\}$

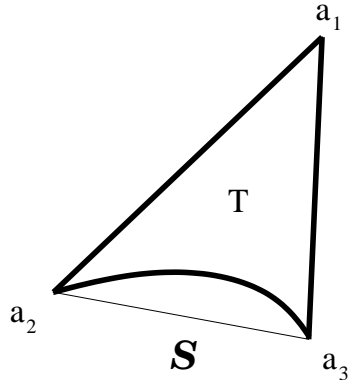


FIG. 4.5 – Bubble function $\lambda_2 \lambda_3$ on the interface \mathcal{S} , in a triangle T . (Bidimensional problems)

- for $d = 3$ by :

$$b_{\hat{F}} = \frac{1}{2}(1 - x_1^2)(1 - x_2^2)(1 - x_3), \quad \forall \hat{x} = (\hat{x}_1, \hat{x}_2, \hat{x}_3) \in [-1, 1]^3,$$

- for $d = 2$ by :

$$b_{\hat{F}} = \frac{1}{2}(1 - x_1^2)(1 - x_2), \quad \forall \hat{x} = (\hat{x}_1, \hat{x}_2) \in [-1, 1]^2.$$

Proposition 4.11. *With $q = 1$ and a bubble stabilization on the interface, the assumption 4.2 is always satisfied with a stability constant independent of the discretization, whatever the relative configuration of the meshes on the interface \mathcal{S} .*

Proof : Let I_m be an approximation operator from $\mathbb{H}_\delta^{1/2}(\Gamma_m)$ to $W_{m;\delta_m}^0$, to be detailed later. For all $v \in \mathbb{H}_\delta^{1/2}(\Gamma_m)$, we define with constants γ_F to be computed later :

$$\pi_m v = I_m v + \sum_{F \in \mathcal{F}_{m;\delta_m}} \gamma_F b_F|_F.$$

Because Lagrange multipliers are piecewise constant, we must have for all $F \in \mathcal{F}_{m;\delta_m}$:

$$\int_F \pi_m v = \int_F v,$$

which imposes :

$$\gamma_F = \frac{\int_F (v - I_m v)}{\int_F b_F}.$$

By a classical change of variable on the reference element \hat{F} :

$$\int_F b_F = \frac{\text{meas}(F)}{\text{meas}(\hat{F})} \int_{\hat{F}} \hat{b} = C \text{meas}(F),$$

and then by Cauchy-Schwartz inequality :

$$|\gamma_F| \leq C \frac{\|v - I_m v\|_{L^2(F)}}{\text{meas}(F)^{1/2}}.$$

Thus, we obtain the following estimate :

$$\begin{aligned} \|\pi_k v\|_{\delta, \frac{1}{2}, m}^2 &= \sum_{F \in \mathcal{F}_{m; \delta_m}} \frac{1}{h(F)} \|\pi_k v\|_{L^2(F)}^2 \\ &\leq C \left(\sum_{F \in \mathcal{F}_{m; \delta_m}} \frac{1}{h(F)} \|I_m v\|_{L^2(F)}^2 + \sum_{F \in \mathcal{F}_{m; \delta_m}} \frac{1}{h(F)} \|v - I_m v\|_{L^2(F)}^2 \frac{\|b_F\|_{L^2(F)}^2}{\text{meas}(F)} \right) \\ &\leq C \left(\sum_{F \in \mathcal{F}_{m; \delta_m}} \frac{1}{h(F)} \|I_m v\|_{L^2(F)}^2 + \sum_{F \in \mathcal{F}_{m; \delta_m}} \frac{1}{h(F)} \|v - I_m v\|_{L^2(F)}^2 \right) \\ &\leq C \left(\sum_{F \in \mathcal{F}_{m; \delta_m}} \frac{1}{h(F)} \|I_m v\|_{L^2(F)}^2 + \sum_{F \in \mathcal{F}_{m; \delta_m}} \frac{1}{h(F)} \|v\|_{L^2(F)}^2 \right). \end{aligned}$$

By chosing the approximation operator I_m as the projection from $\mathbb{H}_\delta^{1/2}(\Gamma_m)$ to $W_{m; \delta_m}^0$ for the inner product :

$$\langle u, v \rangle_{\delta, \frac{1}{2}, m} = \sum_{F \in \mathcal{F}_{m; \delta_m}} \frac{1}{h(F)} \int_F u \cdot v,$$

which ensures that we have :

$$\sum_{F \in \mathcal{F}_{m; \delta_m}} \frac{1}{h(F)} \|I_m v\|_{L^2(F)}^2 \leq \sum_{F \in \mathcal{F}_{m; \delta_m}} \frac{1}{h(F)} \|v\|_{L^2(F)}^2,$$

we conclude :

$$\|\pi_m v\|_{\delta, \frac{1}{2}, m} \leq C \|v\|_{\delta, \frac{1}{2}, m},$$

which ends the proof. \square

4.7.2 A counter example

We show here that the assumption 4.2 can be easily violated when a bubble stabilization is not introduced. For example, let us consider an interface \mathcal{S} whose non-mortar side is

represented on figure 4.6, and equipped with a uniform square mesh. The diameter of the squares is denoted by δ .

We adopt the classical $\mathbb{Q}_1 \times \mathbb{P}_0$ discretization :

$$\begin{cases} M_\delta = \{p \in L^2(\mathcal{S})^d, \quad p|_F \in \mathbb{P}_0(F)^d, \forall F \in \mathcal{F}_\delta\}, \\ W_\delta^0 = \{p \in H_0^1(\mathcal{S})^d \cap \mathcal{C}^0(\mathcal{S})^d, \quad p|_F \in \mathbb{Q}_1(F)^d, \forall F \in \mathcal{F}_\delta\}. \end{cases}$$

If $\lambda_h^* \in M_\delta$ is taken as a checkboard (as shown on figure 4.6), that is :

$$\lambda_h^*|_F = \pm a, \quad a \in \mathbb{R}^d,$$

depending of $F \in \mathcal{F}_\delta$ in the way indicated by figure 4.6, then we have by point symmetry of each shape function around each node :

$$\int_{\mathcal{S}} \phi_h \cdot \lambda_h^* = 0, \quad \forall \phi_h \in W_\delta^0.$$

As a consequence, the inf-sup condition (4.67) cannot be satisfied.

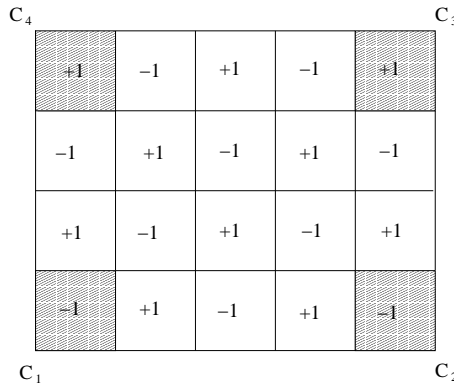


FIG. 4.6 – Uniform square mesh of the interface \mathcal{S} between two subdomains.

Remark 4.17. *The standard assumption 4.2 ensures the well-posedness of the approximate problem (4.7) whatever the relative configuration of the mortar and non-mortar meshes. In particular, it is always strictly stronger than the inf-sup condition (4.9), except in the conforming case, where it is equivalent. The instability shown on figure 4.6 entails that (4.7) is not well-posed for conforming meshes on the interface, but the problem (4.7) could be well-posed for strictly non-conforming interfaces. Indeed, in the inf-sup condition (4.9), the displacement over the interface enters through its jump whereas it only enters in the assumption 4.2 through its value on the non-mortar side. Obviously, the space of jumps over the interface can be considerably richer than the space of the displacements on the non-mortar side if the interface is really non-conforming. This enrichment coming from the non-conformity can make the inf-sup condition (4.9) satisfied, but in such cases, there will be no robustness with respect to the relative position of the interfaces.*

4.7.3 Numerical validation

We propose here a numerical test to check if the inf-sup condition (4.67) is satisfied for a given discretization by mesh-refinement. This test is a simple variant of a test introduced by [BCI00]. For $1 \leq m \leq M$, let us denote by :

$$\beta'_{m;\delta_m} = \min_{\lambda_m \in M_{m;\delta_m} \setminus \{0\}} \max_{\phi_m \in W_{m;\delta_m}^0 \setminus \{0\}} \frac{\int_{\Gamma_m} \lambda_m \cdot \phi_m}{\|\phi_m\|_{\delta,\frac{1}{2},m} \|\lambda_m\|_{\delta,-\frac{1}{2},m}},$$

the discrete inf-sup constant. Then, we have the following result :

Proposition 4.12. *Under the assumption that the family of meshes $(\mathcal{F}_{m;\delta_m})_{\delta_m > 0}$ on the interface Γ_m is quasi-uniform, we have :*

$$\beta'_{m;\delta_m} = O\left(\frac{1}{\delta_m^{d-1}} \lambda_{\min}(\mathbf{B}_m \mathbf{B}_m^t)^{1/2}\right),$$

where \mathbf{B}_m is the matrix associated to the bilinear form b on $W_{m;\delta_m}^0 \times M_{m;\delta_m}$ and $\lambda_{\min}(\mathbf{M})$ the smallest eigenvalue of the matrix \mathbf{M} . We remark that $\lambda_{\min}(\mathbf{B}_m \mathbf{B}_m^t)^{1/2}$ is the smallest positive singular value of \mathbf{B}_m .

Proof : We have $\beta'_{m;\delta_m} = \min_{\lambda_m \in M_{m;\delta_m} \setminus \{0\}} A_{\lambda_m}$ with :

$$A_{\lambda_m} = \max_{\phi_m \in W_{m;\delta_m}^0 \setminus \{0\}} \frac{\int_{\Gamma_m} \lambda_m \cdot \phi_m}{\|\phi_m\|_{\delta,\frac{1}{2},m} \|\lambda_m\|_{\delta,-\frac{1}{2},m}}.$$

Using matrices and vectors representing data in the chosen discrete spaces in a given basis, we have :

$$A_{\lambda_m} = \max_{\Phi_m} \frac{\langle \mathbf{B}\Phi_m, \Lambda_m \rangle}{\langle \mathbf{M}_\Phi \Phi_m, \Phi_m \rangle^{1/2} \langle \mathbf{M}_\Lambda \Lambda_m, \Lambda_m \rangle^{1/2}}.$$

In particular, the matrix \mathbf{M}_Φ (resp. \mathbf{M}_Λ) is the definite positive matrix representing $\|\cdot\|_{\delta,\frac{1}{2},m}$ (resp. $\|\cdot\|_{\delta,-\frac{1}{2},m}$) in the discrete spaces. Let us remark that \mathbf{B} , \mathbf{M}_Φ and \mathbf{M}_Λ depend on h . The vector Φ_m reaches the maximum if :

$$\langle \mathbf{B}\Psi_m, \Lambda_m \rangle - s \langle \mathbf{M}_\Phi \Phi_m, \Psi_m \rangle = 0, \quad \forall \Psi_m,$$

with $\langle \mathbf{M}_\Phi \Phi_m, \Phi_m \rangle = 1$. As a consequence :

$$\Phi_m = \frac{\mathbf{M}_\Phi^{-1} \mathbf{B}^t \Lambda_m}{\langle \mathbf{B} \mathbf{M}_\Phi^{-1} \mathbf{B}^t \Lambda_m, \Lambda_m \rangle^{1/2}},$$

and :

$$\begin{aligned} A_{\lambda_m} &= \frac{\langle \mathbf{B} \mathbf{M}_\Phi^{-1} \mathbf{B}^t \Lambda_m, \Lambda_m \rangle^{1/2}}{\langle \mathbf{M}_\Lambda \Lambda_m, \Lambda_m \rangle^{1/2}} \\ &\leq \frac{1}{\lambda_{\min}(\mathbf{M}_\Phi)^{1/2}} \frac{1}{\lambda_{\min}(\mathbf{M}_\Lambda)^{1/2}} \frac{\langle \mathbf{B} \mathbf{B}^t \Lambda_m, \Lambda_m \rangle^{1/2}}{\langle \Lambda_m, \Lambda_m \rangle^{1/2}}, \quad \forall \Lambda_m. \end{aligned}$$

The last result is a consequence of the inequality :

$$\lambda_{\min}(\mathbf{M}) \langle \Lambda, \Lambda \rangle \leq \langle \mathbf{M} \Lambda, \Lambda \rangle \leq \lambda_{\max}(\mathbf{M}) \langle \Lambda, \Lambda \rangle.$$

Hence we get :

$$\beta'_{m;\delta_m} = \min_{\lambda_m \in M_{m;\delta_m} \setminus \{0\}} A_{\lambda_m} \leq C \frac{1}{\delta_m^{d-1}} \lambda_{\min}(\mathbf{B}_m \mathbf{B}_m^t)^{1/2},$$

using the result from lemma 4.14, because the interface mesh is quasi-uniform.

Conversely, proceeding as previously, we deduce that :

$$\begin{aligned} A_{\lambda_m} &= \frac{\langle \mathbf{B} \mathbf{M}_\Phi^{-1} \mathbf{B}^t \Lambda_m, \Lambda_m \rangle^{1/2}}{\langle \mathbf{M}_\Lambda \Lambda_m, \Lambda_m \rangle^{1/2}} \\ &\geq C \frac{1}{\lambda_{\max}(\mathbf{M}_\Phi)^{1/2}} \frac{1}{\lambda_{\max}(\mathbf{M}_\Lambda)^{1/2}} \frac{\langle \mathbf{B} \mathbf{B}^t \Lambda_m, \Lambda_m \rangle^{1/2}}{\langle \Lambda_m, \Lambda_m \rangle^{1/2}}, \end{aligned}$$

yielding :

$$\beta'_{m;\delta_m} \geq C \frac{1}{\delta_m^{d-1}} \lambda_{\min}(\mathbf{B}_m \mathbf{B}_m^t)^{1/2},$$

using lemma 4.14 on a quasi-uniform mesh. Hence the proof. \square

In the previous proof, we have used the following lemma :

Lemma 4.14. *We assume that $\mathcal{F}_{m;\delta_m}$ is a family of uniform meshes. For all $\phi_m \in W_{m;\delta_m}$, the following inequalities hold :*

$$C \delta_m^{d-2} \langle \Phi_m, \Phi_m \rangle \leq \langle \mathbf{M}_\Phi \Phi_m, \Phi_m \rangle \leq C \delta_m^{d-2} \langle \Phi_m, \Phi_m \rangle,$$

where Φ_m is the vector of the nodal degrees of freedom of ϕ_m in $W_{m;\delta_m}$, and $\langle \mathbf{M}_\Phi \Phi_m, \Phi_m \rangle = \|\phi_m\|_{\delta, \frac{1}{2}, m}^2$. Moreover, for all $\lambda_m \in M_{m;\delta_m}$, we have also :

$$C \delta_m^d \langle \Lambda_m, \Lambda_m \rangle \leq \langle \mathbf{M}_\Lambda \Lambda_m, \Lambda_m \rangle \leq C \delta_m^d \langle \Lambda_m, \Lambda_m \rangle,$$

where Λ_m is the vector of the degrees of freedom of λ_m in $M_{m;\delta_m}$, and $\langle \mathbf{M}_\Lambda \Lambda_m, \Lambda_m \rangle = \|\lambda_m\|_{\delta, -\frac{1}{2}}^2$.

Proof : The proof of this lemma can be found in [EG02] for the L^2 norm and the adaptation to the weighted L^2 norms is straightforward. For completeness, we recall the proof. It proceeds in three steps.

1. First, let us denote by $(\hat{\theta}_1, \dots, \hat{\theta}_n)$ a basis of the finite-element scalar functions defined on the reference element \hat{F} , and define the following application :

$$\begin{aligned} \psi : \mathcal{S}^n &\rightarrow \mathbb{R} \\ \eta &\mapsto \left\| \sum_{i=1}^n \eta_i \hat{\theta}_i \right\|_{L^2(\hat{F})}^2, \end{aligned}$$

over the unit sphere \mathcal{S}^n of \mathbb{R}^n . Because \mathcal{S}^n is compact, ψ admits a minimum \hat{c} and a maximum \hat{C} , which are non-negative, and in fact positive. Indeed, by contradiction, let us assume that $\hat{c} = 0$. It would imply the existence of a $\eta \in \mathcal{S}^n$ such that $\sum_{i=1}^n \eta_i \hat{\theta}_i = 0$, and because the functions $(\hat{\theta}_i)_{1 \leq i \leq n}$ are independent, then $\eta = 0$, which is in contradiction with $\eta \in \mathcal{S}^n$. As a consequence :

$$0 < \hat{c} \leq \hat{C}.$$

For each finite element function $\hat{v} = \sum_{i=1}^n V_i \hat{\theta}_i \neq 0$ on the reference element \hat{F} , we introduce the quantity $\eta = V / \|V\|_n$ with $\|V\|_n^2 = \sum_{i=1}^n V_i^2$. We then have :

$$\psi(\eta) = \frac{\|\hat{v}\|_{L^2(\hat{F})}^2}{\|V\|_n^2},$$

and we conclude from the bounds of ψ that :

$$\hat{c} \|V\|_n^2 \leq \|\hat{v}\|_{L^2(\hat{F})}^2 \leq \hat{C} \|V\|_n^2.$$

2. Let F be a deformed element of the surfacic mesh of Γ_m and $T_F : \hat{F} \rightarrow F$ the affine application transforming the reference element \hat{F} into F . For all $1 \leq i \leq n$ we define by $\theta_i = \hat{\theta}_i \circ T_F^{-1}$ the i -th basis function of the scalar finite-element functions over F . For each function $v = \sum_{i=1}^n V_i \theta_i$ on the element F , we define $\hat{v} = v \circ T_F$ and get classically :

$$\|v\|_{L^2(F)}^2 \leq C \frac{\text{meas}(F)}{\text{meas}(\hat{F})} \|\hat{v}\|_{L^2(\hat{F})}^2,$$

and :

$$\|v\|_{L^2(F)}^2 \geq C \frac{\text{meas}(F)}{\text{meas}(\hat{F})} \|\hat{v}\|_{L^2(\hat{F})}^2,$$

where C denotes various constants independent of F . Using that $\text{meas}(F) \leq Ch(F)^{d-1} \leq C\delta_m^{d-1}$ and by quasi uniformity of the mesh that $\text{meas}(F) \geq C\delta_m^{d-1}$, we conclude from the point **1.** that :

$$c\delta_m^{d-1} \|V\|_n^2 \leq \|v\|_{L^2(F)}^2 \leq C\delta_m^{d-1} \|V\|_n^2,$$

where the constants c and C do not depend on F . By quasi-uniformity of the mesh, we also have :

$$c\delta_m^{d-2}\|V\|_n^2 \leq \frac{1}{h(F)}\|v\|_{L^2(F)}^2 \leq C\delta_m^{d-2}\|V\|_n^2,$$

and :

$$c\delta_m^d\|V\|_n^2 \leq h(F)\|v\|_{L^2(F)}^2 \leq C\delta_m^d\|V\|_n^2.$$

3. Let us generalize to the entire mesh. Let $(\varphi_i)_{1 \leq i \leq N}$ be the basis of the scalar Lagrange finite-element functions over Γ_m . The suffix i makes reference to the node of the mesh, and we introduce the number ζ_i of elements $F \in \mathcal{F}_{m;\delta_m}$ sharing the node i . Obviously, we have $\min_{1 \leq i \leq N} \zeta_i \geq 1$ as each node belongs at least to one element, and $\max_{1 \leq i \leq N} \zeta_i$ is bounded independently of δ_m by regularity of the mesh. Moreover, we denote by Υ_F the set of nodes of the element F . For all the scalar finite-element functions $v = \sum_{i=1}^N V_i \varphi_i$ over Γ_m , we deduce from the point **2.** of the present proof that :

$$c\delta_m^{d-2} \sum_{i \in \Upsilon_F} V_i^2 \leq \frac{1}{h(F)}\|v\|_{L^2(F)}^2 \leq C\delta_m^{d-2} \sum_{i \in \Upsilon_F} V_i^2,$$

and :

$$c\delta_m^d \sum_{i \in \Upsilon_F} V_i^2 \leq h(F)\|v\|_{L^2(F)}^2 \leq C\delta_m^d \sum_{i \in \Upsilon_F} V_i^2.$$

By summing these inequalities over $F \in \mathcal{F}_{m;\delta_m}$, we get :

$$c\delta_m^{d-2} \sum_{F \in \mathcal{F}_{m;\delta_m}} \sum_{i \in \Upsilon_F} V_i^2 \leq \sum_{F \in \mathcal{F}_{m;\delta_m}} \frac{1}{h(F)}\|v\|_{L^2(F)}^2 \leq C\delta_m^{d-2} \sum_{F \in \mathcal{F}_{m;\delta_m}} \sum_{i \in \Upsilon_F} V_i^2,$$

and :

$$c\delta_m^d \sum_{F \in \mathcal{F}_{m;\delta_m}} \sum_{i \in \Upsilon_F} V_i^2 \leq \sum_{F \in \mathcal{F}_{m;\delta_m}} h(F)\|v\|_{L^2(F)}^2 \leq C\delta_m^d \sum_{F \in \mathcal{F}_{m;\delta_m}} \sum_{i \in \Upsilon_F} V_i^2.$$

We remark that :

$$\sum_{F \in \mathcal{F}_{m;\delta_m}} \sum_{i \in \Upsilon_F} V_i^2 = \sum_{i=1}^N \zeta_i V_i^2,$$

and because of the bounds on ζ_i , we obtain :

$$c\delta_m^{d-2} \sum_{i=1}^N V_i^2 \leq \sum_{F \in \mathcal{F}_{m;\delta_m}} \frac{1}{h(F)}\|v\|_{L^2(F)}^2 \leq C\delta_m^{d-2} \sum_{i=1}^N V_i^2,$$

and :

$$c\delta_m^d \sum_{i=1}^N V_i^2 \leq \sum_{F \in \mathcal{F}_{m;\delta_m}} h(F)\|v\|_{L^2(F)}^2 \leq C\delta_m^d \sum_{i=1}^N V_i^2.$$

The proof has been done for scalar functions v , but the same estimates hold for vector functions by summing the previous inequalities over their components $1, \dots, d$. \square

As an illustration, we check numerically the satisfaction of the inf-sup condition (4.67) with piecewise constant $\lambda_h \in M_\delta$ and piecewise linear $\phi_h \in W_\delta^0$ with bubble stabilization. It is done on the same square interface \mathcal{S} used in the previous subsection (counter example). On figure 4.7, we present the quantity $\frac{1}{\delta^2} \lambda_{min}(\mathbf{B}\mathbf{B}^t)^{1/2}$ as a function of δ . In particular, it remains greater than a positive constant as δ goes to 0, proving (4.67).

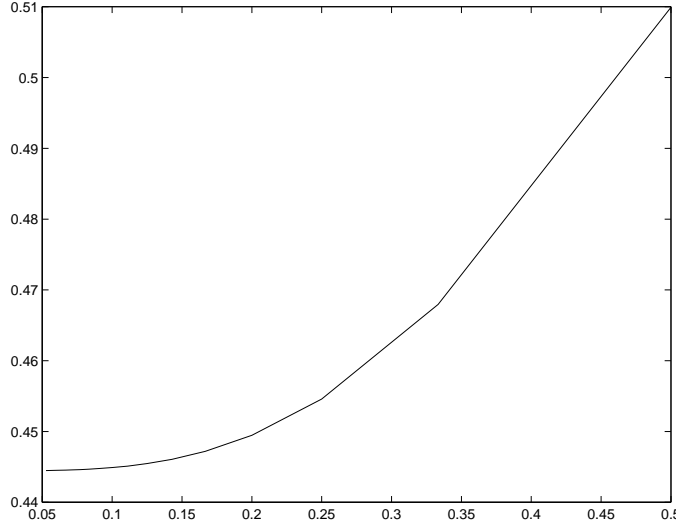


FIG. 4.7 – Numerical computation of $\frac{1}{\delta^2} \lambda_{min}(\mathbf{B}\mathbf{B}^t)^{1/2}$ as a function of δ when $\delta \rightarrow 0$.

4.7.4 A useful lemma

It can be useful to check only a local inf-sup condition on macro-elements, in the way of Boland-Nicolaides [BN83] or Stenberg [Ste84, Ste90] for divergence free problems. We assume that the interface \mathcal{S} is equipped with a family of macro-meshes $(\mathcal{N}_\delta)_{\delta>0}$ constituted of macro-elements. Each macro-element $\omega \in \mathcal{N}_\delta$ is a subset $\omega \subset \mathcal{F}_\delta$ of adjacent elements.

We assume that each element $F \in \mathcal{F}_\delta$ belong to at least one and less than L macro-elements in \mathcal{N}_δ , independently of δ .

Moreover, each $\omega = \cup_i F_i \in \mathcal{N}_\delta$ is assumed to be the image of a reference macroelement $\hat{\omega} = \cup_i \hat{F}_i$ by a mapping J , such that the restrictions $J|_{\hat{F}_i} : \hat{F}_i \rightarrow F_i$ are bounded transformations. The set of reference macro-elements is denoted by $\hat{\mathcal{N}}$.

Lemma 4.15. *Let us assume that for all reference macro-element $\hat{\omega} \in \hat{\mathcal{N}}$, we have with*

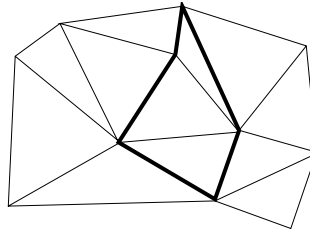


FIG. 4.8 – Example of a macro-element in a mesh.

obvious notations :

$$\inf_{\hat{\lambda} \in M_\delta(\hat{\omega}) \setminus \{0\}} \sup_{\hat{\phi} \in W_\delta^0(\hat{\omega}) \setminus \{0\}} \frac{\int_{\hat{\omega}} \hat{\phi} \cdot \hat{\lambda}}{\|\hat{\phi}\|_{L^2(\hat{\omega})} \|\hat{\lambda}\|_{L^2(\hat{\omega})}} \geq \beta_{\hat{\omega}}. \quad (4.68)$$

Then (4.67) is satisfied for all $k \geq 1$, with a stability constant $\beta'_k \geq C \inf_{\hat{\omega} \in \hat{\mathcal{N}}} \beta_{\hat{\omega}}$.

Proof : Thanks to a change of variable, the local assumptions (4.68) on reference macro-elements can be extended on any macro-element $\omega = J\hat{\omega}$. Indeed, for $\lambda \in M_\delta(\omega)$ and $\phi \in W_\delta^0(\omega)$:

$$\int_{\omega} \lambda \cdot \phi = \sum_i \int_{F_i} \lambda \cdot \phi = \sum_i \frac{\text{meas}(F_i)}{\text{meas}(\hat{F}_i)} \int_{\hat{F}_i} \hat{\lambda} \cdot \hat{\phi} \geq C \sum_i h(F_i)^{d-1} \int_{\hat{F}_i} \hat{\lambda} \cdot \hat{\phi},$$

by regularity of the mesh. Using its quasi-uniformity, we obtain :

$$\int_{\omega} \lambda \cdot \phi \geq C \delta^{d-1} \int_{\hat{\omega}} \hat{\lambda} \cdot \hat{\phi}.$$

We have also :

$$\begin{aligned} \|\phi\|_{\delta, \frac{1}{2}, \omega}^2 &= \sum_i \frac{1}{h(F_i)} \|\phi\|_{L^2(F_i)}^2 \\ &= \sum_i \frac{1}{h(F_i)} \frac{\text{meas}(F_i)}{\text{meas}(\hat{F}_i)} \|\hat{\phi}\|_{L^2(\hat{F}_i)}^2 \\ &\leq C \delta^{d-2} \|\hat{\phi}\|_{L^2(\hat{\omega})}^2, \end{aligned}$$

and similarly :

$$\|\lambda\|_{\delta, -\frac{1}{2}, \omega}^2 \leq C \delta^d \|\hat{\lambda}\|_{L^2(\hat{\omega})}^2.$$

Then, from (4.68), we get for all $\omega \in \mathcal{N}_\delta$:

$$\inf_{\lambda \in M_\delta(\omega) \setminus \{0\}} \sup_{\phi \in W_\delta(\omega) \cap H_0^1(\omega) \setminus \{0\}} \frac{\int_{\omega} \phi \cdot \lambda}{\|\phi\|_{\delta, \frac{1}{2}, \omega} \|\lambda\|_{\delta, -\frac{1}{2}, \omega}} \geq C \beta_{\hat{\omega}}. \quad (4.69)$$

Now, we will prove the global inf-sup condition (4.67). Let $\lambda \in M_\delta$. For all $\omega \in \mathcal{N}_\delta$, the condition (4.69) proves that there exists a function $\phi_\omega \in W_\delta^0(\omega)$ vanishing outside ω such that :

$$\int_\omega \lambda \cdot \phi_\omega \geq C \|\lambda\|_{\delta, -\frac{1}{2}, \omega}^2,$$

with :

$$\|\phi_\omega\|_{\delta, \frac{1}{2}, \omega} \leq \|\lambda\|_{\delta, -\frac{1}{2}, \omega}.$$

Let us define :

$$\phi = \sum_{\omega \in \mathcal{N}_\delta} \phi_\omega.$$

Then, because each element is in a macro-element at least and in less than L :

$$\begin{aligned} \int_S \lambda \cdot \phi &= \sum_{\omega \in \mathcal{N}_\delta} \int_\omega \lambda \cdot \phi_\omega \geq C \sum_{\omega \in \mathcal{N}_\delta} \|\lambda\|_{\delta, -\frac{1}{2}, \omega}^2 \\ &= C \sum_{\omega \in \mathcal{N}_\delta} \sum_{F \in \omega} h(F) \|\lambda\|_{L^2(F)^d}^2 = C \sum_{F \in \mathcal{F}_\delta} \sum_{\omega \ni F} h(F) \|\lambda\|_{L^2(F)^d}^2 \\ &\geq C \sum_{F \in \mathcal{F}_\delta} h(F) \|\lambda\|_{L^2(F)^d}^2 = C \|\lambda\|_{\delta, -\frac{1}{2}}^2, \end{aligned}$$

and :

$$\begin{aligned} \|\phi\|_{\delta, \frac{1}{2}}^2 &\leq \sum_{\omega \in \mathcal{N}_\delta} \|\phi_\omega\|_{\delta, \frac{1}{2}, \omega}^2 \leq \sum_{\omega \in \mathcal{N}_\delta} \|\lambda\|_{\delta, -\frac{1}{2}, \omega}^2 \\ &\leq \sum_{F \in \mathcal{F}_\delta} \sum_{\omega \ni F} h(F) \|\lambda\|_{L^2(F)^d}^2 \leq L \sum_{F \in \mathcal{F}_\delta} h(F) \|\lambda\|_{L^2(F)^d}^2 = L \|\lambda\|_{\delta, -\frac{1}{2}}^2, \end{aligned}$$

which proves (4.67). \square

As a consequence, local inf-sup conditions has only to be checked on reference macro-elements to ensure a global inf-sup compatibility.

4.7.5 Second order stabilized interface elements

We now introduce some stabilized elements achieving second order approximation in displacements and satisfying the local inf-sup condition (4.68).

1D macroelements

For bidimensional problems, we build on the reference interface element $\hat{\omega} = [-1; 1]$, the following spaces :

$$\begin{cases} M_\delta(\hat{\omega}) = \mathbb{P}_1(\hat{\omega})^2, \\ W_\delta^0(\hat{\omega}) = \left(\mathbb{P}_2(\hat{\omega})^2 \oplus \text{span}\{\hat{b}\}^2 \right) \cap H_0^1(\hat{\omega})^2, \end{cases}$$

where the interface bubble function \hat{b} is an odd function over $[-1, 1]$, which satisfies :

$$\int_0^1 x\hat{b}(x) dx \neq 0.$$

Then, the local inf-sup condition (4.68) is satisfied on a macro-element made of the single element $\hat{\omega}$. Indeed, let $\lambda \in M_\delta(\hat{\omega})$ be such that :

$$\int_{\hat{\omega}} \phi \cdot \lambda = 0, \quad \forall \phi \in W_\delta^0(\hat{\omega}).$$

For all $1 \leq i \leq 2$, denoting by λ_i the i th component of λ , we have $\lambda_i(x) = \alpha_i x + \beta_i$ for $x \in \hat{\omega}$, and its integral against any second order polynomial and the bubble \hat{b} vanishes, which implies :

$$\begin{cases} \int_{-1}^1 \lambda_i(x)(1 - x^2) dx = \frac{4}{3}\beta_i = 0 & \implies \beta_i = 0, \\ \int_{-1}^1 \lambda_i(x)\hat{b}(x) dx = 2\alpha_i \int_0^1 x\hat{b}(x) dx = 0 & \implies \alpha_i = 0. \end{cases}$$

Therefore, $\lambda = 0$, which proves that the local inf-sup condition (4.68) is satisfied.

As a bubble \hat{b} , one can take :

$$\hat{b}(x) = x(1 - x^2), \quad x \in \hat{\omega}. \quad (4.70)$$

Obviously, \hat{b} is the trace over $\hat{\omega} \times \{0\}$ of a bubble function \hat{h} defined in a reference element $\hat{K} \subset \mathbb{R}^2$, whose $\hat{\omega} \times \{0\}$ is an edge.

In the case where $\hat{K} = \hat{T}$ is a reference triangle, if $A = (-1, 0)$, $B = (1, 0)$ and $C = (-1, 2)$ are its vertices, the interface bubble function \hat{h} can be defined as :

$$\hat{h}(x, y) = \begin{cases} \left(1 - \frac{y}{2}\right) \hat{b}\left(\frac{2x + y}{2 - y}\right), & \forall (x, y) \in \hat{T} \setminus (-1, 2), \\ 0, & (x, y) = (-1, 2). \end{cases}$$

Such a function \hat{h} is represented on figure 4.9.

In the case where $\hat{K} = \hat{Q}$ is a reference square, if $A = (-1, 0)$, $B = (1, 0)$, $C = (1, 2)$ and $D = (-1, 2)$ are its corners, the interface bubble function \hat{h} can be defined as :

$$\hat{h}(x, y) = \left(1 - \frac{y}{2}\right) \hat{b}(x), \quad \forall (x, y) \in \hat{Q}.$$

Such a function \hat{h} is represented on figure 4.10.

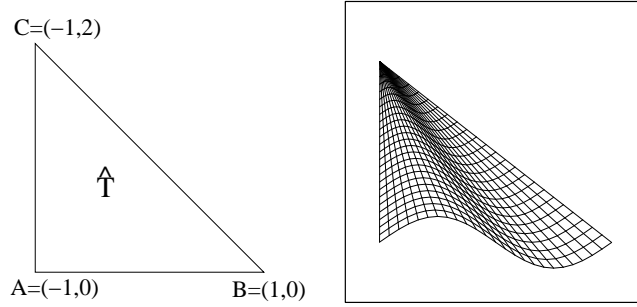


FIG. 4.9 – A reference triangle \hat{T} and a corresponding interface bubble function \hat{h} on the edge $[AB] = \hat{\omega} \times \{0\}$.

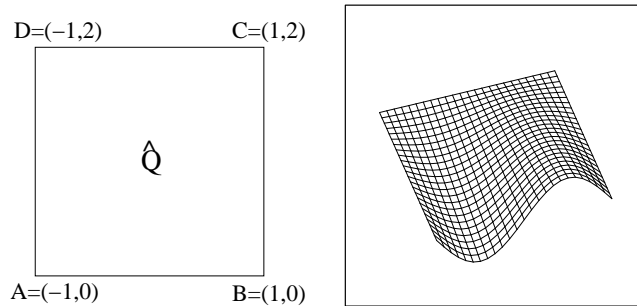


FIG. 4.10 – A reference square \hat{Q} and a corresponding interface bubble function \hat{h} on the edge $[AB] = \hat{\omega} \times \{0\}$.

2D quadrangular interface macroelement

For tridimensional problems, we introduce the following second order 2D quadrilateral interface element. Let $\hat{\omega} = \hat{Q} = [-1, 1]^2$ be a reference quadrilateral, on which we build the following spaces :

$$\begin{cases} M_\delta(\hat{\omega}) = \mathbb{P}_1(\hat{Q})^3, \\ W_\delta^0(\hat{\omega}) = \left(\mathbb{Q}_2(\hat{Q})^3 \oplus \text{span}\{\hat{b}_1, \hat{b}_2\}^3 \right) \cap H_0^1(\hat{\omega})^3, \end{cases}$$

where the bubble functions are defined as follows :

$$\hat{b}_k(x_1, x_2) = x_k(1 - x_k^2)(1 - x_l^2), \quad l \neq k, \quad (4.71)$$

the $(x_k)_{k=1,2}$ being the euclidian coordinates in \mathbb{R}^2 . An illustration of such bubble functions defined on the reference square is shown on figure 4.11.

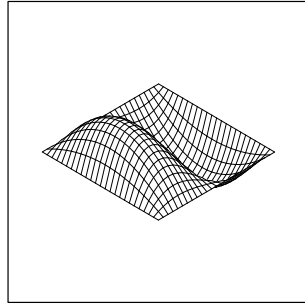


FIG. 4.11 – A bubble function defined by (4.71) on the reference square \hat{Q} .

The corresponding element satisfies the local inf-sup condition (4.68) on a macro-element made of the single element \hat{Q} . Indeed, let $\lambda \in M_\delta(\hat{\omega})$ be such that :

$$\int_{\hat{\omega}} \phi \cdot \lambda = 0, \quad \forall \phi \in W_\delta^0(\hat{\omega}).$$

For all $1 \leq i \leq 3$, denoting by λ_i the i th component of λ , we have $\lambda_i(x_1, x_2) = \alpha_i x_1 + \beta_i x_2 + \gamma_i$ for $(x_1, x_2) \in \hat{\omega}$, and its integral against any second partial order polynomial and bubble vanishes, which implies :

$$\int_{\hat{Q}} \lambda(x_1, x_2)(1 - x_1^2)(1 - x_2^2) dx_1 dx_2 = \frac{16}{9} \gamma_i = 0 \implies \gamma_i = 0,$$

$$\int_{\hat{Q}} \lambda(x_1, x_2)x_1(1 - x_1^2)(1 - x_2^2) dx_1 dx_2 = \frac{16}{45} \alpha_i = 0 \implies \alpha_i = 0,$$

$$\int_{\hat{Q}} \lambda(x_1, x_2)x_2(1 - x_1^2)(1 - x_2^2) dx_1 dx_2 = \frac{16}{45} \beta_i = 0 \implies \beta_i = 0,$$

that is $\lambda = 0$, which proves that the local inf-sup condition (4.68) is satisfied.

As previously, the interface bubble functions $(\hat{b}_k)_{k=1,2}$ are the restrictions to $\hat{Q} \times \{0\}$ of functions $(\hat{h}_k)_{k=1,2}$ defined on a reference cube $\hat{\mathbb{Q}} = \hat{Q} \times [0; 2]$ whose $\hat{Q} \times \{0\}$ is a face. More precisely, we can define for $k = 1, 2$:

$$\hat{h}_k(x_1, x_2, x_3) = \left(1 - \frac{x_3}{2}\right) \hat{b}_k(x_1, x_2), \quad \forall (x_1, x_2) \in \hat{Q}, \forall x_3 \in [0, 2].$$

2D triangular interface macroelement

For tridimensional problems, we introduce the following second order 2D triangular interface element. Let $\hat{\omega} = \hat{T}$ be a triangular element whose vertices are $A = (1, 0)$,

$B = (0, 1)$ and $C = (0, 0)$. We introduce the following spaces :

$$\begin{cases} M_\delta(\hat{\omega}) = \mathbb{P}_1(\hat{T})^3, \\ W_\delta^0(\hat{\omega}) = \left(\mathbb{P}_2(\hat{T})^3 \oplus \text{span}\{\hat{b}_1, \hat{b}_2, \hat{b}_3\}^3 \right) \cap H_0^1(\hat{\omega})^3, \end{cases}$$

where the bubble functions are defined by :

$$\hat{b}_1 = \left(\hat{\lambda}_1 - \frac{1}{2} \right) \hat{\lambda}_1 \hat{\lambda}_2 \hat{\lambda}_3,$$

$$\hat{b}_2 = \left(\hat{\lambda}_2 - \frac{1}{2} \right) \hat{\lambda}_1 \hat{\lambda}_2 \hat{\lambda}_3,$$

$$\hat{b}_3 = \left(\hat{\lambda}_3 - \frac{1}{2} \right) \hat{\lambda}_1 \hat{\lambda}_2 \hat{\lambda}_3,$$

in which $\hat{\lambda}_1$, $\hat{\lambda}_2$ and $\hat{\lambda}_3$ are the barycentric coordinates on \hat{T} , respectively associated to the vertices A , B and C . A typical example of such bubbles is given on figure 4.12.

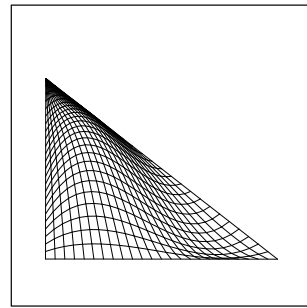


FIG. 4.12 – A bubble function on the reference interface triangle \hat{T} .

The corresponding element satisfies the local inf-sup condition (4.68) on a macro-element made of the single element \hat{T} . Indeed, let $\lambda \in M_\delta(\hat{\omega})$ be such that :

$$\int_{\hat{\omega}} \phi \cdot \lambda = 0, \quad \forall \phi \in W_\delta^0(\hat{\omega}).$$

For all $1 \leq i \leq 3$, denoting by λ_i the i th component of λ , we have $\lambda_i = \alpha_i \hat{\lambda}_1 + \beta_i \hat{\lambda}_2 + \gamma_i \hat{\lambda}_3$, and its integral against any second partial order polynomial and bubble vanishes, which implies :

$$M \begin{pmatrix} \alpha_i \\ \beta_i \\ \gamma_i \end{pmatrix} = \begin{pmatrix} 0 \\ 0 \\ 0 \end{pmatrix}, \quad (4.72)$$

with :

$$M_{kl} = \int_{\hat{T}} \hat{b}_k \hat{\lambda}_l, \quad 1 \leq k, l \leq 3.$$

To compute these coefficients, we use the following lemma (see for example [Lar95], page 57) :

Lemma 4.16. *Let T a non-degenerated triangle in \mathbb{R}^2 and $\lambda_1(x), \lambda_2(x), \lambda_3(x)$ the barycentric coordinates of $x \in \mathbb{R}^2$ with respect to the vertices of T . Then :*

$$\int_T \lambda_1(x)^k \lambda_2(x)^l \lambda_3(x)^m dx = 2 \text{meas}(T) \frac{k! l! m!}{(k+l+m+2)!}.$$

Now, let us calculate the coefficients of the matrix M by using the previous lemma. It is obtained that for $k = 1, 2, 3$:

$$\begin{aligned} M_{kk} &= \int_{\hat{T}} \left(\hat{\lambda}_1 - \frac{1}{2} \right) \hat{\lambda}_1^2 \hat{\lambda}_2 \hat{\lambda}_3 = \int_{\hat{T}} \hat{\lambda}_1^3 \hat{\lambda}_2 \hat{\lambda}_3 - \frac{1}{2} \int_{\hat{T}} \hat{\lambda}_1^2 \hat{\lambda}_2 \hat{\lambda}_3, \\ &= 2 \text{meas}(\hat{T}) \left(\frac{3!}{7!} - \frac{1}{2} \times \frac{2!}{6!} \right) = -\frac{2 \text{meas}(\hat{T})}{7!}, \end{aligned} \quad (4.73)$$

and that for all $k, l \in \{1, 2, 3\}$ such that $i \neq j$:

$$\begin{aligned} M_{kl} &= \int_{\hat{T}} \left(\hat{\lambda}_1 - \frac{1}{2} \right) \hat{\lambda}_1 \hat{\lambda}_2^2 \hat{\lambda}_3 = \int_{\hat{T}} \hat{\lambda}_1^2 \hat{\lambda}_2^2 \hat{\lambda}_3 - \frac{1}{2} \int_{\hat{T}} \hat{\lambda}_1 \hat{\lambda}_2^2 \hat{\lambda}_3 \\ &= 2 \text{meas}(\hat{T}) \left(\frac{2! 2!}{7!} - \frac{1}{2} \times \frac{2!}{6!} \right) = -3 \times \frac{2 \text{meas}(\hat{T})}{7!}. \end{aligned}$$

Then :

$$-\frac{7!}{2 \text{meas}(\hat{T})} M = \begin{pmatrix} 1 & 3 & 3 \\ 3 & 1 & 3 \\ 3 & 3 & 1 \end{pmatrix},$$

and the original linear system (4.72) is equivalent to :

$$\begin{pmatrix} 1 & 3 & 3 \\ 3 & 1 & 3 \\ 3 & 3 & 1 \end{pmatrix} \begin{pmatrix} \alpha_i \\ \beta_i \\ \gamma_i \end{pmatrix} = \begin{pmatrix} 0 \\ 0 \\ 0 \end{pmatrix}.$$

The right hand side matrix is invertible, and the only solution is then $\alpha_i = \beta_i = \gamma_i = 0$ for all $1 \leq i \leq 3$, that is $\lambda = 0$, which proves that the local inf-sup condition (4.68) is satisfied.

As previously, the interface bubble functions $(\hat{b}_k)_{k=1,2,3}$ are the restrictions to $\hat{T} \times \{0\}$ of functions $(\hat{h}_k)_{k=1,2,3}$ defined on a reference tetrahedron $\hat{\mathbb{T}}$ whose $\hat{T} \times \{0\}$ is a face. More precisely, if $\lambda_1, \dots, \lambda_4$ are the barycentric coordinates associated to the vertices of $\hat{\mathbb{T}}$, and

assuming that λ_4 is the barycentric coordinate associated to the node not belonging to $\hat{T} \times \{0\}$, we have for $k = 1, 2, 3$:

$$\hat{h}_k = \lambda_k(\lambda_k - \frac{1}{2})\lambda_l\lambda_m(1 - \lambda_4), \quad \{l, m\} = \{1, 2, 3\} \setminus \{k\}.$$

4.8 Some numerical issues

The practical implementation of mortar elements such as those introduced in the above sections, faces a few technical problems outlined in this section.

4.8.1 Penalized formulation.

One can replace the solution of a saddle-point problem by the solution of a positive definite one, by introducing a penalized formulation for (4.7). It is a very standard solution in many academic and industrial implementations for treating kinematic constraints and non-homogenous essential boundary conditions. Herein, we propose a mesh-dependent penalization term. Introducing the following L^2 inner product :

$$c(\lambda, \mu) = \int_S \lambda \cdot \mu, \quad \forall \lambda, \mu \in M_\delta,$$

and denoting by $\eta > 0$ a small penetration parameter, we propose to replace the problem (4.7) by the symmetric positive definite one :

$$\begin{cases} \tilde{a}(u_h^\eta, v_h) + b(v_h, \lambda_h^\eta) = l(v_h), & \forall v_h \in X_h, \\ b(u_h^\eta, \mu_h) = \eta \delta_{min} c(\lambda_h^\eta, \mu_h), & \forall \mu_h \in M_\delta, \end{cases} \quad (4.74)$$

where the minimum diameter of interface surfacic elements has been denoted by :

$$\delta_{min} = \min_{F \in \mathcal{F}_\delta} h(F).$$

Then, we prove the convergence of the penalized solution of the system (4.74) to the exact constrained solution of (4.7) as η goes to zero :

Proposition 4.13. *We assume that the original mortar formulation (4.7) is well-posed, and denote by $(u_h, \lambda_h) \in X_h \times M_\delta$ its unique solution. Then, for all $\eta > 0$, there exists a unique solution $(u_h^\eta, \lambda_h^\eta) \in X_h \times M_\delta$ of (4.74), and the convergence of the penalized solution to (u_h, λ_h) as $\eta \rightarrow 0$ holds in the sense that :*

$$\|u_h - u_h^\eta\|_X \leq C \eta,$$

$$\|\lambda_h - \lambda_h^\eta\|_{\delta, -\frac{1}{2}} \leq C \eta,$$

where C denotes various constants independent of the penalization coefficient η , of the decomposition into subdomains, and the discretization.

Remark 4.18. *The main difference with the usual penalization strategy used for incompressibility is that \tilde{a} is not coercive on $X_h \times X_h$.*

Proof : The proof is inspired from [EG02], with adequate modifications in order to take the remark 4.18 into account. For convenience, we rewrite (4.74) under the usual operator form with obvious notation :

$$\begin{cases} \tilde{\mathcal{A}}u_h^\eta + \mathcal{B}^t \lambda_h^\eta = \mathcal{L}, & \text{on } X'_h, \\ \mathcal{B}u_h^\eta = \eta \delta_{\min} \mathcal{C}\lambda_h^\eta, & \text{on } M'_\delta. \end{cases} \quad (4.75)$$

and the original problem (4.7) as :

$$\begin{cases} \tilde{\mathcal{A}}u_h + \mathcal{B}^t \lambda_h = \mathcal{L}, & \text{on } X'_h, \\ \mathcal{B}u_h = 0, & \text{on } M'_\delta. \end{cases} \quad (4.76)$$

The present proof is decomposed into 4 parts.

1. **Well-posedness of the penalized problem -** As the bilinear form $c(\cdot, \cdot)$ is coercive and continuous on $M \times M$, with $M = \prod_{m=1}^M L^2(\Gamma_m)^d$, the Lax-Milgram lemma shows the invertibility of \mathcal{C} on $M_\delta \subset M$, and it is obtained from (4.75) that :

$$\underbrace{\left(\tilde{\mathcal{A}} + \frac{1}{\eta \delta_{\min}} \mathcal{B}^t \mathcal{C}^{-1} \mathcal{B} \right)}_{\mathcal{K}_{\eta, \delta_{\min}}} u_h^\eta = \mathcal{L}. \quad (4.77)$$

Moreover, we prove that $\mathcal{K}_{\eta, \delta_{\min}}$ is uniformly coercive with respect to η , to the decomposition into subdomains, and to the discretization. Indeed, for all $u_h \in X_h$:

$$\langle \mathcal{K}_{\eta, \delta_{\min}} u_h, u_h \rangle_{X', X} = \langle \tilde{\mathcal{A}}u_h, u_h \rangle_{X', X} + \frac{1}{\eta \delta_{\min}} \langle \mathcal{B}u_h, \mathcal{C}^{-1} \mathcal{B}u_h \rangle_{M', M},$$

and if $\lambda_h^1 \in M_\delta$ is the unique solution of $\mathcal{C}\lambda_h^1 = \mathcal{B}u_h$ in M'_δ , it follows that :

$$\begin{aligned} \langle \mathcal{K}_{\eta, \delta_{\min}} u_h, u_h \rangle_{X', X} &= \langle \tilde{\mathcal{A}}u_h, u_h \rangle_{X', X} + \frac{1}{\eta \delta_{\min}} \langle \mathcal{C}\lambda_h^1, \lambda_h^1 \rangle_{M', M} \\ &= \langle \tilde{\mathcal{A}}u_h, u_h \rangle_{X', X} + \frac{1}{\eta \delta_{\min}} \|\lambda_h^1\|_M^2 \\ &\geq \langle \tilde{\mathcal{A}}u_h, u_h \rangle_{X', X} + \frac{1}{L} \|\lambda_h^1\|_M^2, \end{aligned}$$

when $\eta \leq 1$ and $\delta_{\min} \leq L$ (which is not a restriction because both η and δ_{\min} are expected to tend to zero), in which L denotes the diameter of the smallest interface. From the definition of π given in section 4.4.3, we get that for all interfaces γ_{kl} :

$$\int_{\gamma_{kl}} \pi[u_h] \cdot \mu = \int_{\gamma_{kl}} [u_h] \cdot \mu = \int_{\gamma_{kl}} \lambda_h^1 \cdot \mu, \quad \forall \mu \in M_{kl},$$

because we have for $\Gamma_m = \gamma_{kl}$, the inclusion $M_{kl} \subset M_{m;\delta_m}$ from assumption 4.3. As a consequence, taking $\mu = \pi[u_h]$ and using Cauchy-Schwarz inequality, it follows that :

$$\|\pi[u_h]\|_M \leq \|\lambda_h^1\|_M.$$

The inequality (4.35) then provides the existence of a coercivity constant $\kappa > 0$ independent of the number of subdomains, of their sizes, and of the discretization, such that :

$$\begin{aligned} \langle \mathcal{K}_{\eta,\delta_{min}} u_h, u_h \rangle_{X',X} &\geq \left\langle \tilde{\mathcal{A}} u_h, u_h \right\rangle_{X',X} + \frac{1}{L} \|\pi[u_h]\|_M^2 \\ &\geq \kappa \|u_h\|_X^2. \end{aligned}$$

The continuity of $\mathcal{K}_{\eta,\delta_{min}}$ holds because for all $u_h, v_h \in X_h$, we have :

$$\begin{aligned} \langle \mathcal{K}_{\eta,\delta_{min}} u_h, v_h \rangle_{X',X} &= \left\langle \tilde{\mathcal{A}} u_h, v_h \right\rangle_{X',X} + \frac{1}{\eta \delta_{min}} \langle \mathcal{C}^{-1} \mathcal{B} u_h, \mathcal{B} v_h \rangle_{M',M} \\ &\leq \|\tilde{\mathcal{A}}\| \|u_h\|_X \|v_h\|_X + \frac{1}{\eta \delta_{min}} \|\mathcal{B} u_h\|_{M'} \|\mathcal{B} v_h\|_{M'} \\ &\leq \|\tilde{\mathcal{A}}\| \|u_h\|_X \|v_h\|_X + \frac{1}{\eta \delta_{min}} \|[\mathcal{B} u_h]\|_M \|[\mathcal{B} v_h]\|_M \\ &\leq C \left(1 + \frac{1}{\eta \delta_{min}} L_{max} \right) \|u_h\|_X \|v_h\|_X, \end{aligned}$$

where $\|\tilde{\mathcal{A}}\|$ is the continuity constant of $\tilde{\mathcal{A}} : X \rightarrow X'$, and L_{max} the diameter of the largest interface. Then, for each penalization coefficient η and each discretization, there exists a unique solution $u_h^\eta \in X_h$ of (4.77) which satisfies the a priori estimate :

$$\|u_h^\eta\|_X \leq \frac{1}{\kappa} \|\mathcal{L}\|_{X'}. \quad (4.78)$$

It is crucial noticing that even if the continuity constant of $\mathcal{K}_{\eta,\delta_{min}}$ depends on η and on the discretization, the coercivity constant does not.

As a consequence of the inf-sup condition (4.9), an upper bound can be established on λ_h^η since :

$$\begin{aligned} \beta \delta_{min}^{1/2} \|\lambda_h^\eta\|_M &\leq \beta \|\lambda_h^\eta\|_{\delta,-\frac{1}{2}} \leq \|\mathcal{B}^t \lambda_h^\eta\|_{X'} \leq \|\mathcal{L} - \tilde{\mathcal{A}} u_h^\eta\|_{X'} \\ &\leq \|\mathcal{L}\|_{X'} + \|\tilde{\mathcal{A}}\| \|u_h^\eta\|_X \\ &\leq \left(1 + \frac{\|\tilde{\mathcal{A}}\|}{\kappa} \right) \|\mathcal{L}\|_{X'}, \end{aligned}$$

resulting in the following estimate :

$$\|\lambda_h^\eta\|_M \leq \frac{1}{\beta \delta_{min}^{1/2}} \left(1 + \frac{\|\tilde{\mathcal{A}}\|}{\kappa} \right) \|\mathcal{L}\|_{X'} \leq C \frac{1}{\delta_{min}^{1/2}}. \quad (4.79)$$

2. First estimate - By subtraction of the penalized system (4.74) to the original one (4.76), we get :

$$\begin{cases} \tilde{\mathcal{A}}(u_h - u_h^\eta) + \mathcal{B}^t(\lambda_h - \lambda_h^\eta) = 0, & \text{on } X'_h, \\ \mathcal{B}(u_h - u_h^\eta) = -\eta \delta_{min} \mathcal{C} \lambda_h^\eta, & \text{on } M'_\delta, \end{cases} \quad (4.80)$$

and deduce by testing the first equation with $u_h - u_h^\eta$ that :

$$\begin{aligned} \langle \tilde{\mathcal{A}}(u_h - u_h^\eta), (u_h - u_h^\eta) \rangle_{X', X} &= \eta \delta_{min} \langle \mathcal{C} \lambda_h^\eta, \lambda_h - \lambda_h^\eta \rangle_{M', M} \\ &\leq \eta \delta_{min} \|\lambda_h^\eta\|_M \|\lambda_h - \lambda_h^\eta\|_M. \end{aligned} \quad (4.81)$$

Moreover, the inf-sup condition (4.9) implies :

$$\begin{aligned} \beta \delta_{min}^{1/2} \|\lambda_h - \lambda_h^\eta\|_M &\leq \beta \|\lambda_h - \lambda_h^\eta\|_{\delta, -\frac{1}{2}} \\ &\leq \|\mathcal{B}^t(\lambda_h - \lambda_h^\eta)\|_{X'} \\ &\leq \|\tilde{\mathcal{A}}(u_h - u_h^\eta)\|_{X'} \quad \text{from (4.80),} \\ &\leq \|\tilde{\mathcal{A}}\| \|u_h - u_h^\eta\|_X, \quad \text{by continuity of } \tilde{\mathcal{A}}, \end{aligned} \quad (4.82)$$

and considering (4.79), it follows from (4.81) that :

$$\langle \tilde{\mathcal{A}}(u_h - u_h^\eta), (u_h - u_h^\eta) \rangle_{X', X} \leq C \eta \|u_h - u_h^\eta\|_X. \quad (4.83)$$

Because $u_h - u_h^\eta \notin V_h$, we cannot conclude directly about the convergence of the displacements.

3. Convergence of displacements - Let us prove now an upper bound for the quantity :

$$\sum_{1 \leq k < l \leq K} \frac{1}{diam(\gamma_{kl})} \int_{\gamma_{kl}} (\pi_{\gamma_{kl}}[u_h - u_h^\eta])^2,$$

with the notation introduced in section 4.4.3. First, because $u_h \in V_h$, we have $\pi[u_h - u_h^\eta] = -\pi[u_h^\eta]$, and :

$$\int_{\gamma_{kl}} \pi[u_h^\eta] \cdot \mu = \int_{\gamma_{kl}} [u_h^\eta] \cdot \mu = \eta \delta_{min} \int_{\gamma_{kl}} \lambda_h^\eta \cdot \mu, \quad \forall \mu \in M_{kl} \quad (\subset M_\delta).$$

By taking $\mu = \pi[u_h^\eta]$, and from Cauchy-Schwarz inequality, we get :

$$\|\pi[u_h^\eta]\|_{L^2(\gamma_{kl})^d} \leq \eta \delta_{min} \|\lambda_h^\eta\|_{L^2(\gamma_{kl})^d},$$

and therefore :

$$\|\pi[u_h - u_h^\eta]\|_{L^2(\gamma_{kl})^d} \leq \eta \delta_{min} \|\lambda_h^\eta\|_{L^2(\gamma_{kl})^d}. \quad (4.84)$$

On the other hand, we get :

$$\int_{\gamma_{kl}} \pi[u_h - u_h^\eta] \cdot \mu = \int_{\gamma_{kl}} [u_h - u_h^\eta] \cdot \mu, \quad \forall \mu \in M_{kl},$$

resulting as above in :

$$\begin{aligned} \|\pi[u_h - u_h^\eta]\|_{L^2(\gamma_{kl})^d} &\leq \|u_h - u_h^\eta\|_{L^2(\gamma_{kl})^d} \\ &\leq C \text{diam}(\gamma_{kl})^{1/2} (\|u_h - u_h^\eta\|_{H^1(\Omega_k)^d} + \|u_h - u_h^\eta\|_{H^1(\Omega_l)^d}), \end{aligned}$$

from the (rescaled) Sobolev trace theorem, and deduce with (4.84) that :

$$\begin{aligned} &\frac{1}{\text{diam}(\gamma_{kl})} \|\pi[u_h - u_h^\eta]\|_{L^2(\gamma_{kl})^d}^2 \\ &\leq C\eta \frac{\delta_{min}}{\text{diam}(\gamma_{kl})^{1/2}} \|\lambda_h^\eta\|_{L^2(\gamma_{kl})^d} (\|u_h - u_h^\eta\|_{H^1(\Omega_k)^d} + \|u_h - u_h^\eta\|_{H^1(\Omega_l)^d}). \end{aligned}$$

From the uniform boundedness with respect to η of $\delta_{min}^{1/2} \|\lambda_h^\eta\|_{L^2(\gamma_{kl})^d}$ shown in (4.79), we deduce :

$$\sum_{1 \leq k < l \leq K} \frac{1}{\text{diam}(\gamma_{kl})} \int_{\gamma_{kl}} (\pi_{\gamma_{kl}}[u_h - u_h^\eta])^2 \leq C\eta \frac{\delta_{min}^{1/2}}{\text{diam}(\gamma_{kl})^{1/2}} \|u_h - u_h^\eta\|_X. \quad (4.85)$$

By summing the inequalities (4.83) and (4.85), and using the coercivity result given by proposition 4.35 (page 138), we deduce for sufficiently small values of $\delta_{min} \leq \text{diam}(\gamma_{kl})$ for all $1 \leq k < l \leq K$ that :

$$\|u_h - u_h^\eta\|_X^2 \leq C\eta \|u_h - u_h^\eta\|_X,$$

leading to the expected convergence result in displacements after division by $\|u_h - u_h^\eta\|_X$.

- 4. Convergence of Lagrange multipliers -** The convergence of Lagrange multipliers is deduced by using the inf-sup condition (4.9) and the first equation in (4.80) :

$$\begin{aligned} \beta \|\lambda_h - \lambda_h^\eta\|_{\delta, -\frac{1}{2}} &\leq \|\mathcal{B}^t(\lambda_h - \lambda_h^\eta)\|_{X'} \leq \|\tilde{\mathcal{A}}(u_h - u_h^\eta)\|_{X'} \\ &\leq \|\tilde{\mathcal{A}}\| \|u_h - u_h^\eta\|_X \leq C\eta. \end{aligned}$$

□

The penalized formulation reinforces the interest in mesh-dependent formulations. We insist on the presence in the penalty term of the minimum diameter of the surfacic interface elements δ_{min} , which is of crucial importance to obtain constants independent of the discretization in convergence estimates with respect to the penalization coefficient η . In spite of the practical computational interest of such a penalized formulation, it is recalled that the condition number classically explodes like $O(1/\eta)$, which suggests that a good compromise should be chosen on the value of the penalization coefficient η .

Remark 4.19. *From the implementation point of view, the penalization strategy classically enables to solve the symmetric positive definite linear system :*

$$\left(\tilde{\mathcal{A}} + \frac{1}{\eta \delta_{min}} \mathcal{B}^t \mathcal{C}^{-1} \mathcal{B} \right) u_h^\eta = \mathcal{L},$$

with operator notation from (4.75).

4.8.2 Exact integration of the constraint

From the numerical point of view, especially in 3D, the accurate calculation of the integral $\int_\Gamma \phi_h \cdot \lambda_h$ is difficult when ϕ_h and λ_h do not live on the same side of the interface Γ , and are therefore defined on completely independent meshes.

The question of approximating this integral by quadrature has been risen in [CLM97, MRW02]. The authors prove that any approximation of this integral by quadrature either on the mortar or non-mortar side is not optimal, leading to a convergence in “ \sqrt{h} ”. This bad behavior will be illustrated in the numerical results to follow. A dissymmetric formulation in which this integral is always approximated by quadrature is proposed.

Herein, we have decided to compute exactly such an integral because the simplest quadrature approach does not lead to accurate simulations as illustrated on figure 4.16 of the next section, and have giving it up using the non-symmetric approach from [CLM97, MRW02].

More precisely, let ϕ_h a finite element displacement living on the mortar side of the interface, and P an interface element on the same side, where ϕ_h does not vanish. Let Q an interface element of the non-mortar side having a non-empty intersection with P , and where the finite element Lagrange multiplier λ_h does not vanish. To compute the integral $\int_{P \cap Q} \phi_h \cdot \lambda_h$, we proceed as follows :

1. We compute the exact intersection of the convex polygons P and Q (see figure 4.13), for which we refer to the book of Joseph O'Rourke [O'R82] for example. The code source in C can be downloaded on his website. It is originally written in integer precision, but can be modified to deal with double precision, and also to detect the complete inclusion of a polygonal into another.
2. We introduce the barycentre G of the n vertices of the intersection polygon $P \cap Q$, and decompose it into n triangles sharing the same vertex G as illustrated on figure 4.13. We denote $P \cap Q = \cup_{i=1}^n T_i$.
3. For all $i = 1, \dots, n$, the integral $\int_{T_i} \phi_h \cdot \lambda_h$ is computed exactly by quadrature, since $\phi_h \cdot \lambda_h$ is a polynomial over T_i . The exact integration is then obtained by :

$$\int_{P \cap Q} \phi_h \cdot \lambda_h = \sum_{i=1}^n \int_{T_i} \phi_h \cdot \lambda_h,$$

the last term being computed thanks to lemma 4.16.

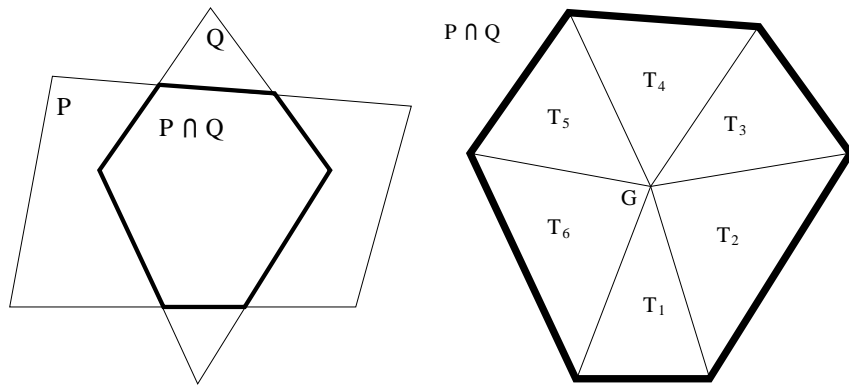


FIG. 4.13 – The exact intersection of the convex polygons P and Q , and its decomposition into triangles.

4.9 Numerical tests for discontinuous mortar-elements

First, we consider an homogeneous beam made with a Hooke's material, whose a tip is clamped on a wall, and whose the other tip is under traction by a uniform negative pressure. All the characteristics are detailed in the table, figure 4.14. For comparison purpose, both non-conforming and conforming meshes are considered, as shown on figure 4.15. They are respectively made of 2926 nodes with 2240 elements and 4225 nodes with 3456 elements.

Young modulus E	5000 Pa
Poisson coefficient ν	0.2
density ρ	1 kg/m ³
traction pressure p	10000 Pa
length L	2 m
thickness l	1 m
extension under static loading	3.97 m
period of the first extensional eigenmode	0.1125 s

FIG. 4.14 – Characteristics of the beam and first numerical estimations.

We test the proposed first order formulation by using a \mathbb{Q}_1 approximation for the displacements on both conforming and non-conforming models, enriched with an interface bubble stabilization (defined on the finer side of the interface) for the non-conforming model together with \mathbb{P}_0 Lagrange multipliers on the finer side of the interface (non-mortar side) as described in section 4.7.1 (page 167). We start by illustrating the non-optimal results obtained when computing the mortar constraint by quadrature on the finer side of the

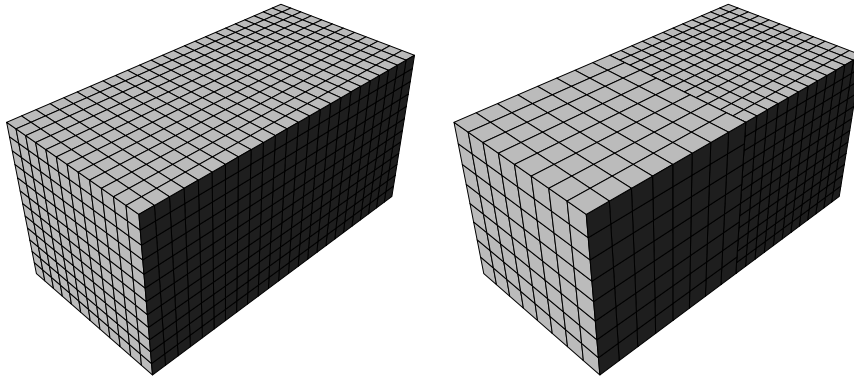


FIG. 4.15 – Conforming (4225 nodes, 3456 elements) and non-conforming (2926 nodes, 2240 elements) meshes of a beam using first order elements.

interface. The quadrature is exact for computing $\int_{\Gamma} \mu_h \cdot v_h$ when both μ_h and v_h live on the finer side of the interface. Such a computation leads to interface oscillations of the displacements, as shown on figure 4.16. This result confirms the work of [CLM97, MRW02], and we will definitively use the exact integration technique described in section 4.8.2.

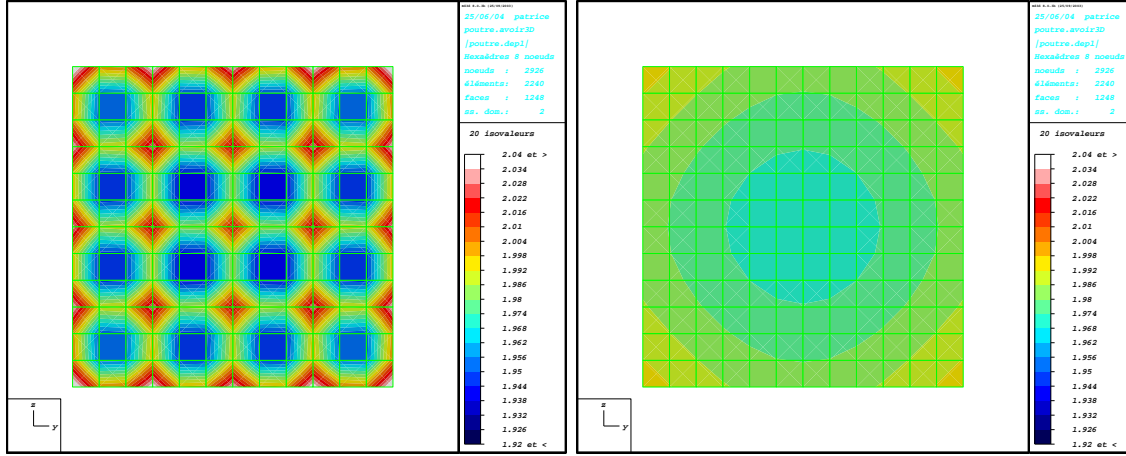


FIG. 4.16 – Interface displacements on the finer side, when using a quadrature approximation (left) and the exact integration (right) of the mortar constraint.

First, we observe the $L^{\infty}(\Omega)^d$ -norm of the error between the displacements obtained on the conforming model and the non-conforming model on which a penalized formulation of the mortar constraint is adopted, that is $\|u_{h,\text{conforming}} - u_{h,\text{non-conforming}}^{\eta}\|_{L^{\infty}(\Omega)^d}$, as a function of the penalization coefficient $1/\eta$. The convergence process is illustrated on

figure 4.17. By the triangular inequality, we have :

$$\begin{aligned} & \|u_{h,\text{conforming}} - u_{h,\text{non-conforming}}^\eta\|_{L^\infty(\Omega)^d} \leq \\ & \leq \|u_{h,\text{conforming}} - u_{h,\text{non-conforming}}\|_{L^\infty(\Omega)^d} + \|u_{h,\text{non-conforming}} - u_{h,\text{non-conforming}}^\eta\|_{L^\infty(\Omega)^d}. \end{aligned}$$

For $1/\eta \leq 10^{10}$, the first term appears to be negligible, and the linear convergence proved in section 4.8.1 is observed. At the penalization limit, the error in displacements between the conforming and non-conforming models is about $5.10^{-6}m$ in L^∞ norm. The corresponding relative error is about 10^{-6} . Concerning Cauchy stresses, a 4.10^{-4} relative gap between the conforming and non-conforming models is observed. This very good agreement is illustrated on figure 4.18, where the computed distribution of σ_{11} stresses is represented.

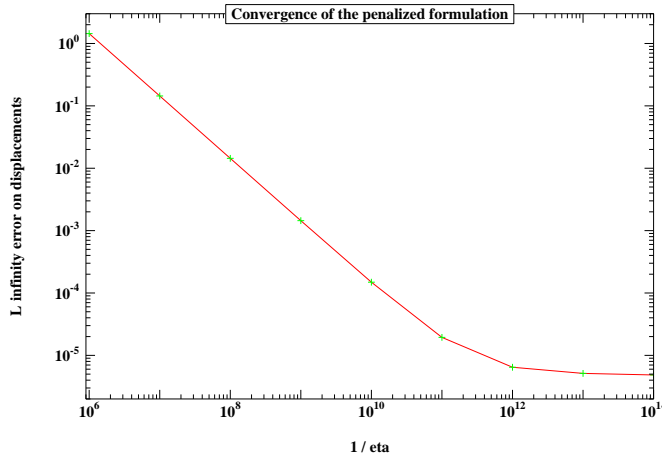


FIG. 4.17 – Error in displacements $\|u_{h,\text{conforming}} - u_{h,\text{non-conforming}}^\eta\|_{L^\infty(\Omega)^d}$ as a function of the penalization coefficient $1/\eta$, with $\|u_{h,\text{conforming}}\|_{L^\infty(\Omega)^d} = 3.97$ m .

Finally, let us discuss the influence of the choice of the non-mortar side (defining the multipliers either on the coarse side, or on the fine one) on the solution. The relative gap of the displacements (resp. of the σ_{11} stresses) in L^∞ norm between the non-conforming solutions computed with these choices is 2.10^{-6} (resp. 8.10^{-4}). As illustrated on figure 4.20, the relative gap of stresses remains concentrated on the elements sharing the interface. The relative gaps in displacements and stresses have the same order than the relative gaps between the conforming and non-conforming solutions. Therefore, the static analysis is confirmed (at least in a homogeneous model) indicating that the choice of the non-mortar side can be done on both sides without affecting the convergence.

The same simulations have been computed for a \mathbb{Q}_2 approximation of the displacements both on conforming and non-conforming models, using the interface stabilization presented

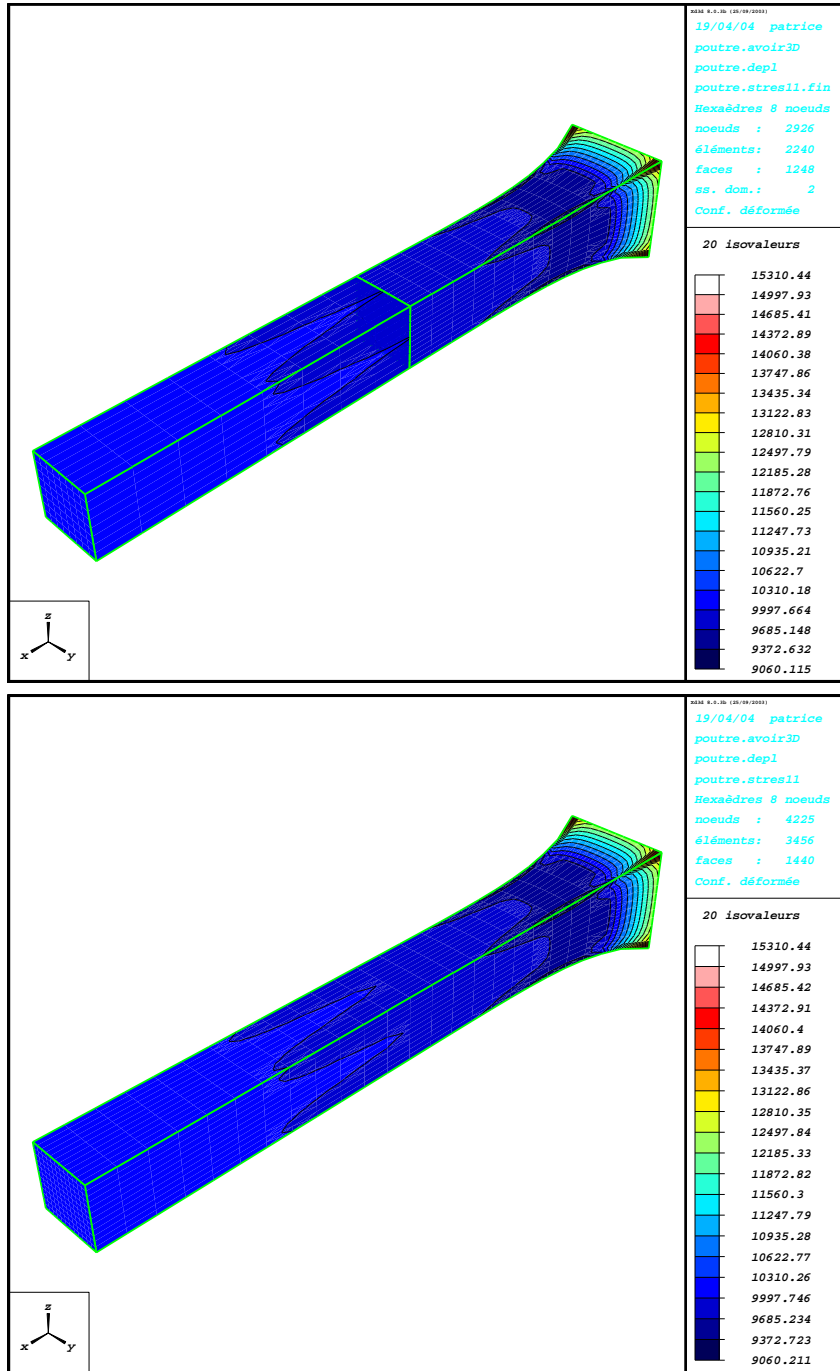


FIG. 4.18 – Distribution of σ_{11} stresses on the deformed configuration of the non-conforming (top) and conforming (bottom) models, by using a first order approximation for the displacements.

in section 4.7.5, and \mathbb{P}_1 Lagrange multipliers. For this second order approximation, we have kept the same number of nodes than the previous first order approximation. Then, the conforming model is made with 4225 nodes and 432 elements, and the non-conforming one with 2926 nodes and 280 elements. We have adopted the value $1/\eta = 10^{11}$ of the penalization coefficient. Then, the relative gap of displacements (resp. maximal stresses) in L^∞ norm between conforming and non-conforming models is 3.10^{-6} (resp. 1.10^{-3}). The distribution of σ_{11} stresses for the conforming and non-conforming models is represented on figure 4.19. Moreover, we show on figure 4.20 that the influence of the choice of the non-mortar side (defining the multipliers either on the coarse side, or on the fine one) is again rather small in this case. Indeed, the relative gap of the σ_{11} stresses between the solutions for the two possible choices of the non-mortar side is always smaller than 2.10^{-3} , keeping the same order than the gap in stresses between the conforming and non-conforming solutions. It is worth noticing that whereas the relative gap of displacements between the first and second order models is 2.10^{-4} in L^∞ norm, the maximal stress has been increased by 10% in the second order model, due to the presence of a singularity at the corners of the fixed tip of the beam.

Let us now consider the elastodynamics problem associated with the previous beam model, by using the trapezoidal time discretization given by (4.52). For comparison purpose, the first order conforming and non-conforming space discretizations used above in the static case are tested. Here, the non-mortar side is the finer one. A constant traction (identical to the static case) is applied at the tip of the beam. As this sollicitation is derived from a potential, oscillations are expected and observed. Some snapshots of the computed dynamics are given on figure 4.21. In order to compare the space non-conforming solution with the conforming one, the horizontal displacement of the central node of the free tip of the beam is represented on figure 4.22 both for non-conforming and conforming approximations when using 20, 50 and 100 time steps per oscillation period. The proximity of the solutions confirms the theoretical result of optimality of the space non-conforming approximation in linear elastodynamics.

Finally, an homogeneous bidimensional cylinder in plane displacements under pressure is considered. It is made with a Hooke's material and its characteristics are given on table, figure 4.24. As previously, for comparison purpose, we consider both conforming and non-conforming meshes, respectively constituted of 1456 nodes with 1350 elements and 973 nodes with 810 elements, shown on figure 4.23. The displacements are approximated by \mathbb{Q}_1 polynomials, together with a bubble interface stabilization and \mathbb{P}_0 Lagrange multipliers, as presented in section 4.7.1 (page 167). In that case, the non-mortar and mortar interfaces do not geometrically match. Then, to formulate the weak-continuity constraint, the displacements of the mortar side are projected on the non-mortar side by elementary plane projections on the non-mortar faces. Of course, the previous analysis do not take this approximation into account. A better approach would have been to consider a \mathbb{Q}_2 approximation for the displacements, with an isoparametric description of the interface as recently analyzed in [FMW04]. Nevertheless, the bold approach presented proves to provide good

results in that simple case. The distribution of maximal stresses over the deformed configuration is represented on figure 4.25, both for conforming and non-conforming first order approximations. The quality of the non-conforming approximation shows here the small influence of the geometric non-conformity. The influence of the choice of the non-mortar side is also studied, and the relative gap of maximal stresses between the two possible choices is represented on figure 4.26. Because of the homogeneity of the material and because the non-conforming interface is not in a high stress region, such an influence remains very small.

From a practical point of view in the case of discontinuous mortar elements, let us underline that when dealing with a penalized formulation of the mortar constraint, or the elimination of the constraint as well, the assembling of the stiffness matrix of the problem in displacements can be done in a purely local way due to the discontinuity of the Lagrange multipliers. Indeed, in the corresponding stiffness operator :

$$\tilde{\mathcal{A}} + \frac{1}{\eta \delta_{min}} \mathcal{B}^t \mathcal{C}^{-1} \mathcal{B} = \tilde{\mathcal{A}} + \frac{1}{\eta \delta_{min}} \sum_{F \in \mathcal{F}_\delta} \mathcal{B}_F^t \mathcal{C}_F^{-1} \mathcal{B}_F,$$

with the notation used in (4.75), the second term can be computed element by element. Moreover, no special treatment is needed on the boundary of the interfaces, which is a great advantage in terms of implementation. The price to pay for these numerical advantages lies in the implementation of the proposed bubble stabilization.

Remark 4.20. *A major practical problem concerns the case when the discretization of the mortar and non-mortar interfaces do not geometrically match. Sometimes, in the case of second order approximation for the displacements, an isoparametric discretization of the interface enables perfect geometric matching and the work done by [FMW04] ensures optimal properties. Nevertheless, in real life cases, such a matching often proves to be impossible and the reformulation of the interface weak-continuity constraint on a regularized interface is crucial, especially when dealing with non-linear elasticity. Indeed, stress singularity on the non-mortar interface may occur during large deformations if this interface is not regularized, and Newton's method convergence is then compromised. Some interesting works regarding these aspects have been published by T. Laursen and M. Puso, and propose Gregory or Hermite patch regularization of the interface (see [PL02, PL03, Pus04]). Such contributions deal also with the treatment of contact surfaces. A comparable regularization approach is proposed and tested in the next chapter of the present work, when considering practical industrial implementation.*

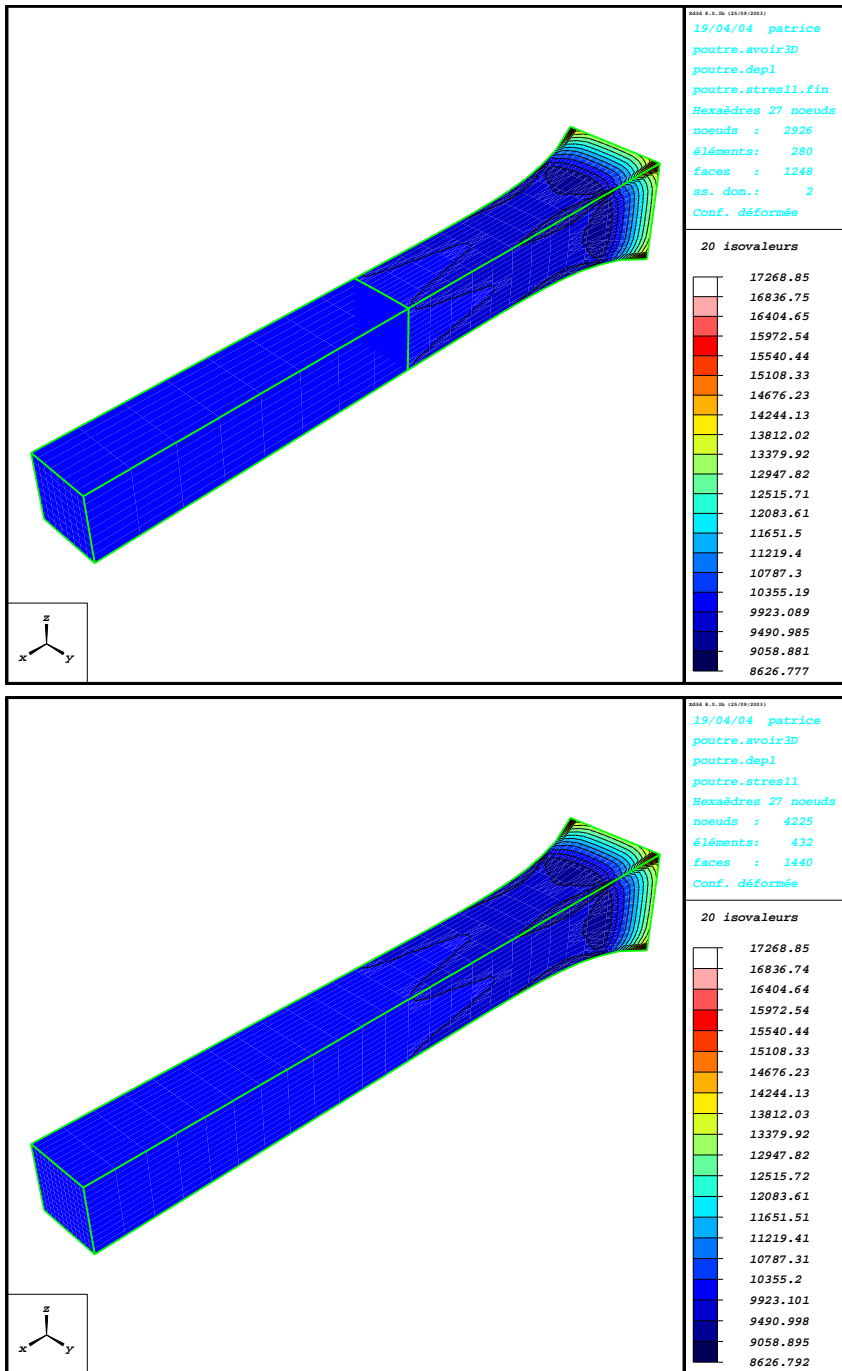


FIG. 4.19 – Distribution of σ_{11} stresses on the deformed configuration of the non-conforming (top) and conforming (bottom) models, by using a second order approximation for the displacements.

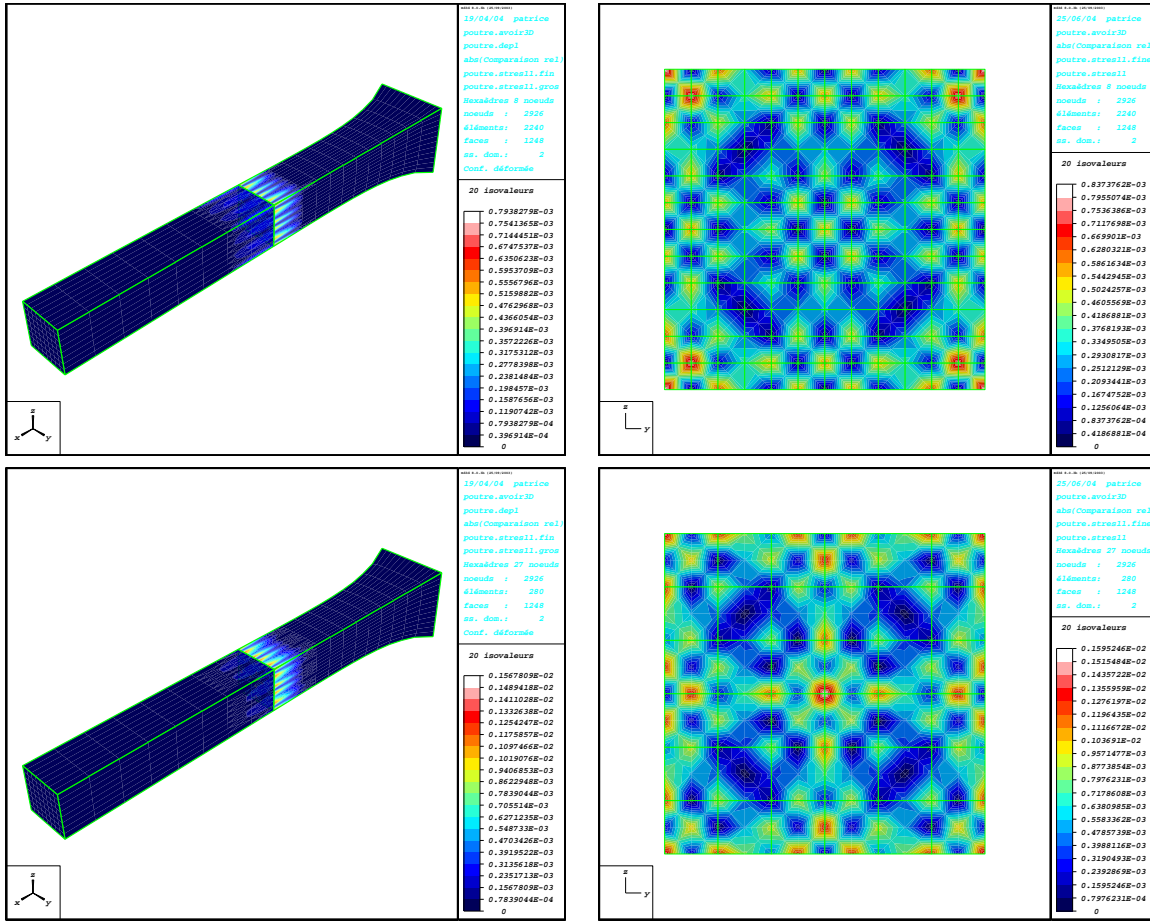


FIG. 4.20 – Relative gap of σ_{11} stresses between the solutions computed on the non-conforming model for the two possible choices of the non-mortar side, when using a first order (top) and a second order (bottom) approximation for the displacements. The pictures on the right column are zooms on the finer side of the interface.

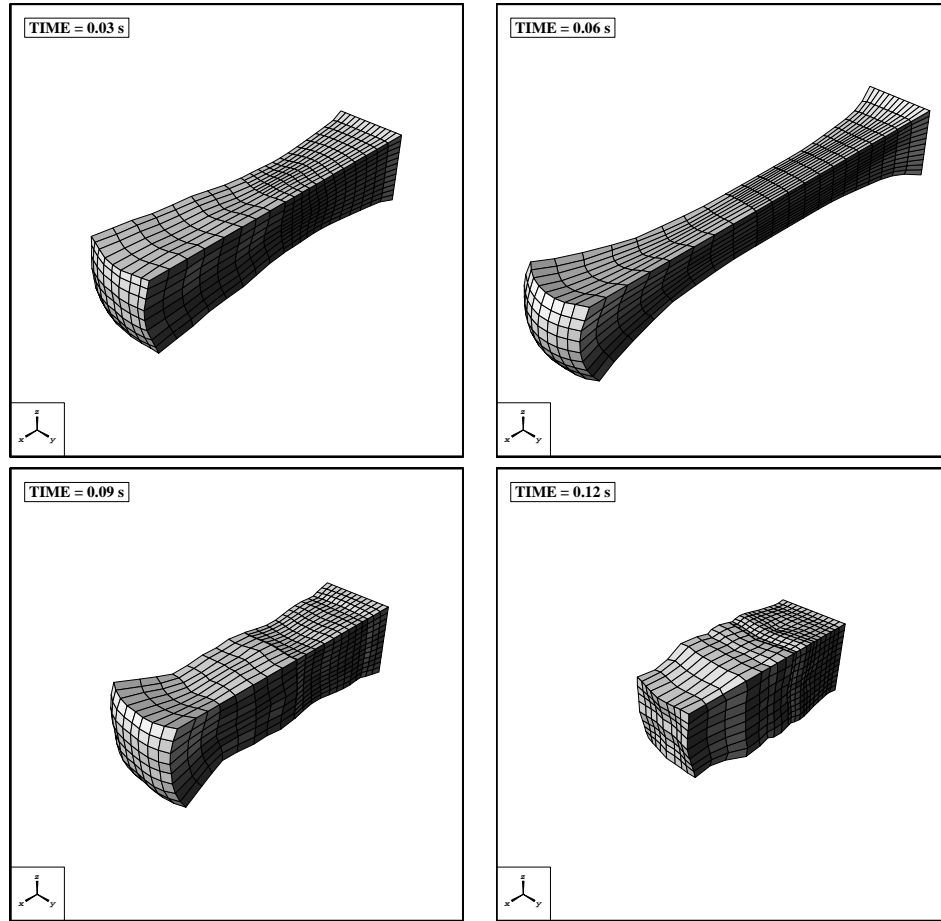


FIG. 4.21 – Snapshots of the computed dynamics of the beam by using a non-conforming first order approximation of the displacements.

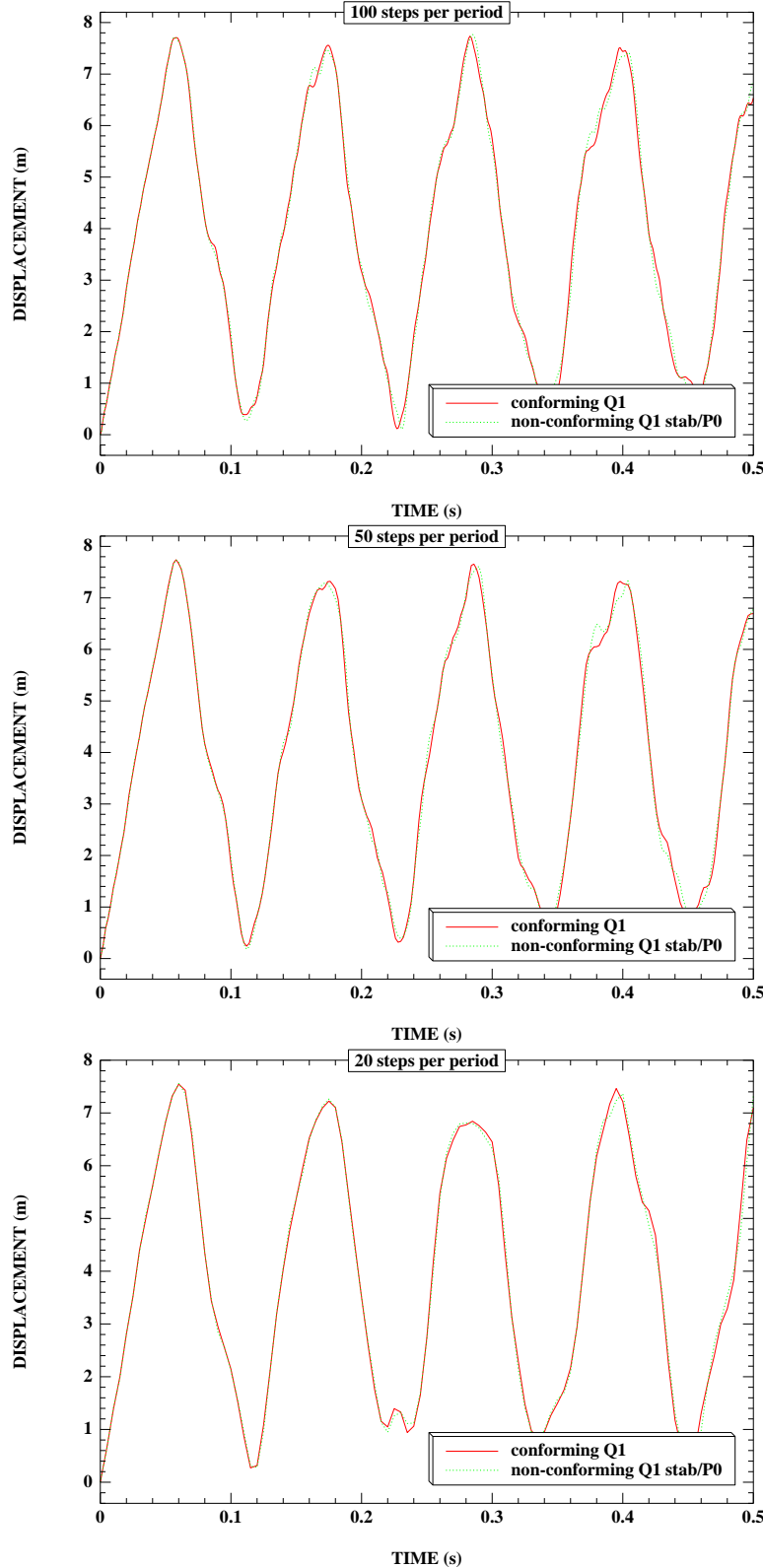


FIG. 4.22 – Horizontal displacement of the central node of the tip of the beam as a function of time, both for the non-conforming and conforming first order space approximation of the beam, together with a trapezoidal approximation in time. Simulations done with 20, 50 and 100 time steps per period. The good agreement confirms the optimality of the non-conforming space approximation.

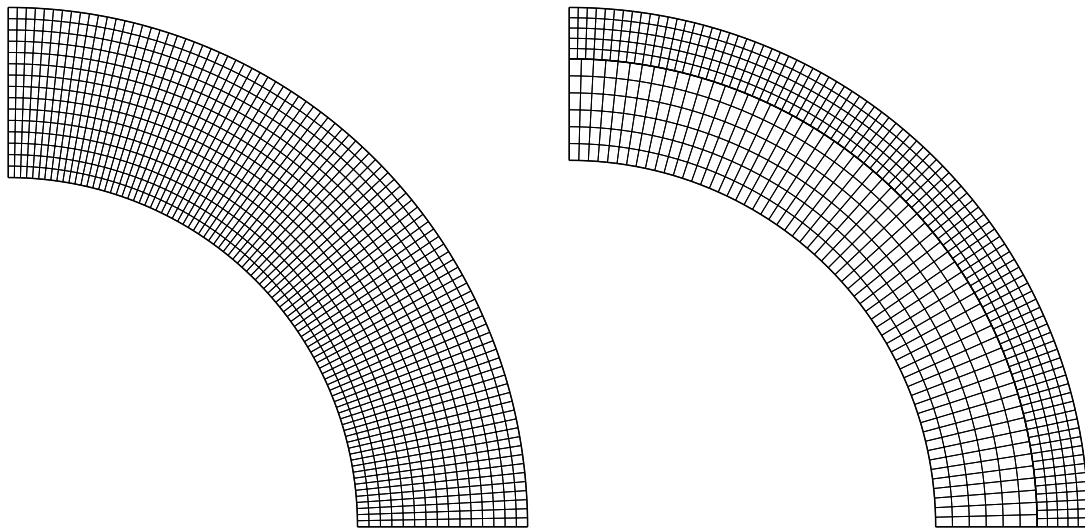


FIG. 4.23 – Conforming (1456 nodes, 1350 elements) and non-conforming (973 nodes, 810 elements) meshes of a cylinder in plane displacements.

Young modulus E	5000 Pa
Poisson coefficient ν	0.2
internal pressure p	100 Pa
internal radius	1.0 m
interface radius	1.33 m
external radius	1.5 m
maximal displacement under loading	0.058 m

FIG. 4.24 – Characteristics of the cylinder.

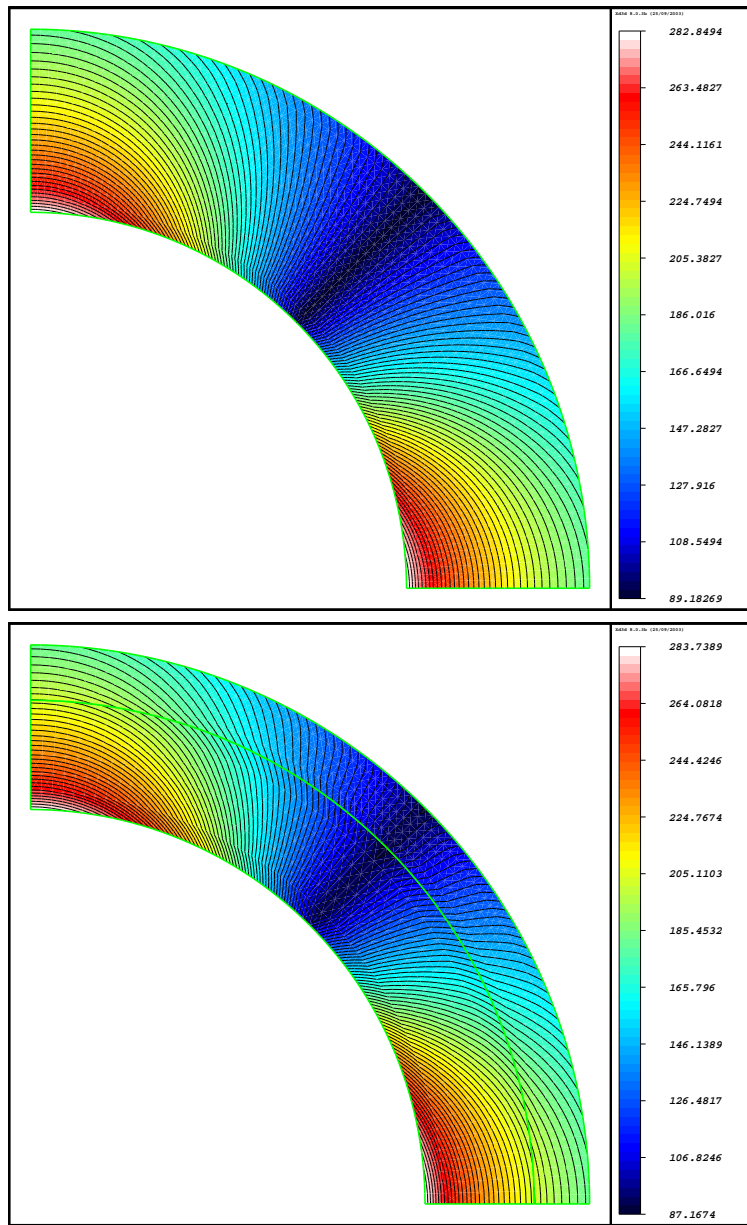


FIG. 4.25 – Distribution of maximal stresses in a cylinder under pressure both for conforming and non-conforming space approximation.

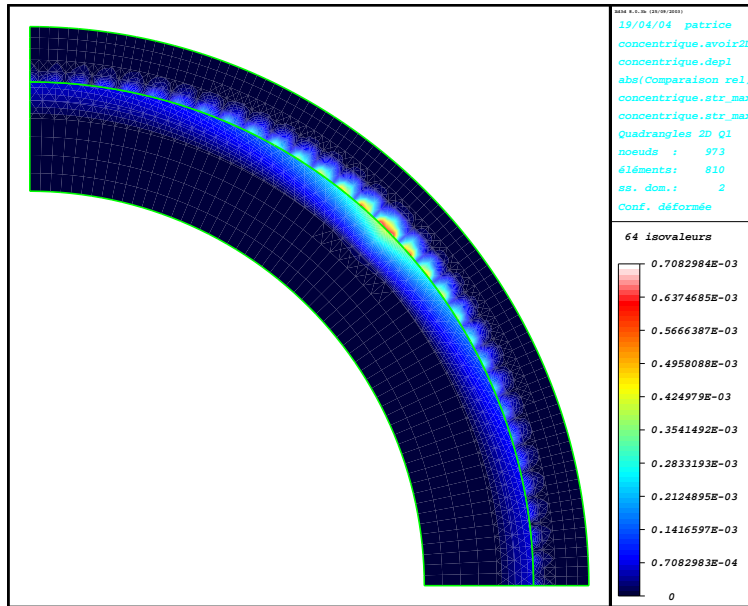


FIG. 4.26 – Relative gap of the σ_{11} stresses between the solutions computed on the non-conforming model for the two possible choices of the non-mortar side, when using a stabilized first order approximation for the displacements and piecewise constant Lagrange multipliers.

4.10 Appendix A : Mesh-dependent norms.

We present here some useful elementary results for the mesh-dependent norms introduced in the text.

First, the duality between the mesh-dependent norms expresses as follows :

Lemma 4.17. *For all $\lambda \in \mathbb{H}_\delta^{-1/2}(\Gamma_m)$, we have :*

$$\|\lambda\|_{\delta, -\frac{1}{2}, m} = \sup_{\phi \in \mathbb{H}_\delta^{1/2}(\Gamma_m)} \frac{\int_{\Gamma_m} \lambda \cdot \phi}{\|\phi\|_{\delta, \frac{1}{2}, m}}.$$

Proof : Let $\lambda \in \mathbb{H}_\delta^{-1/2}(\Gamma_m)$. It is straightforward by a standard Cauchy-Schwarz inequality applied on each face of Γ_m that :

$$\int_{\Gamma_m} \lambda \cdot \phi \leq \|\lambda\|_{\delta, -\frac{1}{2}, m} \|\phi\|_{\delta, \frac{1}{2}, m}, \quad \forall \phi \in \mathbb{H}_\delta^{1/2}(\Gamma_m),$$

hence :

$$\|\lambda\|_{\delta, -\frac{1}{2}} \geq \sup_{\phi \in \mathbb{H}_\delta^{1/2}(\Gamma_m)} \frac{\int_{\Gamma_m} \lambda \cdot \phi}{\|\phi\|_{\delta, \frac{1}{2}, m}}.$$

Conversely, by introducing $\phi = \sum_{F \in \mathcal{F}_{m; \delta_m}} h(F) \lambda|_F$:

$$\sup_{\psi \in \mathbb{H}_\delta^{1/2}(\Gamma_m)} \frac{\int_{\Gamma_m} \lambda \psi}{\|\psi\|_{\delta, \frac{1}{2}, m}} \geq \frac{\int_{\Gamma_m} \lambda \phi}{\|\phi\|_{\delta, \frac{1}{2}, m}} = \|\lambda\|_{\delta, -\frac{1}{2}, m}.$$

□

As the mesh of Γ_m is inherited from the non-mortar side mesh $\mathcal{T}_{k(m); h_{k(m)}}$, we have the following trace result :

Lemma 4.18. *There exist a constant $C > 0$ independent of the discretization such that for all $u \in H^1(\Omega_{k(m)})$:*

$$\|u|_{\Gamma_m}\|_{\delta, \frac{1}{2}, m}^2 \leq C \sum_{\substack{T \in \mathcal{T}_{k(m); h_{k(m)}}, \\ T \cap \Gamma_m \neq \emptyset}} \frac{1}{h(T)^2} \|u\|_{L^2(T)^d}^2 + \|\nabla u\|_{L^2(T)^{d \times d}}^2.$$

Proof : Let us denote by $\phi_m = u|_{\Gamma_m}$. For all $F \in \mathcal{F}_{m; \delta_m}$, by a standard change of variable onto the reference element \hat{F} :

$$\|\phi_m\|_{L^2(F)^d}^2 \leq C \text{meas}(F) \|\hat{\phi}\|_{L^2(\hat{F})^d}^2,$$

and by the standard trace theorem in Sobolev spaces, we have with $T = T(F)$:

$$\begin{aligned}\|\phi_m\|_{L^2(F)^d}^2 &\leq C \operatorname{meas}(F) \left(\|\nabla \hat{u}\|_{L^2(\hat{T})^{d \times d}}^2 + \|\hat{u}\|_{L^2(\hat{T})^d}^2 \right) \\ &\leq C \operatorname{meas}(F) \frac{h(T)^2}{\operatorname{meas}(T)} \left(\|\nabla u\|_{L^2(T)^{d \times d}}^2 + \frac{1}{h(T)^2} \|u\|_{L^2(T)^d}^2 \right).\end{aligned}$$

By regularity of the mesh, we have $\operatorname{meas}(T) \geq Ch(T)^d$ and also $\operatorname{meas}(F) \leq Ch(F)^{d-1} \leq Ch(T)^{d-1}$ so that :

$$\|\phi_m\|_{L^2(F)^d}^2 \leq C h(T) \left(\|\nabla u\|_{L^2(T)^{d \times d}}^2 + \frac{1}{h(T)^2} \|u\|_{L^2(T)^d}^2 \right).$$

Then, by summing over the $F \in \mathcal{F}_{m;\delta_m}$:

$$\begin{aligned}\sum_{F \in \mathcal{F}_{m;\delta_m}} \frac{1}{h(T)} \|\phi_m\|_{L^2(F)^d}^2 &\leq \\ C \sum_{\substack{T \in \mathcal{T}_{k(m)}; h_{k(m)}, \\ T \cap \Gamma_m \neq \emptyset}} \frac{1}{h(T)^2} &\|u\|_{L^2(T)^d}^2 + \|\nabla u\|_{L^2(T)^{d \times d}}^2.\end{aligned}$$

□

Conversely, a lifting result can be established on $W_{m;\delta_m} \cap \mathbb{H}_\delta^{1/2}(\Gamma_m)$. For that purpose, we introduce the definition of discrete extension by zero operators :

Definition 4.2. Let $\phi_m \in W_{m;\delta_m}$, and $(a_i)_i$ the nodes associated to the Lagrange degrees of freedom of the functions in $X_{k(m);h_{k(m)}}$. The discrete extension by zero operator $\mathcal{R}_{m;h_m}$ over $X_{k(m);h_{k(m)}}$ is defined on the non-mortar side by $\mathcal{R}_{m;\delta_m} \phi_k \in X_{k(m);h_{k(m)}}$ such that :

$$\mathcal{R}_{m;\delta_m} \phi_k(a_i) = \begin{cases} \phi_k(a_i), & a_i \in \Gamma_m, \\ 0, & a_i \notin \Gamma_m. \end{cases},$$

and the discrete extension by zero operator $\tilde{\mathcal{R}}_{m;\delta_m}$ over X_h by :

$$\tilde{\mathcal{R}}_{m;\delta_m} \phi_m = \begin{cases} \mathcal{R}_{m;\delta_m} \phi_m, & \text{on } \Omega_{k(m)}, \\ 0, & \text{elsewhere.} \end{cases}$$

Lemma 4.19. There exist a constant $C > 0$ independent of the discretization such that for all $\phi_m \in W_{m;\delta_m} \cap \mathbb{H}_\delta^{1/2}(\Gamma_m)$,

$$\|\mathcal{R}_{m;\delta_m} \phi_m\|_{H^1(\Omega_{k(m)})^d} \leq C \|\phi_m\|_{\delta, \frac{1}{2}, m}.$$

Proof : We have :

$$\|\mathcal{R}_{m;\delta_m} \phi_m\|_{H^1(\Omega_{k(m)})^d}^2 \leq \sum_{F \in \mathcal{F}_{m;\delta_m}} \sum_{T \in \mathcal{T}_{k(m);h_{k(m)}}, T \cap F \neq \emptyset} \|\mathcal{R}_{m;\delta_m} \phi_m\|_{H^1(T)^d}^2.$$

For all $F \in \mathcal{F}_{m;\delta_m}$ the number of elements $T \in \mathcal{T}_{k(m);h_{k(m)}}$ such that $T \cap F \neq \emptyset$ is bounded independently of h by the shape regularity of the mesh. Concerning the tetrahedron $T = T(F)$ whose a face is F , we have :

$$\begin{aligned} \|\mathcal{R}_{m;\delta_m} \phi_m\|_{H^1(T)^d}^2 &= \frac{1}{L_{k(m)}^2} \|\mathcal{R}_{m;\delta_m} \phi_m\|_{L^2(T)^d}^2 + \|\nabla \mathcal{R}_{m;\delta_m} \phi_m\|_{L^2(T)^{d \times d}}^2 \\ &\leq C \left(\frac{\text{meas}(T)}{L_{k(m)}^2} \|\hat{\mathcal{R}}_{m;\delta_m} \hat{\phi}_m\|_{L^2(\hat{T})^d}^2 + \frac{\text{meas}(T)}{h(T)^2} \|\hat{\nabla} \hat{\mathcal{R}}_{m;\delta_m} \hat{\phi}_m\|_{L^2(\hat{T})^{d \times d}}^2 \right), \end{aligned}$$

and since $h(T) < L_{k(m)}$:

$$\leq C \frac{\text{meas}(T)}{h(T)^2} \|\hat{\mathcal{R}}_{m;\delta_m} \hat{\phi}_m\|_{H^1(\hat{T})^d}^2.$$

By equivalence of the norms for discrete functions on \hat{T} , we get :

$$\begin{aligned} \|\mathcal{R}_{m;\delta_m} \phi_m\|_{H^1(T)^d}^2 &\leq C \frac{\text{meas}(T)}{h(T)^2} \|\hat{\phi}_m\|_{L^2(\hat{T})^d}^2 \\ &\leq C \frac{\text{meas}(T)}{h(T)^2} \frac{1}{\text{meas}(F)} \|\phi_m\|_{L^2(F)^d}^2 \leq C \frac{h(T)^{d-2}}{h(F)^{d-1}} \|\phi_m\|_{L^2(F)^d}^2. \end{aligned}$$

Let us consider now a tetrahedron $T \in \mathcal{T}_{k(m);h_{k(m)}}$ sharing only an edge or a vertex with F . The number of these tetrahedras is bounded by regularity of the mesh. The Lagrange finite element nodes on the reference face \hat{F} are denoted by $(\hat{a}_i)_i$. We obtain :

$$\begin{aligned} \|\mathcal{R}_{m;\delta_m} \phi_m\|_{H^1(T)^d}^2 &= \frac{1}{L_{k(m)}^2} \|\mathcal{R}_{m;\delta_m} \phi_m\|_{L^2(T)^d}^2 + \|\nabla \mathcal{R}_{m;\delta_m} \phi_m\|_{L^2(T)^{d \times d}}^2 \\ &\leq C \left(\frac{\text{meas}(T)}{L_{k(m)}^2} \|\hat{\mathcal{R}}_{m;\delta_m} \hat{\phi}_m\|_{L^2(\hat{T})^d}^2 + \frac{\text{meas}(T)}{h(T)^2} \|\hat{\nabla} \hat{\mathcal{R}}_{m;\delta_m} \hat{\phi}_m\|_{L^2(\hat{T})^{d \times d}}^2 \right), \end{aligned}$$

and using that $h(T) < L_{k(m)}$ and the equivalence of the norms for discrete functional spaces :

$$\begin{aligned} &\leq C \frac{\text{meas}(T)}{h(T)^2} \|\hat{\mathcal{R}}_{m;\delta_m} \hat{\phi}_m\|_{H^1(\hat{T})^d}^2 \leq C \frac{\text{meas}(T)}{h(T)^2} \max_i |\hat{\phi}_m(\hat{a}_i)|^2 \\ &\leq C \frac{\text{meas}(T)}{h(T)^2} \|\hat{\phi}_m\|_{L^2(\hat{F})^d}^2 \leq C \frac{\text{meas}(T)}{h(T)^2} \frac{1}{\text{meas}(F)} \|\phi_m\|_{L^2(F)^d}^2 \\ &\leq C \frac{h(T)^{d-2}}{h(F)^{d-1}} \|\phi_m\|_{L^2(F)^d}^2. \end{aligned}$$

Then, the announced result is obtained by using the shape regularity of the mesh and summing the previous inequalities. \square

4.11 Appendix B : Independence of the Korn's constant with respect to the shape of a domain

In this section, we detail a proof for lemmas 4.5 and 4.6, page 125, for regular domains $\Omega_k \subset \mathbb{R}^d$ satisfying items 1 to 6 in Assumption 4.4, page 123. For clarity, we denote here Ω instead of Ω_k , and recall these assumptions :

1. there exists a finite collection of reference domains $(\hat{\Omega}_j)_{1 \leq j \leq J}$ of unit diameter, of compact sets $(\mathcal{K}_j)_{1 \leq j \leq J}$ and of maps $\varphi_j : \hat{\Omega}_j \times \mathcal{K}_j \rightarrow \mathbb{R}^d$, $1 \leq j \leq J$ such that for all $1 \leq j \leq J$:

$$\text{diam}(\varphi_j(\hat{\Omega}_j, p)) = 1, \quad \forall p \in \mathcal{K}_j,$$

and the following application :

$$\begin{aligned} \mathcal{K}_j &\rightarrow W^{1,\infty}(\hat{\Omega}_j)^d, \\ p &\mapsto \varphi_j(\cdot, p), \end{aligned}$$

is continuous,

2. for all $1 \leq j \leq J$, there exists a constant $C_j > 0$ such that :

$$\det \frac{\partial \varphi_j}{\partial \hat{x}}(\hat{x}, p) \geq C_j, \quad \forall p \in \mathcal{K}_j, \text{ for almost all } \hat{x} \in \hat{\Omega}_j,$$

3. there exists a j with $1 \leq j \leq J$ and an element $p \in \mathcal{K}_j$ such that within a scaling factor :

$$\frac{1}{\text{diam}(\Omega)} \Omega = \varphi_j(\hat{\Omega}_j, p).$$

Moreover, we consider that :

4. there exists a finite collection of reference interfaces $(\hat{\gamma}_j)_{1 \leq j \leq J}$, with $\hat{\gamma}_j \subset \partial \hat{\Omega}_j$, $1 \leq j \leq J$, and that the application :

$$\begin{aligned} \mathcal{K}_j &\rightarrow W^{1,\infty}(\hat{\gamma}_j)^d, \\ p &\mapsto \varphi_j(\cdot, p), \end{aligned}$$

is continuous,

5. for all $1 \leq j \leq J$, there exists a constant $C_j > 0$ such that :

$$\det \frac{\partial \varphi_j}{\partial \hat{x}}(\hat{x}, p) \geq C_j, \quad \forall p \in \mathcal{K}_j, \text{ for almost all } \hat{x} \in \hat{\gamma}_j,$$

and when γ is a part of the boundary of $\Omega = \varphi_j(\hat{\Omega}_j, p)$, we assume that :

$$6. \frac{1}{\text{diam}(\gamma)} \gamma = \varphi_j(\hat{\gamma}_j, p).$$

Remark 4.21. Let us notice that the application φ_j and the compact set \mathcal{K}_j can in fact be different when considering the reference domain $\hat{\Omega}_j$ or the part $\hat{\gamma}_j$ of its boundary.

In this section, C will denote various positive constants independent of the domain Ω .

4.11.1 Poincaré-Friedrichs inequalities

As a preliminary, let us prove the following :

Lemma 4.20. *There exists a constant C independent of any domain Ω satisfying assumptions 1,2,3, and of any $\gamma \subset \partial\Omega$ satisfying assumptions 4,5,6 such that :*

$$\frac{1}{diam(\Omega)^2} \|v\|_{L^2(\Omega)^d}^2 \leq C \left(|v|_{H^1(\Omega)^d}^2 + \frac{1}{diam(\Omega)^{2+d}} \left| \int_{\Omega} v \, dx \right|^2 \right), \quad (4.86)$$

$$\frac{1}{diam(\Omega)^2} \|v\|_{L^2(\Omega)^d}^2 \leq C \left(|v|_{H^1(\Omega)^d}^2 + \frac{1}{diam(\Omega)^d} \left| \int_{\gamma} v \, d\sigma \right|^2 \right), \quad (4.87)$$

for all $v \in H^1(\Omega)^d$.

Proof : The two inequalities can be easily proved on $\hat{\Omega}_j$ by a contradiction argument for any function $\hat{v} \in H^1(\hat{\Omega}_j)^d$ and any $1 \leq j \leq J$. Proofs can be found in [Neč67, Wlo87]. For any $v \in H^1(\Omega)^d$, there exists an integer j and a function $\hat{v} \in H^1(\hat{\Omega}_j)^d$ such that $v \circ \varphi_j = \hat{v}$, and by classical changes of variable, it follows from assumptions 2 and 5 that :

$$\begin{cases} \|v\|_{L^2(\Omega)^d}^2 \leq \|\det \nabla \varphi_j\|_{L^\infty(\hat{\Omega}_j)} \|\hat{v}\|_{L^2(\hat{\Omega}_j)^d}^2, \\ |\hat{v}|_{H^1(\hat{\Omega}_j)^d}^2 = \int_{\Omega} \left| \frac{\partial v}{\partial x} \right|^2 \left| \frac{\partial x}{\partial \hat{x}} \right|^2 \det(\nabla \varphi_j)^{-1} \\ \leq \|(\det \nabla \varphi_j)^{-1}\|_{L^\infty(\hat{\Omega}_j)} \|\nabla \varphi_j\|_{L^\infty(\hat{\Omega}_j)^{d \times d}}^2 |v|_{H^1(\Omega)^d}^2 \leq C_j^{-1} \|\nabla \varphi_j\|_{L^\infty(\hat{\Omega}_j)^{d \times d}}^2 |v|_{H^1(\Omega)^d}^2, \\ \left| \int_{\hat{\Omega}_j} \hat{v} \, d\hat{x} \right| \leq \|(\det \nabla \varphi_j)^{-1}\|_{L^\infty(\hat{\Omega}_j)} \left| \int_{\Omega} v \, dx \right| \leq C_j^{-1} \left| \int_{\Omega} v \, dx \right|, \\ \left| \int_{\hat{\gamma}_j} \hat{v} \, d\hat{\sigma} \right| \leq (C_j)^{-1} \|\nabla \varphi_j\|_{L^\infty(\hat{\gamma}_j)^{d \times d}} \left| \int_{\gamma} v \, d\sigma \right|, \end{cases}$$

this latest statement being justified in remark 4.22. Moreover, from the continuity assumption 1 (resp. 4) and the fact that $(\mathcal{K}_j)_{1 \leq j \leq J}$ are compact sets, we obtain the uniform boundedness of $\|\nabla \varphi_j(\cdot, p)\|_{L^\infty(\hat{\Omega}_j)}$ (resp. $\|\nabla \varphi_j(\cdot, p)\|_{L^\infty(\hat{\gamma}_j)}$) with respect to $p \in \mathcal{K}_j$. We obtain as a consequence that :

$$\begin{cases} \|v\|_{L^2(\Omega)^d}^2 \leq C \, diam(\Omega)^d \|\hat{v}\|_{L^2(\hat{\Omega}_j)^d}^2, \\ |\hat{v}|_{H^1(\hat{\Omega}_j)^d}^2 \leq C \, diam(\Omega)^{2-d} |v|_{H^1(\Omega)^d}^2, \\ \left| \int_{\hat{\Omega}_j} \hat{v} \, d\hat{x} \right| \leq C \, diam(\Omega)^{-d} \left| \int_{\Omega} v \, dx \right|, \\ \left| \int_{\hat{\gamma}_j} \hat{v} \, d\hat{\sigma} \right| \leq C \, diam(\Omega)^{1-d} \left| \int_{\gamma} v \, d\sigma \right|. \end{cases} \quad (4.88)$$

This yields, using the inequalities (4.86) and (4.87) written on $\hat{\Omega}_j$:

$$\begin{aligned} \frac{1}{\text{diam}(\Omega)^2} \|v\|_{L^2(\Omega)^d}^2 &\leq C \text{diam}(\Omega)^{d-2} \|\hat{v}\|_{L^2(\hat{\Omega}_j)^d}^2 \\ &\leq C \hat{C}_j \left(|\hat{v}|_{H^1(\hat{\Omega}_j)^d}^2 + \left| \int_{\hat{\Omega}_j} \hat{v} d\hat{x} \right|^2 \right) \text{diam}(\Omega)^{d-2} \\ &\leq C \hat{C}_j \left(|v|_{H^1(\Omega)^d}^2 + \frac{1}{\text{diam}(\Omega)^{2+d}} \left| \int_{\Omega} v dx \right|^2 \right), \end{aligned}$$

and also that :

$$\begin{aligned} \frac{1}{\text{diam}(\Omega)^2} \|v\|_{L^2(\Omega)^d}^2 &\leq C \text{diam}(\Omega)^{d-2} \|\hat{v}\|_{L^2(\hat{\Omega}_j)^d}^2 \\ &\leq C \hat{C}_j \left(|\hat{v}|_{H^1(\hat{\Omega}_j)^d}^2 + \left| \int_{\hat{\gamma}_j} \hat{v} d\hat{x} \right|^2 \right) \text{diam}(\Omega)^{d-2} \\ &\leq C \hat{C}_j \left(|v|_{H^1(\Omega)^d}^2 + \frac{1}{\text{diam}(\Omega)^d} \left| \int_{\gamma} v dx \right|^2 \right), \end{aligned}$$

hence the proof. \square

Remark 4.22. By construction of the jacobian $J = \det \nabla \varphi_j$, we have for all $dM \in \mathbb{R}^d$:

$$J \widehat{dM} \cdot \hat{n} d\hat{\sigma} = dM \cdot n d\sigma,$$

where n (resp \hat{n}) denotes the outward normal unit vector on γ (resp. $\hat{\gamma}$), and $d\sigma$ (resp. $d\hat{\sigma}$) is the surfacic measure over γ (resp. $\hat{\gamma}$). Moreover :

$$J \widehat{dM} \cdot \hat{n} d\hat{\sigma} = dM \cdot n d\sigma = (\nabla \varphi_j \cdot \widehat{dM}) \cdot n d\sigma,$$

yielding by identification :

$$J \hat{n} d\hat{\sigma} = (\nabla \varphi_j)^t \cdot n d\sigma,$$

yielding :

$$d\hat{\sigma} = J^{-1} |(\nabla \varphi_j)^t \cdot n| d\sigma \leq C_j^{-1} \|\nabla \varphi_j\|_{L^\infty(\hat{\Omega}_j)^{d \times d}} d\sigma.$$

4.11.2 Dependence of the constant in Korn's second inequality

We prove the following lemma by using Brenner's equicontinuity argument [Bre04] :

Lemma 4.21. *There exists a constant C such that for any domain Ω satisfying the above assumptions 1,2,3, the following inequality holds :*

$$|v|_{H^1(\Omega)^d} \leq C \left(\|\varepsilon(v)\|_{L^2(\Omega)^{d \times d}} + \frac{1}{\text{diam}(\Omega)^{d/2}} \left| \int_{\Omega} \nabla \times v \right| \right),$$

for all $v \in H^1(\Omega)^d$.

Remark 4.23. *The scaling $\text{diam}(\Omega)^{1-d}$ instead of $\text{diam}(\Omega)^{-d/2}$ which appears in [Bre04] seems to be a mistake. Indeed, it is then straightforward by a rescaling argument that doing so, the best constant C is not independent of $\text{diam}(\Omega)$.*

Proof : Because of scale invariance, we can suppose that $\text{diam}(\Omega) = 1$. Let us first observe that the inequality is true, and can be proved by a contradiction argument and Korn's first inequality (cf. [LM72], page 110). Moreover, the resulting constant is independent of $\text{diam}(\Omega)$ from the adopted scaling of the two sides of the inequality, but a priori depends on the shape of Ω , and we denote it by $C(\Omega)$.

Now, let us fix $1 \leq j \leq J$, and consider the closed subset :

$$\dot{W}^{1,\infty}(\hat{\Omega}_j)^d = \{\phi \in W^{1,\infty}(\hat{\Omega}_j)^d, \text{diam}(\phi(\hat{\Omega}_j)) = 1, \det \hat{\nabla} \phi \geq C_j \text{ almost everywhere on } \hat{\Omega}_j\},$$

endowed with the usual norm of $W^{1,\infty}(\hat{\Omega}_j)^d$. Let us first show that $C(\phi(\hat{\Omega}_j))$ is continuous with respect to $\phi \in \dot{W}^{1,\infty}(\hat{\Omega}_j)^d$, where $C(\phi(\hat{\Omega}_j))$ is given by :

$$\begin{aligned} C(\phi(\hat{\Omega}_j)) &= \sup_{\substack{\hat{v} \in H^1(\hat{\Omega}_j)^d \\ |\hat{v}|_{H^1(\hat{\Omega}_j)^d} = 1}} \frac{|\hat{v} \circ \phi^{-1}|_{H^1(\Omega)^d}}{\|\varepsilon(\hat{v} \circ \phi^{-1})\|_{L^2(\Omega)^{d \times d}} + \left| \int_{\Omega} \nabla \times (\hat{v} \circ \phi^{-1}) \right|} \\ &= \sup_{\substack{\hat{v} \in H^1(\hat{\Omega}_j)^d \\ |\hat{v}|_{H^1(\hat{\Omega}_j)^d} = 1}} R_j(\hat{v}, \phi) = \sup_{\substack{\hat{v} \in H^1(\hat{\Omega}_j)^d \\ |\hat{v}|_{H^1(\hat{\Omega}_j)^d} = 1}} \frac{N_j(\hat{v}, \phi)}{D_j(\hat{v}, \phi)}. \end{aligned}$$

For this purpose, let us detail that both $(N_j(\hat{v}, \phi))_{\hat{v}}$ and $(D_j(\hat{v}, \phi))_{\hat{v}}$ are equicontinuous sets of functions with respect to $\phi \in \dot{W}^{1,\infty}(\hat{\Omega}_j)^d$. Let $F(\phi)$ be given by :

$$F(\phi) = (\hat{\nabla} \phi)^{-1} \left(\det \hat{\nabla} \phi \right)^{1/2} = \frac{(\text{cof } \hat{\nabla} \phi)^t}{\left(\det \hat{\nabla} \phi \right)^{1/2}}.$$

By construction, the map F is continuous with respect to ϕ on $W^{1,\infty}(\hat{\Omega}_j)^d$. From the changes of variable ϕ^{-1} and ψ^{-1} , the triangular inequality, the equivalence of the norms $|A|_2 = \sup_{x \in \mathbb{R}^d, |x|=1} |Ax|_2$ and $|A| = (A : A)^{1/2}$ for any matrix $A \in \mathbb{R}^{d \times d}$, and the fact that

$|A \cdot B|_2 \leq |A|_2 |B|_2$, we obtain that :

$$\begin{aligned}
 \left| |\hat{v} \circ \phi^{-1}|_{H^1(\phi(\hat{\Omega}_j))^d} - |\hat{v} \circ \psi^{-1}|_{H^1(\psi(\hat{\Omega}_j))^d} \right| &= \left\| \|\hat{\nabla} \hat{v} \cdot F(\phi)\|_{L^2(\hat{\Omega}_j)^{d \times d}} - \|\hat{\nabla} \hat{v} \cdot F(\psi)\|_{L^2(\hat{\Omega}_j)^{d \times d}} \right\| \\
 &\leq \left\| \hat{\nabla} \hat{v} \cdot (F(\phi) - F(\psi)) \right\|_{L^2(\hat{\Omega}_j)^{d \times d}} \\
 &= \left(\int_{\hat{\Omega}_j} \left| \hat{\nabla} \hat{v} \cdot (F(\phi) - F(\psi)) \right|^2 d\hat{x} \right)^{1/2} \\
 &\leq C \left(\int_{\hat{\Omega}_j} \left| \hat{\nabla} \hat{v} \right|^2 |F(\phi) - F(\psi)|^2 d\hat{x} \right)^{1/2} \\
 &\leq C \|F(\phi) - F(\psi)\|_{L^\infty(\hat{\Omega}_j)^{d \times d}},
 \end{aligned}$$

because $|\hat{v}|_{H^1(\hat{\Omega}_j)^{d \times d}} = 1$. By the same estimation and the fact that $|A| = |A^t|$ for any matrix $A \in \mathbb{R}^{d \times d}$, we also get :

$$\begin{aligned}
 &\left| \|\varepsilon(\hat{v} \circ \phi^{-1})\|_{L^2(\phi(\hat{\Omega}_j)^{d \times d})} - \|\varepsilon(\hat{v} \circ \psi^{-1})\|_{L^2(\psi(\hat{\Omega}_j)^{d \times d})} \right| \\
 &= \left\| \frac{1}{2} \left(\hat{\nabla} \hat{v} \cdot F(\phi) + F(\phi)^t \cdot (\hat{\nabla} \hat{v})^t \right) \right\|_{L^2(\hat{\Omega}_j)^{d \times d}} - \left\| \frac{1}{2} \left(\hat{\nabla} \hat{v} \cdot F(\psi) + F(\psi)^t \cdot (\hat{\nabla} \hat{v})^t \right) \right\|_{L^2(\hat{\Omega}_j)^{d \times d}} \\
 &\leq \left\| \frac{1}{2} \left(\hat{\nabla} \hat{v} \cdot (F(\phi) - F(\psi)) + (F(\phi) - F(\psi))^t \cdot (\hat{\nabla} \hat{v})^t \right) \right\|_{L^2(\hat{\Omega}_j)^{d \times d}} \\
 &\leq C \|F(\phi) - F(\psi)\|_{L^\infty(\hat{\Omega}_j)^{d \times d}}.
 \end{aligned}$$

Finally, denoting by $\tilde{F}(\phi) = F(\phi) (\det \nabla \phi)^{1/2}$, we get :

$$\begin{aligned}
& \left\| \int_{\phi(\hat{\Omega}_j)} \nabla \times (\hat{v} \circ \phi^{-1}) - \int_{\psi(\hat{\Omega}_j)} \nabla \times (\hat{v} \circ \psi^{-1}) \right\| \\
& \leq \left| \int_{\phi(\hat{\Omega}_j)} \nabla \times (\hat{v} \circ \phi^{-1}) - \int_{\psi(\hat{\Omega}_j)} \nabla \times (\hat{v} \circ \psi^{-1}) \right| \\
& = \frac{1}{2} \left| \int_{\phi(\hat{\Omega}_j)} (\nabla(\hat{v} \circ \phi^{-1}) - (\nabla(\hat{v} \circ \phi^{-1}))^t) - \int_{\psi(\hat{\Omega}_j)} (\nabla(\hat{v} \circ \psi^{-1}) - (\nabla(\hat{v} \circ \psi^{-1}))^t) \right| \\
& \leq \left| \int_{\phi(\hat{\Omega}_j)} \nabla(\hat{v} \circ \phi^{-1}) - \int_{\psi(\hat{\Omega}_j)} \nabla(\hat{v} \circ \psi^{-1}) \right| \\
& = \left| \int_{\hat{\Omega}_j} \hat{\nabla} \hat{v} \cdot (\tilde{F}(\phi) - \tilde{F}(\psi)) \right| \leq C \int_{\hat{\Omega}_j} |\hat{\nabla} \hat{v}| |\tilde{F}(\phi) - \tilde{F}(\psi)| \\
& \leq C |\hat{\Omega}_j|^{1/2} \|\tilde{F}(\phi) - \tilde{F}(\psi)\|_{L^\infty(\hat{\Omega}_j)^{d \times d}} \leq C \|\tilde{F}(\phi) - \tilde{F}(\psi)\|_{L^\infty(\hat{\Omega}_j)^{d \times d}}.
\end{aligned}$$

As a consequence, from the continuity of F and \tilde{F} on $\dot{W}^{1,\infty}(\hat{\Omega}_j)$, $(N_j(\hat{v}, \phi))_{\hat{v}}$ and $(D_j(\hat{v}, \phi))_{\hat{v}}$ are equicontinuous sets of functions in \hat{v} with respect to $\phi \in \dot{W}^{1,\infty}(\hat{\Omega}_j)^d$. We now prove that the ratios $(R_j(\hat{v}, \phi))_{\hat{v}}$ are an equicontinuous set of functions with respect to $\phi \in \dot{W}^{1,\infty}(\hat{\Omega}_j)^d$:

- By equicontinuity of $(D(\hat{v}, \phi))_{\hat{v}}$ with respect to $\phi \in \dot{W}^{1,\infty}(\hat{\Omega}_j)^d$, $\inf_{\hat{v}} D(\hat{v}, \phi)$ is continuous with respect to $\phi \in \dot{W}^{1,\infty}(\hat{\Omega}_j)^d$. Now, let us fix $\phi \in \dot{W}^{1,\infty}(\hat{\Omega}_j)^d$. The standard Korn's second inequality shows that with a shape dependent constant $C_\phi > 0$:

$$\begin{aligned}
D(\hat{v}, \phi) & \geq C_\phi |\hat{v} \circ \phi^{-1}|_{H^1(\phi(\hat{\Omega}_j))^d} \\
& \geq C_\phi \|\hat{\nabla} \phi (\det \hat{\nabla} \phi)^{-1/2}\|_{L^\infty(\hat{\Omega}_j)^{d \times d}},
\end{aligned}$$

and entails that $\inf_{\hat{v}} D(\hat{v}, \phi) > 0$. By continuity of $\inf_{\hat{v}} D(\hat{v}, \psi)$ with respect to $\psi \in \dot{W}^{1,\infty}(\hat{\Omega}_j)^d$, there exists a neighborhood \mathcal{V}_ϕ of $\phi \in \dot{W}^{1,\infty}(\hat{\Omega}_j)^d$ in $\dot{W}^{1,\infty}(\hat{\Omega}_j)^d$, such that there exists a constant $C_\phi^D > 0$ such that :

$$\forall \psi \in \mathcal{V}_\phi, \quad \inf_{\hat{v}} D(\hat{v}, \phi) > C_\phi^D.$$

- By equicontinuity of $(N(\hat{v}, \phi))_{\hat{v}}$ with respect to $\phi \in \dot{W}^{1,\infty}(\hat{\Omega}_j)^d$, $\sup_{\hat{v}} N(\hat{v}, \psi)$ is continuous with respect to $\psi \in \dot{W}^{1,\infty}(\hat{\Omega}_j)^d$, and is therefore bounded by C_ϕ^N on a neighborhood \mathcal{V}_ϕ of $\phi \in \dot{W}^{1,\infty}(\hat{\Omega}_j)^d$ in $\dot{W}^{1,\infty}(\hat{\Omega}_j)^d$, for all $\phi \in \dot{W}^{1,\infty}(\hat{\Omega}_j)^d$.

– We then get :

$$\begin{aligned} |R_j(\hat{v}, \phi) - R_j(\hat{v}, \psi)| &= \left| \frac{N_j(\hat{v}, \phi)}{D_j(\hat{v}, \phi)} - \frac{N_j(\hat{v}, \psi)}{D_j(\hat{v}, \psi)} \right| \\ &= \left| \frac{N_j(\hat{v}, \phi)(D_j(\hat{v}, \phi) - D_j(\hat{v}, \psi))}{D_j(\hat{v}, \phi)D_j(\hat{v}, \psi)} - \frac{N_j(\hat{v}, \phi) - N_j(\hat{v}, \psi)}{D_j(\hat{v}, \psi)} \right| \\ &\leq \frac{C_\phi^N}{C_\phi^D} |D_j(\hat{v}, \phi) - D_j(\hat{v}, \psi)| + \frac{1}{C_\phi^D} |N_j(\hat{v}, \phi) - N_j(\hat{v}, \psi)|. \end{aligned}$$

Hence, the ratios $(R_j(\hat{v}, \phi))_{\hat{v}}$ are an equicontinuous set of functions with respect to $\phi \in \dot{W}^{1,\infty}(\hat{\Omega}_j)^d$.

The supremum $C(\phi(\hat{\Omega}_j))$ of $R_j(\hat{v}, \phi)$ over \hat{v} is therefore a continuous function of $\phi \in \dot{W}^{1,\infty}(\hat{\Omega}_j)^d$.

Because the application :

$$\begin{aligned} \mathcal{K}_j &\rightarrow \dot{W}^{1,\infty}(\hat{\Omega}_j)^d, \\ p &\mapsto \varphi_j(\cdot, p), \end{aligned}$$

is continuous from assumption 1, the function $C(\varphi_j(\hat{\Omega}_j, p))$ is a continuous function of $p \in \mathcal{K}_j$ and since \mathcal{K}_j is a compact, $C(\varphi_j(\hat{\Omega}_j, p))$ reaches its maximum value for a $p \in \mathcal{K}_j$, entailing the existence of a constant C'_j such that :

$$C(\varphi_j(\hat{\Omega}_j, p)) \leq C'_j, \quad \forall p \in \mathcal{K}_j.$$

Hence the proof, and the constant $C = \max_{1 \leq j \leq J} C'_j$ in lemma 4.21. \square

4.11.3 Semi-norm estimates

As introduced in [Bre04], let $\mathfrak{P} : H^1(\Omega)^d \rightarrow \mathcal{R}(\Omega)$ be the rigid motion projection such that for all $v \in H^1(\Omega)^d$, $\mathfrak{P}v \in \mathcal{R}(\Omega)$ is the unique rigid motion such that :

$$\int_{\Omega} (\mathfrak{P}v - v) = 0, \quad \int_{\Omega} \nabla \times (\mathfrak{P}v - v) = 0.$$

The existence and uniqueness comes from the straightforward implication :

$$v \in \mathcal{R}(\Omega), \quad \mathfrak{P}v = 0 \implies v = 0.$$

Lemma 4.22. *Let Φ be a semi-norm satisfying :*

$$|v|_{H^1(\Omega)^d} \leq C \Phi(v), \quad \forall v \in \mathcal{R}(\Omega), \tag{4.89}$$

$$\Phi(v - \mathfrak{P}v) \leq C \|\varepsilon(v)\|_{L^2(\Omega)^{d \times d}}, \quad \forall v \in H^1(\Omega)^d, \tag{4.90}$$

with a constant C independent of any Ω satisfying assumptions 1,2,3. Then there exists a constant C independent of Ω such that :

$$|v|_{H^1(\Omega)^d} \leq C \left(\|\varepsilon(v)\|_{L^2(\Omega)^{d \times d}}^2 + \Phi(v)^2 \right)^{1/2}, \quad \forall v \in H^1(\Omega)^d.$$

Proof : By using the triangular inequality, the property (4.89) of the semi-norm Φ , and lemma 4.21, we get :

$$\begin{aligned} |v|_{H^1(\Omega)^d}^2 &\leq |\mathfrak{P}v + v - \mathfrak{P}v|_{H^1(\Omega)^d}^2 \\ &\leq 2|\mathfrak{P}v|_{H^1(\Omega)^d}^2 + 2|v - \mathfrak{P}v|_{H^1(\Omega)^d}^2 \\ &\leq C \Phi(\mathfrak{P}v)^2 + C \|\varepsilon(v - \mathfrak{P}v)\|_{L^2(\Omega)^{d \times d}}^2 \\ &\leq C \Phi(\mathfrak{P}v)^2 + C \|\varepsilon(v)\|_{L^2(\Omega)^{d \times d}}^2, \end{aligned} \quad (4.91)$$

because $\varepsilon(\mathfrak{P}v) = 0$, $\mathfrak{P}v$ being a rigid body motion. Observing that the triangular inequality and assumption (4.90) entail :

$$\begin{aligned} \Phi(\mathfrak{P}v) &\leq \Phi(v) + \Phi(\mathfrak{P}v - v) \\ &\leq \Phi(v) + C \|\varepsilon(v)\|_{L^2(\Omega)^{d \times d}}, \end{aligned}$$

it is obtained from (4.91) that :

$$|v|_{H^1(\Omega)^d}^2 \leq C \left(\|\varepsilon(v)\|_{L^2(\Omega)^{d \times d}}^2 + \Phi(v)^2 \right),$$

hence the proof. \square

We then have to check the assumptions (4.89) and (4.90) for the particular semi-norms Φ_1 and Φ_2 defined by :

$$\Phi_1(v) = \frac{1}{\text{diam}(\Omega)} \sup_{\substack{r \in \mathcal{R}(\Omega) \setminus \{0\}, \\ \int_{\Omega} r = 0}} \frac{\int_{\Omega} v \cdot r}{\|r\|_{L^2(\Omega)^d}}, \quad \forall v \in L^2(\Omega)^d,$$

and :

$$\Phi_2(v) = \frac{1}{\text{diam}(\Omega)^{1/2}} \sup_{\substack{r \in \mathcal{R}(\Omega) \setminus \{0\}, \\ \int_{\Omega} r = 0}} \frac{\int_{\gamma} v \cdot r}{\|r\|_{L^2(\gamma)^d}}, \quad \forall v \in H^1(\Omega)^d.$$

We obtain indeed the :

Lemma 4.23. Under assumptions 1,3 (resp. assumption 4,6), the semi-norms Φ_1 (resp. Φ_2) satisfy the criterion (4.89).

Proof : Because of scaling, we can restrict ourselves to the case where Ω has a unit diameter, since $\|\varepsilon(v)\|_{L^2(\Omega)^{d \times d}}^2$, $|v|_{H^1(\Omega)^d}^2$ and $\Phi_i^2(v)$ all scale like $diam(\Omega)^{d-2}$. The proof is done in three dimensions ($d = 3$), and can be adapted very simply to the bidimensional case ($d = 2$). Let $t, a \in \mathbb{R}^3$. Thus, $v(x) = t + a \times x$, for all $x \in \Omega$ is a rigid motion. It is a simple exercise to check that $|v|_{H^1(\Omega)^3}^2 = 2|a|^2|\Omega| \leq C|a|^2$, because Ω has a unit diameter.

For all $1 \leq j \leq J$, the following application :

$$\begin{aligned} \mathcal{M}_1^j : \quad \mathbb{R}^3 \times W^{1,\infty}(\hat{\Omega}_j)^d &\rightarrow \mathbb{R} \\ (a, \varphi) &\mapsto \mathcal{M}_1^j(a, \varphi) := \int_{\hat{\Omega}_j} |a \times (\varphi(\hat{x}) - G_{\varphi(\hat{\Omega}_j)})|^2 \det \nabla \varphi(\hat{x}) d\hat{x}, \end{aligned}$$

where $G_{\varphi(\hat{\Omega}_j)}$ is the center of gravity of $\varphi(\hat{\Omega}_j)$ defined as :

$$G_{\varphi(\hat{\Omega}_j)} = \frac{1}{|\varphi(\hat{\Omega}_j)|} \int_{\hat{\Omega}_j} \varphi(\hat{x}) \det \nabla \varphi(\hat{x}) d\hat{x},$$

is continuous. By introducing the compact set $\mathbb{S}^3 := \{a \in \mathbb{R}^3, |a| = 1\} \subset \mathbb{R}^3$, and from assumption 1, it follows by composition that the positive application :

$$\begin{aligned} \mathbb{S}^3 \times \mathcal{K}_j &\rightarrow \mathbb{R} \\ (e, p) &\mapsto \mathcal{M}_1^j(e, \varphi_j(\cdot, p)), \end{aligned}$$

is also continuous, and because both \mathbb{S}^3 and \mathcal{K}_j are compact sets, we deduce the existence of a lower bound. Therefore, there exists a constant $C_j > 0$ such that for all $e \in \mathbb{S}^3$ and all $p \in \mathcal{K}_j$:

$$\mathcal{M}_1^j(e, \varphi_j(\cdot, p)) \geq C_j.$$

By an homogeneity argument, we deduce for all $a \in \mathbb{R}^3$, and all $p \in \mathcal{K}_j$, that :

$$\mathcal{M}_1^j(a, \varphi_j(\cdot, p)) \geq C_j |a|^2 \geq C C_j |v|_{H^1(\Omega)^3}^2.$$

Hence the satisfaction of the criterion (4.89) for Φ_1 with a constant $C' = C \max_{1 \leq j \leq J} C_j$.

We proceed the same concerning Φ_2 , by defining the following application for all $1 \leq j \leq J$:

$$\begin{aligned} \mathcal{M}_2^j : \quad \mathbb{R}^3 \times W^{1,\infty}(\hat{\gamma}_j)^d &\rightarrow \mathbb{R} \\ (a, \varphi) &\mapsto \mathcal{M}_2^j(a, \varphi) := \int_{\hat{\gamma}_j} |a \times (\varphi(\hat{x}) - G_{\varphi(\hat{\gamma}_j)})|^2 m_\varphi(\hat{x}) d\hat{\sigma}(\hat{x}), \end{aligned}$$

where $G_{\varphi(\hat{\gamma}_j)}$ is the center of gravity of $\varphi(\hat{\gamma}_j)$ defined as :

$$G_{\varphi(\hat{\gamma}_j)} = \frac{1}{|\varphi(\hat{\gamma}_j)|} \int_{\hat{\gamma}_j} \varphi(\hat{x}) m_\varphi(\hat{x}) d\hat{\sigma}(\hat{x}),$$

$d\hat{\sigma}$ is the surfacic measure over $\hat{\gamma}_j$, and $m_\varphi(\hat{x})$ is the metric defined as :

$$m_\varphi(\hat{x}) = \det \hat{\nabla} \varphi \left| (\hat{\nabla} \varphi)^{-t} \cdot \hat{n} \right|,$$

in which \hat{n} is the outward normal unit vector on $\hat{\gamma}_j$. The application \mathcal{M}_2^j is continuous. By introducing the compact set $\mathbb{S}^3 := \{a \in \mathbb{R}^3, |a| = 1\} \subset \mathbb{R}^3$, and from assumption 6, it follows by composition that the positive application :

$$\begin{aligned} \mathbb{S}^3 \times \mathcal{K}_j &\rightarrow \mathbb{R} \\ (e, p) &\mapsto \mathcal{M}_2^j(e, \varphi_j(\cdot, p)), \end{aligned}$$

is also continuous, and because both \mathbb{S}^3 and \mathcal{K}_j are compact sets, we deduce the existence of a lower bound. Therefore, there exists a constant $C_j > 0$ such that for all $e \in \mathbb{S}^3$ and all $p \in \mathcal{K}_j$:

$$\mathcal{M}_2^j(e, \varphi_j(\cdot, p)) \geq C_j.$$

By an homogeneity argument, we deduce for all $a \in \mathbb{R}^3$, and all $p \in \mathcal{K}_j$, that :

$$\mathcal{M}_2^j(a, \varphi_j(\cdot, p)) \geq C_j |a|^2 \geq C C_j |v|_{H^1(\Omega)^3}^2.$$

Hence the proof. □

The satisfaction of assumption (4.90) for the semi-norms Φ_1 and Φ_2 is obtained in [Bre04] :

Lemma 4.24. *The semi-norms Φ_1 and Φ_2 satisfy the assumption (4.90).*

Proof : Using the Cauchy-Schwarz inequality, Friedrichs inequality (lemma 4.20) and lemma 4.21, we get :

$$\begin{aligned} \Phi_1(v - \mathfrak{P}v) &\leq \frac{1}{\text{diam}(\Omega)} \|v - \mathfrak{P}v\|_{L^2(\Omega)^d} \\ &\leq C |v - \mathfrak{P}v|_{H^1(\Omega)^d} \\ &\leq C \|\varepsilon(v - \mathfrak{P}v)\|_{L^2(\Omega)^{d \times d}} = C \|\varepsilon(v)\|_{L^2(\Omega)^{d \times d}}. \end{aligned}$$

Concerning Φ_2 , the same result follows by using the Cauchy-Schwarz inequality, the Sobolev trace theorem (lemma 4.25), Friedrichs inequality (lemma 4.20) and lemma 4.21 :

$$\begin{aligned} \Phi_2(v - \mathfrak{P}v) &\leq \frac{1}{\text{diam}(\Omega)^{1/2}} \|v - \mathfrak{P}v\|_{L^2(\gamma)^d} \\ &\leq C \|v - \mathfrak{P}v\|_{H^1(\Omega)^d} \\ &\leq C |v - \mathfrak{P}v|_{H^1(\Omega)^d} \\ &\leq C \|\varepsilon(v - \mathfrak{P}v)\|_{L^2(\Omega)^{d \times d}} = C \|\varepsilon(v)\|_{L^2(\Omega)^{d \times d}}. \end{aligned}$$

Hence the proof. \square

The Sobolev trace theorem with shape independence of the constant is given by the :

Lemma 4.25. *There exists a constant C independent of any domain Ω satisfying assumptions 1,2,3, and of the part γ of its boundary satisfying assumptions 4,5,6, such that :*

$$\frac{1}{\text{diam}(\Omega)} \int_{\gamma} v^2 \leq C \left(|v|_{H^1(\Omega)^d}^2 + \frac{1}{\text{diam}(\Omega)^2} \|v\|_{L^2(\Omega)^d}^2 \right), \quad (4.92)$$

for all $v \in H^1(\Omega)^d$.

Proof : The inequality (4.92) is true for $\Omega = \hat{\Omega}_j$ and $\gamma = \hat{\gamma}_j$ for any $1 \leq j \leq J$, as the standard Sobolev trace inequality. For any $v \in H^1(\Omega)^d$, there exists an integer j and a function $\hat{v} \in H^1(\hat{\Omega}_j)^d$ such that $v \circ \varphi_j = \hat{v}$, and by classical changes of variable, we get as in the proof of lemma 4.20 that :

$$\begin{cases} \int_{\gamma} v^2 \leq \|\text{cof } \nabla \varphi_j\|_{L^\infty(\hat{\gamma}_j)^{d \times d}} \int_{\hat{\gamma}_j} \hat{v}^2, \\ |\hat{v}|_{H^1(\hat{\Omega}_j)^d}^2 \leq \|(\det \nabla \varphi_j)^{-1}\|_{L^\infty(\hat{\Omega}_j)} \|\nabla \varphi_j\|_{L^\infty(\hat{\Omega}_j)^{d \times d}}^2 |v|_{H^1(\Omega)^d}^2 \leq C_j^{-1} \|\nabla \varphi_j\|_{L^\infty(\hat{\Omega}_j)^{d \times d}}^2 |v|_{H^1(\Omega)^d}^2, \\ \|\hat{v}\|_{L^2(\hat{\Omega}_j)^d}^2 \leq \|(\det \nabla \varphi_j)^{-1}\|_{L^\infty(\hat{\Omega}_j)} \|v\|_{L^2(\Omega)^d}^2 \leq C_j^{-1} \|v\|_{L^2(\Omega)^d}^2, \end{cases}$$

Moreover, from the continuity assumption 1 (resp. 4) and the fact that $(\mathcal{K}_j)_{1 \leq j \leq J}$ are compact sets, we obtain the uniform boundedness of $\|\nabla \varphi_j(\cdot, p)\|_{L^\infty(\hat{\Omega}_j)}$ (resp. $\|\nabla \varphi_j(\cdot, p)\|_{L^\infty(\hat{\gamma}_j)}$) with respect to $p \in \mathcal{K}_j$. We obtain as a consequence that :

$$\begin{cases} \int_{\gamma} v^2 \leq C \text{diam}(\Omega)^{d-1} \int_{\hat{\gamma}_j} \hat{v}^2, \\ \|v\|_{L^2(\Omega)^d}^2 \leq C \text{diam}(\Omega)^{-d} \|\hat{v}\|_{L^2(\hat{\Omega}_j)^d}^2, \\ |v|_{H^1(\Omega)^d}^2 \leq C \text{diam}(\Omega)^{2-d} |\hat{v}|_{H^1(\hat{\Omega}_j)^d}^2. \end{cases}$$

This yields, using the inequality (4.92) written on $\hat{\Omega}_j$:

$$\begin{aligned} \frac{1}{\text{diam}(\Omega)} \int_{\gamma} v^2 &\leq C \text{diam}(\Omega)^{d-2} \int_{\hat{\gamma}_j} \hat{v}^2 \\ &\leq C \hat{C}_j \text{diam}(\Omega)^{d-2} \left(\|\hat{v}\|_{L^2(\hat{\Omega}_j)^d}^2 + |\hat{v}|_{H^1(\hat{\Omega}_j)^{d \times d}}^2 \right) \\ &\leq C \hat{C}_j \left(\frac{1}{\text{diam}(\Omega)^2} \|v\|_{L^2(\Omega)^d}^2 + |v|_{H^1(\Omega)^d}^2 \right). \end{aligned}$$

Hence the proof. \square

4.11.4 Conclusion

Lemmas 4.5 and 4.6, page 125, are now proved as a consequence of lemmas 4.22 and 4.20. We recall them in the :

Lemma 4.26. *There exists two constants C_P and C_N , such that for all Ω_k and γ_{kl} satisfying the assumptions 1,2,3,4,5,6, the following inequality holds for all $v \in H^1(\Omega_k)^d$:*

$$\|v\|_{H^1(\Omega_k)^d}^2 \leq C_P \left(\|\varepsilon(v)\|_{L^2(\Omega_k)^{d \times d}}^2 + \frac{1}{\text{diam}(\Omega_k)} \left(\sup_{\mu \in M_{kl}} \frac{\int_{\gamma_{kl}} v \cdot \mu}{\|\mu\|_{L^2(\gamma_{kl})^d}} \right)^2 \right), \quad (4.93)$$

$$\|v\|_{H^1(\Omega_k)^d}^2 \leq C_N \left(\|\varepsilon(v)\|_{L^2(\Omega_k)^{d \times d}}^2 + \frac{1}{\text{diam}(\Omega_k)^2} \left(\sup_{r \in \mathcal{R}(\Omega_k)} \frac{\int_{\Omega_k} v \cdot r}{\|r\|_{L^2(\Omega_k)^d}} \right)^2 \right). \quad (4.94)$$

Proof : From lemma 4.22, which holds due to lemmas 4.23 and 4.24, we have :

$$\begin{aligned} |v|_{H^1(\Omega_k)^d}^2 &\leq C \left(\|\varepsilon(v)\|_{L^2(\Omega_k)^{d \times d}}^2 + \Phi_{1,\Omega_k}(v)^2 \right), \\ &\leq C \left(\|\varepsilon(v)\|_{L^2(\Omega_k)^{d \times d}}^2 + \frac{1}{\text{diam}(\Omega_k)^2} \sup_{r \in \mathcal{R}(\Omega_k)} \frac{\left(\int_{\Omega_k} v \cdot r \right)^2}{\|r\|_{L^2(\Omega_k)^d}^2} \right). \end{aligned} \quad (4.95)$$

On the other hand, using lemma 4.20, we have :

$$\frac{1}{\text{diam}(\Omega_k)^2} \|v\|_{L^2(\Omega_k)^d}^2 \leq C \left(|v|_{H^1(\Omega_k)^d}^2 + \frac{1}{\text{diam}(\Omega_k)^{2+d}} \left| \int_{\Omega_k} v \, dx \right|^2 \right), \quad (4.96)$$

and using here a unit translation r , we deduce :

$$\frac{1}{\text{diam}(\Omega_k)^d} \left| \int_{\Omega_k} v \, dx \right|^2 \leq \sup_{r \in \mathcal{R}(\Omega_k)} \frac{\left(\int_{\Omega_k} v \cdot r \right)^2}{\|r\|_{L^2(\Omega_k)^d}^2}. \quad (4.97)$$

Hence the proof of (4.93) by substituting (4.95) and (4.97) in (4.96) and adding the result to (4.95).

From lemma 4.22, which holds due to lemmas 4.23 and 4.24, we also have :

$$\begin{aligned} |v|_{H^1(\Omega_k)^d}^2 &\leq C \left(\|\varepsilon(v)\|_{L^2(\Omega_k)^{d \times d}}^2 + \Phi_{2,\Omega_k}(v)^2 \right), \\ &\leq C \left(\|\varepsilon(v)\|_{L^2(\Omega_k)^{d \times d}}^2 + \frac{1}{\text{diam}(\Omega_k)} \sup_{r \in \mathcal{R}(\gamma_{kl})} \frac{\left(\int_{\gamma_{kl}} v \cdot r \right)^2}{\|r\|_{L^2(\gamma_{kl})^d}^2} \right). \end{aligned} \quad (4.98)$$

(4.99)

On the other hand, using lemma 4.20, we have :

$$\frac{1}{\text{diam}(\Omega_k)^2} \|v\|_{L^2(\Omega_k)^d}^2 \leq C \left(|v|_{H^1(\Omega_k)^d}^2 + \frac{1}{\text{diam}(\Omega_k)^d} \left| \int_{\gamma_{kl}} v \, dx \right|^2 \right), \quad (4.100)$$

and using here a unit translation r , we deduce :

$$\frac{1}{\text{diam}(\Omega_k)^d} \left| \int_{\gamma_{kl}} v \, dx \right|^2 \leq \frac{1}{\text{diam}(\Omega_k)^2} \sup_{r \in \mathcal{R}(\Omega_k)} \frac{\left(\int_{\gamma_{kl}} v \cdot r \right)^2}{\|r\|_{L^2(\gamma_{kl})^d}^2}. \quad (4.101)$$

Hence the proof of (4.94) by substituting (4.98) and (4.101) in (4.100) and adding the result to (4.98). \square

Chapitre 5

Recollement de maillages incompatibles en contexte industriel

Résumé

Nous présentons dans ce chapitre la formulation d'une contrainte mortier sur interface intermédiaire régularisée par carreaux de Hermite dans l'esprit de [Pus04], mais avec quelques différences quant à la définition des paramètres de la surface et la projection utilisée côté non-mortier. En outre, nous détaillons l'intégration quasi-exacte de cette contrainte. Enfin, nous illustrons l'utilisation de cette technique dans le cadre du recollement de maillages incompatibles en contexte industriel pour la résolution numérique de problèmes d'élastostatique non-linéaire du pneumatique.

Abstract

In this chapter, we present the formulation of a mortar constraint on an intermediate regularized interface by the use of Hermite patches in the way of [Pus04], but with some differences regarding the definition of the parameters of the surface and the projection on the non-mortar side. Moreover, the quasi-exact integration of such a constraint is detailed. Finally, the use of the proposed technique to glue incompatible meshes is illustrated in the tire industry framework for the resolution of nonlinear elastostatics problems.

5.1 Introduction

Le travail effectué en contexte industriel en ce qui concerne le recollement de maillages incompatibles vient compléter celui réalisé par Pascal Landereau et Adeline Eynard [Eyn04],

en proposant la formulation d'une contrainte mortier sur interface courbe régularisée et l'intégration quasi-exacte de cette contrainte.

En effet, l'étude [Eyn04] montre la grande sensibilité de la convergence des itérations de Newton pour la résolution de problèmes d'élastostatique non-linéaires en contexte industriel, en présence de maillages incompatibles et lorsqu'une formulation de recollement de type mortier est adoptée. La raison la plus vraisemblable est que sur l'interface, la présence de facettes incompatibles exerçant des forces sur le maillage mortier induit, des singularités de contraintes surviennent et perturbent dramatiquement la convergence de l'algorithme de Newton. La prise en compte d'une interface bien régulière apparaît alors naturelle. Aussi, si Wohlmuth et al. analysent dans [FMW04] le cas d'interfaces courbes, toute la difficulté demeure dans la définition de telles interfaces. En effet, on ne dispose souvent que des maillages séparés des sous-domaines, et la définition des interfaces courbes doit se faire à partir des données de maillage. Aussi, Laursen et Puso proposent-ils dans [PL02, PL03, Pus04] l'introduction d'une interface intermédiaire de classe G^1 , c'est-à-dire assurant la continuité du champ de normales, et construite par carreaux selon la méthode de Grégory ou Hermite [GF99]. La formulation d'une contrainte de type mortier nécessite alors l'introduction d'applications bijectives entre cette nouvelle interface, et les interfaces discrètes non-coïncidantes.

Par ailleurs, du point de vue de l'approximation de la contrainte mortier, Cazabeau, Maday et leurs collaborateurs montrent dans [CLM97, MRW02] en présence d'interfaces planes, que l'approximation par quadrature des intégrales de contrainte occasionne une dégradation de la convergence de la méthode, qui se fait alors en \sqrt{h} indépendamment du degré d'approximation adopté pour les déplacements ! Une formulation avec quadratures mais non-symétrique est proposée, mais nous choisissons ici de jouer la carte d'une intégration exacte permettant de concilier symétrie et précision.

Enfin, dans le cadre de ce chapitre, on se restreint à la gestion de déplacements Q_1 de part et d'autre de l'interface, contrôlés par des multiplicateurs Q_1 continus ou Q_0 discontinus non-stabilisés, l'absence de stabilisation pouvant être acceptable si les maillages recollés sont "suffisamment incompatibles". En effet, la condition inf-sup usuellement vérifiée dans le cadre des méthodes de mortiers [BMP93] est plus forte que celle strictement nécessaire pour assurer le caractère bien posé du problème, et assure ce caractère bien posé même dans le cas (en fait le pire du point de vue de la constante inf-sup) où les maillages recollés sont compatibles sur leur interface commune. De ce fait, la stabilisation peut s'avérer inutile pour des maillages suffisamment incompatibles. Néanmoins, compte tenu des conclusions de l'étude d'Adeline Eynard relative à des cas test pneus sur les maillages de finesse usuelle, l'utilisation de multiplicateurs de Lagrange Q_1 semble à privilégier numériquement par rapport à des multiplicateurs Q_0 , au moins en l'absence de stabilisation.

Nous introduisons en section 2, une interface intermédiaire par carreaux de Hermite, à l'instar de [Pus04], et formulons une contrainte de type mortier dans l'esprit de [Pus04], mais avec quelques différences de position. Nous détaillons ensuite en section 3, l'intégra-

tion quasi-exacte de cette contrainte. Cette étape nécessitant l'intersection de polygones convexes, nous nous appuierons sur l'algorithme de Rourke [O'R98] qui présente une complexité optimale. Enfin, des tests numériques illustrant la pertinence de la méthode sont présentés en section 4. Pour tout complément quant à des détails plus mathématiques, on se reportera au chapitre précédent.

5.2 Formulation mortier sur une surface courbe

Si l'interface entre deux maillages incompatibles n'est pas plane, le maillage indépendant des sous-domaines conduit à l'obtention de deux interfaces distinctes Γ_h^- et Γ_h^+ entre lesquelles nous souhaitons formuler une continuité faible des déplacements au sens des méthodes de mortier [BMP93]. On notera Γ_h^- l'interface sur laquelle sont définis les multiplicateurs de Lagrange (côté esclave ou non-mortier).

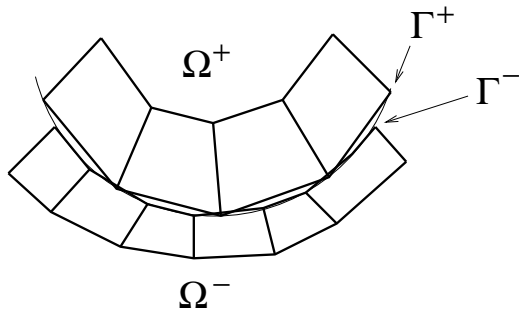


FIG. 5.1 – Configuration dans laquelle les interfaces discrètes Γ^+ et Γ^- des domaines Ω^+ et Ω^- ne se confondent pas en une interface commune.

A l'instar de la technique utilisée par Puso [Pus04], on définit une interface régularisée Γ de classe G^1 , c'est-à-dire assurant la continuité du champ des normales. La motivation pour effectuer une telle construction est double :

- faire en sorte que les déformations de l'interface lisse Γ n'occasionnent pas de singularité de contrainte ,
- faire en sorte que tout noeud de \mathbb{R}^3 admette une projection¹ sur Γ définie selon le champ des normales de la surface Γ ,

ce qui n'est pas le cas sur la surface discrète non-différentiable Γ_h^- . On opte ici pour une construction de Γ par régularisations locales -dites également carreaux (George) ou patches (Laursen, Puso)- en utilisant une approximation tensorielle de Hermite. Dans ce cadre, on se limitera aux cas où la discréétisation de l'interface non-mortier est réalisée en quadrangles.

¹Cette projection étant unique si le noeud est suffisamment proche de Γ , plus précisément à une distance de Γ inférieure à son rayon de courbure local.

Afin de définir la surface Γ , on commence par construire un champ de normales régularisé s'appuyant sur l'interface non-mortier Γ_h^- (sous-section 5.2.1). Chaque élément de l'interface non-mortier est alors déformé par patch Hermite en un élément courbe s'appuyant sur les noeuds de Γ_h^- et possédant en ces noeuds les normales régularisées précédemment définies (sous-section 5.2.2). Enfin, nous proposons une contrainte mortier sur cette interface régularisée, utilisant comme bijections entre Γ et Γ_h^- (resp. Γ_h^+) la déformation de type Hermite des éléments de l'interface non-mortier (resp. la projection selon le champ des normales de Γ).

5.2.1 Construction des espaces tangents

Pour construire l'interface régularisée Γ , il est nécessaire de se donner une information géométrique sur sa courbure. Pour construire une telle information, il faut par exemple définir en chaque noeud du maillage le plan tangent à Γ , ou de façon équivalente la normale à Γ . Soit $F \subset \Gamma_h^-$ un quadrangle de l'interface non-mortier, image de $\hat{F} = [-1; 1]^2$ par l'application φ^F :

$$\varphi^F(\hat{F}) = F.$$

Plus précisément, si les sommets de F sont les $(A_i^F)_{1 \leq i \leq 4} \in \mathbb{R}^3$, on a :

$$\varphi^F(\hat{x}) = \sum_{i=1}^4 A_i^F \hat{\varphi}_i(\hat{x}),$$

où les $\hat{\varphi}_i$ sont les fonctions de forme définies sur l'élément de référence \hat{F} :

$$\begin{aligned}\hat{\varphi}_1(\hat{x}) &= (1 - \hat{x}_1)(1 - \hat{x}_2)/4, \\ \hat{\varphi}_2(\hat{x}) &= (1 + \hat{x}_1)(1 - \hat{x}_2)/4, \\ \hat{\varphi}_3(\hat{x}) &= (1 + \hat{x}_1)(1 + \hat{x}_2)/4, \\ \hat{\varphi}_4(\hat{x}) &= (1 - \hat{x}_1)(1 + \hat{x}_2)/4, \quad \forall \hat{x} = (\hat{x}_1, \hat{x}_2) \in \hat{F} = [-1; 1]^2.\end{aligned}$$

Ainsi, les normales nodales unitaires $(n_i^F)_{1 \leq i \leq 4} \in \mathbb{R}^3$ sont définies par :

$$n_i^F = \frac{t_i^1 \times t_i^2}{\|t_i^1 \times t_i^2\|_2}, \quad 1 \leq i \leq 4,$$

où les vecteurs tangents t_i^1 et t_i^2 à F en A_i sont donnés par :

$$t_i^j = \left[\nabla \varphi^F(\hat{A}_i) \right] \cdot e_j$$

avec $e_1 = (1, 0)$, $e_2 = (0, 1)$, et $\hat{A}_1 = (-1, -1)$, $\hat{A}_2 = (1, -1)$, $\hat{A}_3 = (1, 1)$ et $\hat{A}_4 = (-1, 1)$.
Ensuite, on construit en chaque noeud $A \in \Gamma_h^-$ une normale moyennée :

$$n^A = \sum_{F \subset \Gamma_h^-, \exists j, A_j^F = A} |F| \epsilon_j^F n_j^F,$$

avec $\epsilon_j^F = \pm 1$ afin de pallier au fait que les normales n_j^F , définies sur chaque élément ne sont définies qu'au signe près. $|F|$ désigne la surface du quadrangle d'interface F , et définie par :

$$|F| = \int_{\hat{F}} \det \nabla \varphi^F(\hat{x}) d\hat{x}.$$

Le vecteur normal est ensuite normalisée : $n^A := n^A / \|n^A\|_2$.

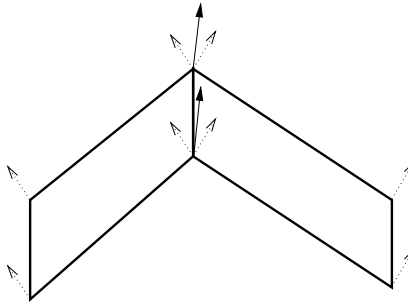


FIG. 5.2 – Construction des normales aux noeuds du maillage.

Remarque 5.1. Une problématique intéressante et assez fondamentale consiste à se demander si la technique de moyenne nodale des normales converge par raffinement de maillage vers l'obtention du champ de normales de la surface continue sur laquelle s'appuie la discrétisation. En réalité, la réponse est non avec la technique proposée qui est cependant répandue (elle est suggérée en particulier dans [GF99]). A l'inverse, des travaux récents, tels [CSM03], proposent des approches plus complexes permettant d'obtenir de bonnes propriétés de convergence du champ des normales par raffinement de maillage. Nous ignorons volontairement ces développements, mais insistons sur leur possible intérêt.

5.2.2 Construction du carreau.

Soit $F \subset \Gamma_h^-$ un quadrangle de l'interface non-mortier, avec les notations de la sous-section précédente. On dispose des quatre sommets $(A_i^F)_{1 \leq i \leq 4} \in \mathbb{R}^3$ et des normales n^A précédemment construites. Nous construisons en chaque noeud A_i^F deux tangentes $(\tilde{t}_i^j)_{1 \leq j \leq 2}$ "régularisées". Si le noeud A_i^F coïncide avec le noeud A du maillage, on définit en A les tangentes à la future interface régularisée intermédiaire Γ par projection sur le plan normal à n^A le long de n^A :

$$\tilde{t}_i^j = t_i^j - (n^A \cdot t_i^j) n^A, \quad 1 \leq j \leq 2.$$

L'élément régularisé que nous utilisons s'appuie sur les noeuds $(A_i^F)_{1 \leq i \leq 4} \in \mathbb{R}^3$ avec les tangentes respectives $(\tilde{t}_i^1, \tilde{t}_i^2)_{1 \leq i \leq 4} \in \mathbb{R}^3$. Nous le définissons comme l'image du carré de référence \hat{F} par l'application $\tilde{\varphi}^F$ donnée par l'expression suivante :

$$\begin{aligned}\tilde{\varphi}^F(\hat{x}) = & A_1^F \psi_1(\hat{x}_1) \psi_1(\hat{x}_2) + A_2^F \psi_2(\hat{x}_1) \psi_1(\hat{x}_2) + A_3^F \psi_2(\hat{x}_1) \psi_2(\hat{x}_2) + A_4^F \psi_1(\hat{x}_1) \psi_2(\hat{x}_2) \\ & + \tilde{t}_1^1 \theta_1(\hat{x}_1) \psi_1(\hat{x}_2) + \tilde{t}_2^1 \theta_2(\hat{x}_1) \psi_1(\hat{x}_2) + \tilde{t}_3^1 \theta_2(\hat{x}_1) \psi_2(\hat{x}_2) + \tilde{t}_4^1 \theta_1(\hat{x}_1) \psi_2(\hat{x}_2) \\ & + \tilde{t}_1^2 \psi_1(\hat{x}_1) \theta_1(\hat{x}_2) + \tilde{t}_2^2 \psi_2(\hat{x}_1) \theta_1(\hat{x}_2) + \tilde{t}_3^2 \psi_2(\hat{x}_1) \theta_2(\hat{x}_2) + \tilde{t}_4^2 \psi_1(\hat{x}_1) \theta_2(\hat{x}_2)\end{aligned}$$

pour $\hat{x} \in [-1; 1]^2$. On a utilisé les fonctions $\psi_1, \psi_2, \theta_1, \theta_2$ qui constituent les fonctions de base usuelles des polynômes de Hermite sur $[-1; 1]$:

$$\psi_1(s) = \frac{1}{4}(s-1)^2(2+s), \quad \psi_2(s) = \frac{1}{4}(s+1)^2(2-s),$$

$$\theta_1(s) = \frac{1}{8}(s+1)(1-s)^2, \quad \theta_2(s) = \frac{1}{8}(s-1)(1+s)^2,$$

pour tout $s \in [-1; 1]$. Elles satisfont les relations suivantes :

$$\psi_1(-1) = 1 \quad \psi_1(1) = 0 \quad \psi'_1(-1) = 0 \quad \psi'_1(1) = 0$$

$$\psi_2(-1) = 0 \quad \psi_2(1) = 1 \quad \psi'_2(-1) = 0 \quad \psi'_2(1) = 0$$

$$\theta_1(-1) = 0 \quad \theta_1(1) = 0 \quad \theta'_1(-1) = 1 \quad \theta'_1(1) = 0$$

$$\theta_2(-1) = 0 \quad \theta_2(1) = 0 \quad \theta'_2(-1) = 0 \quad \theta'_2(1) = 1.$$

Il s'agit d'un carreau tensoriel de Hermite, où on voit qu'on ne prend pas en compte les termes de la forme $\theta_i(\hat{x}_1) \theta_j(\hat{x}_2)$. En conséquence, on ne représente pas le "twist" des éléments (dérivées seconde nulles aux noeuds).

Sur un tel carreau, on définit les vecteurs tangents au point de référence $\hat{x} \in [-1; 1]^2$ par :

$$\tilde{t}^j(\hat{x}) = \frac{\partial \tilde{\varphi}^F}{\partial \hat{x}_j}(\hat{x}), \quad 1 \leq j \leq 2,$$

la normale par :

$$\tilde{n}(\hat{x}) = \frac{\tilde{t}^1(\hat{x}) \times \tilde{t}^2(\hat{x})}{\|\tilde{t}^1(\hat{x}) \times \tilde{t}^2(\hat{x})\|_2},$$

et la métrique riemannienne par :

$$\tilde{m}(\hat{x}) = \|\tilde{t}^1(\hat{x}) \times \tilde{t}^2(\hat{x})\|_2.$$

Dans ces expressions, $\|\cdot\|_2$ désigne la norme euclidienne dans \mathbb{R}^3 . Par construction des carreaux, les espaces tangents se raccordent continûment d'un élément à l'autre. On obtient donc ainsi le pavage d'une variété Γ de classe G^1 .

5.2.3 Projection sur la surface

Ayant précédemment défini la surface régularisée Γ , nous nous attachons ici à définir de façon univoque la projection continue $\mathcal{P}(x) \in \Gamma$ des points $x \in \mathbb{R}^3$ situés dans un voisinage de Γ .

Definition 5.1. On dit que $\mathcal{P}(x) \in \Gamma$ est un projeté de $x \in \mathbb{R}^3$ sur Γ , s'il existe un élément $F \subset \Gamma_h^-$ de l'interface non-mortier, des coordonnées intrinsèques $\hat{p} \in [-1; 1]^2$ et un réel α tels que :

$$x - \tilde{\varphi}^F(\hat{p}) = \alpha \tilde{n}(\hat{p}), \quad (5.1)$$

avec les notations introduites plus haut. On note alors $\mathcal{P}(x) = \tilde{\varphi}^F(\hat{p})$. On utilisera également la notation $\mathcal{P}_F(x)$ pour signifier qu'il s'agit du projeté sur l'élément F .

On obtient alors le :

Lemma 5.1. Pour tout élément $\tilde{F} = \tilde{\varphi}^F(\hat{F})$ de l'interface régularisée Γ , il existe un voisinage fermé $\mathcal{V}(F) \subset \mathbb{R}^3$ de \tilde{F} tel que tout $x \in \mathcal{V}(F)$ admette un unique projeté $\mathcal{P}_F(x)$ sur \tilde{F} . De plus, la projection \mathcal{P}_F est continue.

Preuve : On se donne l'application $f : \mathbb{R} \times \hat{F} \rightarrow \mathbb{R}^3$ définie par :

$$f(\alpha, \hat{p}) = \tilde{\varphi}^F(\hat{p}) + \alpha \tilde{n}(\hat{p}), \quad \forall (\alpha, \hat{p}) \in \mathbb{R} \times \hat{F}.$$

Comme $f \in \mathcal{C}^1(\mathbb{R} \times \hat{F}; \mathbb{R}^3)$ est continûment différentiable, que les points de Γ sont leurs propres projetés :

$$f(0, \hat{p}) = \tilde{\varphi}^F(\hat{p}), \quad \forall \hat{p} \in \hat{F},$$

et que la différentielle :

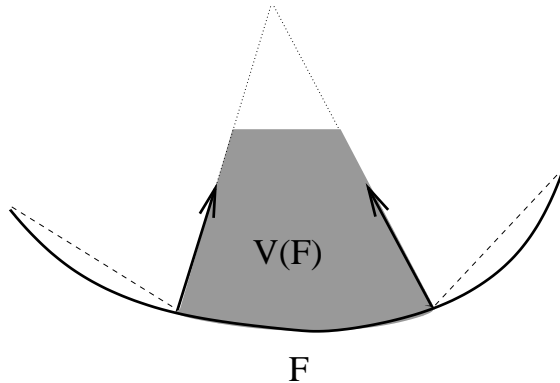
$$df(0, \hat{p}) = \frac{\partial \tilde{\varphi}^F}{\partial \hat{p}} \cdot d\hat{p} + \tilde{n}(\hat{p})d\alpha,$$

est inversible du fait que les vecteurs $t^1(\hat{p}) = \frac{\partial \tilde{\varphi}^F}{\partial \hat{p}} \cdot e_1$, $t^2(\hat{p}) = \frac{\partial \tilde{\varphi}^F}{\partial \hat{p}} \cdot e_2$ et $\tilde{n}(\hat{p})$ sont indépendants par construction, le théorème d'inversion locale [Bou95] assure que pour $x \in \mathbb{R}^3$ assez près de \tilde{F} , il existe un unique projeté de x sur \tilde{F} , et que de plus, l'opération de projection est continue et continûment inversible. \square

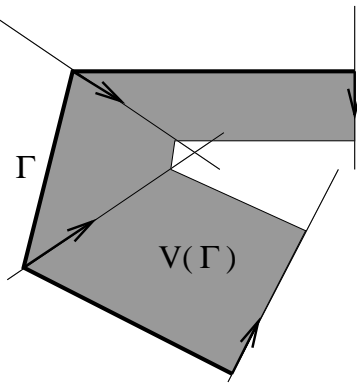
Quitte à restreindre l'épaisseur des voisinages en considérant :

$$\{x \in \mathcal{V}(F), \quad \text{dist}(x, F) \text{ "assez petite"}\}$$

comme nouveau $\mathcal{V}(F)$, on peut toujours supposer que les intersections des intérieurs de tels voisinages pour des éléments distincts sont vides. En effet, les champs de normales sur le bord d'éléments adjacents coïncident et donc les voisinages relatifs à des éléments adjacents sont disjoints, comme cela est illustré ci-dessous :



En jouant sur l'épaisseur des voisinages, on peut donc empêcher toute intersection de voisinages d'éléments d'interface, comme illustré ci-dessous :



On introduit alors le voisinage $\mathcal{V}(\Gamma)$ de Γ comme :

$$\mathcal{V}(\Gamma) = \bigcup_{F \subset \Gamma_h^-} \mathcal{V}(F),$$

dont les $(\mathcal{V}(F))_{F \subset \Gamma_h^-}$ constituent une partition, et la :

Definition 5.2. On note $\mathcal{P} : \mathcal{V}(\Gamma) = \bigcup_{F \subset \Gamma_h^-} \mathcal{V}(F) \rightarrow \Gamma$, la projection définie pour tout $x \in \mathcal{V}(\Gamma)$ par :

$$\mathcal{P}(x) = \mathcal{P}_F(x), \quad \text{si } x \in \mathcal{V}(F).$$

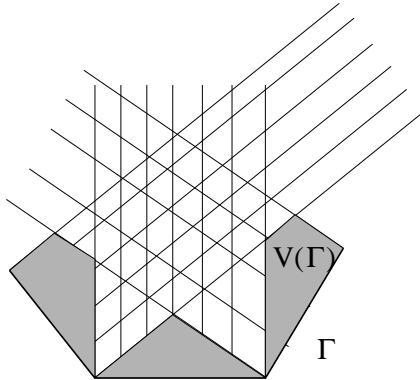
Tout $x \in \mathcal{V}(\Gamma)$ admet donc un unique projeté par construction, d'abord par l'identification d'un voisinage d'élément d'interface, puis par l'unicité de la projection sur l'élément d'interface. De plus, la projection \mathcal{P} est continue par construction du fait de la continuité de \mathcal{P}_F et de la continuité du champ de normales entre deux carreaux adjacents de Γ . Nous

faisons l'hypothèse que l'interface mortier est complètement incluse dans le voisinage $\mathcal{V}(\Gamma)$ de Γ :

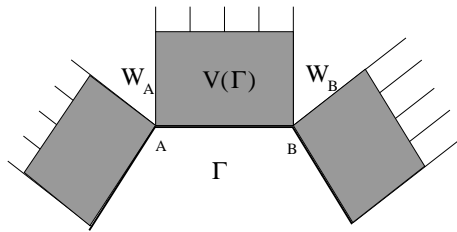
$$\Gamma_h^+ \subset \mathcal{V}(\Gamma),$$

en conséquence de quoi tout point x de Γ_h^+ admet un unique projeté $\mathcal{P}(x)$ sur Γ .

Remarque 5.2. *L'utilisation d'une telle projection sur l'interface G^1 ainsi construite permet d'obtenir la continuité de l'opération de projection. A l'inverse, une projection plane sur chacun des éléments de l'interface facétisée Γ_h^- ne constitue pas une projection globalement continue, et présente de nombreuses zones de non-projectabilité. En particulier, dans le schéma suivant :*



on a représenté en grisé le voisinage $V(\Gamma)$ de l'interface facétisée concave Γ des points admettant un unique projeté sur Γ par projection plane. Ainsi, on observe l'existence de points arbitrairement près de l'interface et n'admettant pas univoquement de projeté. Cette configuration interdit notamment la définition d'une projection continue selon le champ des normales aux facettes. Dans le cas convexe, on observe au contraire l'impossibilité de définir un projeté plan dans certaines zones également arbitrairement près de l'interface.



Quand bien même on adopterait A (resp. B) comme projeté des points de W_A (resp. W_B), rendant la projection continue, on obtiendrait que l'aire sur Γ du projeté de tout volume inclus dans W_A ou W_B est nulle.

Remarque 5.3. *D'un point de vue numérique, l'implémentation de la projection $\mathcal{P}(x)$ se fait par détection de l'élément F par fenêtrage parallélépipédique grossier puis résolution*

de (5.1) par une méthode de Newton.

Avant de définir la contrainte de continuité faible sur l'interface intermédiaire régularisée Γ , nous introduisons l'application \mathcal{Q} comme l'application réciproque de $\mathcal{P}|_{\Gamma_h^+} : \Gamma_h^+ \rightarrow \Gamma$, plus précisément :

Definition 5.3. On notera $\mathcal{Q} : \Gamma \rightarrow \Gamma_h^+$ l'application définie pour tout $x \in \Gamma$ par l'unique solution $\mathcal{Q}(x) \in \Gamma_h^+$ de :

$$\mathcal{Q}(x) - \tilde{\varphi}^F(\hat{x}) = \alpha \tilde{n}(\hat{x}),$$

pour un coefficient α réel à déterminer, x étant situé sur l'élément d'interface $\tilde{F} = \tilde{\varphi}^F(\hat{F})$ et de coordonnées de référence $\hat{x} \in \hat{F}$ en ce sens que $x = \tilde{\varphi}^F(\hat{x})$.

5.2.4 Contrainte mortier

Si $u_h^- \in W_h^-$ et $u_h^+ \in W_h^+$ désignent respectivement les traces des champs des déplacements sur les interfaces non-mortier Γ_h^- et mortier Γ_h^+ , nous imposons la contrainte suivante sur leur saut, intégrée sur la surface intermédiaire régularisée Γ :

$$\int_{\Gamma} [\tilde{u}_h^-(x) - u_h^+(\mathcal{Q}(x))] \cdot \tilde{\mu}_h(x) = 0, \quad \forall \tilde{\mu} \in \tilde{M}. \quad (5.2)$$

Dans cette expression, pour tout $x \in \tilde{F} = \tilde{\varphi}^F(\hat{F})$, nous avons défini le transport des applications u_h^- et μ_h de l'interface non-mortier Γ_h^- sur Γ par l'application de déformation de l'interface $\varphi^F \circ (\tilde{\varphi}^F)^{-1}$:

$$\tilde{u}_h^-(x) = u_h^-(\varphi^F \circ (\tilde{\varphi}^F)^{-1}(x)),$$

$$\tilde{\mu}_h(x) = \mu_h(\varphi^F \circ (\tilde{\varphi}^F)^{-1}(x)),$$

où $\mu_h \in M_h$ est un multiplicateur de Lagrange vivant dans un espace M_h .

Pour chaque élément $F \subset \Gamma_h^-$, et tout $\hat{x} \in \hat{F}$, nous avons :

$$\tilde{u}_h^-(\tilde{\varphi}^F(\hat{x})) = u_h^-(\varphi^F(\hat{x})),$$

$$\tilde{\mu}(\tilde{\varphi}^F(\hat{x})) = \mu_h(\varphi^F(\hat{x})),$$

de sorte que la contrainte se décompose en :

$$\sum_F \int_{\hat{F}} [u_h^-(\varphi^F(\hat{x})) - u_h^+(\mathcal{Q}(\tilde{\varphi}^F(\hat{x})))] \cdot \mu_h(\varphi^F(\hat{x})) \tilde{m}_F(\hat{x}) d\hat{x} = 0, \quad \forall \hat{\mu}_h \in M_h. \quad (5.3)$$

Du point de vue de la condition inf-sup, on obtient très simplement le :

Lemma 5.2. Si la condition inf-sup suivante est satisfaite pour le couple $W_h^- \times M_h$:

$$\inf_{\mu_h \in M_h \setminus \{0\}} \sup_{v_h \in W_h^- \setminus \{0\}} \frac{\int_{\Gamma_h^-} v_h \cdot \mu_h}{\|u^-\|_{\delta, \frac{1}{2}, \Gamma_h^-} \|\mu\|_{\delta, -\frac{1}{2}, \Gamma_h^-}} \geq \beta,$$

elle vaut également pour la contrainte régularisée (5.2) :

$$\inf_{\mu_h \in M_h \setminus \{0\}} \sup_{v_h \in W_h^- \setminus \{0\}} \frac{\int_{\Gamma} \tilde{v}_h \cdot \tilde{\mu}_h}{\|u^-\|_{\delta, \frac{1}{2}, \Gamma_h^-} \|\mu\|_{\delta, -\frac{1}{2}, \Gamma_h^-}} \geq \beta \inf_{F \subset \Gamma_h^-} \inf_{\hat{x} \in \hat{F}} \frac{\tilde{m}_F(\hat{x})}{m_F(\hat{x})}.$$

Preuve : La preuve découle simplement d'un changement de variables à partir de l'expression (5.3) :

$$\begin{aligned} & \sum_F \int_{\hat{F}} u_h^- (\varphi^F(\hat{x})) \cdot \mu_h(\varphi^F(\hat{x})) \tilde{m}_F(\hat{x}) d\hat{x} \\ &= \sum_F \int_{\hat{F}} u_h^- (\varphi^F(\hat{x})) \cdot \mu_h(\varphi^F(\hat{x})) \frac{\tilde{m}_F(\hat{x})}{m_F(\hat{x})} m_F(\hat{x}) d\hat{x} \\ &\geq \inf_{F \subset \Gamma_h^-} \inf_{\hat{x} \in \hat{F}} \frac{\tilde{m}_F(\hat{x})}{m_F(\hat{x})} \sum_F \int_{\hat{F}} u_h^- (\varphi^F(\hat{x})) \cdot \mu_h(\varphi^F(\hat{x})) m_F(\hat{x}) d\hat{x} \\ &= \inf_{F \subset \Gamma_h^-} \inf_{\hat{x} \in \hat{F}} \frac{\tilde{m}_F(\hat{x})}{\det \nabla \varphi^F(\hat{x})} \int_{\Gamma_h^-} u_h^-(x) \cdot \mu_h(x) dx \\ &\geq \inf_{F \subset \Gamma_h^-} \inf_{\hat{x} \in \hat{F}} \frac{\tilde{m}_F(\hat{x})}{\det \nabla \varphi^F(\hat{x})} \beta \|u^-\|_{\delta, \frac{1}{2}, \Gamma_h^-} \|\mu\|_{\delta, -\frac{1}{2}, \Gamma_h^-}. \end{aligned}$$

□

Remarque 5.4. Nous indiquons brièvement les quelques différences entre cette proposition et celle de Michael Puso [Pus04].

- La définition des espaces tangents sur Γ se fait ici à partir d'une moyenne de normales aux noeuds, alors que dans [Pus04], ils sont construits directement par approximation des vecteurs tangents par différences finies entre éléments adjacents. L'avantage de l'approche choisie ici est la réalisation d'un calcul élément par élément, et l'absence de restriction à des maillages réglés.
- C'est la carte locale $\tilde{\varphi}^F$ et non la projection \mathcal{P} que nous utilisons pour appliquer un élément non-mortier de Γ_h^- sur Γ . Cette dernière solution est celle retenue par [Pus04], mais elle apparaît numériquement moins satisfaisante.
- Nous renonçons à l'utilisation des mortiers duals de Barbara Wohlmuth [Woh00]. En effet, l'argument de dualité tel qu'il figure dans [SZ90] ne vaut que sur une interface plane, et il serait particulièrement complexe à généraliser sur la variété Γ . L'avantage de mortiers duals au sens de [Woh00], qui permettent sur une interface plane la diagonalisation de la contrainte, est donc moins clair ici. Nous utiliserons au choix les multiplicateurs \mathbb{Q}_1 de [BMP93] ou les multiplicateurs \mathbb{Q}_0 du chapitre précédent.

5.3 Algorithme d'assemblage

5.3.1 Algorithme

Nous proposons ici un algorithme permettant le calcul de la contrainte cinématique de recollement proposée (5.2) qui est décomposée en :

$$\sum_{F \subset \Gamma_h^-} \sum_{G \subset \Gamma_h^+} \int_{\tilde{F} \cap \mathcal{P}(G)} [\tilde{u}_h^-(x) - u_h^+(\mathcal{Q}(x))] \cdot \tilde{\mu}_h(x) = 0, \quad \forall \tilde{\mu} \in \tilde{M}.$$

Nous détaillons ici le calcul du terme élémentaire :

$$\mathcal{A} = \int_{\tilde{F} \cap \mathcal{P}(G)} [\tilde{u}_h^-(x) - u_h^+(\mathcal{Q}(x))] \cdot \tilde{\mu}_h(x),$$

où F et G désignent respectivement des éléments des interfaces non-mortier Γ_h^- et mortier Γ_h^+ . Un changement de variable fournit :

$$\mathcal{A} = \int_{(\tilde{\varphi}^F)^{-1}(\tilde{F} \cap \mathcal{P}(G))} [u_h^-(\varphi^F(\hat{x})) - u_h^+(\mathcal{Q}(\varphi^F(\hat{x})))] \cdot \mu_h(\varphi^F(\hat{x})) \tilde{m}_F(\hat{x}) d\hat{x}.$$

Remarque 5.5. Une difficulté essentielle pour la détermination de $\tilde{F} \cap \mathcal{P}(G)$ vient de ce qu'on ne peut projeter intégralement G sur Γ en utilisant un seul redressement de Γ . Celà provient de ce que $\mathcal{P}(G)$ déborde sur plusieurs éléments courbes de Γ . En revanche, il est ais  de d terminer le transport de \tilde{F} sur Γ_h^+ par son champ de normales, i.e $\mathcal{Q}(\tilde{F}) \cap G$. La m thode propos e ici utilise la relation :

$$\tilde{F} \cap \mathcal{P}(G) = \mathcal{P}(\mathcal{Q}(\tilde{F}) \cap G),$$

qui vaut parce que $\mathcal{P}|_{\Gamma_h^+} : \Gamma_h^+ \rightarrow \Gamma$ est injective.

Nous détaillons l'évaluation de \mathcal{A} par les étapes suivantes :

1. Détermination de $\mathcal{Q}(\tilde{F}) \cap G$.

Soient $A_i = \varphi^F(\hat{A}_i)$ pour $1 \leq i \leq 4$ les sommets de l' l ment F . Pour tout $1 \leq i \leq 4$, on vient calculer les coordonn es de r f rence \hat{B}_i dans G des $\mathcal{Q}(A_i)$, c'est   dire que :

$$\varphi^G(\hat{B}_i) - A_i = \alpha n^{A_i}, \quad 1 \leq i \leq 4,$$

pour un coefficient α r el  determiner. Cette d termination se fait par une m thode de Newton. Il est bien entendu que tous les \hat{B}_i n'appartiennent pas en g n ral au carr  de r f rence \hat{F} . On note $\hat{H} \subset \mathbb{R}^2$ le polyg ne de sommets $(\hat{B}_i)_{1 \leq i \leq 4}$, et on adopte :

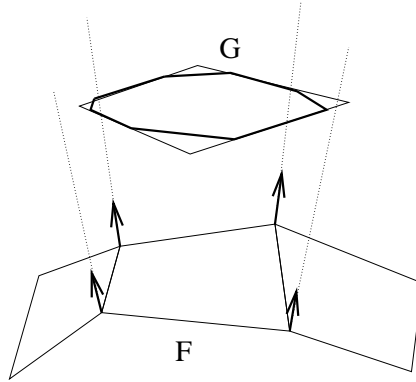
$$(\varphi^G)^{-1}(\mathcal{Q}(\tilde{F}) \cap G) \simeq \hat{H} \cap \hat{F}.$$

Ce faisant on suppose qu'en coordonnées de référence dans G , $\mathcal{Q}(\tilde{F})$ est un polygône, ce qui est faux a priori puisque les arrêtes en sont courbes pour des champs de normales quelconques. Néanmoins, lever cette simplification occasionnerait une algorithmique encore beaucoup plus coûteuse, ce à quoi nous renonçons.

La méthode d'intersection utilisée, travaillant exclusivement sur des polygônes convexes, est celle de Joseph O'Rourke [O'R98]. Le code source original se trouve à l'adresse suivante :

<http://cs.smith.edu/~orourke/books/ftp.html>.

Il a été modifié au cours de ce travail pour traiter des polygônes dont les sommets possèdent des coordonnées non-entières et gérer les exceptions (inclusions de polygônes les uns dans les autres). Les routines correspondantes se trouvent dans `intersec.c`. Les sommets du polygône intersection $\hat{H} \cap \hat{F}$ sont notés $(\hat{C}_i)_{1 \leq i \leq N}$ et on adopte de plus $C_i = \varphi^G(\hat{C}_i)$.



2. Détermination de $\tilde{F} \cap \mathcal{P}(G)$.

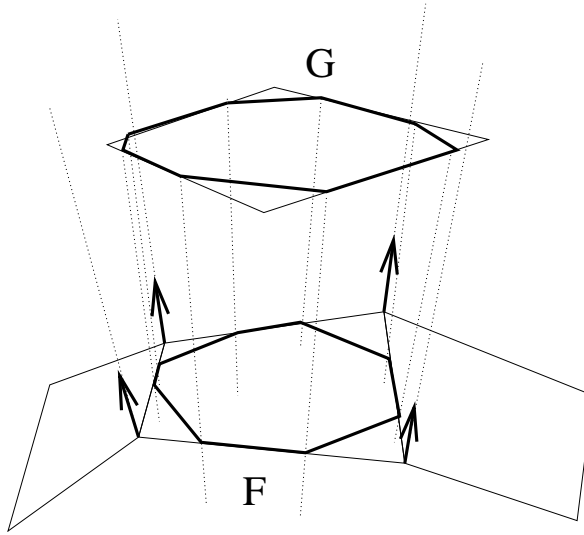
Du fait de l'injectivité de \mathcal{P} , on a :

$$\tilde{F} \cap \mathcal{P}(G) = \mathcal{P}\left(\mathcal{Q}(\tilde{F}) \cap G\right).$$

Pour tout C_i avec $1 \leq i \leq N$, on calcule sa projection $D_i = \mathcal{P}(C_i)$. Plus précisément, on détermine \hat{D}_i et α tels que :

$$C_i - \tilde{\varphi}^F(\hat{D}_i) = \alpha \tilde{n}(\hat{D}_i),$$

par une méthode de Newton. On considère alors en faisant la même approximation qu'à l'étape précédente, que $(\tilde{\varphi}^F)^{-1}(\tilde{F} \cap \mathcal{P}(G))$ est le polygône de sommets \hat{D}_i , inclus dans le carré de référence \hat{F} . Nous notons \hat{R} ce polygône.



3. Intégration.

On découpe le polygone \hat{R} en N triangles partageant le centre du polygone comme sommet commun : $\hat{R} = \bigcup_{j=1}^N \hat{T}_j$, de sorte que maintenant, on adopte :

$$\mathcal{A} \simeq \sum_{j=1}^N \int_{\hat{T}_j} [u_h^- (\varphi^F(\hat{x})) - u_h^+ (\mathcal{Q}(\varphi^F(\hat{x})))] \cdot \mu_h(\varphi^F(\hat{x})) \tilde{m}_F(\hat{x}) d\hat{x},$$

où on vient approcher les intégrales sur les \hat{T}_j par quadrature de Gauss à 12 points afin de conserver suffisamment de précision pour des zones à forte courbure. On intègre ainsi exactement les polynômes de degré total 6 sur les \hat{T}_j alors que le produit de deux fonctions \mathbb{Q}_1 est seulement de degré total 4, et nécessite seulement 6 points de Gauss. Néanmoins, la fonction $u_h^+ \circ \mathcal{Q}$, n'est pas un polynôme \mathbb{Q}_1 sur les \hat{T}_j lorsque les interfaces mortiers et non-mortiers sont géométriquement non-conformes, ce qui légitime la sur-intégration proposée.

5.4 Essais numériques

5.4.1 Recollements au tour de roue

Le fait de considérer des maillages incompatibles permet bien évidemment une économie substantielle de degrés de liberté.

Pour des raisons de convergence des itérations de Newton (l'approche apparaît beaucoup plus robuste en général) et éventuellement d'économie du nombre de relations cinématiques entre noeuds, il reste préférable de définir les multiplicateurs sur le maillage le plus grossier, i.e. celui de l'architecture. En utilisant des multiplicateurs \mathbb{Q}_1 sur l'architecture en présence de la régularisation proposée de l'interface, on obtient les cartes de pressions normales lors

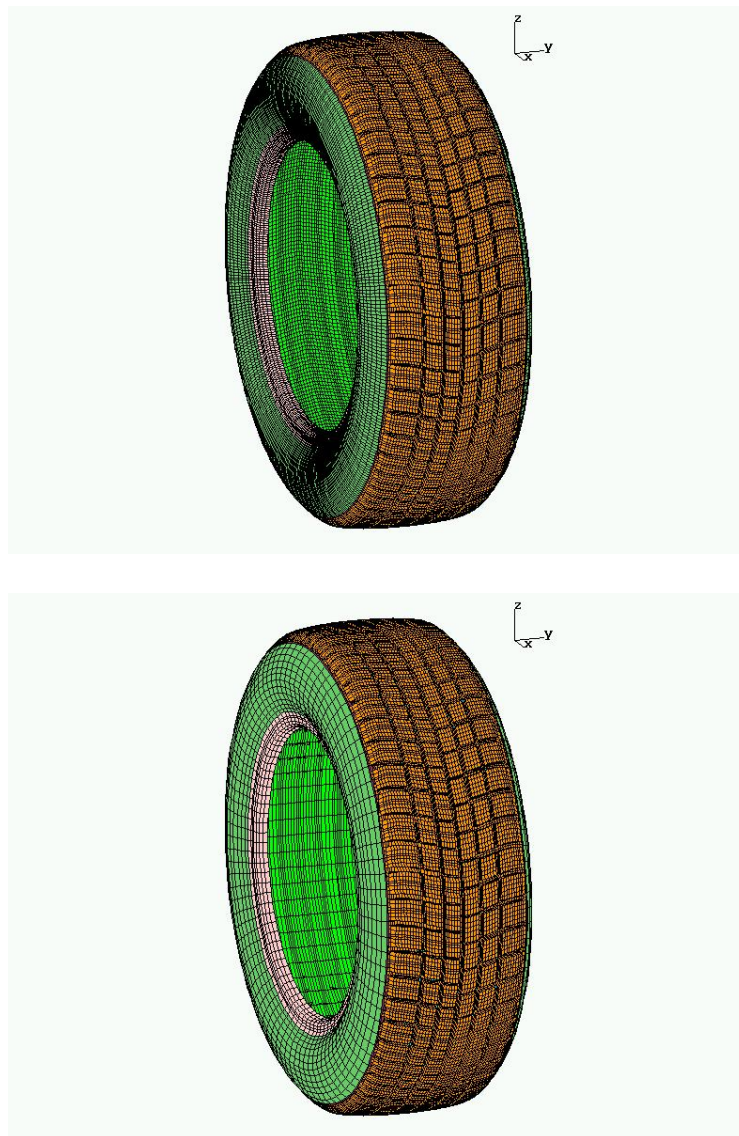


FIG. 5.3 – Maillages compatible et incompatible (ratio 4) d'un pneumatique du projet Roulage 3D, présentant respectivement 240.845 et 128.500 noeuds.

d'un contact glissant représentées ci-après. La précision du calcul réalisé sur le modèle incompatible avec un ratio de maillage de 4 apparaît tout à fait bonne pour la restitution des pressions de contact.

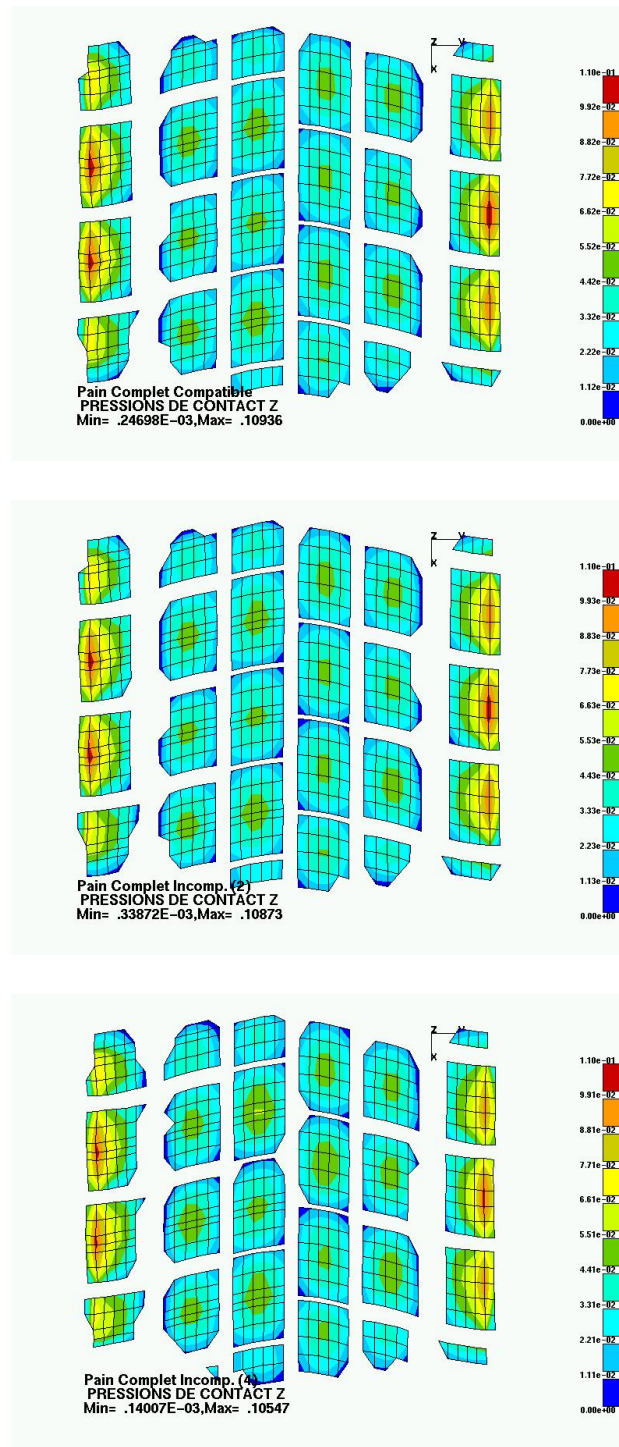
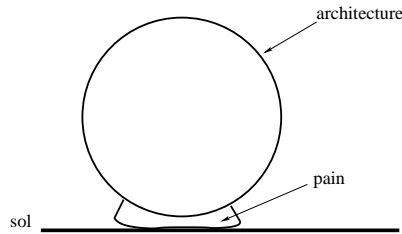


FIG. 5.4 – Cartes de pressions de contact obtenues avec la discréétisation compatible (240.845 noeuds), incompatible d'un ratio 2 (169.000 noeuds, 28.620 relations linéaires) et d'un ratio 4 (128.500 noeuds, 14.310 relations linéaires).

5.4.2 Recollement d'un pain unique

On réalise maintenant le recollement d'un pain de sculpture unique contre une architecture, comme représenté ci-après :



Les déplacements et contraintes σ_{zz} dans l'aire de contact sont représentés figure 5.5. A des fins d'illustration de la régularisation de l'interface architecture/sculpture mise en place ici, on compare l'aire des interfaces régularisées Γ s'appuyant sur Γ_h^- selon que le côté non-mortier choisi est l'architecture ou la sculpture.

	Γ_h	Γ
architecture	48014.	46589.
sculpture	46384.	46536.

L'écart entre les surfaces Γ ainsi construites est bien moindre que celui entre les surfaces anguleuses côté architecture ou sculpture. Ainsi, il apparaît que l'interface régularisée est véritablement une surface intermédiaire.

Si on utilise des multiplicateurs de Lagrange \mathbb{Q}_1 définis sur l'architecture, les contraintes d'interface σ_{zz} sur l'interface sculpture obtenues avec et sans régularisation Hermite sont représentées sur la figure 5.6. Force est de constater que les répartitions sont quasiment identiques. En revanche, dans le cas de multiplicateurs de Lagrange \mathbb{Q}_0 définis sur l'architecture, seule la méthode régularisée permet d'obtenir la convergence de la méthode de Newton, et le champ des contraintes d'interface σ_{zz} sur l'interface sculpture correspondant est représenté sur la figure 5.7.

5.4.3 Mortiers et dynamique

Comme il a été montré au chapitre précédent dans le cadre linéarisé, le recollement de maillages non-conformes par une méthode de mortiers n'altère pas en termes de précision la résolution numérique de la dynamique des structures élastiques. Pour illustrer la véracité de cette assertion, nous considérons les versions compatible (240.845 noeuds) et incompatible d'un ratio 4 (128.500 noeuds, 14.310 relations linéaires) du modèle de pneumatique présenté en section 5.4.1. Après avoir effectué les gonflages, puis écrasements adhérent correspondant, nous réalisons une simulation avec vitesse imposée du centre roue

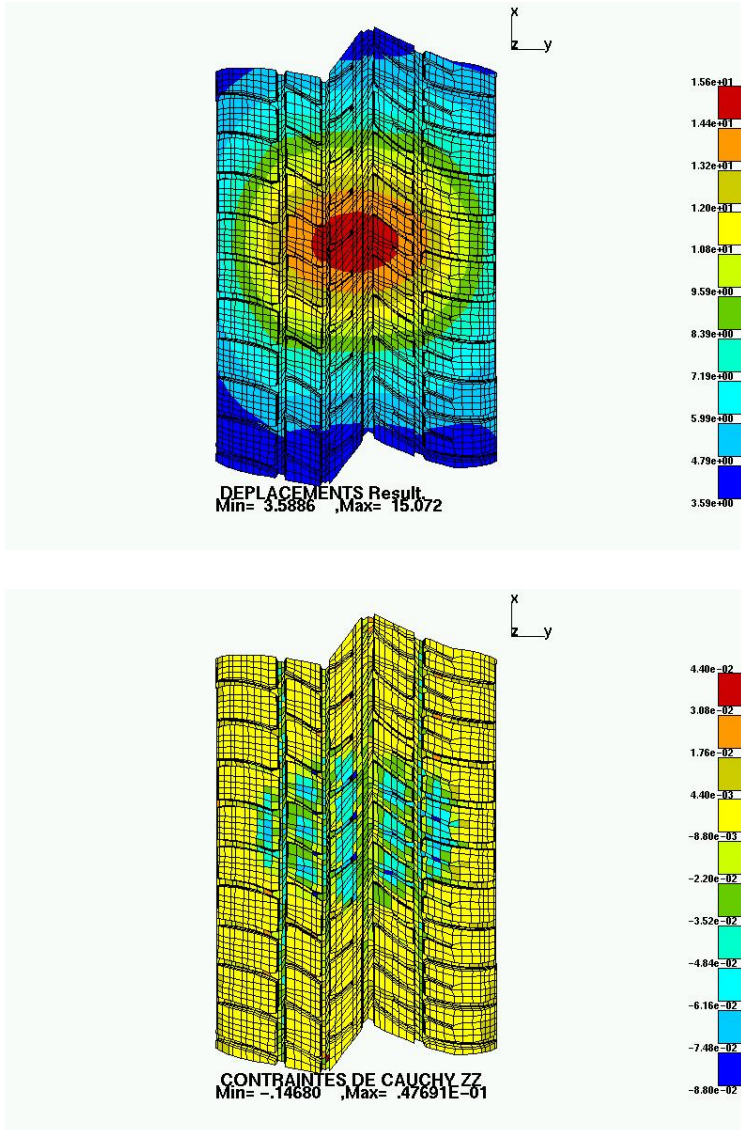


FIG. 5.5 – Cartes de déplacements et de contraintes de Cauchy σ_{zz} dans l'aire de contact d'un pain de sculpture isolé collé contre une architecture et écrasé sur le sol

à 1 km/h. Sans qu'un régime purement stationnaire soit établi, nous extrayons les pressions de contact pour le roulage adhérent des deux modèles. Les résultats sont présentés en figure 5.8. Ils confirment cette affirmation. En outre, la dynamique déterminée à partir du modèle incompatible est sensiblement moins coûteuse à calculer. En effet, on compte un nombre comparable d'itérations de Newton par pas de temps, mais pour un coût de

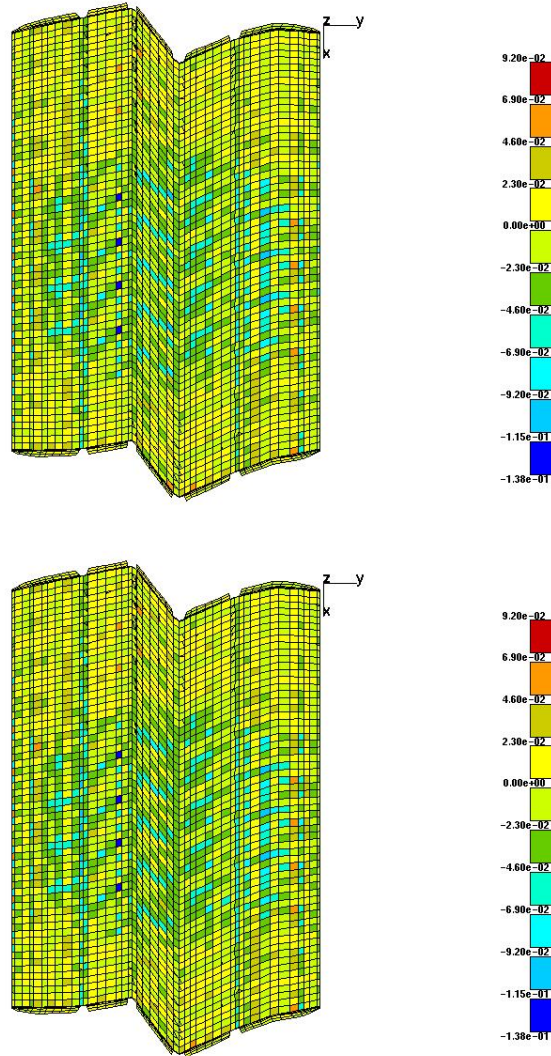


FIG. 5.6 – Contraintes σ_{zz} sur l’interface sculpture sans (en haut) et avec régularisation Hermite (en bas), en présence de multiplicateurs de Lagrange \mathbb{Q}_1 définis sur l’architecture.

16 minutes contre 34 en faveur du modèle incompatible à iso-processeur. Notons néanmoins que ce rapport de temps de calcul est inférieur au carré du rapport des degrés de liberté, en raison du fait que le modèle incompatible nécessite l’inversion d’un système non-symétrique défini positif en l’absence d’élimination préalable de la contrainte.

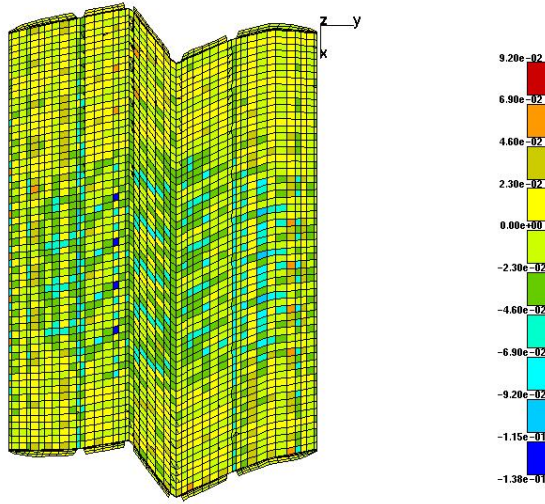


FIG. 5.7 – Contraintes σ_{zz} sur l’interface sculpture avec régularisation Hermite, en présence de multiplicateurs de Lagrange \mathbb{Q}_0 non-stabilisés définis sur l’architecture.

Remarque 5.6. *L’élimination préalable de la contrainte cinématique de recollement permettrait l’obtention d’un système symétrique défini positif, et pourrait sans doute permettre de combler le manque à gagner. En outre, dans le cadre d’une éventuelle implémentation en décomposition de domaine, le caractère symétrique défini positif du problème acquiert encore davantage d’importance. En effet, la difficulté d’une analyse complète dans le cadre non-symétrique est illustrée dans la référence [GGTN04].*

5.5 Conclusion

La présente contribution a consisté en la mise en place d’une régularisation par polynômes de Hermite de l’interface de recollement avec intégration courbe exacte de la contrainte mortier dans le cas de déplacements \mathbb{Q}_1 sur les maillages en vis-à-vis. Quitte à concéder la définition des multiplicateurs de Lagrange sur le maillage le plus grossier, cette formulation permet un gain sensible de robustesse, tout particulièrement pour des calculs stationnaires non-linéaires d’écrasement glissant ou adhérent.

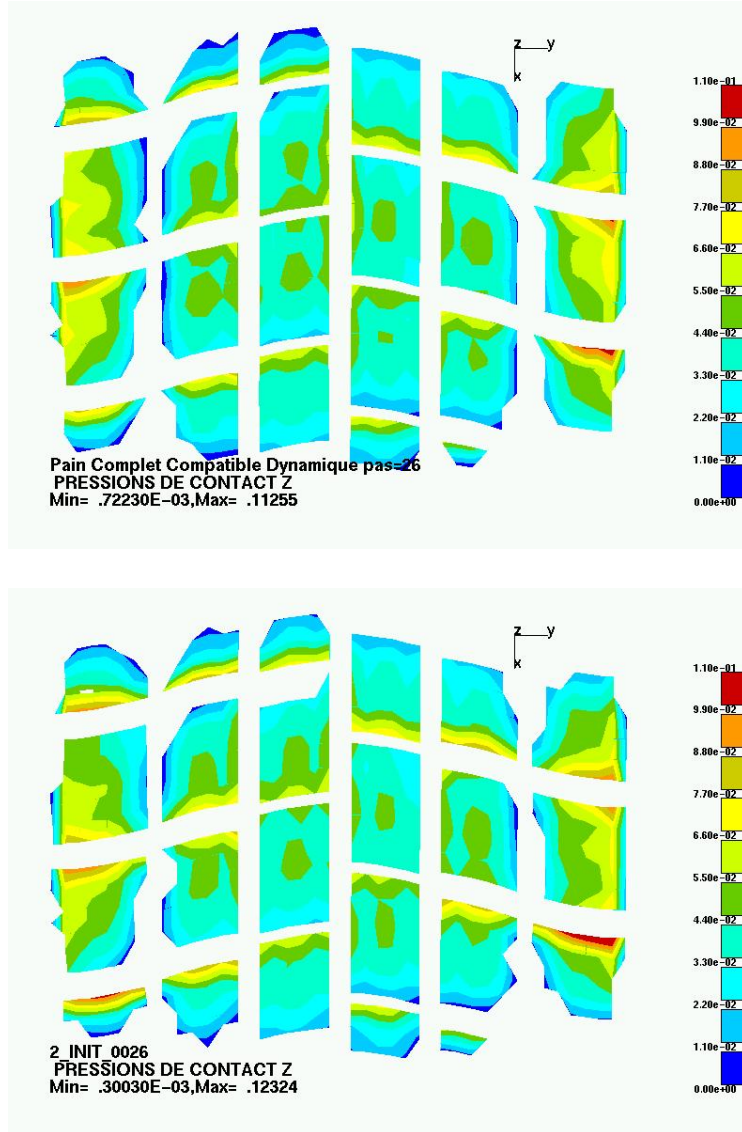


FIG. 5.8 – Cartes de pressions de contact obtenues lors du roulage à 1km/h du pneumatique présenté en section 2.4.1, pour les discrétisations compatible (240.845 noeuds), et incompatible d'un ratio 4 (128.500 noeuds,14.310 relations linéaires) déjà présentées.

Chapitre 6

Two-scale Dirichlet-Neumann preconditioners for elliptic problems with small disjoint geometric refinements on the boundary

Résumé

Dans ce chapitre, nous proposons, analysons et testons deux préconditionneurs de type Dirichlet-Neumann pour la résolution de problèmes d'élasticité sur des domaines présentant de petits détails géométriques sur leur bord, et discrétisés par une méthode de mortiers isolant ces détails. En particulier, nous montrons l'indépendance du conditionnement du système préconditionné par rapport au nombre et à la taille des détails du bord. En outre, nous introduisons pour l'un de ces préconditionneurs un espace grossier permettant de contrer l'influence de conditions aux limites essentielles sur les détails géométriques. Enfin, une méthode de quasi-Newton s'inspirant de ces préconditionneurs est proposée en présence d'élasticité non-linéaire.

Abstract

We propose, analyze and test herein two simple Dirichlet-Neumann preconditioners to solve a non-conforming mortar formulation of elasticity problems presenting small disjoint geometric refinements on the boundary. In particular, we show a two-scale property, that is the independence of the condition number of the preconditioned system in the number and the size of the small details on the boundary. On the other hand, we introduce for one of the preconditioners, a coarse space counterbalancing the effect of essential boundary conditions on the small details. Finally, a quasi-Newton method inspired by these preconditioners is proposed when dealing with nonlinear elasticity.

6.1 Introduction

The present chapter is devoted to the construction of efficient numerical procedures to solve vector elliptic problems with small geometric details on the boundary of the domain, that is where a *localized fine scale* behavior of the solution is expected. In particular, the solution in displacements $u \in \mathbb{R}^d$ of the linearized elastostatics problem will be considered, that is for $d = 2, 3$ the solution of :

$$\begin{cases} -\operatorname{div}(\mathbf{E} : \varepsilon(u)) = f, & \Omega \subset \mathbb{R}^d, \\ u = 0, & \Gamma_D, \\ (\mathbf{E} : \varepsilon(u)) \cdot n = g, & \Gamma_N, \end{cases} \quad (6.1)$$

where the linearized strain tensor is denoted by :

$$\varepsilon(u) = \frac{1}{2} (\nabla u + \nabla^t u),$$

and the fourth order tensor \mathbf{E} is assumed to be elliptic over the set of symmetric matrices :

$$\exists \alpha > 0, \forall \xi \in \mathbb{R}^{d \times d}, \xi^t = \xi, \quad (\mathbf{E} : \xi) : \xi \geq \alpha \xi : \xi.$$

In our framework, we consider that inside the disjoint subsets $(\Omega_k)_{1 \leq k \leq K}$ of Ω , the solution rapidly varies. In applications like tire developments, one could think of geometric refinements or sculptures on the boundary $\partial\Omega$. At the opposite, u slowly varies in $\Omega_0 = \Omega \setminus \overline{(\cup_{1 \leq k \leq K} \Omega_k)}$.

The strategy proposed in this chapter consists in using a non-conforming mortar formulation for (6.1) in order to decompose the physical domain into coarse and fine zones. Then, Dirichlet-Neumann preconditioners are proposed in order to solve the obtained linear system for the approximate cost of inversion of the coarse system, that is the problem set over Ω_0 . To do so, we assume that the computational cost of the solution over each

$(\Omega_k)_{1 \leq k \leq K}$ knowing the solution over Ω_0 is reasonably low when compared to the resolution over Ω_0 . For the proposed strategies, we then show a two-scale property in the sense that the condition number of the preconditioned system remains independent of the number and the size of the small subdomains.

Mortar methods have been introduced for the first time in [BMP93, BMP94] as a weak coupling between subdomains with non-conforming meshes, or between subproblems solved with different approximation methods. The main purpose was to overcome the very sub-optimal “ \sqrt{h} ” error estimate obtained with pointwise matching. The analysis of this method as a mixed formulation can be found in [Bel99]. For the present purpose, various Lagrange multipliers spaces can be indifferently adopted. For example, one can use the original formulation from [BMP93]. It is worth noticing that because of the disjoint character of the small subdomains, no modification of Lagrange multipliers is necessary on the boundary of the interfaces. Indeed, interfaces are only shared by two subdomains : the coarse one, and a fine one. The dual variant from [Woh00] can present the advantage of making the weak continuity constraint diagonal, at least in the case of plane interfaces. It is always nearly diagonal when using discontinuous stabilized Lagrange multipliers as in the previous chapter. In the case of a second order approximation in displacements, one can also adopt the proposal from [Ses98], opting for affine Lagrange multipliers. Moreover, as we have proved in the previous chapter the independence of the coercivity constant of the broken elastostatics bilinear form with respect to the number and the size of the subdomains, there is no limitation in considering here a high number of small subdomains. Indeed, the error estimates remain optimal. A brief review on the non-conforming formulation adopted to discretize (6.1) is done in section 2.

The challenge is then to develop a solver which efficiently handles such situations. In the present framework, the disymmetric roles played by the coarse subdomain and fine ones give greater importance to Dirichlet-Neumann preconditioners (see [QV99, Woh01]), rather than symmetric strategies such as Neumann-Neumann [TRV91] or FETI [FR91], studied in the mortar framework in the references [Tal93, AKP95, AMW99, AAKP99, Ste99]. In section 4, we begin by proposing a basic Dirichlet-Neumann preconditioner and prove that its quality is independent of the number and of the size of the refinements of the boundary. In this sense, we can talk of two-scale preconditioning. Nevertheless, the quality of this first preconditioner deteriorates when an essential boundary condition is imposed on such a boundary refinement. This inconvenient is overcome by considering a special coarse space taking interface rigid motions into account. An enhanced Dirichlet-Neumann preconditioner insensitive to essential boundary conditions is then obtained and analyzed. These preconditioners are tested in section 4 to confirm the previous analysis.

When considering nonlinear problems with soft geometric refinements on the boundary, it is illustrated in section 6 that such preconditioners can be used to build efficient quasi-Newton methods.

6.2 A mortar formulation

6.2.1 Continuous problem

Let $\Omega \subset \mathbb{R}^d$, be an open set partitioned into $K + 1$ subsets $(\Omega_k)_{0 \leq k \leq K}$ satisfying $\overline{\Omega} = \cup_{i=0}^K \overline{\Omega_k}$ and $\Omega_k \cap \Omega_l = \emptyset$ if $k, l \geq 1$. We denote by $\Gamma_{0k} = \overline{\Omega_0} \cap \overline{\Omega_k}$ the interface between Ω_0 and Ω_k , and the skeleton of the internal interfaces is denoted by $\mathcal{S} = \cup_{k=1}^K \Gamma_{0k}$. For the understanding of the situation, let us say that Ω_0 has slowly varying physical properties whereas the disjoint subsets $(\Omega_k)_{1 \leq k \leq K}$ have rapidly varying ones or complex geometries. Moreover, the subdomain Ω_0 has a non-empty intersection with all the sub-domains $(\Omega_k)_{1 \leq k \leq K}$. We will also assume as a simplification that the intersection between two local subdomains Ω_k , $k \geq 1$ is empty. In other words, for the time being, the inclusions are disconnected. On the part Γ_D of the boundary $\partial\Omega$, an homogeneous Dirichlet boundary condition is imposed. Concerning the coefficients of the fourth order elasticity tensor \mathbf{E} , we assume that the stress tensor is symmetric whatever the deformation in the material, namely for almost all $x \in \Omega$:

$$\forall \xi \in \mathbb{R}^{d \times d}, \xi^t = \xi, \quad \mathbf{E}(x) : \xi \text{ is a symmetric matrix.}$$

Moreover, the different materials are spectrally isotropic, namely for all $k \geq 1$, there exists two constants c_k and C_k , such that for almost all $x \in \Omega_k$:

$$\forall \xi \in \mathbb{R}^{d \times d}, \xi^t = \xi, \quad c_k \xi : \xi \leq (\mathbf{E}(x) : \xi) : \xi \leq C_k \xi : \xi. \quad (6.2)$$

For homogeneous isotropic materials, if E_k stands for the Young modulus of the material used in Ω_k , both c_k and C_k are proportional to E_k within a shape dependent constant.

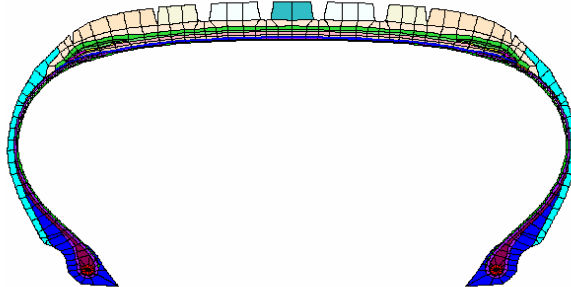


FIG. 6.1 – Example of a structure presenting small geometric refinements on its boundary.

We introduce the following spaces :

$$H_*^1(\Omega) = \{v \in H^1(\Omega)^d, v|_{\Gamma_D} = 0\},$$

$$H_*^1(\Omega_k) = \{v \in H^1(\Omega_k)^d, v|_{\Gamma_D \cap \partial\Omega_k} = 0\},$$

$$X = \left\{ v \in L^2(\Omega)^d, v_k = v|_{\Omega_k} \in H_*^1(\Omega_k), \forall k \right\} = \prod_{k=0}^K H_*^1(\Omega_k),$$

X being endowed with the H^1 broken norm :

$$\|v\|_X = \left(\sum_{k=0}^K \|v\|_{H^1(\Omega_k)^d}^2 \right)^{\frac{1}{2}},$$

and :

$$M = \prod_{k=1}^K L^2(\Gamma_{0k})^d.$$

In the whole paper, for homogeneity reason, the H^1 norm is rescaled, that is :

$$\|v\|_{H^1(\Omega_k)^d}^2 = \frac{1}{(L_k)^2} \|v\|_{L^2(\Omega_k)^d}^2 + \|\nabla v\|_{L^2(\Omega_k)^d}^2,$$

where L_k denotes the diameter of Ω_k .

We are interested in finding $u \in H_*^1(\Omega)$ such that :

$$a(u, v) = l(v), \quad \forall v \in H_*^1(\Omega), \tag{6.3}$$

where the continuous coercive bilinear form a is defined as :

$$a(u, v) = \int_{\Omega} (\mathbf{E} : \boldsymbol{\varepsilon}(u)) : \boldsymbol{\varepsilon}(v), \quad \forall u, v \in H_*^1(\Omega),$$

and the continuous linear form l as :

$$l(v) = \int_{\Omega} f \cdot v + \int_{\Gamma_N} g \cdot v, \quad \forall v \in H_*^1(\Omega),$$

with $f \in L^2(\Omega)^d$ and $g \in L^2(\Gamma_N)^d$. This problem is well-posed from Lax-Milgram lemma, by using the Korn's inequality (see [DL72]) to prove the coercivity of the bilinear form a .

6.2.2 Discretization

We introduce here a domain based non-conforming discretization of the problem using mortar elements. Under standard assumptions, well-posedness results and error estimates are reviewed below.

The mesh

For each $0 \leq k \leq K$, let us consider a family of shape regular meshes $(\mathcal{T}_{k;h_k})_{h_k>0}$ defined over each domain Ω_k , and denote :

$$h_k = \sup_{T \in \mathcal{T}_{k;h_k}} \text{diam}(T).$$

The mesh $\mathcal{T}_{0;h_0}$ defined on Ω_0 is the coarsest, i.e $h_0 > h_k$, for all $1 \leq k \leq K$, and a non-conforming family of meshes $(\mathcal{T}_h)_{h>0}$ over Ω is obtained by :

$$\mathcal{T}_h = \cup_{k=0}^K \mathcal{T}_{k;h_k}, \quad h = \max_{0 \leq k \leq K} h_k.$$

For each $1 \leq k \leq K$, Γ_{0k} inherits from the family of meshes $(\mathcal{F}_{k;\delta_k})_{\delta_k>0}$, obtained as the trace of the fine mesh $(\mathcal{T}_{k;h_k})_{h_k>0}$ over Γ_{0k} . We have adopted the notation :

$$\delta_k = \sup_{F \in \mathcal{F}_{k;\delta_k}} h(F).$$

Then, the family of meshes $(\mathcal{F}_\delta)_{\delta>0}$ can be defined over the skeleton \mathcal{S} by :

$$\mathcal{F}_\delta = \cup_{k=1}^K \mathcal{F}_{k;\delta_k}, \quad \delta = \max_{1 \leq k \leq K} \delta_k.$$

Moreover, the following assumption is made (Figure 6.2).

Assumption 6.1. $F \in \mathcal{F}_\delta$ is always an entire face of an element $T \in \mathcal{T}_h$.

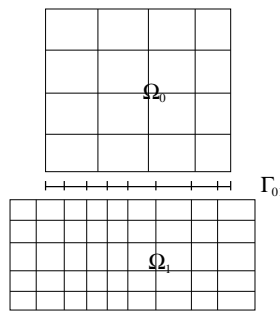


FIG. 6.2 – A situation where the mesh $\mathcal{F}_{1;\delta_1}$ of the interface Γ_{01} is inherited from the mesh $\mathcal{T}_{1;h_1}$ of Ω_1 , and where assumption 1 is violated.

Mesh-dependent spaces

We define here some mesh-dependent spaces, endowed with useful mesh-dependent norms already proposed and used in [AT95, Woh99]. For each $1 \leq k \leq K$, they are defined by :

$$\mathbb{H}_\delta^{1/2}(\Gamma_{0k}) = \{\phi \in L^2(\Gamma_{0k})^d, \|\phi\|_{\delta, \frac{1}{2}, k}^2 = \sum_{F \in \mathcal{F}_{k; \delta_k}} \frac{1}{h(F)} \|\phi\|_{L^2(F)^d}^2 < +\infty\},$$

$$\mathbb{H}_\delta^{-1/2}(\Gamma_{0k}) = \{\lambda \in L^2(\Gamma_{0k})^d, \|\lambda\|_{\delta, -\frac{1}{2}, k}^2 = \sum_{F \in \mathcal{F}_{k; \delta_k}} h(F) \|\lambda\|_{L^2(F)^d}^2 < +\infty\},$$

endowed respectively with the norms $\|\cdot\|_{\delta, \frac{1}{2}, k}$ and $\|\cdot\|_{\delta, -\frac{1}{2}, k}$. The product spaces $\mathbb{W}_\delta = \prod_{k=1}^K \mathbb{H}_\delta^{1/2}(\Gamma_{0k})$ and $\mathbb{M}_\delta = \prod_{k=1}^K \mathbb{H}_\delta^{-1/2}(\Gamma_{0k})$, are then respectively endowed with the norms :

$$\begin{aligned} \|\phi\|_{\delta, \frac{1}{2}} &= \left(\sum_{k=1}^K \|\phi\|_{\delta, \frac{1}{2}, k}^2 \right)^{1/2}, \\ \|\lambda\|_{\delta, -\frac{1}{2}} &= \left(\sum_{k=1}^K \|\lambda\|_{\delta, -\frac{1}{2}, k}^2 \right)^{1/2}. \end{aligned}$$

They can be viewed as dual spaces by means of the the L^2 inner product :

$$\int_S \phi \cdot \lambda \leq \|\lambda\|_{\delta, -\frac{1}{2}} \|\phi\|_{\delta, \frac{1}{2}}, \quad \forall (\phi, \lambda) \in \mathbb{W}_\delta \times \mathbb{M}_\delta.$$

Remark 6.1. *The use of such mesh-dependent spaces instead of $H_{00}^{1/2}(\Gamma_{0k})^d$ and its dual $H^{-1/2}(\Gamma_{0k})^d = (H_{00}^{1/2}(\Gamma_{0k})^d)'$ for example, has several advantages. First, these mesh-dependent norms are computable, which make easier a posteriori estimations (see [Woh99]) and penalized formulations (see the previous chapter). Moreover, their use enables to avoid some technical difficulties for 3D problems.*

Non-conforming approximation

Let us introduce the discrete subspaces of degree q inside each subdomain :

$$X_{k; h_k} = \{p \in H_*^1(\Omega_k) \cap \mathcal{C}^0(\Omega_k)^d, \quad p|_T \in \mathcal{P}_q(T), \forall T \in \mathcal{T}_{k; h_k}\} \oplus \mathcal{B}_{k; h_k},$$

with $\mathcal{P}_q = [\mathbb{P}_q]^d$ or $[\mathbb{Q}_q]^d$, where \mathbb{P}_q (resp. \mathbb{Q}_q) is the space of polynomials of total (resp. partial) degree q , and where we have introduced a possible stabilization space $\mathcal{B}_{k; h_k}$ built with bubbles on the interface as in [BM00] or in the previous chapter. The corresponding product space is denoted by :

$$X_h = \prod_{k=0}^K X_{k; h_k} \subset X.$$

Let us define the following trace spaces on the non-mortar side (small subdomain side herein) :

$$W_{k;\delta_k} = \{p|_{\Gamma_{0k}}, p \in X_{k;h_k}\}, \quad W_{k;\delta_k}^0 = W_{k;\delta_k} \cap H_0^1(\Gamma_{0k})^d,$$

endowed with the mesh-dependent norm $\|\cdot\|_{\delta,\frac{1}{2},k}$.

In order to formulate the weak continuity constraint, we introduce the spaces $M_{k;\delta_k}$ of (possibly discontinuous) Lagrange multipliers defined on the meshes $\mathcal{F}_{k;\delta_k}$. In order to achieve optimal approximation, they must contain all polynomials $[\mathbb{P}_{q-1}]^d$ of degree $q-1$. The product space $M_\delta = \prod_{k=1}^K M_{k;\delta_k}$ is endowed with the mesh-dependent norm $\|\cdot\|_{\delta,-\frac{1}{2}}$. The following bilinear form is then introduced to express the constraint on the jump of the displacements on the non-conforming interfaces :

$$\begin{aligned} b : \quad X \times M &\rightarrow \mathbb{R} \\ (v, \lambda) &\mapsto b(v, \lambda) = \sum_{k=1}^K \int_{\Gamma_{0k}} [v_k] \cdot \lambda_k, \end{aligned}$$

with $[v_k] = v_0 - v_k$, on Γ_{0k} . We denote :

$$\begin{aligned} b(v, \lambda) &= \sum_{k=1}^K \int_{\Gamma_{0k}} v_0 \cdot \lambda_k - \sum_{k=1}^K \int_{\Gamma_{0k}} v_k \cdot \lambda_k \\ &:= \sum_{k=1}^K b_{0k}(v_0, \lambda_k) - \sum_{k=1}^K b_k(v_k, \lambda_k). \end{aligned}$$

Then, the constrained space of admissible displacements can be defined as :

$$V_h = \{u_h \in X_h, \quad b(u_h, \lambda_h) = 0, \quad \forall \lambda_h \in M_\delta\}.$$

In order to formulate the approximate problem, the broken elliptic form \tilde{a} is defined as :

$$\begin{aligned} \tilde{a} : \quad X \times X &\rightarrow \mathbb{R} \\ (u, v) &\mapsto \tilde{a}(u, v) = \sum_{k=0}^K a_k(u_k, v_k), \end{aligned}$$

with :

$$a_k(u_k, v_k) = \int_{\Omega_k} (\mathbf{E} : \boldsymbol{\varepsilon}(u_k)) : \boldsymbol{\varepsilon}(v_k).$$

We are then interested in finding $(u_h, \lambda_h) \in X_h \times M_\delta$, such that :

$$\begin{cases} \tilde{a}(u_h, v_h) + b(v_h, \lambda_h) = l(v_h), & \forall v_h \in X_h, \\ b(u_h, \mu_h) = 0, & \forall \mu_h \in M_\delta. \end{cases} \quad (6.4)$$

In other words, we solve our variational problem on the product space X_h under the kinematic continuity constraint $b(\cdot, \cdot) = 0$.

Fundamental assumptions and error estimates

In order to ensure the well-posedness of the problem (6.4), some fundamental assumptions have to be made. Concerning the compatibility of X_h and M_δ , we assume :

Assumption 6.2. *For each $1 \leq k \leq K$, there exists an operator :*

$$\pi_k : \mathbb{H}_\delta^{1/2}(\Gamma_{0k}) \rightarrow W_{k;\delta_k},$$

such that for all $v \in \mathbb{H}_\delta^{1/2}(\Gamma_{0k})$:

$$\int_{\Gamma_{0k}} (\pi_k v) \cdot \mu = \int_{\Gamma_{0k}} v \cdot \mu, \quad \forall \mu \in M_{k;\delta_k},$$

with :

$$\|\pi_k v\|_{\delta, \frac{1}{2}, k} \leq C \|v\|_{\delta, \frac{1}{2}, k}.$$

This assumption means that the projection perpendicular to the multiplier space onto the trace space $W_{k;\delta_k}$ is continuous. It implies a limitation on the size of M_δ with respect to X_h . If more than two subdomains had a common intersection, the range $W_{k;\delta_k}$ of π_k in assumption 6.2 would be replaced by $W_{k;\delta_k}^0$, in order to enable independent projections on each interface.

The coercivity of \tilde{a} over $V_h \times V_h$ is obtained under the following assumption introduced in the previous chapter :

Assumption 6.3. *For all $1 \leq k \leq K$, we assume that there exists a subspace \tilde{M}_k of the Lagrange multipliers space $M_{k;\delta_k}$ such that $\tilde{M}_k \subset M_{k;\delta_k}$ independently of δ_k . Moreover, we assume that for all $v \in X$ which is locally a rigid motion over all the $(\Omega_k)_{k \geq 1}$ in the sense that :*

$$\tilde{a}(v, w) = 0, \quad \forall w \in X,$$

and satisfying :

$$\int_{\Gamma_{0k}} [v] \cdot \mu = 0, \quad \forall \mu \in \tilde{M}_k, \quad k = 1, \dots, K,$$

then $v = 0$.

Various pairs of spaces $X_h \times M_\delta$ can be chosen to satisfy the assumptions 6.2 and 6.3 :

- The initial formulation from [BMP93, BMP94] proposes discrete displacements of degree q without stabilization, i.e. $\mathcal{B}_{k;h_k} = \emptyset$, and continuous Lagrange multipliers of degree q . In our framework, no modification of the Lagrange multipliers is necessary on the boundaries of the interfaces $(\partial\Gamma_{0k})_{1 \leq k \leq K}$ because they are disjoint. Therefore, with this choice, the displacements trace spaces over the fine subdomains interfaces coincides with Lagrange multipliers spaces, that is $M_{k;\delta_k} = W_{k;\delta_k}$ for all $1 \leq k \leq K$.

- In order to make the mortar weak continuity constraint diagonal, one can adopt the dual Lagrange multipliers from Wohlmuth [Woh00], again without special treatment on the boundaries of the interfaces.
- As shown in [Ses98] for second order approximations of the displacements ($q \geq 2$), the formulation from [BMP93, BMP94] can be modified by using only continuous Lagrange multipliers of degree $q - 1$.
- Discrete displacements of degree q with a proper stabilization are compatible with discontinuous Lagrange multipliers of degree $q - 1$, as proved in the previous chapter, and detailed in the previous chapter.

In this framework, we have proved in propositions 4.5 and 4.6 from chapter 4, the :

Proposition 6.1. *Under assumptions 6.2 and 6.3, the problem (6.4) is well-posed. Moreover, if $u \in \prod_{k=0}^K H^{q+1}(\Omega_k)^d$ is solution of (6.3) with $(\mathbf{E} : \varepsilon(u)) \in \prod_{k=0}^K H^q(\Omega_k)^{d \times d}$ in which $q \geq 1$, and $(u_h, \lambda_h) \in X_h \times M_\delta$ is solution of (6.4), the following error estimates hold :*

$$\begin{aligned} \|u - u_h\|_X &\leq C \left(\sum_{k=1}^K h_k^{2q} |u|_{q+1, \mathbf{E}, \Omega_k}^2 \right)^{1/2}, \\ \|\lambda - \lambda_h\|_{\delta, -\frac{1}{2}} &\leq C \left(\sum_{k=0}^K h_k^{2q} |u|_{q+1, \mathbf{E}, \Omega_k}^2 \right)^{1/2}, \end{aligned}$$

with :

$$|u|_{q+1, \mathbf{E}, \Omega_k}^2 = |u|_{H^{q+1}(\Omega_k)^d}^2 + \frac{1}{C_k^2} \|\mathbf{E} : \varepsilon(u)\|_{H^q(\Omega_k)^{d \times d}}^2.$$

We have denoted the flux over the artificial interfaces by $\lambda = (\mathbf{E} : \varepsilon(u)) \cdot n$, where the normal outward unit vector on $\partial\Omega_0$ is denoted by n . C denotes various constants independent of the decomposition into subdomains and of the discretization.

Remark 6.2 (Choice of the non-mortar side). *In this discretization, as confirmed by assumption 6.2, we have chosen the non-mortar side defining the multipliers as the fine scale side of the interface \mathcal{S} . The main motivation is that in the preconditioners to be defined later, it is crucial to get a stable extension operator over the small scale subdomains, which is the case with the present choice while compatible with the standard assumption 6.1.*

6.3 Two-scale preconditioners.

The previous discretization leads to a well-posed linear discrete problem with optimal error estimates. In this section, we propose and analyze preconditioners to solve this linear system for the approximate computational cost of the coarse scale problem on Ω_0 , provided the solution of the problem over each $(\Omega_k)_{1 \leq k \leq K}$ be at a reasonably low-cost. That is

why we have assumed that the $(\Omega_k)_{1 \leq k \leq K}$ were small and disjoint. Then, the inversions of the fine scale problems on the boundary can be parallelized and are relatively cheap in terms of computation.

Some notation and remarks must first be introduced :

- In this section, all quantities live in finite dimensional spaces. If a is a bilinear form, then \mathbf{A} represents the matrix of a in the discrete space. If u is a function, then U is the vector of its nodal degrees of freedom in the chosen discrete space.
- For all $0 \leq k \leq K$, the bilinear form $a_k(\cdot, \cdot)$ is continuous in $H^1(\Omega_k)^d \times H^1(\Omega_k)^d$ and its continuity constant is C_k , already defined in (6.2).
- When $\Gamma_D \cap \partial\Omega_0$ has a positive measure, $a_0(\cdot, \cdot)$ is coercive in $H_*^1(\Omega_0) \times H_*^1(\Omega_0)$. We denote by α_0 its constant of coercivity, which is proportional to c_0 defined in (6.2), within a shape dependent constant.
- For all $1 \leq k \leq K$ such that Ω_k is fixed on a part of its boundary, the bilinear form $a_k(\cdot, \cdot)$ is coercive over $H_*^1(\Omega_k) \times H_*^1(\Omega_k)$ and its coercivity constant is denoted by α_k . It is proportional to c_k defined in (6.2), within a constant which depends continuously on the shape of Ω_k but not of its size because a_k and the scaled norm of H^1 have the same dependence with respect to a change of scale.

6.3.1 Introduction

With obvious notation, the discrete problem (6.4) leads to the following linear system to solve :

$$\begin{cases} \mathbf{A}_0 U_0 + \sum_{k=1}^K \mathbf{B}_{0k}^t \Lambda_k = F_0, \\ \mathbf{A}_k U_k - \mathbf{B}_k^t \Lambda_k = F_k, \quad 1 \leq k \leq K, \\ \mathbf{B}_{0k} U_0 - \mathbf{B}_k U_k = 0, \quad 1 \leq k \leq K. \end{cases} \quad (6.5)$$

Defining the local extended stiffness matrix of the k -th ($k \geq 1$) subproblem by :

$$\mathbf{K}_k = \begin{pmatrix} \mathbf{A}_k & -\mathbf{B}_k^t \\ -\mathbf{B}_k & 0 \end{pmatrix},$$

the problem (6.5) can be rewritten as :

$$\begin{cases} \mathbf{A}_0 U_0 + \sum_{k=1}^K \mathbf{B}_{0k}^t \Lambda_k = F_0, \\ \mathbf{K}_k \begin{pmatrix} U_k \\ \Lambda_k \end{pmatrix} = \begin{pmatrix} F_k \\ -\mathbf{B}_{0k} U_0 \end{pmatrix}, \quad 1 \leq k \leq K. \end{cases} \quad (6.6)$$

The operator R_k of matrix $\begin{pmatrix} 0, I_{M_k; \delta_k} \end{pmatrix}$ is defined as the canonical restriction from $X_{k; h_k} \times M_{k; \delta_k}$ to $M_{k; \delta_k}$, and therefore, from (6.6), we can obtain Λ_k as a function of U_0 as :

$$\Lambda_k = R_k \mathbf{K}_k^{-1} \begin{pmatrix} F_k \\ -\mathbf{B}_{0k} U_0 \end{pmatrix} = R_k \mathbf{K}_k^{-1} \begin{pmatrix} F_k \\ 0 \end{pmatrix} - R_k \mathbf{K}_k^{-1} R_k^t \mathbf{B}_{0k} U_0.$$

Then, by elimination of Λ_k in the coarse scale problem, (6.6) becomes :

$$\begin{cases} \left(\mathbf{A}_0 - \sum_{k=1}^K \mathbf{B}_{0k}^t R_k \mathbf{K}_k^{-1} R_k^t \mathbf{B}_{0k} \right) U_0 = F_0 - \sum_{k=1}^K \mathbf{B}_{0k}^t R_k \mathbf{K}_k^{-1} \begin{pmatrix} F_k \\ 0 \end{pmatrix}, \\ \mathbf{K}_k \begin{pmatrix} U_k \\ \Lambda_k \end{pmatrix} = \begin{pmatrix} F_k \\ -\mathbf{B}_{0k} U_0 \end{pmatrix}, \quad 1 \leq k \leq K, \end{cases} \quad (6.7)$$

which can be re-written as :

$$\begin{cases} \mathbf{D}_0 U_0 = \overline{F}_0, \\ \mathbf{K}_k \begin{pmatrix} U_k \\ \Lambda_k \end{pmatrix} = \begin{pmatrix} F_k \\ -\mathbf{B}_{0k} U_0 \end{pmatrix}, \quad 1 \leq k \leq K. \end{cases} \quad (6.8)$$

Here, $\mathbf{D}_0 = \mathbf{A}_0 - \sum_{k=1}^K \mathbf{B}_{0k}^t R_k \mathbf{K}_k^{-1} R_k^t \mathbf{B}_{0k}$ is the Schur complement matrix. The problem is now split into a coarse problem defined on Ω_0 , and into fine problems defined on $(\Omega_k)_{1 \leq k \leq K}$ using the coarse solution U_0 . It seems that the calculus on the subdomains are now separated, but the price to pay is in the building of the coarse Schur complement \mathbf{D}_0 . Our aim is to obtain a good preconditioner for this problem, using an approximate coarse operator $\hat{\mathbf{D}}_0$. In other terms, we need to construct an approximate solution $(\tilde{u}, \tilde{\lambda}) \in X_h \times M_\delta$ of (6.8) by :

$$\begin{cases} \tilde{U}_0 = \hat{\mathbf{D}}_0^{-1} \overline{F}_0, \\ \mathbf{K}_k \begin{pmatrix} \tilde{U}_k \\ \tilde{\lambda}_k \end{pmatrix} = \begin{pmatrix} F_k \\ -\mathbf{B}_{0k} \tilde{U}_0 \end{pmatrix}, \quad 1 \leq k \leq K, \end{cases} \quad (6.9)$$

and the main issue is to build an appropriate definition of the Schur inverse $\hat{\mathbf{D}}_0^{-1}$.

6.3.2 Two possible definitions for $\hat{\mathbf{D}}_0$

A symmetrized Dirichlet-Neumann preconditioner

The simplest idea consists in replacing the Schur complement \mathbf{D}_0 by the stiffness of the coarse problem :

$$\hat{\mathbf{D}}_0 = \mathbf{A}_0, \quad (6.10)$$

which reduces the proposed preconditioning to a symmetrized Dirichlet-Neumann iteration. Indeed, solving (6.9) then amounts to solving :

1. Dirichlet problems on the $(\Omega_k)_{1 \leq k \leq K}$ with zero weak trace on the interface to obtain

$$\overline{F}_0 = F_0 - \sum_{k=1}^K \mathbf{B}_{0k}^t R_k \mathbf{K}_k^{-1} \begin{pmatrix} F_k \\ 0 \end{pmatrix},$$

2. a Neumann problem on Ω_0 with the sollicitation \overline{F}_0 to compute U_0 ,

3. Dirichlet problems on the $(\Omega_k)_{1 \leq k \leq K}$ to compute the $(U_k)_{1 \leq k \leq K}$ with right-hand sides

$$\begin{pmatrix} F_k \\ -\mathbf{B}_{0k} U_0 \end{pmatrix}.$$

In section 3.3, we prove that the condition number of the associated preconditioned system is independent of the number and of the size of the fine scale subdomains $(\Omega_k)_{k \geq 1}$. We also prove that the method is efficient when Ω_0 has not a small stiffness in comparison with the $(\Omega_k)_{k \geq 1}$, and when the small subdomains are not fixed on a part of their boundary.

An enhanced symmetrized Dirichlet-Neumannnn preconditioner

The previous simplest choice of preconditioner may lack of efficiency in two simple situations :

- the substructure Ω_k is of small size and is fixed on a part of its boundary. In this situation, because of its size, the substructure will have a rather large stiffness to interface rigid body displacements.
- the substructure Ω_k may have other privileged directions of large stiffness to interface motions (rigid links, incompressibility).

Assuming that these directions of interface localized stiffness be in very small number N_k (this is indeed the case for interface rigid body motions), we propose a modification of the previous preconditioner enabling to correct such a lack of efficiency.

For all $k \geq 1$ such that Ω_k is fixed on a part of its boundary, we denote by $(e_k^i)_{1 \leq i \leq N_k}$ (with $N_k = 6$ in general) the interface rigid motions of Γ_{0k} or rigid links and introduce :

$$\mathring{W}_k = \text{span}\{e_k^i, i = 1, \dots, N_k\}.$$

To each interface rigid body motion e_k^i , we introduce its local a_k -harmonic extension $(u_k^i, \lambda_k^i) \in X_{k;h_k} \times M_{k;\delta_k}$ solution of :

$$\begin{cases} a_k(v, u_k^i) - \int_{\Gamma_{0k}} v \cdot \lambda_k^i = 0, & \forall v \in X_{k;h_k}, \\ - \int_{\Gamma_{0k}} u_k^i \cdot \mu = - \int_{\Gamma_{0k}} e_k^i \cdot \mu, & \forall \mu \in M_{k;\delta_k}. \end{cases} \quad (6.11)$$

These solutions span two small local spaces :

$$\mathring{X}_k = \text{span}\{u_k^i, i = 1, \dots, N_k\} \subset X_{k;h_k},$$

$$\mathring{M}_k = \text{span}\{\lambda_k^i, i = 1, \dots, N_k\} \subset M_{k;\delta_k}.$$

If $k \geq 1$ is such that Ω_k is not fixed on its boundary, we adopt :

$$\mathring{W}_k = \mathring{M}_k = \{0\}.$$

Then, instead of finding U_0 such that $\mathbf{D}_0 U_0 = \overline{F_0}$, we propose to compute $u_0 \in X_{0;h_0}$, $(u_k) \in (\dot{X}_k)_{1 \leq k \leq K}$, $(\lambda_k) \in (\dot{M}_k)_{1 \leq k \leq K}$ solution of the coupled problem :

$$\begin{cases} a_0(u_0, v_0) + \sum_{k=1}^K \int_{\Gamma_{0k}} v_0 \cdot \lambda_k = \overline{l_0}(v_0), & \forall v_0 \in X_{0;h_0}, \\ a_k(u_k, v_k) - \int_{\Gamma_{0k}} v_k \cdot \lambda_k = 0, & \forall v_k \in \dot{X}_k, \quad 1 \leq k \leq K, \\ - \int_{\Gamma_{0k}} u_k \cdot \mu_k = - \int_{\Gamma_{0k}} u_0 \cdot \mu_k, & \forall \mu_k \in \dot{M}_k, \quad 1 \leq k \leq K, \end{cases} \quad (6.12)$$

where $\overline{l_0}$ is the linear form associated to the coarse sollicitation $\overline{F_0}$.

We introduce the matrix $\mathbf{I}_{0k} \in \mathbb{R}^{N_k \times \dim X_{0;h_0}}$ defined for all $v_0 \in X_{0;h_0}$ by :

$$(\mathbf{I}_{0k} V_0)_i = \int_{\Gamma_{0k}} v_0 \cdot \lambda_k^i = \langle \mathbf{B}_{0k} V_0, \Lambda_k^i \rangle, \quad \forall i = 1, \dots, N_k,$$

that is $\mathbf{I}_{0k} = [\Lambda_k^1, \dots, \Lambda_k^{N_k}]^t \mathbf{B}_{0k} = \Lambda_k^t \mathbf{B}_{0k}$, and the restriction $\dot{\mathbf{A}}_k$ of the displacement stiffness matrix \mathbf{A}_k on the local space \dot{X}_k . Thus :

$$(\dot{\mathbf{A}}_k)_{ij} = (U_k^i)^t \mathbf{A}_k U_k^j = a_k(u_k^j, u_k^i) = \int_{\Gamma_{0k}} u_k^j \cdot \lambda_k^i.$$

From (6.11)-1, the system (6.12) can be rewritten as :

$$\begin{cases} \mathbf{A}_0 U_0 + \sum_{k=1}^K \mathbf{I}_{0k}^t \Theta_k = \overline{F_0}, \\ \dot{\mathbf{A}}_k Z_k - \dot{\mathbf{A}}_k^t \Theta_k = 0, \\ -\dot{\mathbf{A}}_k Z_k = -\mathbf{I}_{0k} U_0, \quad 1 \leq k \leq K. \end{cases} \quad (6.13)$$

The new vector Θ_k (resp. Z_k) denotes the component of λ_k (resp. u_k) in \dot{M}_k (resp. \dot{W}_k) appearing in (6.12). From the elimination of Θ_k and Z_k in (6.13), it follows that :

$$\hat{\mathbf{D}}_0 U_0 = \overline{F_0}, \quad (6.14)$$

with a new approximate Schur complement given by :

$$\begin{aligned} \hat{\mathbf{D}}_0 &= \mathbf{A}_0 + \sum_{k=1}^K \mathbf{I}_{0k}^t \dot{\mathbf{A}}_k^{-t} \mathbf{I}_{0k} \\ &= \mathbf{A}_0 + \sum_{k=1}^K \mathbf{B}_{0k}^t \Lambda_k \dot{\mathbf{A}}_k^{-t} \Lambda_k^t \mathbf{B}_{0k}. \end{aligned} \quad (6.15)$$

Its complexity is much smaller than (6.7) because the local problem (6.13)-2,(6.13)-3 for the subproblem $k \geq 1$ is of dimension N_k .

For analysis purpose, this enhanced Dirichlet-Neumann preconditioner corresponds to a Dirichlet-Neumann decomposition where the Dirichlet substructures are defined by :

$$\dot{X}_{k;h_k}^\perp = \{u_k \in X_{k;h_k}, \quad \int_{\Gamma_{0k}} u_k \cdot \mu = 0, \quad \forall \mu \in \dot{M}_k\}, \quad 1 \leq k \leq K,$$

and where the Neumann substructure is defined by :

$$\dot{X}_h = \{u \in X_h, \quad b(u, \mu) = 0, \quad \forall \mu \in \dot{M}_k\}.$$

The analysis of this preconditioner is done in section 4.3, proving now an independence with respect to essential boundary conditions imposed over the small subdomains $(\Omega_k)_{k \geq 1}$. For further analysis, we introduce :

Definition 6.1. For any $v_0 \in X_{0;h_0}$, its “rigid body projection” over Ω_k denoted by $\dot{\pi}_k v_0 \in \dot{X}_k$ is defined as the solution of (6.13)-2,(6.13)-3 for the subproblem k . More precisely $(\dot{\pi}_k v_0, \dot{\lambda}_k) \in \dot{X}_k \times \dot{M}_k$ is such that :

$$\begin{cases} a_k(\dot{\pi}_k v_0, v_k) - \int_{\Gamma_{0k}} \dot{\lambda}_k \cdot v_k = 0, & \forall v_k \in \dot{X}_k, \\ - \int_{\Gamma_{0k}} \dot{\pi}_k v_0 \cdot \mu_k = - \int_{\Gamma_{0k}} v_0 \cdot \mu_k, & \forall \mu_k \in \dot{M}_k. \end{cases} \quad (6.16)$$

In matricial form, we have $\dot{\pi}_k v_0 = \sum_{j=1}^{N_k} z_j u_k^j$ with :

$$-\dot{\mathbf{A}}_k Z = -\mathbf{I}_{0k} V_0,$$

yielding :

$$\dot{\Pi}_k V_0 = \left[U_k^1, \dots, U_k^{N_k} \right] \dot{\mathbf{A}}_k^{-1} \mathbf{I}_{0k} V_0 = \dot{\mathbf{U}}_k \dot{\mathbf{A}}_k^{-1} \mathbf{I}_{0k} V_0,$$

that is :

$$\dot{\Pi}_k = \dot{\mathbf{U}}_k \dot{\mathbf{A}}_k^{-1} \mathbf{I}_{0k}.$$

We then have by construction of $\dot{\mathbf{A}}_k$:

$$\begin{aligned} \dot{\Pi}_k^t \mathbf{A}_k \dot{\Pi}_k &= \mathbf{I}_{0k}^t \dot{\mathbf{A}}_k^{-t} \dot{\mathbf{U}}_k^t \mathbf{A}_k \dot{\mathbf{U}}_k \dot{\mathbf{A}}_k^{-1} \mathbf{I}_{0k} \\ &= \mathbf{I}_{0k}^t \dot{\mathbf{A}}_k^{-t} \dot{\mathbf{A}}_k \dot{\mathbf{A}}_k^{-1} \mathbf{I}_{0k} \\ &= \mathbf{I}_{0k}^t \dot{\mathbf{A}}_k^{-t} \mathbf{I}_{0k}, \end{aligned}$$

and therefore the new preconditioner (6.15) takes the form :

$$\hat{\mathbf{D}}_0 = \mathbf{A}_0 + \sum_{k=1}^K \dot{\Pi}_k^t \mathbf{A}_k \dot{\Pi}_k. \quad (6.17)$$

Also observe from (6.11) that when a_k is symmetric, we have :

$$\dot{\pi}_k e_k^i = u_k^i, \quad 1 \leq i \leq N_k. \quad (6.18)$$

6.4 Condition number analysis

In this section, we establish upper bounds on the condition number of the preconditioned systems based on the two symmetrized Dirichlet-Neumann preconditioners respectively defined in the subsections 6.3.2 and 6.3.2. First, the same factorized form for the original linear system and the preconditioner is introduced. Then, we show the spectral equivalence between $\hat{\mathbf{D}}_0$ and \mathbf{D}_0 , detailing the dependence of the constants on the size of the domains, the stiffness of the materials, and on the mesh sizes, and deduce estimates on the condition number of the preconditioned system.

6.4.1 Factorization

The original system to solve is :

$$\mathbf{A} \begin{pmatrix} U_0 \\ U_1 \\ \Lambda_1 \\ \vdots \\ U_K \\ \Lambda_K \end{pmatrix} = \begin{pmatrix} F_0 \\ F_1 \\ 0 \\ \vdots \\ F_K \\ 0 \end{pmatrix},$$

with :

$$\mathbf{A} = \begin{pmatrix} \mathbf{A}_0 & 0 & \mathbf{B}_{01}^t & \dots & 0 & \mathbf{B}_{0K}^t \\ 0 & \mathbf{A}_1 & -\mathbf{B}_1^t & & & \\ \mathbf{B}_{01} & -\mathbf{B}_1 & 0 & & & \\ \vdots & & & \ddots & & \\ 0 & & & & \mathbf{A}_K & -\mathbf{B}_K^t \\ \mathbf{B}_{0K} & & & & -\mathbf{B}_K & 0 \end{pmatrix}.$$

Now, let us factorize the expression of \mathbf{A} . Introducing the triangular matrix :

$$T = \begin{pmatrix} I & 0 & \dots & 0 \\ \mathbf{K}_1^{-1} R_1^t \mathbf{B}_{01} & I & & \\ \vdots & & \ddots & \\ \mathbf{K}_K^{-1} R_K^t \mathbf{B}_{0K} & 0 & \dots & I \end{pmatrix},$$

and the block diagonal matrix :

$$H = \begin{pmatrix} \mathbf{D}_0 & 0 & \dots & 0 \\ 0 & \mathbf{K}_1 & & \\ \vdots & & \ddots & \\ 0 & & & \mathbf{K}_K \end{pmatrix},$$

it is straightforward to check that $\mathbf{A} = T^t H T$.

The matrix of our preconditioner can be written under the similar form $\mathbf{C} = T^t \hat{H} T$, with the block diagonal matrix :

$$\hat{H} = \begin{pmatrix} \hat{\mathbf{D}}_0 & 0 & \dots & 0 \\ 0 & \mathbf{K}_1 & & \\ \vdots & & \ddots & \\ 0 & & & \mathbf{K}_K \end{pmatrix}.$$

We have then :

$$\mathbf{C} \begin{pmatrix} \tilde{U}_0 \\ \tilde{U}_1 \\ \tilde{\Lambda}_1 \\ \vdots \\ \tilde{U}_K \\ \tilde{\Lambda}_K \end{pmatrix} = \begin{pmatrix} F_0 \\ F_1 \\ 0 \\ \vdots \\ F_K \\ 0 \end{pmatrix}.$$

The matrices \mathbf{A} and \mathbf{C} are not positive, and we introduce the kernel on which the following results hold, and in which \mathbf{A} and \mathbf{C} are definite positive :

$$E = \{U = (U_0, U_1, \Lambda_1, \dots, U_K, \Lambda_K)^t; \mathbf{B}_{0k} U_0 = \mathbf{B}_k U_k, 1 \leq k \leq K\}.$$

Our aim is to bound the condition number $\kappa_{\mathbf{A}, E}(\mathbf{C}^{-1} \mathbf{A})$ in \mathbf{A} -norm on E .

6.4.2 Spectral equivalence for the simple Dirichlet-Neumann

We show herein the spectral equivalence between the Schur complement \mathbf{D}_0 and its approximation $\hat{\mathbf{D}}_0$ for the symmetrized Dirichlet-Neumann preconditioner presented in subsection 6.3.2. For the choice $\hat{\mathbf{D}}_0 = \mathbf{A}_0$ made in section 6.3.2 and corresponding to the simple symmetrized Dirichlet-Neumann preconditioner, we obtain :

Proposition 6.2. *Assuming that \mathbf{A}_0 is invertible that is $\Gamma_D \cap \partial\Omega_0$ has a positive measure, the following spectral equivalence holds for all U_0 :*

$$W_{1,h} \langle \mathbf{D}_0 U_0, U_0 \rangle \leq \langle \mathbf{A}_0 U_0, U_0 \rangle \leq \langle \mathbf{D}_0 U_0, U_0 \rangle,$$

with :

$$\frac{1}{W_{1,h}} = 1 + C \left(\max_{k \in I_1} \frac{C_k}{c_0} + \max_{k \in I_2} \frac{C_k L_0}{\alpha_0 L_k} \right),$$

where I_1 (resp. I_2) is the set of indices $k \geq 1$ such that Ω_k is not fixed on its boundary (resp. is fixed on a part of its boundary). The constant C is independent of the number K and the size of the subdomains.

Observe that the condition number deteriorates for a small fixed subdomain $L_k \ll L_0$, $k \in I_2$, and for very stiff subdomains $C_k \gg \alpha_0$.

The following lemma is needed in the proof :

Lemma 6.1. *Let us assume that Γ_{0k} is of class C^1 . Then, there exists an open set $\Omega'_k \subset \Omega_0$ which is the restriction of a neighborhood of Γ_{0k} to Ω_0 , and a linear extension operator :*

$$\mathcal{D}_k : H^1(\Omega'_k)^d \rightarrow H^1(\Omega_k)^d,$$

such that for all $u \in H^1(\Omega_0)^d$, $\mathcal{D}_k u = u$ on Γ_{0k} , and :

$$\int_{\Omega_k} (\mathcal{D}_k u)^2 \leq C \int_{\Omega'_k} u^2,$$

$$\int_{\Omega_k} (\nabla \mathcal{D}_k u)^2 \leq C \int_{\Omega'_k} (\nabla u)^2,$$

where the constant C does not depend on Ω_k .

The proof of this lemma is rather standard in functional analysis, and the existence of such an extension operator can be found in ([Bré99], page 158) for example. Now, we can prove the proposition.

Proof : [of the proposition] Let U_0 be given. For all $k \geq 1$, let us define (U_k, Λ_k) such that :

$$\begin{pmatrix} \mathbf{A}_k & -\mathbf{B}_k^t \\ -\mathbf{B}_k & 0 \end{pmatrix} \begin{pmatrix} U_k \\ \Lambda_k \end{pmatrix} = \begin{pmatrix} 0 \\ -\mathbf{B}_{0k} U_0 \end{pmatrix}.$$

In other words, we have :

$$\Lambda_k = -R_k \mathbf{K}_k^{-1} R_k^t \mathbf{B}_{0k} U_0,$$

and then by construction of U_k and Λ_k :

$$\begin{aligned} -\langle \mathbf{B}_{0k}^t R_k \mathbf{K}_k^{-1} R_k^t \mathbf{B}_{0k} U_0, U_0 \rangle &= \langle \mathbf{B}_{0k}^t \Lambda_k, U_0 \rangle \\ &= \langle \Lambda_k, \mathbf{B}_k U_k \rangle \\ &= \langle \mathbf{A}_k U_k, U_k \rangle \\ &\geq 0. \end{aligned}$$

We deduce by addition that :

$$\begin{aligned} \langle \mathbf{D}_0 U_0, U_0 \rangle &= \langle \mathbf{A}_0 U_0, U_0 \rangle - \sum_{k=1}^K \langle \mathbf{B}_{0k}^t R_k \mathbf{K}_k^{-1} R_k^t \mathbf{B}_{0k} U_0, U_0 \rangle \\ &\geq \langle \mathbf{A}_0 U_0, U_0 \rangle. \end{aligned}$$

Hence the inequality :

$$\langle \mathbf{A}_0 U_0, U_0 \rangle \leq \langle \mathbf{D}_0 U_0, U_0 \rangle, \quad \forall U_0.$$

Let us now bound \mathbf{A}_0 from below. Let $u_0 \in H_*^1(\Omega)$ be given. For all $k \geq 1$, such that Ω_k has an empty intersection with Γ_D (we denote $k \in I_1$), we decompose u_0 on Ω'_k (as defined in lemma 6.1) into :

$$u_0 = r_k + w_k, \quad \text{on } \Omega'_k,$$

where r_k belongs to the space $\mathcal{R}(\Omega'_k)$ of rigid motions over Ω'_k , and :

$$\int_{\Omega'_k} w_k \cdot r = 0, \quad \forall r \in \mathcal{R}(\Omega'_k). \quad (6.19)$$

We define the function :

$$u_k = r_k + u'_k, \quad \text{on } \Omega_k,$$

where $r_k \in \mathcal{R}(\Omega_k)$ is the natural extension to Ω_k of $r_k \in \mathcal{R}(\Omega'_k)$ (thus $r_k \in \mathcal{R}(\Omega_k \cup \Omega'_k)$), and :

$$u'_k = \mathcal{I}_{k;h_k} \mathcal{D}_k w_k + \mathcal{R}_{k;\delta_k} \pi_k(w_k - \mathcal{I}_{k;h_k} \mathcal{D}_k w_k),$$

where $\mathcal{I}_{k;h_k}$ denotes the Scott-Zhang [SZ90] interpolation over $X_{k;h_k}$, and $\mathcal{R}_{k;\delta_k}$ is the extension by zero operator over the grid points of Ω_k , already defined in the previous chapter. By construction, the mortar condition is satisfied :

$$\int_{\Gamma_{0k}} u_k \cdot \mu = \int_{\Gamma_{0k}} u_0 \cdot \mu, \quad \forall \mu \in M_{k;\delta_k}.$$

Moreover, by using the stability of the extension operator $\mathcal{R}_{k;\delta_k}$ from $W_{k;\delta_k}$ to $H^1(\Omega_k)^d$, the assumption 6.2, the stability of $\mathcal{I}_{k;h_k}$ from $H^1(\Omega_k)^d$ to $H^1(\Omega_k)^d$, the classical estimation (see [SZ90]) :

$$\|u - \mathcal{I}_{k;h_k} u\|_{\delta, \frac{1}{2}, k} \leq C |u|_{H^1(\Omega_k)^d},$$

and the stability property of \mathcal{D}_k in lemma 6.1, we obtain :

$$\begin{aligned} a_k(u_k, u_k) &\leq C_k \int_{\Omega_k} |\nabla u'_k|^2 = C_k |u'_k|_{H^1(\Omega_k)^d}^2 \\ &\leq 2C_k |\mathcal{I}_{k;h_k} \mathcal{D}_k w_k|_{H^1(\Omega_k)^d}^2 + 2C_k |\mathcal{R}_{k;\delta_k} \pi_k(\mathcal{D}_k w_k - \mathcal{I}_{k;h_k} \mathcal{D}_k w_k)|_{H^1(\Omega_k)^d}^2 \\ &\leq 2C_k |\mathcal{I}_{k;h_k} \mathcal{D}_k w_k|_{H^1(\Omega_k)^d}^2 + 2CC_k \|\pi_k(\mathcal{D}_k w_k - \mathcal{I}_{k;h_k} \mathcal{D}_k w_k)\|_{\delta, \frac{1}{2}, k}^2 \\ &\leq 2C_k |\mathcal{I}_{k;h_k} \mathcal{D}_k w_k|_{H^1(\Omega_k)^d}^2 + 2CC_k \|\mathcal{D}_k w_k - \mathcal{I}_{k;h_k} \mathcal{D}_k w_k\|_{\delta, \frac{1}{2}, k}^2 \\ &\leq CC_k |\mathcal{D}_k w_k|_{H^1(\Omega_k)^d}^2 \leq CC_k |w_k|_{H^1(\Omega'_k)^d}. \end{aligned} \quad (6.20)$$

Moreover, the following inequality holds for all $v \in H^1(\Omega'_k)^d$:

$$|v|_{H^1(\Omega'_k)^d}^2 \leq C_{\Omega'_k} \left(\int_{\Omega'_k} \varepsilon(v) : \varepsilon(v) + \frac{1}{\text{diam}(\Omega'_k)^2} \left(\sup_{\substack{r \in \mathcal{R}(\Omega'_k), \\ \int_{\Omega'_k} r = 0}} \frac{\int_{\Omega'_k} v \cdot r}{\|r\|_{L^2(\Omega'_k)^d}} \right)^2 \right), \quad (6.21)$$

with a constant $C_{\Omega'_k}$ independent of the size of Ω'_k from the adopted scaling of the norms, but possibly depending on its shape. The shape independence of this constant can be insured for polyhedral shape regular domains, as shown in section 4.11, page 205, using the arguments from [Bre04]. Therefore, we have from (6.19) by definition of w_k :

$$|w_k|_{H^1(\Omega'_k)^d}^2 \leq C_{\Omega'_k} \int_{\Omega'_k} \varepsilon(w_k) : \varepsilon(w_k).$$

By summing over $k \in I_1$, we get from (6.20) that :

$$\sum_{k \in I_1} a_k(u_k, u_k) \leq C \sum_{k \in I_1} C_k \int_{\Omega'_k} \varepsilon(u_0) : \varepsilon(u_0), \quad (6.22)$$

with a constant C independent of the size of the subdomains. Since by construction $\cup_{k \in I_1} \Omega'_k \subset \Omega_0$, and since there is a bounded number of domains Ω'_k overlapping at a given point, we deduce :

$$\sum_{k \in I_1} a_k(u_k, u_k) \leq C \max_{k \in I_1} (C_k) \int_{\Omega_0} \varepsilon(u_0) : \varepsilon(u_0) \leq \frac{C}{c_0} \max_{k \in I_1} (C_k) a_0(u_0, u_0).$$

For all $k \geq 1$ such that Γ_D is fixed on a part of its boundary (that is $k \in I_2$), we cannot use the extension operator \mathcal{D}_k because it will not satisfy the Dirichlet boundary condition on Γ_D . But, the Sobolev lifting theorem proves the existence of a function \tilde{u}_k whose trace is u_0 on Γ_{0k} and such that :

$$\frac{1}{(L_k)^2} \int_{\Omega_k} |\tilde{u}_k|^2 + \int_{\Omega_k} |\nabla \tilde{u}_k|^2 \leq C \left(\frac{1}{L_k} \int_{\Gamma_{0k}} \langle u_0 \rangle_k^2 + |u_0|_{H^{1/2}(\Gamma_{0k})^d}^2 \right).$$

Here, $\langle u_0 \rangle_k$ denotes the average

$$\langle u_0 \rangle_k = \frac{1}{\text{meas}(\Gamma_{0k})} \int_{\Gamma_{0k}} u_0$$

of u_0 on Γ_{0k} and C is a constant which is independent of the size of Ω_k but which depends on the ratio between L_k and the distance from Γ_{0k} to Γ_D . We then modify \tilde{u}_k to obtain a discrete function satisfying the weak-continuity constraint on Γ_{0k} , and define using our previous notation :

$$u_k = \mathcal{I}_{k;h_k} \tilde{u}_k + \mathcal{R}_{k;\delta_k} \pi_k(\tilde{u}_k - \mathcal{I}_{k;h_k} \tilde{u}_k).$$

By construction, the mortar condition is satisfied :

$$\begin{aligned} \int_{\Gamma_{0k}} u_k \cdot \mu &= \int_{\Gamma_{0k}} (\mathcal{I}_{k;h_k} \tilde{u}_k + \tilde{u}_k - \mathcal{I}_{k;h_k} \tilde{u}_k) \cdot \mu \\ &= \int_{\Gamma_{0k}} u_0 \cdot \mu, \quad \forall \mu \in M_{k;\delta_k}. \end{aligned}$$

From the same argument as in the case $k \in I_1$, we get :

$$\begin{aligned} a_k(u_k, u_k) &\leq CC_k \int_{\Omega_k} |\nabla \tilde{u}_k|^2 \\ &\leq CC_k \left(\frac{1}{L_k} \int_{\Gamma_{0k}} \langle u_0 \rangle_k^2 + |u_0|_{H^{1/2}(\Gamma_{0k})^d}^2 \right) \\ &\leq CC_k \frac{L_0}{L_k} \left(\frac{1}{L_0} \int_{\Gamma_{0k}} \langle u_0 \rangle_k^2 + |u_0|_{H^1(\Omega'_k)^d}^2 \right). \end{aligned}$$

By summation, we have :

$$\begin{aligned} \sum_k \int_{\Gamma_{0k}} \langle u_0 \rangle_k^2 &= \sum_k \text{meas}(\Gamma_{0k}) \langle u_0 \rangle_k^2 \\ &= \sum_k \text{meas}(\Gamma_{0k})^{-1} \left(\int_{\Gamma_{0k}} 1 u_0 \right)^2 \\ &\leq \sum_k \text{meas}(\Gamma_{0k})^{-1} \int_{\Gamma_{0k}} u_0^2 \int_{\Gamma_{0k}} 1 \\ &\leq \sum_k \int_{\Gamma_{0k}} u_0^2 = \int_{\Gamma_0} u_0^2. \end{aligned} \tag{6.23}$$

By summing over $k \in I_2$, we get as before :

$$\begin{aligned} \sum_{k \in I_2} a_k(u_k, u_k) &\leq C \max_{k \in I_2} \left(C_k \frac{L_0}{L_k} \right) \left(\frac{1}{L_0} \int_{\Gamma_0} u_0^2 + |u_0|_{H^1(\partial\Omega_0)^d}^2 \right) \\ &\leq C \max_{k \in I_2} \left(C_k \frac{L_0}{L_k} \right) \|u_0\|_{H^1(\Omega_0)^d}^2 \\ &\leq C \max_{k \in I_2} \frac{C_k L_0}{\alpha_0 L_k} a_0(u_0, u_0). \end{aligned}$$

As a consequence, with this choice of u_k :

$$\langle \mathbf{A}_0 U_0, U_0 \rangle + \sum_{k=1}^K \langle \mathbf{A}_k U_k, U_k \rangle \leq \left(1 + C \max_{k \in I_1} \frac{C_k}{c_0} + C \max_{k \in I_2} \frac{C_k L_0}{\alpha_0 L_k} \right) \langle \mathbf{A}_0 U_0, U_0 \rangle.$$

Now, let us show that for all $(V_k)_{k \geq 1}$ such that $\mathbf{B}_k V_k = \mathbf{B}_{0k} U_0$, we have :

$$\langle \mathbf{D}_0 U_0, U_0 \rangle \leq \langle \mathbf{A}_0 U_0, U_0 \rangle + \sum_{k=1}^K \langle \mathbf{A}_k V_k, V_k \rangle. \tag{6.24}$$

For all $k \geq 1$, we decompose V_k into $V_k = U_k^* + \delta U_k$, where :

$$\begin{pmatrix} \mathbf{A}_k & -\mathbf{B}_k^t \\ -\mathbf{B}_k & 0 \end{pmatrix} \begin{pmatrix} U_k^* \\ \Lambda_k^* \end{pmatrix} = \begin{pmatrix} 0 \\ -\mathbf{B}_{0k} U_0 \end{pmatrix},$$

and $\mathbf{B}_k \delta U_k = 0$. Then, since by construction :

$$\langle \mathbf{A}_0 U_0, U_0 \rangle + \sum_{k=1}^K \langle \mathbf{A}_k U_k^*, U_k^* \rangle = \langle \mathbf{D}_0 U_0, U_0 \rangle,$$

we obtain by symmetry of \mathbf{A}_k :

$$\langle \mathbf{A}_0 U_0, U_0 \rangle + \sum_{k=1}^K \langle \mathbf{A}_k V_k, V_k \rangle = \langle \mathbf{D}_0 U_0, U_0 \rangle + \sum_{k=1}^K 2 \langle \mathbf{A}_k U_k^*, \delta U_k \rangle + \langle \mathbf{A}_k \delta U_k, \delta U_k \rangle.$$

Moreover :

$$\langle \mathbf{A}_k U_k^*, \delta U_k \rangle = \langle \mathbf{B}_k^t \Lambda_k^*, \delta U_k \rangle = \langle \Lambda_k^*, \mathbf{B}_k \delta U_k \rangle = 0,$$

resulting in :

$$\begin{aligned} \langle \mathbf{A}_0 U_0, U_0 \rangle + \sum_{k=1}^K \langle \mathbf{A}_k V_k, V_k \rangle &= \langle \mathbf{D}_0 U_0, U_0 \rangle + \sum_{k=1}^K \langle \mathbf{A}_k \delta U_k, \delta U_k \rangle \\ &\geq \langle \mathbf{D}_0 U_0, U_0 \rangle. \end{aligned}$$

In particular, we can take for all $k \geq 1$, $V_k = U_k$ where U_k has been built above. We conclude that :

$$\langle \mathbf{D}_0 U_0, U_0 \rangle \leq \left(1 + C \max_{k \in I_1} \frac{C_k}{c_0} + C \max_{k \in I_2} \frac{C_k L_0}{\alpha_0 L_k} \right) \langle \mathbf{A}_0 U_0, U_0 \rangle,$$

which ends the proof. \square

6.4.3 Spectral equivalence for the enhanced Dirichlet Neumann

For the enhanced Dirichlet-Neumann preconditioner presented in section 6.3.2, we prove that :

Proposition 6.3. *For all U_0 , the following spectral equivalence holds :*

$$W_{1,h} \langle \mathbf{D}_0 U_0, U_0 \rangle \leq \langle \hat{\mathbf{D}}_0 U_0, U_0 \rangle \leq \langle \mathbf{D}_0 U_0, U_0 \rangle,$$

with :

$$\frac{1}{W_{1,h}} = C \left(1 + \max_{k \in I_1 \cup I_2} \frac{C_k}{c_0} \right),$$

where I_1 (resp. I_2) is the set of indices $k \geq 1$ such that Ω_k is not fixed on its boundary (resp. is fixed on a part of its boundary). The constant C is independent of the number K and the size of the subdomains.

Proof : Let U_0 be given. We proceed as in the last part of the previous proof, and introduce (U_k^*, Λ_k^*) satisfying :

$$\begin{pmatrix} \mathbf{A}_k & -\mathbf{B}_k^t \\ -\mathbf{B}_k & 0 \end{pmatrix} \begin{pmatrix} U_k^* \\ \Lambda_k^* \end{pmatrix} = \begin{pmatrix} 0 \\ -\mathbf{B}_{0k} U_0 \end{pmatrix}. \quad (6.25)$$

We introduce the decomposition $U_k^* = \mathring{U}_k^* + W_k^*$ with $\mathring{U}_k^* = \mathring{\Pi}_k U_0$, and by construction of U_k^* , we get :

$$\begin{aligned} \langle \mathbf{D}_0 U_0, U_0 \rangle &= \left\langle \left(\mathbf{A}_0 - \sum_{k=1}^K \mathbf{B}_{0k}^t R_k \mathbf{K}_k^{-1} R_k^t \mathbf{B}_{0k} \right) U_0, U_0 \right\rangle \\ &= \langle \mathbf{A}_0 U_0, U_0 \rangle + \sum_{k=1}^K \langle \mathbf{A}_k U_k^*, U_k^* \rangle \\ &\geq \langle \mathbf{A}_0 U_0, U_0 \rangle + \sum_{k=1}^K \langle \mathbf{A}_k \mathring{U}_k^*, \mathring{U}_k^* \rangle + 2 \langle \mathbf{A}_k \mathring{U}_k^*, W_k^* \rangle. \end{aligned}$$

But decomposing $\mathring{U}_k^* = \mathring{\Pi}_k U_0 = \sum_{j=1}^{N_k} z_j U_k^j$ we have :

$$\begin{aligned} \langle \mathbf{A}_k W_k^*, \mathring{U}_k^* \rangle &= \sum_{j=1}^{N_k} z_j a_k(w_k^*, u_k^j) \\ &= \sum_{j=1}^{N_k} z_j \int_{\Gamma_{0k}} \lambda_k^j \cdot w_k^*, \quad \text{from (6.11).1,} \\ &= \sum_{j=1}^{N_k} z_j \int_{\Gamma_{0k}} (u_k^* - \mathring{u}_k^*) \cdot \lambda_k^j, \quad \text{by construction of } w_k^*, \\ &= \sum_{j=1}^{N_k} z_j \left[\int_{\Gamma_{0k}} u_k^* \cdot \lambda_k^j - \int_{\Gamma_{0k}} \mathring{u}_k^* \cdot \lambda_k^j \right], \quad \text{from (6.25) and (6.16).2,} \\ &= 0. \end{aligned}$$

This gives :

$$\begin{aligned}
\langle \mathbf{D}_0 U_0, U_0 \rangle &\geq \langle \mathbf{A}_0 U_0, U_0 \rangle + \sum_{k=1}^K \left\langle \mathbf{A}_k \dot{U}_k^*, \dot{U}_k^* \right\rangle \\
&= \langle \mathbf{A}_0 U_0, U_0 \rangle + \sum_{k=1}^K \left\langle \mathbf{A}_k \dot{\Pi}_k U_0, \dot{\Pi}_k U_0 \right\rangle \\
&= \left\langle \left(\mathbf{A}_0 + \sum_{k=1}^K \dot{\Pi}_k^t \mathbf{A}_k \dot{\Pi}_k \right) U_0, U_0 \right\rangle \\
&= \langle \mathbf{A}_0 U_0, U_0 \rangle + \sum_{k=1}^K \left\langle \mathbf{A}_k \dot{U}_k^*, \dot{U}_k^* \right\rangle, \quad \text{from (6.17).}
\end{aligned}$$

Let us prove now a lower bound for $\hat{\mathbf{D}}_0$. For all $1 \leq k \leq K$, as in the proof of the previous proposition, we build a particular function $u_k \in W_{k;\delta_k}$ satisfying the weak continuity constraint on the interface Γ_{0k} . When Ω_k is not fixed on a part of its boundary, which we have denoted by $k \in I_1$, we take the u_k defined in the previous proof by “reflexion” with respect to Γ_{0k} . When Ω_k is fixed on a part of its boundary, namely $k \in I_2$, we proceed differently, and define here $\langle u_0 \rangle_k \in \mathcal{R}(\Gamma_{0k})$ (the trace over Γ_{0k} of a rigid motion) such that :

$$\int_{\Gamma_{0k}} \langle u_0 \rangle_k \cdot r = \int_{\Gamma_{0k}} u_0 \cdot r, \quad \forall r \in \mathcal{R}(\Gamma_{0k}).$$

Then, we introduce :

$$u_k = \mathcal{I}_{k;h_k} \tilde{u}_k + \mathcal{R}_{k;\delta_k} \pi_k [\tilde{u}_k - \mathcal{I}_{k;h_k} \tilde{u}_k] + \dot{\pi}_k \langle u_0 \rangle_k,$$

where \tilde{u}_k is a function whose trace is zero on Γ_D and is $u_0 - \langle u_0 \rangle_k$ on Γ_{0k} satisfying from the Sobolev lifting theorem :

$$\begin{aligned}
\int_{\Omega_k} |\nabla \tilde{u}_k|^2 &\leq C \left[\frac{1}{L_k} \langle u_0 - \langle u_0 \rangle_k \rangle_k + |u_0 - \langle u_0 \rangle_k|_{H^{1/2}(\Gamma_{0k})^d}^2 \right] \\
&= C |u_0 - \langle u_0 \rangle_k|_{H^{1/2}(\Gamma_{0k})^d}^2, \quad \text{by construction of } \langle u_0 \rangle_k.
\end{aligned} \tag{6.26}$$

The mortar condition is indeed satisfied because :

$$\begin{aligned}
\int_{\Gamma_{0k}} u_k \cdot \mu &= \int_{\Gamma_{0k}} (\mathcal{I}_{k;h_k} \tilde{u}_k + \tilde{u}_k - \mathcal{I}_{k;h_k} \tilde{u}_k) \cdot \mu + \int_{\Gamma_{0k}} \dot{\pi}_k \langle u_0 \rangle_k \cdot \mu \\
&= \int_{\Gamma_{0k}} \tilde{u}_k \cdot \mu + \int_{\Gamma_{0k}} \dot{\pi}_k \langle u_0 \rangle_k \cdot \mu \\
&= \int_{\Gamma_{0k}} (u_0 - \langle u_0 \rangle_k + \dot{\pi}_k \langle u_0 \rangle_k) \cdot \mu, \quad \forall \mu \in M_{k;\delta_k},
\end{aligned}$$

and because, since $\langle u_0 \rangle_k$ is a linear combination of rigid body motions e_k^i , we have from (6.18) :

$$\int_{\Gamma_{0k}} (\langle u_0 \rangle_k - \dot{\pi}_k \langle u_0 \rangle_k) \cdot \mu = 0, \quad \forall \mu \in M_{k;\delta_k}.$$

On the other hand, we have for $k \in I_2$:

$$\begin{aligned} a_k(u_k, u_k) &\leq 2a_k(u_k - \dot{\pi}_k \langle u_0 \rangle_k, u_k - \dot{\pi}_k \langle u_0 \rangle_k) \\ &\quad + 2a_k(\dot{\pi}_k \langle u_0 \rangle_k, \dot{\pi}_k \langle u_0 \rangle_k). \end{aligned} \quad (6.27)$$

Using the same argument as in (6.20), we get by construction of u_k :

$$\begin{aligned} a_k(u_k - \dot{\pi}_k \langle u_0 \rangle_k, u_k - \dot{\pi}_k \langle u_0 \rangle_k) &\leq CC_k \int_{\Omega_k} |\nabla \tilde{u}_k|^2 \\ &\leq CC_k |u_0 - \langle u_0 \rangle_k|_{H^{1/2}(\Gamma_{0k})^d}^2, \quad \text{from (6.26),} \\ &\leq CC_k \int_{\Omega'_k} \varepsilon(u_0) : \varepsilon(u_0), \end{aligned} \quad (6.28)$$

from the Sobolev trace theorem and the inequality (6.21). On the other hand, we have from lemma 6.2 :

$$\begin{aligned} a_k(\dot{\pi}_k \langle u_0 \rangle_k, \dot{\pi}_k \langle u_0 \rangle_k) &\leq 2a_k(\dot{\pi}_k(u_0 - \langle u_0 \rangle_k), \dot{\pi}_k(u_0 - \langle u_0 \rangle_k)) \\ &\quad + 2a_k(\dot{\pi}_k u_0, \dot{\pi}_k u_0) \\ &\leq CC_k |u_0 - \langle u_0 \rangle_k|_{H^{1/2}(\Gamma_{0k})^d}^2 + 2a_k(\dot{\pi}_k u_0, \dot{\pi}_k u_0) \\ &\leq CC_k \int_{\Omega'_k} \varepsilon(u_0) : \varepsilon(u_0) + 2a_k(\dot{\pi}_k u_0, \dot{\pi}_k u_0). \end{aligned}$$

We then deduce from (6.22),(6.27) and (6.28) :

$$\begin{aligned} a_0(u_0, u_0) + \sum_{k=1}^K a_k(u_k, u_k) &\leq a_0(u_0, u_0) + C \sum_{k=1}^K C_k \int_{\Omega'_k} \varepsilon(u_0) : \varepsilon(u_0) \\ &\quad + 4a_k(\dot{\pi}_k u_0, \dot{\pi}_k u_0) \\ &\leq \left(4 + \frac{C}{c_0} \max_{k \geq 1}(C_k) \right) \left[a_0(u_0, u_0) + \sum_{k \in I_2} a_k(\dot{\pi}_k u_0, \dot{\pi}_k u_0) \right] \\ &= \left(4 + \frac{C}{c_0} \max_{k \geq 1}(C_k) \right) \langle \hat{\mathbf{D}}_0 U_0, U_0 \rangle. \end{aligned}$$

We deduce from (6.24) and from the mortar conditions satisfied by the $(u_k)_{k \geq 1}$, that :

$$\langle \mathbf{D}_0 U_0, U_0 \rangle \leq \left(4 + \frac{C}{c_0} \max_{k \geq 1}(C_k) \right) \langle \hat{\mathbf{D}}_0 U_0, U_0 \rangle.$$

□

In the above proof, we have used the following lemma :

Lemma 6.2. *If a_k is symmetric, the projection operator $\dot{\pi}_k$ satisfies :*

$$a_k(\dot{\pi}_k w, \dot{\pi}_k w) \leq CC_k \left[\frac{1}{L_k} \int_{\Gamma_{0k}} \langle w \rangle_k^2 + |w|_{H^{1/2}(\Gamma_{0k})^d}^2 \right]$$

Proof : Let \tilde{w} be a lifting function of w with zero trace on Γ_D , with $\tilde{w} = w$ on Γ_{0k} and satisfying the Sobolev lifting theorem :

$$\int_{\Omega_k} |\nabla \tilde{w}|^2 \leq C \left[\frac{1}{L_k} \int_{\Gamma_{0k}} \langle w \rangle_k^2 + |w|_{H^{1/2}(\Gamma_{0k})^d}^2 \right].$$

Let us define as before $\tilde{w}_k = \mathcal{I}_{k;h_k} \tilde{w} + \mathcal{R}_{k;\delta_k} \pi_k(\tilde{w} - \mathcal{I}_{k;h_k} \tilde{w})$ which belongs to $X_{k;h_k}$ and which satisfies by construction :

$$\int_{\Gamma_{0k}} \tilde{w}_k \cdot \mu = \int_{\Gamma_{0k}} \tilde{w} \cdot \mu, \quad \forall \mu \in M_{k;\delta_k}. \quad (6.29)$$

We then have on one hand :

$$\begin{aligned} a_k(\tilde{w}_k, \tilde{w}_k) &= a_k(\dot{\pi}_k w, \dot{\pi}_k w) + a_k(\dot{\pi}_k w - \tilde{w}_k, \dot{\pi}_k w - \tilde{w}_k) \\ &\quad + 2a_k(\dot{\pi}_k w, \dot{\pi}_k w - \tilde{w}_k). \end{aligned} \quad (6.30)$$

Developing $\dot{\pi}_k w_k$ into $\dot{\pi}_k w_k = \sum_{j=1}^{N_k} z_j u_k^j$, we have from (6.11).1

$$\begin{aligned} a_k(\dot{\pi}_k w - \tilde{w}_k, \dot{\pi}_k w) &= \sum_{j=1}^{N_k} z_j a_k(\dot{\pi}_k w - \tilde{w}_k, u_k^j) \\ &= \sum_{j=1}^{N_k} z_j \int_{\Gamma_{0k}} (\dot{\pi}_k w - \tilde{w}_k) \cdot \lambda_k^j \\ &= \sum_{j=1}^{N_k} z_j \left[\int_{\Gamma_{0k}} w \cdot \lambda_k^j - \int_{\Gamma_{0k}} \tilde{w} \cdot \lambda_k^j \right], \quad \text{from (6.16).2 and (6.29)} \\ &= 0. \end{aligned}$$

Plugged back in (6.30), this implies :

$$a_k(\dot{\pi}_k w, \dot{\pi}_k w) \leq a_k(\tilde{w}_k, \tilde{w}_k).$$

But on the other hand, proceeding as in (6.20), we have :

$$a_k(\tilde{w}_k, \tilde{w}_k) \leq CC_k \int_{\Omega_k} |\nabla \tilde{w}|^2 \leq CC_k \left[\frac{1}{L_k} \int_{\Gamma_{0k}} \langle w \rangle_k^2 + |w|_{H^{1/2}(\Gamma_{0k})^d}^2 \right]$$

the last inequality coming from the Sobolev lifting theorem. This concludes the proof. \square

Bound on condition number

We prove now a classical result, using for example the technique from the Matsokin-Nepomniashchik [MN85] framework :

Proposition 6.4. *Let us assume that there exist two positive quantities $W_{1,h}, W_{2,h}$ such that for all U_0 :*

$$W_{1,h} \langle \mathbf{D}_0 U_0, U_0 \rangle \leq \langle \hat{\mathbf{D}}_0 U_0, U_0 \rangle \leq W_{2,h} \langle \mathbf{D}_0 U_0, U_0 \rangle. \quad (6.31)$$

Then, the condition number of $\mathbf{C}^{-1}\mathbf{A}$ in \mathbf{A} -norm on E admits the following upper bound :

$$\kappa_{\mathbf{A},E}(\mathbf{C}^{-1}\mathbf{A}) \leq \frac{\max(1, W_{2,h})}{\min(1, W_{1,h})}.$$

Proof : Knowing that :

$$\kappa_{\mathbf{A},E}(\mathbf{C}^{-1}\mathbf{A}) = \sup_{U \in E} \frac{\langle \mathbf{AU}, \mathbf{C}^{-1}\mathbf{AU} \rangle}{\langle \mathbf{AU}, U \rangle} \left(\inf_{U \in E} \frac{\langle \mathbf{AU}, \mathbf{C}^{-1}\mathbf{AU} \rangle}{\langle \mathbf{AU}, U \rangle} \right)^{-1} = \frac{\lambda_{\max}(\mathbf{C}^{-1}\mathbf{A})}{\lambda_{\min}(\mathbf{C}^{-1}\mathbf{A})},$$

we give an upper bound for the highest eigenvalue $\lambda_{\max}(\mathbf{C}^{-1}\mathbf{A})$ of $\mathbf{C}^{-1}\mathbf{A}$ and a lower bound for its smallest eigenvalue $\lambda_{\min}(\mathbf{C}^{-1}\mathbf{A})$.

Let us begin with the smallest eigenvalue. For all $U \in E$, by using the Cauchy-Schwarz inequality and the factorizations $\mathbf{A} = T^t HT$ and $\mathbf{C} = T^t \hat{H}T$, we obtain that :

$$\begin{aligned} \langle \mathbf{AU}, U \rangle &= \langle T^{-t} \mathbf{AU}, TU \rangle = \langle \hat{H} \hat{H}^{-1} T^{-t} \mathbf{AU}, TU \rangle \\ &\leq \langle \hat{H} TU, TU \rangle^{1/2} \langle \hat{H} \hat{H}^{-1} T^{-t} \mathbf{AU}, \hat{H}^{-1} T^{-t} \mathbf{AU} \rangle^{1/2}, \\ &\leq \langle \hat{H} TU, TU \rangle^{1/2} \langle T^{-t} \mathbf{AU}, \hat{H}^{-1} T^{-t} \mathbf{AU} \rangle^{1/2}, \\ &\leq \langle \hat{H} TU, TU \rangle^{1/2} \langle \mathbf{AU}, \mathbf{C}^{-1}\mathbf{AU} \rangle^{1/2}. \end{aligned}$$

As $U = (U_0, U_1, \Lambda_1, \dots, U_K, \Lambda_K)^t \in E$, it is simple to check that $V = (V_0, V_1, \Lambda'_1, \dots, V_K, \Lambda'_K)^t$ such that $V = TU$ satisfies :

$$V_0 = U_0, \quad \text{and } \mathbf{B}_k V_k = 0, \quad 1 \leq k \leq K.$$

As a consequence, we have by using assumption (6.31) :

$$\begin{aligned} \langle \hat{H} TU, TU \rangle &= \langle \hat{H} V, V \rangle = \langle \hat{\mathbf{D}}_0 U_0, U_0 \rangle + \sum_{k=1}^K \langle \mathbf{A}_k V_k, V_k \rangle \\ &\leq \max(1, W_{2,h}) \left(\langle \mathbf{D}_0 U_0, U_0 \rangle + \sum_{k=1}^K \langle \mathbf{A}_k V_k, V_k \rangle \right) \\ &\leq \max(1, W_{2,h}) \langle HTU, TU \rangle. \end{aligned} \quad (6.32)$$

Using the upper bound (6.32), we now get :

$$\begin{aligned}\langle \mathbf{A}U, U \rangle &\leq \max(1, W_{2,h})^{1/2} \langle HTU, TU \rangle^{1/2} \langle \mathbf{A}U, \mathbf{C}^{-1}\mathbf{A}U \rangle^{1/2}, \\ &\leq \max(1, W_{2,h})^{1/2} \langle \mathbf{A}U, U \rangle^{1/2} \langle \mathbf{A}U, \mathbf{C}^{-1}\mathbf{A}U \rangle^{1/2},\end{aligned}$$

resulting in :

$$\inf_{U \in E} \frac{\langle \mathbf{A}U, \mathbf{C}^{-1}\mathbf{A}U \rangle}{\langle \mathbf{A}U, U \rangle} \geq \frac{1}{\max(1, W_{2,h})}.$$

Concerning the highest eigenvalue, let us begin by applying the Cauchy-Schwarz inequality to get :

$$\langle \mathbf{A}U, \mathbf{C}^{-1}\mathbf{A}U \rangle \leq \langle \mathbf{A}U, U \rangle^{1/2} \langle \mathbf{A}\mathbf{C}^{-1}\mathbf{A}U, \mathbf{C}^{-1}\mathbf{A}U \rangle^{1/2}. \quad (6.33)$$

Moreover, by using the factorizations of $\mathbf{A} = T^t HT$ and $\mathbf{C} = T^t \hat{H}T$ and the Cauchy-Schwarz inequality, we obtain that :

$$\begin{aligned}\langle \mathbf{A}\mathbf{C}^{-1}\mathbf{A}U, \mathbf{C}^{-1}\mathbf{A}U \rangle &= \langle T^t HTT^{-1}\hat{H}^{-1}T^{-t}\mathbf{A}U, T^{-1}\hat{H}^{-1}T^{-t}\mathbf{A}U \rangle \\ &= \langle H\hat{H}^{-1}T^{-t}\mathbf{A}U, \hat{H}^{-1}T^{-t}\mathbf{A}U \rangle.\end{aligned} \quad (6.34)$$

Let us introduce $W = \hat{H}^{-1}T^{-t}\mathbf{A}U = \hat{H}^{-1}HTU$. As $U = (U_0, U_1, \Lambda_1, \dots, U_K, \Lambda_K)^t \in E$, the vector $V = (V_0, V_1, \Lambda'_1, \dots, V_K, \Lambda'_K)^t = TU$ satisfies :

$$V_0 = U_0, \quad \text{and } \mathbf{B}_k V_k = 0, \quad 1 \leq k \leq K.$$

Then, the vector $W = (W_0, W_1, \Lambda''_1, \dots, W_K, \Lambda''_K)^t = \hat{H}^{-1}HV$ satisfies :

$$W_0 = \hat{\mathbf{D}}_0^{-1}\mathbf{D}_0 U_0, \quad \text{and } W_k = V_k, \quad 1 \leq k \leq K,$$

entailing that $\mathbf{B}_k W_k = 0$, for $k \geq 1$. Then :

$$\begin{aligned}\langle \hat{H}W, W \rangle &= \langle \hat{\mathbf{D}}_0 W_0, W_0 \rangle + \sum_{k=1}^K \langle \mathbf{A}_k V_k, V_k \rangle \\ &\geq \min(1, W_{1,h}) \left(\langle \mathbf{D}_0 W_0, W_0 \rangle + \sum_{k=1}^K \langle \mathbf{A}_k V_k, V_k \rangle \right) \\ &\geq \min(1, W_{1,h}) \langle HW, W \rangle.\end{aligned} \quad (6.35)$$

Using this inequality in (6.34) we obtain that :

$$\begin{aligned}\langle \mathbf{A}\mathbf{C}^{-1}\mathbf{A}U, \mathbf{C}^{-1}\mathbf{A}U \rangle &\leq \min(1, W_{1,h})^{-1} \langle \hat{H}\hat{H}^{-1}T^{-t}\mathbf{A}U, \hat{H}^{-1}T^{-t}\mathbf{A}U \rangle \\ &\leq \min(1, W_{1,h})^{-1} \langle \mathbf{A}U, \mathbf{C}^{-1}\mathbf{A}U \rangle,\end{aligned}$$

which gives in (6.33) :

$$\langle \mathbf{A}U, \mathbf{C}^{-1}\mathbf{A}U \rangle \leq \frac{1}{\min(1, W_{1,h})^{1/2}} \langle \mathbf{A}U, U \rangle^{1/2} \langle \mathbf{A}U, \mathbf{C}^{-1}\mathbf{A}U \rangle^{1/2},$$

entailing the following upper bound on the highest eigenvalue of $\mathbf{C}^{-1}\mathbf{A}$:

$$\sup_{U \in E} \frac{\langle \mathbf{A}U, \mathbf{C}^{-1}\mathbf{A}U \rangle}{\langle \mathbf{A}U, U \rangle} \leq \frac{1}{\min(1, W_{1,h})}.$$

We conclude that :

$$\kappa_{\mathbf{A},E} \leq \frac{\max(1, W_{2,h})}{\min(1, W_{1,h})},$$

which ends the proof. \square

We conclude by the main result of that section, which gives an upper bound on the condition number of the preconditioned systems :

Proposition 6.5. *For the symmetrized Dirichlet-Neumann preconditioner given in section 6.3.2, we have :*

$$\kappa_{\mathbf{A},E}(\mathbf{C}^{-1}\mathbf{A}) \leq 1 + C \left(\max_{k \in I_1} \frac{C_k}{c_0} + \max_{k \in I_2} \frac{C_k L_0}{\alpha_0 L_k} \right),$$

and for the enhanced Dirichlet-Neumann preconditioner given in section 6.3.2 :

$$\kappa_{\mathbf{A},E}(\mathbf{C}^{-1}\mathbf{A}) \leq C \left(1 + \max_{k \in I_1 \cup I_2} \frac{C_k}{c_0} \right).$$

Both condition numbers are independent of the number K of fine scale subdomains and of their sizes. In that sense, we can reasonably talk of two-scale preconditioners. The simplest symmetrized Dirichlet-Neumann preconditioner, which imposes the invertibility of \mathbf{A}_0 (i.e. a Dirichlet boundary condition on Ω_0 for example), is strongly affected by the presence of small subdomains that are fixed on a part of their boundary, through the ratio L_0/L_k . The enhanced symmetrized Dirichlet-Neumann preconditioner avoids efficiently this dependence, and its use is not limited to the case where $\Gamma_D \cap \partial\Omega_0$ has a positive measure. Nevertheless, both condition numbers are affected by the presence of stiff fine subdomains in comparison with the coarse domain, through the presence of the ratio C_k/α_0 because C_k (resp. α_0) is proportional to the Young modulus E_k (resp E_0) of the material in Ω_k (resp. Ω_0).

6.5 Algorithm

Before testing these two preconditioners, we summarize herein the algorithm coming from their application. The action of a preconditioner on a right hand side

$$\begin{pmatrix} F_0 \\ F_1 \\ 0 \\ \vdots \\ F_K \\ 0 \end{pmatrix}$$

in the dual of E leads to the following sequence of operations :

1. Compute the equivalent coarse scale sollicitation on Ω_0 :

$$\overline{F}_0 = F_0 - \sum_{k=1}^K \mathbf{B}_{0k}^t R_k \mathbf{K}_k^{-1} \begin{pmatrix} F_k \\ 0 \end{pmatrix},$$

by solving in parallel one Dirichlet problem by small subdomain.

2. Use the equivalent coarse scale operator $\hat{\mathbf{D}}_0$ to determine :

$$\tilde{U}_0 = \hat{\mathbf{D}}_0^{-1} \overline{F}_0.$$

3. Solve the local problems for $1 \leq k \leq K$:

$$\mathbf{K}_k \begin{pmatrix} \tilde{U}_k \\ \tilde{\Lambda}_k \end{pmatrix} = \begin{pmatrix} F_k \\ -\mathbf{B}_0 \tilde{U}_0 \end{pmatrix}.$$

If the computational cost of \mathbf{A}_k^{-1} for $k \geq 1$ is low with respect to the one of \mathbf{A}_0^{-1} , the calculation cost is concentrated in the step 2.

Remark 6.3. *Even if a saddle-point problem is involved, this preconditioner can be used in a Conjugate Gradient because it provides approximations in the constrained space V_h on which the considered problem is elliptic. For practical convenience, the saddle point problem to solve can be penalized with a small parameter of penetration η , even though the condition number of the resulting penalized system explodes like $O(1/\eta)$.*

Remark 6.4. *This preconditioner is multiplicative, in the sense that the two scales cannot be solved simultaneously. Nevertheless, the solutions over the small details can be performed simultaneously in parallel.*

6.6 Numerical tests

6.6.1 A basic two-scale model

Let us consider a two-scale linear model beam whose tips are clamped. We impose a negative constant pressure on the lower face of the small details. A \mathbb{Q}_1 approximation is adopted for displacements, and an example of the resulting deformed configuration of our model is represented on figure 6.3. The Young modulus and the Poisson coefficient are taken constant over the coarse (E_0, ν_0) and the fine (E', ν') subdomains. As assumed above, the non-mortar side is taken as the fine side of the interface and Lagrange multipliers are taken piecewise constant as in the previous chapter, together with an interface bubble stabilization for the displacements. Moreover, the weak-continuity constraint is ensured by a penalization strategy (as described in the previous chapter) and the associated penalization coefficient is taken as :

$$\frac{1}{\eta} = 10^6 E'.$$

On this model, we use the first symmetrized Dirichlet-Neumann preconditioner in a standard Conjugate Gradient algorithm, and the L^2 norm of the successive increments on Lagrange multipliers along the iterations is illustrated on figure 6.4 for different values of the ratio $r = E'/E_0$. Conversely the number of iterations necessary to obtain a 10^{-9} convergence, estimated in terms of the L^2 norm of the current increment on the Lagrange multiplier, is represented on figure 6.5. The degradation of the performance as r grows is in conformity with our predictions.

Let us assume now, that two of the details are clamped on their lower face, leading under the same load to the new deformed configuration illustrated on figure 6.6. The convergence of simple and enhanced Dirichlet-Neumann algorithms are then compared on figure 6.7 for the ratios $r = 10, 100, 1000, 10^6$. Conversely, the number of iterations necessary to reach a 10^{-9} convergence as a function of r is represented on figure 6.8 both for simple and enhanced Dirichlet-Neumann algorithms. We observe a much better performance of the enhanced preconditioner, the number of iterations being typically divided by 3 for an additional computational cost of 6 additional degrees of freedom on the coarse part of the model. Indeed, 3 rigid motions per clamped small structure have been added to the coarse model. The resulting overcost per iteration in terms of computation is negligible.

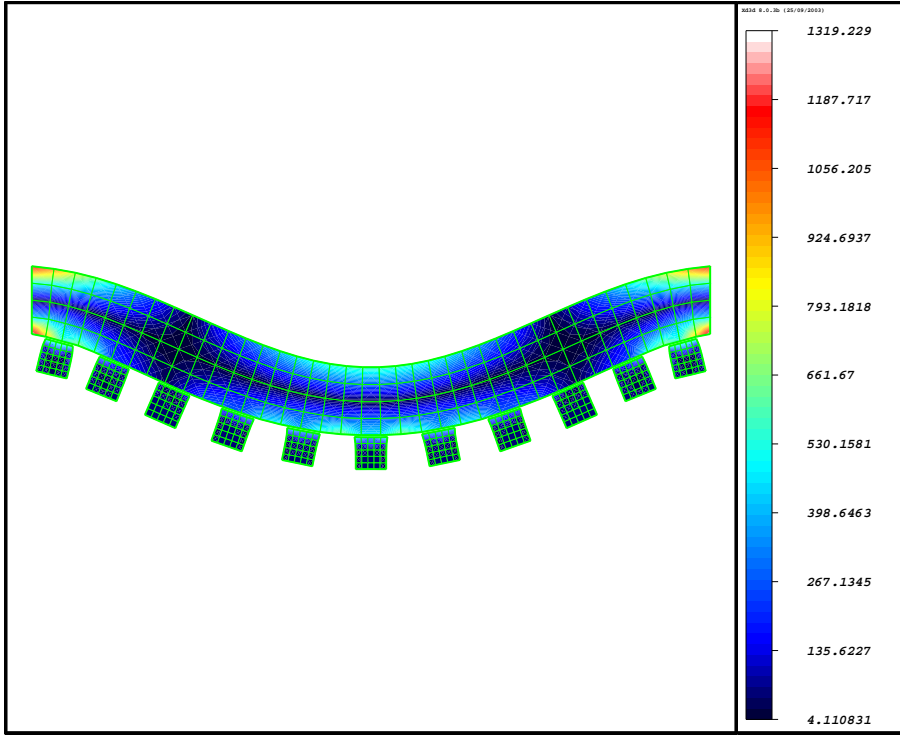


FIG. 6.3 – Maximal stress distribution on a deformed configuration of our two-scale model problem ($E_0 = E'$, $\nu_0 = \nu'$, 497 elements mesh).

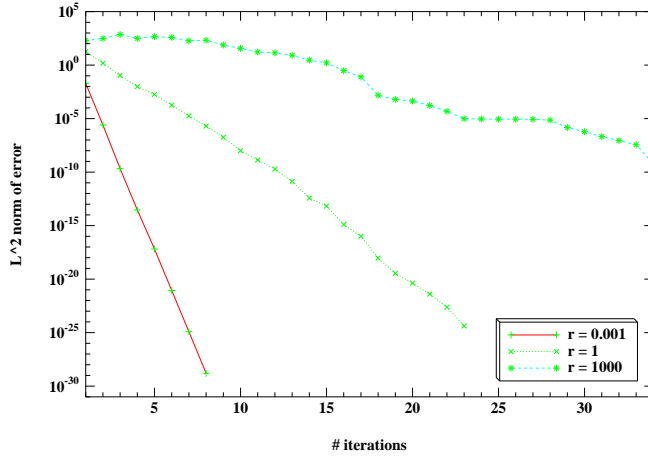


FIG. 6.4 – L^2 norm of the successive increments on Lagrange multipliers along the iterations.

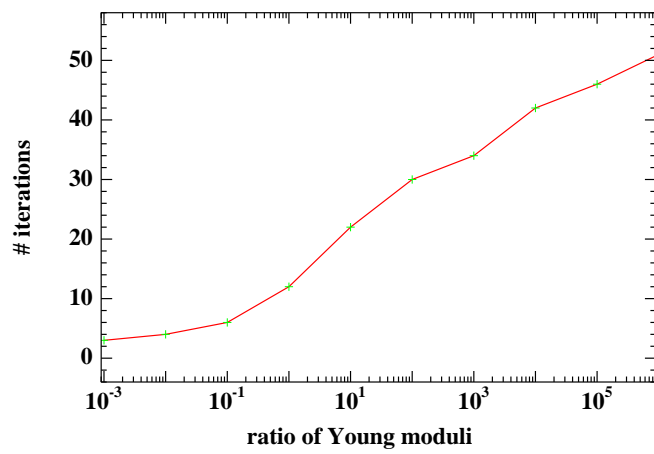


FIG. 6.5 – Number of iterations necessary to obtain a 10^{-9} convergence of the simple Dirichlet-Neumann preconditioned Conjugate Gradient, estimated in terms of the L^2 norm of the current increment on the Lagrange multiplier, as a function of the ratio $r = E'/E_0$.

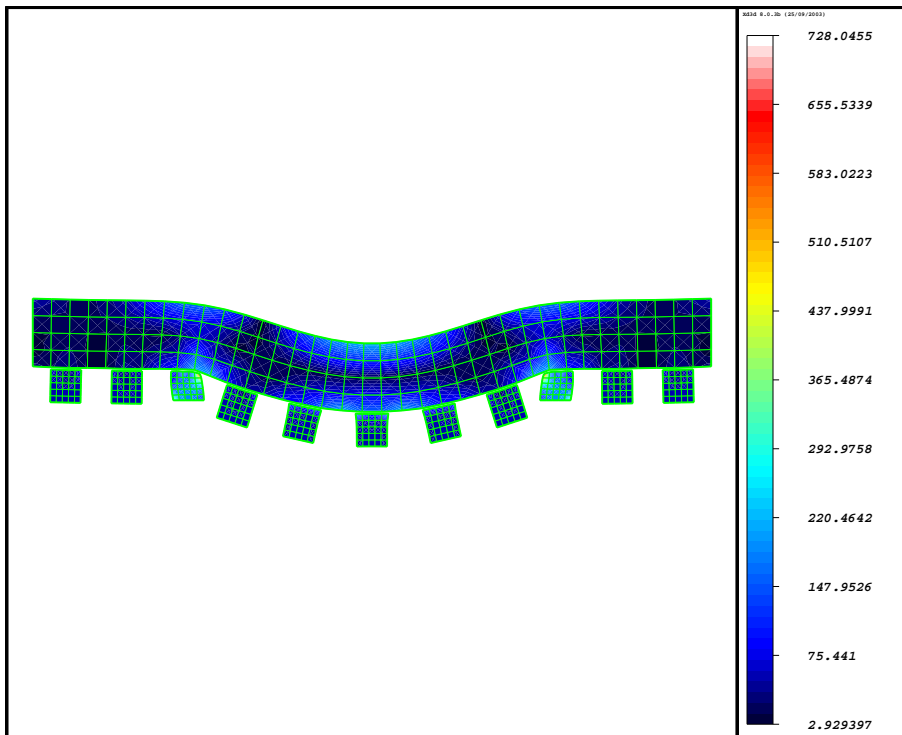


FIG. 6.6 – Maximal stress distribution on a deformed configuration of our two-scale model problem where two of the details are clamped on their lower face ($E_0 = E'$, $\nu_0 = \nu'$, 497 elements mesh).

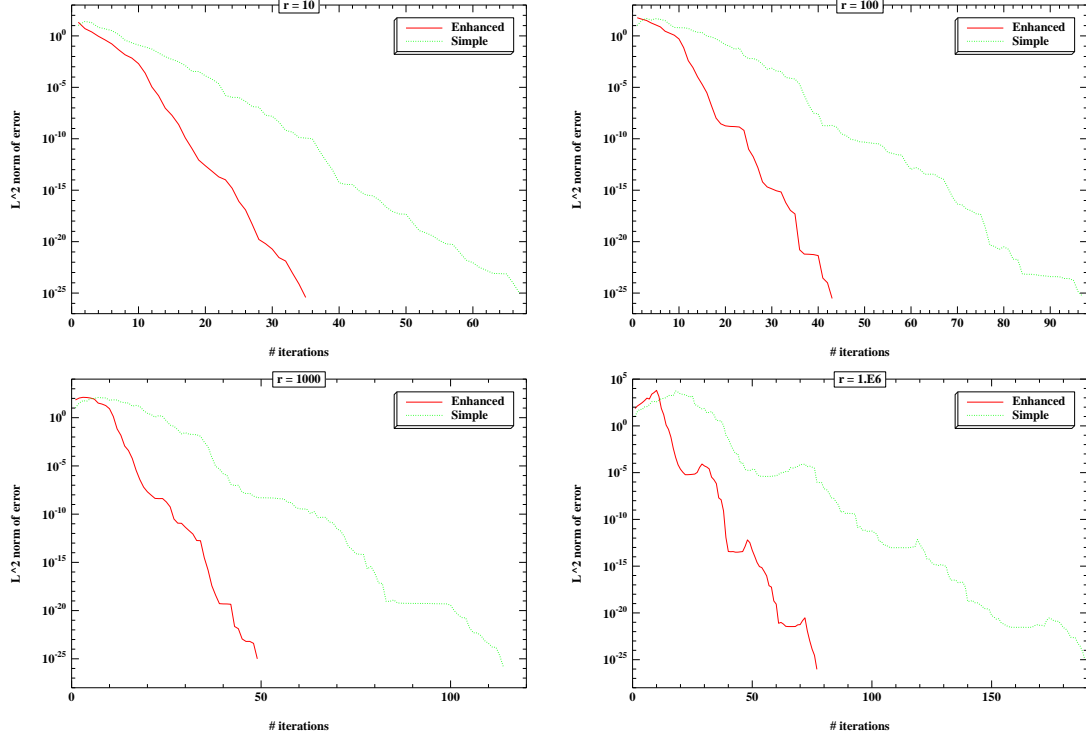


FIG. 6.7 – Convergence of the simple and enhanced Dirichlet-Neumann algorithms for different values of the ratio r of Young moduli.

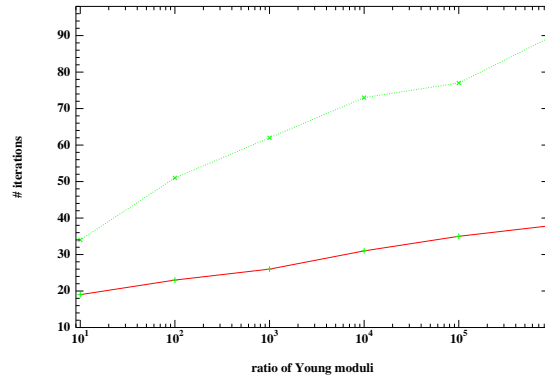


FIG. 6.8 – Number of iterations necessary to obtain a 10^{-9} convergence of the simple and the enhanced Dirichlet-Neumann preconditioned Conjugate Gradient, estimated in terms of the L^2 norm of the current increment on the Lagrange multiplier, as a function of the ratio $r = E'/E_0$.

6.6.2 Extension to a quasi-Newton method

When considering nonlinear problems with soft fine geometrical details on the boundary, the previous preconditioners can be successfully applied to quasi-Newton methods. Instead of solving each tangent problem by a preconditioned Conjugate Gradient method, the idea is to replace the tangent problems by the preconditioning problems. From the implementation point of view, it is no more necessary to keep in memory the non-inverted matrix of the tangent problem. Moreover, the numerical tests show that this strategy entails almost no overcost in terms of iterations of the Newton method.

For example, let us consider the following elastostatics problem :

$$\begin{cases} -\operatorname{div} \frac{\partial \hat{\mathcal{W}}}{\partial F}(id + \nabla u) = f, & \Omega, \\ u = 0, & \Gamma_D, \\ \frac{\partial \hat{\mathcal{W}}}{\partial F}(id + \nabla u) \cdot n = g, & \Gamma_N. \end{cases}$$

Let us assume that the potential $\hat{\mathcal{W}}$ is given by the Saint-Venant-Kirchhoff constitutive law defined by :

$$\hat{\mathcal{W}}(F) = \frac{\lambda}{4} [tr(F^t \cdot F - id)]^2 + \frac{\mu}{8} tr [(F^t \cdot F - id)^2].$$

After a non-conforming finite element discretization, we have then to solve a nonlinear discrete problem of the form :

$$\begin{cases} \mathcal{F}_0(U_0) + \sum_{k=1}^K \mathbf{B}_{0k} \Lambda_k = F_0, \\ \mathcal{F}_k(U_k) - \mathbf{B}_k^t \Lambda_k = F_k, \quad 1 \leq k \leq K, \\ \mathbf{B}_{0k} U_0 - \mathbf{B}_k U_k = 0, \quad 1 \leq k \leq K. \end{cases}$$

A standard Newton algorithm would build two sequences $(U^n)_n$ and $(\Lambda^n)_n$ such that :

$$\begin{cases} U^{n+1} = U^n + \delta U^n, \\ \Lambda^{n+1} = \Lambda^n + \delta \Lambda^n, \end{cases}$$

with :

$$\begin{cases} \partial_{U_0} \mathcal{F}_0(U_0^n) \cdot \delta U_0^n + \sum_{k=1}^K \mathbf{B}_{0k} \delta \Lambda_k^n = F_0 - \mathcal{F}_0(U_0^n) - \sum_{k=1}^K \mathbf{B}_{0k} \Lambda_k^n, \\ \partial_{U_k} \mathcal{F}_k(U_k^n) \cdot \delta U_k^n - \mathbf{B}_k^t \Lambda_k^n = F_k - \mathcal{F}_k(U_k^n) + \mathbf{B}_k^t \Lambda_k^n, \quad 1 \leq k \leq K, \\ \mathbf{B}_{0k} \delta U_0^n - \mathbf{B}_k \delta U_k^n = 0, \quad 1 \leq k \leq K. \end{cases}$$

At iteration n , this linear system can then be written as follows :

$$\mathbf{A} \begin{pmatrix} \delta U_0^n \\ \delta U_1^n \\ \delta \Lambda_1^n \\ \vdots \\ \delta U_K^n \\ \delta \Lambda_K^n \end{pmatrix} = \begin{pmatrix} F_0^n \\ F_1^n \\ 0 \\ \vdots \\ F_K^n \\ 0 \end{pmatrix}.$$

We propose to define the new increments $\delta \tilde{U}^n$ and $\delta \tilde{\Lambda}^n$ as the solutions of :

$$\mathbf{C} \begin{pmatrix} \delta \tilde{U}_0^n \\ \delta \tilde{U}_1^n \\ \delta \tilde{\Lambda}_1^n \\ \vdots \\ \delta \tilde{U}_K^n \\ \delta \tilde{\Lambda}_K^n \end{pmatrix} = \begin{pmatrix} F_0^n \\ F_1^n \\ 0 \\ \vdots \\ F_K^n \\ 0 \end{pmatrix},$$

with the same notations used in section 2. Our two-scale quasi-Newton method is then defined by :

$$\begin{cases} U^{n+1} = U^n + \delta \tilde{U}^n, \\ \Lambda^{n+1} = \Lambda^n + \delta \tilde{\Lambda}^n. \end{cases}$$

Let us consider the same model problem as in the previous section, under a dead pressure of $p = 100Pa$. We have adopted the following Lamé coefficients :

$$\lambda_0 = E_0 \frac{\nu_0}{(1 + \nu_0)(1 - 2\nu_0)} = 1389Pa, \quad \mu_0 = \frac{E_0}{2(1 + \nu_0)} = 2083Pa,$$

$$\lambda' = r\lambda_0, \quad \mu' = r\mu_0 Pa,$$

respectively for the coarse and the fine subdomains, characterized by the stiffness ratio :

$$r = \frac{E_0}{E'} = \frac{\lambda_0}{\lambda'} = \frac{\mu_0}{\mu'}.$$

The solution remains unchanged when p , λ_0 , E_0 , λ' and μ' are multiplied by the same coefficient. We have observed numerically that for $r \geq 10$, the quasi-Newton method does not converge well, as shown on the table on figure 6.9. Whereas, the convergence becomes extremely slow with $r = 1$, the method does not converge any more with $r = 100$. The convergence of the Newton-Raphson method is represented as a comparison. Nevertheless, when the ratio r remains sufficiently small, the proposed quasi-Newton method appears to be interesting, even though the convergence is no more quadratic. The overcost in terms of iterations compared with a Newton-Raphson method is low, as shown in the table, on

it.	$r = 1$		$r = 100$	
	quasi-Newton	Newton	quasi-Newton	Newton
1	0.6193E+01	0.5839E+01	0.6187E+01	0.5224E+01
2	0.1904E+01	0.1649E+01	0.1380E+02	0.1401E+01
3	0.1013E+01	0.9821E+00	0.6958E+03	0.7683E+00
4	0.6684E+00	0.6221E+00	0.1283E+04	0.4046E+00
5	0.3309E+00	0.3032E+00	0.3672E+04	0.2419E+00
6	0.8885E-01	0.8811E-01	0.1847E+04	0.1454E+00
7	0.4654E-02	0.8719E-02	0.9162E+03	0.1096E+00
8	0.5162E-02	0.1591E-03	0.6159E+03	0.5302E-01
9	0.4352E-02	0.8287E-07	0.1027E+04	0.5350E-01
10	0.3714E-02		0.6719E+03	0.7019E-02
11	0.3155E-02		0.8720E+03	0.3277E-02
12	0.2716E-02		0.5561E+03	0.3023E-04
13	0.2334E-02		0.6285E+03	0.3357E-07
14	0.2023E-02		0.8873E+03	
15	0.1753E-02		0.5120E+03	
16	0.1528E-02		0.5499E+03	
17	0.1333E-02		0.6496E+03	
18	0.1167E-02		0.9376E+03	
19	0.1023E-02		0.3581E+03	
20	0.8981E-03		0.3805E+03	
21	0.7895E-03		0.5372E+03	
22	0.6950E-03		0.8865E+03	
23	0.6123E-03		0.7312E+03	
24	0.5399E-03		0.7739E+03	
25	0.4764E-03		0.7279E+03	

FIG. 6.9 – Slow convergence of the method for $r = 1$, and lack of convergence for $r = 100$.

figure 6.10. Finally, we represent on figure 6.11 the different evolutions of the L^2 norm of the residual for the proposed quasi-Newton method along the iterations, depending on the value of the ratio r .

This kind of quasi-Newton Dirichlet-Neumann strategy has been recently used with success in fluid-structure interactions problems and specially hemodynamics, as developed in [GV03] where a simplified model for the fluid is adopted in the preconditioner.

it.	L^2 norm of the residual with	
	Newton algorithm	two-scale quasi-Newton
1	0.6192E+01	0.6249E+01
2	0.1775E+01	0.1811E+01
3	0.1061E+01	0.1075E+01
4	0.6671E+00	0.6747E+00
5	0.3254E+00	0.3292E+00
6	0.8096E-01	0.7836E-01
7	0.5036E-02	0.3414E-02
8	0.2010E-04	0.8871E-05
9	0.3750E-09	0.5000E-06
10	converged	0.1387E-07
11	converged	0.3629E-08

FIG. 6.10 – Convergence of the exact Newton and two-scale quasi-Newton algorithm using the preconditioner (6.10). We have chosen $E_0/E' = 10$ and the convergence criterion is that the L^2 norm of the residual become $\leq 10^{-9}$.

6.7 Conclusion

In this paper, we have introduced, analyzed and tested two symmetrized Dirichlet-Neumann preconditioners that can be used efficiently together with a non-conforming mortar formulation to solve elliptic problems with small geometrical details on the boundary. This method is well-adapted to the case where the details are localized enough to make their resolution relatively cheap. In the case where the small structures would not be so localized to satisfy this assumption, one can imagine a Neumann-Neumann domain decomposition approach [TRV91] to solve the Dirichlet part of the present Dirichlet-Neumann method. Finally, we have deduced a quasi-Newton method which is well-adapted for soft details in the framework of nonlinear problems.

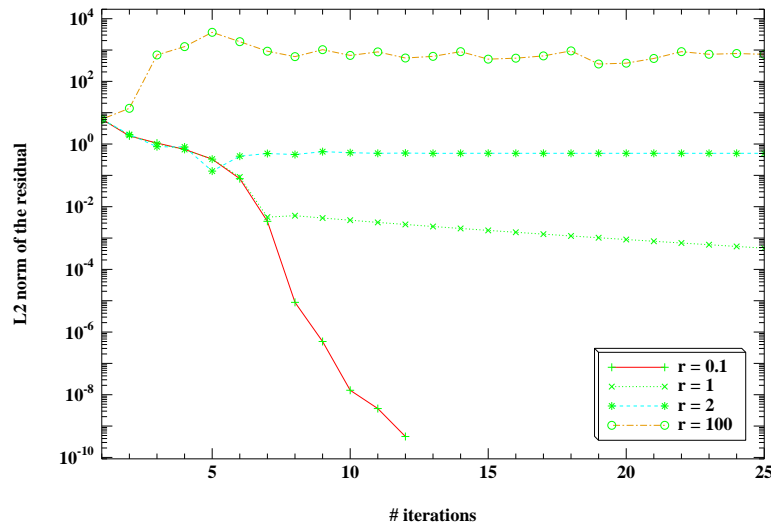


FIG. 6.11 – Evolutions of the L^2 norm of the residual for the proposed quasi-Newton method along the iterations, depending on the value of the ratio r .

Chapitre 7

Conclusion

Le présent travail a permis l'analyse détaillée du comportement énergétique de quelques schémas d'intégration en temps usuels dans le cadre non-linéaire incompressible, et a débouché sur la formulation, l'analyse et le test d'une méthode d'intégration en temps à dissipation réglable, jamais accrétive, et inspirée du travail de Gonzalez [Gon00] et de la présente analyse de conservation pour le schéma de Hilber-Hughes-Taylor [HHT77]. La méthode proposée inclut également une formulation pénalisée conservative des forces de contact normales, utilisant les contraintes de Kuhn et Tucker usuelles aux pas de temps entiers, problématique soulevée dans [LL02]. Les contributions de ce troisième chapitre ont fait l'objet d'implémentations et de validations académiques et industrielles, et permettent l'initialisation et la simulation du roulage instationnaire de pneumatiques.

Le troisième chapitre a également été l'occasion de proposer une méthode d'intégration en temps adaptée à un comportement viscoélastique non-linéaire (issu de [TRK93]) du matériau, et présentant dans ce cadre un bilan énergétique discret exact. Nous avons également montré dans [TH03a] la possible extension de telles techniques conservant l'énergie, aux problèmes en interaction fluide-structure.

Afin d'accroître la modularité de la discrétisation en espace des problèmes d'élastodynamique, nous avons proposé au chapitre 4 l'utilisation de formulations mortiers de recollement de maillages incompatibles, introduites dans [BMP93], et utilisant ici des multiplicateurs de Lagrange discontinu et une stabilisation des déplacements sur l'interface, étendant les idées de [BM00]. Nous avons également montré l'indépendance de la constante de coercivité du problème d'élasticité linéarisé vis-à-vis du nombre et de la taille des sous-domaines, et avons étendu l'analyse statique désormais classique [Woh01] au cadre de l'élastodynamique linéaire. La méthode proposée a fait l'objet d'implémentations académiques et industrielles ayant débouché sur sa validation. En outre, nous avons proposé et testé au chapitre 5, une formulation de la contrainte mortier adaptée au cas d'interfaces géométriquement non-conformes, dans l'esprit de [Pus04], et permettant d'obtenir une certaine amélioration de la robustesse du recollement mortier en contexte industriel.

Enfin, dans le cadre de problèmes à deux échelles, et plus précisément dans le cas où de

petits sous-domaines constituent un raffinement géométrique du bord d'une structure plus grossière, nous avons proposé au chapitre 6, l'utilisation de deux préconditionneurs de type Dirichlet-Neumann [QV99] permettant de résoudre le problème discrétisé par une technique de mortiers isolant les structures fines. Nous avons montré le caractère à deux échelles de ces méthodes, c'est-à-dire l'indépendance du nombre de conditionnement du système préconditionné par rapport au nombre et à la taille des détails géométriques. En outre, nous avons proposé l'utilisation d'un espace grossier (dans l'esprit de [Tal94a, TSV94]) permettant de s'affranchir en termes de qualité du préconditionnement, de la présence de conditions aux limites essentielles sur les détails géométriques. Ces méthodes ont fait l'objet d'une implémentation et d'une validation académiques, et ont également permis de définir une méthode de quasi-Newton efficace dans le cas de détails peu rigides.

En complément du travail réalisé ici, l'implémentation et le test des méthodes proposées dans le cadre de problèmes non-linéaires viscoélastiques, mais également en interaction fluide-structure, pourrait se révéler intéressante et ouvrir encore le champ d'application des méthodes conservatives, déjà fort étudiées pour des raisons de stabilité.

S'agissant des méthodes de mortiers appliquées aux problèmes d'élasticité, quoique déjà très étudiées, quelques développements semblent nécessaires. Tout d'abord, leur utilisation dans le cadre de modèles présentant de fortes discontinuités de coefficients sur les interfaces de recollement reste toujours délicate, et une étude approfondie serait sans doute utile. En outre, leur mise en pratique se heurte sans cesse à des questions de non-conformité géométrique en ce sens que les surfaces à recoller ne coïncident pas. Aussi, si on doit à [FMW04] une analyse récente de la question supposant connue l'interface courbe de recollement, une étude mathématique des méthodes de recollement par patch de Puso et Laursen [PL02, PL03, Pus04] serait sans doute instructive.

Du point de vue des futurs défis à relever, mentionnons qu'un des axes majeurs demeure la compréhension et l'élaboration de techniques de simulation pour des problèmes dynamiques (éventuellement non-linéaires) présentant deux échelles de temps et d'espace. En effet, la présence de phénomènes dynamiques présentant des temps caractéristiques très brefs par rapport au phénomène principal étudié, occasionne des temps de calcul d'autant plus importants que le rapport des temps caractéristiques est grand. Si l'approche par homogénéisation (cf. [All97]) présente l'avantage d'une certaine simplicité en termes de simulation, elle impose une certaine restriction à des problèmes linéaires avec distribution périodique des détails inférieurs. Des alternatives pourraient alors se trouver dans des méthodes dites d'homogénéisation numérique [HW97, MS01], ou dans des techniques récentes considérant comme stochastique la contribution des détails les plus fins (voir le récent travail de [Lel04]).

Bibliographie

- [AAKP99] G. Abdulaiev, Y. Achdou, Y. Kuznetsov, and C. Prudhomme. On a parallel implementation of the mortar element method. *M2AN*, 33(2), 1999.
- [AKP95] Y. Achdou, Y. Kuznetsov, and O. Pironneau. Substructuring preconditioners for the Q_1 mortar element method. *Numerische Mathematik*, 71 :419–449, 1995.
- [All97] G. Allaire. Homogenization and two-scale convergence. *SIAM J. Math. Anal.*, 23(6) :1482–1518, 1997.
- [AMW99] Y. Achdou, Y. Maday, and O. Widlund. Substructuring preconditioners for the mortar method in dimension two. *SIAM Journal of Numerical Analysis*, 32(2) :551–580, 1999.
- [AP98] F. Armero and E. Petöcz. Formulation and analysis of conserving algorithms for frictionless dynamic contact/impact problems. *Comput. Methods Appl. Mech. Engrg.*, 158 :269–300, 1998.
- [AR01a] F. Armero and I. Romero. On the formulation of high-frequency dissipative time-stepping algorithms for nonlinear dynamics. part i : low-order methods for two model problems and nonlinear elastodynamics. *Comput. Methods Appl. Mech. Engrg.*, 190(20-21) :2603–2649, February 2001.
- [AR01b] F. Armero and I. Romero. On the formulation of high-frequency dissipative time-stepping algorithms for nonlinear dynamics. part ii : second-order methods. *Comput. Methods Appl. Mech. Engrg.*, 190(51-52) :6783–6824, October 2001.
- [Arn89] V.I. Arnold. *Mathematical methods of classical mechanics*. Springer-Verlag, 1989.
- [AT95] A. Agouzal and J.M. Thomas. Une méthode d’éléments finis hybrides en décomposition de domaines. *RAIRO M2AN*, 29 :749–764, 1995.
- [Aub87] J.-P. Aubin. *Analyse fonctionnelle appliquée*, volume 1 and 2. Presses universitaires de France, 1987.
- [Bab73] I. Babuska. The finite-element method with lagrangian multipliers. *Numerische Mathematik*, 20 :179–182, 1973.

- [Bat82] K-J. Bathe. *Finite element procedures in engineering analysis*. Prentice-Hall, 1982.
- [BB99] O.A. Bauchau and C.L. Botasso. On the design of energy preserving schemes for flexible, nonlinear multibody systems. *Comput. Methods Appl. Mech. Engrg.*, 169 :61–79, 1999.
- [BBC02] C.L. Botasso, O.A. Bauchau, and J.Y. Choi. An energy decaying scheme for nonlinear dynamics of shells. *Comput. Methods Appl. Mech. Engrg.*, 191 :3099–3121, 2002.
- [BBT01a] M. Borri, C.L. Botasso, and L. Trainelli. Integration of elastic multibody systems by invariant conserving/dissipating algorithms. part i : Formulation. *Comput. Methods Appl. Mech. Engrg.*, 190 :3669–3699, 2001.
- [BBT01b] M. Borri, C.L. Botasso, and L. Trainelli. Integration of elastic multibody systems by invariant conserving/dissipating algorithms. part ii : Numerical schemes and applications. *Comput. Methods Appl. Mech. Engrg.*, 190 :3701–3733, 2001.
- [BBT03] M. Borri, C.L. Botasso, and L. Trainelli. Robust integration schemes for flexible multibody systems. *Comput. Methods Appl. Mech. Engrg.*, 192 :395–420, 2003.
- [BCI00] K.J. Bathe, D. Chapelle, and A. Iosilevich. An inf-sup test for shell finite elements. *Computers and Structures*, 75(5) :439–456, 2000.
- [BD98] D. Braess and W. Dahmen. Stability estimates of the mortar finite element method for 3-dimensional problems. *East-West J. Numer. Math.*, 6 :249–263, 1998.
- [Bel99] F. Ben Belgacem. The mortar finite element method with lagrange multipliers. *Numer. Math.*, 84 :173–197, 1999.
- [BH70] J.H. Bramble and S.R. Hilbert. Estimation of linear functionals on sobolev spaces with application to fourier transforms and spline interpolation. *SIAM J. Numer. Anal.*, 7(1) :112–124, 1970.
- [BJ99] O.A. Bauchau and T. Joo. Computational schemes for nonlinear elastodynamics. *Int. J. Num. Meth. Engr.*, 45(693-719), 1999.
- [BLP78] Bensoussan, Lions, and Papanicolaou. *Homogenization of periodic structures*. North Holland, Amsterdam, 1978.
- [BM97] F. Ben Belgacem and Y. Maday. The mortar element method for three dimensional finite element. *M2AN*, 31 :289–303, 1997.
- [BM00] F. Brezzi and D. Marini. Error estimates for the three-field formulation with bubble stabilization. *Math. Comp.*, 70 :911–934, 2000.
- [BMP93] C. Bernardi, Y. Maday, and A.T. Patera. *Asymptotic and numerical methods for partial differential equations with critical parameters*, chapter Domain decomposition by the mortar element method., pages 269–286. 1993.

- [BMP94] C. Bernardi, Y. Maday, and A.T. Patera. *Nonlinear partial differential equations and their applications.*, chapter A new nonconforming approach to domain decomposition : the mortar element method., pages 13–51. Pitman, Paris, 1994.
- [BMR01] A. Buffa, Y. Maday, and F. Rapetti. A sliding mesh-mortar method for two dimensional eddy currents model for electric engines. *M2AN*, 35(2) :191–228, 2001.
- [BN83] J. Boland and R. Nicolaides. Stability of finite elements under divergence constraint. *SIAM Numer. Anal.*, 20(4) :722–731, 1983.
- [Bou95] J-P. Bourguignon. *Calcul variationnel*. Ellipses, 1995.
- [Bre74] F. Brezzi. On the existence, uniqueness and approximation of saddle-point problems arising from lagrangian multipliers. *RAIRO Analyse Numérique, Série Rouge*, 8 :129–151, 1974.
- [Bré99] H. Brézis. *Analyse fonctionnelle*. Dunod, 1999.
- [Bre03] S. Brenner. Poincaré-friedrichs inequalities for piecewise H^1 functions. *SIAM J. Numer. Anal.*, 41(1) :306–324, 2003.
- [Bre04] S. Brenner. Korn’s inequalities for piecewise H^1 vector fields. *Mathematics of Computation*, 73 :1067–1087, 2004.
- [BT96] O.A. Bauchau and N.J. Theron. Energy decaying schemes for nonlinear beam models. *Comput. Methods Appl. Mech. Engrg.*, 134 :37–56, 1996.
- [Bui03] Q.V. Bui. Energy dissipative time finite elements for classical mechanics. *Comput. Methods Appl. Mech. Engrg.*, 192 :2925–2947, 2003.
- [Cia88] P-G. Ciarlet. *Mathematical Elasticity*. North Holland, 1988.
- [Cia92] P-G. Ciarlet. *Introduction à l’analyse numérique matricielle et à l’optimisation*. Dunod, 1992.
- [CLM97] L. Cazabœuf, C. Lacour, and Y. Maday. Numerical quadratures and mortar methods. In John Wiley and Sons, editors, *Computational Science for the 21st Century*, pages 119–128, 1997.
- [Cri97] M.A. Crisfield. *Nonlinear finite element analysis of solids and structures*, volume 2 : Advanced topics. Wiley, 1997.
- [CSM03] David Cohen-Steiner and Jean-Marie Morvan. Restricted delaunay triangulations and normal cycle. In *SoCG’03*, San Diego, California, USA, June 2003.
- [DL55] J. Deny and J.-L. Lions. Les espaces du type Beppo-Levi. *Annales de l’Institut Fourier (Grenoble)*, 5 :305–370, 1955.
- [DL72] G. Duvaut and J-L. Lions. *Les inéquations en Mécanique et en Physique*. Dunod, 1972.

- [EG02] A. Ern and J-L. Guermond. *Eléments finis : théorie, applications, mise en oeuvre*, volume 36 of *collection Mathématiques et Applications*. Springer-Verlag, 2002. Also available in english as the reference [EG04].
- [EG04] A. Ern and J.-L. Guermond. *Theory and Practice of Finite Elements*, volume 159 of *Applied Mathematical Series*. Springer-Verlag, New York, 2004.
- [Eyn04] A. Eynard. Application de la méthode des mortiers à la simulation pneumatique. Rapport de stage de fin d'études, ISIMA, 2004.
- [Fer02] Anca Ferentă. *Conception et analyse d'éléments finis de coques minces adaptés à l'inclusion dans un milieu tridimensionnel*. PhD thesis, Ecole Polytechnique, 2002.
- [FLT98] C. Farhat, M. Lesoinne, and P. Le Tallec. Load and motion transfer algorithms for fluid/structure interaction problems with non-matching discrete interfaces : Momentum and energy conservation, optimal discretization and application to aeroelasticity. *Comp. Meth. Appl. Mech. Eng.*, 157(1-2) :95–114, 1998.
- [FMW04] B. Flemisch, J.M. Melenk, and B. Wohlmuth. Mortar methods with curved interfaces. Technical report, Max Planck Institute, 2004. Preprint.
- [FR91] C. Farhat and F-X. Roux. A method of finite element tearing and interconnecting and its parallel solution algorithm. *Int. J. Num. Meth. Engr.*, 32 :1205–1228, october 1991.
- [GF99] Paul-Louis George and Pascal Jean Frey. *Maillages*. Germes Science publications, 1999.
- [GGTN04] L. Gerardo-Giorda, P. Le Tallec, and F. Nataf. A Robin-Robin preconditioner for advection-diffusion equations with discontinuous coefficients. *Computer Methods in Applied Mechanics and Engineering*, 193 :745–764, March 2004.
- [GLB03] J.-F. Gerbeau, T. Lelièvre, and C. Le Bris. Simulation of MHD flows with moving interfaces. *Journal of Computational Physics*, 184 :163–191, 2003.
- [Gon96] O. Gonzalez. Time integration and discrete hamiltonian systems. *Journal of Nonlinear Science*, 6 :449–467, 1996.
- [Gon00] O. Gonzalez. Exact energy and momentum conserving algorithms for general models in nonlinear elasticity. *Comput. Methods Appl. Mech. Engrg.*, 190(13-14) :1763–1783, December 2000.
- [Gop99] J. Gopalakrishnan. *On the Mortar Finite Element Method*. PhD thesis, Texas A and M University, August 1999.
- [GR86] V. Girault and P-A. Raviart. *Finite element methods for Navier-Stokes equations : theory and algorithms*. 1986.
- [GR93] M. Gérardin and D. Rixen. *Théorie des vibrations : application à la dynamique des structures*. Masson, 1993.

- [GV03] J.-F. Gerbeau and M. Vidrascu. A quasi-Newton algorithm based on a reduced model for fluid-structure interaction problems in blood flows. *Mathematical Modelling and Numerical Analysis (M2AN)*, 37(4) :663–680, 2003.
- [GvL83] G.H. Golub and C.F. van Loan. *Matrix computations*. John Hopkins University Press, Baltimore, 1983.
- [Hau04] P. Hauret. Intégration en temps pour la dynamique hyperélastique des structures non-linéaires incompressibles. Technical report, Manufacture Française des Pneumatiques Michelin, 2004. Confidentiel industrie.
- [HHT77] H.M. Hilber, T.J.R. Hughes, and R.L. Taylor. Improved numerical dissipation for time integration algorithms in structural dynamics. *Earthquake Engin. and Struct. Dynamics*, 5 :283–292, 1977.
- [HLC78] T.J.R. Hughes, W.K. Liu, and Caughey. Transient finite element formulations that preserve energy. *Journal of Applied Mathematics*, 45 :366–370, 1978.
- [HLW02] E. Hairer, C. Lubich, and G. Wanner. *Geometric Numerical Integration*. Springer-Verlag, 2002.
- [HT02] P. Hauret and P. Le Tallec. Conservation analysis for integration schemes in quasi-incompressible nonlinear elastodynamics. Technical Report 499, CMAP, october 2002.
- [HT04a] P. Hauret and P. Le Tallec. Dirichlet-neumann preconditioners for elliptic problems with small disjoint geometric refinements on the boundary. Technical Report 552, CMAP, september 2004.
- [HT04b] P. Hauret and P. Le Tallec. A stabilized discontinuous mortar formulation for elastostatics and elastodynamics problems, part i : abstract framework. Technical Report 553, CMAP, september 2004.
- [HT04c] P. Hauret and P. Le Tallec. A stabilized discontinuous mortar formulation for elastostatics and elastodynamics problems, part ii : discontinuous lagrange multipliers. Technical Report 554, CMAP, september 2004.
- [Hug87] T.J.R. Hughes. *The Finite Element Method, Linear Static and Dynamic Finite Element Analysis*. Prentice-Hall, 1987.
- [HW97] T.Y. Hou and W-H. Wu. A multiscale finite element method for elliptic problems in composite materials and porous media. *J. Comput. Phys.*, 134(1) :169–189, june 1997.
- [Joh85] K.L. Johnson. *Contact Mechanics*. Cambridge University Press, 1985.
- [KMOW00] C. Kane, J.E. Marsden, M. Ortiz, and M. West. Variational integrators and the Newmark algorithm for conservative and dissipative mechanical systems. *International Journal for Numerical Methods in Engineering*, 49 :1295–1325, 2000.
- [Lar95] B. Larrouy-Dulis. *Méthodes numériques pour les sciences de l'ingénieur*. Cours de l'Ecole Polytechnique, 1995.

- [Lau02] T.A. Laursen. *Computational contact and impact mechanics*. Springer, 2002.
- [LB99] R.S. Langley and P. Bremner. A hybrid method for the vibration analysis of complex structural-acoustic systems. *Journal of the Acoustical Society of America*, 150(3) :1657, March 1999.
- [LC97] T.A. Laursen and V. Chawla. Design of energy conserving algorithms for frictionless dynamic contact problems. *International Journal for Numerical Methods in Engineering*, 40 :863–886, 1997.
- [Lel04] T. Lelièvre. *Modèles multi-échelles pour les fluides viscoélastiques*. PhD thesis, Ecole Nationale des Ponts et Chaussées, 2004.
- [LL02] T.A. Laursen and G.R. Love. Improved implicit integrators for transient impact problems; geometric admissibility within the conserving framework. *Int. J. Num. Meth. Engr.*, 53(2) :245–274, January 2002.
- [LL03] G.R. Love and T.A. Laursen. Improved implicit integrators for transient impact problems; dynamic frictional dissipation within the conserving framework. *Comput. Methods Appl. Mech. Engrg.*, 192(19) :2223–2248, May 2003.
- [LM72] J-L. Lions and E. Magenes. *Non homogeneous boundary value problems and applications*. Springer-Verlag, 1972.
- [LM01] T.A. Laursen and X.N. Meng. A new solution procedure for application of energy-conserving algorithms to general constitutive models in nonlinear elastodynamics. *Computer Methods in Appl. Mech. and Eng.*, 190 :6309–6322, September 2001.
- [Lue84] David G. Luenberger. *Linear and Nonlinear Programming*. Addison-Wesley Publishing Company, 1984.
- [MH83] J.E. Marsden and T.J.R. Hughes. *Mathematical foundations of elasticity*. Prentice-Hall, 1983.
- [MK99] H. Munthe-Kass. High order runge-kutta methods on manifolds. *Applied Numerical Mathematics*, 29 :115–127, 1999.
- [MN85] A. Matsokin and S. Nepomniaschik. A Schwarz alternating method in a subspace. *Sov. Math.*, 29 :78–84, 1985.
- [MR94] J.E. Marsden and T.S Ratiu. *Introduction to mechanics and symmetry*. Springer-Verlag, 1994.
- [MRW02] Y. Maday, F. Rapetti, and B. Wohlmuth. The influence of quadrature formulas in 3d mortar methods. In *Recent Developments in Domain Decomposition Methods, Lecture Notes in Computational Science and Engineering*, volume 23, pages 203–221. Springer, 2002.
- [MS01] A-M. Matache and C. Schwab. *Lecture Notes in Computational Science and Engineering*, volume 20, chapter Generalized FEM for Homogenization Problems, pages 197–239. Springer-Verlag, 2001.

- [MW01] J.E. Marsden and M. West. *Acta Numerica*, chapter Discrete mechanics and variational integrators, pages 357–514. Cambridge University Press, 2001.
- [Neč67] J. Nečas. *Les méthodes directes en théorie des équations elliptiques*. Masson, Paris, 1967.
- [NNR77] E. Naug, O.S Nguyen, and A.L De Rouvray. An improved energy conserving implicit time integration algorithm for nonlinear dynamic structural analysis. In *Proceedings of the Fourth Conference on Structural Mechanics in Reactor Technology*, San Francisco, August 1977.
- [O'R82] J. O'Rourke. A new linear algorithm for intersecting convex polygons. *Comput. Graph Image Processing*, 19 :384–391, 1982.
- [O'R98] J. O'Rourke. *Computational geometry in C*. Cambridge University Press, 2nd edition, 1998.
- [PL02] M.A. Puso and T.A. Laursen. A 3d contact smoothing method using gregory patches. *International Journal for Numerical Methods in Engineering*, 54 :1161–1194, 2002.
- [PL03] M.A. Puso and T.A Laursen. Mesh tying on curved surfaces in 3d. *Engineering Computations*, 20 :305–139, 2003.
- [Pus04] M.A. Puso. A 3d mortar method for solid mechanics. *Int. J. Num. Meth. Engr.*, 59 :315–336, 2004.
- [QV99] A. Quarteroni and A. Valli. *Domain Decomposition Methods for Partial Differential Equations*. Oxford University Press, 1999.
- [RT98] P-A Raviart and J-M. Thomas. *Introduction à l'analyse numérique des équations aux dérivées partielles*. Dunod, 1998.
- [Sal88] J. Salençon. *Mécanique des milieux continus*. Ellipses, 1988.
- [Sca04] G. Scarella. *Analyse mathématique et numérique des équations de l'élastodynamique en présence de contact unilatéral*. PhD thesis, Université Paris Dauphine, 2004. contrat de collaboration E.D.F.-L.M.A.-I.N.R.I.A.
- [Sch66] L. Schwartz. *Théorie des distributions*. Hermann, 1966.
- [Ses98] P. Seshaiyer. *Non-conforming hp finite element methods*. PhD thesis, University of Maryland, 1998.
- [SG93] J.C. Simo and O. Gonzalez. Assessment of energy-momentum and symplectic schemes for stiff dynamical systems. In *American Society of Mechanical Engineers, ASME Winter Annual Meeting, New Orleans, Louisiana*, 1993.
- [SL92] J.C. Simo and T.A. Laursen. Augmented lagrangian treatment of contact problems involving friction. *Comput. Struct.*, 42 :97–116, 1992.
- [SSC94] J.M. Sanz-Serna and M.P. Calvo. *Numerical Hamiltonian Problems*. Chapman & Hall, 1994.

- [ST92] J.C. Simo and N. Tarnow. The discrete energy-momentum method. conserving algorithms for non linear elastodynamics. *Z angew Math Phys*, 43 :757–792, 1992.
- [Ste84] R. Stenberg. Analysis of mixed finite element methods for the stokes problem : a unified approach. *Math. of Comp.*, 42 :9–23, 1984.
- [Ste90] R. Stenberg. A technique for analysing finite element methods for viscous incompressible flow. *Int. J. Num. Meth. Fluids*, 11 :935–948, 1990.
- [Ste99] D. Stefanica. *Domain decomposition methods for mortar finite elements*. PhD thesis, Courant Institute of Mathematical Sciences, New York University, 1999.
- [Str73] G. Strang. *The Mathematical Foundations of the Finite Element Method*, chapter Variational crimes in the finite element method, pages 689–710. Academic Press, New York, 1973.
- [SZ90] L.R. Scott and S. Zhang. Finite element interpolation of nonsmooth functions satisfying boundary conditions. *Math. Comp.*, 54(190) :483–493, april 1990.
- [Tal81] P. Le Tallec. Compatibility condition and existence results in discrete finite incompressible elasticity. *Computer Methods in Applied Mechanics and Engineering*, 27 :239–259, 1981.
- [Tal93] P. Le Tallec. Neumann-Neumann domain decomposition algorithm for solving 2d elliptic problems with nonmatching grids. *East-West J. Numer. Math.*, 1(2) :129–146, 1993.
- [Tal94a] P. Le Tallec. *Computational Mechanics Advances*, volume 1, chapter Domain Decomposition Methods in Computational Mechanics, pages 123–217. North Holland, 1994.
- [Tal94b] P. Le Tallec. *Handbook of Numerical Analysis*, volume 3. North Holland, 1994. Part 2 : Numerical methods for solids.
- [Tal99] P. Le Tallec. *Introduction à la dynamique des structures*. Ecole Polytechnique, 1999.
- [TH03a] P. Le Tallec and P. Hauret. Energy conservation in fluid-structure interactions. In P. Neittanmaki Y. Kuznetsov and O. Pironneau, editors, *Numerical methods for scientific computing, variational problems and applications*, CIMNE, Barcelona, 2003.
- [TH03b] P. Le Tallec and P. Hauret. Nonlinear schemes and multiscale preconditioners for time evolution problems in constrained structural dynamics. In K.-J. Bathe, editor, *Proceedings of the 2nd MIT Conference on Computational Fluid and Solid Mechanics*, pages 19–22, Boston, June 2003.
- [THR02] P. Le Tallec, P. Hauret, and A. Rezgui. Efficient solvers for the dynamic analyses of nonlinear multiscale structures. In H.A Mang, F.G. Rammerstorfer, and J. Eberhardsteiner, editors, *Proceedings of the Fifth World Congress*

- on *Computational Mechanics WCCM V*, Vienna, Austria, July 2002. Vienna University of Technology, Austria. ISBN 3-9501554-0-6, full paper available at <http://wccm.tuwien.ac.at>, abstract page II-61.
- [TM00] P. Le Tallec and S. Mani. Numeric analysis of a linearized fluid-structure interaction problem. *Numerische Mathematik*, 87 :317–354, 2000.
- [TM01] P. Le Tallec and J. Mouro. Fluid structure interaction with large structural displacements. *Comp. Meth. Appl. Mech. Eng.*, 190(24-25) :3039–3068, 2001.
- [TP93] R.L. Taylor and P. Papdopoulos. On a finite element method for dynamic contact impact problems. *International Journal for Numerical Methods in Engineering*, 36 :2123–2140, 1993.
- [TRK93] P. Le Tallec, C. Rahier, and A. Kaiss. Three-dimensional incompressible viscoelasticity in large strains : Formulation and numerical approximation. *Comput. Methods Appl. Mech. Engrg.*, 1993.
- [TRV91] P. Le Tallec, Y.H. De Roeck, and M. Vidrascu. Domain decomposition methods for large linearly elliptic three dimensional problems. *J. Comput. Appl. Math.*, 34 :93–117, 1991.
- [TSV94] P. Le Tallec, T. Sassi, and M. Vidrascu. Three-dimensional domain decomposition methods with nonmatching grids and unstructured coarse solvers. In D. Keyes and al., editors, *Domain decomposition methods in scientific and engineering computing. Proceedings of the 7th international conference on domain decomposition*, pages 61–74. American Mathematical Society, 1994.
- [Wlo87] J. Wloka. *Partial differential equations*. Cambridge University Press, UK, 1987.
- [Woh99] B.I. Wohlmuth. Hierarchical a posteriori error estimators for mortar finite element methods with lagrange multipliers. *SIAM J. Numer. Anal.*, 36 :1636–1658, 1999.
- [Woh00] B.I. Wohlmuth. A mortar finite element method using dual spaces for the lagrange multiplier. *SIAM J. Numer. Anal.*, 38 :989–1012, 2000.
- [Woh01] B.I. Wohlmuth. *Discretization methods and iterative solvers based on domain decomposition*. Springer, 2001.
- [Wri02] P. Wriggers. *Computational Contact Mechanics*. John Wiley and Sons, 2002.
- [Yos65] Yosida. *Functional Analysis*. Springer, 1965.